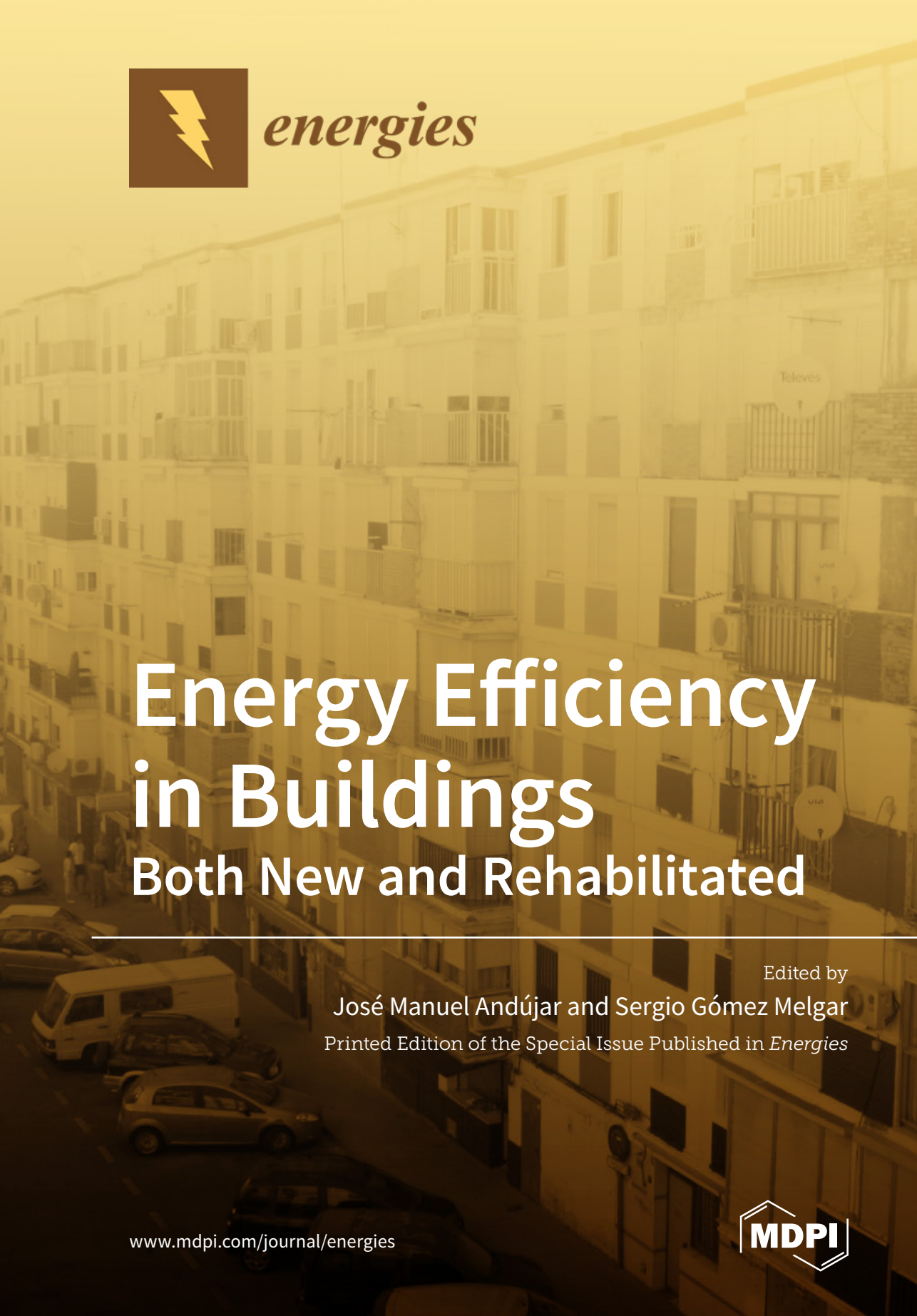

energies

Energy Efficiency in Buildings

Both New and Rehabilitated

Edited by

José Manuel Andújar and Sergio Gómez Melgar

Printed Edition of the Special Issue Published in *Energies*

www.mdpi.com/journal/energies

MDPI

Energy Efficiency in Buildings

Energy Efficiency in Buildings

Both New and Rehabilitated

Special Issue Editors

José Manuel Andújar
Sergio Gómez Melgar

MDPI • Basel • Beijing • Wuhan • Barcelona • Belgrade • Manchester • Tokyo • Cluj • Tianjin

Special Issue Editors
José Manuel Andújar
University of Huelva
Spain

Sergio Gómez Melgar
University of Huelva
Spain

Editorial Office
MDPI
St. Alban-Anlage 66
4052 Basel, Switzerland

This is a reprint of articles from the Special Issue published online in the open access journal *Energies* (ISSN 1996-1073) (available at: https://www.mdpi.com/journal/energies/special_issues/efficiency_buildings).

For citation purposes, cite each article independently as indicated on the article page online and as indicated below:

LastName, A.A.; LastName, B.B.; LastName, C.C. Article Title. *Journal Name* **Year**, *Article Number*, Page Range.

ISBN 978-3-03928-702-4 (Pbk)
ISBN 978-3-03928-703-1 (PDF)

Cover image courtesy of Sergio Gómez Melgar.

Contents

About the Special Issue Editors

José Manuel Andújar Márquez got his PhD in 2000. He is currently a Full Professor of Systems Engineering and Automatic Control at the University of Huelva, Spain. Throughout his professional life he has received 27 awards and academic honors. He has supervised 12 doctoral theses, eight of them prize winning, and has 15 international patents. He has more than 100 papers published in indexed journals in the ISI Journal Citation Reports. In particular, he has 55 quartile Q1 publications in 24 different journals, most being among the top 10 and several being number one. He has led or co-led 61 research projects funded by public institutions and companies. His main research interests are control engineering, renewable energy systems, remote piloted aircraft systems applications, and engineering education.

Sergio Gómez Melgar got his PhD in 2017. He is currently an Associate Professor of Structural Engineering at the University of Huelva (Spain), a Visiting Professor at Nanjing University (China) and the CEO_Architect for LAR Arquitectura (Spain). His research is in the field of sustainable architectonical design and energy efficiency in buildings, communities, and cities. His work utilizes uhuMEB—a new methodology for the design, construction and operation of minimal energy buildings (MEB), both new and retrofitted—to introduce the BIM/BEM standard from the first steps of the architectonical design, as part of the necessary holistic approach. This meethod uses on-site real measurements of physical variables (temperature, humidity, air quality, solar radiation, energy, etc.) and renewable sources (solar, geothermal, and hydrogen) integrated in the architecture of the building.

energies

MDPI

Review

Green Building Rating Systems and the New Framework Level(s): A Critical Review of Sustainability Certification within Europe

Antonio Sánchez Cordero [1], Sergio Gómez Melgar [2,*] and José Manuel Andújar Márquez [2]

[1] Programa de Ciencia y Tecnología Industrial y Ambiental, Escuela Técnica Superior de Ingeniería, Universidad de Huelva, CP. 21007 Huelva, Spain; antonio.sanchez443@alu.uhu.es

[2] TEP192 Control y Robótica, Escuela Técnica Superior de Ingeniería, Universidad de Huelva, CP. 21007 Huelva, Spain; andujar@uhu.es

* Correspondence: sergomel@uhu.es

Received: 11 November 2019; Accepted: 18 December 2019; Published: 21 December 2019

Abstract: Increasing problems regarding pollution and climate change have long been demonstrated by scientific evidence. An important portion of carbon emissions are produced by the building sector. These emissions are directly related not only to the building's energy consumption, but also other building attributes affecting the construction and operation of existing buildings: materials selection, waste management, transportation, water consumption, and others. To help reduce these emissions, several green building rating system (GBRSs) have appeared during the last years. This has made it difficult for stakeholders to identify which GBRSs could be more suitable to a specific project. The heterogeneity of the GRBS scenario requires the creation of a transparent and robust indicator framework that can be used in any country within the European Union (EU), which is a common EU framework of core sustainability indicators for office and residential buildings Level(s) with the goal to provide a solid structure for building sustainability certification across all countries of the EU. This paper provides a comprehensive review of the most common GBRSs within the EU: Building Research Establishment Assessment Method (BREEAM), Deutsche Gesellschaft für Nachhaltiges Bauen (DGNB), Haute Qualité Environnementale (HQE), and Leadership in Energy & Environmental Design (LEED), and a bottom up comparison of the influence in the final score produced by the indicators stated by Level(s). The indicators studied show a different influence of Level(s) indicators on every GBRS, where LEED and BREEAM were most affected while HQE and DGNB were less so. This paper demonstrates the heterogeneity of current GRBSs in the EU scenario and the difference between sustainability assessments, where DGNB seems to be more aligned to the current EU framework. Finally, the paper concludes with the need to work to achieve alignment between the GBRS and Level(s).

Keywords: Level(s); green building rating systems; Building Research Establishment Assessment Method (BREEAM); Deutsche Gesellschaft für Nachhaltiges Bauen (DGNB); Haute Qualité Environnementale (HQE); Leadership in Energy & Environmental Design (LEED)

1. Introduction

The world's global energy consumption has been steadily increasing during the last several years, which has consequently produced an equivalent growth in atmospheric CO_2 emissions [1]. The constant urbanization process of developing countries and worldwide development of the building construction sector have been defined as some of the most important causes of the growth in pollution [2]. At the same time, as the construction rate of cities and buildings keeps steadily growing, buildings in developed countries keep on increasing their energy demands to satisfy the inhabitant's needs [3,4].

It is a proven fact that human activity is the driven force of current climate change [5], and there is no time to lose to mitigate its impacts. Although some countries are making interesting efforts to improve energy performance, others are not [6,7], thus the only option to succeed seems to be a coordinated global effort. On 25 September, 2015, The 70th General Assembly of the United Nations approved the 2030 Agenda for Sustainable Development: Transforming our world (2030 Agenda) [8]. There, the committee established an action plan of 17 sustainable development goals (SDG) and 169 targets for planet and prosperity that must be followed by the signatory countries.

The EU had already been working along the same direction before signing the 2030 Agenda as it is included in its action plan [9], and measured by the United Nations Economic Commission for Europe (UNECE) [10]. Among the ten priorities defined by the EU to converge with the 2030 Agenda, the first one of them, A new Boost for jobs, growth and investment, is based on the principle of circular economy, which is included in the EU 2015 Circular Economy Action Plan [11] and confirmed in the EU 2017 Work Programme [9]. It contains the adoption of several SDGs: SDG6, SDG8, SDG9, SDG11, SDG12, SDG13, SDG14, and SDG15. However, how these SDG can be achieved and how can they be measured, evaluated, and compared requires the introduction of specific tools and frameworks.

In 2014, the European Commission (EC) released the Communication on Resource Efficiency Opportunities in the Building Sector—COM (2014) 445 [12], which declared the need for a common European approach to improve the environmental performance of buildings throughout their whole lifecycle. In fact, this is a policy maker response with the objective to organize the complex GBRS ecosystems worldwide and specifically within the EU. According to different authors, there are between 70 [13] and 600 [14] GBRSs working at the moment.

In the construction environment where buildings trends are to gradually reduce its energy consumption to become minimum energy buildings (MEB) [15], different areas of building design, construction, and operation like materials selection [16] or waste management [17,18] are producing a proportionally higher impact, which introduces the need to provide comprehensive tools that go beyond energy benchmarking.

As Doan et al. [19] defines, GBRSs are focused on the measurement of environmental aspects like energy, land, water, and materials. These provide more affordable and realistic measurements for the industry than others called sustainable building rating systems, justifying a discussion to replace the word green for sustainability [20]. Although it is not yet widely accepted and these two words are still far from convergence, it reveals terms that must be used carefully due to its transcendence. Today, there is not a single accepted definition about what is sustainability and what aspects it includes, but it is commonly accepted that it contains no less than three aspects that are environmental (ENV), economic (ECO), and social (SOC), as stated by Brundtland in 1987 [21]. From there, other pillars were included: a fourth pillar called institutional (INS), which is not usually commented [22], and later, in 2010, The United Cities and Local Government (UCLG) enounced the fifth pillar: culture [23]. Therefore, there is uncertainty about what concepts will include sustainability in the future, but it is still the environmental impact that weighs more in current GBRSs [14,24–27]. Due to the uncertain definition of what we refer to with regard to sustainability, the term green will prevail for the moment.

In 1990, the first version of The Building Research Environmental Assessment Method (BREEAM) [28] was launched in the United Kingdom. This was considered the first GBRS published in the world [13]. From then, many others like the Leadership in Energy and Environmental Design (LEED) [29], *Deutsche Gesellschaft für Nachhaltigies Bauen* (DGNB) [30], and *Haute Qualité Environnementale* (HQE) [31] have followed with similar purpose: to provide reliable assessment for buildings through an indicator system with several different criteria. Now, most have spread wide from the underground to mainstream, and figures of building's certified worldwide have exponentially increased from just a few at the end of the 20th century to dozens of thousands today [32].

Among them, LEED and BREEAM are described as the most popular, although DGNB and HQE have a certain degree of international success. The Comprehensive Assessment System for Built Environment Efficiency (CASBEE) [33], and GREEN STAR [34], which are not used within

the EU, also have international versions and are widely used in other regions outside the EU [13]. The Environmental Standard for Green Buildings (ESGB) [35], which is released and controlled by the Ministry of Urban Housing and Rural Development of the People's Republic of China (MOUHURD), has no international version, but due the size of China, it is obviously used by many stakeholders [36]. Apart from BREEAM, DGNB, HQE, and LEED, many countries in the EU have developed their own GBRSs [13] based on four different strategies (see Table 1 and Figure 1):

- A local adaptation of BREEAM INT GBRS made by national institutes [37] like BREEAM ES [38], BREEAM NL [39], BREEAM DE [40], BREEAM NOR [41], and BREEAM SW [42].
- A local adaptation of an SBTool, made by a national member of The World Green Building Council (WGBC, London, UK) such as SBToolCZ [43], SBToolPT [25,44], *Instituto per l'innovazione e trasparenza degli appalti e lacompatibilita ambientale* (ITACA) [14,45,46], VERDE [47,48], and the *Total quality building assessment* (TQB) [49].
- A new GBRS developed by a national member of the WGBC like DGNB, HQE, Miljoyggnad, and Minergie ECO [50].
- Independent attempts to create a holistic transparent and regionally adaptable GBRS like Open House [51], which can be seen as the first step of LEVEL(s).

Table 1. List of the most representative GBRS within the EU.

Country	GBRS Name	Organization	Starting	Version	References
Austria	TQB 2010	OGNB	2010	National	[52]
	BREEAM AT	DIFNI		National	[37,53]
Czech Republic	SBToolCZ	IISBE Czech/CIDEAS	2010	National	[43]
France	HQE	HQE	1997	International	[31]
Germany	DGNB	German Sustainable Building Council	2008	International	[54]
	BREEAM DE	TÜV SÜD DIFNI	2011	National	[37,40]
Italy	LEED Italia	Italy GBC	2006	National	[55]
	ITACA	IISBE Italia	2004	National	[45]
The Netherlands	BREEAM NL	Dutch GBC	2011	National	[37]
Norway	BREEAM NW	Norwegian GBC	2011	National	[37]
Portugal	SBToolPT	iiSBE PT	2009	National	[25,44]
Spain	VERDE	Spanish GBC	2011	National	[48]
	BREEAM ES	ITG	2010	National	[37]
Sweden	BREEAM SE	Swedish GBC	2011	National	[37]
	Miljöbyggnad		2011	National	[56]
Switzerland	BREEAM CH	DIFNI	2011	National	[37]
	Minergie ECO	MINERGIE	1998	National	[50]
United Kingdom	BREEAM	BRE	1990	International	[37]
	HQM		2015	National	[57]
	CEEQUAL		2011	International	[58]

The whole picture represents a total of more than 37 international and 54 EU certificates with more than 500 different indicators [51,59] working in the EU at the same time, which creates a heterogeneous system that is difficult to manage for policy makers and stakeholders. Therefore, this scenario requires the creation of a transparent and robust framework of indicators that can be used by policy makers and stakeholders in any country within the EU. As a consequence, in August 2017, Level(s), a voluntary reporting framework to improve the sustainability of buildings within the EU, was launched [60]

and its full development process can be followed through the website of the Joint Research Centre (JRC) [61]. The framework is still in its beta version, and has been tested by 136 projects in 21 different countries applied to buildings from different typologies such as residential and others, but the JRC has already established spring 2020 as the official end of the testing period, and the date for the launch of the final version [62].

The Level(s) indicators proposed are organized in six different categories: emissions, resources, water, wellbeing and comfort, resilience, and adaptation to climate change [61]. This categorization serves as a basis for a comparison between the most popular GBRSs in the EU. This paper provides a comprehensive top-down critical review between most used GBRSs in the EU and Level(s) to identify potentially emerging conflicts in the application of the new framework. Furthermore, the specific objectives were to:

- Establish a comparison between the most widely used GBRSs in the EU: BREEAM, DGNB, HQE, LEED, and describe the main differences according to regional adaptation and the indicators included as well as stages covered.
- Provide a comparison between those indicators stated by Level(s) and similar ones included in BREEAM, DGNB, HQE, and LEED.
- Identify similarities and conflicts between Level(s) and current GBRSs in EU to find areas that may be considered in both future versions of the framework, and the mentioned GBRS.

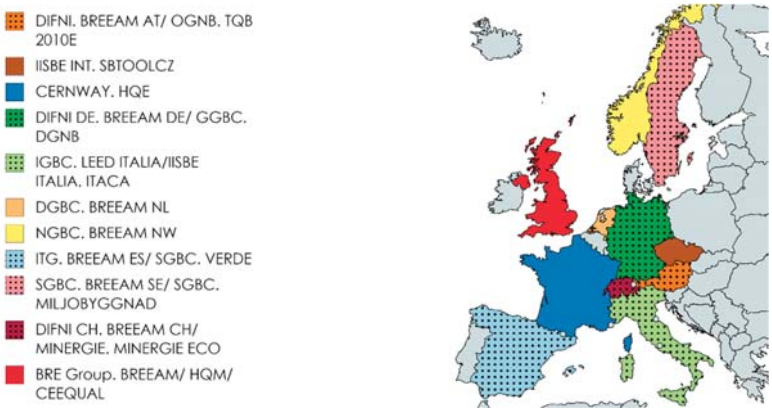

Figure 1. Map of most representative GBRS within the EU.

2. Methodology

2.1. Materials and Methods

Due to the nature of this research, which is mainly a critical revision paper, software tools were the only material used. No other materials like hardware devices, surveys, or others were used. These software tools will be explained in detail in the following section.

In summary, this research used a 5-step methodology to provide a comprehensive review of the current status of GBRS within the EU (Figure 2).

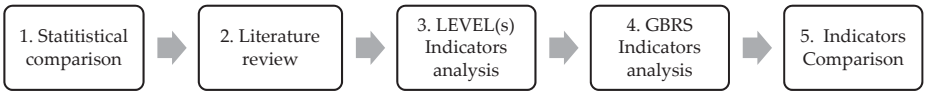

Figure 2. The 5-step methodology flux diagram.

The indicator system is the core of the sustainability assessment process. This research was conducted in a double way: a bibliographic review from up–down to determine the most interesting topics in the current research as well as a bottom–up technical manuals review focused on indicator systems as described in the following sections.

2.2. GBRS Statistical Comparison

According to the objective of this research paper, a ranking of the most used GBRSs within the EU must be defined to proceed with a consistent methodology that can be applied for every GBRS carried out in any of the EU members. Therefore, the establishment of the aforementioned ranking was defined as the first step of this methodology. As can be seen in Figure 3, the statistical comparison carried out includes both registered and certified GBRSs.

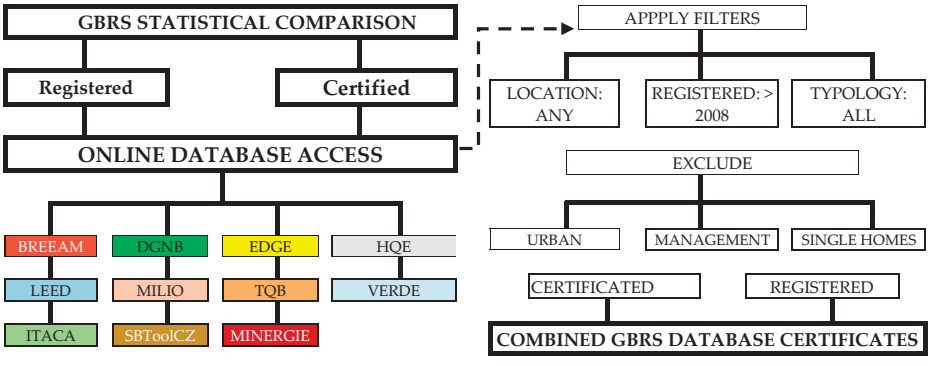

Figure 3. GBRS methodology for statistical comparison.

To obtain reliable data on the number of certificates from the most representative GBRSs in the EU, this research gathered data from official websites like BREEAM [37], DGNB [54], HQE [63], LEED [64], MILJOYGGNAD [56], MINERGIE [50], and TQB-2010 [52]. For those with no available data on their websites, it was necessary to proceed with a consultation process [64–68], carried out on 31 July, 2019. EDGE [69] and VERDE [48] responded with a detailed list of certified and registered buildings as requested. Some others neither published detailed data on the website nor sent requested information, like ITACA and SBToolCZ. Fortunately, there were only a few of them and most likely those with a smaller number of certificates across the whole EU. Future updates of this work will probably include more comprehensive data about these minoritarian GBRSs.

According to the objective of this research, and to provide consistent requirements with Section 2.2 that can be easily compared, some exclusions were applied: data before 2008, single homes, urban developments, and building management certification (Figure 3).

2.3. GBRS Literature Review

Once the major worldwide GBRSs were defined, a literature review research was conducted. The aim of this second step was to (a) observe the development of research in green rating systems; (b) find out how popular they are in the research community; (c) discover through previous scientific papers which methodologies can be used to compare GBRS; and (d) identify which GBRSs still received less attention from researchers, even when they had an strong market presence.

Scopus (SCO) and Web of Science (WOS) were selected as the research databases, according to their relevance in the scientific field [70]. According to the objective of this paper and the results from Section 3.1, the following acronyms were defined as keywords: BREEAM, DGNB, HQE, LEED and Levels in the main search fields as the title, abstract, and keywords. Later, some filters were applied to narrow the results given by search: only journal articles, published after 2008, in the English language.

Finally, an author's personal revision was applied to discard inadequate results that may arise when using the LEED acronym because of its ambiguous significance in other disciplines. The results from both SCO and WOS were finally merged into a single database managed with Mendeley software (Figure 4).

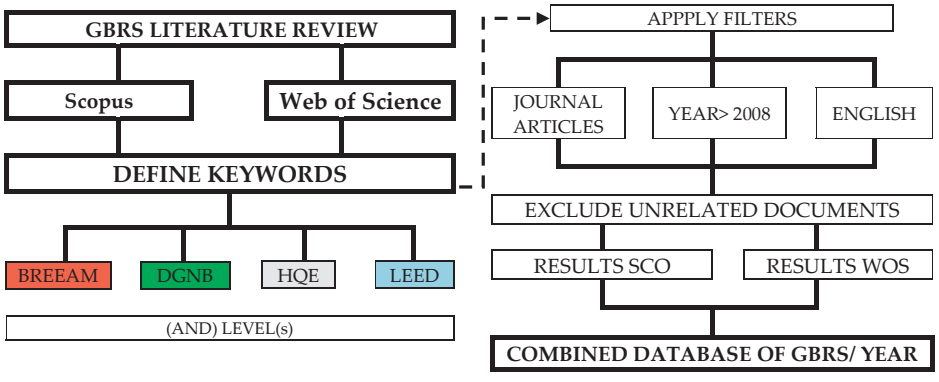

Figure 4. GBRS methodology for the literature review.

2.4. Indicator Analysis

Most common GBRSs like BREEAM, DGNB, HQE, and LEED are based on an hierarchical structure with a top–down organization as follows: categories systems (CAS), Issue System (ISS), Criteria System (CRS), and Indicators system (IDS) [71]. Terms like CAS, CRE, CRS, and IDS are commonly used by different technical manuals and authors [36]. BREEAM terms for structure classification were adopted in this paper [28], as can be seen in Table 2. CAS is defined as a Macro-objective in Level(s), Topic in DGNB, and Theme in HQE. ISS is called the target in HQE [72], requirement in LEED [73], and criteria group in DGNB [30]. Finally, CRS is called the core indicator in Level(s), Criteria in DGNB, Sub-Target in HQE, and Requirements in LEED. From all of these items, the user operation item (UOI) defines the element that must be addressed to obtain the score. This concept is relevant to the methodology because it shows the difficulties in accurately comparing scoring systems of different GBRSs.

Table 2. Summary of elements included in the methodology and user operation item.

GBRS	Category (CAS)	Issue (ISS)	Criteria (CRS)	Indicator (IDS)
Level(s)	Macro-objective		Core indicator	Indicator [1]
BREEAM	Category	Issue	Criteria [1]	Indicator
DGNB	Topic	Criteria group	Criteria	Indicator [1]
HQE	Theme	Target	Sub-target	Indicator [1]
LEED	Category	Credit	Requirements [1]	Indicator

[1] User operation item (UOI).

Most of the common GBRS scoring methods are summarized in Figure 5, where the structure follows BREEAM and LEED details in terms of the UOI. According to a bottom–up scoring system, points obtained by criteria accomplishment provide each category score. In BREEAM, the score is weighted by a different coefficient per category while in LEED the coefficient is 1. The DGNB and HQE scoring system is similar to BREEAM and LEED, however their UOI is an indicator. Later, a cumulative scoring process was carried out to obtain the global mark that these IDS would produce in theory.

Due to the geographical scope of this research, only the international version of technical manuals for BREEAM, DGNB, HQE, and LEED were considered (see Table 2).

According to the heterogeneity of different methods, this research suggests an open methodological approach (see Table 3) where each GBRS version listed in Table 3 is presented to determinate the

comparison framework. Second, the same GBRS versions were separated into CAS, ISS, and IDS or CRS, at each depth system of that presented in Figure 5. Finally, a comparison matrix between the indicators covered by Level(s) and BREEAM, DGNB, HQE, and LEED are presented.

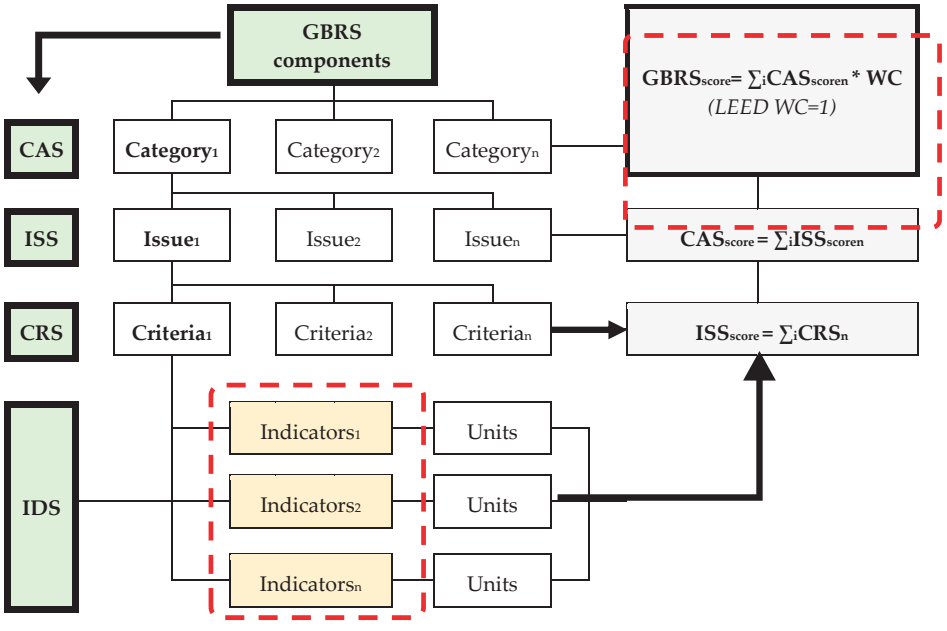

Figure 5. GBRS scoring process overview (not applicable to DGNB and HQE).

Table 3. Selected manuals of Level(s), BREEAM, DGNB, HQE and LEED.

GBRS	Version	Published	References
Level(s)	v1.0	2017	[74,75]
BREEAM	INT NC SD233 v2.0	2016	[28]
DGNB	INT 2014	2014	[76]
HQE	v1.01	2016	[72]
LEED	BD + C v4.1	2019	[73]

New construction and restoration of residential and office buildings.

3. Results

3.1. Most Used GBRS within the EU

According to the methodology explained in Figure 3, consultations and web searches provided a comprehensive spreadsheet that was transformed into Figures 6 and 7. Figure 6 includes a comparison between registered buildings (9145) and those that finally obtained certification (11,365). On the right side, Figure 7 includes a GBRS certification breakdown including the most widely used GBRSs within the EU: BREEAM (65.00%), HQE (13.58%), DGNB (6.49%), LEED (5.46%), Miljobyggnad (4.02%), EDGE (3.61%), TQB (1.52%), and VERDE (0.35%). These results form the basis that support the GBRS selected for this research.

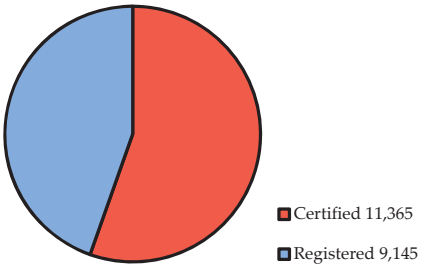

Figure 6. Registered vs. certified GBRS in the EU.

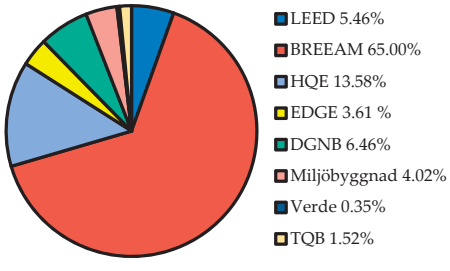

Figure 7. GBRS distribution in Europe.

3.2. GBRS Literature Review

A total of 1169 papers were obtained from the scientific search made via SCO and WOS through the methodology proposed in Figure 3. These results were combined into a spreadsheet to create two working databases:

1. A comprehensive database with whole number of papers per GBRS and year, which was used to produce Figures 8 and 9. In Figure 8, the coloured lines show the total amount of research papers by GBRS/year as well as a cumulative of the four together bar per year. This gives an idea of both the full number of GBRS research papers, but also the proportion of each GBRS studied. Figure 9 shows the number of papers/years, which combined two, three, or four of the GBRSs included.

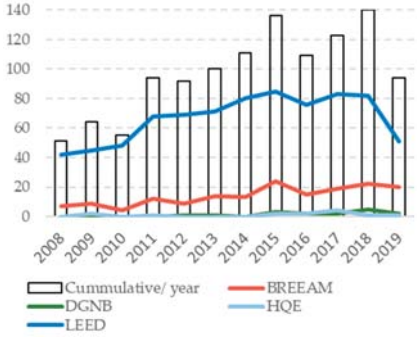

Figure 8. GBRS papers in SCO and WOS.

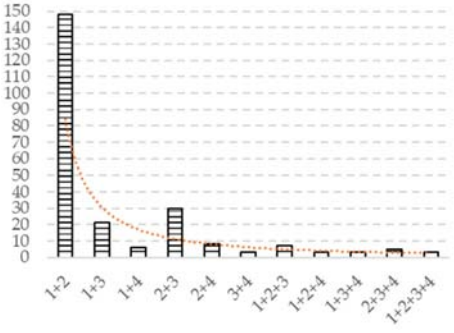

1 = BREEAM 2 = LEED 3 = DGNB 4 = HQE

Figure 9. GBRS papers in SCO and WOS.

2. A reduced database including only papers published in the second quartile (Q1 and Q2) [77,78]. with six or more papers published on GBRSs from 2008 to 2019. These were used to produce Figure 10, where the coloured line chart shows the GBRS published per journal each year. Included journals were: *Architectural Design*, *Building Research and Information*, *Facilities*, *Journal of Cleaner production*, *Sustainable Cities and Society*, *Building and Environment*, *Energy and Buildings*, *International Journal of Sustainable Building Technology and Urban Development*, *Sustainability*, and *Journal of Management in Engineering*.

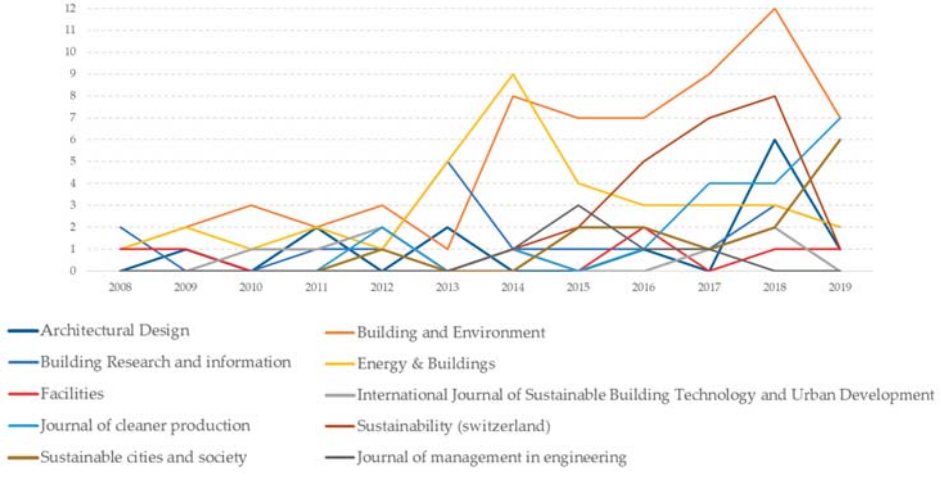

Figure 10. Evolution of published papers in the Q1 and Q2 journals.

Data from Figure 10 have been presented in Table 4, where more relevant journals according to its quartile classification [78] have been organized by study areas: Architecture; Building and construction; Renewable energy, sustainability and the environment, and Engineering [77].

Most relevant papers within the database obtained from the literature review can be classified into three groups (see Figure 11), according to their research objective: those providing New Tools (NT), Frameworks, or Regional Adaptation (RA) of current GBRS, see Appendix A, Table A1; those providing a comparison between different GBRSs (GBRSC), see Appendix A, Table A2; and finally, other papers that cannot be included in any of the preceding categories.

Papers from all regions were analysed to determine the kinds of comparisons that authors have conducted. As mentioned in Figure 11, the GBRS score was structured into the CAS, ISS, and IDS. Therefore, Figure 12 presents the proportion of papers focused on these systems. There, it can be seen that few authors provided a category system comparison, while the research objective for most authors was focused on CRS or IDS.

Table 4. Number of papers on the selected journals.

Areas	Journal	H Index	Quartile	Papers
Architecture	Architectural design	19	2	13
Building and Construction	Building and environment	124	1	62
	Building research and information	72	1	18
	Energy and buildings	147	1	36
	Facilities	38	2	7
	International journal of sustainable building technology and urban development	11	2	8
Renewable energy, sustainability and environment	Journal of cleaner production	150	1	19
	Sustainability	53	2	24
	Sustainable cities and society	34	2	14
Engineering	Journal of management in engineering—ASCE	55	1	61

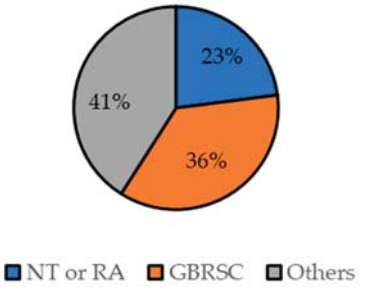

Figure 11. GBRS relevant papers between 2008 and 2019 classified by main objective.

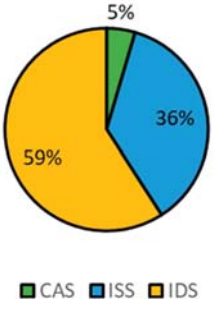

Figure 12. GBRS relevant papers between 2008 and 2019 classified by depth of comparison.

According to the geographical context of this research, which is the EU, selected research papers were classified by areas included into the study, as seen in Figure 13. GBRSs are highly affected by local conditions, and this is a matter of importance for many authors who work with the aim to provide improvements based on regional adaptations. Asia shows the highest figure, while North America (NA) had the lowest, with the EU and the Middle East and North Africa (MENA) in the middle.

Looking at the whole picture, 33 out of 46 papers provided a geographical contextualization while 13 out of 46 did not. Therefore, the majority of authors published papers focused on a region.

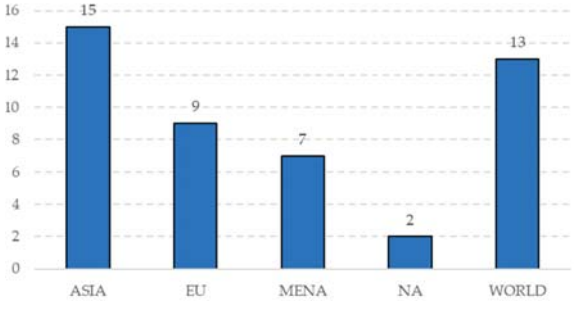

Figure 13. GBRS relevant papers between 2008 and 2019 classified by region of study.

3.3. Level(s)

Level(s) is a voluntary tool developed by the Joint Research Centre of the EU. Although it is still in a beta version, its official release is expected by spring 2020 [60], with the aim to provide transparency and robustness to European sustainability policies. Instead of describing a set of mandatory requirements, Level(s) is based on the concept of Levels of deepness from beginners to experts. These are Level (1), Level (2), and Level (3). Level (1) is a common assessment, Level (2) is a comparative assessment, and finally Level (3) is an optimization assessment. This approach is based on a progressive accuracy increase of the tools involved, which allows all kinds of stakeholders, from less educated to experts, to work within the same framework.

The framework is organized into six categories, called macro-objectives, and 14 indicators (see Table 5), which are defined as the UOI. It also provides a set of Life Cycle (LC) tools and a value risk rating. Level(s) can be used directly or via another GBRS aligned with the G17 Alliance [79]. As a framework, the Level(s) score will vary depending on regional conditions. Level(s) is based on a performing situation where 136 case studies were selected to provide results with the aim to refine the indicators. Later, national governments are expected to set values and limits to core indicators that can be finally transformed into a final score. Some EU GBRS, like the latest version of DGNB have already included specific sections to provide interaction with Level(s). It is expected that there will be a progressive adaptation by the other GBRSs developed in the EU to this framework, or at least GBRSs depending on the members of the G17 Alliance.

3.4. GBRS Manuals Revision

3.4.1. BREEAM

BREEAM, which was first launched in 1990 in the UK by *The Building Research Establishment* (BRE) [80], released its international version in 2008. Since then, 7387 buildings have been certified with BREEAM, from the whole data of 13,824 registered buildings. Data were obtained until July 2019 according to the methodology depicted in Figure 3. The scoring system was based on a bottom–up methodology as described in Figure 5 including nine CAS, 52 ISS, 76 CRS, and their corresponding IDS as UOI. Each criterion group provides a certain number of points that makes the sum per category. Later, a percentage-weighting factor was assigned to each category to obtain the final score. According to the number of points, the awarded buildings can be rated as: unclassified (<30 points), pass (≥30 points), good (≥45 points), very good (≥55 points), excellent (≥70 points), and outstanding (≥85 points).

CAS are management (MAN), health and wellbeing (HEA), energy (ENE), transport (TRA), water (WT), materials (MAT), waste (WAS), land use and ecology (USE), pollution (POL), and innovation (INV).

BREEAM, which was originally applied in the UK, incorporates several measures to enhance local adaptation to different countries. First, BREEAM is the only GBRS to include a local assessor, who acts as both a consultant and an on-site auditor. Second, it is organized in categories, which are weighted according to site conditions [78]. Finally, in locations where the volume of certified buildings is high, BRE boosts cooperation with local institutes to adapt BREEAM INT to local conditions, language, and regulations.

The scoring system has a maximum score of 100 points, plus there are up to 10 additional points for an extra category, which includes innovation criteria.

Table 5. Summary of CAS, CRS and IDS in Level(s).

CAS	Greenhouse Gas Emissions along a Building's Life Cycle (LC)	Resource Efficient and Circular Material LC	Efficient Use of Water Resources	Healthy and Comfortable Spaces	Adaptation and Resilience to Climate Change	Optimised LC Cost and Value
CRS 1	Use stage energy performance	LC tool: Building bill of materials	Total water consumption	Indoor air quality	LC tools: scenarios for projected future climatic conditions	LC costs
CRS 1.1	Primary energy demand					
CRS 1.2	Delivered energy demand					
CRS 2	LC warming potential	LC tools: scenarios for building lifespan, adaptability and deconstruction		Time outside of thermal comfort range		Value creation and risk factors
CRS 3		Construction and demolition waste and materials				
CRS 4		Overarching assessment tool: Cradle to grave LC Assessment				

3.4.2. DGNB

DGNB was launched in 2009 by the *Deutsche Gesellschaft für Nachhaltiges Bauen* (DGNB). In 2014, an international version was released [13], but its latest versions was only just released in November 2019, coinciding with the writing of this paper. According to data obtained through the methodology explained in Figure 3, in July 2019, it showed 924 registered buildings including 734 already certified buildings, which ranks it in fourth position of the GBRS in terms of the number of certified buildings. The DGNB system includes three equally weighted categories regarding three of the most commonly accepted sustainability pillars [13,14,19,81], which are environmental, economic, sociocultural, and functional quality (see Figure 14). The DGNB system includes three other categories with less importance as the weighting factors: technical, process, and site quality. Furthermore, 10 ISS and 38 CRS with corresponding IDS are included. IDS acts as the UOI in the DGNB. The final score depends on the weighting methodology as stated in Figure 5. Weighting of these criteria is different according to the building typology.

The maximum score is 100%, and certification can be rated as: DGNB Bronze (≥35 points), DGNB Silver (≥50 points), DGNB Gold (≥65 points), and DGNB Platinum (≥80 points).

Figure 14. Weighting factors of the DGNB categories from the DGNB 2020 international version.

3.4.3. HQE

HQE was launched in 1994 in France with the aim of guaranteeing the high environmental quality of buildings. Since 2013, the HQE international version has been available and CERWAY is the organization in charge of supporting worldwide [72]. In July 2019, there were 1543 certified buildings from a total number of 2139, according to the methodology in Figure 3. The scoring system is based on four themes, 14 CAS, 37 ISS, 53 CRS, and IDS (>53). In HQE, indicators act as UOI and each category has the same importance so there are no weighting coefficients. The target provides points to each category that can achieve three performing Levels: prerequisite, performing, and high performing. To finally become certified, a building must achieve the high performing Level in at least three categories and the basic Level in a maximum of seven categories.

The CAS considered are site, components, worksite, energy, water, waste, maintenance, hygrothermal comfort, acoustic comfort, visual comfort, spaces quality, air quality, and water quality.

3.4.4. LEED

LEED was first launched in 1998 in the USA by The US Green Building Council (USGBC). Although it is one of the most popular GBRSs in the world, its figures in the EU are significantly smaller than other European GBRSs. In July 2019, it showed 1973 registered buildings including 621 already certified buildings. Data were obtained through the methodology explained in Figure 3.

The scoring system is based on a bottom–up methodology like that described in Figure 5, but there are no weighting factors, therefore, the final score is directly obtained by simple criterion addition (see Figure 15). In LEED, these criterion act as UOI.

Figure 15. The LEED scoring system that does not include a weighting factor.

The LEED scoring system includes seven CAS, 62 ISS with 16 of them defined as prerequisite (not valid for scoring), and CRS (76) and IDS (>76) [73]. According to the number of points awarded, buildings can be rated as: Unclassified (<40 points), Certified (≥40 points), Silver (≥50 points), Gold (≥60 points), and Platinum (≥80 points).

The CAS are location and transportation (LT), sustainable sites (SS), water efficiency (WE), energy and atmosphere (EA), materials and resources (MR), indoor environmental quality (IE), and innovation and regional priority (RP).

The scoring system has a maximum score of 100 points, plus there are up to 10 additional bonus points for complying with two special categories: innovation and regional priority, which is the only site adequation that LEED provides.

3.4.5. Weight Per UOI on Each GBRS

In Figure 16, the results show the percentage of influence by UOI per category. In more advanced GBRSs like DGNB and HQE, the results are shown by IDS while the results in the BREEAM graph are shown by CRS. Finally, LEED results are not influenced by any weighting coefficient, thus all CRS provide the same influence.

BREEAM materials and land use and ecology are the most relevant UOI in terms of final scoring, with more than 1.5% final score influence. On the other hand, management, transport, and waste are less relevant with less than 0.5% of the final weight. DGNB economic quality UOI are the most relevant to the final score with an influence of 1.9%, while process quality only provides 0.2% of the final weight. The HQE health category UOI provides 1.0% of the final weight to become the most important category by weight, while energy is the least important with less than 0.5%. As previously stated, in LEED, all UOI are same importance in terms of final score. As presumed, those GBRSs with a higher number of UOI, DGNB, and HQE, provided less weight per UOI than those with GBRS, BREEAM, and LEED, which had a smaller number of them.

(a) BREEAM: Weight/CRS

(**b**) DGNB: Weight/IDS

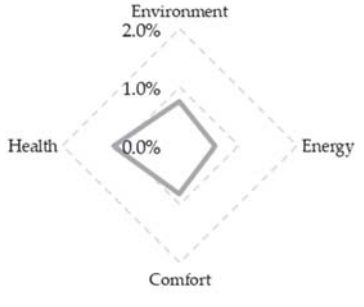

(**c**) HQE: Weight/IDS

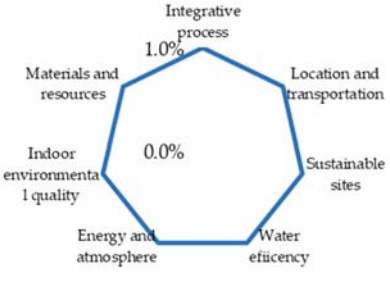

(**d**) LEED: Weight/CRS

Figure 16. Weight associated with UOI: (**a**) CRS in BREEAM; (**b**) IDS in DGNB; (**c**) IDS in HQE; (**d**) CRS in IDS.

3.5. Synergies between Level(s) and Other GBRSs

The results were compiled with the objective to show a comparison between Level(s) and BREEAM, DGNB, HQE, and LEED. As detailed before in Section 3.4, the scoring process is different from one GBRS to another, thus synergies between GBRSs cannot be fully estimated in the same conditions. DGNB and HQE provide full details about their IDS, thus their results can be considered to be highly accurate, specifically, the latest version of DGNB, which provides a comprehensive description of the synergies between it and Level(s). On the other hand, the IDS from BREEAM and LEED were obtained by author interpretation because they use different methodologies where the UOI are CRS instead of IDS (see Table 2). These results could be considered as less accurate than those obtained in DGNB and HQE, thus it will be carefully discussed in the following section.

In Table 6, the synergies between GBRS and Level(s) are described in groups of two columns. For each GBRS, the column on the left explains the percentage influenced by Level(s), while the column on the right shows if this CAS is included within every GBRS. As described in the table, DGNB is the only GBRS to include six CAS described in Level(s). BREEAM includes all CAS, except Optimised life cycle cost and value. LEED and HQE include only four CAS, and do not include either the CAT 5 Adaptation and resilience to climate change or CAT 6 Optimised life cycle cost and value.

Table 4 and Figure 17 show the IDS influence breakdown, where the percentage of every GBRS in line with Level(s) is included. Figures inside the table are later shown in the graphs of the above-mentioned figure. Here, the final score influences were 21.1% in DGNB, 39.2% in HQE, 42.6% in BREEAM, and 66.0% in LEED.

Table 6. Synergies between the GBRS and Level(s).

Level(s)			BREEAM		DGNB		HQE		LEED	
CAS	**CRS**	**IDS**	**%**	**INC**	**%**	**INC**	**%**	**INC**	**%**	**INC**
Greenhouse gas emissions along a building's life cycle	1	2	20.0	●	3.60	●	5.03	●	33.0	●
Resource efficient and circular material life cycles	4	1	8.9	●	11.25	●	5.77	●	13.0	●
Efficient use of water resources	1	1	7.0	●	0.64	●	7.14	●	11.0	●
Healthy and comfortable spaces	2	1	6.1	●	4.35	●	16.1	●	9.0	●
Adaptation and resilience to climate change	1	1	0.6	●	0.86	●				
Optimised life cycle cost and value	2	1			0.36	●				
	11	7	42.6		21.1		39.2		66.0	

● Indicators from Level(s) included (INC) in each GBRS.

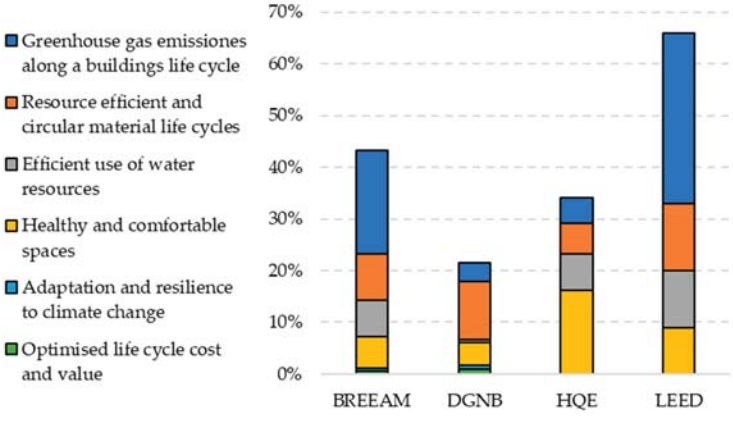

Figure 17. UOI weight breakdown per GBRS showing LEVEL(s) influence on the final score.

4. Discussion

4.1. Assessment Trends in GBRS within the EU

The results shown in Figure 6 from Section 3.1 indicate a significant difference between the number of buildings that finally obtained a certification with those only registered. This may happen due to several reasons, highlighting the difficulty of the process in time, cost, and professional skills needed [82]. It is not yet certain as to whether the appearance of Level(s) will provide an increase in the already existing GBRS assessments, or, on the contrary, may produce a displacement from the current ones to it. As mentioned in Section 3.3, Level(s) is available in direct or indirect use [61], which would still allow stakeholders to freely decide about which GBRS would be better suited for their building assessment.

In Figure 7 in Section 3.1, the data reflects which one of the existing GBRSs within the EU are more widely used by stakeholders, where BREEAM, HQE, LEED and DGNB in this order are the most accepted. This seems to be related to the maturity of the process, but also with the strength of the organization supporting the GBRS. According to Section 3.4, BREEAM was born in 1990, HQE in 1997, and LEED in 1998. This is why it is likely that they already had a strong presence in the market before the appearance of the other GBRS. However, DGNB started in 2009 and grew fast to become the fourth ranked GBRS in the EU in terms of the number of buildings assessed. BREEAM in the UK, DGNB in Germany, HQE in France, and LEED in the USA, are supported by BRE, DGNB, CERNWAY and the US GBC. DGNB and HQE are members of the G17 Alliance, born with the aim of helping with the successful application of the UN SDGs [79]. Additionally, other councils included in Figure 6 such as the SGBC in Spain and OGNB in Austria are members of the G17 Alliance. This may produce a different response into two different kinds of GBRS: on one hand, those members of the G17 Alliance with the aim to enhance homogeneity of some common indicators, but on the other hand, those truly internationally implanted (BREEAM and LEED), which will probably keep on developing their own methodologies to pursue SDGs, but without converging with Level(s) indicators.

Finally, the results in this section are influenced by the range defined in the methodology (see Section 2.1), thus any modification to it by introducing urban developments or in use assessments may provide significant changes, but these would not be included in the typologies covered by Level(s). As soon as Level(s) enlarges the scope of its included typologies, the results within this section should be revised carefully.

4.2. Research Trends and Critical Review of Current GBRS within the EU

Trends on research from 2008 are included in Section 3.2. There, only BREEAM, DGNB, HQE and LEED were included, according to the aims of this research. The total number of papers carefully analysed, 1169, provides the first conclusion: most of research papers in English since 2008 were focused on LEED while BREEAM was in the medium range, and only a few included DGNB and HQE. Despite the results in Figure 8, the data in Figure 9 show the evident conclusion that there were only very few papers that included a comparison between BREEAM, DGNB, HQE, and LEED in any possible combination. Usually, papers including DGNB and HQE provide a comparison between them and others. Language filter may be one reason, thus future research should consider the impact on the search using different languages, mainly French and German. Level(s) was included in this search but it produced no results, which may be because it is still a work in progress whose first draft was released in 2018 [61].

From all of the data classified, only those belonging to journals with SCI classified Q1 and Q2 were considered for this research, and more relevant journals are presented in Figure 10 and Table 2 to provide a classification of them. These may have influenced this research; thus, future research could include some exceptional works appearing in less relevant journals. In any case, the quartile of a journal is not a still photo, since it can vary from year to year.

4.3. RA and NT in GRBS Assessment

As Figure 13 shows, most of the relevant research from 2008 was focused in Asia, the EU, or MENA regions and less in NA. BREAM (UK) and LEED (US) had an earlier development and the research is probably more mature than in other regions. Research focused on developing regions like Asia and MENA as well as those focused on small developed countries within the EU seem to need adaptations of current GBRSs to local conditions. This means that 41% of relevant papers were focused on RA or NT development (see Figure 11). The RA of existing GBRSs has lately been a trend for researchers in locations like Jordan [83], Saudi Arabia [84,85], Pakistan [86], and Iran [87]. These studies usually use BREAM, LEED, or SBTool as a source to define scoring methodology and IDS. In particular, LEED includes a regional priority category that may bring four extra points [88], which is less than 4% of the final score. On the contrary, BREEAM seems fully adapted to some countries via cooperation agreements with local institutes, but there are only a few (see Table 1). For those countries where there is still no cooperation agreement between BREEAM and local institutions, it includes specific weightings per country as well as some climatic influence applied to credit scores [28]. The amount of RA research has created doubt on the validity of the most common used GBRS at the international Level and if they can improve their RA. Level(s) is somehow a public effort to create a wide framework that can mitigate the need for continuous adaptations of GBRSs per country. Its use may reduce the need for national stakeholders to develop a new GBRS. Considering this scenario with many GBRS and different versions, some authors are working on the need to provide some helping tools for stakeholders to choose the most appropriate GRBS for each project, depending on factors such as location [84], project delivery attributes [82], and available credits [89]. These will probably be affected by the introduction of Level(s) because of two reasons: first, Level(s) provides a framework of simplicity and transparency in comparison with the other GBRS, and second, it is pushing the EU GBRS to make convergence efforts.

Other authors have proceeded with the improvement of current GBRSs in terms of holistic sustainability [81]. LEED and BREEAM, as pioneers, have focused on ENV sustainability, thus these authors are working on an improvement of SOC [90,91] and ECO [92] sustainability. In contrast, the HQE score is highly influenced by SOC sustainability and the latest version of DGNB already states a similar weight for the ENV, SOC, and ECO pillars. Certainly, it is the first GBRS to achieve a robust score system that is truly holistic. Level(s) was also developed with the idea to also provide holistic sustainability and so it is not as mature as DGNB in this field. From the 13 IDS included in it, eight correspond to ENV, two to SCO, and three to ECO sustainability pillars. However, these may be amended through the introduction of some weighting factors.

4.4. Trends in GRBS Assessment Comparison

Instead of using a NT or RA approach, 36% of authors focused in providing GBRSC (see Figure 12), and according to their research, deepness was classified into 5% CAS, 36% ISS, and 59% IDS, as defined in Section 2.3. A sub-category comparison and the way holistic sustainability is reached [15,20] was not considered in this research due to its main objective. Authors have considered establishing a GBRSC at the IDS Level focused on a specific category [16,93,94] or case study [46,94–97]. According to Level(s), IDS analysis is a matter of importance when trying to compare other GBRSs. It requires organizing the BREEAM, DGNB, HQE, and LEED into a similar structure composed of CAS, ISS, CRS, and IDS, which is not easy when the UOI changes from one to another. DGNB and HQE have a LCA approach more like Level(s) (see Sections 3.4.2 and 3.4.3), while the BREEAM and LEED structure is quite different. These differences in proceedings causes some difficulties in quantifying the synergies between Level(s) and the other GBRSs. This is likely to be done with some development of any of these GBRS, especially BREEAM and LEED, to improve the adequacy to Level(s). Only DGNB in its latest version includes a *synergies* section with Level(s). HQE does not include a Level(s) synergies section, but according to its methodology, it has been easier to provide a comparison with Level(s).

4.5. Level(s) Scoring Influence on (IDS) of the Existing GBRS

According to the results in Table 6, DGNB is the only GBRS that includes in its UOI all IDS from Level(s). BREEAM includes only five of them, and HQE and LEED include only four. Even with this in mind, DGNB seems to be less affected by Level(s) (21.1%) than HQE (39.2%), BREEAM (42.6%), and LEED (66.0%), which is a significant deviation. This may have been produced by an accumulative mistake when the methodology was applied to compare the GBRS. In Figure 17, the UOI weight breakdown shows which Level(s) category presented a more significant deviation. In BREEAM and LEED, Greenhouse gas emissions along a building's life cycle had an influence of 20.0% and 33.0%, respectively, which is consistent with the methodology applied. The *Energy* CAS in BREEAM and *Energy an Atmosphere* CAS in LEED were considered as fully affected. Additionally, HQE *Healthy and comfortable spaces* had a 16.1% influence on the HQE final score because the weight of the *Comfort* CAS in IT. As LEED, BREEAM, and HQE do not provide specific synergies, results from the methodology in Section 2.3 assigned influence at every IDS with a potential relationship. Future versions of BREEAM, HQE, and LEED may include an alignment section with Level(s).

5. Conclusions

Level(s) intends to improve building sustainability within the EU region and comes at time of maturity but confusion. Several GBRSs have already been established with thousands of assessments already provided, but their processes are not the same. Usually, this provides confusion to stakeholders, which slows down the spread of the sustainability process.

This paper demonstrates the heterogeneity of current GRBS in the EU scenario and the difference between sustainability assessments, where DGNB seems to be more aligned with the current EU framework.

Efforts to provide knowledge, regional adaptation, or helping tools for the most relevant GBRS have been undertaken by researchers, which gives the impression of the difficulty to give universal solutions.

The Level(s) proposal is intended to partially solve this confusing scenario with a simple structure of common indicators based on EU regulations, proceedings, and tools of common use by professionals. At least it seems to be producing a boosting effect in other GBRSs to search for European alignment. DGNB is the first of its class that has specifically introduced a section focused on synergies with Level(s) and it will probably not be the only one as the G17 Alliance is intended for that, especially HQE, whose methodology seems to be easily adaptable to it.

Considering the last international version of the GBRS manual, BREEAM and LEED are more influenced by Level(s). Their current structure is not intended to provide holistic sustainability because they still provide much more weight to the environmental pillar than to the others. Although every GBRS provides a differentiated structure with a different number of CAS and IDS, all of them rely on a UOI that can be compared. Trends in GBRS seem to lead to a simplification based on three macro-categories with a similar weight: environmental, economic and social, and a better alignment between the GBRS and EU policies.

Several interesting questions worth expanding in the future have arisen from the results obtained in this research.

Attention to upcoming versions of Level(s) as well as BREAM, HQE, and LEED has a vital interest in supervising the alignment of these GBRSs to the new EU framework and determine if this guide to the simplification and homogenization of the sustainability assessment process will succeed. This will definitively help to find a way to pursue a circular economy and the fulfilment of the SDGs proposed by the UN.

In light of these big challenges, future research should focus on the development of specific CAS that allow for a deeper comparison between UOI. Detailed research on specific topics will increase the alignment and robustness of the whole process, thus helping to strengthen existing GBRSs and Level(s).

Author Contributions: A.S.C. wrote the article, S.G.M. checked the manuscript and carried out the revision, and J.M.A.M. supervised and reviewed all of work and manuscript. All authors have read and agreed to the published version of the manuscript.

Funding: This research received no external funding.

Acknowledgments: The authors gratefully acknowledge the contribution of several institutions: EDGE and GBCE provided us a comprehensive list of certified buildings with EDGE and Verde, and DGNB GmbH provided us DGNB 2020 international version.

Conflicts of Interest: The authors declare no conflicts of interest.

Abbreviation

BRE	Building research establishment
BREEAM	Building research establishment environmental assessment method
DGNB	Deutsche gesellschaft für nachhaltigies bauen
CAS	Categories system
CASBEE	Comprehensive assessment system for built efficiency
CRS	Criterion systems
EC	European commission
ECO	Economic
ENV	Environmental
ESGB	Evaluation standard for green buildings
EU	European Union
GBC	Green building council
GBRS	Green building rating system
HQE	Haute qualité environnementale
IDS	Indicators system
INS	Institutional
ISS	Issues system
ITACA	Instituto per l'innovazione e trasparenza degli appalti e la compatibilita ambientale
LEED	Leadership in Energy and Environmental Design
JRC	Joint research centre
MEB	Minimum energy buildings
MENA	Middle East and North Africa
MOUHURD	Ministry of Urban Housing and Rural Development
NA	North America
NT	New tool
RA	Reginal adaptation
SBTool	Sustainable building tool
SCO	Scopus
SDG	Sustainable Development Goals
SOC	Social
TQB	Total quality building assessment
UCLG	United cities and local government
UNECE	United Nations Economic Commission for Europe
UOI	Users operation item
WGBC	World Green Building Council
WOS	Web of Science

Appendix A

Table A1. Most Relevant Authors According to New Development Tools and/or Regional Adaptation from 2008 to 2019.

Authors	Year	Scope of the GBRS Included		Other			Notes
		EU Most Used	Others	Region	BT [1]	SC [2]	
B. Aktas, B. Ozorhon	2015	LEED		MENA	●		New GBRS tool for existing buildings based on 6 LEED case studies from Turkey
H. Ali, -S. Al Nsairat	2009	BREEAM, LEED	SABA, CASBEE, SBTooL	MENA	●		New GBRS tool for residential buildings in Jordan, based on indicators from other GBRS implemented through an AHP method.
Banani et al.	2016	BREEAM, LEED	GS, CASBEE, Estidama	MENA	●		New GBRS tool for Saudi Arabia, based on indicators from other GBRS implemented through an AHP method.
Choi et al.	2015	LEED	LDRI	World			new GBRS tool for stakeholders pursuing LEED certification based on an AHP method.
de Klijn et al.	2017	BREEAM		EU		●	BREEAM NL Materials category analysis from an office building case study.
Ferreira et al.	2014	BREEAM, LEED	Lidera, SBTool	EU		●	Energy analysis of several Portuguese GBRS, from case study perspective.
Kreiner et al.	2015	DGNB		EU	●		New systemic approach to improve GBRS performance for office buildings based on office case study from Austria.
Mahmoud et al.	2019			World			New GBRS tool for existing buildings based on indicators system.
Olakitan Atanda J.	2019	LEED		World			New GBRS social sustainability framework using AHP method based on indicators from several GBRS.
Papajohn et al.	2017			World			New meta-framework of key criteria from most representative GBRS tested on ENVISION
Brinker, C.	2019	DGNB		EU			LCA proposal as database for GBRS benchmarks at early design stage.
Seyis S, Ergen E	2017			World	●		New GBRS MADM tool for selecting green building certification credits based on project delivery attributes.
Ullah et al.	2018	BREEAM, LEED		Asia	●		New GBRS framework for residential buildings in Pakistan using AHP method based on indicators from several GBRS.
Zarghami et al.	2018	BREEAM, LEED	SBTool, CASBEE	MENA	●		Regional adaptation of existing GBRS for Iranian residential buildings with a MCMD method.

● Main research objective included: [1] Building typology focused (BT), [2] Single category focused (SC).

Table A2. Most Relevant Authors According to GBRS Comparison from 2008 to 2019.

Authors	Year	Scope of the GBRS Included		GBRSC				Notes
		EU Most Used	Others	Region	CAS [1]	ISS [2]	IDS [3]	
Asdrubali et al.	2015	LEED	Itaca	EU	●	●	●	LEED and ITACA methodology comparison from a residential case study.
Awadth O.	2017	BREEAM, LEED	Estidama, GSAS	MENA	●	●	●	Energy and water categories comparison.
Bernardi et al.	2017	BREEAM, DGNB, HQE, LEED	CASBEE, SBTool	World	●	●		Overview of most representative GBRS in the world.
Chen H, Lee WL	2013	LEED	BEAM Plus	Asia	●	●	●	LEED and BEAM Plus methodology comparison from a office building case study perspective focused in energy category.
Dat Tien Doan et al.	2017	BREEAM, LEED	CASBEE. GS	World	●	●	●	Sub-Categories comparison of most representative GBRS

Table A2. *Cont.*

Dias et al.	2017			World	●	●	●	Dependences among LEED indicators from 10 office building case study perspective.
He et al.	2018	LEED	GS, ASGB	Asia	●	●	●	Design influence of LEED, GS and ASGB, from case study perspective of an educational building.
Hu et al.	2017	LEED	Living Building Challenge	NA	●	●	●	Energy category comparison of several GBRS from different cases study perspective.
Illankoon et al.	2017	BREEAM, LEED	GS, GM, CASBEE, BEAM Plus, GBI, IGBC	Asia	●	●	●	key criteria comparison of most representative GBRS in the Asia, to provide foundations of new GBRS tools in the future.
Ismaell W.	2018	BREEAM, LEED DGNB	GS, GG, GBTooL CASBEE	World	●	●		Comparison of most representative GBRS, with special attendance to midpoint and endpoint methodology.
Komurlu et al.	2015	LEED	Estidama, TNGBC	MENA	●	●	●	Energy category comparison of several GBRS in Turkey
Lee, W.L.	2013	BREEAM, LEED	ESGB, BEAM Plus, CASBEE	Asia	●	●	●	Categories comparison of metrics of most representative GBRS in the Asia.
Lee, W.L.	2012	BREEAM, LEED	BEAM-Plus, CASBEE	Asia	●	●	●	Energy category comparison of several GBRS in Asia
Lee et al.	2008	BREEAM, LEED	BEAM-Plus	Asia	●	●	●	Energy category comparison of several GBRS from a residential building case study perspective.
Li et al.	2017		CASBEE, GS, SBTool, BEAM Plus	Asia	●	●		Categories comparison of most representative GBRS in the Asia.
Lu et al.	2019	LEED	GBEL, BEAM Plus	Asia	●	●		Waste categories comparison.
Mansour et al.	2016			World				Case study of 6 office buildings with focused on environmental impacts.
Mattoni et al.	2018	BREEAM, LEED	Itaca, CASBEE, GS	World	●	●		Categories comparison of most representative GBRS, thorough macro-aggregation process.
Nguyen B. K., Hasim A.	2011	BREEAM, LEED	CASBEE, GS, BEAM-Plus	Asia	●			Comparison of most representative GBRS from stake holders survey methodology.
Park et al.	2017	BREEAM, LEED	CASBEE, LBC, SEED	Asia	●	●	●	Material categories comparison.
Seinre et al.	2014	BREEAM, LEED		EU	●	●		Categories weighting improvement for existing GBRS in Estonia, from an office case study perspective.
Stender et al.	2019	DGNB		EU				Social impacts in urban communities from a DGNB case study assessment.
Zhang et al.	2019	BREEAM, LEED	ESGB, EEWH	Asia	●	●		Categories comparison between GBRS in China.
Zou Y.	2019	BREEAM	ESGB	Asia	●	●		Comparison between LEED and ESGB, with special attendance to Chinese market evolution.

● Main research objective included: [1] Category system (CAS), [2] Issues system (ISS), [3] Indicator system (IDS).

References and Note

1. Nejat, P.; Jomehzadeh, F.; Taheri, M.M.; Gohari, M.; Majid, M.Z.A. A global review of energy consumption, CO_2 emissions and policy in the residential sector (with an overview of the top ten CO_2 emitting countries). *Renew. Sustain. Energy Rev.* **2015**, *43*, 843–862. [CrossRef]
2. Martínez-Zarzoso, I.; Maruotti, A. The impact of urbanization on CO_2 emissions: Evidence from developing countries. *Ecol. Econ.* **2011**, *70*, 1344–1353. [CrossRef]
3. Pérez-Lombard, L.; Ortiz, J.; Pout, C. A review on buildings energy consumption information. *Energy Build.* **2008**, *40*, 394–398. [CrossRef]
4. Li, M.; Li, L.; Strielkowski, W. The impact of urbanization and industrialization on energy security: A case study of China. *Energies* **2019**, *12*, 2194. [CrossRef]

5. Edenhofer, O.; Pichs-Madruga, R.; Sokona, Y.; Farahani, E.; Kadner, S.; Seyboth, K.; Adler, A.; Baum, I.; Brunner, S.; Eickemeier, P.; et al. *Climate Change 2014: Mitigation of Climate Change. Contribution of Working Group III to the Fifth Assessment Report of the Intergovernmental Panel on Climate Change*; Cambridge University Press: Cambridge, UK; New York, NY, USA, 2014.
6. Wang, C.N.; Ho, H.X.T.; Hsueh, M.H. An integrated approach for estimating the energy efficiency of seventeen countries. *Energies* **2017**, *10*, 1597. [CrossRef]
7. Wang, L.W.; Le, K.D.; Nguyen, T.D. Assessment of the energy efficiency improvement of twenty-five countries: A DEA approach. *Energies* **2019**, *12*, 1535. [CrossRef]
8. Assembly, T.G.; Goals, T. 271015_EN_A_RES_70_1_transforming_our_world. 16301, October, 1–35, 2015.
9. European Commission. European Action for Sustainability: Next Steps for a Sustainable European Future. In Proceedings of the Communication from the Commission to the European Parliament, the Council, the European Economic and Social Committee and the Committee of the Regions, Strasbourg, France, 22 November 2016.
10. United Nations Economic Commission for Europe. SDG Priorities. 2019. Available online: https://www.unece.org/sustainable-development/sdg-priorities.html (accessed on 22 October 2019).
11. European Commission. Circular Economy. Implementation of The Circular Economy Action Plan. 2019. Available online: https://ec.europa.eu/environment/circular-economy/index_en.htm (accessed on 26 October 2019).
12. European Commission. Resource efficiency opportunities in the building sector. In Proceedings of the Communication from the Commission to the European Parliament, the Council, the European Economic and Social Committee and the Committee of the Regions, Brussels, Belgium, 1 July 2016.
13. Bernardi, E.; Carlucci, S.; Cornaro, C.; Bohne, R.A. An Analysis of the Most Adopted Rating Systems for Assessing the Environmental Impact of Buildings. *Sustainability* **2017**, *9*, 1226. [CrossRef]
14. Mattoni, B.; Guattari, C.; Evangelisti, L.; Bisegna, F.; Gori, P.; Asdrubali, F. Critical review and methodological approach to evaluate the differences among international green building rating tools. *Renew. Sustain. Energy Rev.* **2018**, *82*, 950–960. [CrossRef]
15. Melgar, S.G.; Bohórquez, M.Á.M.; Márquez, J.M.A. UhuMEB: Design, construction, and management methodology of minimum energy buildings in subtropical climates. *Energies* **2018**, *11*, 2745. [CrossRef]
16. De Klijn-Chevalerias, M.; Javed, S. The Dutch approach for assessing and reducing environmental impacts of building materials. *Build. Environ.* **2017**, *111*, 147–159. [CrossRef]
17. Lu, W.; Chi, B.; Bao, Z.; Zetkulic, A. Evaluating the effects of green building on construction waste management: A comparative study of three green building rating systems. *Build. Environ.* **2019**, *155*, 247–256. [CrossRef]
18. Eriksson, O.; Finnveden, G. Energy recovery from waste incineration—The importance of technology data and system boundaries on CO_2 emissions. *Energies* **2017**, *10*, 539. [CrossRef]
19. Doan, D.T.; Ghaffarianhoseini, A.; Naismith, N.; Zhang, T.; Ghaffarianhoseini, A.; Tookey, J. A critical comparison of green building rating systems. *Build. Environ.* **2017**, *123*, 243–260. [CrossRef]
20. Berardi, U. Clarifying the new interpretations of the concept of sustainable building. *Sustain. Cities Soc.* **2013**, *8*, 72–78. [CrossRef]
21. Friedmann, W.; Munro, L. United Nations. *Int. J.* **2010**, *16*, 102. [CrossRef]
22. Littig, B.; Griessler, E. Social sustainability: A catchword between political pragmatism and social theory. *Int. J. Sustain. Dev.* **2006**, *8*, 65. [CrossRef]
23. *Culture: Fourth Pillar of Sustainable Development*; United Cities Local Government Policy Statement: Barcelona, Spain, 2010.
24. Awadh, O. Sustainability and green building rating systems: LEED, BREEAM, GSAS andEstidama critical analysis. *J. Build. Eng.* **2017**, *11*, 25–29. [CrossRef]
25. Ferreira, J.; Pinheiro, M.D.; de Brito, J. Portuguese sustainable construction assessment tools benchmarked with BREEAM and LEED: An energy analysis. *Energy Build* **2014**, *69*, 451–463. [CrossRef]
26. Qian, W.; Kaur, A.; Schaltegger, S. Managing Eco-Efficiency Development for Sustainability: An Investigation of Top Carbon Polluters in Australia. In *Accounting for Sustainability: Asia Pacific Perspectives*; Springer: Cham, Switzerland, 2018; Volume 33, pp. 103–124.
27. Lee, W.L. Benchmarking energy use of building environmental assessment schemes. *Energy Build.* **2012**, *45*, 326–334. [CrossRef]

28. BRE Global. *BREEAM International New Construction 2016*; BRE Global: Watford, UK, 2017; Available online: https://hbreavis.com/wp-content/uploads/2017/06/BREEAM-International-New-Construction-2016.pdf (accessed on 18 October 2019).
29. U.S. Green Building Council. *LEED v4.1|USGBC*. 2019. Available online: https://new.usgbc.org/leed-v41 (accessed on 12 September 2019).
30. *DGNB System—Certificate for Sustainable and Green Building*; DGNB GmbH: Stuttgart, Germany, 2019.
31. Cerway. HQE Certification. 2019. Available online: https://www.behqe.com/# (accessed on 18 October 2019).
32. Varma, C.R.S.; Palaniappan, S. Comparision of green building rating schemes used in North America, Europe and Asia. *Habitat Int.* **2019**, *89*, 101989. [CrossRef]
33. *CASBEE Certification System*; Japan Sustainable Building Consortium: Tokyo, Japan, 2019.
34. Green Building Council Australia. Green Star Rating System | Green Building Council of Australia. 2019. Available online: https://new.gbca.org.au/green-star/rating-system/ (accessed on 12 September 2019).
35. Ding, Z.; Fan, Z.; Tam, V.W.; Bian, Y.; Li, S.; Illankoon IC, S.; Moon, S. Green building evaluation system implementation. *Build. Environ.* **2018**, *133*, 32–40. [CrossRef]
36. Zhang, X.; Zhan, C.; Wang, X.; Li, G. Asian green building rating tools: A comparative study on scoring methods of quantitative evaluation systems. *J. Clean. Prod.* **2019**, *218*, 880–895. [CrossRef]
37. Building Research Establishment Group. BREEAM Worlwide. 2019. Available online: https://www.breeam.com/worldwide/ (accessed on 18 October 2019).
38. Building Research Establishment Environmental Assessment Method ES. 2019. Available online: http://www.breeam.es/ (accessed on 4 November 2019).
39. Dutch Green Building Council. BREEAM-NL. 2019. Available online: https://www.breeam.nl/ (accessed on 4 November 2019).
40. TÜV SÜD Industrie Service GmbH. DIFNI. BREEAM DE. 2019. Available online: https://difni.de/breeam/breeam-de/ (accessed on 18 October 2019).
41. Norwegian Green Building Council. BREEAM NW. 2019. Available online: https://byggalliansen.no/sertifisering/ (accessed on 18 October 2019).
42. Stahan, K. Energy-efficient architecture in sustainable urban tourism. *Prostor* **2014**, *22*, 279–290.
43. CR, G.B.C. SBToolCZ. 2018. Available online: https://www.sbtool.cz/cs/ (accessed on 18 October 2019).
44. Andrade, J.; Braganca, L. Sustainability assessment of dwellings—A comparison of methodologies. *Civ. Eng. Environ. Syst.* **2016**, *33*, 125–146. [CrossRef]
45. Italia, I. ITACA. 2019. Available online: http://www.iisbeitalia.org/ (accessed on 18 October 2019).
46. Asdrubali, F.; Baldinelli, G.; Bianchi, F.; Sambuco, S. A comparison between environmental sustainability rating systems LEED and ITACA for residential buildings. *Build. Environ.* **2015**, *86*, 98–108. [CrossRef]
47. Macias, M.; Garcia Navarro, J. VERDE, a methodology and tool for a sustainable building assessment. *Inf. LA Constr.* **2010**, *62*, 87–100.
48. Green Building Council España. GBCe | Certificación VERDE. 2019. Available online: https://gbce.es/certificacion-verde/ (accessed on 12 September 2019).
49. Austrian Institute for Building Biology and Ecology. ASBC TQB Assessment. 2019. Available online: https://www.oegnb.net/en/tqb.htm (accessed on 12 September 2019).
50. Minergie. Minergie ECO. 2019. Available online: https://www.minergie.ch/it/ (accessed on 18 October 2019).
51. Peyramale, V.; Eberl, S.; Essig, N. OPEN HOUSE: An online platform for a transparent and open methodology to assess the sustainability of buildings. *Int. J. Sustain. Build. Technol. Urban. Dev.* **2012**, *3*, 316–321. [CrossRef]
52. ÖGNB. TQB Certification. 2019. Available online: https://www.oegnb.net/ablauf.htm (accessed on 18 October 2019).
53. DIFNI. BREEAM AT. 2019. Available online: https://difni.de/breeam/breeam-at/ (accessed on 18 October 2019).
54. German Sustainable Building Council GmbH. DGNB System—Scheme overview. 2019. Available online: https://www.dgnb-system.de/en/schemes/scheme-overview/ (accessed on 12 September 2019).
55. Green Building Council Italia. LEED Italia. 2019. Available online: http://www.gbcitalia.org/leed (accessed on 18 October 2019).
56. Swedish Green Building Council. Miljobyggnad Certification. 2019. Available online: https://www.sgbc.se/certifiering/miljobyggnad/ (accessed on 18 October 2019).
57. Building Research Establishment Group. HQM Certification. 2019. Available online: https://www.homequalitymark.com/ (accessed on 18 October 2019).

58. Building Research Establishment Group. CEEQUAL Certification. 2019. Available online: https://www.ceequal.com/ (accessed on 18 October 2019).
59. Reader, L. *Guide to Green Building Rating Systems: Understandung LEED, Green Globes, Energy Star, the National Green Building Standard, and More. Residential Rating Systems: A Comparison*; John Wiley & Sons: Hoboken, NJ, USA, 2011; pp. 1–25.
60. European Commission. *LEVEL(S) Taking Action on the Total Impact of the Construction Sector*; Publications Office of the European Union: Luxembourg, 2019.
61. Joint Reseach Centre. LEVEL(s) A Common EU Framework of Core Sustainability Indicators. 2019. Available online: https://susproc.jrc.ec.europa.eu/Efficient_Buildings/documents.html (accessed on 26 October 2019).
62. Pushkar, S.; Verbitsky, O. Strategies for leed certified projects: The building layer versus the service layer. *Can. J. Civ. Eng.* **2018**, *45*, 1065–1072. [CrossRef]
63. Cerway. Cerway—HQE Certification—High Environmental Quality—Référent Training. 2019. Available online: https://www.behqe.com/home (accessed on 12 September 2019).
64. U.S. Green Building Council. Projects | U.S. Green Building Council. 2019. Available online: https://www.usgbc.org/projects (accessed on 31 July 2019).
65. Building Research Establishment. BREEAM Projects. 2019. Available online: https://tools.breeam.com/projects/explore/map.jsp?sectionid=0&projectType=&rating=&certNo=&buildingName=&client=&developer=&certBody=&assessor=&addressPostcode=&countryId=&partid=10023&Submit=Search (accessed on 31 July 2019).
66. German Sustainable Building Council GmbH. DGNB Pre-Certified and Certified Projects. 2019. Available online: https://www.dgnb-system.de/en/projects/ (accessed on 31 July 2019).
67. Certivea. CertiBOX. 2019. Available online: http://certibox.certivea.fr/system_certivea/axxone.php?TUFQL3BnZS1NQVBfYWNjdWVpbC5waHA= (accessed on 31 July 2019).
68. Nguyen, T.H.; Toroghi, S.H.; Jacobs, F. Automated Green Building Rating System for Building Designs. *J. Archit. Eng.* **2016**, *22*, 4. [CrossRef]
69. International Finance Corporation. *EDGE Methodology Report | EDGE Buildings*; International Finance Corporation: Washington, DC, USA, 2019.
70. Aghaei Chadegani, A.; Salehi, H.; Yunus, M.; Farhadi, H.; Fooladi, M.; Farhadi, M.; Ale Ebrahim, N. A comparison between two main academic literature collections: Web of science and scopus databases. *Asian Soc. Sci.* **2013**, *9*, 18–26. [CrossRef]
71. Wu, Z.; Shen, L.; Yu, A.T.W.; Zhang, X. A comparative analysis of waste management requirements between five green building rating systems for new residential buildings. *J. Clean. Prod.* **2016**, *112*, 895–902. [CrossRef]
72. Cerway. *Assessment Scheme for the Environmental Performance of Non-Residential Building under Construction*; Cerway: Paris, France, 2016.
73. Council, U.G.B. *LEED v4.1 for Building Design and Construction*; US Green Building Council: Washington, DC, USA, 2019.
74. Dodd, N.; Cordella, M.; Traverso, M.; Donatello, S. *Level(s)—A Common EU Framework of Core Sustainability Indicators for Office and Residential Buildings: Parts 1 and 2, EUR 28899EN*; Publications Office of the European Union: Luxembourg, 2017.
75. Dodd, N.; Cordella, M.; Traverso, M.; Donatello, S. *Level(s)—A Common EU Framework of Core Sustainability Indicators for Office and Residential Buildings: Part 3, EUR 28898 EN*; Publications Office of the European Union: Luxembourg, 2017.
76. German Sustainable Building Council. *DGNB System International 2014 Version*; DGNB GmbH: Stuttgart, Germany, 2014.
77. SCIMAGO LAB. SJR: Scientific Journal Rankings. 2019. Available online: https://www.scimagojr.com/journalrank.php (accessed on 31 July 2019).
78. Falagas, M.E.; Kouranos, V.D.; Arencibia-Jorge, R.; Karageorgopoulos, D.E. Comparison of SCImago journal rank indicator with journal impact factor. *FASEB J.* **2008**, *22*, 2623–2628. [CrossRef] [PubMed]
79. G17. G17—European Green Building Councils Alliance Network. 2019. Available online: https://www.g17.eu/ (accessed on 8 November 2019).
80. Building Research Establishment Group. Our History | BRE Group. 2019. Available online: https://www.bregroup.com/about-us/our-history/ (accessed on 31 July 2019).
81. Keeble, B.R. The Brundtland Report: 'Our Common Future'. *Med. War* **1988**, *4*, 17–25. [CrossRef]

82. Seyis, S.; Ergen, E. A decision-making support tool for selecting green building certification credits based on project delivery attributes. *Build. Environ.* **2017**, *126*, 107–118. [CrossRef]
83. Ali, H.H.; Al Nsairat, S.F. Developing a green building assessment tool for developing countries—Case of Jordan. *Build. Environ.* **2009**, *44*, 1053–1064. [CrossRef]
84. Alyami, S.H.; Rezgui, Y. Sustainable building assessment tool development approach. *Sustain. Cities Soc.* **2012**, *5*, 52–62. [CrossRef]
85. Banani, R.; Vahdati, M.M.; Shahrestani, M.; Clements-Croome, D. The development of building assessment criteria framework for sustainable non-residential buildings in Saudi Arabia. *Sustain. Cities Soc.* **2016**, *26*, 289–305. [CrossRef]
86. Ullah, W.; Noor, S.; Tariq, A. The development of a basic framework for the sustainability of residential buildings in Pakistan. *Sustain. Cities Soc.* **2018**, *40*, 365–371. [CrossRef]
87. Zarghami, E.; Azemati, H.; Fatourehchi, D.; Karamloo, M. Customizing well-known sustainability assessment tools for Iranian residential buildings using Fuzzy Analytic Hierarchy Process. *Build. Environ.* **2018**, *128*, 107–128. [CrossRef]
88. Pushkar, S. The effect of regional priority points on the performance of LEED 2009 certified buildings in Turkey, Spain and Italy. *Sustainability* **2018**, *10*, 3364. [CrossRef]
89. Choi, J.O.; Bhatla, A.; Stoppel, C.M.; Shane, J.S. LEED credit review system and optimization model for pursuing LEED certification. *Sustainability* **2015**, *7*, 13351–13377. [CrossRef]
90. Olakitan Atanda, J. Developing a social sustainability assessment framework. *Sustain. Cities Soc.* **2019**, *44*, 237–252. [CrossRef]
91. Stender, M.; Walter, A. The role of social sustainability in building assessment. *Build. Res. Inf.* **2019**, *47*, 598–610. [CrossRef]
92. Seinre, E.; Kurnitski, J.; Voll, H. Quantification of environmental and economic impacts for main categoriesof building labeling schemes. *Energy Build.* **2014**, *70*, 145–158. [CrossRef]
93. Park, J.; Yoon, J.; Kim, K.-H. Critical review of the material criteria of building sustainability assessment tools. *Sustainability* **2017**, *9*, 186. [CrossRef]
94. He, Y.; Kvan, T.; Liu, M.; Li, B. How green building rating systems affect designing green. *Build. Environ.* **2018**, *133*, 19–31. [CrossRef]
95. Lee, W.L.; Burnett, J. Benchmarking energy use assessment of HK-BEAM, BREEAM and LEED. *Build. Environ.* **2008**, *43*, 1882–1891. [CrossRef]
96. Mahmoud, S.; Zayed, T.; Fahmy, M. Development of sustainability assessment tool for existing buildings. *Sustain. Cities Soc.* **2019**, *44*, 99–119. [CrossRef]
97. Castellano, J.; Ribera, A.; Ciurana, J. Integrated system approach to evaluate social, environmental and economic impacts of buildings for users of housings. *Energy Build.* **2016**, *123*, 106–118. [CrossRef]

energies

MDPI

Review

Simulation Tools to Build Urban-Scale Energy Models: A Review

Alaia Sola *, Cristina Corchero, Jaume Salom and Manel Sanmarti

IREC Catalonia Institute for Energy Research, 08930 Sant Adrià de Besòs, Spain; ccorchero@irec.cat (C.C.); jsalom@irec.cat (J.S.); msanmarti@irec.cat (M.S.)

* Correspondence: asola@irec.cat; Tel.: +34-933-562-615

Received: 31 October 2018; Accepted: 16 November 2018; Published: 23 November 2018

Abstract: The development of Urban-Scale Energy Modelling (USEM) at the district or city level is currently the goal of many research groups due to the increased interest in evaluating the impact of energy efficiency measures in city environments. Because USEM comprises a great variety of analysis areas, the simulation programs that are able to model urban-scale energy systems actually consist of an assemblage of different particular sub-models. In order to simulate each of the sub-models in USEM, one can choose to use either existing specific simulation engines or tailor-made models. Engines or tools for simulation of urban-scale energy systems have already been overviewed in previous existing literature, however the distinction and classification of tools according to their functionalities within each analysis area in USEM has not been clearly presented. Therefore, the present work aims at reviewing the existing tools while classifying them according to their capabilities. The ultimate goal of this classification is to expose the available resources for implementing new co-simulation approaches in USEM, which may reduce the modelling effort and increase reliability as a result of using established and validated simulation engines.

Keywords: urban modelling; co-simulation; simulation engines; building stock energy demand

1. Introduction

Cities have proved to be one of the largest energy consumer groups and emitters of greenhouse gases in the world [1]. Consequently, urban areas offer a large potential for energy efficiency improvement and greenhouse gases mitigation. One of the key aspects to evolve towards a more sustainable city energy system is to develop integrated or multi-energy systems, where electricity, heating, cooling, and transport interact with each other at various levels. This new urban energy paradigm presents challenges and uncertainty of systems interaction. In order to assess the behavior of urban energy systems, the research field of multi-domain Urban-Scale Energy Modelling (USEM) has experienced a considerable progress in the recent years. USEM platforms are being developed and used as means of anticipating the resulting performance of different scenarios and/or finding the optimal scenario according to given criteria. In fact, USEM comprises a great variety of analysis areas, thus USEM platforms (i.e., simulation programs able to model urban-scale energy systems) actually represent an assemblage of different particular sub-models, as depicted in Figure 1. A sub-model in this context is defined as a model developed specifically to reproduce the behavior of a sub-system within the urban context, aiming at estimating the performance of a simpler system compared to the more complex overall urban-scale energy system.

Based on the previous statements, modelling tools are defined as either specific simulation engines or tailor-made models capable of simulating one part of the urban energy system (one or multiple sub-models). In contrast, heterogeneous USEM platforms are capable of simulating a broad urban energy system including different sub-models. It has been noticed by the authors that the distinction

between the existing modelling tools and the existing heterogeneous USEM platforms has been partly omitted in existing reviews. However, it is believed that these two concepts must be differentiated. Towards this end, the present review article aims at strictly focusing on the state-of-the-art of the relevant available simulation engines for each sub-model in USEM.

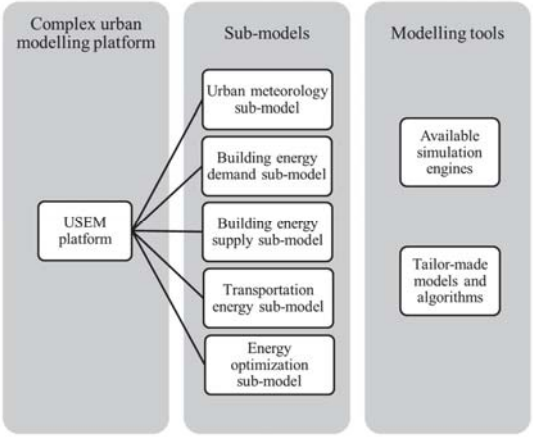

Figure 1. Sub-models in Urban-Scale Energy Modelling platforms.

Engines or tools for the simulation of urban-scale energy systems have already been overviewed in previous existing literature [2,3]. However, the classification of the tools by their functionalities for the simulation of each sub-model (i.e., each basic analysis area) that a complete USEM platform should include has not been clearly presented. Therefore, the present work aims at reviewing the existing tools while classifying them according to their capabilities related to each sub-model in USEM. The ultimate goal of this classification is to expose the available resources for implementing new co-simulation approaches in USEM, which may reduce the modelling effort and increase reliability due to the use of established simulation engines able to build multi-domain USEM platforms. Several modelling tools have been published to date offering the capabilities to simulate one or more of the multiple sub-models that an USEM platform may incorporate. As an example, EnergyPlus simulation engine [4] is used as the tool for the building stock energy demand model in broader USEM platforms such as HUES [5] and Urban Modelling Interface (umi) [6]. In fact, it has been found that existing reviews on urban energy modelling tend to focus on the tools for the simulation of the building stock energy demand, e.g., in [7,8]. On the contrary, the present paper intends to provide researchers with an overview of the existing tools for all the analysis areas.

The paper is presented as follows. We begin by offering a description of our review methodology (Section 2). Tools for the simulation of each of the five sub-models of an USEM platform are then reviewed in turn. Tools for urban meteorology analysis are introduced in Section 3. The review of tools for building energy systems modelling is divided in Sections 4 and 5, i.e., tools for building energy demand and supply analysis, respectively. Transportation energy modelling is reviewed in Section 6. Tools for energy optimization modelling are discussed in Section 7. Conclusions are presented in Section 8. Finally, the selection of tools and simulation engines in this study is also classified in different Tables which indicate the main capabilities of each tool concerning topics such as the analyses of the environment, energy demand, energy generation, energy distribution, and optimization in an urban-scale energy system.

2. Review Methodology

The subject area of Urban-Scale Energy Modelling encompasses numerous techniques and application domains. We therefore conducted a dedicated survey of the literature in order to identify the diversity of the existing engines or tools that have been used for the simulation of urban-scale energy systems. The work is based on the academic experiences of the authors besides the literature survey. The analysis performed with literature review includes findings from the sources SCOPUS and Google Scholar. Since the work has been structured in various sections dedicated to each of the sub-models in USEM, different combinations of terms were used in the search engines depending on the target of the article crawl.

Article crawls were performed within the period of 1997 (first articles on image-processing software for urban-scale environmental model) to early 2018. The identified papers primarily represent the past decade and confirm that the review is an assessment of current practice. Also, in order to identify a manageable subset of papers, the results were filtered by excluding subject areas irrelevant to the aim of our work, such as biological and health sciences. The remaining studies were reviewed and classified. These studies generally belong to the fields of urban climate studies, building simulation, district networks simulation, micro- and macrosimulation of transportation, and optimization engines, all with relevance to energy systems.

3. Tools for Urban Meteorology Analysis

Energy systems in cities interact with the atmosphere over a wide range of scales. This fact together with the increasing share of humans living in cities has promoted the research on urban meteorology (the study of the effect of urban areas on local weather variables) during the last decades. It is therefore known that in order to develop an accurate USEM platform, the context data—meteorological and environmental—is of great importance. Accordingly, some of the available tools aimed at modelling the main physical processes that characterize the urban meteorology are discussed in this section.

3.1. Meteorological Data

Meteorological data is commonly used in hourly values for building simulation. There are many meteorological data sources available on the web, both from national meteorological services and commercial data bases (such as Meteonorm [9]). The first kind of data source is based on measured data, whereas the second one is rather synthetic data that are constructed from monthly values with models.

Although it is well known that there is a great sensitivity of building heating and cooling demands to climate change, the standard weather files rarely consider this phenomenon. In order to cope with this limitation, additional tools are required, i.e., climate change weather file generator tools. Two available tools with wide industry recognition are CCWorldWeatherGen [10] and WeatherShift™ [11]. CCWorldWeatherGen is a freely available tool that integrates future climate scenarios into the widely used weather file formats within simulation TMY2 and EPW. In a similar way, the commercial WeatherShift™ toolkit produces EPW weather files adjusted for changing climate conditions. These tools are based on different general circulation models and different Assessment reports by the Intergovernmental Panel on Climate Change (IPCC) on the emission scenarios that provide projections of possible future climate change.

3.2. Urban Climate Modelling

Besides climate change, the urbanized areas themselves are another factor that should be included in an urban meteorology sub-model. The morphology of buildings and their heat emissions influence local temperatures and air circulation and alter the formation of precipitation and the frequency and intensity of thunderstorms [12]. More in detail, with the presence of a very dense building stock, more shortwave radiation is absorbed, less longwave radiation is emitted, and the mean wind speed is lower, so that the mean air temperature is higher. This is the so-called Urban Heat Island (UHI) effect,

which is fostered by anthropogenic heat sources and the relative lack of vegetated surfaces in urban areas. UHI is the main factor influencing the variations in building stock energy demand between urban and rural areas [13]. Due to this fact, the meteorological data usually available in commercial databases may not be representative enough to model the energy use in urban areas. At this point, the urban climate modelling (i.e., the modelling of the ways in which cities influence atmospheric thermodynamics) becomes essential to reveal the trend of the urban heat load.

Urban climate assessment tools can be classified under mesoscale and microclimate models. On one hand, a modelling tool classified within the mesoscale modelling approach is well suited to predicting phenomena in the city block scale, i.e., 100 km order with the smallest applicable mesh size being about 1 km. On the other hand, the microclimate modelling approach is useful to predict detailed spatial distributions of flow, temperatures, and scalar fields inside complex urban areas at building or district scale [14]. Mesoscale and microclimate models may be used separately or simultaneously, depending on the targeted resolution level. However, in general terms, in order to evaluate the energy use in city districts, microclimate models are of great use. Urban microclimate modelling ranges from radiation analyses that take focus on the short and longwave radiant exchange within the urban geometries (e.g., in reference [15]) to more detailed multi-scale atmospheric flow modelling by means of three-dimensional computational fluid dynamics (CFD) (e.g., in reference [16]).

The urban microclimate assessment tool ENVI-met [17] is a CFD-based tool that takes into account shortwave and longwave radiation, transpiration, evaporation and sensible heat flux from vegetation and water, as well as heat exchange with the soil. The ENVI-met 4.0 works with prescribed dynamic boundary conditions (temperature, wind velocity, humidity) and in such way generates 'corrected' urban climatologic parameters. Furthermore, it includes 3D modelling and allows the user to specify each element's physical properties on the building's façades [18]. In addition to ENVI-met, several urban microclimate models exist that are freely available and could be applied to urban meteorology and climatology. The RayMan model [19] is a tool for the simulation of radiation flux densities and mean radiant temperature from the three-dimensional surroundings in simple and complex environments. RayMan allows calculating sunshine duration with or without sky view factors; estimating daily mean, max or summing of global radiation; and calculating shadows for existing or future complex environments. SkyHelios [20] is a tool to calculate global radiation, sunshine duration, shade, roughness, wind speed, and sky view factors in high spatial and temporal resolution by using a graphic processor. Additionally, it provides an interface to RayMan and other models, as well as import possibility of GIS files and formats. MUKLIMO_3 [21] is a non-hydrostatic climate model which can be considered a mesoscale model in contrast to ENVI-met, SkyHelios and RayMan tools (which are considered as microscale models). As an urban climate model, MUKLIMO_3 was developed to simulate the near-surface meteorology of urban areas [22]. It simulates the atmospheric temperature, humidity and wind field on a 3D grid. Being a mesoscale model, the spatial resolution of the model can vary from a few meters with resolved buildings to several hundred meters with parametrized building environments. One simulation tool extensively applied for solar and daylighting studies is the non-commercial software Radiance [23]. This tool includes a model that uses vector data to calculate solar energy incident on buildings, accurately calculates luminance and radiance, and models both electric light and daylight, all based on urban obstructions in a volumetric 3D model. Radiance is used, for example, in the urban modelling platforms URBANopt [24] and umi [6]. The modelling tool Urban Weather Generator (UWG) [25,26] calculates air temperatures inside urban canyons from measurements at an operational weather station located in an open area outside a city. The tool can be used alone (as a data pre-processing step) or coupled to existing programs (thus using the co-simulation approach). Therefore, UWG calculates the hourly values of urban air temperature and humidity by modelling UHI, based on neighborhood-scale energy balances. An application of the UWG is presented in [27], where UWG is combined with a parametric simulation module that works either stand-alone or together with the urban platform umi in Rhinoceros 3D software [28].

In general, and at the present stage of USEM development, the use of a variety of sub-models for urban climate modelling is well-established in either an integrated manner (including at source-code level the mathematical modelling of urban climate) or in a sequential manner (using a simulation engine or model to pre-process the meteorological data that will be subsequently input to other sub-models of the USEM platform). In fact, the main observed approach in USEM is the sequential use of existing urban climate modelling tools. For example, this capability is implemented in CitySim platform [13] with the use of three climate models developed by [29] (i.e., a macro, meso and an urban canopy model) to predict temperature, wind and pressure field in the city considering the building stock. The urban climate models are run as a pre-process to modify the climatic inputs to the other sub-models in CitySim.

4. Tools for Building Energy Demand Modelling

Over the last decades, detailed individual building energy modelling has become an established mode of analysis for building designers. Consequently, there are a large number of modelling tools (simulation engines or software) available to simulate the energy demand of a building. At an urban level, the analysis of the energy demand of buildings includes both a characterization of the building stock itself and the simulation of the energy demand of the buildings integrating this stock.

4.1. Building Stock Characterization

Building stock characterization consists of two steps: First, the building typology (or also called building archetype) identification and, second, its topological (geometry) definition and eventually representation. This characterization is one of the critical points, especially in case of analyzing existing urban areas, since the information must be extracted from existing data sets. The problem complexity is significantly reduced in case of neighborhoods in planning phase due to the more complete information on both typologies and thermal characteristics of the buildings, where characterization may be generated from scratch.

Firstly, the building typology (also called 'archetype') identification comprises the definition of a set of parameters (use, age and shape) for each building. Given the diversity of building constructions, systems and occupancy patterns in a city, the typology characterization is normally done by grouping a set of buildings and defining them with the average properties of a real building sample with the same characteristics. Secondly, the building topological (geometry) definition acquires the information from cadastral data bases, statistical estimates, sampling and remote sensing by image processing technologies. Digital image processing is the process of assigning a pixel (or groups of pixels) of remote sensing image to a land cover or land use class. In fact, digital image processing has been recognized for a wide scope of applications (not limited to urban energy modelling), which has led to an important progress on this field (see e.g., references [30–32]). An application example is the LT Urban method developed by references [33,34], which uses digital image processing in order to obtain the urban geometries of non-residential buildings for the simplified energy demand model. LT Urban uses Digital Elevation Models derived from ortophotos. In a similar way, this approach was used by references [35,36] to obtain environmental parameters, such as shadowing distribution, daylight availability, sky view factors and so on. In this case, the authors used the Image Processing Toolbox within Matlab [37]. Other approaches include the laser scanning for building characterization applied by reference [38] and the satellite images and aerial photos used by reference [39]. It is interesting to note that reference [39] deduced the building construction period by comparing satellite images taken in different years. Both methodologies have been applied to study possible improvements or feasibility of district heating systems in what may be considered as low-density settlements. These kinds of tools have been shown to be of great utility, especially in areas with low quality cadastral information.

Data for building geometry definition may be combined from two disparate data streams. In order to complement the use of digital image processing, the integration of this approach and Geographical Information Systems (GIS) technologies has been applied widely for building geometry

characterization. GIS are computer programs for the acquisition, storage, analysis and display of geographic data, which allow withdrawing information regarding the geometry and typology of the existing buildings. The most frequently used tools for such purposes are ArcGIS, e.g., used in references [40,41], and the open source free Quantum GIS or QGIS, e.g., used in references [42,43]. Some of these tools can be coupled to 3D modelling tools in order to project a 2D geometry onto a complex 3D surface, e.g., ArcGIS can be coupled to Sketchup [44], as done in reference [45]. The use of 3D GIS software like SketchUp or ESRI CityEngine [46] is common and mostly used for data creation focused on building geometry (without semantic information). In practice, most of the GIS models are relatively poorly attributed when referring to semantical information acquisition. In order to address this constraint, a framework for integrating the Building Information Modelling (BIM) technology into GIS is proposed in the literature [47]. BIM is a process involving the generation and management of digital representations of both physical and functional characteristics of a building, but it is mostly used in small scale projects. The integration of BIM into GIS leads to the concept of City Information Modelling (CIM). An example of a well-developed and established semantic model in digital city is CityGML (City Geography Markup Language) [48]. CityGML is an open standardized data model and exchange format to store digital 3D models of cities and landscapes, which is quickly being adopted (mainly in Europe) as an international exchange format standard [49]. This kind of approach has been used in several platforms for city-scale building load simulation in order to gain accuracy in volumetric/geometric definition of existing building stock. Examples of the use of CityGML for building stock characterization are the 3D city model of the city of Ludwigsburg by reference [50], the 3D modelling of the city of Essen by reference [51], the tool TEASER by reference [52], or the web-based data and computing platform CityBES by reference [53]. Finally, the geometric modelling of the building stock can be done as a computer-aided design (CAD) representation ('manual' drawing) of each building or typology, for example with common CAD tools such as AutoCAD [54]. Many of these tools offer the feature of using Google Earth [55] to import GIS information in order to subsequently analyze, place, and orient the design of the buildings.

4.2. Building Energy Demand Modelling

The sub-model for building stock energy demand calculation within USEM has broadly used well-known commercial or public-domain software. In fact, it is common to find urban platforms that put an emphasis on the demand side of the urban energy system and ignore the energy supply side. In this case, models can be classified as Urban Building Energy Modelling (UBEM) platforms, which mostly simulate the demand endogenously, that is, by including equations that provide the demand under different conditions as an output of the model).

The tools for building energy demand simulation analyzed in this study follow a bottom-up approach. Such approach extrapolates the estimated energy consumption of a representative set of individual building archetypes to a wider urban area [56], thus merging detailed individual building energy models and large-scale building stock models. The opposite approach for energy demand modelling is the so-called top-down approach, which treats the residential sector as energy sink and is not concerned with individual end-uses. The latter utilizes historic aggregate energy values and from them computes the energy consumption of the housing stock as a function of top-level variables (e.g., gross domestic product, unemployment, inflation), energy price, and general climate [56]. In general, models for energy conversion inside a building (e.g., models for HVAC equipment, boilers and storage devices) are relatively simple and typically based on heat and mass balance equations and equipment performance parameters or curves. Notwithstanding this, it must be noted that detailed building energy demand modelling is a key element for the subsequent evaluation of different energy supply systems at a district or city level.

Bottom-up modelling methodologies applied in UBEM can be classified in two main categories: Statistical and engineering modelling methods. An overview of these two different energy demand modelling methodologies is done in reference [56]. On the one hand, engineering models estimate

the dynamic energy demand by taking into account building physics, climate, occupancy, usage of equipment, etc. and can provide profiles of individual (typical) buildings with high temporal resolution. For example, this kind of model is used in the USEM platform HUES [5]. On the other hand, statistical methods result from regression analyses which establish the relationship between building energy consumption and its defined end-uses and climatic conditions.

There are many representative review papers which compare the features of the major existing building-level energy simulation tools used for UBEM [6,57,58]. For the aim of the present work, a selection of the most representative building energy demand simulation tools based on the engineering modelling approach and employed in both UBEM and USEM platforms has been done. The categorization and technical attributes of the selected tools are summarized in Table 1.

- DOE-2 [59], used for example to simulate the heating and cooling loads and energy usage for 144 residential and 120 commercial prototypes/climate combinations in reference [60]. It models building heating, cooling and electricity demand.
- eQUEST [61] (derived from DOE-2), used for example in reference [62] in conjunction with DOE-2 to obtain day-specific estimates of electricity and natural gas consumption within the residential and commercial sectors in a city. eQUEST has an extensive library of default values for building characteristics for several building types in the United States.
- ESP-r [63], used for example by reference [64] for the calculation of space heating and cooling of 17,000 houses in the Canadian hybrid residential end-use energy and emissions model (CHREM). It models building heating, cooling, appliances, lighting and domestic hot water demand.
- EnergyPlus [4] (partly based on DOE-2 software), used for instance by reference [43] for thermal building simulations at large urban scale, as well as in the USEM platforms previously mentioned HUES and umi. It models building heating, cooling, appliances, lighting and domestic hot water demand.
- HASP/ACLD [65], widely used by Japanese authors, e.g., used in reference [66] to simulate the energy use in buildings in a representative district. It models the indoor temperature, humidity and building thermal loads. A comparison of HASP/ACLD features and capabilities with the EnergyPlus software in terms of air-conditioning evaluation of buildings is done by reference [67].
- HOT2000 [68], mainly used by Canadian authors, e.g., used in reference [69] to perform batch simulations for 8767 house files based on the Canadian stock. Similar to HASP/ACLD, it models building heating and cooling demand.
- TRNSYS [70], used by references [71,72] for example to couple it with urban microclimate engines to include the effects of urban microclimate in building energy performance simulations of the building stock. TRNSYS is designed to simulate the transient performance of thermal energy systems while building input data is entered through a dedicated visual interface (TRNBuild).
- Modelica [73] is an object-oriented simulation language that offers an extensive set of standard libraries, with models for control, thermal, electrical and mechanical systems. These are used to develop the base for modelling highly-specialized applications. Examples of relevant Modelica libraries within urban energy modelling are the Building library by reference [74] and the AixLib library by reference [75]. Several multi-domain modelling and simulation solutions existing in USEM are based on Modelica, e.g., the work presented in reference [76]. Some of simulation tools able to execute Modelica are Dymola, MathModelica, MapleSim, and Open-Modelica.
- PolySun [77] models building heating, cooling and domestic hot water demand. Thermal and electrical models are presented all in one tool. An example of the use of PolySun for urban energy modelling is presented in reference [78].
- IDA ICE or IDA Indoor Climate and Energy [79], used by reference [80] in order to assess the effect of urban modifications on indoor air temperature and the building cooling load. It consists of thermal simulation software that models heating, cooling, ventilation, and lighting systems in a building.

These simulation engines may also be used in a sequential manner, thus the output of one of them is subsequently used as the input for the other one. For instance, in the model developed by reference [81], DOE-2 building loads are simplified and used in a sequential manner as input for TRNSYS simulations, which are in turn used to model the energy supply system. TRNSYS and Modelica simulation environments were combined by reference [82] in order to benefit from the advantages of employing the specialized modelling capabilities of TRNSYS together with the ability of performing rapid prototyping within Modelica for large-scale energy systems modelling. Similarly, a model that allows EnergyPlus to conduct co-simulation with various simulation tools (e.g., with Modelica) is presented in reference [83]. Another approach for co-simulation of whole-building energy modelling is OpenStudio cross-platform [84]. This platform is a collection of software tools that interface with EnergyPlus input and output files and manage the simulations. In this case, the tool supports the co-simulation with advanced daylight analysis using Radiance software, and it includes graphical interfaces (such as a plug-in to Google SketchUp) to create building geometry [85].

As for the tools based on bottom-up statistical techniques, these are applied to determine the energy demand contribution of end-uses in buildings (normally including behavioral aspects) based on data obtained from energy bills, simple surveys, or others [56]. Common programming languages for this kind of simulation tools are Matlab, R [86], GradeStat [87], Python [88], or Java [89]. Examples of the use of statistical techniques to create forecasting models of energy consumption and load demand peak are described in references [90–92].

Table 1. Characteristics of reviewed simulation tools for building energy demand in USEM.

	Transient/ Static	Radiation Analysis	Coupling with GIS	Building Geometry	Energy Demand Modelling Approach	Energy Demand Modelling	Types of Building Energy Demand	Impact of User Behavior on Energy Demand	Modelling of Energy Generation	District Thermal Network	Electricity Network	Gas Network	Building Design Optimization	Time Scale	Availability	References
DOE-2	T	x	-	x	Eng	Endo	H, C, V, L	-	PV, GSHP, TES, boiler, chiller	-	-	-	x [1]	hourly	free	[59]
eQUEST	T	x	x	x	Eng	Endo	H, C, V, L	-	PV, GSHP, TES, boilers, chillers	-	-	-	x [1]	hourly	free	[61]
ESP-r	T	x	-	x	Eng	Endo	H, C, A, L, DHW	x	PV, solar thermal, boilers, chillers	-	-	-	x [1]	sub-hourly	free, open-source	[63]
EnergyPlus	T	x	x	x	Eng	Endo	H, C, A, L, DHW	x	PV, BIPV, cogeneration, boilers, chillers	-	-	-	x [1]	sub-hourly	free, open-source	[4]
HASP/ACLD	T	-	-	x	Eng	Endo	H, C	-	-	-	-	-	-	hourly	free	[65]
HOT2000	T	-	-	x	Eng	Endo	H, C	-	-	-	-	-	-	annual	free	[68]
TRNSYS	T	x	x	x	Eng	Endo	H, C, V	x	PV, solar thermal, GSHP, TES, boilers, chillers	x	-	-	x [1]	sub-hourly	commercial, open-source	[70]
Modelica	T	x	-	x	Eng	Endo	H, C, A, L	x	PV, GSHP, boilers, chillers	x	x	-	x	sub-hourly	open-source, free, commercial	[73]
Polysun	T	x	-	x	Eng	Endo	H, C, E, DHW	x	PV, solar thermal, wind, GSHP	x	x	-	x [2]	sub-hourly	commercial	[77]
IDA ICE	T	x	-	x	Eng	Endo	H, C, V, L	x	PV, GSHP	x	-	-	x [1]	sub-hourly	commercial, open-source	[79]

S = Steady-state; T = Transient; Eng = Engineering model; Sta = Statistical model; Endo = Endogenous; Exo = Exogenous; H = Heating; C = Cooling; V = Ventilation; A = Appliances; L = Lighting; E = Electricity, DHW = Domestic Hot Water; PV = Photovoltaics; GSHP = Ground-source heat pump; CHP = Combined Heat&Power; BIPV = Building Integrated Photovoltaics; HP = Heat Pump; TES = Thermal Energy Storage; [1] Coupled with generic optimization programs; [2] Coupled with Matlab & Polysun Inside (a Polysun plug-in).

5. Tools for Building Energy Supply Modelling

In order to fully simulate the energy system of a city or district, the modelling of the supply side is also of high importance. The relationship between the performance of energy supply systems and the energy demand profiles of buildings determines the main energy flows of the district or city. Therefore, one of the main goals of urban energy simulation should be to help forecasting potential problems of supply and demand mismatch and propose scenarios to overcome barriers. In order to achieve this, the energy supply system sub-model should simulate both the energy generation plants (how they dynamically behave related to their efficiency and weather-dependency) and the energy distribution networks (to observe potential network capacity overloads and/or help sizing the networks themselves).

In general, the simulation of district energy systems requires the calculation of the energy flows of networks and grids by considering the energy supply from both central systems and distributed systems (if included in the analysis). On the one hand, typical building electricity supply systems are composed of two sources: Grid electricity from central systems and the so-called Distributed Energy Resource Systems (DERs) (which allow an energy system to be partially or completely independent from the grid). On the other hand, the same concept may be considered for the thermal supply, as heating and cooling can be sourced from both a thermal district network supplied by a central system and/or from distributed thermal energy generation. Different tools to simulate building energy supply systems have been reviewed by references [93–95]. The categorization and technical attributes of the selected tools for the present study are provided in Table 2.

5.1. Energy Generation Modelling

Modelling of both central and decentralized energy conversion or generation plants may be done by developing a customized model, or also by using standard libraries of available simulation engines or tools. The use of TRNSYS, DOE-2, and Modelica for this purpose is frequent. Some examples are the use of Modelica for thermal simulation of natural gas cogeneration power plants, absorption chillers and thermal solar collectors described in reference [43], or the use of TRNSYS for analyzing different energy supply scenarios including Combined Heat and Power (CHP) units, ground- and water-source heat pumps, and boilers found in [81].

Focusing on DERs evaluation tools, a variety of reviews on software for design and optimization of DER technology can be found in the literature [3,95,96]. Some of the most known tools for DERs simulation are energyPRO [97], HOMER [98], DER-CAM [99], RETScreen [100], or EnergyPLAN [101]. Differently to tools such as TRNSYS, DOE-2, and Modelica, this type of simulation engines is more focused on techno-economic analysis of the consequences of different energy investments in relation to the availability of distributed energy resources, rather than on the specific physical impact of DERs technologies on the distribution grids and networks. This kind of software do not normally model detailed building stock energy demand as the tools described in Section 4 do, but they generally utilize real load profiles or load profiles generated by other tools for their analysis.

5.2. Energy Distribution Modelling

The proper modelling of the dependency of energy demand systems on the electrical grid and thermal district networks is desirable, as the energy carrier infrastructures are a significant element in the potential for optimization of district energy systems. Modelling of distribution systems will provide information on the possibility for reduction of transmission losses and problems related to congestion in distribution systems, as well as the possibility of interaction between the building energy consumers/producers and the distribution systems. However, until now many USEM published in the literature ignored this sub-model, as they focus on building energy demand modelling and local energy generation, assuming all the rest of the required energy by the building stock is guaranteed on a district scale. Therefore, one aspect to emphasize for the future development of USEM is the

consideration of the detailed modelling of the energy infrastructures. Indeed, there are a variety of available simulation engines for energy infrastructure modelling, thus energy distribution modelling within more complex USEM platforms should take advantage of the available tools.

An existing review of a quite large number of software tools for district heating modelling is presented in reference [102]. One such tool is Modelica, used by [43] in their simulation of the thermal energy distribution network in an urban area. Yet, it is not documented how detailed the model is in this case. Generally, the simplified models of the district thermal energy network tend to focus on the calculation of heat losses. However, the simulation of other aspects may also be of interest, as e.g., network storage capability, inertia (time delays in the network), distribution temperature, or operation strategies that involve dynamic temperature control [103]. These other parameters are especially of interest if a more interactive network is foreseen in order to upgrade the system performances or to deal with very low energy demand buildings [104]. In this sense, it is advisable to pay attention to the capabilities of commercial district energy models such as TERMIS [105]. This software can create models of both simple and complex district energy pipeline systems besides including multiple generation plants, heat exchangers, pumps, valves and other equipment that affect pipeline operation. In addition to TERMIS, examples of other commercial tools for district heating and cooling (DHC) calculations are NetSim [106] and PolySun [77]. NetSim can perform accurate district network calculations considering parameters such as pressure, velocity, and temperature. PolySun (although not originally designed for network simulations) can provide detailed hydraulics modelling to simulate energy flows and pumping power requirements for district heating networks with decentralized pumps. Other available software is Apros [107], which can be used to model and analyze district heating networks and also long-distance district heat transmission circuits. TRNSYS has been used in more than one work [108–113] for thermal energy networks simulation, mainly by developing new models in the TRNSYS library to better simulate the hydronic systems for space heating, DHW and district heating systems. Also, the UBEM tool CityBES (despite being focused on the simulation of building stock energy demand) allows the evaluation of the feasibility of advanced DHC systems through the co-simulation between DHC models in Modelica and building models in EnergyPlus [53].

Other than thermal energy networks simulation, there are simulation tools in the market that have electricity and/or gas distribution modelling capabilities. NEPLAN [114] is a tool that performs optimization of electrical, water, gas, and district heating networks. It can perform flow and energy loss calculations for microgrids as well as hydraulic modelling of district heating networks.

Focusing on power grid simulation, there is a large variety of free, open-source and commercial software packages available because of the engineering requirements of the industry and providers. Power system modelling is a broad field and consequently the type of models and assumptions used varies considerably among software packages. Existing simulation tools can differ in time-scale of the simulations (steady-state vs. transient), and in domain (power generation, transmission, platforms and the classification of their capabilities is presented in [115]. Examples of widely used commercial software packages for power system design and operation applications are DigSILENT PowerFactory [116], MODEST [117], the Matlab tool MATPOWER [118], PyPower (a port of MATPOWER to the Python programming language) [119], ETAP [120], IPSA 2 [121].

Table 2. Characteristics of reviewed simulation tools for building energy supply in USEM.

	Transient/ Static	Coupling with GIS	Endogenous/ Exogenous Energy Demand Modelling	Types of Building Energy Demand Considered	Modelling of Energy Generation	Thermal Network	Electricity Network	Gas Network	Energy System Optimization	Time Scale	Availability	References
HOMER	T	-	Exo	T, E	PV, wind, hydro, biomass, microturbines, fuel cells, batteries, hydrogen storage	x	x	-	x	sub-hourly	commercial	[97]
TERMIS	S	-	Exo	T	Exogenously	x	-	-	x	-	commercial	[105]
NetSim	S	x	Exo	T	Exogenously	x	-	-	x	-	commercial	[106]
Apros	T	-	Exo	T, E	Solar thermal, cogeneration, thermal power plants	x	x	-	x	hourly	commercial	[107]
NEPLAN	T	x	Exo	T, E	Exogenously	x	x	x	x	hourly	commercial, open-source	[114]
DigSILENT PowerFactory	T	-	Exo	E	Exogenously	x	-	-	x	hourly	commercial	[116]
MODEST	T	-	Exo	T, E	Wind, hydro, biomass, HP, CHP, boilers	x	-	x	x	hourly	commercial	[117]
MATPOWER	S	-	Exo	E	Exogenously	-	x	-	x	-	free, open-source	[118]
PYPOWER	S	-	Exo	E	Exogenously	-	x	-	x	-	free, open-source	[119]
ETAP	T	x	Exo	E	PV, wind, batteries	-	x	-	x	hourly	commercial	[120]
IPSA 2	T	x	Exo	E	PV, wind, generator, battery	-	x	-	x	sub-hourly	commercial	[121]

S = Steady-state; T = Transient; Endo = Endogenous; Exo = Exogenous; T = Thermal demand; E = Electrical demand; PV = Photovoltaics; CHP = Combined Heat & Power; HP = Heat Pump.

6. Tools for Transportation Energy Demand Modelling

There are numerous transport modelling software products available on the market. The approach followed by these simulation engines may be either macroscopic (statistical dispersion models, freeway traffic models, etc.) or microscopic (multi-agent simulation, particle system simulation, etc.) [122]. Therefore, in general terms, there are two classes of models for transportation energy demand calculation: vehicle-based models that predict energy consumption based on the result of a microsimulation model, and macrosimulation models that use aggregate energy consumption data to predict transportation energy consumption with low spatial and temporal resolutions. The choice between both approaches will be based on the required level of detail since each approach has its own advantages and disadvantages. As stated in the review on traffic simulation software in reference [122], macrosimulation models do not examine the impacts a single vehicle may have in the traffic network, while microsimulation models are very detailed but may present issues with the use of computer memory. Similarly, from the energy consumption point of view, macroscopic models (based on average speed philosophy) relate the fuel consumption by transport to the average speed of links, while microsimulation models provide more accurate estimates of fuel consumption for a limited network application context. There is a wide spectrum of reviews on traffic simulation tools in the literature (e.g., [122,123]). Some examples of the mostly used micro- and macrosimulation tools introduced in these reviews are CUBE Dynasim [124], Paramics [125], EMME [126], SimTraffic [127], AIMSUN [128], VISSIM [129], and MatSIM [130]. Details on the characteristics of these tools are presented in Table 2. It must be noted that, in most of the cases, the environmental impact and thus energy consumption in the form of fossil fuel consumption is not directly assessed by the transport simulation tool but this calculation is exogenously done instead as a post-process with the use of fuel consumption factors/ratios).

An example of an USEM co-simulation platform which integrates transportation modelling by using an existing transport modelling tool is the urban platform CitySim [13]. This platform exogenously (specified by the user as a model input) integrates a stochastic transport model by using the MatSIM tool [130]. MATSim is a mesoscopic tool or low-fidelity microsimulation tool, as it has the intention of modelling very large scenarios and does not simulate so detailed models as microsimulation models do. Another example is LakeSIM urban platform [131], which includes the modelling suite for transportation system POLARIS [132] in order to facilitate the assessment of proposed transportation infrastructure. Also, non-motorized trips have been integrated in USEM. The USEM platform umi performs walkability evaluations of complete neighborhoods based on the sustainable transportation module developed by [133]. Walkability is calculated for each building based on a grid of streets and pedestrian pathways as well as amenities using custom Python scripts [6].

A thorough review on computer tools for modelling electric vehicle energy requirements and their impact on power distribution networks is presented in reference [123]. In their work, the authors include a vast list of simulation engines capable of simulating vehicle systems and control, renewable energy and vehicle-to-grid integration, impact analysis, traffic system simulation, etc. As concluded in reference [123], in most situations none of the reviewed tools will be adequate for analyzing and optimizing all aspects of the electric vehicle and the grid interaction. Accordingly, the capabilities of each of the tools are specified in reference [123] in order to find possible synergies among them. A selection of tools is presented on Table 3, together with the classification of some of their main modelling characteristics.

Table 3. Characteristics of reviewed simulation tools for transport energy demand modelling.

	Transient/Static	Supports GIS Integration	Transport Energy Demand Modelling	Traffic Signal Timing Optimization	Time Scale	Availability	References
CUBE Dynasim	T	x	Micro-simulation	x	sub-hourly	commercial	[124]
Paramics	T	-	Micro-simulation	x	sub-hourly	commercial	[125]
EMME/2	S	x	Micro-simulation	x	-	commercial	[126]
SimTraffic	T	-	Micro-simulation	x	sub-hourly	commercial	[127]
AIMSUN	T	x	Micro- and Macro-simulation	x	sub-hourly	commercial	[128]
VISSIM	T	x	Micro-simulation	x	sub-hourly	commercial	[129]
MATSim	T	x	Micro-simulation	x	sub-hourly	free, open-source	[130]
POLARIS	T	x	Micro-simulation	x	sub-hourly	free, open-source	[132]

7. Tools for Energy Optimization Modelling

As USEM platforms have a great number of variables and input parameters, the number of possible combinations is very large. The probability of identifying a multi-objective optimal configuration of these variables by manual trial and error or simple parametric studies is correspondingly small. In order to overcome this problem, simulation-based optimization may be used. Within system optimization studies, the best performing set of parameters and technologies is identified by considering the accomplishment of a set of desired multi-objective criteria. Here, different optimization objectives (Objective functions) may be chosen, e.g., the minimization of primary energy demand, or the minimization of the cost of providing the entire energy supply system (like e.g., implemented in the SynCity urban model [134]). Also, different constraints (environmental emissions, resources) can be fixed in the objective function.

Optimizers coupled with simulation tools allow performing a scientific exploration of alternatives. Global Optimization algorithms have been in use for building thermal performance simulation for long. For example, the Generic Optimization Program GenOpt [135], freeware, can be customized for the minimization of a cost function that is evaluated by an external simulation program. It has been used for conducting optimization calculations with TRNSYS, Dymola, IDA ICE, ESP-r, EnergyPlus and DOE-2, among others [136,137]. Two comprehensive reviews on the most used optimization programs on building performance optimization and their key capabilities are presented in references [138,139]. The survey in reference [138] concludes that EnergyPlus and TRNSYS are the mostly used building simulation programs in building optimization studies, while the mostly used optimization engines or tools seem to be GenOpt and Matlab optimization toolboxes applied to building design optimization. Among the listed optimization tools, some more examples of commercial and free optimization solvers are: Altair HyperStudy, DAKOTA, GoSUM, iSIGHT, LionSolver, MOBO, MultiOpt, Opt-E-Plus, and TRNOPT (a GenOpt interface). Within the scope of building design optimization, fully-functional simulation–optimization tools have also been developed. An example of such platforms is the software BEopt [140], which is designed to find optimal building designs along the path to Zero Net Energy buildings. BEopt uses DOE-2 and EnergyPlus simulation engines to calculate the energy use of the building, and TRNSYS to calculate water-heating loads and energy savings for solar water heating and annual electrical energy production from a grid-connected PV system.

When extrapolating from single building design to the urban system scale, Global Optimization algorithms can also be applied to perform optimization studies. BEopt was used to assess the impact of DER technologies in an urban area by optimizing three defined building prototypes and extrapolating them to the city scale [141]. The CitySim platform uses a hybrid evolutionary algorithm to manipulate the geometric form of groups of buildings to optimize the potential utilization of solar energy by passive and active means [142] and therefore reduce the heating and cooling consumption of the buildings. The effectiveness of this new algorithm was validated in reference [143] by comparing its results against other global optimization algorithms such as the ones behind GenOpt. Another tool to apply Global Optimization algorithms to urban scale energy modelling is Galapagos [144]. This tool is used combined with Walkscore [145] (a tool for walkability metrics that yields the proximity of buildings to amenities) to enhance land-use allocation in a neighborhood with respect to minimizing transportation needs by car, and its output is used in the urban platform umi. Both previous examples relate to the use of global optimization techniques for the minimization of energy consumption (building energy demand and transport energy demand, respectively) in a district or city. Notwithstanding, optimization tools can also be applied to energy supply systems.

In terms of tools for the optimization of energy generation systems, a very detailed review on this topic is presented in reference [146]. Additionally, some of the tools introduced in Section 5.1 are able to perform both the simulation and the optimization of energy generation systems, i.e., HOMER, DER-CAM, RETScreen, or EnergyPLAN. Normally, these tools model energy supply and storage systems at a wide scale and find the optimal DER investments by minimizing the total energy costs, carbon dioxide emissions, or a combination of both criteria. However, it must be noted that a focus on

the generation systems may not be sufficient when optimizing energy supply systems, as other issues need to be simultaneously optimized, e.g., distribution networks layout and costs. The optimization model presented in reference [147] overcomes this limitation by considering both the optimization of the logistics of energy resources/products and the networks layout between consumers and suppliers (both the electrical and thermal distribution).

In general, there are several tools in the market which have been developed for the optimization of energy distribution systems (both for the electricity sector and district thermal systems). The goal of the optimization in this case can be, for instance, to produce the most economical fuel combination by considering a variety of costs, or find the physical equilibrium of the energy distribution network. Examples of simulation tools that include optimization algorithms among the tools presented in Section 5.2 are NEPLAN, TERMIS, DIgSILENT PowerFactory). Also, many of the tools for transport energy demand simulation presented in Section 6 (e.g., Paramics, EMME, SimTraffic, and AIMSUN) include the optimization of traffic signal timings to minimize the total travel time of users and/or reduce the fuel consumption.

Regarding the overall energy-economics in USEM, Multi-Objective Energy System Optimization tools have been under development for long time. For example, the MARKAL/TIMES family [148] are energy/economic/environmental model generators to represent the evolution over a period of usually 20–50 years of a specific energy-environment system at the global, multi-regional, national, state/province, or community level. The main goal of this type of energy models is the identification of the least-cost energy systems and investment strategies or the identification of cost-effective responses to restrictions on environmental emissions and resource constraints. Even if MARKAL tools do not deal with 'fine grade' demand assessment, the energy-economy concepts they integrate may be useful for future USEM development.

8. Conclusions

The assessment and prediction of urban energy systems using Urban-Scale Energy Modelling platforms is becoming increasingly important. The main driver for this work was the fact that, even though there are a significant number of review articles on the topic, they do not normally differentiate specific existing simulation engines (able to tackle one or few analysis areas in the urban energy system) from published USEM platforms (expressly developed to cover several analysis areas in the urban energy system). In addition, not many review papers classify the available simulation engines according to their capabilities and the analysis area(s) of the urban energy system they cover.

In this paper, a general introduction and classification of relevant simulation engines aimed at building each of the sub-models in Urban-Scale Energy Modelling platforms has been provided, backed by the pertinent literature review of major publications on the topic. The selection of both free and commercial simulation tools for USEM has been classified in Tables 1–3, indicating the main capabilities of each tool concerning the analysis of the environment, energy demand, energy generation, energy distribution, and optimization. The preceding sections have shown that there is a very wide range of simulation engines available for the modelling of each of the analysis areas or sub-models that a complete USEM platform may include.

Firstly, both commercial and freely-available simulation engines for urban climate modelling can easily be found. However, the integration of these tools with building performance simulation software is mainly done in a sequential manner (where the microclimate is a predetermined boundary condition), whereas it should be considered that the strong interaction between the local microclimate and the buildings' energy demand may be better represented by co-simulation approaches.

The analysis of building stock energy demand at the urban level needs both the characterization of building stock itself and the simulation of the energy demand of such buildings. For building geometry characterization, the integration of tools for digital image processing and GIS has been widely applied. Nevertheless, due to the limitations of most of the GIS tools in terms of poorly attributed building semantical information, City Information Modelling (CIM) tools are being developed. An example of

a well-developed and established semantic model in digital city is CityGML, a tool for the modelling and exchange of 3D city and landscape models, which is quickly being adopted (mainly in Europe) as an international standard for representing and storing 3D city models. Well-known commercial or public-domain building performance simulation software have been broadly used to compute the results of the building energy demand sub-model in USEM. Accordingly, there are a significant number of available simulation engines as well as representative review papers on this topic. In fact, it is common to find urban platforms that use such tools and put an emphasis on the bottom-up building demand generation of the urban energy system.

Notwithstanding this, a complete simulation of a district energy system requires the calculation of the energy flows of networks and grids by considering the energy supply from both central systems and distributed systems. Indeed, there are a variety of available simulation engines for energy infrastructure modelling (mainly for district heating networks and electrical grids), thus energy distribution modelling within more complex USEM platforms should take advantage of the available tools. In the specific case of power grid simulation, there is a meaningful variety of free and commercial software packages available (due to the engineering requirements of the industry), which could be coupled to other sub-models within USEM.

Transportation modelling has been widely developed in the last decades. This implies that well-established transportation modelling tools are available, although their focus is not the modelling of transportation energy consumption. In general terms, macroscopic transportation modelling tools calculate the transport fuel consumption based on the average speed of links, while microsimulation modelling tools provide more accurate estimates of fuel consumption for a limited network application context. In any of the cases, this calculation is commonly done in an exogenous manner (as a post-process with the use of fuel consumption factors/ratios). To date, transportation modelling tools have been scarcely integrated in wider urban-scale energy models. The vast majority of these tools focus on modelling the individual traffic behavior and include optimization based on specific criteria, as for example the optimization of signal timings to reduce fuel consumption.

Finally, simulation-based optimization tools have also been in use for building thermal performance simulation for a long time. When extrapolating from single building design to urban system scale, Global Optimization algorithms can also be applied. There are existing tools that allow the use of global optimization techniques for the minimization of energy consumption (building energy demand and transport energy demand) in a district or city, as well as the optimization of energy supply systems. It is also common to find optimization tools in the market aimed at producing the most economical fuel combination by considering a variety of costs, or finding the physical equilibrium of the distribution networks. In a different time and physical boundary scales, Multi-Objective Energy System Optimization tools have been under development for long time in the form of energy/economic/environmental model generators. They represent the evolution over a period of usually 20–50 years of a specific energy-environment system at the global, multi-regional, national, state/province, or community level. The main goal of this type of energy models is the identification of the least-cost energy systems and investment strategies, or the identification of cost-effective responses to restrictions on environmental emissions and resource constraints.

With the present work, the ambition is that the given information can help users in academia and in industry with the selection of suitable simulation tools to address Urban-Scale Energy Modelling problems. In contrast to some of the existing USEM reviews which are focused on tools for the simulation of building stock energy demand, the present paper additionally reviews tools for urban meteorology analysis, building energy supply modelling, transportation energy demand modelling, and energy optimization.

Author Contributions: Conceptualization, A.S., C.C., J.S., M.S.; Methodology, A.S., C.C., J.S., M.S.; Software, A.S., C.C., J.S., M.S. All authors have equal contribution.

Funding: This research was funded by the research and innovation program Horizon 2020 of the European Union under the grant agreement nr. 646456 (GrowSmarter) as well as the GEIDI project (ref. TIN2016-78473-C3-3-R)

financed by the Ministry of Economy and Competitiveness of Spain. C. Corchero work is supported by the grant IJCI-2015-26650 (MICINN).

Conflicts of Interest: The authors declare no conflict of interest.

References

1. Masanet, E.R.; Poponi, D.; Bryant, T.; Burnard, K.; Cazzola, P.; Dulac, J.; Pales, A.F.; Husar, J.; Janoska, P.; Munuera, L. *Energy Technology Perspectives 2016-Towards Sustainable Urban Energy Systems*; International Energy Agency: Paris, France, 2016; ISBN 92-64-25234-7.
2. Allegrini, J.; Orehounig, K.; Mavromatidis, G.; Ruesch, F.; Dorer, V.; Evins, R. A review of modelling approaches and tools for the simulation of district-scale energy systems. *Renew. Sustain. Energy Rev.* **2015**, *52*, 1391–1404. [CrossRef]
3. Manfren, M.; Caputo, P.; Costa, G. Paradigm shift in urban energy systems through distributed generation: Methods and models. *Appl. Energy* **2011**, *88*, 1032–1048. [CrossRef]
4. Crawley, D.B.; Lawrie, L.K.; Winkelmann, F.C.; Buhl, W.F.; Huang, Y.J.; Pedersen, C.O.; Strand, R.K.; Liesen, R.J.; Fisher, D.E.; Witte, M.J. EnergyPlus: Creating a new-generation building energy simulation program. *Energy Build.* **2001**, *33*, 319–331. [CrossRef]
5. Bollinger, L.A.; Evins, R. HUES: A holistic urban energy simulation platform for effective model integration. In Proceedings of the International Conference CISBAT 2015 Future Buildings and Districts Sustainability from Nano to Urban Scale, Lausanne, Switzerland, 9–11 September 2015; LESO-PB: Lausanne, Switzerland; EPFL: Lausanne, Switzerland, 2015; pp. 841–846.
6. Reinhart, C.F.; Dogan, T.; Jakubiec, J.A.; Rakha, T.; Sang, A. Umi-an urban simulation environment for building energy use, daylighting and walkability. In Proceedings of the 13th Conference of International Building Performance Simulation Association, Chambery, France, 26–28 August 2013.
7. Harish, V.S.K.V.; Kumar, A. A review on modeling and simulation of building energy systems. *Renew. Sustain. Energy Rev.* **2016**, *56*, 1272–1292. [CrossRef]
8. Li, W.; Zhou, Y.; Cetin, K.; Eom, J.; Wang, Y.; Chen, G.; Zhang, X. Modeling urban building energy use: A review of modeling approaches and procedures. *Energy* **2017**, *141*, 2445–2457. [CrossRef]
9. Remund, J.; Kunz, S. *METEONORM: Global Meteorological Database for Solar Energy and Applied Climatology*; Meteotest: Bern, Switzerland, 1997.
10. Jentsch, M.F.; James, P.A.; Bourikas, L.; Bahaj, A.S. Transforming existing weather data for worldwide locations to enable energy and building performance simulation under future climates. *Renew. Energy* **2013**, *55*, 514–524. [CrossRef]
11. Dickinson, R. Generating future weather files for resilience. In Proceedings of the International Conference on Passive and Low Energy Architecture, PLEA 2016–Cities, Buildings, People: Towards Regenerative Environments, Los Angeles, CA, USA, 11–13 July 2016.
12. Baklanov, A.; Grimmond, C.S.B.; Carlson, D.; Terblanche, D.; Tang, X.; Bouchet, V.; Lee, B.; Langendijk, G.; Kolli, R.K.; Hovsepyan, A. From urban meteorology, climate and environment research to integrated city services. *Urban Clim.* **2018**, *23*, 330–341. [CrossRef]
13. Robinson, D.; Haldi, F.; Kämpf, J.; Leroux, P.; Perez, D.; Rasheed, A.; Wilke, U. CitySim: Comprehensive micro-simulation of resource flows for sustainable urban planning. In Proceedings of the Building Simulation, Glasgow, Scotland, 27–30 July 2009; pp. 1614–1627.
14. Ooka, R. Recent development of assessment tools for urban climate and heat-island investigation especially based on experiences in Japan. *Int. J. Climatol. J. R. Meteorol. Soc.* **2007**, *27*, 1919–1930. [CrossRef]
15. Robinson, D. 15 Integrated resource flow modelling of the urban built environment. *Build. Perform. Simul. Des. Oper.* **2011**, 441.
16. Yang, X.; Zhao, L.; Bruse, M.; Meng, Q. An integrated simulation method for building energy performance assessment in urban environments. *Energy Build.* **2012**, *54*, 243–251. [CrossRef]
17. Bruse, M. Modelling and strategies for improved urban climates. In *Proceedings International Conference on Urban Climatology & International Congress of Biometeorology*; Citeseer: Gaithersburg, MD, USA, 1999; pp. 8–12.
18. Huttner, S.; Bruse, M. Numerical modeling of the urban climate–a preview on ENVI-met 4.0. In Proceedings of the 7th International Conference on Urban Climate ICUC-7, Yokohama, Japan, 29 June–3 July 2009; Volume 29.

19. Matzarakis, A.; Rutz, F.; Mayer, H. Modelling radiation fluxes in simple and complex environments: Basics of the RayMan model. *Int. J. Biometeorol.* **2010**, *54*, 131–139. [CrossRef] [PubMed]
20. Matzarakis, A.; Fröhlich, D.; Gangwisch, M.; Ketterer, C.; Peer, A. Developments and applications of thermal indices in urban structures by RayMan and SkyHelios model. In Proceedings of the ICUC9 9th International Conference on the Urban Climate Jointly with the 12th Symposium on the Urban Environment, Freiburg, Germany, 23 April 2015.
21. Sievers, V. *The Model MUKLIMO_3, Special Aspects and Extensions*; Deutscher Wetterdienst: Offenback, Germany, 2001.
22. Simon, H. *Modeling Urban Microclimate: Development, Implementation and Evaluation of New and Improved Calculation Methods for the Urban Microclimate Model ENVI-Met*; 2016.
23. Larson, G.W.; Shakespeare, R. *Rendering with Radiance: The Art and Science of Lighting Visualization*; Booksurge Llc: Charleston, SC, USA, 2004; ISBN 0-9745381-0-8.
24. Polly, B.; Kutscher, C.; Macumber, D.; Schott, M.; Pless, S.; Livingood, B.; Van Geet, O. *From Zero Energy Buildings to Zero Energy Districts*; NREL (National Renewable Energy Laboratory): Golden, CO, USA, 2016.
25. Bueno, B.; Norford, L.; Hidalgo, J.; Pigeon, G. The urban weather generator. *J. Build. Perform. Simul.* **2013**, *6*, 269–281. [CrossRef]
26. Bueno, B.; Roth, M.; Norford, L.; Li, R. Computationally efficient prediction of canopy level urban air temperature at the neighbourhood scale. *Urban Clim.* **2014**, *9*, 35–53. [CrossRef]
27. Nakano, A. *Urban Weather Generator User Interface Development: Towards a Usable Tool for Integrating Urban Heat Island Effect within Urban Design Process*; Massachusetts Institute of Technology: Cambridge, MA, USA, 2015.
28. McNeel, R.; Rhinoceros. NURBS Modleing for Windows. 2015. Available online: http://www.rhino3d.com/jewelry.htm (accessed on 30 October 2018).
29. Rasheed, A. *Multiscale Modelling of Urban Climate*; EPFL: Lausanne, Switzerland, 2009.
30. Ledoux, H.; Meijers, M. Extruding building footprints to create topologically consistent 3D city models. In *Urban and Regional Data Management*; CRC Press: Boca Raton, FL, USA, 2009; pp. 51–60.
31. Ledoux, H.; Meijers, M. Topologically consistent 3D city models obtained by extrusion. *Int. J. Geogr. Inf. Sci.* **2011**, *25*, 557–574. [CrossRef]
32. Ghawana, T.; Zlatanova, S. *Data Consistency Checks for Building of 3D Model: A Case Study of Technical University, Delft Campus, The Netherlands*; Geospatial World: Rotterdam, The Netherlands, 2010.
33. Ratti, C. LT Urban-The energy modeling of urban form. *Proc. PLEA2000* **2000**, 660–665.
34. Ratti, C.; Baker, N.; Steemers, K. Energy consumption and urban texture. *Energy Build.* **2005**, *37*, 762–776. [CrossRef]
35. Richens, P. Image processing for urban scale environmental modelling. In *Proceedings 5th Intemational IBPSA Conference: Building Simulation 97*; University of Bath: Bath, UK, 1997; pp. 163–171.
36. Ratti, C.; Di Sabatino, S.; Britter, R. Urban texture analysis with image processing techniques: Winds and dispersion. *Theor. Appl. Climatol.* **2006**, *84*, 77–90. [CrossRef]
37. Gonzalez, R.C.; Woods, R.E.; Eddins, S.L. *Digital Image Processing Using MATLAB*; Pearson-Prentice-Hall Upper Saddle River: Saddle River, NJ, USA, 2004; Volume 624.
38. Neidhart, H.; Sester, M. Identifying building types and building clusters using 3-D laser scanning and GIS-data. *Int. Arch. Photogramm. Remote Sens. Spatial Inf. Sci.* **2004**, *35*, 715–720.
39. Geiß, C.; Taubenböck, H.; Wurm, M.; Esch, T.; Nast, M.; Schillings, C.; Blaschke, T. Remote sensing-based characterization of settlement structures for assessing local potential of district heat. *Remote Sens.* **2011**, *3*, 1447–1471. [CrossRef]
40. Massimo, D.E.; Barbalace, A.; Marzo-Micale, A. GIS, 3D city modeling and green urban conservation. In Proceedings of the 30th Esri International User Conference, San Diego, CA, USA, 12–16 July 2010.
41. Reiter, S.; Wallemacq, V. City energy management: A case study on the area of Liège in Belgium. In Proceedings of the International Conference GEOProcessing, Valencia, Spain, 29 January–4 February 2011; IARIA: Barcelona, Spain, 2011; pp. 1–6.
42. Kulkarni, S.; Banerjee, R. Renewable energy mapping in Maharashtra; India using GIS. In Proceedings of the World Renewable Energy Congress-Sweden, Linköping, Sweden, 8–13 May 2011; Linköping University Electronic Press: Linköping, Sweden, 2011; pp. 3177–3184.

43. Huber, J.; Nytsch-Geusen, C. Development of modeling and simulation strategies for large-scale urban districts. In Proceedings of the Building Simulation, Sydney, Australia, 14–16 November 2011; Volume 2011, pp. 1753–1760.
44. Sketchup Software. Available online: https://www.sketchup.com/ (accessed on 30 October 2018).
45. Saygi, G.; Agugiaro, G.; Hamamcıoğlu-Turan, M.; Remondino, F. Evaluation of GIS and BIM roles for the information management of historical buildings. *ISPRS Ann. Photogramm. Remote Sens. Spat. Inf. Sci.* **2013**, *2*, 283–288. [CrossRef]
46. Hu, X.; Liu, X.; He, Z.; Zhang, J. *Batch Modeling of 3D City Based on ESRI Cityengine*; IET: Stevenage, UK, 2013.
47. Xu, X.; Ding, L.; Luo, H.; Ma, L. From building information modeling to city information modeling. *J. Inf. Technol. Constr. (ITcon)* **2014**, *19*, 292–307.
48. Kolbe, T.H.; Gröger, G.; Plümer, L. CityGML: Interoperable access to 3D city models. In *Geo-Information for Disaster Management*; Springer: New York, NY, USA, 2005; pp. 883–899.
49. Gröger, G.; Kolbe, T.H.; Nagel, C.; Hafele, K.H. *OpenGIS City Geography Markup Language (CityGML) Encoding Standard (OGC 12-019)*; Version 2.0. 0. OGC 12-019; Open Geospatial Consortium: Wayland, MA, USA, 2014.
50. Nouvel, R.; Zirak, M.; Dastageeri, H.; Coors, V.; Eicker, U. Urban energy analysis based on 3D city model for national scale applications. In Proceedings of the IBPSA Germany Conference, Aachen, Germany, 22–24 September 2014; Volume 8.
51. Monien, D.; Strzalka, A.; Koukofikis, A.; Coors, V.; Eicker, U. Comparison of building modelling assumptions and methods for urban scale heat demand forecasting. *Future Cities Environ.* **2017**, *3*, 2. [CrossRef]
52. Remmen, P.; Lauster, M.; Mans, M.; Osterhage, T.; Müller, D. CityGML Import and Export for Dynamic Building Performance Simulation in Modelica. In Proceedings of the Building Simulation and Optimization Conference (BSO16), Newcastle University, Newcastle upon Tyne, UK, 12–14 September 2016; pp. 329–336.
53. Hong, T.; Chen, Y.; Lee, S.H.; Piette, M.A. CityBES: A web-based platform to support city-scale building energy efficiency. *Urban Comput.* **2016**. [CrossRef]
54. Autodesk AutoCAD Software. Available online: https://www.autodesk.es/ (accessed on 30 October 2018).
55. Google Earth. Available online: https://www.google.com/earth/ (accessed on 30 October 2018).
56. Swan, L.G.; Ugursal, V.I. Modeling of end-use energy consumption in the residential sector: A review of modeling techniques. *Renew. Sustain. Energy Rev.* **2009**, *13*, 1819–1835. [CrossRef]
57. Crawley, D.B.; Hand, J.W.; Kummert, M.; Griffith, B.T. Contrasting the capabilities of building energy performance simulation programs. *Build. Environ.* **2008**, *43*, 661–673. [CrossRef]
58. Reinhart, C.F.; Davila, C.C. Urban building energy modeling–A review of a nascent field. *Build. Environ.* **2016**, *97*, 196–202. [CrossRef]
59. Birdsall, B.; Buhl, W.F.; Ellington, K.L.; Erdem, A.E.; Winkelmann, F.C. *Overview of the DOE-2 Building Energy Analysis Program, Version 2.1 D*; U.S. Department of Energy: Washington, DC, USA, 1990.
60. Huang, Y.J.; Brodrick, J. *A Bottom-up Engineering Estimate of the Aggregate Heating and Cooling Loads of the Entire US Building Stock*; Lawrence Berkeley National Laboratory: Guangdong, China, 2000.
61. Hirsch, J.J. eQuest, the QUick Energy Simulation Tool. 2006. Available online: http://www.doe2.com/equest (accessed on 30 October 2018).
62. Heiple, S.; Sailor, D.J. Using building energy simulation and geospatial modeling techniques to determine high resolution building sector energy consumption profiles. *Energy Build.* **2008**, *40*, 1426–1436. [CrossRef]
63. ESRU, O. *The ESP-r System for Building Energy Simulation: User Guide Version 10 Series*; University of Strathclyde: Glasgow, Scotland, 2003.
64. Swan, L.; Ugursal, V.I.; Beausoleil-Morrison, I. Implementation of a Canadian residential energy end-use model for assessing new technology impacts. In *Proceedings of Building Simulation, Glasgow*; Citeseer: Gaithersburg, MD, USA, 2009; pp. 1429–1436.
65. Matsuo, Y. HASP/ACLD/ACSS 8501. In *Tokyo: Japan Building Mechanics Engineers Association*; 1985.
66. Shimoda, Y.; Fujii, T.; Morikawa, T.; Mizuno, M. Development of residential energy end-use simulation model at city scale. In Proceedings of the Eighth International IBPSA Conference, Eindhoven, The Netherlands, 11–14 August 2003.
67. Yuan, J.; Farnham, C.; Emura, K.; Alam, M.A. Proposal for optimum combination of reflectivity and insulation thickness of building exterior walls for annual thermal load in Japan. *Build. Environ.* **2016**, *103*, 228–237. [CrossRef]
68. *NRCan HOT2000 V. 7.10 User's Manual for DOS and MacIntosh Computers*; 1995.

69. Guler, B.; Ugursal, V.I.; Fung, A.S.; Aydinalp-Koksal, M. Impact of energy efficiency upgrade retrofits on the residential energy consumption and Greenhouse Gas emissions in Canada. *Int. J. Environ. Technol. Manag.* **2008**, *9*, 434–444. [CrossRef]
70. Klein, S.A. TRNSYS-A transient system simulation program. In *University of Wisconsin-Madison, Engineering Experiment Station Report*; National Library of Australia: Canberra, Australia, 1988; pp. 12–38.
71. Salom, J. Study of the Residential Building Sector in the Plan for Energy Improvement of Barcelona. In *Proceedings EuroSun2002-Congress*; ISES-Europe: Bologna, Italy, 2002.
72. Perini, K.; Palme, M.; Salvati, A. UWG -TRNSYS Simulation Coupling for Urban Building Energy Modelling. 7. Available online: https://bura.brunel.ac.uk/bitstream/2438/16798/1/Fultext.pdf (accessed on 30 October 2018).
73. Fritzson, P.; Engelson, V. Modelica—A unified object-oriented language for system modeling and simulation. In *European Conference on Object-Oriented Programming*; Springer: New York, NY, USA, 1998; pp. 67–90.
74. Wetter, M.; Zuo, W.; Nouidui, T.S.; Pang, X. Modelica buildings library. *J. Build. Perform. Simul.* **2014**, *7*, 253–270. [CrossRef]
75. Lauster, M.; Teichmann, J.; Fuchs, M.; Streblow, R.; Mueller, D. Low order thermal network models for dynamic simulations of buildings on city district scale. *Build. Environ.* **2014**, *73*, 223–231. [CrossRef]
76. Baetens, R.; De Coninck, R.; Van Roy, J.; Verbruggen, B.; Driesen, J.; Helsen, L.; Saelens, D. Assessing electrical bottlenecks at feeder level for residential net zero-energy buildings by integrated system simulation. *Appl. Energy* **2012**, *96*, 74–83. [CrossRef]
77. Lacoste, B.; Wolf, A.; Witzig, A.; Märklin, A. Polysun: PV, Wind and Power-Heat-Cogeneration in one Design Tool. In Proceedings of the 5th European PV-Hybrid and Mini-Grid Conference by OTTI, Tarragona, Spain, 29–30 April 2010; pp. 29–30.
78. Bornatico, R.; Pfeiffer, M.; Witzig, A.; Guzzella, L. Optimal sizing of a solar thermal building installation using particle swarm optimization. *Energy* **2012**, *41*, 31–37. [CrossRef]
79. Kalamees, T. IDA ICE: The simulation tool for making the whole building energy and HAM analysis. *Annex* **2004**, *41*, 12–14.
80. Krüger, E.; Pearlmutter, D.; Rasia, F. Evaluating the impact of canyon geometry and orientation on cooling loads in a high-mass building in a hot dry environment. *Appl. Energy* **2010**, *87*, 2068–2078. [CrossRef]
81. Courchesne-Tardif, A.; Kummert, M.; Demark, S.; Butler, T.; Pearl, D.; Jones, S.; Charneux, R.; Genest, F.; Picard, D. Assessing community-scale energy supply scenarios using TRNSYS simulations. In *Proceedings of Building Simulation*; Citeseer: Gaithersburg, MD, USA, 2011.
82. Elsheikh, A.; Widl, E.; Pensky, P.; Dubisch, F.; Brychta, M.; Basciotti, D.; Müller, W. Modelica-enabled rapid prototyping via TRNSYS. In Proceedings of the 13th International Conference of the International Building Performance Simulation Association, Chambéry, France, 25–28 August 2013.
83. Nouidui, T.; Wetter, M.; Zuo, W. Functional mock-up unit for co-simulation import in EnergyPlus. *J. Build. Perform. Simul.* **2014**, *7*, 192–202. [CrossRef]
84. DOE OpenStudio Website. Available online: https://www.openstudio.net/ (accessed on 30 October 2018).
85. Guglielmetti, R.; Macumber, D.; Long, N. OpenStudio: An open source integrated analysis platform. In Proceedings of the 12th Conference of International Building Performance Simulation Association, Sydney, Australia, 14–16 November 2011.
86. R Core Team. *A Language and Environment for Statistical Computing*; R Foundation for Statistical Computing: Vienna, Austria, 2015.
87. Wiech, M.; Szczesny, W. Gradestat–Noncommercial statistical application using grade algorithms and methods to make synthesis of information. In *Information Systems in Management III*; 2009; p. 121.
88. Van Rossum, G.; Drake, F.L. *The Python Language Reference Manual*; Network Theory Ltd.: Eastbourne, UK, 2011; ISBN 1-906966-14-1.
89. Arnold, K.; Gosling, J.; Holmes, D. *The Java Programming Language*; Addison Wesley Professional: Boston, MA, USA, 2005; ISBN 0-321-34980-6.
90. Gajowniczek, K.; Nafkha, R.; Ząbkowski, T. Electricity peak demand classification with artificial neural networks. In Proceedings of the 2017 Federated Conference on Computer Science and Information Systems (FedCSIS), Prague, Czech Republic, 3–6 September 2017; pp. 307–315.

91. Ząbkowski, T.; Gajowniczek, K.; Szupiluk, R. Grade analysis for energy usage patterns segmentation based on smart meter data. In Proceedings of the 2015 IEEE 2nd International Conference on Cybernetics (CYBCONF), Gdynia, Poland, 24–26 June 2015; p. 234.
92. Monari, F.; Strachan, P. CALIBRO: An R package for the automatic calibration of building energy simulation models. In Proceedings of the Building Simulation 2017, San Francisco, CA, USA, 7–9 August 2017.
93. Best, R.E.; Flager, F.; Lepech, M.D. Modeling and optimization of building mix and energy supply technology for urban districts. *Appl. Energy* **2015**, *159*, 161–177. [CrossRef]
94. Keirstead, J.; Jennings, M.; Sivakumar, A. A review of urban energy system models: Approaches, challenges and opportunities. *Renew. Sustain. Energy Rev.* **2012**, *16*, 3847–3866. [CrossRef]
95. Connolly, D.; Lund, H.; Mathiesen, B.V.; Leahy, M. A review of computer tools for analysing the integration of renewable energy into various energy systems. *Appl. Energy* **2010**, *87*, 1059–1082. [CrossRef]
96. Gao, Y.; Meng, X.; Gao, W.; Long, E. A review of technologies and evaluation softwares for distributed energy source system. *Procedia-Soc. Behav. Sci.* **2016**, *216*, 398–408. [CrossRef]
97. Energypro. Available online: https://www.emd.dk/energypro/ (accessed on 30 October 2018).
98. Homer, N. *HOMER Computer Software, Version 2.68 Beta*; HOMER Energy LLC: Boulder, CO, USA, 2011.
99. Firestone, R. *Distributed Energy Resources Customer Adoption Model Technology Data*; Berkeley Lab: Berkeley, CA, USA, 2004.
100. Leng, G.J. RETScreen^{TM} international: A decHOMER Energy LLCision support and capacity building tool for assessing potential renewable energy projects. *Ind. Environ. Paris* **2000**, *23*, 22–23.
101. Lund, H. Energyplan-advanced energy systems analysis computer model. *Doc. Version* **2011**, *9*.
102. Olsthoorn, D.; Haghighat, F.; Mirzaei, P.A. Integration of storage and renewable energy into district heating systems: A review of modelling and optimization. *Sol. Energy* **2016**, *136*, 49–64. [CrossRef]
103. Gabrielaitienė, I. Numerical simulation of a district heating system with emphases on transient temperature behaviour. In Proceedings of the the 8th International Conference of Environmental Engineering, Ilnius, Lithuania, 19–20 May 2011.
104. Dalla Rosa, A.; Christensen, J.E. Low-energy district heating in energy-efficient building areas. *Energy* **2011**, *36*, 6890–6899. [CrossRef]
105. Termis District Energy Optimization Software. Available online: http://software.schneider-electric.com/products/termis/ (accessed on 30 October 2018).
106. NetSim Software. Available online: https://www.vitecsoftware.com/en/product-areas/energy/products/netsim-grid-simulation/ (accessed on 30 October 2018).
107. Silvennoinen, E.; Juslin, K.; Hänninen, M.; Tiihonen, O.; Kurki, J.; Porkholm, K. The APROS software for process simulation and model development. In *Technical Research Centre of Finland. Research Report*; 1989.
108. Fan, J.; Furbo, S.; Svendsen, S. *TRNSYS Simulation of the Consumer Unit for Low Energy District Heating Net*; Technical University of Denmark (DTU): Lyngby, Denmark, 2008.
109. Heymann, M.; Rühling, K.; Felsmann, C. Integration of Solar Thermal Systems into District Heating–DH system simulation. *Energy Procedia* **2017**, *116*, 394–402. [CrossRef]
110. Schafer, K.; Schlegel, F.; Pauschinger, T. Decentralized feed-in of solar heat into district heating networks–a technical analysis of realized plants. In Proceedings of the Book of Papers of the 2nd International Solar District Heating Conference, Hamburg, Germany, 3–4 June 2014; pp. 3–4.
111. López Villada, J. *Integración de Sistemas de Refrigeración Solar en Redes de Distrito de Frío y de Calor*; Universitat Rovira i Virgili: Tarragona, Spain, 2010; ISBN 84-693-9443-6.
112. Lozano, M.A.; Anastasia, A.; Palacín, F.; Serra, L.M. *Simulation Study and Economic Analysis of Large-Scale Solar Heating Plants in Spain*; EUROSUN: Graz, Austria, 2010.
113. Deschaintre, L. Development of a solar district heating online calculation tool. *Energy Procedia* **2014**, *48*, 1065–1075. [CrossRef]
114. Neplan Software. Available online: https://www.neplan.ch/ (accessed on 30 October 2018).
115. Hay, S.; Ferguson, A. *A Review of Power System Modelling Platforms and Capabilities*; The Institute of Engineering and Technology: Stevenage, UK, 2015.
116. DIgSILENT Power Factory Website, DIgSILENT GmbH. Available online: https://www.digsilent.de/en/powerfactory.html (accessed on 30 October 2018).
117. Henning, D. MODEST: Model for optimization of dynamic energy systems with time dependent components and boundary conditions. In *Interdisciplinary Energy System Methodology*; 2011; p. 44.

118. Zimmerman, R.D.; Murillo-Sánchez, C.E.; Thomas, R.J. MATPOWER: Steady-state operations, planning, and analysis tools for power systems research and education. *IEEE Trans. Power Syst.* **2011**, *26*, 12–19. [CrossRef]
119. PyPower Sotware. Available online: https://pypi.org/project/PYPOWER/ (accessed on 30 October 2018).
120. ETAP Website. Available online: http://etap.com/electrical-power-systemsoftware/etap-products.htm (accessed on 30 October 2018).
121. IPSA Website. Available online: http://www.ipsa-power.com/ (accessed on 30 October 2018).
122. Kotusevski, G.; Hawick, K.A. *A Review of Traffic Simulation Software*; Massey University: Wellington, New Zealand, 2009.
123. Mahmud, K.; Town, G.E. A review of computer tools for modeling electric vehicle energy requirements and their impact on power distribution networks. *Appl. Energy* **2016**, *172*, 337–359. [CrossRef]
124. CITILABS CUBE–Transportation & Land-Use Modeling Software. Available online: http://www.citilabs.com/software/cube/ (accessed on 30 October 2018).
125. Quadstone Paramics Software. Available online: http://www.paramics-online.com/index.php (accessed on 30 October 2018).
126. EMME Software. Available online: https://www.inrosoftware.com/en/products/emme/ (accessed on 30 October 2018).
127. Trafficware Software. Available online: http://www.trafficware.com/blog/category/simtraffic (accessed on 30 October 2018).
128. Aimsun Software. Available online: http://www.aimsun.com/site/ (accessed on 30 October 2018).
129. PTV Group Website. Available online: http://vision-traffic.ptvgroup.com/en-us/products/ptv-vissim/ (accessed on 30 October 2018).
130. MATSim Website. Available online: https://matsim.org/ (accessed on 30 October 2018).
131. Bergerson, J.; Muehleisen, R.T.; Rodda, W.B.; Auld, J.A.; Guzowski, L.B.; Ozik, J.; Collier, N. Designing future cities: LakeSIM integrated design tool for assessing short and long term impacts of urban scale conceptual designs. *ISOCARP Rev.* **2015**, *11*.
132. Auld, J.; Hope, M.; Ley, H.; Sokolov, V.; Xu, B.; Zhang, K. POLARIS: Agent-based modeling framework development and implementation for integrated travel demand and network and operations simulations. *Transp. Res. Part C Emerg. Technol.* **2016**, *64*, 101–116. [CrossRef]
133. Rakha, T.; Reinhart, C.F. A carbon impact simulation-based framework for land use planning and non-motorized travel behavior interactions. In Proceedings of the Building Simulation, Chambéry, France, 25–28 August 2013; pp. 25–28.
134. Keirstead, J.; Samsatli, N.; Shah, N. SynCity: An integrated tool kit for urban energy systems modelling. In *Energy Efficient Cities: Assessment Tools and Benchmarking Practices*; 2010; pp. 21–42.
135. GenOpt Website. Available online: https://simulationresearch.lbl.gov/GO/ (accessed on 30 October 2018).
136. Wetter, M. *GenOpt (R), Generic Optimization Program, User Manual, Version 2.0.0*; 2003.
137. Wetter, M.; Wright, J. A comparison of deterministic and probabilistic optimization algorithms for nonsmooth simulation-based optimization. *Build. Environ.* **2004**, *39*, 989–999. [CrossRef]
138. Nguyen, A.-T.; Reiter, S.; Rigo, P. A review on simulation-based optimization methods applied to building performance analysis. *Appl. Energy* **2014**, *113*, 1043–1058. [CrossRef]
139. Evins, R. A review of computational optimisation methods applied to sustainable building design. *Renew. Sustain. Energy Rev.* **2013**, *22*, 230–245. [CrossRef]
140. Christensen, C.; Anderson, R.; Horowitz, S.; Courtney, A.; Spencer, J. BEoptTM Software for Building Energy Optimization: Features and Capabilities. In *National Renewable Energy Laboratory (NREL) Technical Report*; 2006.
141. Burdjalov, D.; Daukoru, S.M.; Duer, A. Assessing Aggregated Impacts of Distributed Energy Resources (DERs): A Building Stock Model Approach.
142. Kämpf, J.H.; Robinson, D. Optimisation of building form for solar energy utilisation using constrained evolutionary algorithms. *Energy Build.* **2010**, *42*, 807–814. [CrossRef]
143. Kämpf, J.H. On the modelling and optimisation of urban energy fluxes. **2009**. [CrossRef]
144. Rutten, D. *Evolutionary Principles Applied to Problem Solving Using Galapagos*; AAG10: Vienna, Austria, 2010.
145. Walkscore Website. Available online: http://www.walkscore.com (accessed on 30 October 2018).

146. Bazmi, A.A.; Zahedi, G. Sustainable energy systems: Role of optimization modeling techniques in power generation and supply—A review. *Renew. Sustain. Energy Rev.* **2011**, *15*, 3480–3500. [CrossRef]
147. Fazlollahi, S.; Becker, G.; Maréchal, F. Multi-objectives, multi-period optimization of district energy systems: III. Distribution networks. *Comput. Chem. Eng.* **2014**, *66*, 82–97. [CrossRef]
148. MARKAL/TIMES Website. Available online: https://www.energyplan.eu/othertools/national/markaltimes/ (accessed on 30 October 2018).

energies

MDPI

Review

A Review of Heat Pump Systems and Applications in Cold Climates: Evidence from Lithuania

Rokas Valancius [1,*], Rao Martand Singh [2], Andrius Jurelionis [1] and Juozas Vaiciunas [1]

[1] Faculty of Civil Engineering and Architecture, Kaunas University of Technology, Studentų str. 48, LT-51367 Kaunas, Lithuania; andrius.jurelionis@ktu.lt (A.J.); juozas.vaiciunas@ktu.lt (J.V.)

[2] Department of Civil and Environmental Engineering, University of Surrey, Thomas Telford Building, Guildford GU2 7XH, Surrey, UK; r.singh@surrey.ac.uk

* Correspondence: rokas.valancius@ktu.lt

Received: 3 October 2019; Accepted: 8 November 2019; Published: 13 November 2019

Abstract: Similar to other cold climate countries, space heating and domestic hot water (DHW) accounts form the largest share of household energy demand in Lithuania. Heat pump technology is considered to be one of the environmentally friendly solutions to increase energy efficiency and reduce the carbon footprint of buildings. Heat pumps have been finding their way into the Lithuanian market since 2002, and currently there are many good practice examples present in the country, especially in the residential and public sectors. Heat pump use is economically advantageous in the Baltic Region, and the market share of these systems is growing. Studies have reported seasonal performance factor (SPF) ranges within 1.8 and 5.6. The lower SPF values are typically attributable to air source heat pumps, whereas the higher efficiency is achieved by ground or water source heat pump applications. While the traditional heat pump techniques are well established in the region, there is a slow uptake of new technologies, such as solar-assisted heat pumps, absorption heat pumps and heat pumps integrated into foundations, tunnels or diaphragm walls. This paper provides a critical review of different heat pump technologies, using Lithuania as a cold climate case study to overview the market trends within the European context. Potential trends for the heat pump technology development in terms of application areas, cost-benefit predictions, as well as environmental aspects, are discussed.

Keywords: space heating; domestic hot water (DHW); air, ground and water source heat pump (ASHP, GSHP and WSHP); coefficient of performance (COP); seasonal performance factor (SPF); energy pile; energy tunnel

1. Introduction

The building sector accounts for 40% of the final energy consumption and 36% of carbon dioxide (CO_2) emissions in Lithuania and other European Union (EU) countries [1]. About 26% of all final energy consumption in the EU is needed for space heating and DHW [2]. In recent years, the European Commission (EC) has set a new target of reducing carbon dioxide emissions by 90% for the building sector by the year 2050 [3]. As reported in the 2014/15 European work program, more than 17% of the primary energy savings potential of the EU for 2050 [4] is related to the building retrofit.

The Heat Pump (HP) is an environmentally friendly and renewable energy technology that exploits renewable heat energy from the ground, air or water for building or industrial applications by reversing the natural heat flow from a lower to a higher useful temperature [5]. In an electrically-powered HP, the amount of transferred heat can be three or four times larger than the electrical power consumed, resulting in a coefficient of performance (COP) value of 3 to 4. The seasonal coefficient of performance (SCOP) describes the average COP during a heating season.

Alongside the COP and SCOP, another important parameter should also be considered when describing the energy performance of HPs, namely their seasonal performance factor (SPF). This SPF is

the 'net seasonal coefficient of performance in active mode' defined as the ratio between annual usable energy provided by the HP and the annual energy supplied to the whole heating and/or DHW system under real operating conditions [6].

As reported by Zimny et al. [7], the theoretical understanding of the HP system allows the construction of the first device in the second half of the nineteenth century; however, industrial-scale applications were only introduced after World War I. At this time electric drivers for compressors became a standard, making smaller-sized devices possible.

In 1945, John Sumner, the City Electrical Engineer for Norwich, installed an experimental water-source HP (WSHP). It fed the central heating system, using a nearby river to heat new Council administrative buildings [8]. It demonstrated a seasonal coefficient of performance (SPF) of 3.42 and average thermal delivery of 147 kW, as well as a peak output of 234 kW. Despite the efficiency and effectiveness of the system, it was not widely accepted in the UK because of the relative availability of low-cost fossil fuels, such as coal at the time, and later North Sea oil and gas.

The new technology was widely adopted in Switzerland due to the shortage of fossil fuels. One HP of a 100 kW output was installed in the Zurich City Hall in 1938, and 35 HP devices were installed in Switzerland between 1938 and 1945 [9]. The development of HP technologies decreased due to the drop in fossil fuel prices after the World War II, demonstrating further growth only after the oil crises in 1973 and 1979 [10,11]. Within the next two decades, several countries launched programs supporting research on HP technologies, national HP associations were created, quality guidelines and certification protocols of products were developed, leading to more technologically mature products appearing in the market.

The European Heat Pump Association (EHPA) in 2018 reported that the European HP sales grew by more than 10% for the third year in a row in 2017. After 1.1 million HP units sold in Europe in 2017, the total number of units in the continent reached 10.6 million within 20 years, with a 5% total share of installed capacity in the building market. Contribution from these installations led to the reduction of carbon emissions by 29.8 Mt, while generating 116 TWh of energy. This in turn accounted for 148 TWh of energy saved, while creating a total of 54,000 full-time equivalent jobs in Europe. France, Italy and Spain are the leaders in Europe's HP markets, with a 50% share of total units sold. The top 10 countries, including Sweden, Germany, Norway, Finland, Denmark, Switzerland and Austria as well, sell 90% of all units. In terms of market penetration, Norway, Estonia and Finland are the leaders of sales on a per capita basis [12].

The first Lithuanian study on HP was presented at the end of the twentieth century when A. Zukauskas [13] reported the monograph entitled "Energy transfer process in heat pumps". That was the beginning of HP research in Lithuania. At the beginning of this twenty-first century, a series of different studies were conducted [5,14–22], mainly due to the price increase of energy produced in conventional ways (i.e., district heating, solid fuels and natural gas). These studies were focused on the potential energy savings and environmental aspects of HPs.

In Lithuania the HP market emerged only in 2002 and its popularity has been constantly increasing. However, the market was still limited at the time, and it did not grow significantly until 2013, when due to other factors resulting from the global financial crisis of 2007–08, the HP market recorded substantial growth. Financial confidence of households has led to increased acquisition of relatively more expensive and yet easier to maintain systems. Growing housing completions also helped the market to boost the usage of HPs. Price decrease and stimulating economic factors pushed up the market growth [5,23].

According to the study published in 2016 [5], the majority of end-users were affluent, and the obtaining of HPs was an issue of status and comfort. Approximately one-third of HPs sold in 2013 were installed into new buildings, which constitutes to approximately 4% of all new heating systems installations. The new housing segment share decreased moderately compared to the previous decade. HPs nowadays are technologically well-developed and therefore popular between consumers. The technology has found its way to industrial and transport applications as well [7].

The aim of this paper is to provide a critical review of HP technologies in buildings, using Lithuania as a cold climate case study, to outline the factors hindering HP market growth, as well as provide insights on the new technologies unlocking new potential uses for HP technology.

In Section 2 we discuss the main characteristics of HPs. In Section 3 we provide an overview of the climatic, technical and legal aspects of the HP market in Lithuania, as well as introduce detailed case studies on several HP installations. In Section 4 we discuss performance and application issues with regard to the heat source, looking into ASHPs, GSHPs and WSHPs. Future trends for HP technology development and applications are discussed in Section 5, and the conclusions are provided in Section 6.

2. Classification, Operating Principles and Performance Efficiency of HPs

HP technology is commonly classified according to its source, function, type of energy and application as described below:

- heat source: air, ground, water, solar heat, waste water etc.
- function: cooling, heating, cooling and heating, DHW heating etc.
- type of energy supplied to a HP: electric, mechanical, thermally driven (natural gas, propane, solar heated water, geothermal heated water etc.).
- application: residential, commercial, industrial, district heating etc.

The operation principle of the HP is shown in Figure 1. Energy transfer in the HP is based on the phase change of refrigerant under the constant thermodynamic cycle. The heat is extracted from the source and transferred to the building energy systems. Reverse cycle HPs have a cooling ability as well, by changing the flow direction of the refrigerant, resulting in heat extraction from the building and rejection to the outside source [24,25].

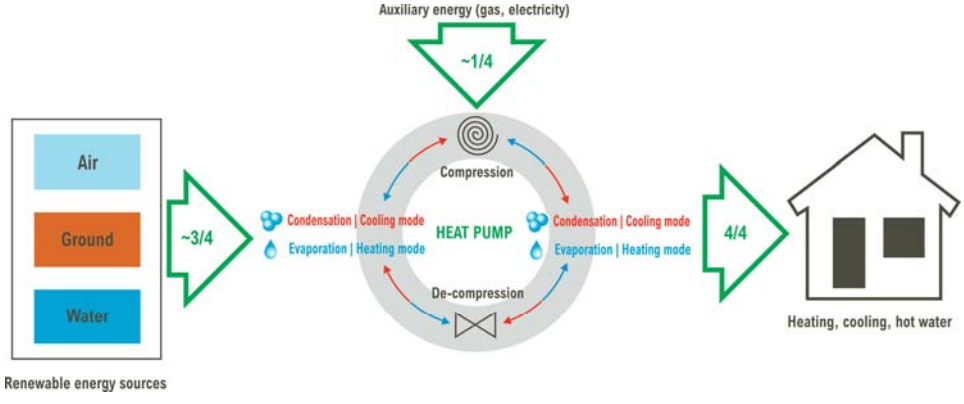

Figure 1. Operation principle of the HP in heating (clockwise/red) or cooling (counter clockwise/blue) mode.

Four main components incorporated within the HP are: the compressor, an expansion valve and two heat exchangers for evaporation and condensation (Figure 1). The main auxiliary components are fans, piping, controls and housing. HP for heating purposes operates as per the following steps:

1. In the evaporator, the liquid refrigerant extracts heat from a heat source and evaporates. After the evaporator refrigerant is in the state of low-pressure vapor, then the temperature increases slightly.
2. The refrigerant in vapor state flows into the electrical compressor; here the pressure is increased, resulting in the increase of the temperature.
3. High temperature vapor flows to the condenser. The heat transfer to the building's heating system causes the refrigerant to cool down and condensate to high pressure and temperature liquid.

4. Hot liquid runs through an expansion valve, where its pressure is reduced, in turn lowering the temperature. The refrigerant returns to the evaporator and the cycle is repeated.

Desuperheaters are included in some HPs performing as an auxiliary heat exchanger supplying heat to a DHW tank (up to 65–70 °C). The desuperheater is placed at the compressor's exit; it transfers thermal energy of compressed vapor to water that circulates through a hot water tank, therefore reducing or eliminating the energy required for DHW heating [25].

The most common type of HP classification is according to the heat source. In general, there are three principal types of HPs based on heat source: an air source heat pump (ASHP), ground source heat pump (GSHP) and the water source heat pump (WSHP), and they are described in the following sections.

The other heat sources are worth mentioning too: waste water, industrial waste heat, geothermal water flue gas, district cooling or solar heat. These HP technologies are very promising, but still have limited use.

2.1. Air Source Heat Pump (ASHP)

Air Source Heat Pump (ASHPs) use the ambient air as a heat source. ASHPs (air to air or air to water) utilizing ambient heat are less efficient compared to other types of HPs, when the outside air temperature is lower than −10 °C. They can also be noisy according to the study [26] performed in Sweden, reporting the average sound level of tested ASHP outdoor units of 61 dB. However, the performance of the ASHP has improved significantly in recent years. Due to better performance of compressors, heat exchangers and refrigerants, modern ASHPs can operate at outside air temperatures as low as −15 °C to −30 °C, subject to the manufacturer and region of distribution. These features, alongside the lower investments and easier installation, made ASHPs more cost-effective in recent years. These units are widely used in residential houses in Scandinavian countries [27–30]. In recent years this is also reflected in the sales of HPs in Lithuania [5,12].

However, as reported in [31], in the Finnish cold climate, typical SPF values of ASHP were: 1.8–2.2 for air to air HPs. The study in Canada [25] showed that equivalent COPs of ASHPs for various heating systems are 2.3–3.5. The analysis of ASHP system in the single family building in Latvia showed that the system can reach an SPF of 3.43, with a lowest COP of 2.6 during the coldest month of January [32]. The other case studies in Latvia [33] showed that the SPF of an ASHP varies from 2.45 to 2.62 for average outside air temperatures, respectively, within +2.4 °C and +6.0 °C. These studies suggest that during the cold months ASHPs can operate with an average SPF from 2.93 to 3.2 in a cold climate.

The current level of technical development of ASHP units still suggests these HPs are to be used as a supportive heating source in cold climates. In most cases, ASHP-based systems must be equipped with an additional electric heater or other source of energy to be utilized during the coldest periods of winter.

2.2. Ground Source Heat Pump (GSHP)

The Ground Source Heat Pump (GSHP) uses the ground as a heat source; therefore it consists of heat exchanging loops installed in a horizontal, vertical or oblique fashion. A much lower variation of the source temperature on a daily basis throughout the year is common for GSHP installations compared to the ambient air installations [34]. The threshold depth of relatively stable ground temperature is considered 0.8 m [35], yet it depends on such factors as solar radiation patterns, air temperature variations, average snow cover, precipitation and the thermal properties of the soil [25]. It has been also reported that ground temperature variations are more pronounced on a seasonal basis rather than on a daily basis [36]. When the range between inside and outside temperatures is large, as is the case for the ASHP, more energy is required to provide the same amount of heat, which reduces the COP [37]. Operation of GSHPs are usually less affected by excessive temperature differences.

The studies in Finland and Canada showed that typical SPF values for GSHP are 2.6–3.6, while the equivalent COP of GSHP for various heating systems can vary between 3 and 5 in cold climates [25,31].

Higher installation cost of GSHP due to drilling compared to ASHP in most cases is compensated by higher performance. However, the cost also depends upon soil properties, and because Lithuania has mainly soft soils, this results in affordable drilling [5].

2.3. Water Source Heat Pump (WSHP)

A typical WSHP uses water as a heat source brought directly to the HP unit. If there is no barrier between the water heat source (ground water or surface water body) and the evaporator of the HP, the term "open-loop" is applied for this type of HP.

Several factors need to be considered in open-loop installations, and water quality is one of the most important ones. It affects the operation of the heat exchanger between the refrigerant and groundwater, and may lead to its fouling, corrosion and blockage. The second important factor is the adequacy of available water volume and flow rate. The required flow rate through the primary heat exchanger between the refrigerant and groundwater is usually within 5.5 and 11 l/min per system cooling ton (0.027 and 0.054 L/s-kW) [38]. The demand of water amount can be significant, and it can be regulated by local water resource regulations. The third important factor is handling of the discharged water. There are two options: The groundwater can be re-injected into the ground through separate wells, or it can be discharged into the surface water basins, i.e., rivers, lakes, etc. The feasibility of open-loop systems depends on the local codes and regulations [39].

The main advantage of WSHP in comparison to GSHP is lower installation costs. Also, it has better thermodynamic performance than closed-loop systems because of wells that supply groundwater at ground temperature and the heat exchanger delivers heat-transfer liquid at temperatures other than ground temperature. Also, the system can be combined with a potable water supply well, in turn decreasing operating costs if water was already pumped for other purposes, such as irrigation [39].

The study in Romania [40] showed that the average COP of WSHPs is similar to that of the GSHPs, reaching up to 4.

3. HPs Technology in Lithuania

Lithuania is situated in a colder climate zone where the use of HPs is mainly for heating and DHW, with a limited cooling application. Because of low traditional energy prices and a well-developed district heating network, the HPs were mainly adopted on the Lithuanian market only at the beginning of this century, and then they demonstrated slow growth in the number of installations.

3.1. Climatic Conditions in Lithuania

The Lithuanian climate is considered typical of the central and Nordic European continental climate. Summers are warm and dry, while winters are cold and sometimes severe. The coldest month is January; its daytime temperatures are usually around −5 °C, but for shorter periods air temperatures can be around −20 °C. Heavy snowfall or even snowstorms are usually expected. Because of the proximity to the Baltic Sea, weather is windy, cold and humid. Air temperature in summer during the day reaches 20–25 °C and can go over 30 °C for a period of a few days or weeks. The warmest month of the year is July, with its average temperature of 20 °C.

On the other hand, climate change is evident, and winters in Lithuania are getting warmer with only a few days or weeks of snowfall within the past decade. However, according to the study published by Nikulin et al. [41], in the future, climate change will result in more frequent strong winter frosts, while the day temperature range is expected to splay out.

According to Lithuanian building codes, climatic data for the heating, ventilation, and air conditioning (HVAC) design has not changed since the 1990s [42]. The average temperatures in Kaunas City, located in central Lithuania, and the average groundwater temperature, are presented in Figure 2. These temperatures are representative of the average temperature of the whole of Lithuania.

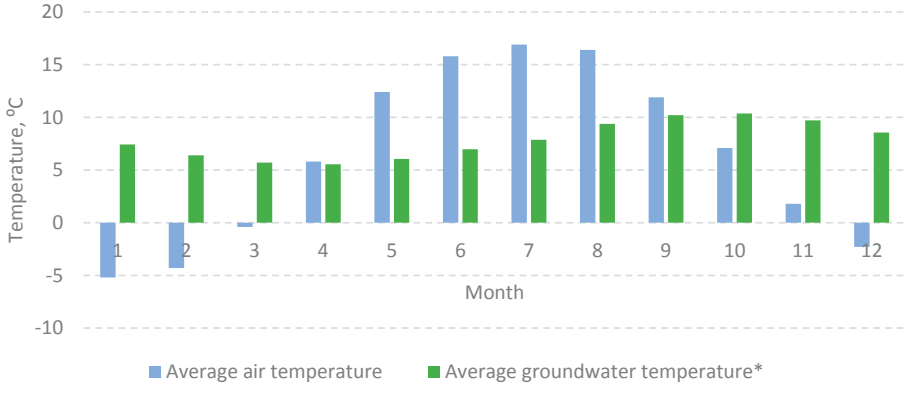

Figure 2. Average air temperature (1961–1990) in Kaunas City, Lithuania [RSN 156-94] and average groundwater temperature (2005–2015) near Zuvintas Lake at the depth of 1.26 m. (data from the Lithuania geological survey under the Ministry of the Environment).

3.2. HP Related Environmental, Technical and Legal Aspects of Lithuanian Market

The biggest part of the building stock in Lithuania was built in the second part of the twentieth century. About 60% of the Lithuanian population resides in multi-apartment buildings constructed during 1961–1990. About 40% of people live in one or two-family buildings. Only about 0.2% buildings are non-residential. Compared to the other EU countries with similar climate conditions, energy consumption for residential heating is approximately 1.8 times higher in Lithuania [43]. Many thousands of twentieth century buildings need renovation for better energy efficiency.

The district heating network in Lithuania covers more than 55% of the total thermal market, and the average price is 0.048 €/kWh, excluding 9% VAT (1 September 2019). In recent years, the district heating energy price dropped by about 12% [44]. Switching from natural gas to bio fuel reduced the district heating energy price significantly in the last five years. Due to a dramatic decline in oil and natural gas prices, conventional fuel prices decreased by up to 35% in the last five years as well. About 25% of thermal energy in Lithuania is produced by burning bio fuels, followed by natural gas and oil, with the share of 12% and 5%, respectively. Electrical heating is rarely used as a main source for space heating.

In 2019 natural gas prices in Lithuania varied from 0.37 to 0.55 €/m^3 excluding 21% VAT, depending on consumption per calendar year. Electricity prices varied from 0.072 to 0.122 €/kWh, excluding 21% VAT, depending on a selected tariff [45]. Despite a small fluctuation in recent years, evidence shows that conventional energy prices are on a growing curve at the moment.

According to Lithuanian legislation it is recommended to start the heating season after three consecutive days with an average outdoor air temperature below +10 °C. At present, the heating season starts by October the fifteenth and ends by April the fifteenth. During this period, the average outdoor air temperature is approx. 0 °C [46]. Indoor air temperature for residential and public buildings should be within +18 to +22 °C.

The survey performed in 2016 showed that major Lithuanian cities and two thirds of the population use district heating, while 18% are using gas heating and 15% has solid fuel-based systems, wood logs and charcoal [47]. Other heat sources such as electricity, geothermal heating or pellet burning were indicated by a very small proportion of the population.

According to the results of the survey, the choice of the heating method is influenced by the price, availability and convenience. Accordingly, the priority for these heating criteria, heating and availability, was provided by 42% and 39% of respondents during the survey. The comfort was especially emphasized by those residents whose home was heated by natural gas (44%), but the price was also a very important factor for them (38%) [47].

Costs of heating and other energy needs for buildings are of the most important factors that influence the renewable energy market. It is evident that in most cases the growth of these markets depends upon subsidies. In Lithuania, limited subsidy systems and funds for renewable energy installations existed since 2005. Depending on a project, it is possible to apply for a subsidy covering from 40% to 100% of initial costs. For example, it is possible to get a subsidy up to 50% for a single family building, up to 40% for a multifamily building and up to 100% for hospitals.

About 8938 units of different HPs were sold in 2017 in Lithuania [12], a country with a population of three million. It shows that HPs have become the most popular choice within newly constructed, single-family residential buildings and their owners. Current trends indicate that HPs are also slowly replacing gas and solid fuel boilers, as well as district heating in existing buildings. Compared to previous years the sales of HPs in 2017 increased significantly. This growth can be attributed to increased efficiency and reduced capital expenses for ASHP installations. On the other hand, the price reduction of solar photovoltaic systems and new storage technologies helped to grow, not only installations of solar photovoltaic systems, but HPs as well.

According to the study from 2016 [5] it is anticipated that the market of the HP will be consistent in Lithuania until 2020, and within the next five years the adoption rate will remain steady. This is the result of the increasing popularity of HP technology and its competitive life-cycle costs.

A new Lithuanian HP and ventilation association with 20 members has been founded at the beginning of 2017, striving to promote the technical and economic progress of the Lithuanian HP industry. One of the main tasks of the newly established association is to develop and promote a fair and favorable public opinion about HPs, and to raise awareness about the environmental benefits of these systems.

3.3. Case Studies—Representative Implementation of HPs in Lithuania

Despite the HP market in Lithuania appeared only at the beginning of this century, it is growing slowly, and some studies and good practice examples are presented in the following sections.

3.3.1. Small Capacity Single-Family Building HP Installations

In last decade some studies of HPs in single family buildings in Lithuania were presented. A case study by Jonynas et al. [16] presented an SPF for a real GSHP system. This GSHP system was designed and installed in 2006 for an individual house of 180 m^2 with a low temperature underfloor heating system and DHW preparation (Figure 3). The investment in the 11 kW GSHP was 15,292 € in 2006. The main purpose of the research study was to explore the seasonal SPF of GSHP. Manufacturer and installer documented COP for the equipment to be 4.5 or even higher. The results of 20-month analysis showed that the SPF has reached 3.02 only and the price of heat energy was 0.031 €/kWh in 2009. In this case there was no economic benefit to use GSHP compared to conventional heating systems.

It is evident that the analyzed GSHP system was not a good design, probably the main problem was the insufficient horizontal ground collector system. On the other hand, this GSHP is still in operation with the 10 years SPF of 2.47 with no significant maintenance expenditure during the last decade (see Figure 3).

A study performed by Zekas and Martinaitis [17] reported the use of a GSHP of 15.9 kW capacity in an individual house of 175 m^2 with a low temperature underfloor heating system and DHW supply. The study showed that prevailing COP was from 3.7 to 3.9 which was reached during various characteristic periods of the heating season. In this case the higher efficiency of GSHP was reached due to some important energy needs being excluded, namely energy for DHW, circulation pumps, control equipment, as well as heat losses of the DHW storage tank.

Aleksandravicius and Zinevicius [18] presented a comparison of an HP and gas boiler heating system with investments of 9372 € for the 13.0 kW GSHP and 1100 € for the gas boiler heating system. The systems were analyzed for the heating purposes of a single-family house of 175 m^2. The calculations were carried out using the prices of the natural gas, electricity and equipment of the

year 2012. Results showed that the operation cost of the HP system was 495 €/year and that of the gas boiler system was 3735 €/year. The SPF over the heating season (from October 2007 to April 2008) was 3.95. The study reported that in the short run the gas boiler system looked more financially attractive, but in the long run (10 years) it will be 2.6 times more expensive.

Figure 3. A Ground Source Heat Pump (GSHP) system in a single-family building.

It can be observed that in this study the investments of GSHP were 37% lower than it was presented by other researches [16,17] and the calculation method of SPF was not reported.

In 2015 one study [19] of a 7.4 kW variable-speed low temperature ASHP showed that for the heating mode the COP varied from 1.98 to 3.05 as the outdoor temperature changed from −7.0 °C to +5.0 °C. In this case, at the end of the heating season (heating season was assumed to begin on October 1st and end on May 21st) the total electricity consumption turned out to be 1737 kWh and the total heating output was 5927 kWh, leading to an SPF of 3.41 without taking frosting into account. Consideration of frosting in a simulation model was proven to be significant, resulting in the SPF decrease to 2.86.

A study in 2016 [47] of different heating systems for a B-class energy performance single family building of 150 m^2 with four inhabitants and with total energy needs for heating and DHW of 20 MWh, showed that solid fuel is still the cheapest way to heat the building in Lithuania. As expected, comparison of capital expenses for solid fuel, natural gas, pellet burning system installations and HP systems was unfavorable to HPs. Nevertheless, HPs outperform conventional systems from the perspective of 10 years' operating expenses, equal to 0.034 €/kWh. The study in 2018 of seven different heating systems for an A-class energy performance single-family building of 150 m^2 with total energy needs for heating and DHW of 15 MWh showed almost the same results [48].

3.3.2. Multifamily and Public Building Installations

Some analyses and good practice examples of HP systems in multifamily buildings and public buildings in recent years are presented here.

In 2011 the analysis of ASHP usage in an Alytus City multifamily building was presented [20]. It showed that compared to district heating prices, the use of ASHP for heating needs in apartment buildings is not economically viable. Without the full building retrofit, in the analyzed case ASHP could save from 7 to 9% of heating cost per multifamily building per year, depending on the interest rate on the loan. In spite of their technical development in most cases, ASHP can be used only as a supportive

heating source in Lithuania for a standard but not renovated multifamily building. However, in recent years a series of different ASHPs and even GSHPs were installed in renovated multifamily buildings.

A case study of GSHP installation for heating and cooling purposes in the building of logistics center was presented in 2015 [21]. A new approach was applied to the construction of the logistic center with the underfloor heating area of 5200 m^2 and a total building volume of 42,000 m^3. A shallow geothermal plant consisted of two HP units (total capacity of 134 kW), using 16 boreholes of 150 m depth with "U-type" heat exchanging loops. Fan coils were applied for cooling for the office part of the building. Total investment was 251,000 €. The commitment to the customer was that the heating and cooling expenses shall not exceed 10,000 €/year at an electricity price of 0.13 €/kWh.

The heating season of 2013/2014 was relatively warm and was characterized by 3200 degree-days instead of the average annual value of 3870. Heating in the logistics center started in October 2013, before the finalizing of the construction work. The temperatures in the office and warehouse spaces were set at 21 °C and 18.5 °C, respectively. The supply water temperature of the heating system in the office did not exceed 30 °C, and 28 °C in the stock. Stable indoor temperatures were maintained, according to the normal heating curve algorithm, additionally adjusting the temperature in every room by thermostatic valves of the floor heating system. The average temperature of water-glycol in the shallow geothermal loop was at least 4 °C. The HP system was automatically shut down at an average three days outdoor temperature of 14 °C.

Energy performance of the building during the heating season was evaluated by the set of energy meters. It showed that the production of thermal energy by HPs was 178.8 MWh, consumption of electricity by HPs was 29.5 MWh, resulting in a COP value of 6.06, excluding the energy used by the circulation pump. Considering the energy for circulators, the SPF of one heating season was 5.57. Total heating expenses for space heating was 4170 € for the whole heating season.

Seventeen projects with ASHP systems (from 15 to 90 kW) and solar thermal systems (from 20 to 210 m^2) were implemented in Lithuanian hospital buildings by using Swiss and Lithuanian state funding in 2016. Most of these systems were designed only for DHW applications. All of these systems were fully automated with solar thermal systems used as the primary energy source, and HPs in operation as a supportive system (Figure 4).

Analysis of three different systems in 2018 showed that the SPF of HPs varies from 2.42 to 2.61, due to the requirements of the high temperature of DHW (50–60 °C) [49]. Systems for DHW and swimming pool heating were the most efficient (SPF-2.61). However, in the analyzed cases HPs operate only up to the outdoor temperature of −10 °C. When the temperature is lower than −10 °C it is more efficient to use district heating or gas boiler energy.

The sanatorium Grand SPA Lithuania in Druskininkai City has the biggest installation of an HP system in the Baltic region. The project was funded using local and EU funds. The total heated area of this sanatorium complex is 20,000 m^2. HPs (1300 kW) and the passive cooling system have been installed in the facility. The system's purpose is heating, DHW, the preparation of hot mineral water and the heating of swimming pool water. Heating and cooling demand is satisfied by the combination of ASHP and brine/water HPs, that efficiently recover the energy of wastewater, exhaust air and geothermal energy (boreholes).

The systems implemented in the complex have the following features: brine/water HP with a total nominal power of 1014 kW; the field of geothermal bores (the total depth of 8320 m); natural cooling system using ground (the total capacity of 539 kW); DHW heating system; hot mineral water (up to 80 m^3 of hot water per day) and mud technology heat preparation systems; ASHP with a total nominal power of 264 kW (the exhaust air heat from recuperative ventilation system was used); and heat recovery from complex waste water system (power up to 400 kW) [5].

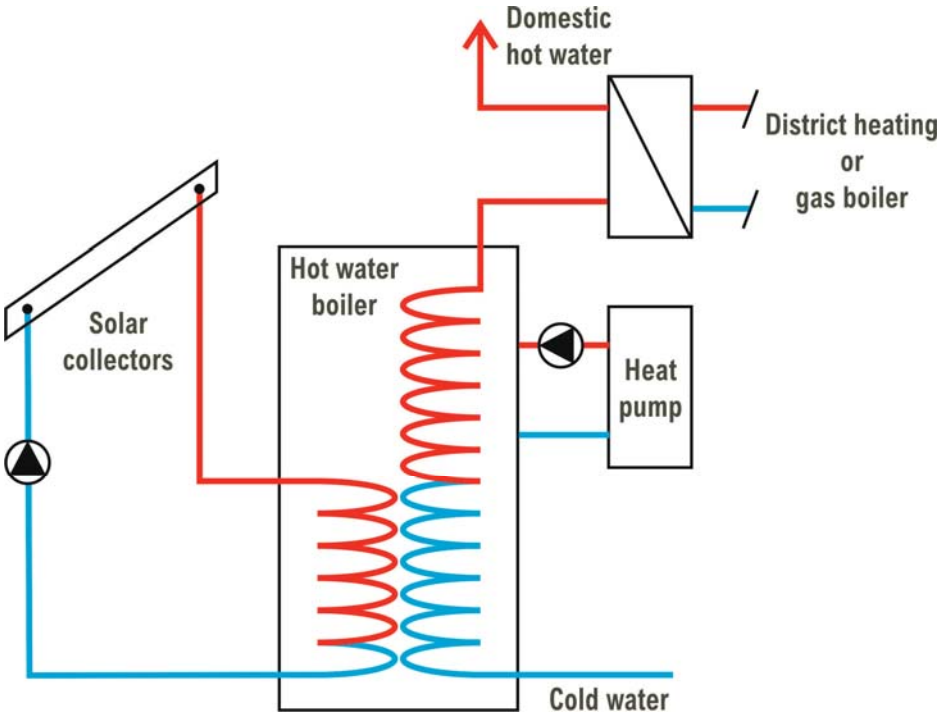

Figure 4. Principle scheme of combined Air Source Heat Pump (ASHP) and solar thermal system in the case study Lithuanian hospitals.

The complex still has a possibility to use heating from a district heating network in the case of very low outdoor temperature or lower price compared to the HP system. HPs are covering more than 80% of the heating demand and 100% of the cooling demand, with a passive cooling capacity of approx. 500 kW.

Recently to the many small or medium size projects some new big HP projects in Lithuania were launched in 2018, including a possibility study for HP usage for district heating in Panevezys City. The aim of this study was to reduce the district heating production price. Two cases were analyzed: usage of return energy for HP and usage of wastewater energy for HP. Another 1 MW waste water HP project is going to be implemented in the company "Rokiskio Suris" by using company and EU funds for cheese production technology with an expected COP of more than 4.

4. Comparison of ASHP, GSHP and WSHP

The advantages and disadvantages of ASHP, GSHP and WSHP are presented in Table 1. The SPF spread is large because of different equipment, design and installation quality, as well as maintenance. In general, ASHP requires lower installation cost and less space for installation. For example, horizontal GSHP requires a lot of space, since the pipes are spread out over a large surface area. Depending on soil and drilling depth, vertical boreholes typically cost in Lithuania between 20 to 35 EUR per meter depth. On the other hand, the installation cost of WSHP can be even lower than ASHP if the water source is suitable and near the heat sink.

One of the biggest disadvantages beside lower efficiency at low outdoor temperatures of ASHP is the loud noise caused. GSHP and WSHP have lower running cost compared with ASHP. In most

cases GSHP and WSHP characterize as longer lifespan (up to 50 years) of outdoor components than an ASHP.

Table 1. Comparison of Air Source Heat Pump (ASHP), Ground Source Heat Pump (GSHP) and Water Source Heat Pump (WSHP).

Item	ASHP	GSHP and WSHP
SPF	1.8–3.4	2.5–5.6
Lower installation cost	Yes	No
Requires less space for installation	Yes	No
Better efficiency at low outdoor temperatures	No	Yes
Less noise	No	Yes
Lower running cost	No	Yes
Longer lifespan	No	Yes

5. Future Trends for HPs Usage

While the traditional ASHP, GSHP and WSHP techniques are well established, continuing research and development is focused on reducing installation costs, i.e., speed/ease of installation, solar heat HP, waste water HP, absorption/adsorption HP, combined photovoltaic and HP system efficiency, large-scale district cooling as well as foundations, diaphragm walls and a tunnel lining use for HP.

A study by David et al. [50] in 2017 presented a review and roadmap of large-scale HP in district heating systems. The review found 149 units, operating at almost 80 locations in 11 European countries with an output capacity of 1580 MW. Approximately 1000 MW of the large-scale HP build in Sweden the 1980s were still operational. These HP could supply temperatures over 70 °C or even 90 °C, while still achieving a COP over 3. This comprehensive study demonstrates that the technical level of the existing large-scale HP is mature enough to make them suitable for replication in other countries such as Lithuania, where district heating networks are well developed.

Very promising technology and a new type of HP for residential systems is absorption/adsorption HP. These HPs use heat as their energy source and can be driven with a wide variant of heat sources, such as natural gas, propane, solar heat or geothermally-heated water.

A review of absorption heating technologies [51] showed that they are becoming more and more important in energy conservation and emissions reduction. Large scale application has adopted absorption HPs relativity early, but civil applications developed less rapidly because of dependence on traditional heating systems and the popularity of electric-driven HPs. Significant work is still required before absorption heating systems are widely adopted.

A review by Saha et al. [52] showed that adsorption HP systems are considered as a promising alternative to the mechanical systems. The environmental benefits of these thermally-driven HP are impressive. Difficulties in improving its performance are overcome day by day with the development of innovative adsorbents and system design.

Building foundations, diaphragm walls and tunnels have potential for the incorporation of a geothermal HP system into a structure. A construction of a building's foundation requires excavation and/or drilling. Incorporation of a ground heat exchanger into the foundation excavation or boreholes significantly lowers the cost of installations in comparison with an installation of a conventional ground heat exchanger.

The use of foundations, diaphragm walls, tunnel linings, anchors and other underground geotechnical structures as energy geostructures significantly increases in Europe and all around the world. At first a foundation's bearing slabs and a basement walls were used for energy exchange, afterwards bearing piles quickly followed (mid-1980s), diaphragm walls (mid-1990s) and then tunnels (early-2000s) [53–55]. Each of these types is described in more detail in the following.

5.1. Energy Foundations and Diaphragm Walls

Pile foundations and diaphragm walls perform the dual function of exchanging heat and providing structural support, and are only installed at sites where pile foundations are already required; these systems provide the thermal performance of shallow geothermal energy systems at no additional drilling costs (Table 2). There is a significant amount of cost saving if underground structures can be utilized as an energy source. Heat exchanging loops (absorber pipes) are installed within the reinforcement horizontally in slabs and pile rafts and vertically in diaphragm walls and pile foundations.

Underground energy geotechnical structures have the dual role of providing structural support and transfer heat with the surrounding ground to supply heat energy for the heating and cooling of buildings and deicing structures such as roads and bridges. The heat exchange is achieved by installing loops in the underground energy structures, in which heat is extracted or injected from or into the ground by a circulating fluid pumped by HP. These systems are categorized as low enthalpy geothermal energy systems and indeed work with HP technology [56].

Table 2. Cost comparison of bore-hole GSHPs and energy piles (modified from Amis [57]).

Item	Bore Hole Heat Exchanger	Geothermal Energy Pile
Diameter	125 mm	600 mm
Length	100 m	30 m
Number of loops	1	3
Loop length	200 m (3.5 kW)	6 × 30 = 180 m (3.5 kW)
Drilling bore hole cost	38 €/m × 100 m = 3800 €	0 (no extra boring)
Thermal grout cost	5.5 €/m × 100 m = 550 €	Not required
Pipe 32 mm diameter	3.2 €/m × 200 = 640 €	3.2 €/m × 180 = 576 €
Total	4990 €	576 €

Energy piles also known as pile heat exchangers (PHEs) and thermal piles have particularly gained popularity in Europe due to their easy and quick installation. Existing pile installation techniques such as the driven technique (for precast pile) and bored technique (for cast in-situ pile) have been modified slightly to accommodate the installation of absorber pipes with reinforcement. Precast concrete energy piles with hollow central spaces can be built into the soil before installing the energy loops in the hollow space and filling it with cement mortar to ensure a good contact between these loops and the concrete pile. A typical cross-section of a precast energy pile is shown in Figure 5. Steel piles can also be driven and filled with concrete. Additionally, the coring technique could also be employed to fit absorber pipes in the case of hardened concrete piles already installed in the ground.

In the bored technique, holes are bored in the ground and supported by a casing (in case of loose soil), followed by installing the reinforcement cage with absorber pipes attached prior to concreting. The loops (absorber pipes) are attached the reinforcement cage, either to the inner or outer surface, and the loops' length is matched with the length of the reinforcement cage rather than the design thermal load in the bored piles, as shown in Figure 6. Contiguous flight auger (CFA) piles intended for energy purposes consist of energy loops attached to a central steel bar to provide support to the loops when they are being pushed into fresh concrete. CFA piles are more common due to their fast installation. The pipes are pressurized and maintained at a nominal pressure of 8 bars (800 kPa), to prevent collapse due to concrete-imposed load during concreting in bored piles or when pipes are being pushed into concrete in CFA piles.

A large number of energy pile/wall installations are already operational, especially in the United Kingdom, Switzerland, Austria and Germany [57–65]. However, deep and shallow foundations, energy piles and diaphragm walls bring new challenges to geotechnical pile design. During a heat exchange operation, the pile will expand and contract relative to the soil as heat is injected and extracted, respectively. These relative movements have the potential to alter the shear transfer mechanism at the pile-soil interface. Furthermore, the range of temperature increases near the pile surface, and though

limited by practical operational guidelines, this can have a significant effect on pore pressure generation and soil strength.

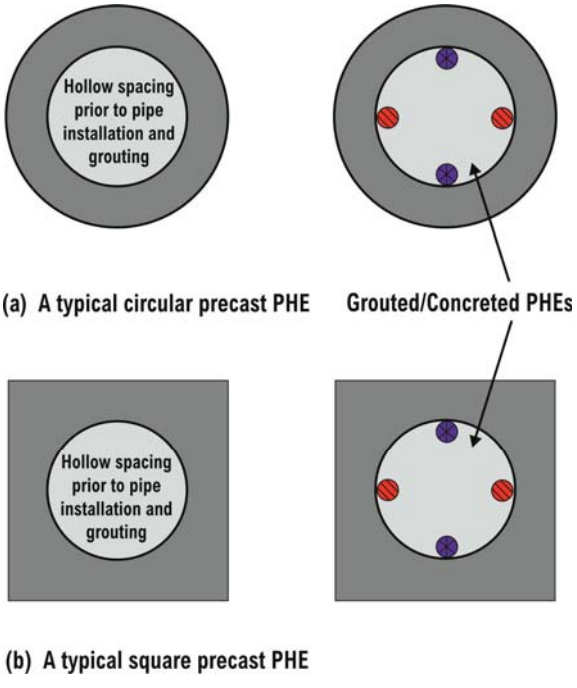

Figure 5. Precast energy pile.

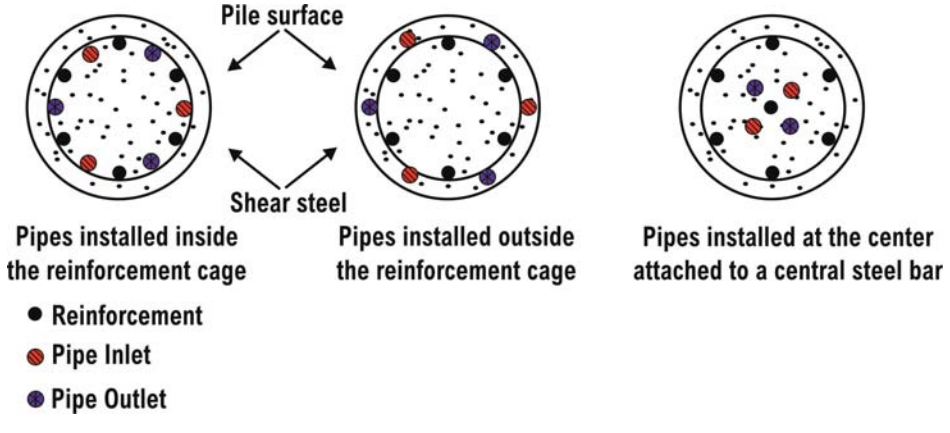

Figure 6. Absorber pipe locations within the energy pile.

5.2. Energy Tunnels

An innovative and very promising technology is the use of energy from tunnels. In this case heat exchanging loops can be installed in a tunnel lining to allow heat exchange either with air or surrounding ground (Figure 7). There are various tunnel techniques such as cut and cover, the tunnel

boring method (TBM) and the new Austrian tunneling method (NATM). Energy loops (absorber pipes) can be installed on site and as a precast tunnel segment.

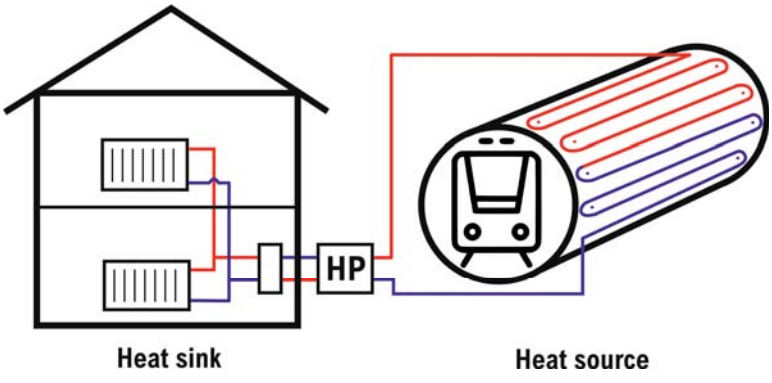

Figure 7. Principle scheme of energy usage from metro tunnels.

Energy tunnels have the advantage of using a larger volume of ground and surface for heat exchange in comparison to energy piles/walls. There are two types of energy tunnels, viz. cold and hot. In the case of a cold tunnel, the air temperature inside the tunnel is similar to the surrounding ground temperature, while in the hot tunnel, it is higher due to the movement of trains and applying brakes. The ventilation system required for hot tunnels can be partially substituted by a geothermal system [55].

However, the practical implementation of energy tunnel technology is limited at the moment, and only few experimental energy tunnels have been trialed in Austria, Germany and Italy. This is a new technology which requires a business model to utilize the heat from energy tunnels by neighboring buildings and also the initial installation cost and the energy extraction strongly depends upon a specific site [59,66,67].

Presently, design guidelines are not well defined, which can guide contractors to install heat exchanging loops in the tunnel lining without compromising the safety and serviceability of the tunnel. A number numerical studies have been reported which highlight various aspects of the energy tunnel behavior that should be taken into account by both contractors and design engineers planning and undertaking a project [68].

6. Conclusions

The HPs in Lithuania and similar cold climate countries are accepted as one of the most outstanding technologies of heating in both residential and commercial buildings, because they provide high SPF, 1.8–3.4 for ASHP and 2.5–5.6 for GSHP and WSHP. However, the spread is large, because of different equipment, design and installation quality as well as maintenance. HP efficiency has increased significantly in last decade, particularly that of ASHP. This has influenced a growing popularity of these HPs in the residents' building market.

While the traditional ASHP, GSHP and WSHP techniques are conventional, the ongoing research and development works are focused on the reduction of installation costs; i.e., decreasing of installation time and complexity, solar heat HP, waste water HP, absorption/adsorption HP, foundations, diaphragm walls, tunnel linings used for HP. Presently comprehensible design guides and standards are missing. These manuals have to cover a methodology for the establishing of thermal actions; how they should be performed in terms of safety and serviceability of the energy geostructure. There is an ongoing need to demonstrate the efficacy of building pile foundations as energy piles and energy

tunnel systems considering investments, heat exchange potential and the impact of heat exchange operations on the structure itself.

The main factor hindering market growth in Lithuania is the high initial cost of these HPs. The payback period of HP systems in most cases is too long to ensure the stable growth of HP applications without governmental grants. Despite the long payback period the market of HP systems is slowly growing, and the trend continues towards larger HP systems in multifamily buildings, hospitals, hotels and other large complexes due to support from EU and other funds.

Author Contributions: Conceptualization, R.V., R.M.S. and A.J.; methodology, R.V. and R.M.S.; validation, R.V., R.M.S. and A.J.; formal analysis, R.V.; data curation, R.V. and J.V.; writing—original draft preparation, R.V.; writing—review and editing, R.V., R.M.S., A.J.; visualization, J.V.

Funding: This research received no external funding.

Acknowledgments: This work has been supported by the COST Action TU1405—"European Network for Shallow Geothermal Energy Applications in Buildings and Infrastructure" (GABI).

Conflicts of Interest: The authors declare no conflict of interest.

References

1. Eurostat. European Commission. *Consumption of Energy.* Available online: https://ec.europa.eu/energy/en/topics/energy-efficiency/buildings (accessed on 8 November 2017).
2. Bosh, J.; Johnson, F.X.; Mertens, R.; Roubanis, N.; Loesoenen, P.; Gikas, A.; Gorton, J. *Panorama of Energy: Energy Statistics to Support EU Politics and Solutions*; Eurostat: Luxembourg, 2008.
3. European Commission. *COM (2011) 112 Final. Commission Communication. Roadmap to a Competitive Low Carbon Economy in 2050*; European commission: Brussels, Belgium, 2011.
4. European Commission. *Draft Horizon 2020 Work Programme 2014–2015 in the Area of Secure, Clean and Efficient Energy*; European commission: Brussels, Belgium, 2015.
5. Gaigalis, V.; Skema, R.; Marcinauskas, K.; Korsakiene, I. A review on heat pumps implementation in Lithuania in compliance with the national energy strategy and EU policy. *Renew. Sustain. Energy Rev.* **2016**, *53*, 841–858. [CrossRef]
6. European Parliament. *Directive 2009/28/EC of the European Parliament and of the Council of 23 April 241 2009 on the Promotion of the use of Energy from Renewable Sources and Amending and Subsequently 242 Repealing Directives 2001/77/EC and 2003/30/EC*; Off J Eur Union L 140: Brussels, Belgium, 2009.
7. Zimny, J.; Michalak, P.; Szczotka, K. Polish heat pump market between 2000 and 2013: European background, current state and development prospects. *Renew. Sustain. Energy Rev.* **2015**, *48*, 791–812. [CrossRef]
8. The History of Heat Pump Technology. Available online: https://finn-geotherm.co.uk/the-history-of-heat-pumps/ (accessed on 19 November 2018).
9. Zogg, M. History of heat pumps Swiss contributions and international milestones. In Proceedings of the 9th International IEA Heat Pump Conference, Zurich, Swizerland, 20–22 May 2018.
10. Arentsen, M.J.; Dinica, V. *Sustainable Electricity Supply in the European Union Achieving Sustainable Development, the Challenge of Governance Across Social Scales*; Praeger: London, UK, 2003; pp. 235–256.
11. Goetzler, W.; Zogg, R.; Lisle, H.; Burgos, J. Ground-Source Heat Pumps: Overview of Market Status, Barriers to Adoption, and Options for Overcoming Barriers. Navigant Consulting; 2009. Available online: https://www1.eere.energy.gov/geothermal/pdfs/gshp_overview.pdf (accessed on 19 November 2018).
12. Heat Pumps. *Integrating Technologies to Decarbonise Heating and Cooling*; European Copper Institute: Woluwe-Saint-Pierre, Belgium, 2018.
13. Bubelis, E.; Makarevičius, V. *Energy Transfer Processes in Heat Pumps*; Mokslas: Vilnius, Lithuania, 1990.
14. Bubelis, E.; Marcinauskas, K.; Skema, R. Heat pumps and district heating systems. In Proceedings of the IV Minsk International Seminar "Heat Pipes, Heat Pumps, Refrigerators", Minsk, Belarus, 4–7 September 2000.
15. Marcinauskas, K.; Bubelis, E. Silumos siurbliai individualiose sodybose Lietuvoje: Prielaidos ir prognozes. *Energetika* **2002**, *3*, 56–66.
16. Jonynas, R.; Valancius, R.; Suksteris, V. Realus silumos siurblio sezoninis energijos transformacijos koeficientas. *Mokslas Lietuvos Ateitis Pastatu Inzinerines Sistemos* **2009**, *1*, 35–37. [CrossRef]

17. Zekas, V.; Martinaitis, V. Realiai veikiancio silumos siurblio efektyvumo tyrimas. *Mokslas Lietuvos Ateitis Pastatu Inzinerines Sistemos* **2009**, *1*, 68–71. [CrossRef]
18. Aleksandravicius, T.A.; Zinevicius, F. Single family house: Heat pump or gas boiler? *Energetika* **2012**, *58*, 195–199. [CrossRef]
19. Januskevicius, K.; Streckiene, G.; Bielskus, J.; Martinaitis, V. Validation of unglazed transpired solar collector assisted air source heat pump simulation model. *Energy Procedia* **2016**, *95*, 167–174. [CrossRef]
20. Suksteris, V.; Jonynas, R. Silumos Siurblio Panaudojimo Alytaus Daugiabuciame Name Analize. Available online: http://lsta.lt/files/studijos/2011%20metu/A-60Alytaus%20%C5%A0S%20analize_Suksterio.pdf (accessed on 23 November 2018).
21. Zinevicius, F.; Sliaupa, S.; Mazintas, A.; Dagilis, V. Geothermal energy use in Lithuania. In Proceedings of the World Geothermal Congress 2015 Melbourne, Melbourne, Australia, 19–25 April 2015.
22. Tamasauskas, R.; Monsvilas, E.; Bliūdzius, R.; Banionis, K.; Miskinis, K. Comparison of calculation methods of renewable energy generated by electric heat pumps. *J. Sustain. Archit. Civ. Eng.* **2015**, *2*, 41–51. [CrossRef]
23. The European Heating Product Market Report. *Lithuania Full Options. Heat Pumps Lithuania. BRG Buildings Solutions*. 2014, p. 114. Available online: http://issuu.com/sanistaal/docs/lt_heating_full_report_may_2014 (accessed on 6 October 2018).
24. Hepbasli, A.; Kalinci, Y. A review of heat pump water heating systems. *Renew. Sustain. Energy Rev.* **2009**, *13*, 1211–1229. [CrossRef]
25. Self, S.J.; Reddy, B.V.; Rosen, M.A. Geothermal heat pump systems: Status review and comparison with other heating options. *Appl. Energy* **2013**, *101*, 341–348. [CrossRef]
26. Nakos, H.; Haglund, S.C.; Andersson, K.; Lidbom, P.; Thyberg, S. Air-to-air heat pumps evaluated for Nordic climates-trends and standards. In Proceedings of the 11th IEA Heat Pump Conference 2014, Montreal, QC, Canada, 12–16 May 2014.
27. Campaign for Take Off for Renewable Heat Pumps in Ireland. Country Report—Experiences with the Development of the Heat Pump Market in Austria, Germany, Sweden and Switzerland. Arsenal Research. April 2004. Available online: https://www.seai.ie/uploadedfiles/FundedProgrammes/CountryReportlastversion.pdf (accessed on 18 November 2018).
28. HP Outlook 2012—Finland. Finnish Heat Pump Association SULPU. 2012. Available online: http://www.sulpu.fi/documents/184029/189661/HP%20Outlook,%20%20Finland%202012-1.pdf (accessed on 18 November 2018).
29. IEAHPP Annex 41, Cold Climate Heat Pumps, Task 1: Critical Literature Survey. Japan Country Report International Energy Agency, April 2013. Available online: http://www.hptcj.or.jp/Portals/0/data0/hpp%20annex/annex41/documents/Annex41Task1CountryReportDraftasofMay2013.pdf (accessed on 17 November 2018).
30. Hirvonen, J. The heat pump market, its market drivers and how to have an impact on them in Finland. In Proceedings of the 12th IEA Heat Pump Conference, Rotterdam, The Netherlands, 15–18 May 2017.
31. Honkapuro, S.; Koreneff, G. *Heat pumps and other DER technologies in Finland. IEA DSM Agreement. Task XVII Integration of DSM, DG, RES and storages. Workshop in Sophia Antipolis, France*. 2011. Available online: http://www.ieadsm.org/ViewTask.aspx?ID=16&Task=17&Sort=0 (accessed on 17 November 2018).
32. "Oras-Vanduo" Silumos Siurbliai—Perversmas Sildymo Technikos Rinkoje. Available online: http://www.manonamai.lt/praktiniai-patarimai/namui-butui/oras-vanduo-silumos-siurbliai-perversmas-sildymo-technikos-rinkoje.d?id=67722480 (accessed on 23 November 2018).
33. Kazjonovs, J.; Sipkevics, A.; Jakovics, A.; Dancigs, A.; Bajare, D.; Dancigs, L. Performance analysis of air-to-water heat pump in Latvian climate conditions. *Environ. Clim. Technol.* **2014**, *14*, 18–22. [CrossRef]
34. Lee, C.K. Effects of multiple ground layers on thermal response test analysis and ground-source heat pump simulation. *Appl. Energy* **2011**, *88*, 4405–4410. [CrossRef]
35. Dowlatabadi, H.; Hanova, J. Strategic GHG reduction through the use of ground source heat pump technology. *Environ. Res. Lett.* **2007**, *2*, 1–8.
36. Michopoulos, A.; Papakostas, K.T.; Kyriakis, N. Potential of autonomous ground coupled heat pump system installations in Greece. *Appl. Energy* **2011**, *88*, 2122–2129. [CrossRef]
37. Healy, P.F.; Ugursal, V.I. Performance and economic feasibility of ground source heat pumps in cold climates. *Int. J. Energy Res.* **1997**, *21*, 857–870. [CrossRef]
38. Doty, S.; Turner, W.C. Energy management. In *Handbook*, 7th ed.; The Fairmont Press, Inc.: Lilburn, GA, USA, 2009.
39. Abdeen, M.O. Ground-source heat pumps systems and applications. *Renew. Sustain. Energy Rev.* **2008**, *12*, 344–371.

40. Sarbu, I.; Sebarchievici, C. General review of ground-source heat pump systems for heating and cooling of buildings. *Energy Build.* **2014**, *70*, 441–454. [CrossRef]
41. Nikulin, G.; Kjellström, E.; Hansson, U.; Strandberg, G.; Ullerstig, A. Evaluation and future projections of temperature, precipitation and wind extremes over Europe in an ensemble of regional climate simulations. *Tellus* **2011**, *63*, 41–55. [CrossRef]
42. RSN 156-94. *Statybine Klimatologija*; Renkon: Vilnius, Lithuania, 1994.
43. Streimikiene, D. Residential energy consumption trends, main drivers and policies in Lithuania. *Renew. Sustain. Energy Rev.* **2014**, *35*, 285–293. [CrossRef]
44. Lietuvos Šilumos Tiekėjų Asociacija. Vidutinė Šilumos Kaina Gyventojams (Po Perskaičiavimų). Available online: http://lsta.lt/lt/pages/apie-silumos-uki/silumos-kainos (accessed on 2 September 2019).
45. Regula 2019. Valstybinė Kainų ir Energetikos Kontrolės Komisija. Visuomeniniai Tarifai AB "Energijos Skirtymo Operatorius" nuo 2019 m. Sausio 1 d. Available online: https://www.regula.lt/Puslapiai/default.aspx (accessed on 2 September 2019).
46. Silumos Vartotojo Vadovas. Pirmas Priedas. Available online: http://lsta.lt/files/Leidiniai/SILUMOS_vartotojo_vadovas/Silumos_vadovo_Priedas%20koreg.pdf (accessed on 3 September 2019).
47. Tyrimas: Kiek Kainuoja Namu Siluma? Available online: http://www.eso.lt/lt/ziniasklaida/tyrimas-kiek-kainuoja-namu-siluma.html (accessed on 23 November 2018).
48. Cerneckiene, J.; Valancius, R.; Stasiulienė, L.; Perednis, E.; Vaiciunas, J. Analysis of the criteria for selecting heating systems for residential buildings in cold climate. *J. Sustain. Archit. Civil Eng.* **2018**, *23*, 69–78.
49. Valancius, R.; Cerneckiene, J.; Singh, R.M. Review of combined solar thermal and heat pump systems installations in Lithuanian hospitals. In Proceedings of the EuroSun 2018 Conference of ISES Europe, Rapperswil, Switzerland, 10–13 September 2018.
50. David, A.; Mathiesen, B.V.; Averfalk, H.; Werner, S.; Lund, H. Heat roadmap Europe: Large-scale electric heat pupms in district heating systems. *Energies* **2017**, *10*, 578. [CrossRef]
51. Wei, W.; Wang, B.; Wenxing, S.; Xianting, L. Absorption heating technologies: A review and perspective. *Appl. Energy* **2014**, *130*, 51–71.
52. Saha, B.B.; Uddin, K.; Pal, A.; Thu, K. Emerging sorption pairs for heat pump applications: An overview. *JMST Adv.* **2019**, *1*, 161–180. [CrossRef]
53. Laloui, L.; Di Donna, A. *Energy Geostructures: Innovation in Underground Engineering*; ISTE Ltd and John Wiley & Sons Inc.: Hoboken, NJ, USA, 2013.
54. Brandl, H. Energy foundations and other thermo-active ground structures. *Géotechnique* **2006**, *56*, 81–122. [CrossRef]
55. Adam, D. Tunnels and foundations as energy sources—practical applications in Austria. In Proceedings of the 5th International Symposium on Deep Foundations on Bored and Auger Piles (BAP V), Ghent, Belgium, 8–10 September 2008; pp. 337–342.
56. Barla, M.; Donna, A.L.; Perino, A. Application of energy tunnels to an urban environment. *Geothermics* **2016**, *61*, 104–113. [CrossRef]
57. Amis, T. Energy Foundation in the UK. Ground Source Live Sustainable Heating & Cooling: Peterborough, UK. Available online: https://www.gshp.org.uk/GroundSourceLive2011/TonyAmisPilesgsl.pdf (accessed on 1 October 2018).
58. Adam, D.; Markiewicz, R. Energy from earth-coupled structures, foundations, tunnels and sewers. *Géotechnique* **2009**, *59*, 229–236. [CrossRef]
59. Bourne-Webb, P.; Amatya, B.; Soga, K.; Amis, T.; Davidson, C.; Payne, P. Energy pile test at Lambeth College, London: Geotechnical and thermodynamic aspects of pile response to heat cycles. *Géotechnique* **2009**, *59*, 237–248. [CrossRef]
60. Pahud, D. A case study: The Dock Midfield of Zurich Airport. In *Energy Geostructures: Innovation in Underground Engineering*; Laloui, L., DiDonna, A., Eds.; ISTE Ltd. and John Wiley & Sons Inc.: Hoboken, NJ, USA, 2013; pp. 281–295.
61. Riederer, P.; Evers, G.; Gourmez, D.; Jaudin, F.; Monnot, P.; Pertenay, V.; Pincemin, S.; Wurtz, E. *Conception de Fondations Geothermiques*; brgm: Paris, France, 2007.
62. SIA DO 190. Utilisation de la chaleur du sol par des ouvrages de fondation etde soutènement en béton. In *Guide Pour la Conception, la Realization et Lamaintenance, Switzerland*; Société Suisse des Ingénieurs et des Architects: Zurich, Switzerland, 2005.

63. Brandl, H. Energy piles and diaphragm walls for heat transfer from and into ground. In Proceedings of the 3rd International Symposium on Deep Foundations on Bored and Auger Piles (BAP III), Ghent, Belgium, 19–21 October 1998; pp. 37–60.
64. Gao, J.; Zhang, X.; Liu, J.; Li, K.; Yang, J. Numerical and experimental assessment of thermal performance of vertical energy piles: An application. *Appl. Energy* **2008**, *85*, 901–910. [CrossRef]
65. Suryatriyastuti, M.; Mroueh, H.; Burlon, S. Impact of transient heat diffusion of a thermoactive pile on the surroundings soil. In *Energy Geostructures: Innovation in Underground Engineering*; Laloui, L., Di Donna, A., Eds.; ISTE Ltd. and John Wiley & Sons Inc.: Hoboken, NJ, USA, 2013; pp. 193–209.
66. Schneider, M.; Moormann, C. GeoTU6—a Geothermal Research Project for Tunnels. *Tunnel* **2010**, *2*, 14–21.
67. Franzius, J.N.; Pralle, N. Turning segmental tunnels into sources of renewable energy. *Proc. ICE Civil Eng.* **2011**, *164*, 35–40. [CrossRef]
68. Bourne-Webb, P.; Burlon, S.; Javed, S.; Kürten, S.; Loveridge, F. Analysis and design methods for energy geostructures. *Renew. Sustain. Energy Rev.* **2016**, *65*, 402–419. [CrossRef]

energies

MDPI

Article

uhuMEBr: Energy Refurbishment of Existing Buildings in Subtropical Climates to Become Minimum Energy Buildings

Sergio Gómez Melgar *, Miguel Ángel Martínez Bohórquez and José Manuel Andújar Márquez

Escuela Técnica Superior de Ingeniería, Universidad de Huelva, Campus de El Carmen, 21007 Huelva, Spain; bohorquez@uhu.es (M.Á.M.B.); andujar@uhu.es (J.M.A.M.)

* Correspondence: sergomel@uhu.es; Tel.: +34-687-880-714; Fax: +34-959-217-304

Received: 27 December 2019; Accepted: 1 March 2020; Published: 5 March 2020

Abstract: Today, most countries in the world have mandatory regulations, more or less strict, regarding energy efficiency in buildings. However, a large percentage of the buildings already built were constructed under lax or non-existing regulations in this regard. Therefore, many countries are facing the energy refurbishment of their existing buildings to reduce their carbon footprint. Depending on ambient weather conditions where a building settles, its operation with respect to the achievement of maximum energy efficiency should usually be different. This happens in subtropical climates when, during the year and depending on the season, the building needs to conserve heat, evacuate it or even make an exchange with the outside to take advantage of favorable environmental conditions. This paper presents a complete methodology for conducting building energy efficiency refurbishments in subtropical climates in order to convert them into minimum energy buildings. The proposed methodology is illustrated by a case study in a dwelling that includes all the stages, from the analysis of the existing dwelling to the refurbishment works, showing the final results and the subsequent dwelling operation.

Keywords: energy efficiency; subtropical climate building; Minimum-Energy Building (MEB); building refurbishment; building rehabilitation; building renovation; envelope airtightness; envelope thermography; envelope transmittance

1. Introduction

The construction sector is responsible for 40% of greenhouse gas production in the European Union (EU) [1]. Governments, building associations and construction companies have been making significant efforts in reducing this impact, thus, improving the energy efficiency of the new buildings. EU mandatory building regulations have already incorporated, in recent years, some of the best research findings in this field. Examples of this are reflected by the directives on the energy performance of the buildings [2], and their subsequent updates [3–5]. Not only for legal reasons, but for corporative responsibility (and maybe for marketing proposes), most successful developers and building sector entrepreneurs want to offer the best product to their customers, both from the social point of view [6] and sale perspective [7], because the market demands increasingly efficient buildings.

EU, Directives [4] and [5] establish a specific mandatory requirement for member states to draw up national plans to increase the number of nearly zero energy buildings (nZEB). According to both directives, the member states' national plans must include the detailed definition of the nZEB concept, as it is reflected in the EU Directive [7], in such a way that their national, regional, and local conditions are reflected, and a numerical indicator of the primary energy use must be included and expressed in kWh/m^2 per year. However, leaving in the hands of each country the specific definition (this means

numerical values of all the intervening parameters) of the nZEB, can lead to multiple norms in EU. In any case, taking into account the different climate zones in Europe, and within them, their specific sub-climate conditions (altitude, proximity to the sea, humidity, etc.), it seems logical to establish the nZEB concept for the entire EU, but not its specific development. For this reason or others, among which are the economic ones, of course, several green building rating systems (GBRs) have appeared during the last years [8]. Perhaps so many that, today, stakeholders are probably having difficulties to choose the most suitable for their projects. Although some GBRs are more used than others, none of the current ones is a European standard, i.e., reference for the entire EU. In Reference [9], the authors of this paper carried out a critical review of the most common GBRSs within the EU. The conclusion was that there is a confusion and heterogeneity within current GRBS, as well as the need to provide regional adaptations to cover the specificities of the different EU zones. Anticipating these conclusions, the authors of this article proposed a year earlier [10] a set of parameter values for new construction in subtropical climates, focused on the Spanish case, but easily applicable to EU Mediterranean countries, specifically to their temperate climate areas.

However, recently constructed buildings in the EU under energy efficiency criteria are only a small part of the current park of buildings, which consist mainly of buildings that are several decades old, long before the first EU energy efficiency directives.

In the EU, during the 1950s, 1960s and the early 1970s, the period, including the big reconstruction after the World War II and before the first petrol crisis in the mid 1970s, most of the new peripheries around big cities were built up with social neighborhoods without considering the minimal energy performance of the building. If required, the inhabitants of those social houses could use electrical systems for heating or cooling their houses, because electricity in that period used to be affordable and inexpensive. Those owners have found themselves with insufficient funds to retrofit and improve the quality of the materials used in the original construction, so most buildings have remained in the same state as they were built, becoming obsolete and converting their dwellings in energy sinks [11], causing significant energy waste and even energy poverty for those who cannot afford the cost of the electricity they need to maintain their homes in comfortable conditions. Examples of this are [12,13] for the cases of Spain and Greece, respectively, and [14] for a general study. This has led to the current situation: In the EU, depending on the country, between the 70 and 90% of the buildings are energy inefficient, i.e., consume more energy than necessary.

Specifically, in the case of Spain, which can be extrapolated to other EU countries, more than half of the housing stock was built before 1980. This means that around 13 million dwellings were built without any energy efficiency measure. So, this may be indicative of the huge amount of housing stock that needs energy refurbishment. However, Spain only represents around 9% of the EU population, while the need for energy refurbishment in the EU can exceed 100 million dwellings.

In Spain, buildings account for 31% of energy consumption, which is partly due to the fact that 84% of its buildings are energy inefficient. In fact, a very efficient building (class A in Spain, in a descending range from A to G) can consume 10 times less energy than a highly inefficient one (class G).

Spain has a subtropical climate, but with different and varied sub-climates, which complicates strategy options to face energy refurbishment, because, in large areas, such as the case study, it is necessary to deal with the twofold problem entailed by the fact that the same built solution must solve the heat loss in winter and the heat gain in summer. This problem was previously studied in References [15,16] for the Chinese case, Reference [17] for the Indian case and Reference [18] for a general case. Even more, it is highly recommended to take advantage of mild weather days during spring, autumn, winter mid-days and summer nights; a sample is [19]. Therefore, in practice, in large areas of a subtropical climate, the building, in order to achieve its maximum energy efficiency, should be adapted to 3 different climate conditions as follows:

(1) In order to face the cold period successfully one must obtain the best insulated and hermetic outer envelope, without exchanging air with the outside, but with high efficiency heat recovery mechanical ventilation to keep the best indoor air quality. In that sense, Reference [20] carries out a review on integrations between energy performance and indoor environment quality, on the other hand, Reference [21] it is a good example of the influence of the building envelope in the best use of the energy.
(2) The heat gains produced inside the building (such as solar radiation through windows and skylights, human metabolism, household appliances, etc.) favor the efficiency of the final result, as shown in Reference [22].
(3) In order to face the hot period successfully one must undertake the same strategy related to insulation and air tightness of the external envelope, but with the difference that now, the internal heat gains act against the efficiency of the final result. In periods of heat, it can be interesting to open the windows in the night hours in order to take advantage of the natural and free cooling. This, apart from renovating overheated inner air, temper the dwelling to delay the advance of the thermal wave at daytime. This effect, commonly called the Mediterranean climate, is studied in Reference [23] for external walls of nZEB buildings, in Reference [24] with respect to the effect of high thermal insulation, and in Reference [25], regarding the effect of thermal transmittance.
(4) In order to face the mild weather period successfully, it is necessary for the external envelope of the building to operate dynamically, i.e., enclosed or partially open, depending on the outside weather.

To give an optimal constructive and operative solution to achieve the best building response in terms of the three different climate strategies explained represents a great challenge for architectural and engineering designers. If this can be challenging in new construction, it is even more of a predicament in the building refurbishment field, where the degree of freedom to intervene in an existing building is considerably lower. So, except in very favorable conditions, the only way to approach the accomplishment of the three established strategies, is through a very well-studied building refurbishment. In fact, a good building refurbishment requires a proper mix (not always in the same proportion) between insulation (to prevent heat loss in the winter and gains in summer), facilities (to provide, with the most efficiency use of resources, the greatest degree of comfort to its inhabitants), renewable energy systems (RES, to make the building sustainable with the environment) and smart technologies that ensure the proper functioning of building systems and facilities, the comfort of its users and the energy exchange management of the building with its surroundings throughout the year.

In Reference [10], a new methodology (uhuMEB) for the design, construction and management of minimum energy buildings (MEB) in subtropical climate was proposed for the authors of this paper. An MEB was defined as a building concept in which energy waste is not allowed, even if it has been produced in a renewable way. Different MEB grades were defined, but all with the same energy efficiency; the difference between them is only the capacity of the MEB to produce its own energy, which must also be renewable. In this way, the lowest MEB degree was defined as an optimized nZEB, i.e., a building with very high energy optimization through passive construction criteria, but consuming, totally or partially, electrical energy from the grid. From here, depending on the renewable electrical energy production capability of the building, an MEB can grow up to zero energy building (ZEB, produces its whole energy demand) and even to +ZEB (the building is a net renewable electrical energy producer; so, it could sell energy to the grid). It is very important to highlight that according to the methodology proposed in Reference [10], the transition from nZEB to +ZEB has to be done exclusively through RES.

In this paper, the authors propose to complement the uhuMEB (of application to new construction) methodology to include the energy refurbishment of existing buildings (called uhuMEBr). The developed methodology presents step-by-step guidelines to convert an existing energy inefficient building or dwelling into a MEB. Different energy efficiency requirements must be met at each

methodological step. However, the available degrees of freedom for the refurbishment of an existing building is not usually the desired ones; so, the practice implies that, usually, each building refurbishment project requires its own construction and facility-based solution. Notwithstanding, the construction and facility-based solution to the specific refurbishment problem of each building or even each dwelling is not the aim of this paper nor of the uhuMEBr methodology, i.e., this article is not intended to provide research in construction or facilities, although both fields are necessary to comply with the proposed methodology. Even more, the paper does not cover the solutions to get a MEB, which can be very varied, but focused on the accomplishment of its requirements.

As an application example of the proposed uhuMEBr methodology, a case study, will be shown in the paper. Among other building refurbishment projects carried out by the authors, this has been chosen because of its intrinsic difficulties and the social performance that they represent. In many Spanish cities, as in other EU countries, there was an important exodus from the countryside to the city in the decade of the 50s. People were looking for an improvement in their standard of living by working in factories, and taking advantage of the additional possibilities offered by cities as opposed to the countryside. This brought with it a huge need for low-cost housing, which gave away to the many suburbs that surround many European cities (obviously this situation can be found in other parts of the world). In those years, there were no laws legislating buildings' energy efficiency, whereby these suburbs constitute today true energy sinks. Now and for obvious reasons, European governments are very interested in the refurbishment of, energetically speaking, these suburbs, and in general, existing buildings.

This paper is structured as follows. In Section 2, the set of materials and methods used in this research is introduced. Some of them are commercial, while others are specific, although they are not part of the topic of this paper. Section 3 explains the uhuMEBr methodology, focused on energy efficient refurbishment of existing buildings. The actual implementation of the methodology is presented through a case study carried out in Section 4. The results of this section are discussed in detail in Section 5. The paper ends with the main conclusions that are drawn from the research done.

2. Materials and Methods

In this section, all the materials and methods used in this research are described. Some of them are commercial, but others are specific developments by the research group to which the authors belong (Control y Robótica, TEP192, from the University of Huelva, Huelva, Spain, https://www.controlyrobotica.com/). These developments are not the subject of this research, so in this section, they will only be briefly described, referring the reader to the specific bibliography of the authors where these developments are explained in detail.

As indicated in the introduction, the case study has focused on the energy refurbishment of social housing. Specifically, a dwelling of 106.74 m^2 built, located on the fifth floor of a six-story building (named *Casa del Carmen*); its exterior facade is oriented to the south and the interior one to a backyard. The building, built in the late 1960s, consists of a ground floor of commercial space and two dwellings per floor, amounting to a total number of twelve. This work was part of a pilot project (Code G-GI3000/IDI_TEP192) funded by the Andalusian regional government (Spain) whose goal was to get true data over real dwellings subjected to actual refurbishments.

The *Casa del Carmen* building is located in a social residential neighborhood in the city of Huelva, in the southwest corner of Spain, at 37° latitude in the northern hemisphere. The climate of the area is typical subtropical. Specifically, according to the Köppen-Geiger climate classification, it is included in the Csa climate zone: Temperate and rainy winters, dry and hot summers and variable springs and autumns, both in terms of temperature and rainfall. The annual average temperature is around 18 °C. In winter, the coldest months are December, January and February, with average low temperatures of 7.6, 5.9 and 7 °C, respectively (in spite of the average temperature in these months are 9.3, 10.3 and 10.8, respectively; which it means large temperature changes during the day). Regarding relative humidity, the same months, December, January and February, with average values of 78, 77 and 74%,

respectively, are the wettest. An important aspect that increases the cold sensation in these months, is the dominant wind direction, which comes from the north and usually gusty. The rest of the year, the dominant wind direction is west-southwest. In the summer, the warmest months are June, July, August and September, with average high temperatures of 29, 32.7, 32.4, and 29.4 °C, respectively (in spite of the average temperature in these months are 22.8, 25.8, 25.7, and 23.3 °C, respectively; which again, means large temperature changes during the day). Regarding relative humidity, the same months are the least wet, with average values of 57, 51, 55, and 61%, respectively. Heating degree days (HDD) and cooling degree days (CDD), defined relative to 15.5 °C base temperature for the EU in Huelva station—AN, ES (6.91 W, 37.28 N) ID 08383-, are, respectively, 595 and 1550.

Then, from the above and following the stated in the introduction of the paper, it seems clear that over the year the building needs to work in three different climatic conditions, i.e., three months (December, January and February) as in cold climate, four months (June, July, August and September) as in warm climate, and the rest of the year (five months), as in mild climate, where, depending on the outside weather, the building must operate enclosed or partially open, exchanging heat with the outside to take advantage of favorable environmental conditions.

From the above, it is important to highlight that the energy efficient refurbishment of a building in this geographical zone is not an easy task.

The characteristics of the construction and facilities in the case study dwelling were: Concrete structure, 12 cm thick brick external walls with no insulation, sliding windows with iron frames and single glazing, no cooling or heating facilities and a single gas boiler (butane) for hot water supply.

Following with the materials and methods, the specialized software in environmental and energy simulation used for the case study was DesignBuilder™ (version 5.4.0) from DesignBuilder™ Software Ltd. This tool, probably one of the best in the world in its field, enables the evaluation of aspects, such as comfort levels, energy consumption and carbon emissions, among many others. The program has a modular structure around a core that is an advanced 3D modeler. Each of the modules allows a specific type of analysis; in this research, the following modules were used: Display (virtual models with photo-realistic textures), simulation (integrates the EnergyPlus™, a whole building energy simulation program), natural lighting (allows to evaluate and optimize natural light in buildings), cost (allows to evaluate the cost of construction, energy and those associated with the building life cycle), optimization (evaluates the different solutions to help decision making in the construction—new or refurbished—process), heating ventilation and air conditioning (HVAC—allows simulating a wide range of heating, ventilating and air conditioning—HVAC—systems) and CFD (computational fluid dynamic; among other utilities, it allows to predict the movement of air and the distribution of temperature in architectural spaces).

The building information modelling (BIM) used for the case study has been Archicad™ (version 20.0) from the Graphisoft™ Company. The project building information protocol used is based on the model of the American Institute of Architects (AIA™). BIM is a collaborative work methodology for the creation and management of a construction project. BIM incorporates geometric (3D), time (4D), cost (5D), environmental (6D) and maintenance (7D) information. This allows BIM to go beyond the design phases, covering the execution of the project and extending throughout the life cycle of the building, allowing its management and reducing operating costs.

Following the developed methodology, the first step has been the data collection (which will be analyzed in Section 3.1 and schematized in Figure 1). The sensors and measurement systems used are briefly described below. Some of them ended up being part of the home automation system (HAS) of the refurbished dwelling.

The temperature and solar irradiance sensors used in this work are not commercial. Both have been developed and patented by our research group. Specifically, the temperature sensor is based on the DS 18B20 integrated circuit from Maxim Integrated™, which, together with the encapsulation used, constitute the PCT/ES2009/000543 patent. More information on its assembly, use and programming can be consulted and expanded in References [26,27]. As for the solar irradiance sensor or pyranometer

used, it is based on a BPW 21 photodiode with digital output and thermostatting. This device is also patented under the number PCT/ES2008/000736. Further information can be found in Reference [28]. The CO_2 environmental concentration is measured by the GAS SENSING SOLUTIONS™ sensor.

Thermographic measurements were carried out by the TESTO™ 875-1i camera and the dwelling envelope airtightness measurements by the Minneapolis Blower Door™ System (with DG-700) from TEC™. The procedures followed for the cited measurements can be found in Reference [10]. Finally, thermal transmittance (*u*-value) measurements were carried out with their own development and procedure explained in References [29,30].

Data collected from actual measurements of the dwellings were used, in combination with DesignBuilder™ simulations, to make an optimized decision about the scope and type of refurbishment to be performed. In what follows, the chosen solutions for insulation, HVAC, RES and HAS are described.

For the improvement of the external envelope, an external thermal insulation composite system (ETICS) from Isover™ (called *Isofex*) were used. It accomplishes with the EU standards UNE 13,500 y ETAG 004. The ETICS consist in a fastening layer of cement mortar applied to the existing external coating, 10 cm thick mineral wool disposed in two layers of 5 cm each screwed with polyamide fixings, and a final coating of acrylic mortar with a polyethylene grid inside. Among the different alternatives of insulation material on the market, a waterproof rockwool with 0.036 W/m^{2}K was chosen.

New windows installed in the case study dwelling consists of seven chambers PVC window frames (thermal transmittance = 1.1 W/m^{2}K), with a total thickness of 82 mm. Regarding the glass, a 6/15/6/15/6 (thermal transmittance = 0.6 W/m^{2}K) with double insulation chamber were installed. They incorporate low emissive film, and they are filled with 90% argon gas.

In party walls, a self-supporting double plasterboard partition from Placo™ with 8 cm (double layer 4 + 4 cm) thick glass wool inside has been installed.

Regarding the ceiling slab, it was improved by a single layer of 4 cm thick glass wool attached with profile aluminum for screwing single gypsum plasterboard.

The floor slab was improved by a single flexible panel of 8 mm thick composite carpet, consisting in three layers of extrude polyethylene, air bubbles and aluminum film. This carpet was installed over the existing cladding, serving as a base for the new floor, consisting in laminated wood.

For the improvement of the building envelope airtightness, a continuous layer of plastered gypsum mortar in the inner part of it was applied. The weak points in the joints between the windows and the masonry were solved with self-expanded bands and polyurethane foam from Soudal™.

Regarding the dwelling ventilation, a double duct heat recovery facility from Paul™ has been installed. The efficiency of the heat recovery is 93%, and the maximum air volume exchange is 450 m^3/h. Indoor pipes are made of polyethylene, 15 × 10 cm size. Intake and exhaust pipes are made of *expanded polyethylene* (EPS), Φ100 mm size.

For air conditioning and heat pump (ACHP), the 4MXM68N equipment from Daikin™ was installed. It consists of an exterior unit and four splits (indoor units for wall mounting). Its capacity is 6800 W/8600 W in cooling/heating with power consumption that only 1540 W/1790 W. It has inverter technology and uses R-32 gas.

Regarding RES, the ESCOSOL FMAX 300l 2.0/2 from Salvador Escoda™ was installed for domestic hot water (DHW). It is a compact thermosiphon unit with flat solar collectors and 300 L capacity. With respect to the photovoltaic facility, it consists of eight photovoltaic panels (PV) of 250 Wp each from SACLIMA™ that make up a 2 kWp facility. The electronics of the PV facility is from Atersa™.

The installed HAS is an own development whose instrumentation/control system (the only module used in this research) is explained in Reference [10].

3. uhuMEBr Methodology

The uhuMEBr methodology is based on the uhuMEB methodology presented in Reference [10], but specifically oriented to the energy efficient refurbishment of existing buildings. Really, uhuMEBr

complements and completes uhuMEB, but is significantly different. In a new construction, the building project could theoretically be designed based on ideally free design criteria. However, in an existing building, this is not possible, even more, there are cases where the refurbishment scope shall be reduced, due to the imposed restrictions (historical, urban, normative, budgetary, and those related to space, use, etc.). On the other hand, before carrying out an energy refurbishment project, the following question must be answered: What energy efficiency does the existing building have? This can only be accurately assessed by taking measurements (envelope thermal transmittance, envelope airtightness, thermal bridges, etc.) and analyzing consumptions (electricity, gas, etc.). From the analysis of real data, accurate simulations can be performed to develop an optimized refurbishment project. Simulations will not only allow to make decisions about the best solutions for projected energy efficiency, but also on the consumption savings achieved. With this and the necessary investment, a good approach for the investment payback can be found. Of course, refurbishment works must have a permanent measurement program to ensure that the projected matches what is actually built.

A pivotal element in the uhuMEBr methodology is the MEB concept, whose requirements, proposed by the authors, are derived from the quantification of Directive in Reference [3] that sets the qualitative requirements for an nZEB building. In summary, the MEB mandatory requirements to be met are (see Table 1):

(1) The energy demand for HVAC of the building for comfort conditions must be less than 10 kWh/m^2 year.
(2) The total primary energy demand (HVAC + DHW + appliances + lighting + home automation (or domotics) system of the building must be less than 80 kWh/m^2 year.
(3) The CO_2 concentration (indoor air quality level in the building; pivotal control in case of very high thermally insulated buildings) should be kept below 1.000 ppm.
(4) The annual percentage of thermal discomfort time (heat or cold) inside the building, expressed in terms of equivalent temperature, must be less than 10%. uhuMEBr considers thermal comfort between 20 °C and 24 °C in winter (the inhabitants of the house will be more sheltered) and between 24 °C and 26 °C in summer (the inhabitants of the house will be more unsheltered). The gap is due to the fact that thermal sensation depends on the relative humidity. If it is of 50%, the thermal comfort in winter is 22 °C and in summer 25 °C.
(5) The building envelope airtightness test (air changes rate per hour at a differential pressure of 50 Pa, n50-value) should be lower than 0.6 h^{-1}.
(6) The thermographic study of the complete building envelope must confirm that there are no significant thermal bridges.
(7) At least 90% of the DHW needs must be covered by renewable energy.

If the building refurbishment is carried out following the MEB requirements, at the end of the process, the building must accomplish the above 7 mandatory quantitative values. From here, it must keep the MEB rating during its life cycle; for this, the following four additional requirements should be met after energy efficient refurbishment (see Table 1):

(8) The average daily occupancy of the building should give true utility to it, which is, of course, highly dependent on its intended use. In any case, it must be greater than 10^{-2} people/m^2.
(9) The building must have a proper HAS, at least to measure the mandatory MEB values.
(10) The HAS data analysis on electric consumption, RH, temperature and air quality in the operative phase of the building must validate points 1, 2, 3, and 4 annually.
(11) The building must be operated and maintained by MEB qualified technicians.

The uhuMEBr methodology is summarized by an algorithm in Figure 1. Essentially it consists of three stages: one before building refurbishment called *existing building energy evaluation stage*; another, the refurbishment itself, called *existing building energy refurbishment*; and finally, after refurbishment

and for the rest of the building life cycle, the so-called *refurbished building energy management*. These three stages are connected by a decision-making branch that allows to decide if the building really needs refurbishment or if the detected problems can be solved simply by means of corrective maintenance.

Table 1. Minimum energy buildings (MEB) mandatory requirements.

Parameter	Mandatory Requirements	
1. Total energy demand for HVAC	≤10 kWh/m^2year	**MEB requirements that the building must reach through the energy efficiency refurbishment**
2. Total primary energy demand	≤80 kWh/m^2year	
3. Indoor air quality	≤1000 ppm CO_2	
4. Annual percentage of thermal discomfort time	≤10%	
5. Building envelope airtightness test	≤0.6 h^{-1} (50 Pa)	
6. Thermal bridges	No significant	
7. DHW	≥90% by renewable energy	
8. Average daily occupancy	≥10^{-2} people/ m^2	MEB requirements that must satisfy the building after energy efficiency refurbishment
9. HAS incorporated	At least for MEB parameters measurement	
10. By the HAS: annual compliance with the MEB requirements	1, 2, 3 and 4 parameters	
11. Operation and maintenance of the building	By MEB qualified technicians	

3.1. Existing Building Energy Evaluation Stage

Because uhuMEBr is applied to an existing building (it could be in use or not), before making decisions about the necessary energy efficiency refurbishment, it is mandatory to carry out the *existing building energy evaluation* (Figure 1). This stage allows assessing whether the building meets the MEB requirements. It consists of different steps that lead to the *existing building energy report*, which is the result of a *measurement campaign* (it is important to highlight that it is not based in software simulations, but in on-site instrumentation) and the obtained *data analysis*. If the building is already running under the uhuMEB methodology, it must have an *annual operation certification* that informs of its proper running. However, today this situation is practically impossible because uhuMEB is brand new. So, this paper is focused on the energy efficient refurbishment of any existing building, regardless of the methodology used in its construction and its use.

Ideally, the *measurement campaign* should last a year (in order to cover all the seasons), but if it is possible to extrapolate data, it could last less. After the *measurement campaign* (and partly also coinciding with its development), the obtained data must be analyzed in order to have a complete idea of the energy efficiency state of the existing building, in order to plan in the best way, the necessary refurbishment. This leads to the *existing building energy report* (see Figure 1) and completes the *existing building energy evaluation* stage.

In the case of the existing building, according to the results of the *existing building energy report*, it fully fits the MEB requirements; thus, it does not need to be refurbished. Nothing else has to be done in terms of improving the energy efficiency performance of the building. Obviously, this situation is really improbable in the case of an old existing building.

The *existing building energy report* will reveal the energy shortcomings of the building, and consequently, the required degree of refurbishment.

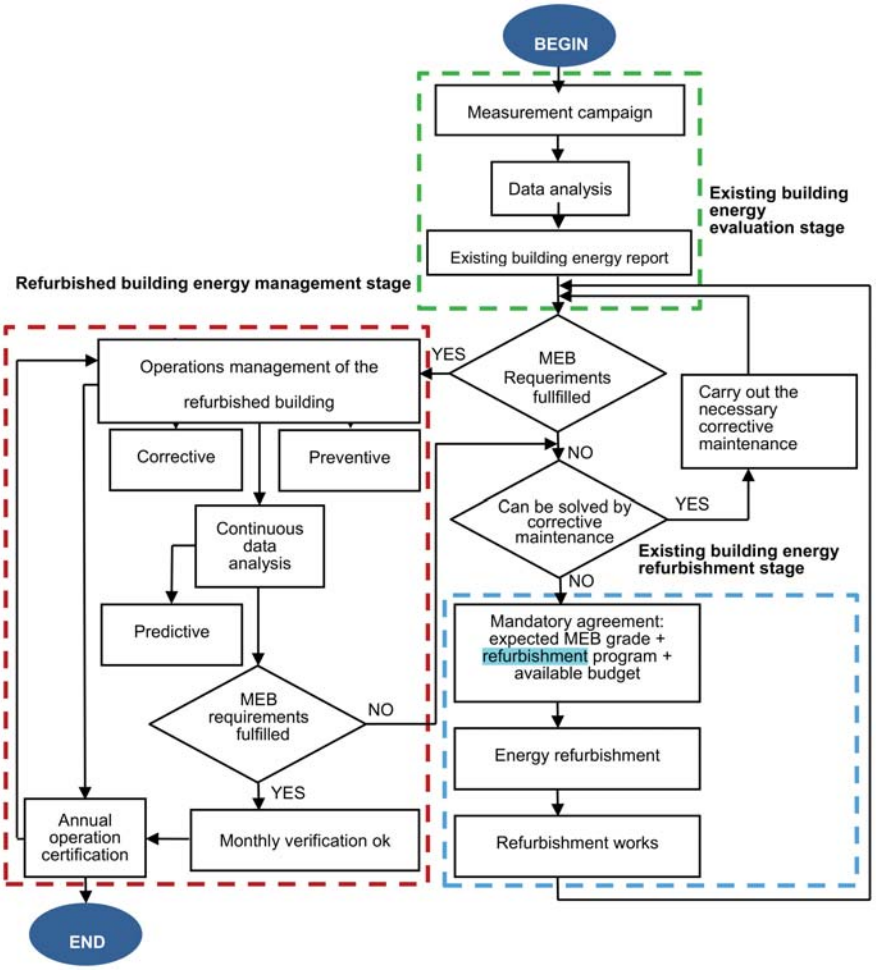

Figure 1. uhuMEBr algorithm.

3.2. Existing Building Energy Refurbishment Stage

As has already been said, before executing this stage (see Figure 1), it is necessary to check if the existing energy efficiency defects can be resolved simply by means of corrective maintenance (it is under the criteria and decision of the technicians specialized in MEB), in which case the building does not need to be refurbished. If this is not the case, the *existing building energy refurbishment* stage needs to be implemented.

At this point and considering that one is dealing with an existing building, little can be done in terms of aesthetic issues (except exceptional cases that require exceptional treatment), except, perhaps, preserving the original appearance of the building. However, very important decisions need to be made at the beginning, even before starting the energy refurbishment project, regarding the expected MEB grade: nZEB, ZEB, or +ZEB; the refurbishment program (deadlines, architectural possibilities, geographical location of the building, application regulations, etc.), and obviously, the available budget. Of course, the three requirements above may be incompatible between them; for example, to obtain a ZEB or + ZEB MEB, a larger budget and a longer period of work together with favorable architectural conditions will normally be required; but it is even likely that, with all this solved, the applicable

regulations do not allow such deep refurbishment, due to the aesthetic changes and other modifications they could cause. Another issue to consider is the geographical situation of the building itself with, perhaps, poor orientation regarding the sun, shadows of other buildings, etc. Obviously, the diversity in specific cases can be huge, making it is impossible to contemplate it in its entirety. Notwithstanding, the deal among the expected MEB grade, refurbishment program and the available budget is, together with the *existing building energy report*, the starting information to move to the *energy refurbishment project*.

Finally, before entering with the explanation of the different phases of the *existing building energy refurbishment* stage, it is necessary to remark that all of them are controlled and coordinated by means of the BIM methodology, with different levels of development (LOD) of each BIM module (one different for each phase).

3.2.1. Energy Refurbishment Project

Figure 2 shows the algorithm that implements the *energy refurbishment project* phase. It is important to keep in mind that, mentioned before, in building refurbishment the variety of cases can be significant; so, uhuMEBr cannot set all the paths to achieve MEB requirements, but only if they are reached or not. It should be noted that, even in the case of typical and apparently uniform residential buildings, it is possible that over time some dwellings may have undergone refurbishments and others may have not; a typical example is the carpentries. Therefore, when facing the complete refurbishment of a building, the actual situation of each dwelling must be taken into account. That is why the previous *measurement campaign* and *data analysis* is so important (Figure 1).

The algorithm begins with the necessary commitment that conjugates the extent of the refurbishment expected with the actual possibilities and the budget available. From here, and taking into account at all times the restrictions imposed, technicians can carry out their work. First, facing the *architectural refurbishment design* phase (see Figure 2) where, by following exclusively passive criteria (without facilities), they must achieve an HVAC total energy demand that does not exceed 10 kWh/m^{2}year. The required LOD in this phase is LOD200, which means that it is graphically represented within the BIM as a generic system, object, or assembly with approximate quantities, size, shape, location, and orientation.

The MEB *architectural refurbishment design* parameter's values are shown in Table 2. In a newly designed building, this can be conceived to accomplish each one of the parameter's value of Table 2; however, in an existing building, the freedom degrees regarding these parameters are very limited (the *form factor* is a clear example), so the *architectural refurbishment design* must put effort in those parameters that can be significantly improved. Clear examples of this can be the carpentry (frames and glasses); the transmittance improvement of the building both from the inside, and if it is possible, from the outside; etc.

The proper *architectural refurbishment design* must guarantee that the HVAC total energy demand is ≤10 kWh/m^{2}year (see Table 2). At this point in the refurbishment project, this can only be guaranteed by simulation. The key to getting this small value is that due to the exterior envelope isolation to an air and heat exchange with the outside, the thermal gap that the ACHP must overcome to reach comfort temperature is that only a few degrees. Therefore, the ACHP to be installed does not need to have high power or operate for a long time.

The following phase is the *facilities and systems engineering retrofitting design*, for which mandatory parameter's values for an MEB building are shown in Table 3. Now, the freedom degrees can grow, making it easier to reach the necessary values. The required LOD in this phase is LOD300, which means that it is graphically represented within the BIM as a specific system, object, or assembly in terms of quantity, size, shape, location, and orientation. The proper design of the facilities and systems must guarantee that the total primary energy demand of the building be ≤80 kWh/m^{2}year (see Table 1). At this point in the refurbishment project, this can only be guaranteed by simulation,

and perhaps, if a laboratory or test bench is available (including those of the manufacturers), by some experimental tests.

Table 2. MEB architectural refurbishment design requirements.

Parameter	Explanation
Sunshine	To avoid heat gains by incoming direct solar in hot months, but do just the opposite in cold months.
u-value < 0.3 Wm^2/K	Envelope thermal transmittance (rate of heat transfer through the building envelope), i.e., the combined transmittance of the opaque and opening building envelope.
F < 0.8 m^2/m^3	Form factor. The ratio between outer envelope surface and the inner volume enclosed.
N_{50}-value < 0.6 h^{-1}	Envelope airtightness without infiltration points. Air changes per hour at a differential pressure of 50 Pa in an airtightness test.
S_{of} > 0.05	Natural ventilation. Measured as the ratio between practicable and constructed surfaces.
No thermal bridges	To avoid structural and envelope building parts with a higher thermal conductivity than the surrounding materials.
S_{gf} > 0.1	Natural lighting in order to minimize the need for artificial lighting. The ratio between glazed and constructed surfaces.
HVAC ≤ 10 kWh/m^2 year	As a result of the accomplishing of the above parameters, it is the limit for HVAC requirements.

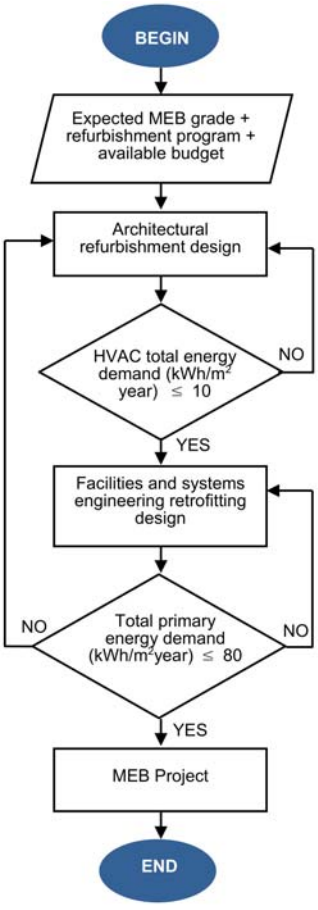

Figure 2. Energy refurbishment project algorithm.

The *facilities and systems engineering retrofitting design* phase must ensure that all parameters in Table 3 are within the allowed range. Thus, with respect to HVAC systems, there are many varied solutions: completely renewable, plugged into the grid or mixed. Obviously, the choice will depend on

the possibilities of the site (for example, if it is possible to use geothermal energy [S]) or of the building itself (for example, if there is enough roof for solar collectors or if the building is not often under shadows, etc.), and of course, everything is subject to the available budget.

Regarding DHW, the most common solution is to use thermal solar panels. However, it is not the only one, since, in case of not having enough roof or when the building has many shadows or simply by aesthetics, there are other solutions as the use of aerothermal energy (according to the European Union directive 2009/28/EC of April 2009 is considered a renewable energy source) for example.

Following with the parameters in Table 3, appliances and lighting are included as facilities and systems; however, except in very special cases (aesthetic for example), they do not require any design. Today there are many commercial solutions for efficient appliances and lighting.

Then, when all the primary energy (this means that, for example, a charging point for an electric vehicle does not consume primary energy, it is extra energy) needs are computed, the total primary energy demand must be ≤80 kWh/m^{2}year

As Figure 1 shows, in the *refurbished building energy management stage*, the success that it continues being MEB over time depends largely on the continuous data analysis of its pivotal energy efficiency variables. Specifically, and each room: indoor and outdoor temperature, indoor relative humidity, indoor air quality and electrical consumption of the building separated by circuits. Together with them and depending on the characteristics of MEB, other measurements may be necessary, such as solar irradiance or wind speed, for example. These measurements (obtained by their corresponding sensors) and the subsequent data analysis can be considered, and in fact, the authors do so, part of the building HAS.

Regarding RES, it deserves special attention. Strictly, in a MEB, RES are not mandatory because its lowest step (nZEB) must be reached only by means of passive or architectural embodiments.

However, it is increasingly common for different countries' legislation to incorporate RES requirements depending on the surface of the buildings and their use. Therefore, either because of this or because the building under refurbishment expect to reach ZEB or +ZEB grade, the incorporation of RES to a greater or lesser degree is practically mandatory in today's building, even in refurbishment as well.

There are many commercial RES solutions: two of them practically available worldwide (those based on solar energy, for ACHP, DW and/or producing electricity through photovoltaic panels (PV) and those based on aerothermal energy, for ACHP and DW), and depending on the geographical location, wind, geothermal energy (in different grades, from high to low enthalpy), etc., may be available.

In any case, either because the availability of renewable energy on-site or because the expected MEB grade or because the legislation to apply or because the building morphology or because all these factors together or part of them, each refurbishment project will require a specific RES study and the solutions of one project can hardly be extrapolated to another.

Table 3. MEB facilities and systems engineering retrofitting design requirements.

Parameter	Explanation
HVAC systems ≤ 10 kWh/m^{2}year	The systems were chosen for HVAC must meet the MEB limit.
DHW ≤ 90% renewable	The need for domestic hot water in the building must be covered by renewable energy, at least 90%.
Appliances ≤ A++	The efficiency energy of the appliances must be at least A++ which is the second highest energy label in Europe.
Lighting ≤ A++	The efficiency energy of the lighting must be at least A++. Today it is easy to reach with the long-lasting efficient LED available in the market.
Total primary energy demand ≤ 80 kWh/m^{2}year	As a result of the accomplishing the above parameters, it is the limit for total primary energy demand.
HAS incorporated	Home automation system (HAS) at least to measure, after refurbishment, the mandatory MEB values. This is pivotal for the *refurbished building management* stage.
RES incorporated	Optional. The first MEB grade (nZEB) must be achieved only with passive performances. So, RES are only necessary if the *refurbished* MEB will become a zero (ZEB) or a net energy generator building (+ZEB); or if the application forms require it.

Finally, with respect to Figure 2, it may be surprising that from the *facilities and systems engineering retrofitting design* phase it is possible to return to the *architectural refurbishment design* phase (NO* in the decision branch); however, this freedom degree of the algorithm is necessary: think for example that the necessary RES facilities do not fit on the roof of the building or on its terraces.

Once the algorithm in Figure 2 is fully executed, the building project obtains the *MEB project certification* (nZEB, ZEB, or +ZEB), which guarantees the MEB rating of the existing building in the project phase.

3.2.2. Refurbishment Works Management

Figure 3 shows the algorithm that implements the *refurbishment works management* phase. The required LOD, in this case, is LOD400, which means that it is graphically represented within the BIM as a specific system, object, or assembly in terms of size, shape, location, quantity, and orientation with detailing, fabrication, assembly, and installation information. The MEB *refurbishment works management* parameter values are shown in Table 4.

The algorithm in Figure 3 is a conceptual framework proposed by the authors to carry out the refurbishment work management in an orderly manner. Of course, this phase of the refurbishment process can be done in a different way. Actually, it is truly important to obtain the required parameter values, and in general, the proper functioning of the installed facilities.

The algorithm in Figure 3 begins with the output of the previous phase: *MEB project certification*, i.e., the certified energy refurbishment project. From it begins the *construction management*. At this point, it is necessary to emphasize something already said in the introduction of the article: the refurbishment process itself or the way to carry out the necessary construction works, and facilities is not part of the uhuMEBr methodology. It only monitors that in each of its steps the energy efficiency requirements be met, in order to obtain the corresponding certifications. So, probably (the case study is an example of this), the refurbishment paths to reach an MEB can be different and all valid. Then, the construction manager, in charge of *construction management* (Figure 3), must ensure that, in terms of energy efficiency, the refurbishment works are carried out in accordance with the *MEB Project certification*.

Following the order, shown in Figure 3 (not mandatory), the first test to perform is the thermal transmittance. The envelope thermal transmittance (rate of heat transfer through the building envelope), i.e., the combined transmittance of the opaque and opening building envelope must be less than 0.3 Wm^2/K. Of course, in the event that this requirement is not accomplished, it is mandatory to act on the building envelope until it is achieved. If not, the building could lose its MEB rating because it could have an energy demand above the established limit (see Table 1).

On the other hand, the *envelope thermography test* must confirm that the building has not significant thermal bridges. If present and significant, they must be corrected, as they can move the building away from accomplishing the MEB energy consumption requirements (see Table 1).

Regarding the envelope airtightness test, it must show the proper degree of airtightness of the building. Each air exhaust orifice causes a waste of energy, therefore, it is very important to avoid them, and if detected, cover them.

The construction manager must certify that MEB facilities and systems installed in the refurbished building have been executed in agreement with the project certification and functioning properly according to MEB parameters (see Tables 3 and 4).

Finally, if during the construction phase important modifications of the original *energy refurbishment project* are carried out, they must be reflected in the project and a new MEB project certification must be obtained (see, in this order, Figures 2 and 3).

The refurbishment works management algorithm ends with the *MEB as-refurbished certification*, which guarantees the MEB level (nZEB, ZEB, or +ZEB) of the refurbished building.

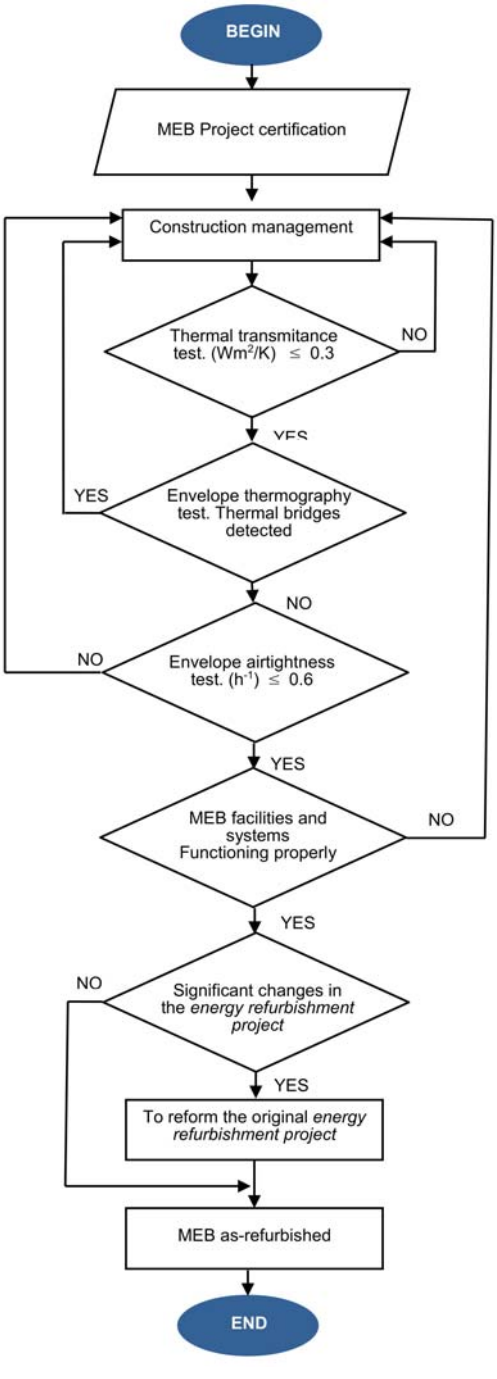

Figure 3. Refurbishment works management algorithm.

Table 4. MEB refurbishment works management requirements.

Parameters	Explanation
$U_e < 0.3\ Wm^2/K$	Tested by specific measurements in the building envelope as described in Reference [30].
No thermal bridges	Tested by thermography of the facades.
n_{50}-value $< 0.6\ h^{-1}$	Tested by airtightness test envelope.
MEB facilities and systems	Check that the building facilities and systems (separate electrical circuits, sensors for the required measurements, appliances, lighting, RES, etc.) meet the MEB requirements and that the HAS working properly for the MEB needs.

3.3. Refurbished Building Energy Management Stage

The uhuMEBr (see Figure 1) is applicable throughout the life cycle of the building. The goal is clear: it is so important that a refurbished building can reach the MEB classification as long as it can be maintained over time. Therefore, the building needs continuous monitoring during its life cycle. That is why the information obtained through the HAS and the analysis of the collected data is so important.

This stage is also controlled and coordinated by means of the BIM methodology, specifically under the LOD500 (it is a field-verified representation in terms of size, shape, location, quantity, and orientation) under the operation manager's direction. The operations management of the refurbished building, as well as the MEB life cycle management requirements, are shown in Table 5.

Each refurbished building must have its own maintenance program. In this case, and as far as uhuMEBr is concerned, it is focused exclusively on the energy efficiency issue, i.e., not considering the maintenance of a lift, for example.

Regarding maintenance, see Table 5, the *corrective maintenance* is intended for the repair or replacement of devices, equipment, machinery or building infrastructure based on the damage detected. It is the oldest type of maintenance and only acts when the fault is already present.

Preventive maintenance is devoted to avoiding unexpected faults. The way to get it is by programming maintenance tasks (cleaning, greasing, eye inspection, measurements, etc.), while the devices, equipment, machinery or building infrastructure are still properly working. Well-programmed preventive maintenance decreases the corrective maintenance frequency.

Table 5. Operations management of the refurbished building. MEB life cycle management requirements.

Tasks	Explanation
Corrective maintenance	Repair or replacement of devices, equipment, machinery or building infrastructure based on the damage detected.
Preventive maintenance	Regular and programed maintenance intended to avoid unexpected faults. So, it is performed, while the devices, equipment, machinery or building infrastructure are still properly working.
Predictive maintenance	It is advanced maintenance intended for preventing failures through data analysis to identify patterns and predict issues before they happen.
Continuous data analysis	Predictive maintenance needs data collection and processing.
Monthly verification	It means that the previous month the MEB has functioned as expected.
Annual operation	It means that the previous year the MEB has functioned as expected; it becomes a certification.

Finally, the brand new and advanced maintenance is the predictive one. In order to carry it out, it is necessary to have data available. Indeed, this is one of the fundamental tasks of the HAS in the refurbished building: to deliver functioning data. *Predictive maintenance* acts in advance of the maintenance itself, i.e., it saves costs on preventive maintenance because maintenance tasks are not scheduled; they are only carried out when justified. To do this, it is necessary to have

much information about the devices, machinery or infrastructure in maintenance, since it needs to estimate their degradation. Through data collection and processing (usually using artificial intelligence techniques), predictive maintenance allows early fault detection, time for failure prediction and resource optimization.

Finally, continuing with Figure 1 and Table 5, if the MEB requirements are fulfilled monthly, this leads to monthly verification ok; if not, the refurbished building energy management stage goes to the decision branch that leads to a corrective maintenance (the usual) or to a new refurbishment whose scope will depend on the magnitude of the problem detected. The correct monthly verification for one year leads to the annual operation certification of the refurbished building.

4. Results

Now, as has been introduced in Section 2 of this paper, the application of uhuMEBr to the energy efficient refurbishment of a dwelling in the *Casas del Carmen* building will be explained.

4.1. Existing Building Energy Evaluation stage

As depicted in Figure 1, the uhuMEBr methodology begins with the *existing building energy evaluation stage*, i.e., a measurement campaign devoted to get information from the first six parameters of Table 1: Total energy demand for HVAC, total primary energy demand, indoor air quality, annual percentage of thermal discomfort time, dwelling envelope airtightness (measured by an airtightness test) and thermal bridges (measured by thermographies). In addition to the above parameters, it is necessary to measure another aspect that has significant influence on energy demand: it is about thermal transmittance (see Table 2), measured by a specific test. Airtightness test, thermal bridges test and thermal transmittance test inform about the behavior of the outer building envelope.

To collect the data from the first four parameters of Table 1, a HAS (introduced in Section 2) was installed for a whole year (from January to December 2016) in the dwelling to control its energy efficiency behavior.

4.1.1. Total Energy Demand for HVAC

Figure 4 shows, for example, the dwelling energy consumption obtained along 24 h in a cold day (16 December 2016) and a hot day (10 August 2016). This analysis for a year yielded the data of 36 kWh/m^2 as total energy demand for HVAC. This value is more than triple the MEB requirement (see Table 1).

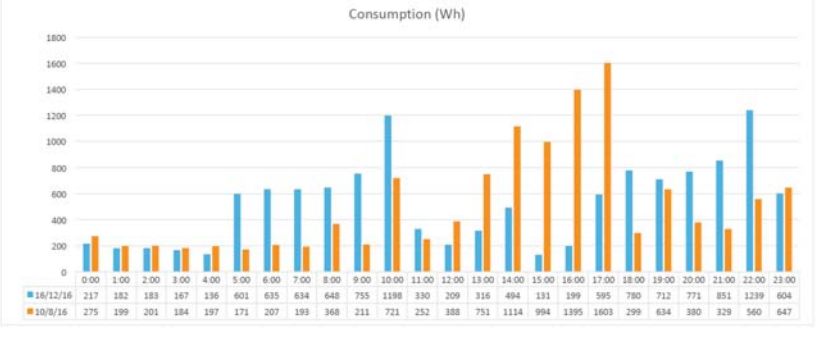

Figure 4. Examples of the dwelling energy consumption in a winter and summer day before refurbishment.

4.1.2. Total Primary Energy Demand

Figure 5 shows the annual dwelling primary energy demand. The obtained value was 526.29 kWh/m^{2}year. This value is far away from the MEB of Table 1. The most demanded month was January with a total of 5800.47 kWh; the less demanded months were April and May with a total of 3510.04 and 3480.62 kWh, respectively.

Figure 5. Monthly energy consumption in a whole year (2016) before refurbishment.

4.1.3. Indoor Air Quality

During the monitored year, the dwelling remained the parts per million (ppm) of CO_2 in the air in an average of 600 ppm. At no time during the year, the percentage of CO_2 exceeded the MEB limit of 1000 ppm. (Table 1).

4.1.4. Thermal Discomfort

During the monitored year, the dwelling remained at a thermal discomfort time of an average of 23%. The maximum thermal discomfort time percentage was recorded during winter (months of December, January and February) and summer (months of July, August and September) with average values of 32.5% and 35%, respectively.

4.1.5. Building Envelope Airtightness Test

The envelope airtightness test in the dwelling yielded a result of 2.85 h^{-1} for 50 Pa (620 m^3/h for a total inner air volume of 217.70 m^3). Figure 6 shows different dwelling leakage values according to each pressure difference (from 25 to 70 Pa) obtained from the test.

4.1.6. Envelope Thermography Test

Figure 7a shows the thermal behavior of the dwelling exterior façade (enclosed in red). Notice the weak points in windows and shutter boxes. Moreover, observe the behavior of a dwelling on the bottom right (enclosed in blue) in the same building. This dwelling (Figure 7b) has a very deteriorated façade (enclosed in blue), unlike the one that is enclosed in red that is freshly painted. Figure 8 shows the thermal behavior of the dwelling façade that overlooks the backyard. Notice, again, the weak points in windows and shutter boxes. Note also that the interior I (Figure 8a) is more deteriorated than the exterior (Figure 8b). Figures 7 and 8 show the poor thermal behavior of the dwelling and its need to improve it.

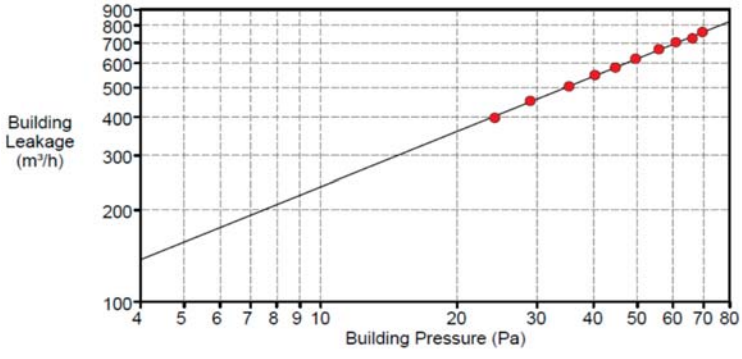

Figure 6. Dwelling envelope airtightness test before refurbishment.

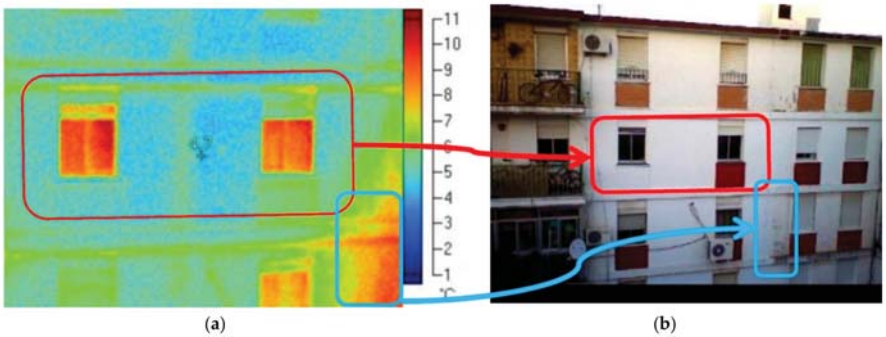

Figure 7. (**a**) Thermal behavior of the dwelling exterior façade; (**b**) Visual aspect.

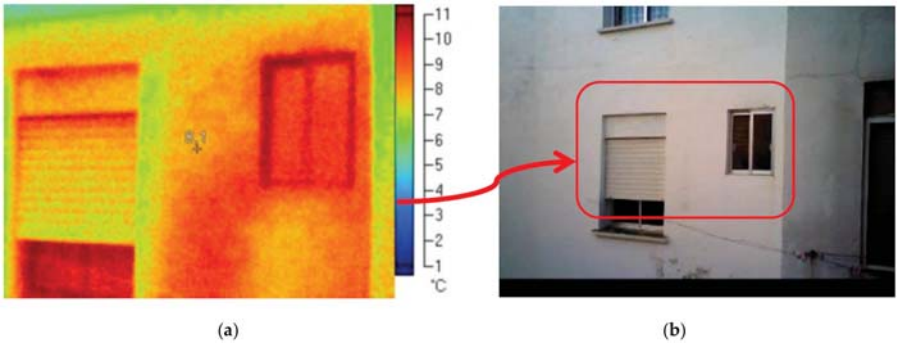

Figure 8. (**a**) Thermal behavior of the dwelling façade that overlooks the backyard; (**b**) Visual aspect.

4.1.7. Thermal Transmittance Test

The existing building energy evaluation stage finished with the thermal transmittance test (Figure 9). The measured *u*-value was 2.73 W/m^{2}K; which is well above the 0.3 Wm^2/K required for a MEB. Once the dwelling's weak points were detected, an existing building energy report was drafted (Figure 1). Its study by the technicians led to the decision that it was impossible to solve the multiple dwelling failures (in the field of the energy efficiency only) through corrective maintenance, so the decision to carry out energy refurbishment was made (see Figure 1).

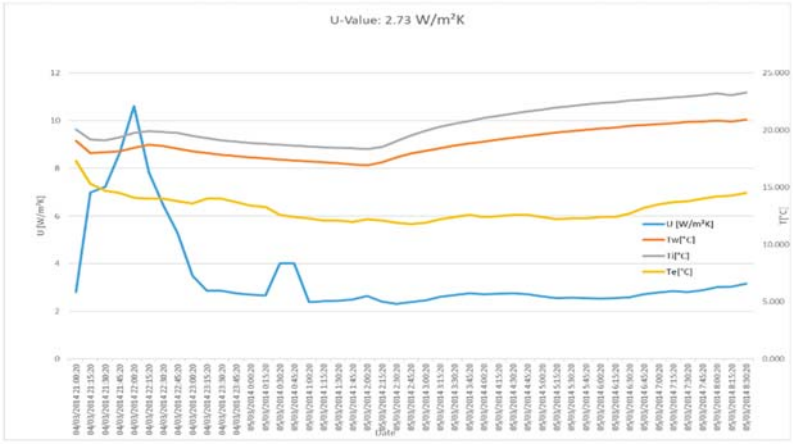

Figure 9. Dwelling envelope thermal transmittance test before refurbishment.

4.2. Existing Building Energy Refurbishment Stage

Taking advantage of the *energy refurbishment project* (Figures 1 and 2), the owners carried out rooms reforms in the dwelling but, from the point of view of uhuMEBr, the only interest is on energy efficiency reforms.

Figure 1 shows that the refurbishment works begin with a mandatory agreement: expected MEB grade + refurbishment program + available budget. In this case, due to the nature of the action, is a pilot project subsidized by the administration, the objective was to know the actual refurbishment cost of a dwelling and the obtained actual result, to extend it later, in a first phase, to the whole building, and in a second, to the whole neighborhood, since it was composed of similar buildings, such as the refurbished one.

With the above in mind, the starting hypothesis was, as uhuMEBr establish, to get a nZEB MEB dwelling only by architectural design (of course, keeping the continuity of the extIfacade since it was mandatory), and later, depending on the necessary commitment between the cost and the possibilities of the building (especially roof and balconies available), to try, by renewable facilities, an approach to ZEB. With this initial framework, the *energy refurbishment project* was faced.

4.2.1. Energy Refurbishment Project

The *Casa del Carmen* building responds to a type of massive construction (not prefabricated) with a mixed steel-reinforced concrete structure and external masonry envelope. This and their respective variants represent the predominant construction technology in subtropical countries, such as Spain, and in general, southern Europe.

In order to accomplish the MEB architectural refurbishment design requirements of Table 2, the algorithm presented in Figure 2 was implemented.

Architectural Refurbishment Design

Regarding this phase, the aim was to accomplish each one of the parameters of Table 2. Thereby, the concepts of *sunshine* and envelope thermal transmittance were faced together (this means that improving one of them would improve the other). The reason for proceeding in this way was that nothing could be done regarding the orientation of the building, nor on the exterior façade (the dwelling also has an interior façade that overlooks a backyard), which should be preserved in its current appearance; so, the only path to face sunshine and thermal transmittance was to improve

carpentries (frame and glasses), as well as thermal insulation from outside (from the inside would significantly reduce the useful area in the dwelling) of the dwelling, in façade walls.

For a better understanding and monitoring of the explanations, the dwelling floor plan is shown in Figure 10.

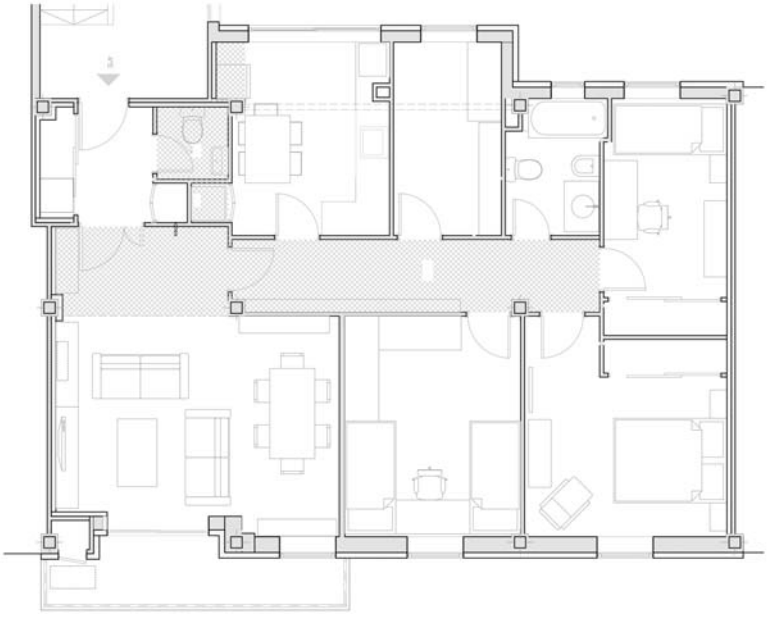

Figure 10. Dwelling floor plan.

At this point, it is necessary to point out that the dwelling exterior façade is oriented to the south, so the pivotal goal was to prevent the penetration of direct solar radiation most of the year. After simulations, new window glasses with solar factor (or *g*-value that measures the percentage of heat that passes through the glass) of 0.5 (the lower the solar factor, the higher the solar protection) were chosen. This combined with electric sliding shutters governed by the HAS would allow to take advantage of the sun in winter and avoid it in summer. The final solution implemented on façade windows and balcony door was practicable seven chambers PVC carpentry (transmittance = 1.1 W/m^2K) housing glasses with double insulation chamber, incorporating low emissive film and both filled with 90% argon gas. The new glazing installed was 6/15/6/15/6 (transmittance = 0.6 W/m^2K).

The windows solution needed to be combined with a solution for the rest of the façade (exterior walls) in order to obtain an envelope thermal combined transmittance <0.3 Wm^2/K. To achieve it, considering the losses in windows and balcony door (booth transmittances were above 0.3 W/m^2K), it was necessary to devise an outdoor isolation system with a transmittance lower than 0.3 Wm^2/K. After simulations, the commitment between thickness, composition and cost were to design an external thermal insulation composite system (ETICS) with 10 cm (5 + 5) thick rockwool (transmittance = 0.036 W/m^2K). Of course, the color and relief of the façade should be preserved. Why rockwool? Because of its fire resistance, thermal properties, acoustic performance, sturdiness, aesthetic, water behavior and circularity, since it can be obtained from waste from other industries. The simulations show that with this solution, the façade's combined transmittance was quite less than 0.3 Wm^2/K.

Once the façades were solved (the same solutions described above to the exterior façade were applied to the interior one), it was the turn of the party walls. In this case, obviously, the solution had to be carried out from inside the dwelling under refurbishment. Specifically, it was designed

a self-supporting double plasterboard partition with 8 cm (double layer 4 + 4 cm) thick inner glass wool (an insulating material made from fibers of glass, with very good thermal and acoustic insulation properties, in addition to repelling water).

It was finally the turn of the floor and ceiling. For the improvement of the ceiling slab, a 4 cm thick glass wool attached with profile aluminum for screwing single gypsum plasterboard was designed. For the improvement of the floor slab, an 8 mm thick composite carpet, consisting in three layers of extrude polyethylene, air bubbles and the aluminum film was designed. This carpet should extend over the existing cladding, serving as the basis for the new floor, which it was going to be made of laminated wood.

Continuing with Figure 1 and Table 2, regarding dwelling *form factor* (F) it is very good because the outer envelope surface is 43.45 m^2 and the inner volume enclosed is 217.70 m^3, so $F = 0.20\ m^2/m^3$, widely fulfilling the MEB requirement. However, it is not a merit of the refurbishment project, but one that is innate to the housing because of its location in the building.

With regard to airtightness, it is mainly a constructive issue because it is mandatory to seal any gap (carpentry joints, shutter boxes, wires, etc.) that can connect the exterior and interior of the dwelling. Avoiding this, the simulations showed that the airtightness MEB requirements might be reached. Nevertheless, in order to improve the sealing of the dwelling, the application of a continuous layer of gypsum-cement mortar on the inner side of the thermal envelope was prescribed.

As for natural ventilation, again, in an innate way and without the need for refurbishment, the dwelling can comfortably provide natural ventilation during temperate seasons. In fact, the existence of two opposite facades, street and courtyard, facilitates the cross ventilation when the windows and doors are opened. The dwelling meets the requirement of $S_{of} > 0.05$ (Table 2). The obtained exact value was 0.11 (11.75 m^2 practicable opening surface in a constructed area of 106.74 m^2). However, what happens in non-temperate seasons, as the coldest days of winter or, worse at this latitude, summer days? In this case, the necessary commitment between insulation and ventilation must be resolved by a specific facility that can solve the ventilation without losing the indoor/outdoor temperature isolation. The adopted solution (in the next section is explained) was a double duct ventilation facility with high efficiency heat recovery. This facility is completely independent of the ACHP.

With regard to avoid thermal bridges, the façade and party walls, isolation systems must be applied in two layers of 5 and 4 cm each. The first placed between the original wall and the steel frame, and the second inside it, perfectly filling the gaps between the steel frames.

Finally, and again in an innate way, the dwelling natural lighting accomplish the MEB requirements (Table 2) since $S_{gf} > 0.1$, specifically 0.13. This value corresponds to a 13.46 m^2 glazed in a constructed area of 106.74 m^2.

According to the software simulation carried out (under normal comfort condition, from 22 to 25 °C and RH around 50%), the total HVAC consumption was 8.87 kWh/m^2 year, below the value of 10 demanded by the uhuMEB methodology (see Table 2).

Facilities and Systems Engineering Retrofitting Design

Once the passive design of *Casas del Carmen* was completed (*architectural* refurbishment *design*, see Figure 1 and Table 2) with all the MEB requirements satisfied, the *Facilities and systems engineering retrofitting design* phase followed.

The first challenge was how to resolve the ventilation system. It was necessary to find out the place for the heat recovery ventilation facility (fan box and pipes), something that is not easy in a 2.35-m-high dwelling.

Despite it, a double duct ventilation facility with high efficiency heat recovery (93%) was introduced in the dwelling. There are a general intake and exhaust for the air in inner yard facade, over de kitchen window and separated both a distance of 2 m. The renewed air is introduced inside the house through the ventilation facility using blinds located over the doors of the living room and bedrooms.

The wasted air is exhausted from the kitchen and the bathrooms, but exchanging first its heat with the incoming air. This double flow ventilation system, plus the air filters (F8, fine filter—average particle retention efficiency of 0.4µm, between 90% and 95%—for the incoming air and G4—average dust retention better than 60%—for the exhaust air) located in the fan, creates a proper air circuit that improves the indoor air quality.

Following Table 3, regarding HVAC, but now focused on the ACHP, the key was to achieve a consumption under 10 kWh/m^{2}year. Then, considering the proposed outer envelope insulation, this was not a problem because the small thermal gap that had to be overcome, both in winter and in summer, allowed using a low power system that, in addition, was expected to work for short periods of time. Specifically, a multisplit with a single exterior unit commercial system was prescribed. Since dwelling had three bedrooms and living room, four wall splits were required. Regarding the cooling/heating capacity, around 7000/9000 W. For this capacity and considering an A++ energy efficiency system, its power consumption should not exceed 2000 W.

With respect to DHW, the adopted renewable solution has been two conventional flat solar thermal collectors. This is probably the cheapest and easiest solution because the *Casa del Carmen* building has a large roof available and lacks shadows from adjoining buildings. The entire facility was sized to meet 100% of the DHW demand. On this site, with such high solar radiation (65 kWh/m^2 in the worst month—December—and 240 kWh/m^2 in the best month—July) it is easy to cover all the yearly DHW needs taking advantage of the sun; the only precaution is to connect an overheating valve to avoid overpressure in the hottest months, when solar radiation is higher.

Regarding appliances, a market solution was adopted following Table 3 guidelines. However, to improve the efficiency of the set of appliances working together, an ingenious solution was adopted: the refrigerator and induction cooker have been installed on opposite walls, thus, avoiding heat transfer between them. In addition, the washing machine and dishwasher have separate hot and cold water inlets, thus, avoiding the need for electric heating. Finally, in order to avoid the loss of dwelling airtightness, the extractor hood is not connected to the outdoor; instead, an activated carbon grid filter has been used.

As for the lighting, the house is fully equipped with LED lamps, fully complying with the requirements of Table 3.

At this point, according to the software simulation carried out (including DHW, appliances and lighting), the total primary energy demand was reduced by 88%, from 526.29 kWh/m^{2}year (see Section 4.1.2) to 67.34 kWh/m^2 year Now, it was completely within the MEB value of ≤80 kWh/m^{2}year (see Table 3).

Following with Table 3, the used HAS was developed by the authors (the reason is that with the owner's permission, the dwelling serves as a real-time laboratory (thorough an INTERNET connection, and of course, without cameras) on the actual behavior of the refurbished dwelling. MEB data is received in our research laboratory. The HAS allows for all the MEB requirements, i.e., consumption for each electrical circuit, RH and temperature in each room and outside the home, and indoor air quality. Based on these measurements, it runs the electrical sliding shutters, the double duct ventilation facility and warns the residents when it is convenient to open the windows. The HAS also monitors the RES facility.

Special mention deserves the RES. In addition to the HDW facility, the dwelling incorporates a photovoltaic panel (PV) facility on the roof of the building. Specifically, 8 PV of 250 Wp each that make up a 2 kWp facility. This power does not allow the dwelling to move from nZEB to ZEB, but brings it closer.

4.2.2. Refurbishment Works Management

As stated in Section 3.2.2, the construction manager must ensure that, in terms of energy efficiency, the works are carried out in accordance with the MEB Project certification (Figure 3). Then, following the energy refurbishment project (previous section), the work done will be shown.

Figure 11a,b shows the ETICS. In Figure 11a, the balcony façade, still under construction, is enclosed in blue line and the rest of the façade, already finished, is enclosed in red line. Notice the window openings still no frames or glass, and because it is mandatory, the color and relief of the façade have been preserved. Figure 11b shows the balcony façade detail with the thick rockwool that is part of the ETICS.

Figure 12 shows the internal thermal insulation composite system (applied in party walls): (a) under construction and (b) finished. Figure 13 shows an example of the new façade windows with double insulation chamber glasses and electric sliding shutter.

(a) (b)

Figure 11. (**a**) Exterior façade of the dwelling under refurbishment; (**b**) Balcony façade detail.

(a) (b)

Figure 12. (**a**) Internal thermal insulation composite system; (**b**) Finished.

Figure 13. New façade windows.

To achieve the dwelling airtightness, a continuous layer of gypsum-cement mortar on the inner side of the thermal envelope has been applied. The facilities holes were sealed with the same mortar, applying silicone to the inside of the corrugated tubes and cable entries. Joints between carpentry and walls were filled with special joints and high-durability flexible self-expanding polyurethane foam

(Figure 14). The shutters' airtightness was improved with silicone (boxes) and brush gaskets, getting airtight the entire set.

Figure 14. Special joints and high-durability flexible self-expanding polyurethane foam used.

Regarding the double duct ventilation facility, almost all its air pipes go through the corridor ceiling (Figure 15), which was raised down 20 cm to 2.15 high—just over the door flashings—to hide them. It was a big concern can do it in a social house without affecting its habitability. With respect to ACHP, the solution to be installed was simple: an exterior unit with four wall splits, one for each room, so nothing special is worth commenting on it after what was said.

Taking advantage of the building roof availability, all the RES facilities were mounted there. Figure 16 depicts the installed RES facilities.

Figure 15. Double duct ventilation facility installed in the dwelling.

With respect to the HAS, it meets the MEB requirements and takes measurements from the RES as well. It uses sensors and data acquisition systems developed by the authors' research group [26–28]. Figures 17 and 18 show, for example, a couple of HAS screens with the ACHP off. The HAS can be consulted and monitored, with the appropriate access permission, from any device with an Internet connection.

Now, following Figure 3, the construction manager must carry out or supervise the different tests to ensure that the *refurbishment works management* runs as established by the *energy refurbishment project*.

Figure 19 shows the dwelling measured *u*-value after refurbishment. The result was 0.30 W/m^{2}K, which met the corresponding MEB value (Table 2).

Figure 16. (**a**) Flat solar thermal collectors; (**b**) Photovoltaic panel facility.

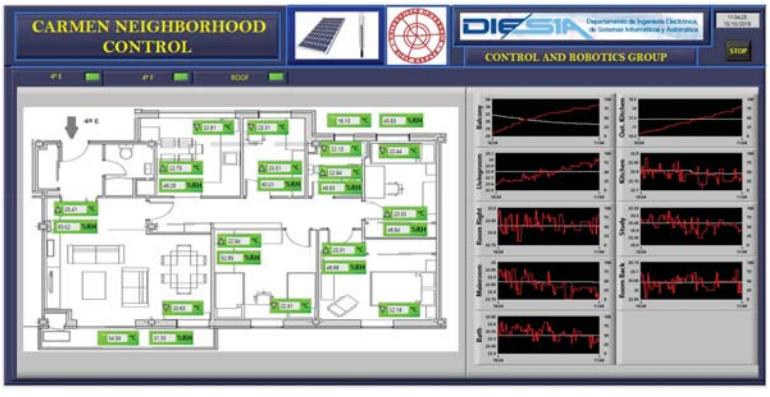

Figure 17. HAS screen. Left: Dwelling plan with measurements of temperature, relative humidity and air quality. Right: Measurements versus time for each room.

Figure 18. HAS screen. Left: Photovoltaic facility and its production. Right: Electrical circuits of the dwelling.

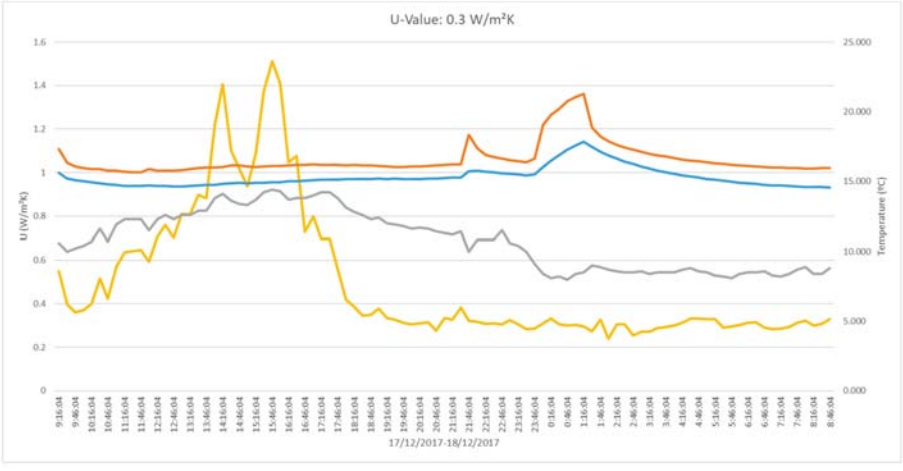

Figure 19. Dwelling envelope thermal transmittance test after refurbishment.

Regarding thermal envelope behavior, Figure 20a shows the difference between the part of the envelope that has been retrofitted with ETICS and new windows (encircled in white color in Figure 20b) and the original building envelope. Thermal bridges caused by concrete columns and slab borders can be clearly seen in the façade below the refurbished dwelling. This part of the façade is radiating energy out, i.e., losing energy.

Finally, the standard procedure EN 13829 BDT was followed to check the building envelope airtightness. Figure 21 shows the test results. The average value was 0.59 h^{-1}, which is lesser than 0.60 h^{-1} that is the maximum allowed for an MEB (Table 2).

Once it was verified that all MEB facilities and systems were functioning properly and that it was not necessary to make any important modifications to the *energy refurbishment project*, the *as-refurbished certification* was approved by the project manager.

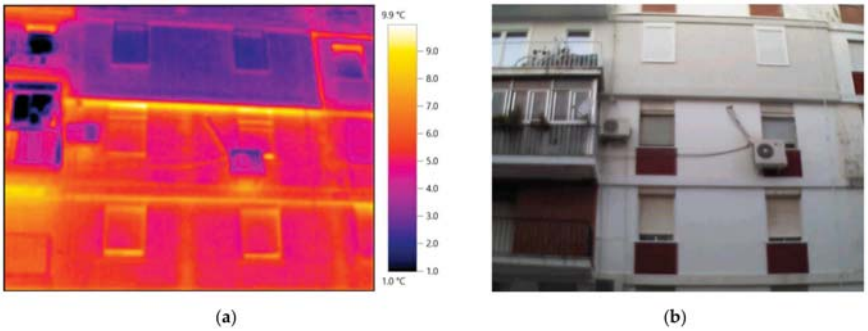

Figure 20. (**a**) Dwelling thermography test after refurbishment; (**b**) Visual aspect.

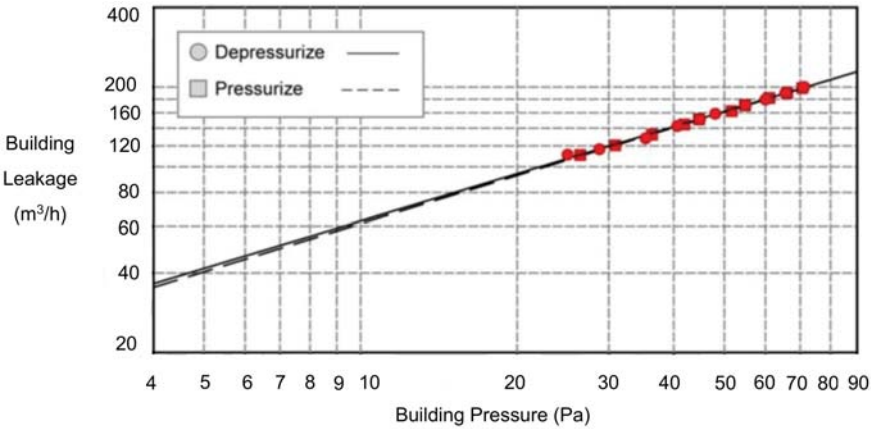

Figure 21. Dwelling envelope airtightness test after refurbishment.

4.3. Refurbished Building Energy Management Stage

This last stage of the proposed methodology (see Figure 1) is currently underway. The recent completion of refurbishment works, about a year, means that the *refurbished building energy management stage* is in its beginnings; so, no maintenance works are in progress, but there are data availability from the HAS. Figures 22 and 23 show the hourly evolution of the temperature and relative humidity in the dwelling (temperature and humidity average, i.e., taking into account all the measurements points (Figure 17) in two random days of summer and winter with the ACHP off. Figure 24 shows the amount of energy generated and sold (the surplus is sold to the grid) monthly (2018) by the PV facility. The production peak (May-September) happens during hotter months, coinciding with the more irradiance ones (Figure 25).

The maintenance of the building, see Figure 1, is being carried out since the end of the refurbishment works. As dwelling functions as a real laboratory for our research group, this task is being carried out by us. At the end of 2018, the dwelling obtained its first *annual operation certification* (Figure 1). As expected, the dwelling perfectly met the MEB requirements. This year will be the first full year after refurbishment, and up to now, the monthly verification has been satisfactory.

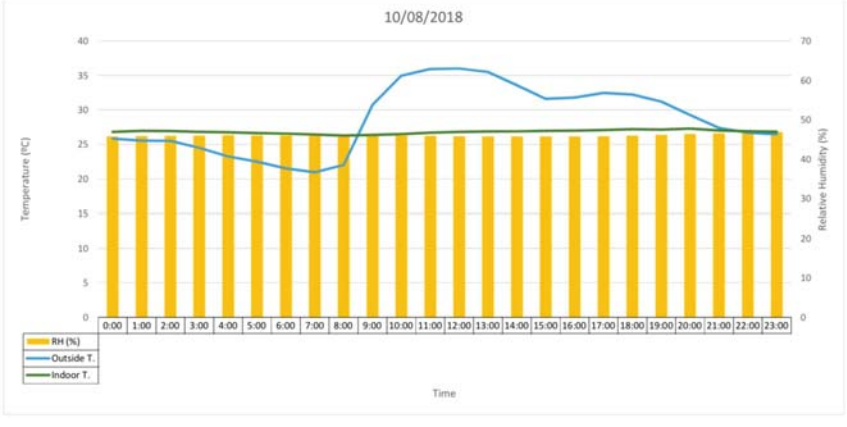

Figure 22. Hourly evolution of temperature and relative humidity after refurbishment in a random summer day.

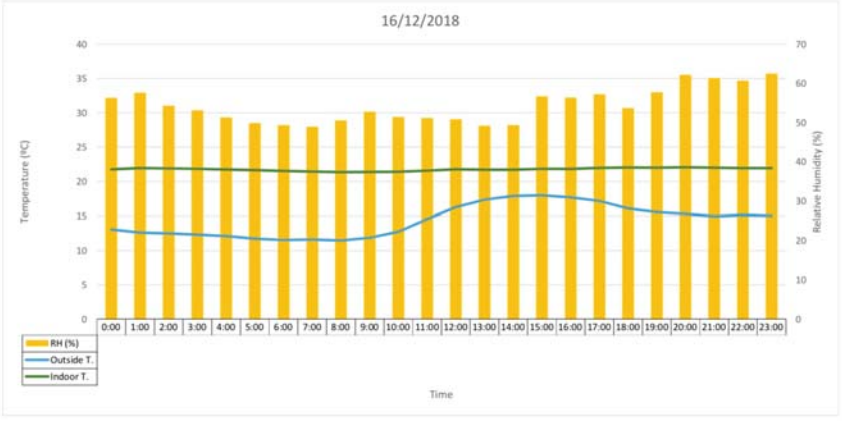

Figure 23. Hourly evolution of temperature and relative humidity after refurbishment in a random winter day.

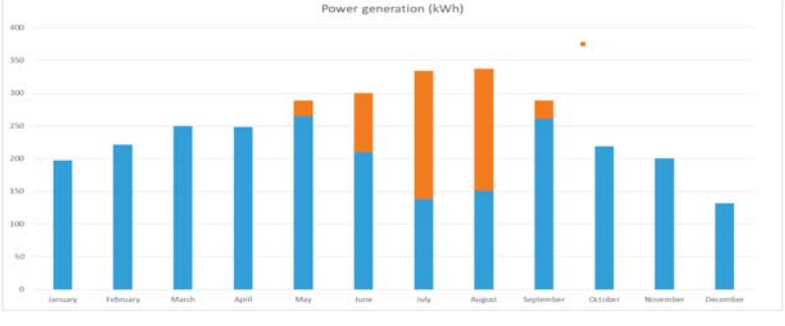

Figure 24. Monthly energy generated (blue + orange) and surplus (orange) in a whole year (2018) after refurbishment.

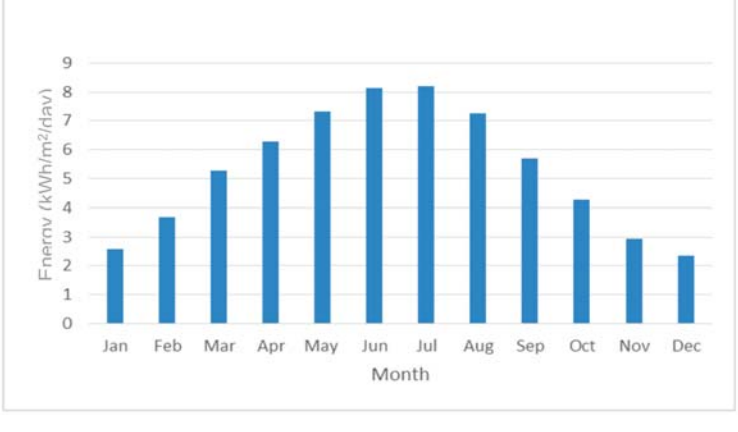

Figure 25. Monthly global solar irradiance during 2018 at *Casa del Carmen* location.

5. Discussion

Based on the results obtained in the previous section, the proposed uhuMEBr methodology summarized in Figures 1–3 and Tables 1–5, is discussed below.

The *existing building energy evaluation* stage (Figure 1), compulsory because is the only way (at least effective) that the true efficiency of the building in its current state can be known, shows which energy efficiency parameters are out of range (following Tables 1 and 2). From here and once the corresponding report has been delivered, the technicians must have enough information to make the best decision on whether the building can solve its energy efficiency problems thorough maintenance tasks or it needs a refurbishment.

Using their own HAS that the authors, together with their research group, have developed, as well as thorough different tests carried out on the site, the energy efficiency operation of the dwelling under study was analyzed. In that way, information about the following parameters was collected:

- *Total energy demand for HVAC* and *total primary energy demand*: Much higher than allowed for a MEB. This found a clear explanation later, when the tightness and thermal behavior of the outer envelope was checked. Figure 4 shows how in winter, the period of time with the highest consumption (heating mainly), corresponds with the normal operation according to the dwelling inhabitants' habits. First thing in the morning until the inhabitants of the dwelling leave it and from late afternoon to the late evening, when the inhabitants are again at home. However, in summer (August is usually a holiday month for students and workers in Spain), consumption skyrockets (mainly due to air conditioning) because the inhabitants are at home at the hottest hours. Figure 5 shows that the months with less demand correspond to those with more pleasant weather because there is no need for HVAC nor artificial lighting.
- *Indoor air quality*: Very good, as a result of the house not being well sealed. Then, regardless of whether the windows and doors are closed, the exchange of air with the outside is maintained.
- *Thermal discomfort*: As one would expect, the months with the highest electricity consumption are those with the greatest thermal discomfort (see Table 1 and the parameter four explanation).
- *Building envelope airtightness test* and *thermal bridges test*. Both tests explain that due to the poor behavior of the outer envelope and its lack of airtightness (Figures 6–8), the dwelling needs more electrical energy than that required in an MEB to achieve thermal comfort. In the dwelling, all original windows were sliding type, which is inconvenient to obtain airtightness. Even more, the main access door was made of wood and without sealing elements; in addition, the kitchen had two vents to evacuate the gases from the gas cooker and the DHW gas boiler.
- Regarding the behavior of the thermal envelope, Figures 7 and 8 explain the influence of the façade state. As expectIe worst the facade state is the worst thermal behavior presents.
- *Thermal transmittance test*: This test explains the heat transfer through the outer dwelling envelope. Obviously, to prevent heat escapes from the dwelling in winter and heat inputs in summer, the outer envelope thermal transmittance must be low enough. In this case, it was poor, about nine times greater what is allowed for an MEB (Figure 9). This also helps explain the dwellings high electricity consumption.

Since the *existing building energy report* (Figure 1) shown that virtually all parameters were outside the mandatory MEB values, the only way to convert the dwelling into an MEB was to perform a specific energy refurbishment.

The first step of the *existing building energy refurbishment stage* requires a mandatory agreement between the owners and the technicians in order to establish the refurbishment degree based on the expected MEB degree (nZEB, ZEB or +ZEB) that must comply with the applicable regulations, work planning, and of course, the available budget. It is important to point out that uhuMEBr does not deal with an architectural refurbishment, due to aesthetic or to new distribution or usage changes. The methodology is only interested in the aspects that influence energy efficiency.

From the above, the *existing building energy refurbishment stage* goes to the technicians exclusively. Then, following Figures 1 and 2, the first phase was to carry out the *energy refurbishment project*, which involves architectural refurbishment, but also facilities and systems engineering retrofitting.

The *energy refurbishment project* must design all the works and procedures to carry out in the building (during the stage of refurbishment works) to comply with the parameter's values of Tables 2 and 3. In the case study shown in this paper, all the proposed solutions have been commercial, and they have been carefully explained in the manuscript. Of course, this is always advisable because they are generally cheaper solutions, and as important as the previous one, they are proven.

A very important aspect to consider when carrying out the *energy refurbishment project* is that technicians must have solid training in energy simulation tools. At this phase of the uhuMEBr, the only way to verify the designs and proposals (that lead to the *MEB project certification*) is by means of simulation, hence, the importance of their knowledge and domain. In the best case, perhaps it will be possible to complement simulations with some specific tests on a specialized laboratory.

Completed and certified the refurbishment project (Figure 2) the refurbishment works began (Figure 3). From the architectural point of view, following what was prescribed in the project, the main actions (explained by Figures 11–14) consisted of:

- Installation of an ETICS on the façades.
- Insulation actions in the interior of the dwelling: party walls, floor and ceiling slabs.
- Works to install double duct ventilation.
- New carpentry (windows and balcony door) with electric sliding shutters.

Regarding airtightness, it is a constructive aspect that should be treated carefully, specifically the window and door fittings. In this regard, shutter boxes are a traditional source of problems. In fact, workers were trained on the site to best apply the products for joints and insulators.

From the facilities and systems point of view, following what was prescribed in the project, the main actions (explained by Figures 15–18) have consisted of:

- Installation of a double duct ventilation with heat recovering.
- Installation of the rest of the HVAC system, i.e., the ACHP.
- Installation of a RES facility with two goals: to solve the HDW by flat solar collectors and generate renewable electricity by PV panels.
- Installation of a non-commercial HAS (a specific design by the research group of the authors). It is composed of sensors, hardware, software and communication capabilities via Wi-Fi and internet.
- Installation of electric sliding shutters governed by the HAS in all windows and balcony door.
- Ensuring that appliances and lighting meet at least the requirements of class A ++.

The double duct ventilation with heat recovery solves the necessary observance of air quality in a tightness dwelling, but without losing (winter) or gaining (summer) heat from the outside. As for ACHP, the adopted solution has been very simple and cheap; really with the airtightness degree achieved for dwelling, nothing superior and more expensive was needed.

With respect to the RES facility, the large solar radiation at this latitude makes it possible to cover all the yearly DHW by this energy, and if enough PV panels are installed (it was not the case), also the required electrical energy.

As the dwelling (its operation regarding energy efficiency), with the corresponding owner permission, is serving as a permanent laboratory for our research group, a specific HAS adapted to the needs is being used. It can measure all mandatory MEB variables, as well as those of RES; moreover, it can control the sliding shutters depending on whether the dwelling can take advantage of solar radiation and natural lighting. Additionally, measuring the gap between the external temperature and the internal comfort temperature can warn the dwelling inhabitants that is advisable to open the windows. Obviously, this avoids the use of double duct ventilation that the HAS disconnects in this

situation. Figures 17 and 18 show a couple of current HAS screens (15 October 2019) with the ACHP off. The first one presents the real-time environmental conditions of the dwelling with measurements of temperature, RH and air quality (ppm CO_2). Note that, while the outside temperature ranges between 18.3 °C (backyard) and 19.09 °C (front facade), the indoor temperature ranges only between 22.13 °C and 23.53 °C, i.e., within the comfort temperature. This demonstrates the excellent behavior of the outer dwelling envelope.

Figure 17 shows the real-time behavior of the generation/consumption of electrical energy in the dwelling. FV panels are supplying 0.1200 kWh (by a power of 1440.71 W) of which the dwelling is consuming only 0.1117 kWh (by a power of 1340.9 W). The surplus after losses (0.0047 kWh by a power of 56.5846 W) is sold to the grid. Obviously, as the dwelling electrical facility registers an energy surplus, the external grid consumption is zero. As can be seen, the ACHP is off, and the only consumption is due to the electric kitchen.

The works checking finished with the following tests: thermal transmittance (measured on outer envelope walls), outer envelope thermal behavior (by thermographies) and outer envelope airtightness (varying the pressure between inside and outside the dwelling).

The transmittance test (Figure 19) showed the behavior of the outer envelope with respect to the heat exchange between the interior and exterior of the dwelling. The test implies that the measurement, to be valid, needs to reach steady-state conditions, which means that the average u-value remains substantially constant over time.

Attending Figure 19, it can be observed that practically in the last 13 h the average transmittance value remained constant, which means that the steady-state has been reached and the measured transmittance value was 0.30 W/m^{2}K, which fulfilled the corresponding MEB value (Table 2). A comparison between Figures 9 and 19 shows that the improvement of the envelope transmittance thanks to the ETICS and the carpentry was from 2.73 W/m^{2}K to 0.3 W/m^{2}K, i.e., about nine times smaller.

Figure 20 complements the results reflected in Figure 19 with respect to thermographies. This Figure shows the dwelling thermography test. It is easy to appreciate the drastic change of the outer envelope thermal behavior after the refurbishment. In fact, if a comparison between Figures 7, 8 and 20 is carried out, immediately it can be observed that, after the refurbishment, the dwelling practically does not lose energy thorough its outer envelope (façades).

Regarding the last test (envelope airtightness) showed in Figure 21, the improvement achieved with the refurbishment is notorious because in Figure 6, before refurbishment, was 2.85 h^{-1} and in Figure 21, after refurbishment, is nearly five times smaller, i.e., now the dwelling is considerably more hermetic. This immediately translates into a lower need for ACHP to reach the comfort temperature in the dwelling. The results are shown in Figures 19–21 justify the suitability of the ETICS, window glasses and frames chosen.

The last stage of the proposed methodology is the *refurbished building energy management stage* (Figure 1), i.e., the monitoring and control of the dwelling behavior in operation, with its inhabitants inside carrying out their usual life. The goal is to extend the MEB requirements achieved by the refurbishment thorough the entire dwelling life cycle. Obviously, the refurbishment has been so recent that there are still no maintenance needs; however, the HAS is continuously delivering data for analysis. In that sense and as examples, Figures 22 and 23 show the hourly evolution of the temperature and humidity (both average, taking into account all the measurements points, please see Figure 17) in two specifics days of summer and winter with the ACHP off. The first Figure demonstrates the optimal functioning of the dwelling regarding its outer envelope and airtightness. The outside temperatures in the summer day ranged around 21 °C at 7:00 to a peak of 36 °C from 10:30 to 13:00, and then fell gradually. However, in the face of an external thermal jump around 15 °C, the average temperature in the dwelling is around 26 °C throughout the day; with a thermal jump not greater than 2 °C. Figure 23 demonstrates the same, but in winter; in this case, the outdoor temperature ranged around 12 °C at 6:00 to a peak of 18 °C from 13:00 to 17:00. However, the indoor temperature remains constant at around 22 °C throughout the day. So, the excellent behavior of the outer dwelling

envelope allows that, if necessary, with little ACHP power consumption, the dwelling can permanently maintain a comfortable temperature.

With respect to the PV facility, the analysis of Figure 24 shows that in summer, the production is maximized, due to the greater solar radiation (please see Figure 25). This, together with the fact that July and August are usually vacation months with less electricity consumption (in this year, 2018, the inhabitants were outside most of the time, on the beach and travelling), creates a considerable surplus that is sold to the external network. This does not mean that in the remaining months, the PV facility can meet the dwelling needs. The graph represents the total energy, but not per hour; so throughout the entire day (and night of course), since there is no energy storage (the facility has no batteries), sometimes there may be a surplus of energy, but other deficits, so the connection to the external grid is mandatory because it guarantees the consumption needs. In fact, the dwelling consumes from the external grid thorough the year, obviously much more in winter because the PV facility production is lower.

6. Conclusions

In this paper, a new methodology for building energy efficient refurbishment in subtropical climates has been proposed. It is called uhuMEBr because it complements the uhuMEB methodology already published by the authors that are dedicated to new buildings. In this case, the goal is to convert an existing building into a minimum energy building.

Regarding energy efficiency, the operation of a building in a subtropical climate must meet part of the year with the goal of cold climates (usually in winter and part of spring and autumn depending on latitude, height and proximity to the sea), i.e., to prevent heat from escaping from the building. However, the rest of the year must meet with the goal of tropical climates, i.e., to prevent heat from entering the building. Even, depending on the site, some days (or part of them) of the year (usually in spring, autumn and summer nights) it should take advantage of the comfort of the outside weather to exchange with it.

All the above conditions complicate the process of refurbishment and operation of a building in a subtropical climate. With this in mind, the proposed methodology develops all the necessary steps to convert an energy inefficient building in an efficient one. However, the methodology does not end when the refurbishment is carried out, since it continues the rest of the life cycle of the building, maintaining its efficiency.

The methodology comprises the following three stages: the *existing building energy evaluation*, where its energy efficient operation is measured and analyzed, which allows the knowledge of the refurbishment degree that the building needs; the *existing building energy refurbishment* which ranges from the architectural and engineering project to the refurbishment works themselves; and finally, the *refurbished building energy management*, which covers the entire operation of the refurbished building, including its maintenance, in order to maintain its condition as a minimum energy building for the rest of its life cycle.

The proposed methodology has been illustrated with an actual case study that shows step by step its practical application. The case study has been carefully chosen because it is social housing with very poor insulation, limited refurbishment capabilities and located in a low-income neighborhood, so it was a challenge in itself.

In terms of energy efficiency, from an initial (before refurbishment) HVAC energy demand of 36 kWh/m^{2}year, the refurbishment carried out achieved a 75% reduction, up to 8.87 kWh/m^{2}year, entirely within the uhuMEBr requirement of ≤10 kWh/m^{2}year. In addition, from an initial (before refurbishment) primary energy demand of 526.29 kWh/m^{2}year, the developed refurbishment achieved a 88% reduction, falling to 67.34 kWh/m^{2}year; again, entirely within the uhuMEBr requirement of ≤80 kWh/m^{2}year.

Author Contributions: S.G.M. wrote the article, M.Á.M.B. carried out the experimentation, and J.M.A.M. supervised and reviewed all work and the manuscript. All authors have read and agreed to the published version of the manuscript.

Funding: This work has been funded by the DPI2017-85540-R Project supported by the Spanish Ministry of Economy and Competitiveness and by the European Union Regional Development Fund. Some parts of the study have been funded by the resources of the research team "Control y Robótica (TEP192)" from the University of Huelva (Spain).

Acknowledgments: This work is a contribution of the DPI2017-85540-R Project supported by the Spanish Ministry of Economy and Competitiveness and by the European Union Regional Development Fund. It was also supported by the Project Code G-GI3000/IDI_TEP192, of the Andalusia regional government (Spain).

Conflicts of Interest: The authors declare no conflict of interest.

Abbreviations

ACHP	Air Conditioning and Heat Pump
AIA	American Institute of Architects
BDT	Blower Door Test
BIM	Building Information Modeling
DHW	Domestic Hot Water
ETICS	External Thermal Insulation Composite System
EPS	Expanded Polyethylene
EU	European Union
HAS	Home Automation System
HVAC	Heating, Ventilating and Air Conditioning
LOD	Level of Development
LED	Light Emitting Diode
MEB	Minimun Energy Building
nZEB	Nearly Zero Energy Building
PPM	Parts Per Million
PV	Photovoltaic Panels
PVC	Poly Vinyl Chloride
RES	Renewable Energy Systems
RH	Relative Humidity
uhuMEB	University of Huelva Minimum Energy Building
uhuMEBr	University of Huelva Minimum Energy Building Refurbished
ZEB	Zero Energy Building
+ZEB	Net Energy Generator Building

References

1. Eurostat, & Union Européenne. *Eurostat, Energy, Transport and Environment Indicators*; Eurostat, Ed.; E. Pocketbooks: Luxembourg, 2014.
2. European Parliament. *Directive 2002/91/EU of the European Parliament and of the Council of 16 December 2002 on the Energy Performance of Buildings*; European Parliament: Brussels, Belgium, 2002; pp. 65–71.
3. European Parliament. *Directive 2010/31/EU of the European Parliament and of the Council of 19 May 2010 on the Energy Performance of Buildings*; European Parliament: Brussels, Belgium, 2010; pp. 13–35.
4. European Parliament. *Directive 2012/27/EU of the European Parliament and of the Council of 25 October 2012 on Energy Efficiency, Amending Directives 2009/125/EC and 2010/30/EU and Repealing Directives 2004/8/EC and 2006/32/EC*; European Parliament: Brussels, Belgium, 2012; pp. 1–56.
5. European Parliament. *Directive 2018/844/EU of the European Parliament and of the Council of 30 May 2018 Amending Directive 2010/31/EU on the Energy Performance of Buildings and Directive 2012/27/EU on Energy Efficiency*; European Parliament: Brussels, Belgium, 2018; pp. 75–91.
6. Yang, X.; Zhang, J.; Zhao, X. Factors affecting green residential building development: Social network analysis. *Sustainability* **2018**, *10*, 1389. [CrossRef]

7. Encinas, F.; Marmolejo-Duarte, C.; Wagemann, E.; Aguirre, C. Energy-efficient real estate or how it is perceived by potential homebuyers in four Latin American countries. *Sustainability* **2019**, *11*, 3531. [CrossRef]
8. Mattoni, B.; Guattari, C.; Evangelisti, L.; Bisegna, F.; Gori, P.; Asdrubali, F. Critical review and methodological approach to evaluate the differences among international green building rating tools. *Renew. Sustain. Energy Rev.* **2018**, *82*, 950–960. [CrossRef]
9. Cordero, A.S.; Melgar, S.G.; Márquez, J.M.A. Green Building Rating Systems and the New Framework Level(s): A Critical Review of Sustainability Certification within Europe. *Energies* **2019**, *13*, 66.
10. Melgar, S.G.; Bohórquez, M.A.M.; Márquez, J.M.A. uhuMEB: Design, construction, and management methodology of minimum energy buildings in subtropical climates. *Energies* **2018**, *11*, 2745. [CrossRef]
11. Hughes, S.; Yordi, S.; Bescoes, l. The Role of Pilot Projects in Urban Climate Change Policy Innovation. *Policy Stud. J.* **2020**. [CrossRef]
12. Aranda, J.; Zabalza, I.; Conserva, A.; Millán, G. Analysis of energy efficiency measures and retrofitting solutions for social housing buildings in Spain as a way to mitigate energy poverty. *Sustainability* **2017**, *9*, 1869. [CrossRef]
13. Boemi, S.N.; Papadopoulos, A.M. Energy poverty and energy efficiency improvements: A longitudinal approach of the Hellenic households. *Energy Build.* **2019**, *197*, 242–250. [CrossRef]
14. Mrówczyńska, M.; Skiba, M.; Bazan-Krzywoszańska, A.; Bazuń, D.; Kwiatkowski, M. Social and infrastructural conditioning of lowering energy costs and improving the energy efficiency of buildings in the context of the local energy policy. *Energies* **2018**, *11*, 2302.
15. Fu, X.; Qian, X.; Wang, L. Energy efficiency for airtightness and exterior wall insulation of passive houses in hot summer and cold winter zone of China. *Sustainability* **2017**, *9*, 1097.
16. Ge, J.; Wu, J.; Chen, S.; Wu, J. Energy efficiency optimization strategies for university research buildings with hot summer and cold winter climate of China based on the adaptive thermal comfort. *J. Build. Eng.* **2018**, *18*, 321–330. [CrossRef]
17. Bing, X.; Jiaqi, W. A comparative research on energy efficiency of atrium morphological types in hot-summer and cold-winter zone. *IPPTA Q. J. Indian Pulp Paper Tech. Assoc.* **2018**, *30*, 165–178.
18. Lu, M.Y.; Ge, J.; Shen, T.T. Strategies for energy efficiency renovation and evaluation system of Existing Residential Building in hot summer and cold winter zone. *Lowl. Technol. Int.* **2015**, *17*, 111–120. [CrossRef]
19. Zhang, Y.; Wang, X.; Hu, E. Optimization of night mechanical ventilation strategy in summer for cooling energy saving based on inverse problem method. *Proc. Inst. Mech. Eng. Part A J. Power Energy* **2018**, *232*, 1093–1102. [CrossRef]
20. Wang, Y.; Kuckelkorn, J.; Zhao, F.Y.; Spliethoff, H.; Lang, W. A state of art of review on interactions between energy performance and indoor environment quality in Passive House buildings. *Renew. Sustain. Energy Rev.* **2017**, *72*, 1303–1319. [CrossRef]
21. Anderson, J.S. Energy use excellence and the building envelope. *J. Green Build.* **2019**, *14*, 179–204. [CrossRef]
22. Schnieders, J.; Eian, T.D.; Filippi, M.; Florez, J.; Kaufmann, B.; Pallantzas, S.; Paulsen, M.; Reyes, E.; Wassouf, M.; Yeh, S.C. Design and realisation of the Passive House concept in different climate zones. *Energy Effic.* **2019**. [CrossRef]
23. Baglivo, C.; Congedo, P.M.; Fazio, A.; Laforgia, D. Multi-objective optimization analysis for high efficiency external walls of zero energy buildings (ZEB) in the Mediterranean climate. *Energy Build.* **2014**, *84*, 483–492. [CrossRef]
24. Stazi, F.; Bonfigli, C.; Tomassoni, E.; Di Perna, C.; Munafò, P. The effect of high thermal insulation on high thermal mass: Is the dynamic behaviour of traditional envelopes in Mediterranean climates still possible? *Energy Build.* **2015**, *88*, 367–383. [CrossRef]
25. Rodrigues, E.; Fernandes, M.S.; Gaspar, A.R.; Gomes, Á.; Costa, J.J. Thermal transmittance effect on energy consumption of Mediterranean buildings with different thermal mass. *Appl. Energy* **2019**, *252*, 113437. [CrossRef]
26. Bohórquez, M.A.M.; Gómez, J.M.E.; Márquez, J.M.A. A new and inexpensive temperature-measuring system: Application to photovoltaic solar facilities. *Sol. Energy* **2009**, *83*, 883–890. [CrossRef]
27. Martínez, M.A.; Andújar, J.M.; Enrique, J.M. Temperature measurement in PV facilities on a per-panel scale. *Sensors* **2014**, *14*, 13308–13323. [CrossRef] [PubMed]
28. Martínez, M.A.; Andújar, J.M.; Enrique, J.M. A new and inexpensive pyranometer for the visible spectral range. *Sensors* **2009**, *9*, 4615–4634. [CrossRef] [PubMed]

29. Andújar Márquez, J.M.; Martínez Bohórquez, M.Á.; Gómez Melgar, S. Ground thermal diffusivity calculation by direct soil temperature measurement. Application to very low enthalpy geothermal energy systems. *Sensors* **2016**, *16*, 306.
30. Andújar Márquez, J.M.; Martínez Bohórquez, M.Á.; Gómez Melgar, S. A New Metre for Cheap, Quick, Reliable and Simple Thermal Transmittance (*U-Value*) Measurements in Buildings. *Sensors* **2017**, *17*, 2017.

energies

MDPI

Article

Energy and Economic Analysis for Greenhouse Ground Insulation Design

James Bambara * and Andreas K. Athienitis

Department of Building, Civil and Environmental Engineering, Concordia University, Montreal, QC H3G 1M8, Canada; aathieni@encs.concordia.ca

* Correspondence: j_bamba@encs.concordia.ca; Tel.: +1-514-848-2424 (ext. 7080)

Received: 29 October 2018; Accepted: 16 November 2018; Published: 20 November 2018

Abstract: Energy and life cycle cost analysis were employed to identify the most-cost effective ground envelope design for a greenhouse that employs supplemental lighting located in Ottawa, Ontario, Canada (45.4° N). The envelope design alternatives that were investigated consist of installing insulation vertically around the perimeter and horizontally beneath the footprint of a greenhouse with a concrete slab and unfinished soil floor. Detailed thermal interaction between the greenhouse and the ground surface is achieved by considering 3-dimensional conduction heat transfer within the TRNSYS 17.2 simulation software. The portion of total heat loss that occurred through the ground was approximately 4% and permutations in ground insulation design reduced heating energy consumption by up to 1%. For the two floor designs, the highest net savings was achieved when perimeter and floor zone horizontal insulation was installed whereas a financial loss occurred when it was also placed beneath the crop zone. However, in all cases, the improvement in economic performance was small (net savings below $4000 and reduction in life cycle under 0.2%). Combined energy and life cycle cost analysis is valuable for selecting optimal envelope designs that are capable of lowering energy consumption, improving economics and enhancing greenhouse durability.

Keywords: greenhouse; floor envelope design; ground heat transfer; thermal insulation; energy modeling; life cycle cost analysis

1. Introduction

Heating is a major operating expense for greenhouses that are located in mid-to-high latitude locations. In addition, heating is commonly achieved by burning fossil fuels, which contribute to greenhouse gas emissions and environmental degradation. Since most of heat loss occurs through the envelope (walls, roof and floor), optimal designs, which reduce energy use while addressing economics concerns, are required.

Much of the prior work regarding ground heat transfer has been performed for buildings [1–3] whereas only a few studies have been performed for greenhouses. Most of the research for greenhouses ground heat transfer consists of case studies [4–6] or the potential for design improvements such as ground-source heat exchangers [7,8]. Various levels of modeling resolution have been employed for representing the thermally massive ground. Most studies have separated the ground into one or more relatively thin earth layer and energy transfer is solved using 1-dimensonal (1D) heat transfer equations [9–11]. The advantage of 2-dimensional (2D) heat transfer is that it enables interaction with the greenhouse edge/perimeter. For instance, a numerical study using computational fluid dynamics enables visualization of the ground temperature profile [12]. However, the entire footprint (and interaction with the perimeter) can only be studied when 3-dimensional (3D) discretization of the ground is performed, whereby the ground is divided into control volumes so that overall heat transfer can be solved analytically or numerically. The only study that employed 3D analysis of ground heat

transfer in greenhouses used the WUFI software to compare thermal energy use for a greenhouse located above, below and at ground level [13]. However, these studies did not consider economic implications of employing ground insulation. To determine the most cost-effective design, a combined energy and economic analysis must be performed. To our best knowledge, there has not been any previously published work regarding the detailed 3D energy analysis and economic analysis for the design of a greenhouse floor envelope.

The aim of this paper is to demonstrate how integrated thermal-daylight energy analysis and life cycle cost analysis (LCCA) can be employed to identify the most-cost effective ground insulation design for a greenhouse that controls light to a consistent daily integral located in Ottawa, Ontario, Canada (45.4° N, mid-latitude, 4560 heating degree-days).

2. Energy and Economic Analysis

For greenhouses that supplement daylight with horticultural lighting, the choice of cover materials may alter the daylight availability and lighting electricity use. The effect of such alterations must be transferred to the module which calculates the thermal energy consumption. In theory, modifying the envelope design for greenhouses that control light to a consistent daily integral (e.g., for producing leafy green vegetables year-round near the consumer) should not affect crop growth as the supplemental lighting and heating system control will adjust and compensate for any changes in the indoor climate. Consequently, the analysis of this type of greenhouse will be carried out by omitting biological aspects.

The decision-making process for envelope design requires both energy and economic analysis. The performance obtained through energy simulation is not sufficient for determining a cost-optimal design. From an investor's perspective, the incremental cost of alternative claddings should be outweighed by operational savings. This study employs LCCA and the net savings method was selected for comparing envelope design alternatives. The net savings method can provide detailed economic analysis in a time efficient manner (it only requires economic aspects that are impacted by a design variation to be quantified).

2.1. Greenhouse Characteristics

A schematic of the 929.03 m^2 (10,000 ft^2) greenhouse considered for this study is provided in Figure 1. It has an equal length and width of 30.48 m, and a height of 3.66 m. The floor surface consists of a crop zone located between two identical floor areas (floor zone). Heating and ventilation are used to control inside humidity and temperature. The greenhouse does not utilize humidification, cooling is provided by mechanical ventilation only, and condensation is ignored in this study. The artificial lights (AL) are the only internal gain considered in the model.

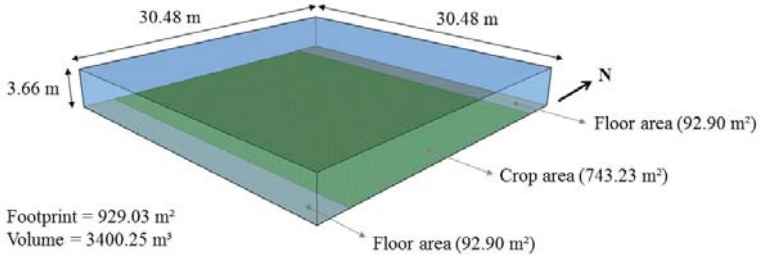

Figure 1. Schematic showing the modeled greenhouse.

2.2. Energy Analysis

TRNSYS 17.2 was selected for the transient simulation of the greenhouse climate [14]. Type 56 multizone building model was used to create the greenhouse energy model [15]. Figure 2 depicts the three most common locations for ground insulation of greenhouse: vertical along the perimeter, slanted

wing, and horizontal beneath the floor. Slanted wing insulation is excluded from the analysis because of modeling limitations of the TRNSYS software (Version 17.2, Solar Energy Laboratory, Madison, WI, USA).

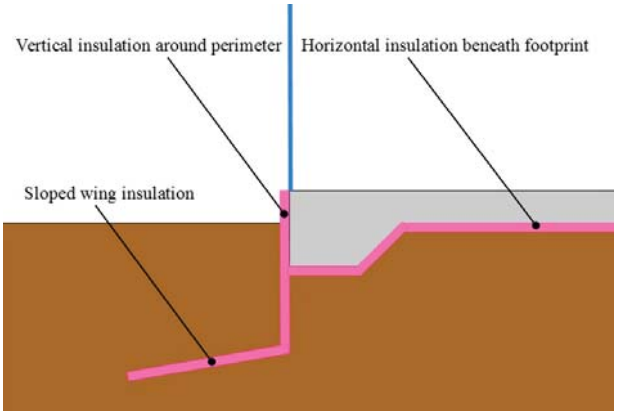

Figure 2. Common locations for ground insulation on buildings.

This study compares a base case greenhouse (BCGH) without thermal insulation to alternative designs (AGH) that consist of: (1) perimeter insulation; (2) perimeter insulation and horizontal insulation beneath the both floor zones; (3) perimeter insulation and horizontal insulation beneath both floor zones and the crop zone; and (4) perimeter insulation and horizontal insulation beneath the crop zone. Installing horizontal insulation alone is not considered because it is unlikely that it would be a viable option if perimeter insulation is not. The objective of this study is to determine whether the most cost-effective envelope design for the floor is no insulation, perimeter insulation, or a combination of perimeter and horizontal insulation. The investigation will consider two types of greenhouse floor designs: one with a concrete slab over soil (Figure 3) and another with unfinished soil (Figure 4). For the greenhouse with a ground consisting of unfinished soil, the concrete slab is replaced with a single layer of soil whose thickness is satisfactory for root development. As depicted in Figure 4, when thermal insulation is installed, it is assumed to be located beneath this layer of arable soil.

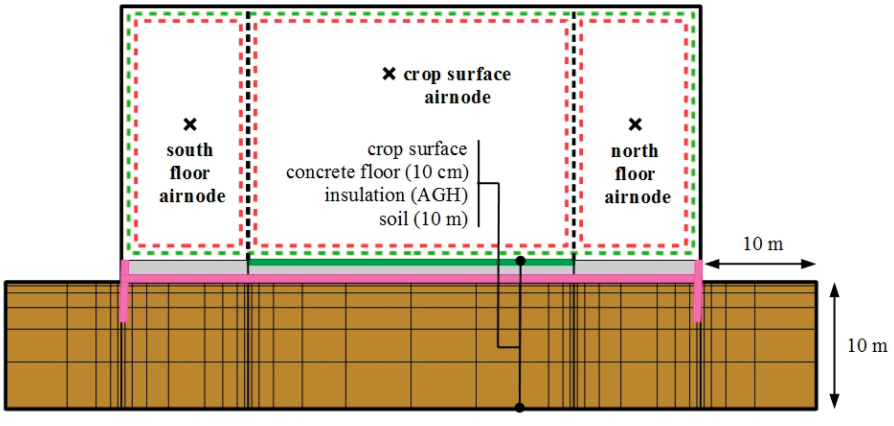

Figure 3. Greenhouse model with three airnodes and discretized ground zones.

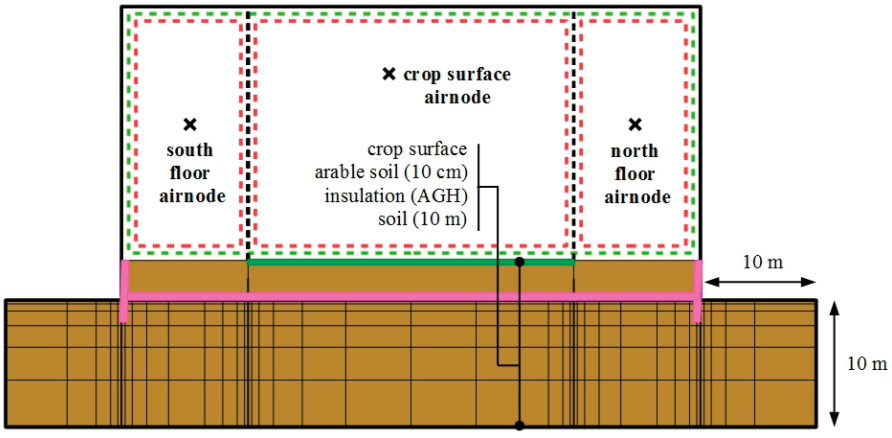

Figure 4. Same greenhouse model as Figure 3 but with a floor consisting of unfinished soil.

The two models which enable detailed 3D ground heat transfer in TRNSYS consist of Type 49 [16] and Type 1244 [17]. When these ground heat transfer models are selected for interaction with Type 56, each floor area must be associated with a dedicated thermal zone or airnode. Therefore, the adopted solution for enabling 3D ground heat transfer with multiple floor areas within a single zone is to separate the greenhouse into multiple airnodes. The volume associated with each airnode is dictated by the ground area which is belongs to.

The modeled greenhouse has three floor surfaces (two for the floor and one for crop zone) and therefore the single greenhouse zone is separated into three airnodes. The surface between the airnodes is defined as a "virtual" surface (shown in Figure 5), which enables unobstructed radiation heat transfer. Meanwhile, mass and energy flow between airnodes is specified by air "coupling" to maintain the well-mixed assumption (that is commonly achieved using horizontal airflow fans in greenhouses). Figures 3 and 4 illustrate the three airnode greenhouse models with the discretization of the ground into control volumes. A user defined volume of soil is specified in the model so that 3D heat transfer can be calculated within this "ground zone". Each airnode contains a certain volume of soil beneath the area that is in contact with the ground, with smaller discretization of the layers around the perimeter that are in contact with adjacent airnodes. The same concept is applied for the areas in contact with the exterior environment.

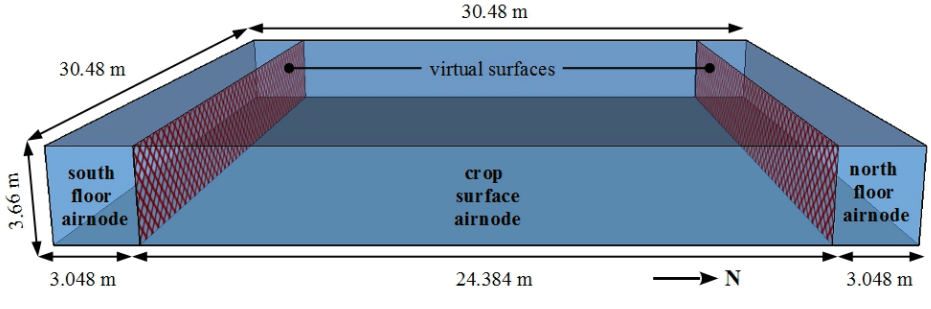

Figure 5. Schematic showing the two virtual surfaces that separate the three airnodes.

Annual and design day energy simulations of the model are performed to obtain the energy-related inputs that are needed for conducting the LCCA. The energy analysis is separated into daylight, artificial light and thermal modules. The analysis method for the daylight and artificial light modules is the same as presented by the authors in [18].

2.2.1. Thermal Module

The purpose of the thermal module is to determine the heating energy consumption and peak demand, with artificial lighting as a dynamic input. Figure 6 illustrates the major mass and energy fluxes that are considered in the three airnode greenhouse model. The energy balances are presented for the crop surface airnode that is located between the two floor airnodes (north and south sides of the greenhouse).

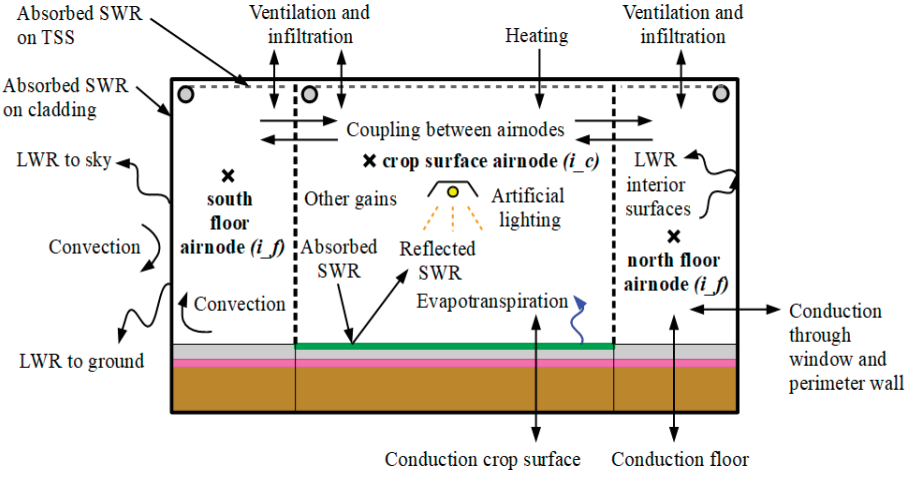

Figure 6. Schematic showing the mass and energy fluxes considered in the three airnode greenhouse model.

The mass balance for the crop surface airnode (i_c) is given by:

$$X_m \cdot \rho_a \cdot V_{i\_c} \cdot (\partial \omega_{i\_c} / \partial t) = m_{vent} + m_{inf} + m_{ET} + m_{m\_cpl} \quad (1)$$

where:

X_m is the moisture capacitance multiplier (dimensionless)
ρ_a is the density of air (kg m^{-3})
V_{i_c} is the volume of the crop zone airnode (m^3)
$\partial \omega_{i\_c}$ is the rate of change of the inside air humidity ratio (kg$_{water}$ kg$_{dry_air}{}^{-1}$)
∂t_i is the rate of change of time (s)
m_{vent} is the mass transfer rate of water due to ventilation (kg hr^{-1})
m_{inf} is the mass transfer rate of water due to infiltration (kg hr^{-1})
m_{ET} is the mass transfer rate of water due to evapotranspiration (kg hr^{-1})
m_{cpl} is the mass transfer rate of water due air movement between the airnodes (kg hr^{-1}).

The energy balance for the crop surface airnode is written as:

$$X_{th} \cdot \rho_a \cdot c_{p\_a} \cdot V_{i\_c} \cdot (\partial T_{i\_c} / \partial t) = Q_{conv\_si} + Q_{vent} + Q_{inf} + Q_{TSS} + Q_{AL} + Q_{heat} + Q_{cpl} \quad (2)$$

where:

X_{th} is the thermal capacitance multiplier (dimensionless)
c_{p_a} is specific heat of air at constant pressure (kJ kg^{-1} °C^{-1})
∂T_{i_c} is the rate of change of the inside air temperature (°C)
Q_{conv_si} is the energy flux due to convection (W)

Q_{vent} is the energy flux due to ventilation (W)
Q_{inf} is the energy flux due to infiltration (W)
Q_{TSS} is the energy flux from the thermal shading screen (W)
Q_{AL} is the energy flux from artificial lighting (W)
Q_{heat} is the energy flux from auxiliary heating (W)
Q_{cpl} is the energy flux due air movement between the airnodes (W).

The energy balance for the inside surface (*si*) of the cover and an opaque surface is expressed as:

$$0 = Q_{cond} + Q_{conv\_si} + Q_{swr\_si} + Q_{lwr\_si} \quad (3)$$

where:

Q_{cond} is the energy flux due to conduction (W)
Q_{swr_si} is the energy flux due to absorbed shortwave radiation (W)
Q_{lwr_si} is the energy flux due to longwave radiation (W).

The energy balance for the outside surface (*so*) of the cover and an opaque surface is described by:

$$0 = Q_{cond} + Q_{conv\_so} + Q_{swr\_so} + Q_{lwr\_sky} + Q_{lwr\_gnd} \quad (4)$$

where:

Q_{conv_so} is the energy flux due to convection (W)
Q_{swr_so} is the energy flux due to absorbed shortwave radiation (W)
Q_{lwr_sky} is the longwave radiation energy flux to the sky (W)
Q_{lwr_gnd} is the longwave radiation energy flux to the ground (W).

Neglecting chemical energy conversion by photosynthesis, the energy balance for the crop interior surface is defined as:

$$0 = Q_{cond} + Q_{swr\_c} + Q_{swr\_c\_AL} + Q_{conv\_si} + Q_{lwr\_si} - Q_{ET} \quad (5)$$

where:

$Q_{swr\_c\_AL}$ is the energy flux due to absorbed shortwave radiation on the crop surface (W)
Q_{ET} is the energy flux due to evapotranspiration (W).

The mass balance for each floor airnode (*i_f*) is given by:

$$X_m \cdot \rho_a \cdot V_{i\_f} \cdot \left(\partial \omega_{i\_f} / \partial t \right) = m_{vent} + m_{inf} + m_{cpl} \quad (6)$$

The energy balance for each floor airnode is written as:

$$X_{th} \cdot \rho_a \cdot c_{p_a} \cdot V_{i\_f} \cdot \left(\partial T_{i\_f} / \partial t \right) = Q_{conv\_si} + Q_{vent} + Q_{inf} + Q_{TSS} + Q_{cpl} \quad (7)$$

The energy balance for the floor inside surface is expressed as:

$$0 = Q_{cond} + Q_{swr\_si} + Q_{conv\_si} + Q_{lwr\_si} \quad (8)$$

2.2.2. Energy Modeling Key Assumptions

The details and assumptions for calculating the variables in the above energy and mass balance equations, when different than the values provided in [18], are presented below:

Weather data: A typical meteorological year weather file for Ottawa, Ontario, Canada (45.4° N, which represents mid-latitude climatic conditions) was used to run the simulations and obtain the

energy performance over a one-year period. The temperature of the far-field soil is set using the Kasuda correlation which estimates the temperature of the soil at a given depth given the time of year, the soil properties, the average annual soil surface temperature, the amplitude of the annual soil surface temperature, and the day of the year at which the minimum annual surface temperature occurs [19]. Type 15 calculates the sky temperature for longwave radiation calculations [16]. A simulation timestep (Δt) of 15 min was selected. The energy model was simulated for 638 days, with the first nine months of results discarded to eliminate the initial condition transient effects. For an analysis at peak heating design conditions, no solar radiation, a wind speed of 10 m s^{-1}, exterior air relative humidity of 20%, exterior air temperature of −21.8°C, sky temperature of −52 °C, and ground temperature of 8 °C were selected [20].

Ground heat transfer: The ground surface is divided in two floor zones and one crop zone (80% of footprint). The moisture effects are not accounted for in the model. The type of crop produced is a leafy green vegetable (e.g., lettuce, kale). The crop layer is approximated as a smooth and uniform surface located directly above the concrete slab or soil surface and its thermal resistance and capacitance are ignored.

Several models with varying levels of detail exists in TRNSYS for calculating heat transfer with the ground. Type 49 and 1244 are the most detailed models because they enable 3D heat transfer to be calculated between the Type 56 multi-zone building model and the ground surface. A user defined volume of soil is considered for ground heat transfer and divided into control volumes that are assumed to be cubic in shape so there are six unique heat transfers to analyze per control volume. There are several other available methods to solve coupled 3D differential heat transfer equations using iterative methods. Type 49 uses an approximate analytical solution [16] whereas Type 1244 uses finite difference [21]. The analytical solution is timestep independent but does require an iterative solution inside the subroutine to solve the coupled differential equations.

Type 49 assumes that the ground surface is flat, that the soil has homogenous thermal properties, and that the temperature of the ground surface is not affected by the presence of the building and is instead set from long term averages. In contrast, Type 1244, does not impose the assumption of a soil surface temperature unaffected by the building and can model cases where the zone is underground. A major limitation of Type 1244 is that is cannot model perimeter insulation when the building ground level is the same as the exterior. Since perimeter insulation is a practical ground insulation technique for greenhouses, Type 49 was selected to calculate 3D heat transfer between the greenhouse and the ground.

A "map" of the soil surface was created. This map file indicates to the model whether the surface of the soil control volume is covered by one of the multi-zone building floors or whether the surface is exposed to the exterior environment. This model calculates the average surface temperature of the soil directly underneath each of the floors of the multi-zone building. These average surface temperatures are then passed to Type 56 as boundary temperature inputs for each of the floors. Based on the boundary floor temperatures provided to Type 56 by this model, Type 56 calculates the rate of energy that passes from the floors of each zone into the soil. With the soil heat transfer for each zone provided by Type 56, the thermal history of the soil field and the properties of the soil known, the temperatures of each of the control volumes of the 3D soil field can be calculated by this model. Based on the calculated soil temperatures and the zone heat flows, the average zone surface temperatures can be calculated and passed back to Type 56. This iterative methodology is then solved with the standard TRNSYS convergence algorithms.

The size of the control volumes were multiplied by a factor of two as they expanded away from the perimeter of the greenhouse airnodes. The near field/far field boundary is conductive and the temperature of the far field is set by the Kasuda correlation for the x, y and z axes. The deep ground temperature is assumed to be equal to the yearly average outside air temperature. The amplitude of the annual surface temperature profile of the soil is assumed to be equal to the maximum monthly soil surface temperature minus the average annual soil surface temperature. The soil temperature was

assumed to be unaffected by the building at a distance of 10 m beneath the ground surface (in the vertical direction) and 10 m from the edge of the greenhouse (in the horizontal direction).

Coupling mass and energy transfer: Air movement is specified between the three airnodes of the air thermal zone so that they are all nearly at the same temperature (well-mixed assumption). For airflow from the crop airnode (*i_c*) to a floor airnode (*i_f*), the thermal (Q_{cpl} in W) and moisture (m_{m_cpl} in kg hr^{-1}) gains due to coupling are calculated from:

$$Q_{cpl} = m_{cpl} \cdot c_{p\_a} \cdot \left(T_{i\_c} - T_{i\_f} \right) / 3.6 \tag{9}$$

$$m_{m\_cpl} = m_{cpl} \cdot \left(\omega_{i\_c} - \omega_{i\_f} \right) \tag{10}$$

where:

m_{cpl} is coupling mass flow of air between the airnodes (kg hr^{-1})

The factor 3.6 serves to convert units kJ hr^{-1} to W.

Similarly, for airflow from a floor airnode to the crop airnode, the thermal gains due to coupling are defined as:

$$Q_{cpl} = m_{cpl} \cdot c_{p_a} \cdot \left(T_{i\_f} - T_{i\_c} \right) / 3.6 \tag{11}$$

$$m_{m\_cpl} = m_{cpl} \cdot \left(\omega_{i\_f} - \omega_{i\_c} \right) \tag{12}$$

where the coupling mass flow rate is selected so that the airnode temperature become nearly identical due to mixing.

2.2.3. Values of Greenhouse Design Parameters

The values of properties for different materials and components used in the case study that are different than the values provided in [18] are given in Table 1.

Table 1. Parameter values of different materials/components used in the greenhouse model.

Material/Component	Parameter	Symbol	Value	Reference
Soil	Depth of arable soil layer	D_{soil_ar}	0.7 m	Assumed
	Depth of ground zone and far-field distanced	D_{soil}	10 m	Assumed
	Smallest control volume size	CV_{min}	0.1 m	Assumed
	Specific heat	c_{p_soil}	0.84 kJ kg^{-1} K^{-1}	[15]
	Density	ρ_{soil}	3200 kg m^{-3}	
	Thermal conductivity	k_{soil}	2.42 W m^{-1} K^{-1}	
	Emissivity	ε_{soil}	0.9	[22]
	Solar reflectance	ρ_{soil}	0.75	[23]
	Deep earth temperature	T_{de_soil}	5.9 °C	[20]
	Amplitude of surface temperature	Amp	15.3 °C	
	Time shift	ts	32 d	[16]
EPS ground insulation	Thickness	l_{ins}	50 mm	Assumed
	Thermal conductivity	k_{ins}	0.036 W m^{-1} K^{-1}	[24]
	Specific heat	c_{p_ins}	1.5 kJ kg^{-1} K^{-1}	
	Density	ρ_{ins}	20 kg m^{-3}	
	Depth of vertical perimeter insulation	D_{per_ins}	0.61 m	Assumed

2.3. Economic Analysis

The economic analysis follows the same method presented by the authors in [18]. The details of the terms presented in the net savings formula, as it applies to the case study, follows:

Change in energy cost (ΔE): The real discount rate (d in %) can be derived from:

$$d = (1 + D)/(1 + I) - 1 \tag{13}$$

where:

D is the nominal discount rate (%)
I is the inflation rate (%).

The present value of the annually recurring cost for natural gas consumed heating (PV_{E_gas} in \$) is calculated by:

$$PV_{E\_gas} = C_{gas} \cdot m_{gas\_yr} \cdot (1 + e_{gas}) / (d - e_{gas}) \cdot \left[1 - \left[(1 + e_{gas}) / (1 + d)\right]^n\right] \quad (14)$$

where:

C_{gas} is the natural gas price (\$ m^{-3})
e_{gas} is the electricity cost escalation rate (%)
n is the study period (yr).

Modifying the ground insulation design does not impact the indoor lighting and its associated cost. The savings in energy cost is the difference between that of the AGH and BCGH (ΔE in \$) expressed as:

$$\Delta E = \left[PV_{E\_gas}\right]_{BCGH} - \left[PV_{E\_gas}\right]_{AGH} \quad (15)$$

Change in water cost: It is assumed that no difference in water consumption occurs between the AGH and BCGH.

Change in operation, maintenance and replacement cost (O&MR): It is assumed that no difference in OM&R cost occurs between the AGH and BCGH.

Change in initial investment cost (ΔInv): The additional material and installation cost for the added rigid insulation (ΔC_{ins} in \$) is determined as follows:

$$\Delta C_{ins} = A_{ins} \cdot (C_{ins\_mat} + C_{ins\_inst}) \quad (16)$$

where:

A_{ins} is the area with replaced with permanent or movable insulation (m^2)
C_{ins_mat} is the material cost of insulation (\$ m^{-2})
C_{ins_inst} is the installation cost of insulation (\$ m^{-2}).

The AGH envelope designs reduce the peak heating energy demand and this may cause the size and associated cost of the boiler to decrease. The change in material and installation cost for the boiler (ΔC_{boil} in \$) is computed as:

$$\Delta C_{boil} = \left[Q_{p\_heat} \cdot (C_{boil\_mat} + C_{boil\_inst})\right]_{AGH} - \left[Q_{p\_heat} \cdot (C_{boil\_mat} + C_{boil\_inst})\right]_{BCGH} \quad (17)$$

where:

Q_{p_heat} is the rated thermal output of the nearest commercially available boiler that can satisfy the simulated peak thermal energy demand (kW)
C_{boil_mat} is the material cost of the boiler (\$ kW^{-1})
C_{boil_inst} is the boiler installation cost (\$ kW^{-1}).

The total additional initial investment cost (ΔInv in \$) is determined as follows:

$$\Delta Inv = \Delta C_{ins} + \Delta C_{boil} \quad (18)$$

Change in capital replacement cost ($\Delta Repl$): The replacement period for rigid insulation is assumed to be the same as the study period and is ignored in the LCCA. Since indoor lighting is not affected by

modifying the ground envelope design, the replacement costs for artificial lighting is the same in the AGH and BCGH and can be ignored.

The cost for replacing a boiler ($Repl_{boil}$ in \$) is equal to:

$$Repl_{boil} = Q_{p\_heat} \cdot \left(C_{boil\_mat} + C_{boil\_lab\_repl} \right) / (1+d)^{P_{boil}} \quad (19)$$

where P_{boil} is the boiler lifespan (yr).

The total additional capital replacement cost ($\Delta Repl$ in \$) is the difference between that of the AGH and BCGH is expressed as:

$$\Delta Repl = [Repl_{boil}]_{AGH} - [Repl_{boil}]_{BCGH} \quad (20)$$

Change in residual value (ΔRes): The residual value for the boilers (Res_{boil} in \$) is approximated by:

$$Res_{boil} = Q_{p\_heat} \cdot (C_{boil\_mat}) \cdot [roundup(n/P_{boil}, 0) - n/P_{boil}] / (1+d)^{n} \quad (21)$$

The total residual value (ΔRes in \$) is the difference between that of the AGH and BCGH given by:

$$\Delta Res = [Res_{boil}]_{AGH} - [Res_{boil}]_{BCGH} \quad (22)$$

Initial investment cost (Inv): The initial investment cost of the greenhouse (Inv in \$) is taken as the sum of the structure (framing, foundation, floor, covering and TSS), HVAC (ventilation and heating system) and AL components.

$$Inv = A \cdot (C_{stru\_tot} + C_{HVAC\_tot} + C_{AL\_tot}) \quad (23)$$

where:

C_{stru_tot} is the installed cost of the greenhouse structure per unit area (\$ m^{-2})
C_{HVAC_tot} is the installed cost of the HVAC system per unit area (\$ m^{-2})
C_{AL_tot} is the installed cost of the AL system per unit area (\$ m^{-2}).

Values of Greenhouse LCCA Parameters

The relevant cost data (in \$CAD 2017) that is not presented in [18] is provided in Table 2.

Table 2. Values of the cost data used in the LCCA.

Parameter	Symbol	Value	Reference
Initial investment cost of greenhouse	Inv	\$712,700 (concrete floor) \$655,200 (soil floor)	Calculated based on [18]
EPS insulation cost	C_{ins_mat}	6.51 \$ m^{-2}	[25]
EPS insulation installation cost	C_{ins_inst}	5.76 \$ m^{-2}	[25]

3. Results and Discussion

3.1. Portion of Heat Loss through Ground

The average heat loss pathways for the BCGH with a concrete slab in January, were determined to be: 18.6% for infiltration, 21.9% for ventilation, 37.7% from the roof, 17.8% from the walls and 4.0% from the ground. These results are from sunset to sunrise because the ground becomes a source of heat gain when sunlight exists. The portion of the envelope heat loss (walls, roof and ground) that occurred through the ground was approximately 7%. Consequently, permutations in the ground envelope design will have a small impact on the overall greenhouse energy savings.

3.2. Net Savings Achieved by the Ground Insulation Configurations

The present-value costs, residual value, NS (in $CAD 2017), and change in LCC for the AGH and BCGH are provided in Table 3. The two main design alternatives for ground insulation consist of adding vertical insulation around the greenhouse perimeter and horizontal insulation beneath the floor and/or crop zones. The perimeter insulation is considered as the first design alternative because it is the most likely to provide NS. It should be noted that perimeter insulation also has the added benefit of foundation frost protection and improved crop root zone temperatures and therefore, there may be an incentive to apply it even if it does not result in NS. If NS are obtained for perimeter insulation, then the next design alternatives will be to consider horizontal insulation beneath the floor zone. If perimeter insulation does not provide NS, then subsequent designs would only consider horizontal insulation, although it is unlikely that horizontal insulation would be cost effective if perimeter insulation is not. Based on this economic result, two possibilities for subsequent envelope designs will be considered. If combined perimeter and floor zone insulation provides higher NS crop zone insulation (entire footprint). If not, the case of perimeter and crop zone insulation will be assessed. The use of ground insulation had a negligible impact on the peak energy demand for heating and therefore changes in the heating system cost are not considered.

Table 3. Present-value costs, residual value, NS, and change in LCC for the greenhouse models.

Floor Type	Insulation Location and Thickness	Energy Cost	Incremental Initial Investment Cost	Capital Replacement Cost	Residual Value	NS	Change in LCC
Concrete slab	BCGH (no insulation)	$1,582,202	$0	$84,949	$25,586	-	-
	Vertical perimeter	$1,579,716	$912	$84,949	$25,586	$1575	−0.1%
	Vertical perimeter and horizontal floor zones	$1,577,112	$3192	$84,949	$25,586	$1899	−0.1%
	Vertical perimeter and horizontal floor plus crop zones	$1,577,726	$12,311	$84,949	$25,586	−$7835	0.3%
Soil floor	BCGH (no insulation)	$1,567,120	$0	$84,949	$25,586	-	-
	Vertical perimeter	$1,564,725	$912	$84,949	$25,586	$1483	−0.1%
	Vertical perimeter and horizontal floor zones	$1,560,546	$3192	$84,949	$25,586	$3382	−0.2%
	Vertical perimeter and horizontal floor plus crop zones	$1,560,371	$12,311	$84,949	$25,586	−$5562	0.2%

For the concrete slab and soil floor greenhouse designs, the economic results were improved when perimeter insulation is applied (NS of $1575 and $1483, respectively and the LCC decreased by 0.1% for both). When horizontal floor insulation is added, the NS increased by 20.6% for the greenhouse with a concrete slab and 128.0% for the greenhouse with a soil floor. When horizontal crop zone insulation was added, a financial loss of $7835 (0.3% increase in LCC) was observed for the greenhouse with a concrete slab and $5562 (0.2% increase in LCC) for the greenhouse with a soil floor. Therefore, the most cost-effective design for the greenhouses with a concrete slab and soil floor is when perimeter and floor zone horizontal insulation are applied. Although this analysis provided insight into the most cost-effective greenhouse ground insulation design for Ottawa, the NS are negligible compared to the greenhouse LCC (decrease in LCC of 0.1% and 0.2% for the greenhouse with a concrete slab and soil floor, respectively).

3.3. Impact of Insulation on Energy Consumption

Table 4 gives the annual lighting electricity use and fuel consumed for heating. The BCGH with the soil floor consumed 0.7% more electricity for lighting than the concrete floor BCGH due to the

higher solar absorptance of soil compared to concrete. Meanwhile, the increased thermal energy storage in the soil caused heating energy use to decrease by 2.9%. It is interesting to note that for the concrete greenhouse, the heating energy use was lowest for the case of perimeter and floor zone insulation (natural gas use of 61,466 m^3 yr^{-1}), whereas it slightly increased to 61,519 m^3 yr^{-1} when crop zone insulation was also employed. This demonstrates how, in certain cases, the use of ground insulation can be detrimental to energy conservation efforts because it reduces the potential for passive solar heating. For the designs that achieved the highest NS, heating energy was reduced by 0.6% for the greenhouse with a concrete slab and 1.0% for the soil floor. Therefore, employing ground insulation produced negligible energy savings and economic benefit for the location that was investigated. It should be noted that a single insulation thickness was selected for this study. The analysis could be repeated for different thicknesses of EPS insulation to identify the optimal level.

Table 4. Energy consumption for the greenhouse models.

Floor Type	Insulation Level	Lighting Electricity Consumption (kWh yr^{-1})	Natural gas Consumption for Heating (m^3 yr^{-1})
Concrete slab	BCGH (no insulation)	114,971	61,903
	Vertical perimeter	114,971	61,690
	Vertical perimeter and horizontal floor zones	114,971	61,466
	Vertical perimeter and horizontal floor plus crop zones	114,971	61,519
Soil floor	BCGH (no insulation)	115,755	60,105
	Vertical perimeter	115,755	59,900
	Vertical perimeter and horizontal floor zones	115,755	59,541
	Vertical perimeter and horizontal floor plus crop zones	115,755	59,526

3.4. Sensitivity of Net Savings to Energy Model Input Parameter Values

The energy model input parameters to be considered are those that significantly impact energy consumption and whose value carries considerable uncertainty. In this study, the interior surface convective heat transfer coefficients for the floor and crop zones will be assessed because they may have a significant impact on predicted heating energy use and their values are not well known.

Therefore, the analysis was repeated using model parameter values that would result in higher/extreme heating energy use. An interior ground surface convective heat transfer coefficient (CHTC) value of 20 W m^{-2} $°C^{-1}$ (representing high-mixing of greenhouse air using horizontal airflow fans) was selected for the comparison. Table 5 presents the results for ground surface CHTC for the greenhouse with a concrete slab. A higher CHTC increased the heating energy consumption by 13.7% for the BCGH and 13.3% for the AGH design with the highest net savings. Although its effect on heating energy use is relatively small, the net savings increased significantly (190.8%). Therefore, the inside floor surface CHTC is a modeling parameter that greatly influences the economic result. By overestimating its value, the predicted net savings could be too optimistic. Consequently, efforts should focus on accurately determining this parameter for the specific ground cover and airflow patterns that exist inside the greenhouse.

Table 5. Effect of ground surface CHTC for the greenhouse with a concrete slab.

Item	Insulation Level	Internal Calculation of CHTC	CHTC Increased to 20 W m^{-2} $°C^{-1}$	% Change
Natural gas consumption for heating (m^3 yr^{-1})	BCGH	61,903	70,359	13.7%
	50 mm vertical perimeter and horizontal floor plus crop zones	61,466	69,611	13.3%
Net savings	50 mm vertical perimeter and horizontal floor plus crop zones	$1899	$5521	190.8%

3.5. Sensitivity of Net Savings to Economic Parameter Values

It is impossible to know for certain what the price of energy, materials, labor and equipment will actually be over the next 25 years or so. To identify the critical input values in the LCCA, several parameters were individually varied by ±5 and ±10% and plotted against the resulting percent changes in net savings. When one variable is modified, all others remain at their default values. Figure 7 provides the results for the envelope design with highest net savings for the greenhouse with a concrete floor. Based on Figure 7, the critical input values (which provoke a change in NS greater than ±1% when varied by ±10%) in the LCCA include the natural gas price, natural gas cost escalation rate, the discount rate, and the insulation material and installation cost. A 10% increase in the natural gas price, natural gas cost escalation rate, discount rate, insulation material and installation cost caused the net savings to change by 26.8%, 24.3%, −11.0%, −8.9% and −7.9%, respectively. The electricity price and cost escalation does not impact net savings because the electricity consumption for lighting is not affected by design permutations of the ground envelope for a given greenhouse design. Varying the replacement cost of artificial lights did not affect the net savings because, for all cases studied, they were replaced at the maximum fixture lifespan (15 years) rather than the bulb lifespan (50,000 h).

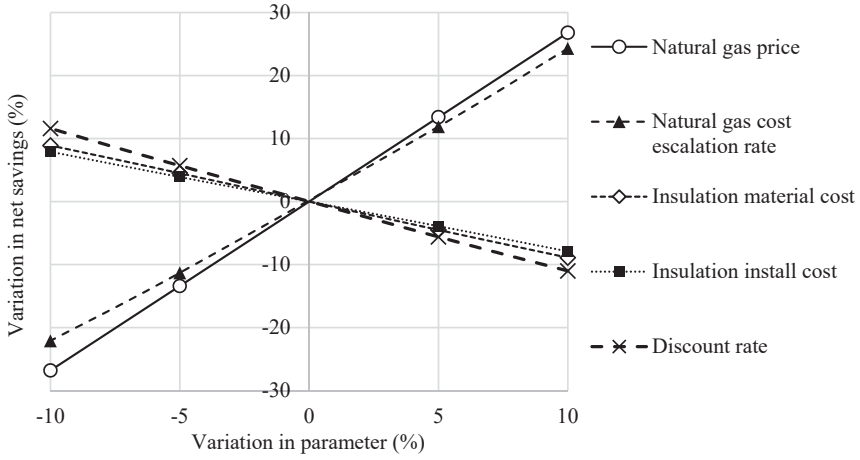

Figure 7. Sensitivity analysis for percentage change in NS given percent change in parameter—Envelope design with highest net savings for greenhouse with concrete floor.

4. Conclusions

This paper demonstrates how the combination of integrated thermal-daylight energy analysis and life cycle cost analysis can be employed to compare envelope designs for greenhouses. To the best of the author's knowledge, it is the first time that a 3D ground heat transfer model was used to compare floor envelope designs for a greenhouse that controls light to a consistent daily integral, based on local climatic and economic conditions.

The methodology was applied to determine the most cost-effective ground insulation design for a greenhouse located in Ottawa, ON, Canada. Two types of floor designs were investigated (concrete slab and unfinished soil floor) and the insulation installation configurations were vertical around the perimeter and horizontal beneath the footprint. The portion of total heat loss that occurred through the ground was approximately 4% and permutations in ground insulation design reduced heating energy consumption by up to 1%. For both of the floor designs considered, the greenhouses produced a higher NS when insulation was applied to both the perimeter and the surface beneath the floor zone then when it was applied to the perimeter alone. Meanwhile, adding insulation beneath the crop zone was not a viable option because it increased the LCC. In all cases, the improvement in economic

performance was small (NS below $4000 and reduction in life cycle under 0.2%). Therefore, a design with perimeter insulation may be the best option because it uses the least amount of material resources and provides some cost savings in addition to frost protection, reduced risk of condensation and improved thermal comfort for the crops.

The development of a 3D ground heat transfer model (that would ideally be compatible with commercially available simulation tools such as TRNSYS and EnergyPlus) which can simultaneously handle vertical perimeter insulation (for both basements and slab on grade), horizontal insulation and wing insulation would be useful for comparing all possible ground insulation configurations. Combined energy and life cycle cost analysis is valuable for determining optimal envelope designs that are capable of lowering energy consumption, improving economics and enhancing greenhouse durability.

Author Contributions: Methodology, formal analysis, writing, J.B.; Supervision, review and editing, A.K.A.

Funding: This research received no external funding.

Acknowledgments: The authors acknowledge the financial support of the Natural Sciences and Engineering Research Council of Canada (NSERC) through the Alexander Graham Bell Canada Graduate Scholarship, the NSERC Smart Net Zero Energy Buildings Strategic Research Network and the Concordia Institute for Water, Energy and Sustainable Systems. Thanks to Laura Bambara for editing this paper.

Conflicts of Interest: The authors declare no conflict of interest.

References

1. Deru, M.; Judkoff, R.; Neymark, J. Whole-building energy simulation with a three-dimensional ground-coupled heat transfer model. *ASHRAE Trans.* **2002**, *109*, 557–565.
2. Andolsun, S. *Comparison of DOE-2.1 E with EnergyPlus and TRNSYS for Ground Coupled Residential Buildings in Hot and Humid Climates Stage 3*; Technical Reports; Energy Systems Laboratory: College Station, TX, USA, 2012.
3. Chen, Y. Methodology for Design and Operation of Active Building-Integrated Thermal Energy Storage Systems. Ph.D. Thesis, Concordia University, Montréal, QC, Canada, 2013.
4. Nawalany, G.; Bieda, W.; Radoń, J.; Herbut, P. Experimental study on development of thermal conditions in ground beneath a greenhouse. *Energy Build* **2014**, *69*, 103–111. [CrossRef]
5. Al-Kayssi, A.W. Spatial variability of soil temperature under greenhouse conditions. *Renew. Energy* **2002**, *27*, 453–462. [CrossRef]
6. Kittas, C.; Karamanis, M.; Katsoulas, N. Air temperature regime in a forced ventilated greenhouse with rose crop. *Energy Build.* **2005**, *37*, 807–812. [CrossRef]
7. Ghosal, M.K.; Tiwari, G.N.; Srivastava, N.S.L. Thermal modeling of a greenhouse with an integrated earth to air heat exchanger: An experimental validation. *Energy Build.* **2004**, *36*, 219–227. [CrossRef]
8. Hepbasli, A. Low exergy modelling and performance analysis of greenhouses coupled to closed earth-to-air heat exchangers. *Energy Build.* **2013**, *64*, 224–230. [CrossRef]
9. Pieters, J.G.; Deltour, J.M. Performances of greenhouses with the presence of condensation on cladding materials. *J. Agric. Eng. Res.* **1997**, *68*, 125–137. [CrossRef]
10. Gupta, M.J.; Chandra, P. Effect of greenhouse design parameters on conservation of energy for greenhouse environmental control. *Energy* **2002**, *27*, 777–794. [CrossRef]
11. Bastien, D. Methodology for Enhancing Solar Energy Utilization in Solaria and Greenhouses. Ph.D. Thesis, Concordia University, Montréal, QC, Canada, 2015.
12. Tong, G.; Christopher, D.M.; Li, B. Numerical modelling of temperature variations in a Chinese solar greenhouse. *Comput. Electron. Agric.* **2009**, *68*, 129–139. [CrossRef]
13. Nawalany, G.; Radon, J.; Bieda, W.; Sokolowski, P. Influence of Selected Factors on Heat Exchange with the Ground in a Greenhouse. *Trans. ASABE* **2017**, *60*, 479–487.
14. Klein, S.A.; Duffie, J.A.; Mitchell, J.C.; Kummer, J.P.; Thornton, J.W.; Bradley, D.E.; Kummert, M. *TRNSYS 17: A Transient System Simulation Program*; Solar Energy Laboratory, University of Wisconsin-Madison: Madison WI, USA, 2014.

15. TRANSSOLAR. *TRNSYS 17. Volume 5. Multizone Building Modeling with Type56 and TRNBuild*; Solar Energy Laboratory, University of Wisconsin-Madison: Madison WI, USA, 2005.
16. Klein, S.A.; Duffie, J.A.; Mitchell, J.C.; Kummer, J.P.; Thornton, J.W.; Bradley, D.E.; Kummert, M. *TRNSYS 17. Volume 4. Mathematical Reference*; Solar Energy Laboratory, University of Wisconsin-Madison: Madison WI, USA, 2014.
17. *Component Libraries for the TRNSYS Simulation Environment*; Thermal Energy System Specialists: Madison, WI, USA, 2012.
18. Bambara, J.; Athienitis, A.K. Energy and economic analysis for the design of greenhouses with semi-transparent photovoltaic cladding. *Renew. Energy* **2019**, *131*, 1274–1287. [CrossRef]
19. Kasuda, T.; Archenbach, P.R. *Earth Temperature and Thermal Diffusivity at Selected Stations in the United States*; National Bureau of Standards: Washington, DC, USA, 1965; Volume 71.
20. RETScreen. *Clean Energy Project Analysis Software*; Version 4; Ministry of Natural Resources: Ottawa, ON, Canada, 2013.
21. TESS Technical Support Team (Madison, WI, USA). Personnel communication, 2017.
22. Cengal, Y.A. *Heat and Mass Transfer: A Practical Approach*, 3rd ed.; McGraw-Hill: New York, NY, USA, 2007.
23. Reagan, J.A.; Acklam, D.M. Solar reflectivity of common building materials and its influence on the roof heat gain of typical southwestern USA residences. *Energy Build.* **1979**, *2*, 237–248. [CrossRef]
24. Yucel, K.T.; Basyigit, C.; Ozel, C. Thermal insulation properties of expanded polystyrene as construction and insulating materials. In Proceedings of the 15th Symposium in Thermophysical Properties, Boulder, CO, USA, 22–27 June 2003.
25. *RSMeans Building Construction Cost Data*; The Gordian Group: Rockland, MA, USA, 2017.

energies

MDPI

Article

Optimization of Performance Parameter Design and Energy Use Prediction for Nearly Zero Energy Buildings

Xiaolong Xu, Guohui Feng *, Dandan Chi, Ming Liu and Baoyue Dou

Shenyang Jianzhu University, Shenyang 110168, China; xuxiaolong@stu.sjzu.edu.cn (X.X.)
879769327@stu.sjzu.edu.cn (D.C.); liuming2018@stu.sjzu.edu.cn (M.L.); wangyue522@stu.sjzu.edu.cn (B.D.)
* Correspondence: Hj_fgh@sjzu.edu.cn; Tel.: +86-02424691899

Received: 18 October 2018; Accepted: 20 November 2018; Published: 22 November 2018

Abstract: Optimizing key parameters with energy consumption as the control target can minimize the heating and cooling needs of buildings. In this paper we focus on the optimization of performance parameters design and the prediction of energy consumption for nearly Zero Energy Buildings (nZEB). The optimal combination of various performance parameters and the Energy Saving Ratio (ESR)are studied by using a large volume of simulation data. Artificial neural networks (ANNs) are applied for the prediction of annual electrical energy consumption in a nearly Zero Energy Building designs located in Shenyang (China). The data of the energy demand for our test is obtained by using building simulation techniques. The results demonstrate that the heating energy demand for our test nearly Zero Energy Building is 17.42 KW·h/(m^2·a). The Energy Saving Ratio of window-to-wall ratios optimization is the most obvious, followed by thermal performance parameters of the window, and finally the insulation thickness. The maximum relative error of building energy consumption prediction is 6.46% when using the artificial neural network model to predict energy consumption. The establishment of this prediction method enables architects to easily and accurately obtain the energy consumption of buildings during the design phase.

Keywords: nearly zero energy building; artificial neural network; performance parameter design; energy saving ratio; dynamic simulation

1. Introduction

The world is confronted with climate change and greenhouse gas emission issues [1]. Nowadays, the energy consumption in the building sector accounts for 40% of the world's total energy consumption, which suggests huge energy saving potential. Therefore, it is essential to identify and investigate the main factors which can have the most significant impact on building energy consumption [2,3]. Additionally, not only can lower greenhouse gas emissions be delivered by reducing building energy consumption, but also the economic development, the innovation of clean technology, and the mitigation of environmental and public health issues can be promoted [4].

Hence, green and energy efficient buildings such as nearly Zero Energy Buildings (nZEB) have attracted governments' attention, and various building energy conservation standards and regulations have been established and implemented across different countries. For example, the Passive House Standard is a sustainable construction standard, which has been called for its implementation and enforcement by all member states by 2021. On 17 November 2009 the European Parliament and the Council fixed 2020 as a deadline for all new buildings to be nZEBs [5]. The European Union has decided that by year 2020 the building energy consumption will be cut down by 20% and greenhouse gas emission by up to 20% [6]. For the first time, the Ministry of Housing and Urban-Rural Development has made a clear demand of nZEBs development, which envisages huge market demand and the

broad prospects in China of promoting nZEBs actively, and the goal is 10 million m^2 by the end of 2020 compared with 500 thousand m^2 now. nZEBs show high thermal comfort and low energy consumption. The required energy in nZEB can be provided from a variety of renewable energy resources including energy from renewable sources produced on-site nearby. International Energy Agency joint Solar Heating and Cooling Task 40 and Energy Conservation in Buildings and Community systems Annex 52 titled "Towards Net Zero Energy Solar Buildings" is making an international effort on the standardization of the Net Zero Energy Building definition [7].

The parametric design of the program stage plays a key role in the shape and performance of the building, which is also the source of the building's energy-saving design. The energy saving potential that exists in decision making at different stages of design will progressively reduce as construction progresses [8]. There are many factors that influence the energy consumption of buildings, during architectural concept design. The building characteristics include parameters relating to geometry, services, glazing, activity, site, construction year, and weather.

Wilde [9] surveyed 67 buildings, where 57% of the technical measures needed to be implemented during the planning and design stage in the application of 303 green building technologies. Since the potential of building energy conservation can be previewed and examined flexibly on the data of heating and cooling loads obtained through simulations at design stage, the optimization of building envelops through parametric design has been attracting much more attentions from the building research community [10]. Based on the literature, the influence factors of the building envelope can be generally categorized into four aspects, namely the outline dimension, orientation, glazing area and thermo-physical properties of the construction materials [11].

Musall et al. [12] have studied energy saving measures applied in net Zero Energy Buildings. Advanced thermal insulation, solar thermal domestic hot water heating and heat recovery are widely used in passive houses, followed by passive technologies such as advanced daylighting, sun shading, passive cooling or ventilation. Bajc et al. [13] constructed and optimized Trombe walls using different types of glazing on the outside of the wall. The Trombe wall is designed with openings with flaps in its concrete core. Temperature distribution under the influence of Trombe wall in both the concrete core and the room are simulated, as well as velocity fields. After that, an analysis of the energy conservation potential iwas conducted. Daouas [14] studied the optimum insulation thickness in walls, energy savings and payback period in Tunisian buildings based on both cooling and heating loads. Yearly transmission loads are rigorously estimated using an analytical method based on Complex Finite Fourier Transform. The result suggests that wall orientation only has a small influence on optimal insulation thickness. The south appears to be the most economical orientation, however the energy conservation reaches the maximum, 23.78 TND/m^2 , when the wall is east-oriented. Özkan D B et al. [15] have investigated the effect of external wall areas and window alternations on the optimal insulation thickness and heating energy demands. Besides, effects of different insulation thicknesses and fuel consumption on emission of pollutants such as CO_2 and SO_2 are also evaluated.

There are many similar studies on the impact of windows on energy consumption. Susorova et al. [16] evaluated the influence of various geometry factors on building energy performance, including window orientation, window to wall ratio, and room width to depth ratio. Energy simulations were performed for six climate zones in the United States using a commercial office building model created in Design Builder. The most energy-efficient solution is when the window-to-wall ratio (WWR) to the north is 20%–30%, and WWR to the south is 50%–80% in cold climates. Thalfeldt et al. [17] simulated a generic open-plan office single floor model. Cost optimal and most energy efficient facade solutions, including window properties, external wall insulation, WWR and external shading were determined. At the cost optimal performance level, the best energy performance was as follows: In the direction of south, east, and north, they have three panes without external shading; WWR is 23.9%; external wall insulation reaches 200 mm; in the north, WWR is 37.5%.

Evidently, low and nearly zero energy buildings will need more careful design to optimize the performance design parameters. Energy consumption data is the basis for promoting energy

conservation in science. Using simulation software to aid program design is an effective solution. However, the dynamic calculation of parameter settings and the calculation process are too complicated and difficult to grasp for the general engineering staff. The calculation and analysis of various schemes still takes a long time, especially for architectural design optimization. That involves the performance evaluation of many groups of programs. It requires a tool during architectural concept design that quickly and accurately evaluates the performance of the architectural scheme.

Artificial neural networks (ANNs) have been widely used in many problem domains, such as computer vision, speech recognition, machine translation, social network filtering, playing board and video games and medical diagnosis. With its flexible structures and powerful 'learning' ability, ANNs has become one of the most popular artificial intelligence models in the prediction of building energy consumption. Inspired by the structure of interconnected neurons in human brain, ANNs demonstrates a superior performance in solving non-linear problems with high-dimensional datasets compared to other AI models [18]. The network is constructed with different layers of neurons, with output layer connected to input and hidden layers to formulate a directed, weighted graph. The network will then be trained repeatedly or recursively to leverage the input dataset and identify the reasonable weights distribution for all neurons in the network. The whole process of modifying weights and functions for activation is called learning, and governed by specific rules [19].

In order to identify the optimal solution from energy optimization functions and improve the accuracy and performance of data-driven energy modelling, Banihashemi [20] proposed a unified approach by introducing an improved hybrid energy objective function and integrating both ANN and Decision Trees, which expands the applicability and enables the model to deal with both continuous and categorical data. Paterson [21] explored an alternative way of predicting building energy consumption by using machine learning methods rather than following the traditional path of physics-based building performance simulation. In this presented model, previously collected thermal comfort and electricity consumption data subject to corresponding certain design parameters are used as inputs to train ANNs model. The mean absolute percentage errors of ANNs model are 22.9% and 22.5% for the prediction of thermal energy usage and electricity consumption respectively. Zhai [22] proposed a systematic model for the optimization of heating, ventilation, and air conditioning (HVAC) systems subject to two adversary fundamental requirements, the less energy consumption and the guarantee of indoor thermal comfort. The model is constructed based on extreme learning machines and neural networks. Then the well-trained models are subsidized by two metaheuristic algorithms, namely sparse firefly algorithm and sparse augmented firefly algorithm (AFA). With the assistance of AFA, the highest potential energy saving rate can reach up to 30% whereby the indoor thermal comfort can still be maintained reasonably well. Ahn [23] proposed another ANN-based control models which can explore and identify optimal parameter settings for supply air by taking into account both the air amount and its temperature simultaneously. Based on research results, the developed ANN controller can effectively avoid control errors by 88% and reduce the energy consumption by 2% compared to conventional on/off controllers.

The gap that is being addressed by this study is integrated design. The performance parameters included 12 parameters relating to geometry, glazing, activity, WWR, and envelope insulation. Integrated design is conducive to understanding the whole process of the project. ANN model is an energy consumption prediction model under the influence of multiple factors. The aim of this study is to optimize building design parameters and predict building energy consumption. The research aim can be achieved by following two major steps. In the first step, the geometric model of our test building was first established in SketchUp, and thermal zones being characterized and divided as well. Then, thermal properties are furnished into the model of the building and weather condition loaded in EnergyPlus. The optimal combination of various performance parameters and the Energy Saving Ratio (ESR) are studied on the basis of a large quantity of simulation data. The second step served to establish ANN model. ANNs were trained to predict the energy consumption of nZEB design.

The training data included energy consumption gathered through energy simulation software and measured building characteristics.

The reminder of the paper is organized as follows: Section 2 describes the methodologies of the studies. Section 2.1 presents the description of nZEB about collected building characteristics and systems description. Section 2.2 gives an overview of ANN model. Section 3 presents the simulation results and analysis from the models developed. The results to validate the proposed technique are discussed in Section 4. Finally, Section 5 reports the conclusions and outlook for future studies.

2. Materials and Methods

EnergyPlus is currently United States Department of Energy flagship whole-building energy simulation engine developed with the active involvement of many participating individuals and organizations since 1995, and is posted open-source on GitHub [24]. First of all, a physical model of the nZEB was built in SketchUp, and then a HVAC system and control strategy were established in OpenStudio [25]. Finally, the IDF files containing technical data about the building envelope materials and HVAC system were imported into EnergyPlus for simulation and optimization of various performance parameters.

EnergyPlus is widely used as an effective and powerful tool among the HVAC research community and engineers to improve and optimize building performance at all stages based on the simulated results about the holistic performance measurements and compositions of sub-sector energy consumptions. OpenStudio is a powerful tool developed by National Renewable Energy Laboratory used for building performance analysis. As a plugin in SketchUp and a visualization interface for EnergyPlus, OpenStudio not only absorbs all merits in building modeling from SketchUp, but also greatly simplifies the modelling of HVAC systems with its abundant component libraries and visualized window. HVAC systems in OpenStudio are mainly divided into Air Loop and Plant Loop. Air Loop is composed of the whole heat exchanger, heating coil, cooling coil, and fan. Plant Loop is composed of hot water loop, cold water loop, and water-side loop.

Building characteristics and systems description as well as the climate conditions are collected, and the geometric model was first established in SketchUp. The OpenStudio Application is a fully featured graphical interface to OpenStudio models including envelope, loads, schedules, and HVAC. Then, exported idf file is calculated in EnergyPlus. The impact of each variable on building energy consumption was analyzed through a large number of simulation calculations. The value of each key parameter is determined with energy consumption as a constraint. These 302 sets of data would be used as training and test data for the nZEB energy consumption forecasting model. A flow chart is given in Figure 1 to illustrate the analysis procedure of this study.

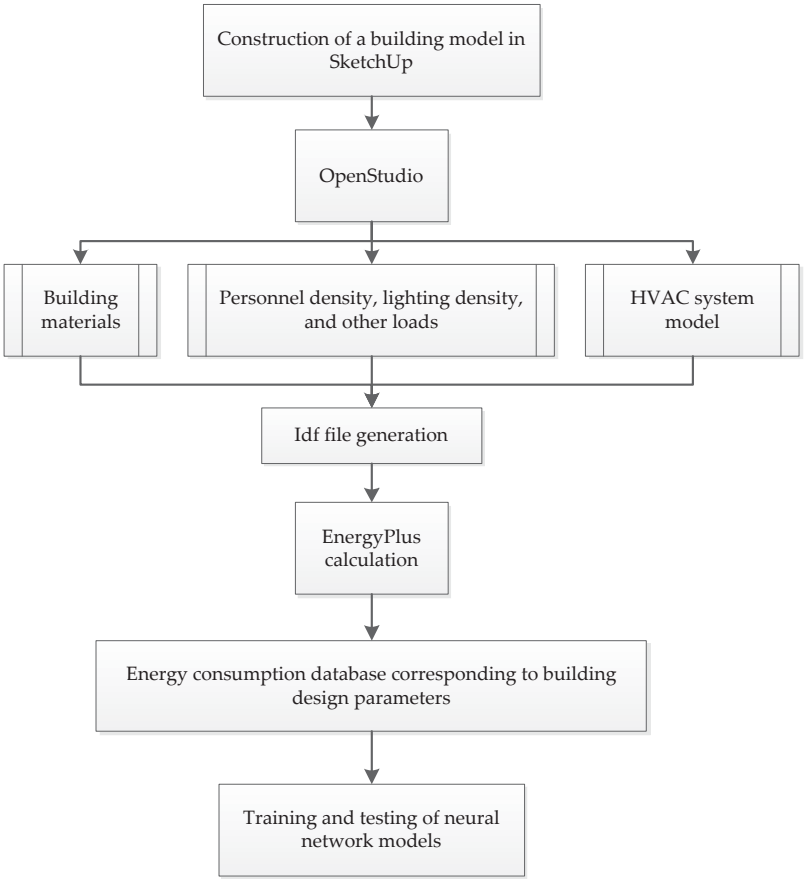

Figure 1. Flow chart of research methodology.

2.1. Description of the nZEB

2.1.1. Description of the research model

The Shenyang Jianzhu University nearly zero energy residential building demonstration center, shown in Figure 2a, is located in Shenyang, China.

(**a**)

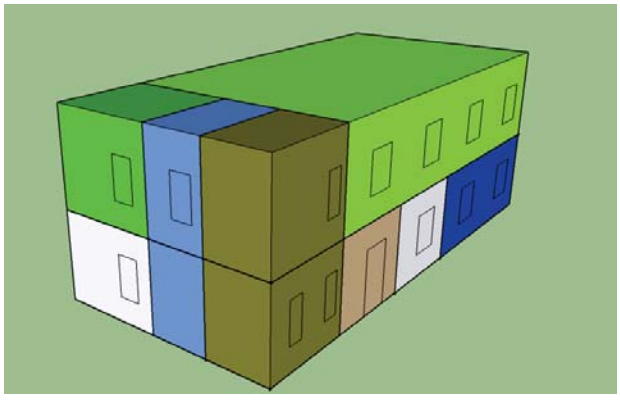

(**b**)

Figure 2. Overview of nZEB from SJZU campus: (**a**) Aerial photo; (**b**) Simulated in EnergyPlus.

The climate zone is a cold climate zone. The building shape is rectangular. The main structure is an H-shaped steel structure with poured polystyrene foam concrete. The shape factor is 0.54, and the total area is 302.4 m^2. Figure 3 shows two floors. The space in first floor is occupied by a hall, equipment room, control room, bedroom, kitchen, bathroom and stairs, and the second floor by two offices and one toilet. Characterized as essential parameters for building performance and energy consumption, the heat transmission properties of each element of envelope (exterior wall, window, door, roof and ground floor.), are summarized in Table 1.

The geometric model of our studied building was established and thermal properties being characterized in SketchUp and EnergyPlus. Figure 2b depicts Thermal Zone in EnergyPlus simulation. The same function room is set as a thermal zone. The status of each thermal zone is always uniform, that is, the thermal zone of air temperature and humidity parameters are the same. Stairwell and the engine room are not set for heating or cooling, so they were set to non-air conditioning area, and the remaining thermal zone as air-conditioned area.

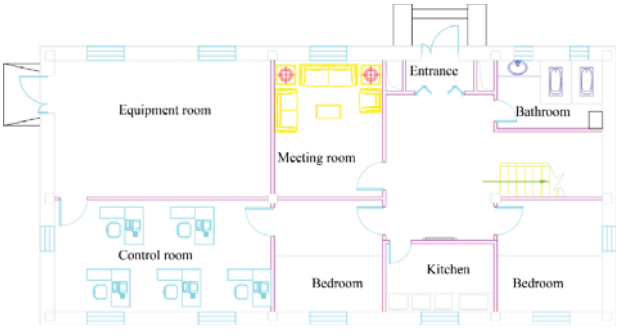

(**a**)

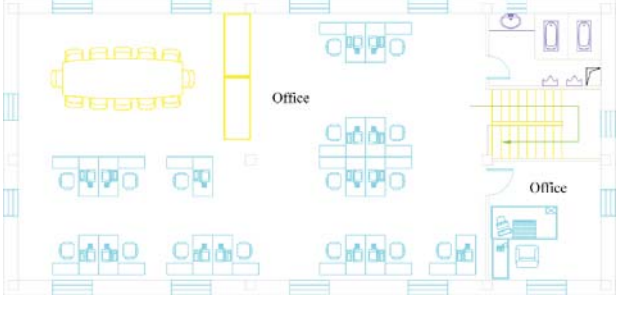

(**b**)

Figure 3. Building plan: ground floor (**a**); (**b**) second floor.

Table 1. U values and thickness of each construction elements.

Component of Buildings	Elements of Construction	Thickness (mm)	*U* Value (W/m·k)
Exterior Wall	Polymer cracking mortar	5.00	0.930
	Expanded polystyrene board	300.00	0.033
	Self-insulation wall	120.00	0.100
	Calcium silicate board	10.00	0.240
	U value 0.099 [W/(m^2·k)]		
Roof	Waterproof materials	5.00	0.930
	Cement mortar	20.00	0.930
	Extruded polystyrene	280.00	0.028
	Autoclaved lightweight concrete	120.00	0.130
	U value 0.090 [W/(m^2·k)]		
Ground floor	Surface layer	20.00	0.930
	Concrete	100.00	1.300
	Extruded polystyrene	240.00	0.028
	Concrete cushion layer	80.00	1.300
	U value 0.113 [W/(m^2·k)]		
Windows	Low emissivity, filled Argon	-	-
	U value 1.0 [W/(m^2·k)]		

2.1.2. Building Systems Description

The system used in the nZEB for heating and cooling includes Water Source Heat Pump System, Solar Water Heating system, as shown in Figure 4.

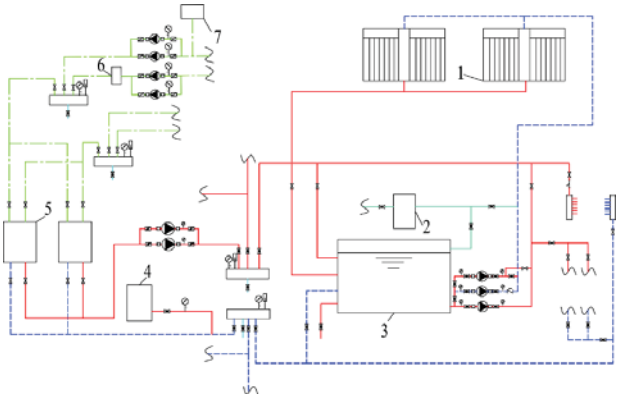

Figure 4. Heating and cooling system. (1) Solar collector; (2) Water softening device; (3) Hot water tank; (4) Constant pressure tank; (5) Water source heat pump; (6) Grit separator; (7) Replenishment device.

The water source heat pump system bears most of the building's heat load and full cooling load. The buried pipe outlet temperature is at 16 °C in summer, and the temperature difference between supply and return is 5 °C. The buried pipe outlet temperature is 12 °C in winter. The hot water loop provides hot water for a radiant floor heating system and the end of the heating coil in the air loop. Outlet temperature of hot water loop is 40 °C, and the temperature difference between supply and return is 8 °C. Also, there are several groups of solar collectors used for domestic hot water and heating. Mechanical Ventilation Heat Recovery Unit (MVHR) is the necessary system for nZEB [5]. It has 81% efficiency for sensible heat recovery and 73% efficiency for latent heat recovery. MVHR need not bear indoor heat load and moisture load. Fan open time is set to 8:00 to 21:00. Nighttime ventilation mode is turned on when the building has no heating or cooling needs. Figure 5 shows the MVHR.

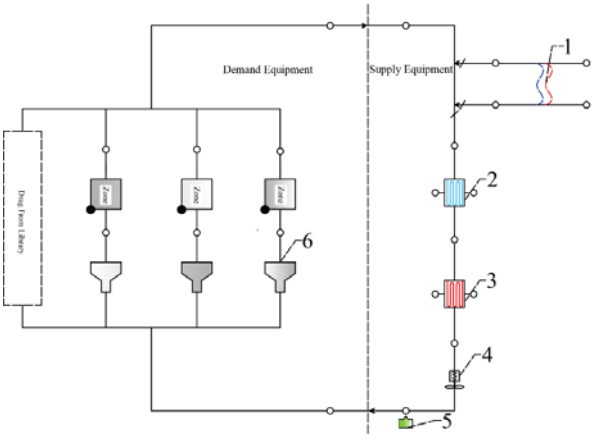

Figure 5. Mechanical Ventilation Heat Recovery Unit in EnergyPlus. (1) Air-to-Air Heat Exchanger; (2) Evaporator Loop-Cooling; (3) Evaporator Loop-Heating; (4) Fan; (5) Node; (6) Diffuser.

2.2. ANN Approach

2.2.1. Overview

ANN models are effective when dealing with complex, nonlinear problems [26,27]. ANN's are used for estimating heating/cooling loads, total electricity consumption and sub-level components' operation and optimization [28]. The Back Propagation (BP) algorithm is the workhorse of learning in neural networks. BP algorithm trains a given feed-forward multilayer neural network for a given set of input patterns with known classifications [29]. As all instances from training dataset are inputted, the networks start to propagate forward till reaching the output layer, then output response according to the pattern of initial dataset will be compared with ground truth and the deviations being calculated. Based on the calculated deviations, the weights of neurons across the whole network will be calibrated and redistributed to mitigate the deviation, this process is considered as back propagation. BP algorithm [30] is based on Widrow-Hoff delta learning rule in which the weight adjustment is done through mean square error of the output response to the sample input. The sets of these sample patterns are repeatedly presented to the network until the error value is minimized. Three types of neurons in an ANN are shown in Figure 6; input nodes, hidden nodes, and output nodes [31].

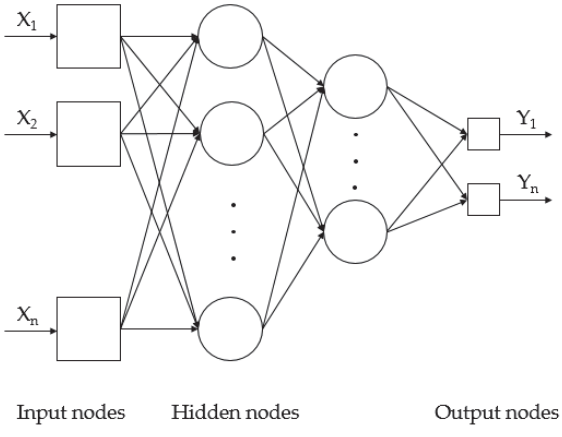

Figure 6. Neural networks structure based on Back Propagation.

MATLAB 7.13 was used to create the ANNs in this research [32]. Each neuron as one dimension in the input layer represents a parameter in the building characteristics dataset, and the single neuron in the output layer represents energy consumption. These data are given in Table 2.

Table 2. Building characteristic parameters.

Parameter (Input Set)	Description Summary	Data Interval	Data Range
Exterior wall heat transfer coefficient	The proportionality constant between the heat flux and the thermodynamic driving force for the flow of heat	Insulation thickness, 20 mm	140–400 mm
Roof heat transfer coefficient		Insulation thickness, 20 mm	140–400 mm
Ground floor heat transfer coefficient		Insulation thickness, 20 mm	140–400 mm
Windows heat transfer coefficient		0.1 or 0.2 ($W/m^2 \cdot K$)	0.6-1.1 ($W/m^2 \cdot K$)
SHGC	Solar heat gain coefficient	It is up to the thermal performance of the window	It is up to the thermal performance of the window
window-to-wall ratio on east facades	The total area of all the east window openings divided by the east facades area	2.5%	5%–30%
window-to-wall ratio on west facades	The total area of all the west window openings divided by the west facades area	2.5%	5%–30%
window-to-wall ratio on south facades	The total area of all the south window openings divided by the south facades area	2.5%	5%–45%
window-to-wall ratio on north facades	The total area of all the north window openings divided by the north facades area	2.5%	5%–25%
Lighting	Indoor lighting electricity	1 W/m^2	3–7 W/m^2
electrical appliances	Indoor technology equipment electricity	1 W/m^2	2–6 W/m^2
personnel activities	Impact of personnel activities	1 m^2/person	5-10 m^2/person

2.2.2. Training

The whole data sets obtained from experiments are randomly divided into two parts for training and testing, respectively, thus 227 data sets are used as training data for the BP neural network model while 75 data sets are retained as testing data to validate the trained model. It should be noted that the divisions of data are formulated in a random manner and the cross validations are also applied to improve the ability of generalization of the model. Regarding limited volume of data samples, the model developing strategy adopted in this study can fully realize the potential of available data sets, therefore more likely to obtain a reasonable energy consumption predictive model under the topology of BP neural networks.

The input neurons of the established Back Propagation network model contain exterior wall heat transfer coefficient, roof heat transfer coefficient, ground floor heat transfer coefficient, windows heat transfer coefficient, solar heat gain coefficient (SHGC), WWR on east facades, WWR on west facades, WWR on south facades, WWR on north facades, indoor lighting, electrical equipment, and personnel activities. With twelve input variables required to predict energy consumption in this study, there are twelve neurons in the input layer corresponding to each variable. Similarly, as the sole purpose of this study is to predict building energy consumption, only one neuron is implemented in the output layer. The rest of the items were assigned the value of benchmark building when a certain performance parameter was changed to calculate the building energy consumption value.

Building energy consumption can be contributed by various factors including building construction, equipment, and occupancy characteristics and so on. A BP neural network with three layers is established in this study as an attempt to explore and quantify the possible relationship between various parameters and building energy consumptions. The input data are normalized into the scale of -1 to 1 based on Premnmx function provided in Matlab at preprocessing stage.

We use the newff function to create a feed-forward backpropagation network. The general syntax has been recorded in Table 3 [33]. The syntax of BP network is presented in Table 4. In neural networks transfer functions are used to calculate a layer's output from its net input. In this study the Hyperbolic Tangent Sigmoid Transfer Function (Tansig) is chosen as transfer function, while Traingdx is selected as training algorithm. Traingdx is a network training function that updates weight and bias values according to gradient descent momentum and an adaptive learning rate. The function traingdx combines adaptive learning rate with momentum training. Traingdx can be applied to train any network as long as its weight, net input, and transfer functions have derivative functions.

Table 3. General syntax.

Net = Newff
net = newff (PR, [S1 S2 ... SNl], {TF1 TF2 ... TFNl}, BTF, BLF, PF)
Description
net = newff creates a new network with a dialog box.
newff (PR, [S1 S2 ... SNl], {TF1 TF2 ... TFNl}, BTF, BLF, PF) takes,
PR—R x 2 matrix of min and max values for R input elements
Si—Size of ith layer, for Nl layers
TFi—Transfer function of ith layer, default = 'tansig'
BTF—Backpropagation network training function, default = 'traingdx'
BLF—Backpropagation weight/bias learning function, default = 'learngdm'
PF—Performance function, default = 'mse'

Table 4. BP network syntax.

net = newff (dx, [12-13-1], {'tansig', 'tansig', 'purelin'}, 'traingdx');
Syntax: A = tansig (N)
N: S-by-Q matrix of net input (column) vectors, the S-by-Q matrix of N's elements squashed into $[-1, 1]$.
Algorithms: tansig (n) = $2/(1 + \exp(-2 * n)) - 1$

3. Results

3.1. Energy Consumption Simulation of Benchmark Building

The model built in OpenStudio mentioned in the previous paragraph was converted to the file (.idf). This file was loaded into EnergyPlus to run in Shenyang's climatic conditions. To improve the predicting accuracy, the schedule of occupancy is extremely important since occupant behaviors can influence building energy consumption in a direct and intuitive way. Simulation was performed for a period of one year using a time step of 1 h. The schedule for different rooms of the entire building adopts the default value in EnergyPlus. Between 9:00 AM and 5:00 PM, the house is occupied, so that the energy consumed during this period of time is maximal. House heating starts in November and continues up to March (i.e. for 5 months), whereas, house cooling starts in June and continues up to August.

Another research interest in this study is to pinpoint the influence factors and their characteristics for each category of energy consumptions, including heating, cooling, lighting, electrical appliances, fans, water pump, and MVHR. A detailed analysis of the energy consumed by the nZEB was performed for the whole year. Table 5 illustrates the energy demand for each area separately for the nZEB simulated.

Table 5. Energy consumption summary of benchmark building.

Statistical Classification	Heating	Cooling	Lighting	Electrical appliances	Fans	Water Pump	MVHR
Energy consumption KW·h/(m^2·a)	17.42	9.77	8.62	8.43	2.34	4.81	2.54
The proportion of total energy consumption	32.31%	18.12%	15.97%	15.63%	4.34%	8.92%	4.70%
Total energy consumption KW·h/(m^2·a)				53.93			

The total energy consumption for heating in nZEB was 5267.81 KW·h for the entire building surface of 302.4 m^2, which equals to17.42 KW·h/(m^2·a) if divided by area. Another large portion of the energy is consumed by the cooling system in the house which is 9.77 KW·h/(m^2·a), then followed by the lighting and electrical appliances.

The total energy demand is as low as 53.93 KW·h/(m^2·a), which should be mainly accredited to the superb insulation of the house. Figure 7 displays average month temperature distribution for Shenyang, the minimum and maximum values of monthly temperature distribution. The highest annual temperature is 25.67 °C in July and the lowest temperature is −11.46 °C in January.

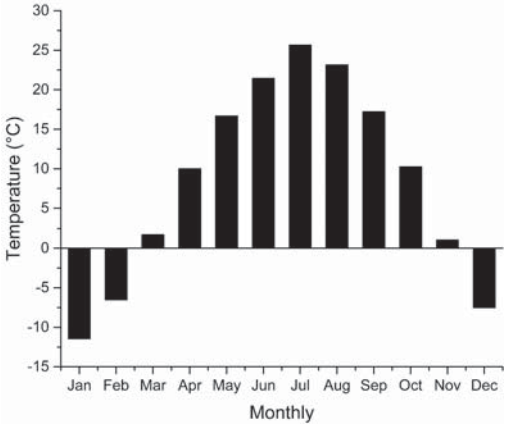

Figure 7. Average monthly temperature distribution for Shenyang, China.

Additionally, Figure 8 presents temperature curve changes of the office on the second floor during the heating season. During the time it is occupied, the room temperature ranges between 19 °C and 22 °C. January is the coldest season in Shenyang.

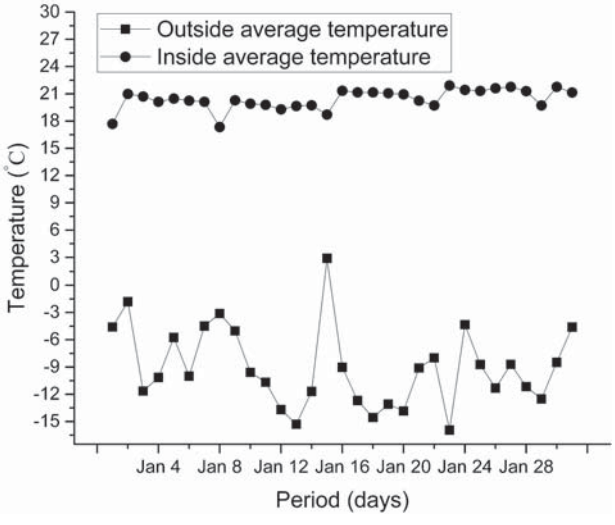

Figure 8. Indoor temperature for office in January.

3.2. Optimal Building Characteristic Parameters

3.2.1. Optimal Envelope Insulation Thickness

Technical guidelines [34] require heat transfer coefficient of exterior wall and roof of nearly zero energy residential buildings to be between 0.1 W/(m^2·K) and 0.2 W/(m^2·K). Heat transfer coefficient of ground floor is between 0.1 W/(m^2·K) and 0.25 W/(m^2·K).

Therefore, insulation thickness was set to 140–400 mm in EnergyPlus. The simulated variable step size was 20 mm. The exterior wall heat transfer coefficient corresponding to this setting was between 0.189 W/(m^2·K) and 0.079 W/(m^2·K). Roof heat transfer coefficient was between 0.164 W/(m^2·K) and 0.065 W/(m^2·K). Ground floor heat transfer coefficient was between 0.188 W/(m^2·K) and 0.068 W/(m^2·K). Heating energy dominates in total energy consumption no matter what the insulation thickness is, as shown in Figure 9. The total energy consumption does not exceed the 60 KW·h/(m^2·a) specified in the technical guidelines when insulation thickness is between 140 mm and 400 mm.

It can be clearly seen from Figure 9 that with the increase in thickness of the external wall and the roof insulation, the total energy consumption shows a downward trend. The change curve of the external wall is more obvious, but the change in energy consumption with increase in the thickness of the ground insulation is relatively small. The impact of thickness of the exterior wall on energy consumption is the largest, followed by the roof thickness, and the last is thickness of the floor insulation.

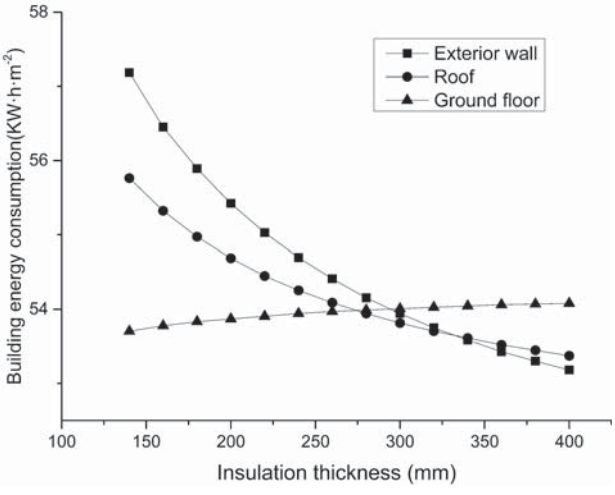

Figure 9. Energy consumption for different envelope insulation thicknesses.

3.2.2. Optimal Glazing Variants

The description of all glazing variants studied is shown in Table 6. Technical guidelines stipulate that U-value of window is between 0.7 W/(m^2·K) and 1.2 W/(m^2·K). There are few windows with heat transfer coefficient lower than 1.2 W/(m^2·K) in the market. We contacted different manufacturers to identify 5 windows used in nearly zero energy residential buildings. Among them, the first window has been produced but not applied.

Table 6. Typical windows summary of nZEBs in severely cold area.

Window Conding	U-value, W/(m^2·K)	SHGC	Visible Light Transmittance	Tightness	Watertight	Wind Pressure	Initial Investment (yuan/m^2)
A-P160	0.6	0.424	0.567	0.30/9 level	700/6 level	5000/9 level	5999
A-P120	0.8	0.439	0.629	0.30/9 level	700/6 level	5000/9 level	3999
B-PAS125	0.9	0.450	0.670	0.20/8 level	600/5 level	5000/9 level	2900
B-78	1.0	0.523	0.710	0.20/8 level	600/5 level	5000/9 level	2700
A-S86	1.1	0.533	0.650	0.30/9 level	700/6 level	5000/9 level	2599

Figure 10 shows that the total primary energy changed little when the U-value increased from 0.6 W/(m^2·K) to 0.9 W/(m^2·K). However, Table 6 shows that the price difference between the two is 3000 yuan/m^2. Change in energy consumption is very obvious when U-value increased from 0.9 W/(m^2·K) to 1.0 W/(m^2·K). In terms of cost, the difference between the two windows is 200 yuan/m^2.

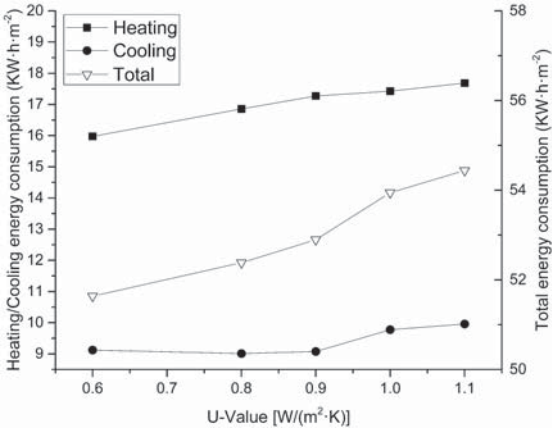

Figure 10. Energy consumption for glazing variants.

3.2.3. Optimal WWR

As previous studies have shown, lowering WWR increases energy efficiency, but on the other hand it also reduces daylighting efficiency. Therefore, it is important to set lower limits to window sizes [17]. Design code for residential buildings (GB 50096-2011) states that daylight factor should not be below 1% in bedroom, living room (hall), and the kitchen. Furthermore, the daylight factor should not be below 0.5% when the light window is set near/on a staircase. Energy conservation design standard for heating in new residential buildings (JGJ26-2010) states WWR of each orientation. East and west WWR should be less than or equal to 30%. South WWR should be less than or equal to 45%. North WWR should be less than or equal to 25%. Simulated variables for WWR are shown in Table 2. East and west energy consumption curve is the steepest, followed by the south, while north energy consumption curve is the most gradual, as shown in Figure 11. This trend also represents the impact of WWR on energy consumption of nZEB in cold regions.

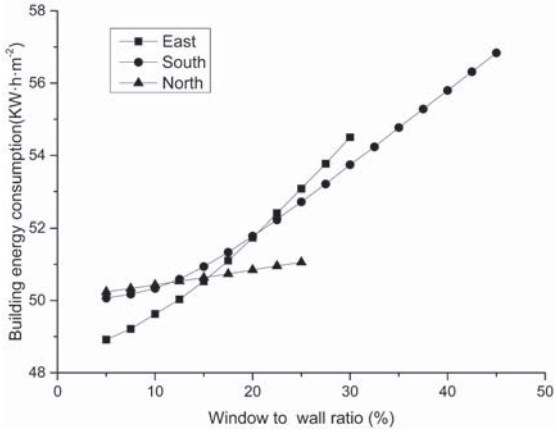

Figure 11. Energy consumption for WWR of different orientation.

3.2.4. Indoor Thermal Disturbance

Not only objective design factors but also artificial subjective factors have an impact on energy consumption. This paper studies the effect of indoor thermal disturbance on the energy consumption

of nZEB in cold regions. Indoor thermal disturbance includes staff density, lighting density and electrical appliances. Staff density was set to 5–10 m^2/person in simulation according to the actual use of the building. The result is shown in Figure 12. With the reduction of indoor personnel, heating energy consumption, cooling energy consumption and total energy consumption all show a downward trend. The downward trend of heating energy consumption curve is relatively flat. Cooling energy consumption and total energy consumption are affected more.

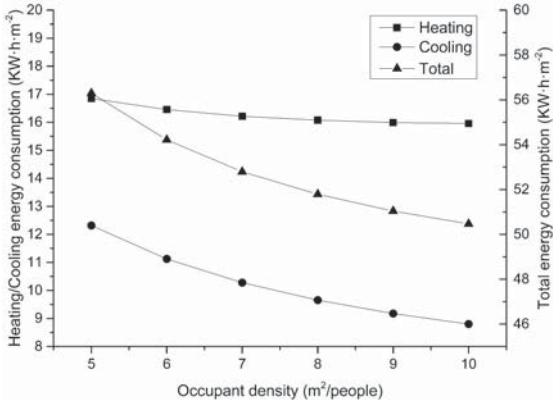

Figure 12. Energy consumption for occupant density.

The Technical Guide points out that the design value of lighting power density is 3 W/m^2. In addition, Heat generated by electrical appliances is 2 W/m^2. The effect of lighting density on energy consumption is shown in Figure 13. The lighting energy consumption is equal to the cooling energy consumption when the lighting density is 3.5 W/m^2. When the lighting density is 5.6 W/m^2, the lighting energy consumption is equal to the heating energy consumption. Although the energy consumption of heating decreased linearly at this time, the total energy consumption showed a straight upward trend. So the lighting density should be minimized under the conditions to satisfy the needs of indoor lighting.

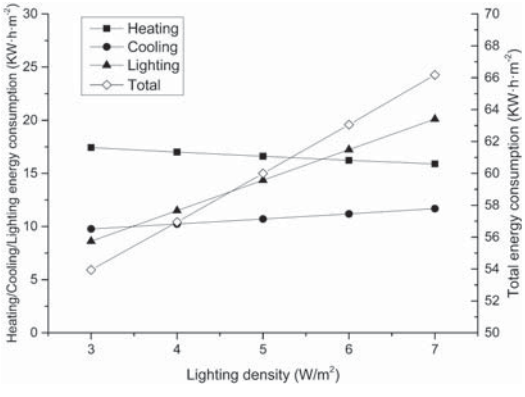

Figure 13. Energy consumption for lighting density.

Figure 14 depicts the effect of electrical appliances load on energy consumption. The impact of electrical appliances load is similar to lighting density. The electrical appliances' energy consumption is equal to the cooling energy consumption when the electrical appliances load is 2.4 W/m^2.

When electrical appliances load is 3.9 W/m^2, the electrical appliances' consumption is equal to the heating energy consumption. The total energy consumption increases linearly with the increase of electrical appliances load. Therefore, the impact of electrical appliances cannot be ignored in design.

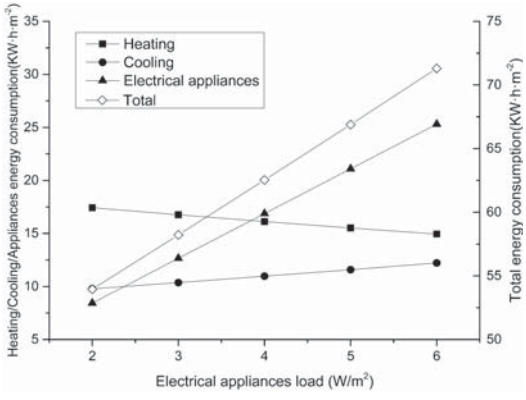

Figure 14. Energy consumption for electrical appliances load.

3.3. ANN Training

The BP network was trained and tested using the processed data in Section 2.2.2. Best training performance is 0.0022624 at epoch 49989. As shown in Figure 15, the network training is over when the function converges. The mean squared error (MSE) assesses the quality of an estimator or a predictor. Definition of an MSE differs according to whether one is describing an estimator or a predictor. For each fold, the ANN with the lowest mean squared error for the testing data was saved and the generalization errors were determined. MSE is given in Equation (1) [21]:

$$E(MSE) = \frac{1}{n}\sum_{i=1}^{n}\left(\hat{Y}_i - Y_i\right)^2 \quad (1)$$

where $\hat{Y}_i$ is the target output, and Y_i is the predicted output, for the training, validation or testing data configuration i, and n is the total number of configurations in the training, validation, or testing data.

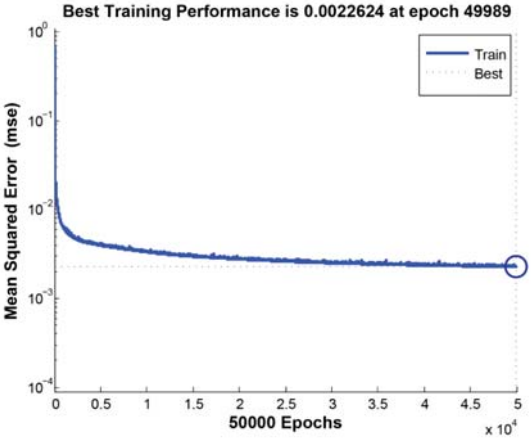

Figure 15. Error reduction curve.

Figure 16 shows the BP neural network model training process. Degree of fitting between BP neural network training results and actual results is high after repeated training. This shows that BP network training meets the expected requirements. Then the test data was predicted using the trained BP network model. The result is shown in Figure 17. The maximum relative error of building energy consumption prediction is 6.46%. Prediction accuracy is high when using BP network model to predict energy consumption.

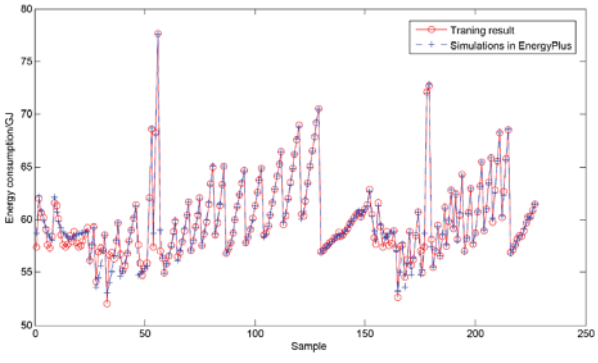

Figure 16. Training process of BP neural network model.

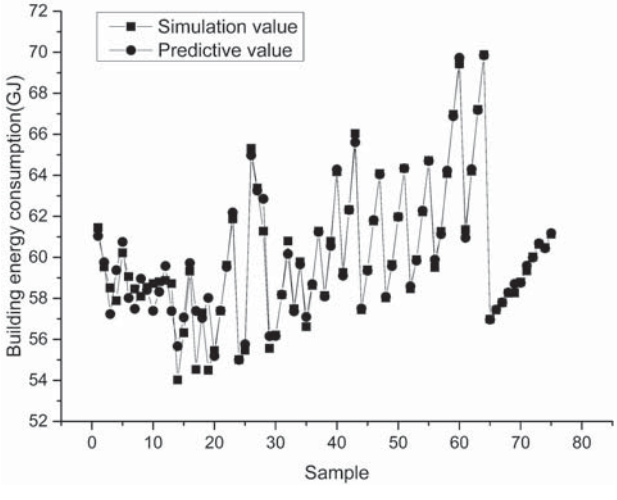

Figure 17. Comparison of simulation results and predictive results.

4. Discussion

The Ministry of Housing and Urban-Rural Development of the People's Republic of China drew on the experience of foreign passive houses and nearly zero energy buildings, combined with the existing engineering practices in our country to compile the "Passive low energy consumption of green building technology guidelines" [34]. Shenyang is in a cold climate in China. In this cold climate such a building has the following characteristics:

- Annual space heat requirement of 18 KW·h/(m^2·a);
- Total energy consumption for heating, cooling and lighting should not exceed 60 KW·h/(m^2·a);
- Leaked air volume must not be higher than 0.6 of the house volume per hour as measured at a pressure of 50Pa;

As is shown from Table 5, the heating energy consumption of the building in the annual energy consumption simulation results is 17.42 KW·h/(m^2·a). This value is less than 18 KW·h/(m^2·a). The annual building energy consumption is 53.93 KW·h/(m^2·a). This value is also within the scope of the Technical Guidelines. Taking the open office area as an example, indoor average temperature reached 19–22 °C during heating in winter, as shown in Figure 8, which represents a comfortable temperature for the occupants. This nZEB possesses a high thermal inertia which in a way protects the indoor environment from the invasion of outdoor disturbance so as to maintain indoor temperature at a comfortable level for occupants, which further reduces the energy consumption induced by the requirement for heating. The energy demand of passive house in Bucharest was simulated using the energyplus software [6]. Building characteristics and system description are similar to benchmark building, including climatic conditions. Simulated demand of energy for heating was 14.1 KW·h/(m^2·a).Bucharest 's climate is milder than Shenyang, so heating demand is smaller.

However, when the exterior wall insulation thickness is less than 260 mm, equivalent to the heat transfer coefficient being greater than 0.115 W/(m^2·K), the heating energy consumption exceeds the required value of 18 KW·h/(m^2·a). The same is true for the roof. When the roof insulation thickness is less than 220 mm, the energy consumption of heating will also exceed the standard value. Thus, it can be seen that even if the heat transfer coefficient of the exterior wall and roof meets the requirements of the technical guidelines, the energy consumption in the final operation may exceed the standard. Therefore, in the program design stage, we can't blindly follow standard values, which may lead to excessive energy consumption.

In any case, it is very important for economic evaluation to be run in parallel with energy simulations, as a cost-optimal solution can really change the design. PAS25 series of windows with U-Value of 0.9 W/(m^2·K) would be the best choice from the cost optimal and energy efficient viewpoint. After simulation optimization, it can be seen that the WWR of each orientation in the scheme stage is 11.59%–15% in the east (west) direction and 9.93%–17.5% in the south direction. The WWR of north facade should try to take a small value on the premise of meeting lighting requirements and ventilation requirements. ESR has been introduced to quantitatively analyze the energy saving effect. In this paper, ESR is defined as Equation (2) [22]:

$$ESR(E_i) = \frac{E_i - E_{bench}}{E_{bench}} \times 100\% \quad (2)$$

where E_i is the energy consumption at given optimization parameter. E_{bench} is the benchmark energy consumption.

The benchmark energy consumption in Section 3.1 for heating, cooling, and electricity is 53.93 KW·h/(m^2·a). E_i is the optimal energy consumption value after changing a key performance parameter. In this paper, the key parameters are as follows: exterior wall insulation thickness, roof insulation thickness, window thermal performance parameters, and WWR for each orientation of the building. Table 7 shows that WWR optimization has the most significant potential for energy saving, followed by the window thermal performance parameters, and finally the envelope insulation thickness.

There is a great association with sample data whether prediction of the artificial neural network model is correct or not. The efficiency of network learning and the accuracy of prediction will be better when the sample data can better represent the characteristics of the predicted problem. On the other hand, when the noise of the sample is too much, the network will learn a lot of useless experiences, which greatly reduces the learning rate and affects the accuracy of the network prediction. The energy consumption of buildings is affected by several characteristics, such as geometry, services, glazing, activity, and weather. However, artificial neural network model has the characteristic of self-learning. It can be based on the different parameters of the building as an input, and then the neural network will automatically adjust the weight, thereby accurately predicting the building's energy consumption.

Table 7. Summary of optimizations results on ESR.

Parameters	Ranges	E_i [KW·h/(m^2·a)]	ESR(E_i)
Exterior wall insulation thickness	280 mm	54.15	0.41
	300 mm	53.94	0.02
	320 mm	53.75	−0.33
Roof insulation thickness	260 mm	54.09	0.30
	280 mm	53.94	0.02
	300 mm	53.81	−0.22
Window thermal performance parameters	Similar PAS125	52.90	−1.91
WWR for East	12.5%	50.03	−7.23
	15%	50.53	−6.30
WWR for South	10%	50.33	−6.68
	12.5%	50.59	−6.19
	15%	50.94	−5.54
	17.5%	51.33	−4.82

The influence of the key performance parameters on the energy consumption of nZEB during the design stage was analyzed through EnergyPlus simulation. 302 sets of data were obtained as training and testing data of BP network model. At the same time, BP model input neurons were identified, including 12 variables: building envelope thermal performance parameters, window-to-wall ratios, indoor thermal disturbance, as shown in Table 2. There is one output neuron in the model, that is, annual energy consumption per unit area of construction. The training parameters of 3-layer BP neural network and network model are determined. Figure 17 shows that the model can predict the energy consumption better. Nearly zero energy buildings will need more careful design to promote energy conservation. The establishment of this prediction method enables architects to easily and accurately obtain the energy consumption of buildings during the design phase. We can adjust the design parameters at any time based on the prediction of energy consumption.

Kang [35] analyzed Equations for Energy Consumption Prediction using Analysis of Variance and multiple regression analysis.The tests also applied an EnergyPlus simulation. The criterion used for the improvement of the prediction was the coefficient of determination. It is expressed as a decimal number between 0.00 and 1.00. 1.00 means perfect prediction in the model. This coefficient is 0.753 for heating energy consumption and 0.602 for cooling energy consumption.

5. Conclusions

This paper presents a study of the nZEB, built in China's cold climate conditions, in accordance with the passive low energy consumption of green building technology guidelines. This nearly zero energy building demonstrates a high thermal inertia which in a way protects the indoor environment from the invasion of outdoor disturbance so as to maintain indoor temperature at a comfortable level for occupants, which further reduces the energy consumption induced by the requirement for heating. Key performance parameters in architectural design stage were optimized based on nZEB energy requirements. The optimal combination of various performance parameters and the ESR were studied on the basis of a large quantity of simulation data. These data were used as training data for artificial neural networks. ANNs were trained to predict the energy consumption of nZEB design.

The heating energy consumption of the building in the annual energy consumption simulation results is 17.42 KW·h/(m^2·a), which is the dominant factor in total building energy consumption. The annual building energy consumption is 53.93 KW·h/(m^2·a). These values are also within the scope of the Technical Guidelines. This building maintains good thermal comfort while meeting energy efficiency standards. We get the following conclusions for the optimization of key performance parameters.

The optimal thickness of exterior wall insulation is 280-320 mm, and corresponding total annual energy consumption is 53.75–54.15 KW·h/(m^2·a). The ESR is about 0.33%. The optimal thickness of roof insulation is 260-300 mm, and corresponding total annual energy consumption is 53.81–54.09 KW·h/(m^2·a). The ESR is about 0.22%. The typical window optimization results are similar to the B-PAS125, and corresponding total annual energy consumption is 52.90 KW·h/(m^2·a). The ESR is about 1.91%. The optimal WWR for the east or west is 12.5%–15%, and corresponding total annual energy consumption is 50.03–50.53 KW·h/(m^2·a). The ESR is about 7.23%. The optimal WWR for the south is 10–17.5%, and corresponding total annual energy consumption is 50.33–51.33 KW·h/(m^2·a). The ESR is about 6.68%. In terms of energy saving potential, this shows that the energy-saving effect of WWR optimization is the most obvious, followed by thermal performance parameters of the window, and finally the insulation thickness.

The maximum relative error of building energy consumption prediction is 6.46%. Prediction accuracy is high when using BP network model to predict energy consumption. The neural network model's calculation process is relatively simple compared with the dynamic calculation method. Therefore, it is easier for engineering designers to learn and apply. In addition, the target optimization process involves a large number of iterative calculations. The energy consumption of the building needs to be evaluated for each iteration. This method takes less time than the dynamic calculation method. The establishment of this prediction method enables architects to easily and accurately obtain the energy consumption of buildings during the design phase.

Additionally, the Ministry of Housing and Urban-Rural Development of the People's Republic of China has mandated that more than 10 million square meters of ultra-low energy consumption, nearly zero energy building demonstration projects will be completed by the year 2020. This study provides essential information that can be used in the future for nZEBs or energy-efficient buildings that will be built in cold climates in China.

In the future, thermal comfort of the nZEBs will be considered. Air temperature, mean radiant temperature, relative humidity, air velocity, dressing style, human activity will be designed. Multi-objective optimization will also be carried out.

Author Contributions: Conceptualization, X.X.; Software, X.X. and D.C.; Validation, M.L.; Formal analysis, D.C.; Data curation, X.X.; Writing—original draft preparation, X.X.; Writing—review and editing, X.X.; Visualization, B.D.; Project administration, G.F.; Funding acquisition, G.F.

Funding: This research was funded by 13th Five-Year National Key R&D Plan Project Nearly-ZEB key strategies and technologies development 2017-2020, grant number 2017YFC0702600.

Conflicts of Interest: The authors declare no conflict of interest.

Abbreviations

The following abbreviations are used in this manuscript:

Acronyms	Description
nZEB	nearly zero energy building
WWR	window-wall ratio
U-value	heat transfer coefficients or thermal transmittances
ANN	artificial neural network
AFA	augmented firefly algorithm
ESR	energy saving rate
SJZU	Shenyang Jianzhu University
MVHR	mechanical ventilation heat recovery unit
HVAC	heating, ventilation, and air conditioning
IDF	file format in EnergyPlus
BP	back Propagation
SHGC	solar heat gain coefficient
MSE	mean squared error

References

1. Park, K.S.; Kim, M.J. Energy Demand Reduction in the Residential Building Sector: A Case Study of Korea. *Energies* **2017**, *10*, 1506. [CrossRef]
2. Ma, Z.; Cooper, P.; Daly, D.; Ledo, L. Existing building retrofits: Methodology and state-of-the-art. *Energy Build.* **2012**, *55*, 889–902.
3. Virote, J.; Neves-Silva, R. Stochastic models for building energy prediction based on occupant behavior assessment. *Energy Build.* **2012**, *53*, 183–193.
4. Marasco, D.E.; Kontokosta, C.E. Applications of machine learning methods to identifying and predicting building retrofit opportunities. *Energy Build.* **2016**, *128*, 431–441. [CrossRef]
5. Passive House—Passivhaus Institut (PHI). Available online: https://passivehouse.com/ (accessed on 22 October 2018).
6. Mihai, M.; Tanasiev, V.; Dinca, C.; Badea, A.; Vidu, R. Passive house analysis in terms of energy performance. *Energy Build.* **2017**, *144*, 74–86. [CrossRef]
7. IEA. SHC Task 40/ECBCS Annex 52, Towards Net Zero Energy Solar Buildings, IEA SHC Task 40 and ECBCS Annex 52. 2008. Available online: http://task40.iea-shc.org/ (accessed on 23 October 2018).
8. Garud, R.; Karnøe, P. Bricolage versus breakthrough: distributed and embedded agency in technology entrepreneurship. *Res. policy.* **2003**, *32*, 277–300. [CrossRef]
9. De Wilde, P. The gap between predicted and measured energy performance of buildings: A framework for investigation. *Autom. Constr.* **2014**, *41*, 40–49. [CrossRef]
10. Pacheco, R.; Ordóñez, J.; Martínez, G. Energy efficient design of building: A review. *Renew. Sustain. Energy Rev.* **2012**, *16*, 3559–3573. [CrossRef]
11. Wang, W.; Tian, Z.; Ding, Y. Investigation on the influencing factors of energy consumption and thermal comfort for a passive solar house with water thermal storage wall. *Energy Build.* **2013**, *64*, 218–223. [CrossRef]
12. Musall, E.; Weiss, T.; Lenoir, A.; Donn, M.; Cory, S.; Garde, F. Net Zero energy solar buildings: An overview and analysis on worldwide building projects. In Proceedings of the EuroSun conference, Graz, Austria, 28 November–1 October 2010.
13. Bajc, T.; Todorović, M.N.; Svorcan, J. CFD analyses for passive house with Trombe wall and impact to energy demand. *Energy Build.* **2015**, *98*, 39–44. [CrossRef]
14. Daouas, N. A study on optimum insulation thickness in walls and energy savings in Tunisian buildings based on analytical calculation of cooling and heating transmission loads. *Appl. Energy.* **2011**, *88*, 156–164. [CrossRef]
15. Özkan, D.B.; Onan, C. Optimization of insulation thickness for different glazing areas in buildings for various climatic regions in Turkey. *Appl. Energy.* **2011**, *88*, 1331–1342. [CrossRef]
16. Susorova, I.; Tabibzadeh, M.; Rahman, A.; Clack, H.L.; Elnimeiri, M. The effect of geometry factors on fenestration energy performance and energy savings in office buildings. *Energy Build.* **2013**, *57*, 6–13. [CrossRef]
17. Thalfeldt, M.; Pikas, E.; Kurnitski, J.; Voll, H. Facade design principles for nearly zero energy buildings in a cold climate. *Energy Build.* **2013**, *67*, 309–321. [CrossRef]
18. Haykin, S. *Neural Networks: A Comprehensive Foundation*; Prentice Hall PTR: Upper Saddle River, NJ, USA, 1994.
19. Zell, A.; Mache, N.; Huebner, R.; Mamier, G.; Vogt, M.; Herrmann, K.; Schmalzl, M.; Sommer, T.; Hatzigeorgiou, A.G.; Doring, S.; et al. SNNS (stuttgart neural network simulator). In *Neural Network Simulation Environments*; Skrzypek, J., Ed.; Springer: Boston, MA, USA, 1994.
20. Banihashemi, S.; Ding, G.; Wang, J. Developing a hybrid model of prediction and classification algorithms for building energy consumption. *Energy Procedia* **2017**, *110*, 371–376. [CrossRef]
21. Paterson, G.; Mumovic, D.; Das, P.; Kimpian, J. Energy use predictions with machine learning during architectural concept design. *Sci. Technol. Built Environ.* **2017**, *23*, 1036–1048. [CrossRef]
22. Zhai, D.; Soh, Y.C. Balancing indoor thermal comfort and energy consumption of ACMV systems via sparse swarm algorithms in optimizations. *Energy Build.* **2017**, *149*, 1–15. [CrossRef]
23. Ahn, J.; Cho, S. Dead-band vs. machine-learning control systems: Analysis of control benefits and energy efficiency. *J. Build. Eng.* **2017**, *12*, 17–25. [CrossRef]
24. Energyplus Documentation. Available online: https://www.energyplus.net/ (accessed on 25 October 2018).

25. OpenStudio Documentation. Available online: http://nrel.github.io/OpenStudio-user-documentation/ (accessed on 25 October 2018).
26. Panja, P.; Velasco, R.; Pathak, M.; Deo, M. Application of artificial intelligence to forecast hydrocarbon production from shales. *Petroleum* **2018**, *4*, 75–89. [CrossRef]
27. Gupta, A.K.; Kumar, P.; Sahoo, R.K.; Sahu, A.K.; Sarangi, S.K. Performance measurement of plate fin heat exchanger by exploration: ANN, ANFIS, GA, and SA. *J. Comput. Des. Eng.* **2017**, *4*, 60–68.
28. Azadeh, A.; Saberi, M.; Anvari, M.; Mohamadi, M. An integrated artificial neural network-genetic algorithm clustering ensemble for performance assessment of decision making units. *J. Intell. Manuf.* **2011**, *22*, 229–245. [CrossRef]
29. Werbos, P. Beyond regression: New Tools for Prediction and Analysis in the Behavior Sciences. Ph.D. Thesis, Harvard University, Cambridge, MA, USA, 1974.
30. Rumelhart, D.; McClelland, J. *Parallel Distributed Processing: Explorations in the Microstructure of Cognition*; MIT Press: Cambridge, MA, USA, 1986.
31. Lippman, R.P. *An Introduction to Computing with Neural Nets*; IEEE Computer Society Press: Los Alamitos, CA, USA, 1987.
32. MathWorks. MATLAB R2018b. Available online: http://www.mathworks.com (accessed on 25 October 2018).
33. Pascal, W.; Michael, L. *Matlab for Neuroscientists*; Academic Press: Burlington, MA, USA, 2009; pp. 307–317, ISBN 978-0-12-374551-4.
34. Passive Ultra-Low Energy Green Building Technical Guidelines. Available online: http://www.mohurd.gov.cn/wjfb/201511/t20151113_225589.html (accessed on 1 July 2018).
35. Kang, H.J. Development of an nearly Zero Emission Building (nZEB) life cycle cost assessment tool for fast decision making in the early design phase. *Energies* **2017**, *10*, 59. [CrossRef]

energies

MDPI

Article

Parametric Analysis of Buildings' Heat Load Depending on Glazing—Hungarian Case Study

Gábor L. Szabó and Ferenc Kalmár *

Department of Building Services and Building Engineering, Faculty of Engineering, University of Debrecen, 4028 Debrecen, Hungary; l.szabo.gabor@eng.unideb.hu

* Correspondence: fkalmar@eng.unideb.hu; Tel.: +36-52-415-155

Received: 29 October 2018; Accepted: 23 November 2018; Published: 25 November 2018

Abstract: The share of cooling is rising in the energy balance of buildings. The reason is for increasing occupants' comfort needs, which is accentuated by the fact that the number and the amplitude of heat waves are increasing. The comfortable and healthy indoor environment should to be realized with the minimum amount of energy and fossil fuels. In order to meet this goal, designers should know the effect of different parameters on the buildings' energy consumption. The energy need for cooling is mainly influenced by the glazed ratio and orientation of the facades, the quality of glazing and shading. In this paper the heat load analysis was done by assuming different types of summer days and surface cooling, depending on the glazing ratio, shading factor and solar factor of glazing. It was proven that, for a certain parameter, the sensitivity of the heat load depends on the orientation and chosen summer day. If the glazing area is doubled, the heat load increases with about 30%. Decreasing the glazed area to 50%, the heat load decreases with about 10%. The heat load decreases with about 3% if the g factor is lowered with 25% or the shading factor is reduced with 60%.

Keywords: building; energy; heat load; sensitivity; glazing; surface cooling

1. Introduction

Mitigation of greenhouse gas emissions is a global goal and countries make important efforts to successfully meet this purpose [1–3]. Increasing the energy efficiency and reducing the energy demand have a priority in each sector. Significant results might be obtained through the energy conscious design of buildings. It was already shown that by proper thermal insulation of the buildings' envelope and rational integration of renewable energy sources important energy savings can be obtained, see for example [4,5]. However, climate change does not help people in their pursuit of reducing the energy use in buildings. In countries with continental temperate climate 60–70% of the total energy consumption of a building was used for heating. In recent decades strict requirements related to the thermal properties of the buildings' envelope and energy performance of buildings were introduced [6–8]. Besides the better thermal properties of the envelope, the warmer winters lead to the decrease of the heating energy demand. At the same time, because of the thermal comfort needs, the number of air conditioned buildings increased considerably. The share of energy use for cooling in the building's energy balance increased in recent decades [9–12]. This is accentuated by the fact that, in recent decades, the number and the amplitude of heat waves during summer have been increasing [13]. By a proper design of thermal mass and heat storage capacity, the heat load of buildings might be reduced [14–21]. However, special attention has to be paid to the asymmetry of the solar radiation [22]. Cooling systems has to be chosen and designed in order to assure proper thermal comfort in closed spaces. In buildings, the required operative temperatures should be provided, minimizing the energy use and avoiding thermal discomfort. Integration of renewable energy sources can be efficiently done by low exergy cooling systems [23–27]. By choosing carefully the surface

temperatures, air temperatures and air velocities in the occupation zone, then draught and asymmetric radiation can be avoided [28–30]. There are different methods and systems available to remove the heat load in a closed space [31–34]. However, to properly choose the cooling system, the heat load has to be determined as precisely as possible. Standard ISO 13790 and standard ISO 52016 give the calculation algorithm and methodology to determine the heat load of a building [35,36]. In the calculations, specific meteorological data have to be taken into account. Furthermore, the building configurations, the space shapes, the used building materials and energy performance requirements are specific for a region or country. In this paper the parametric analysis of building's heat load was done taking into account solar radiation and temperature data from recent years registered in Debrecen, Hungary. It was decided to focus our study on the transparent area of the façade (glazing ratio, orientation, solar factor and shading ratio). Previously, it was demonstrated that the effect of windows *U* value on the buildings' summer heat load is negligible in comparison to the effects of other physical properties of the glazing [37]. Furthermore, the heat gains through the opaque elements are negligible as well, if the envelope is properly insulated, even though there is an ageing process of the insulation material, which has to be taken into account [38].

2. Objectives and Hypothesis

Buildings' heat load is influenced by a series of parameters. Some of these parameters are building dependent; others depend on the climate. The main goal of our research was to analyze the heat load variation in function of glazed ratio of the facades, orientation of glazing, solar factor of glazing and shading type. It was assumed that the sensitivity of the heat load in function of a certain building parameter is the highest for the South orientation of the facade.

3. Practical Implications

Proper design of buildings should result in low energy use and high comfort level. To reach the optimal solutions, complex analysis has to be done. The results of the present research may help practitioners, giving some insights on the buildings' heat load sensitivity to different glazing parameters and on the influence of surface cooling type on the heat load of a conditioned space.

4. Methods

The heat load was determined using the calculation algorithm given by standard ISO 52016. According to this Standard the hourly values of the heat load are calculated in the following steps [28]:

- At first the installed cooling capacity in the analyzed room ($\Phi_{HC,ld,un,ztc,t}$) is assumed to be zero (the room is not cooled);
- The operative temperature ($\theta_{int,op,0,ztc,t}$) is calculated in the room (the cooling system is not in operation);
- If the calculated operative temperature exceeds the set point value ($\theta_{int,op,set,ztc,t}$) required in the room, than the cooling load has to be calculated;
- Firstly, the output of the cooling system is assumed to be ten times higher than the useful area of the room $\Phi_{HC,upper,ztc,t} = 10 \times A_{use,ztc}$. With this theoretical cooling capacity the new operative temperature is calculated $\theta_{int,op,upper,ztc,t}$.
- The output of the cooling system will be:

$$\Phi_{HC,ld,un,ztc,t} = \Phi_{HC,upper,ztc,t} \cdot \frac{\theta_{int,op,set,ztc,t} - \theta_{int,op,0,ztc,t}}{\theta_{int,op,upper,ztc,t} - \theta_{int,op,0,ztc,t}} \quad (1)$$

The operative temperature is calculated as the average of the air temperature of the room and mean radiant temperature of the building elements (practically, the convective heat transfer coefficient and radiative heat transfer coefficient are considered to be equal).

The mean radiant temperature is calculated with Equation (2):

$$\theta_{int,r,mn,ztc,t} = \frac{\sum_{eli=1}^{eln}\left(A_{eli}\cdot\theta_{pli=pln,eli,t}\right)}{\sum_{eli=1}^{eln}A_{eli}} \quad (2)$$

where:

$\theta_{int,r,mn,ztc,t}$ is the mean radiant temperature, in °C;
A_{eli} is the area of building element *eli*, in m^2;
$\theta_{pli\ =\ pln,eli,t}$ is the temperature at node *pli* = *pln* of the building element *eli*, in °C

- The indoor air temperature and the internal surface temperatures of the conditioned space are calculated based on the energy balance of the zone and energy balance of the building elements;
- The energy balance equation of the zone is:

$$\begin{aligned}\left[\frac{C_{int,ztc}}{\Delta t}+\sum_{eli=1}^{eln}\right. & \left.(A_{eli}\cdot h_{ci,eli})+\sum_{vei}^{ven}H_{ve,vei,t}+H_{tr,tb,ztc}\right]\cdot\theta_{int,a,ztc,t}-\sum_{eli=1}^{eln}\left(A_{eli}\cdot h_{ci,eli}\cdot\theta_{pln,eli,t}\right)\\ &=\frac{C_{int,ztc}}{\Delta t}\cdot\theta_{int,a,ztc,t-1}+\sum_{vei}^{ven}\left(H_{ve,vei,t}\cdot\theta_{sup,vei,t}\right)+H_{tr,tb,ztc}\cdot\theta_{e,a,t}+f_{int,c}\\ &\cdot\Phi_{int,ztc,t}+f_{sol,c}\cdot\Phi_{sol,ztc,t}+f_{H/C,c}\cdot\Phi_{HC,ztc,t}\end{aligned} \quad (3)$$

where:

$C_{int,ztc,t}$ is the internal thermal capacity of the zone, in J/K;
Δt is the length of the time interval, t in s;
$\theta_{int,a,ztc,t}$ is the internal air temperature, in °C
$\theta_{int,a,ztc,t\ -\ 1}$ is the internal air temperature in the zone at previous time interval $(t-\Delta t)$, in °C;
A_{eli} is the area of building element *eli*, in m^2;
$h_{ci,eli}$ is the internal convective surface heat transfer coefficient of the building element *eli*, in W/m^{2}K;
$\Theta_{pln,eli,t}$ is the internal surface temperature of the building element *eli*, in °C;
$H_{ve,k,t}$ is the overall heat exchange coefficient by ventilation flow element k, in W/K;
$\Theta_{sup,k,t}$ is the supply temperature of ventilation flow element k, in °C;
$\Theta_{e,a,t}$ is the external air temperature, in °C;
$H_{tr,tb,ztc}$ is the overall heat transfer coefficient for thermal bridges, in W/K;
$f_{int,c,ztc}$ is the convective fraction of the internal gains;
$f_{sol,c,ztc}$ is the convective fraction of the solar radiation;
$f_{H/C,c,ztc}$ is the convective fraction of the cooling system;
$\Phi_{int,ztc,t}$ is the total internal heat gains, in W;
$\Phi_{HC,ztc,t}$ is the cooling load (if negative), in calculation zone *ztc*, at time interval t, depending on type of application of the calculation, in W;
$\Phi_{sol,ztc,t}$ is the directly transmitted solar heat gain into the zone, summed over all window *wi*, in W;

- Building elements are divided into three parts: inner side, inside and outer side and the energy balance equations are to be written for all three nodes;
- The energy balance equation for internal side of a building element ("internal surface node"):

$$\begin{aligned}-(h_{pli-1,eli}\cdot & \quad \theta_{pli-1,eli,t})+\left[\frac{\kappa_{pli,eli}}{\Delta t}+h_{ci,eli}+h_{ri,eli}\cdot\sum_{elk=1}^{eln}\left(\frac{A_{elk}}{A_{tot}}\right)+h_{pli-1,eli}\right]\cdot\theta_{pli,eli,t}\\ &-h_{ci,eli}\cdot\Theta_{int,a,zt,t}-\sum_{elk=1}^{eln}\left(h_{ri,eli}\cdot\frac{A_{elk}}{A_{tot}}\cdot\theta_{pli,elk,t}\right)\\ &=\frac{\kappa_{pli,eli}}{\Delta t}\cdot\theta_{pli,eli,t-1}+\frac{1}{A_{tot}}\\ &\cdot[(1-f_{int,c})\cdot\Phi_{int,ztc,t}+(1-f_{sol,c})\cdot\Phi_{sol,ztc,t}+(1-f_{H/C,c})\cdot\Phi_{HC,ztc,t}]\end{aligned} \quad (4)$$

where:

A_{elk} is the area of (this or other) building element *elk*, in zone *ztc*, in m^2;
A_{tot} is the sum areas A_{elk} of all building elements *elk* = 1, . . . ,*eln*, in m^2;
$\theta_{pli,eli,t}$ is the temperature at node *pli*, in °C;
$\theta_{pli-1,eli,t}$ is the temperature at node $pli - 1$, in °C;
$\theta_{int,a,ztc,t}$ is the internal air temperature in the zone, in °C;
$h_{pli-1,eli,t}$ is the conductance between node *pli* and node $pli - 1$, in W/m^2K;
$\kappa_{pli,eli}$ is the real heat capacity of node *pli*, in J/m^2K;
$h_{ci,eli}$ is the internal convective surface heat transfer coefficient, in W/m^2K;
$h_{ri,eli}$ is the internal radiative surface heat transfer coefficient, in W/m^2K;
$\theta_{pli,eli,t-1}$ is the temperature at node *pli*, at previous time interval $(t - \Delta t)$ in °C.

- The energy balance equation inside the building element:

$$-h_{pli-1,eli}\cdot\theta_{pli-1,eli,t} + \left[\frac{\kappa_{pli,eli}}{\Delta t} + h_{pli,eli} + h_{pli-1,eli}\right]\cdot\theta_{pli,eli,t} - h_{pli,eli}\cdot\theta_{pli+1,eli,t} = \frac{\kappa_{pli,eli}}{\Delta t}\cdot\theta_{pli,eli,t-1} \quad (5)$$

where:

$\theta_{pli+1,eli,t}$ is the temperature at node *pli* + 1, in °C;
$h_{pli,eli,t}$ is the conductance between node *pli* + 1 and node *pli*, in W/m^2K;

- The energy balance equation for the external side of a building element is:

$$\begin{aligned}\left(\tfrac{\kappa_{pli,eli}}{\Delta t} + h_{ce,eli} \quad + h_{re,eli} + h_{pli,eli}\right)\cdot\theta_{pli,eli,t} - h_{pli,eli}\cdot\theta_{pli+1,eli,t} \\ = \tfrac{\kappa_{pli,eli}}{\Delta t}\cdot\theta_{pli,eli,t-1} + (h_{ce,eli} + h_{re,eli})\cdot\theta_{e,t} + \alpha_{sol,pli,eli} \\ \cdot\left(I_{sol,dif,eli,t} + I_{sol,dir,eli,t}\cdot F_{sh,obst,eli,t}\right) - \theta_{sky,eli,t}\end{aligned} \quad (6)$$

where:

$\theta_{e,a,t}$ is the temperature of external environment, in °C;
$h_{ce,eli}$ is the external convective surface heat transfer coefficient, in W/m^2K;
$h_{re,eli}$ is the external radiative surface heat transfer coefficient, in W/m^2K;
$\alpha_{sol,eli}$ is the solar absorption coefficient at the external surface, in W/m^2K;
$I_{sol,dif,eli,t}$ is the diffuse part (including circumsolar) of the solar irradiance on the element with tilt angle β_{eli} and orientation angle γ_{eli};
$I_{sol,dir,eli,t}$·is the direct part (excluding circumsolar) of the solar irradiance on the element with tilt angle β_{eli} and orientation angle γ_{eli};
$F_{sh,obst,eli,t}$ is the shading reduction factor for external obstacles for the element;
$\theta_{sky,eli,t}$ is the (extra) thermal radiation to the sky, in W/m^2;
β_{eli} is the tilt angle of the element (from horizonal, measured upwards facing), in degrees;
γ_{eli} is the orientation angle of the element, in degrees.

- For external opaque elements, five calculation nodes were taken into account (one on the internal side, one on the external and three inside the structure);
- For external transparent elements two calculation nodes were taken into account (one inside and one on the outer side);
- For internal building elements there are no prescriptions for the number of calculation nodes (we have calculated with nodes placed between the layers of the structures).
- In the calculation, the heat storage capacity is taken into account depending on the heat storage class of the building structure:

Class I. (mass concentrated at internal side):

$$\kappa_{pl5,eli} = \kappa_{m,eli} \quad (7)$$

$$\kappa_{pl1,eli} = \kappa_{pl2,eli} = \kappa_{pl3,eli} = \kappa_{pl4,eli} = 0 \quad (8)$$

Class E (mass concentrated at external side)

$$\kappa_{pl1,eli} = \kappa_{m,eli} \quad (9)$$

$$\kappa_{pl2,eli} = \kappa_{pl3,eli} = \kappa_{pl4,eli} = \kappa_{pl5,eli} = 0 \quad (10)$$

Class IE (mass divided over internal and external side)

$$\kappa_{pl1,eli} = \kappa_{pl5,eli} = \frac{\kappa_{m,eli}}{2} \quad (11)$$

$$\kappa_{pl2,eli} = \kappa_{pl3,eli} = \kappa_{pl4,eli} = 0 \quad (12)$$

Class D (equally distributed)

$$\kappa_{pl1,eli} = \kappa_{pl5,eli} = \frac{\kappa_{m,eli}}{8} \quad (13)$$

$$\kappa_{pl2,eli} = \kappa_{pl3,eli} = \kappa_{pl4,eli} = \frac{\kappa_{m,eli}}{4} \quad (14)$$

Class M (mass concentrated in side)

$$\kappa_{pl3,eli} = \kappa_{m,eli} \quad (15)$$

$$\kappa_{pl1,eli} = \kappa_{pl2,eli} = \kappa_{pl4,eli} = \kappa_{pl5,eli} = 0 \quad (16)$$

where: $\kappa_{m,eli}$ is the real heat capacity of opaque element *eli*, in J/m^{2}K.

It was assumed that surface cooling systems are used in the conditioned room. The convective ratio ($f_{C,c,ztc}$) was considered 40% in the case of wall, and 30% in the case of ceiling cooling.

4.1. The Analyzed Room

In order to perform the calculations, a reference room was taken into consideration, and placed on an intermediate floor an office building (Figure 1).

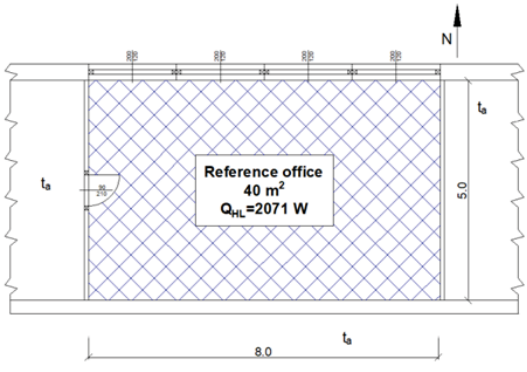

Figure 1. Layout of the analyzed room.

The room height is 3.5 m and has suspended ceiling (0.5 m). The slabs structure is: 2.0 cm lime plastering; 20 cm reinforced concrete, 6 cm concrete 0.6 cm tiles. The internal wall (opposite to the external wall) has the following structure: 2.0 cm lime plastering, 30 cm brick, 1.5 cm lime plastering. In the analyzed office, 10 persons are working between 8:00–17:00. Fresh air is 100% outdoor air and it is introduced in the room without changing its physical parameters. It is assumed that the fresh air flow is 30 m^3/(h·person). The overall heat transfer coefficient of the external wall is 0.24 W/(m^2·K),

while the window has an overall heat transfer coefficient of 1.1 W/(m^2·K) (these values are currently required for a nearly zero energy building in Hungary). The heat storage capacity of the room is: 318110 J/m^{2}K, (Class I). In the reference case, the glazed ratio of the external wall is 40% and the g value of glazing is 0.67.

4.2. Meteorological Parameters

The incident solar radiation and the outdoor temperature in summer were analyzed for recent years. It was observed that in contrast with the previously used Hungarian 04140 Standard (which provides the solar radiation and temperature data for heat load calculation until 2012) the solar radiation does not show symmetry for East and West orientation. In most cases, the incident solar radiation intensity and the solar energy yield for East orientation exceeds the data registered for West orientation. These days were considered asymmetric days [14]. It was decided to analyze the heat load for one symmetric and two asymmetric days. Two extreme hot days were chosen (one symmetric and one asymmetric) and one extreme torrid asymmetric day. Those days are considered extreme hot days, which have an average outdoor temperature in the warmest hour higher than 30 °C. If the mean outdoor temperature in the warmest hour is higher than 35 °C, the day is called extreme torrid. The outdoor temperature variation and the incident solar radiation intensity for the chosen days can be seen in Figure 2. In Figure 2a the data for the extreme hot symmetric day is presented. Figure 2b shows the data for the extreme hot asymmetric day and in Figure 3c, the data for the extreme torrid asymmetric day can be found.

It was decided to analyze the heat load variation depending on the glazed ratio, total solar transmittance of the glazing and shading factor of glazing (Table 1).

Table 1. Input parameters ("*" denotes reference case data).

Changed Parameter	**Analyzed Cases**			
Orientation	North	East	West	South
Meteorological parameters	Extremely warm symmetric day (standard 04140)	Extremely warm asymmetric day (2012.06.30)		Extremely hot asymmetric day (2011.07.10)
Shading	No shading (F_{obst} = 1.0) *	Partial shading (F_{obst} = 0.7)		Strong shading (F_{obst} = 0.4)
Glazing	Triple glazing, Low-e on both sides (g = 0.5; U_w = 0.82 W/(m^2·K))	Double glazing, Low-e on the outer side (g = 0.67; U_w = 1.1 W/(m^2·K)) *		Triple glazing (g = 0.7; U_w = 1.0 W/(m^2·K))
Glazed ratio	G_r = 20%	G_r = 40% *		G_r = 80%

As seen in the first column, the orientation, the meteorological parameters, the shading factor of the transparent surfaces, the glazing type (U and g values) and the glazed ratio of the facade were chosen as variables in the parametric study. We have four orientations of the facade, three days with different meteorological parameters, three types of shading, three types of glazing and three values for glazing ratio. The calculations were done for each combination of these parameters, so the heat load was computed for 648 cases (324—wall cooling; 324—ceiling cooling).

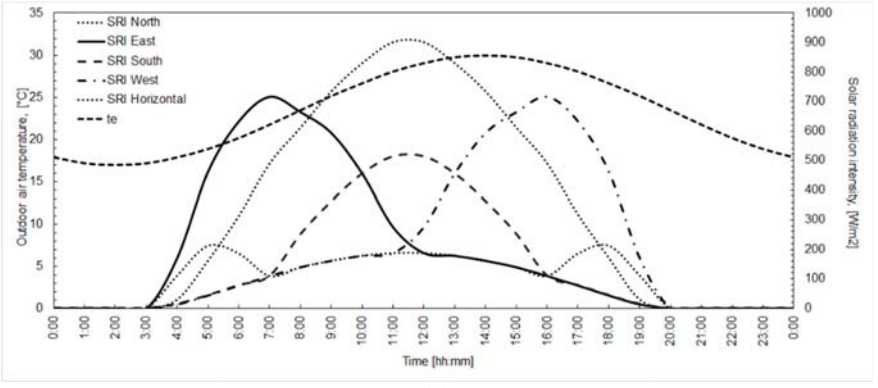

(**a**)

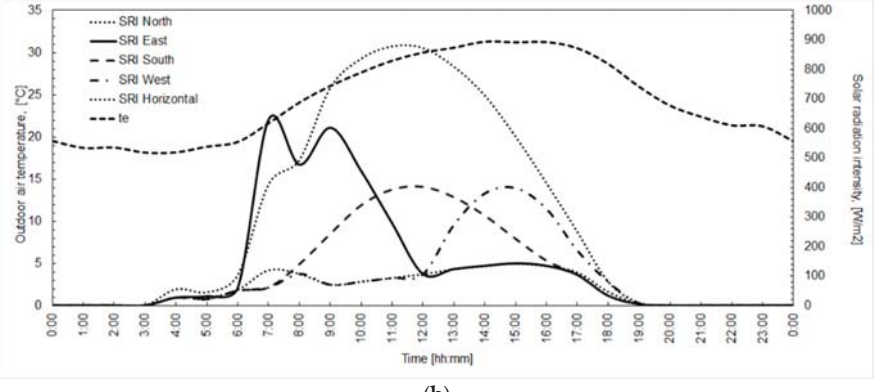

(**b**)

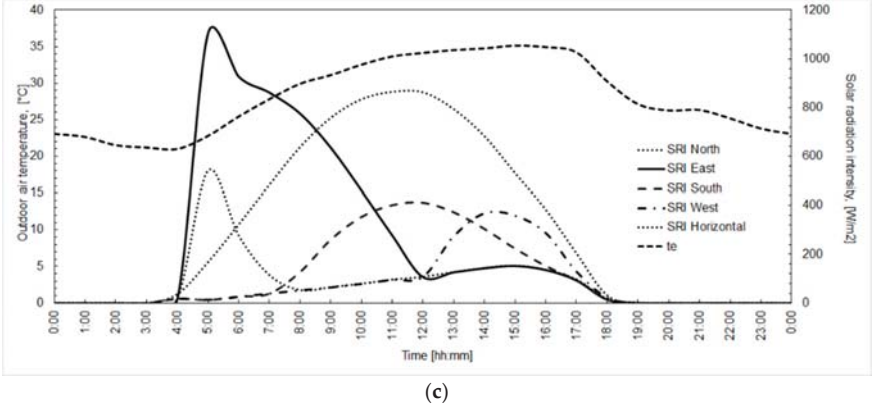

(**c**)

Figure 2. Outdoor temperature and incident solar radiation intensity. (**a**) Extreme hot symmetric day (data from standard 04140); (**b**) Extreme hot asymmetric day (2012.06.30) [39]; (**c**) Extreme torrid asymmetric day (2011.07.10) [39].

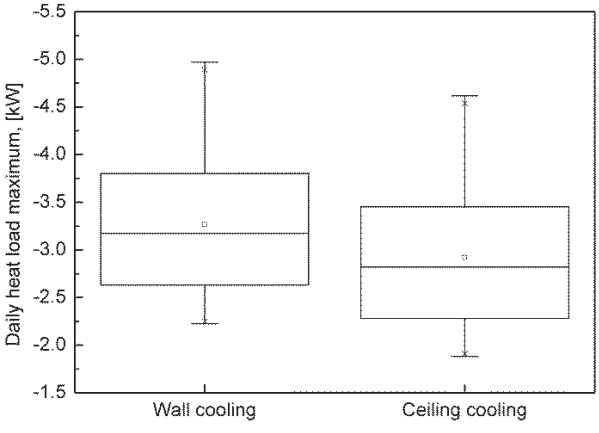

Figure 3. Box chart of the maximum heat load values.

5. Results

In practice, the cooling equipments are chosen for the maximum value of the heat load. In our calculus the heat load variation for the whole day was determined, but from practical reasons in the following the maximum values will be presented and discussed. For the analyzed 648 cases, the computed maximum values of the daily heat load are presented in Figure 3.

The obtained daily maximum heat load values (324 for wall cooling and 324 for ceiling cooling) were classified into six classes (Table 2).

Table 2. Heat load classes.

Heat Load Class	Wall Cooling			Ceiling Cooling		
	Interval		No. of values	Interval		No. of values
1st class	−4971	−4513	18	−4617	−4161	18
2nd class	−4512	−4056	24	−4160	−3705	24
3rd class	−4055	−3598	85	−3704	−3250	87
4th class	−3597	−3140	38	−3249	−2794	36
5th class	−3139	−2683	65	−2793	−2338	65
6th class	−2682	−2225	94	−2337	−1882	94

It can be observed that 55% of the obtained values are found in the 3rd and 6th classes, both for wall and ceiling cooling. The maximum values of the indoor operative temperatures can be seen in Table 3.

Table 3. Maximum indoor operative temperatures [°C].

Operative Temperature	Wall	Ceiling
Minimum	25.82	25.80
Maximum	26.26	26.21
Median	26.17	26.14
Mean	26.13	26.10
Standard Deviation	0.102	0.100

The effects of the glazed ration and orientation on the heat load can be seen in Figure 4.

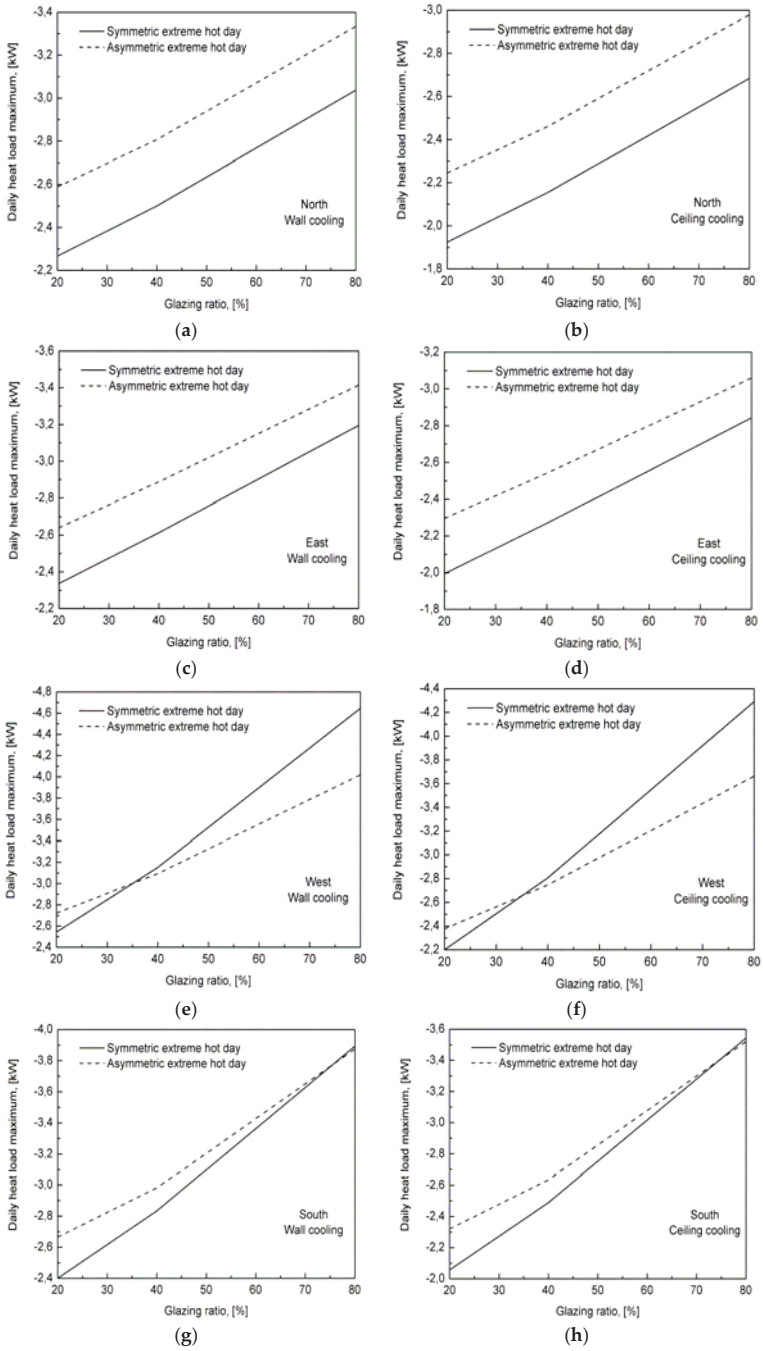

Figure 4. Interrelation between glazing ratio and the maximum of the daily heat load. (**a**) North orientation and wall cooling; (**b**) North orientation and ceiling cooling; (**c**) East orientation and wall cooling; (**d**) East orientation and ceiling cooling; (**e**) West orientation and wall cooling; (**f**) West orientation and ceiling cooling; (**g**) South orientation and wall cooling; (**h**) South orientation and ceiling cooling.

The effects of the shading ratio, solar factor and glazing ratio on the heat load for West orientation of the facade are shown in Figure 5. On the abscissa, the variation of the analyzed parameter can be observed in [%]. The 0 value on the abscissa corresponds to the reference values of the solar factor, glazing ratio and shading ratio. It can be observed that the glazing ratio was increased and decreased, while the solar factor and the shading ratio were only decreased. The reason is that the reference value of the shading ratio was 1 (no shading), so this value cannot be increased further. Similarly, the reference value of the solar factor was 0.67 (this value is around the highest, which characterize the currently used windows).

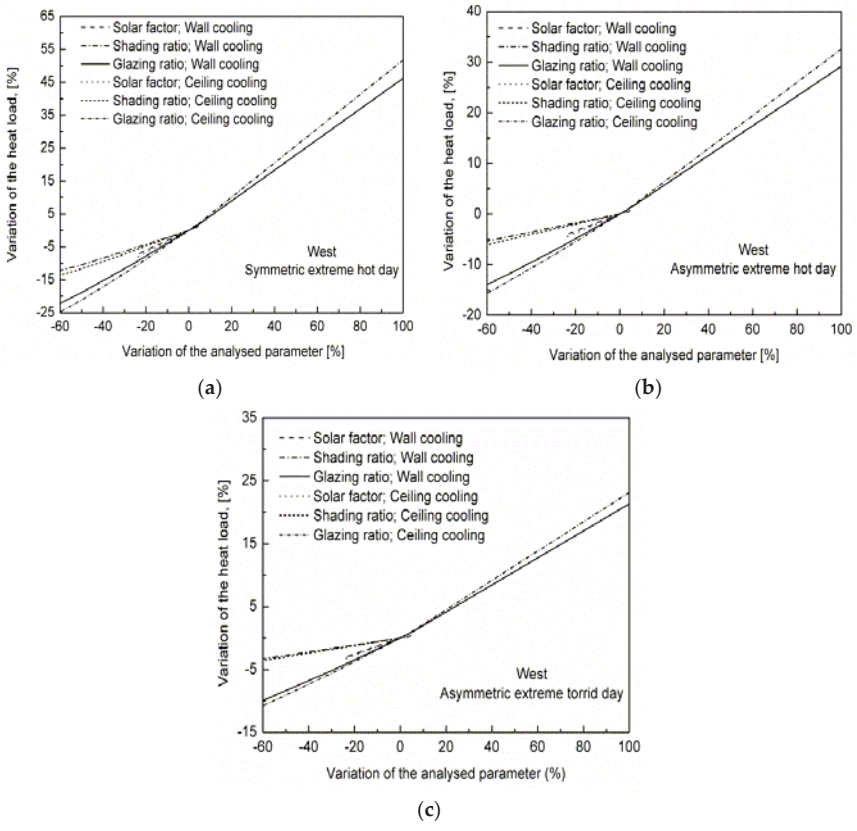

Figure 5. Sensitivity of the heat load depending on the glazing ratio, solar factor and shading ratio (West orientation of the facade). (**a**) Symmetric extreme hot day; (**b**) Asymmetric extreme hot day; (**c**) Asymmetric extreme torrid day.

It can be observed that the variation of glazing ratio, solar factor and shading ratio lead to a linear variation of the heat load maximum values if the calculation methodology given by Standard ISO 52016 is used. The variation of the heat load (in comparison to the reference case) for North, East and South orientation is given in Tables 4–6. In these tables, the heat load variation is shown both for wall and ceiling cooling. For each variable (F_{obst}, g-value and Gr) two values are presented. In the reference case the shading factor is 1. In the tables the heat load variation can be seen if the shading factor was decreased with 30% and 60% respectively. For solar factor, the reference value was decreased with 25.37% and increased with 4.48%. The glazing ratio of the facade was decreased with 50% and increased with 100%. It can be observed that the variation of the glazing ratio has the highest impact

on the heat load. Furthermore, the highest variations of the heat load were obtained for symmetric hot day.

Table 4. Variation of the heat load for North orientation of the facade [%].

Day Type	Wall Cooling						Ceiling Cooling					
	ΔF_{obst} [%]		Δg [%]		ΔG_r [%]		ΔF_{obst} [%]		Δg [%]		ΔG_r [%]	
	−30	−60	−25.37	4.48	−50	100	−30	−60	−25.37	4.48	−50	100
SHD	−0.1	−0.3	−2.9	0.4	−9.2	21.1	−0.1	−0.3	−3.3	0.5	−10.5	24.1
AHD	0.0	0.0	−2.2	0.2	−7.7	18.6	0.0	0.0	−2.5	0.2	−8.7	20.8
ATD	−0.2	−0.4	−2.1	0.1	−5.9	13.6	−0.2	−0.4	−2.3	0.1	−6.4	14.7

Table 5. Variation of the heat load for East orientation of the facade [%].

Day Type	Wall Cooling						Ceiling Cooling					
	ΔF_{obst} [%]		Δg [%]		ΔG_r [%]		ΔF_{obst} [%]		Δg [%]		ΔG_r [%]	
	−30	−60	−25.37	4.48	−50	100	−30	−60	−25.37	4.48	−50	100
SHD	−1.2	−2.5	−3.8	0.5	−10.4	21.8	−1.5	−2.9	−4.3	0.6	−11.8	24.8
AHD	−0.8	−1.6	−2.8	0.3	−8.5	18.0	−0.9	−1.8	−3.2	0.4	−9.6	20.1
ATD	−1.2	−2.3	−2.8	0.2	−7.0	18.3	−1.3	−2.6	−3.1	0.2	−7.6	20.8

Table 6. Variation of the heat load for South orientation of the facade [%].

Day Type	Wall Cooling						Ceiling Cooling					
	ΔF_{obst} [%]		Δg [%]		ΔG_r [%]		ΔF_{obst} [%]		Δg [%]		ΔG_r [%]	
	−30	−60	−25.37	4.48	−50	100	−30	−60	−25.37	4.48	−50	100
SHD	−3.6	−7.3	−5.8	0.9	−14.9	36.3	−4.1	−8.3	−6.6	1.1	−16.9	41.0
AHD	−2.1	−3.5	−3.9	0.5	−10.3	29.2	−2.4	−4.1	−4.4	0.6	−11.6	32.7
ATD	−1.6	−3.2	−3.2	0.3	−8.2	21.4	−1.8	−3.5	−3.5	0.3	−9.0	23.1

6. Discussion

The variation of the heat load depending on the glazing ratio, solar factor and shading is linear and can be characterized by the angle between the line of the heat load and horizontal axis. The higher angle means higher sensitivity. The angle values calculated for chosen days and each orientation are presented in Table 7.

It can be seen that in all cases, the heat load shows the highest angle (sensitivity) depending on the glazing ratio. Furthermore, it can be observed that for a certain orientation of the façade the sensitivity of the heat load is higher in case of ceiling cooling in comparison with the wall cooling. For all analyzed parameters, the highest sensitivity was obtained for symmetric hot day. The asymmetric hot day shows higher sensitivity than the asymmetric torrid day. For a certain parameter, day and surface cooling type the highest sensitivity is observed for West orientation. However, in the case of asymmetric days the sensitivity of the heat load for West and South orientation are almost similar.

The calculations were done assuming 70% heat exchange through radiation in the case of ceiling cooling and 60% in the case of wall cooling. In Figure 6. the sensitivity variation is presented for asymmetric extreme torrid day and West orientation of the faced for all analyzed parameters, taking into account other values for the radiation ratio (1296 simulations were done in total). For a certain parameter, (shading ratio, solar factor or glazing ratio) it can be seen that the highest sensitivity of the heat load is given by the ideal case (100% heat exchange by radiation). Decreasing the radiation ratio, the sensitivity shows lower values. If the glazing area is doubled, then the heat load increases with about 30%. Decreasing the glazed area to half, the heat load decreases with about 10%. The sensitivity of the heat load is almost similar in the case of solar factor and shading ratio. For real values of the radiation ratio the heat load decreases with about 3% if the g factor is lowered with 25% or the shading factor is reduced with 60%.

Table 7. Angle of the heat load variation [°].

Analyzed Day	Cooling Type	Orientation	G_r	g	F_{obst}
SHD	Ceiling cooling	N	13.0	7.2	0.3
		E	13.7	9.4	2.8
		W	25.9	18.6	12.8
		S	21.1	14.3	7.9
	Wall cooling	N	11.4	6.2	0.3
		E	12.1	8.2	2.4
		W	23.5	16.7	11.4
		S	18.8	12.7	6.9
AHD	Ceiling cooling	N	11.1	5.3	0.0
		E	11.2	6.8	1.7
		W	17.0	10.3	5.8
		S	16.4	9.6	3.9
	Wall cooling	N	9.9	4.6	0.0
		E	10.0	6.0	1.5
		W	15.3	9.2	5.1
		S	14.7	8.5	3.4
ATD	Ceiling cooling	N	8.0	4.5	0.4
		E	10.7	6.4	2.4
		W	12.1	7.3	3.4
		S	12.1	7.3	3.3
	Wall cooling	N	7.4	4.1	0.4
		E	9.6	5.8	2.2
		W	11.2	6.7	3.2
		S	11.2	6.7	3.0

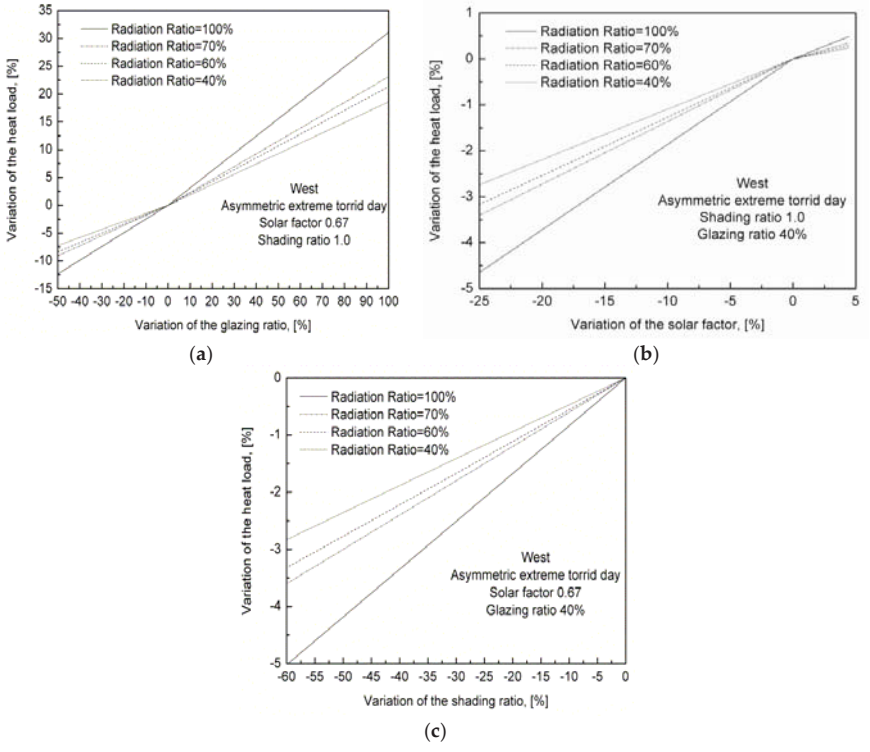

Figure 6. Heat load sensitivity in function of the radiation ratio. (**a**) g = 0.67, F_{obst} = 1.0; (**b**) F_{obst} = 1.0, Gr = 40%; (**c**) g = 0.67; Gr = 40%.

The limitations of our research are as follows:

- We have taken into account windows which can be found on the market. The U and g values are specific for these products;
- It was assumed an office with certain geometry and the number of occupants was set to 10. So, the internal heat loads were constant during the working hours;
- The used global radiation and temperature values were measured in Debrecen, Hungary;
- Surface cooling systems were taken into account. It was assumed that the fresh air (100% outdoor air) is provided in the conditioned room without changing its temperature and relative humidity.

7. Conclusions

In summer, the indoor thermal comfort in buildings is provided using air conditioning systems. The all-air cooling systems usually are using refrigerants and compressors and these systems are operating using electricity. By moving the cold air in the rooms, draught may lead to discomfort. Wall and ceiling cooling systems may avoid draught and the operation temperatures allow for the utilization of renewable energies. In order to obtain the highest performance of the cooling systems, the heat load ought to be determined as accurately as possible. The analysis performed clearly shows that the glazing ratio has the biggest influence on the heat load of a closed space. Considering windows widely used in practice (real values of the shading ratio and solar factor) the sensitivity of the heat load depending on these parameters is lower than 10% in the case of asymmetric days. The highest sensitivity values were obtained for symmetric days (rarely met in practice, but widely used for heat load calculations). The West and South orientations of the glazing leads to highest sensitivity values. The differences between the heat loads sensitivities obtained for different orientations were minimal in the case of asymmetric torrid days. The sensitivity of the maximum values of the heat load shows a linear variation depending on the analyzed parameters (glazing ratio, solar factor and shading ratio).

Author Contributions: Concetualization, F.K.; Methodology, F.K. and G.L.S.; Software, G.L.S.; Validation, F.K. and G.L.S.; Formal Analysis, F.K.; Investigation, G.L.S.; Resources, G.L.S.; Data Curation, G.L.S.; Writing-Original Draft Preparation, F.K. and G.L.S.; Writing-Review & Editing, F.K.; Visualization, G.L.S.

Funding: The research was financed by the Higher Education Institutional Excellence Programme of the Ministry of Human Capacities in Hungary, within the framework of the Energetics thematic program of the University of Debrecen.

Acknowledgments: Authors would like to express their gratitude to András Zöld for his kind comments and observations.

Conflicts of Interest: The authors declare no conflict of interest.

Nomenclature

- SHD—symmetric extreme hot day;
- AHD—asymmetric extreme hot day;
- ATD—asymmetric extreme torrid day;
- N—North;
- E—East;
- W—West;
- S—South;
- Q_{HL}—heat load of the room, [W];
- t_e—outdoor temperature, [°C];
- SRI—solar radiation intensity, [W/m^2];
- Gr—glazing ratio of the façade, [%];
- U_w—overall heat transfer coefficient of windows, [W/m^2·K];
- g—solar factor of glazing, [-];
- F_{obst}—shading factor, [-];
- ΔGr—variation of the glazed ratio of the facade, [%];
- Δg—variation of the solar factor of glazing, [%];
- ΔF_{obst}—variation of the shading factor, [%];

- $\theta_{int,r,mn,ztc,t}$ is the mean radiant temperature, in °C;
- A_{eli} is the area of building element *eli*, in m2;
- $\theta_{pli\,=\,pln,eli,t}$ is the temperature at node $pli = pln$ of the building element *eli*, in °C
- $C_{int,ztc,t}$ is the internal thermal capacity of the zone, in J/K;
- Δt is the length of the time interval, t in s;
- $\theta_{int,a,ztc,t}$ is the internal air temperature, in °C
- $\theta_{int,a,ztc,t\,-\,1}$ is the internal air temperature in the zone at previous time interval $(t-\Delta t)$, in °C;
- A_{eli} is the area of building element *eli*, in m2;
- $h_{ci,eli}$ is the internal convective surface heat transfer coefficient of the building element *eli*, in W/m^{2}K;
- $\Theta_{pln,eli,t}$ is the internal surface temperature of the building element *eli*, in °C;
- $H_{ve,k,t}$ is the overall heat exchange coefficient by ventilation flow element k, in W/K;
- $\Theta_{sup,k,t}$ is the supply temperature of ventilation flow element k, in °C;
- $\Theta_{e,a,t}$ is the external air temperature, in °C;
- $H_{tr,tb,ztc}$ is the overall heat transfer coefficient for thermal bridges, in W/K;
- $f_{int,c,ztc}$ is the convective fraction of the internal gains;
- $f_{sol,c,ztc}$ is the convective fraction of the solar radiation;
- $f_{H/C,c,ztc}$ is the convective fraction of the cooling system;
- $\Phi_{int,ztc,t}$ is the total internal heat gains, in W;
- $\Phi_{HC,ztc,t}$ is the cooling load (if negative), in calculation zone *ztc*, at time interval t, depending on type of application of the calculation, in W;
- $\Phi_{sol,ztc,t}$ is the directly transmitted solar heat gain into the zone, summed over all window *wi*, in W;
- A_{elk} is the area of (this or other) building element *elk*, in zone *ztc*, in m^2;
- A_{tot} is the sum areas A_{elk} of all building elements $elk = 1, \ldots, eln$, in m^2;
- $\theta_{pli,eli,t}$ is the temperature at node *pli*, in °C;
- $\theta_{pli\,-\,1,eli,t}$ is the temperature at node $pli - 1$, in °C;
- $\theta_{int,a,ztc,t}$ is the internal air temperature in the zone, in °C;
- $h_{pli\,-\,1,eli,t}$ is the conductance between node *pli* and node $pli - 1$, in W/m^{2}K;
- $\kappa_{pli,eli}$ is the real heat capacity of node *pli*, in J/m^{2}K;
- $h_{ci,eli}$ is the internal convective surface heat transfer coefficient, in W/m^{2}K;
- $h_{ri,eli}$ is the internal radiative surface heat transfer coefficient, in W/m^{2}K;
- $\theta_{pli,eli,t\,-\,1}$ is the temperature at node *pli*, at previous time interval $(t - \Delta t)$ in °C.
- $\theta_{pli\,+\,1,eli,t}$ is the temperature at node $pli + 1$, in °C;
- $h_{pli,eli,t}$ is the conductance between node $pli + 1$ and node *pli*, in W/m^{2}K;
- $\theta_{e,a,t}$ is the temperature of external environment, in °C;
- $h_{ce,eli}$ is the external convective surface heat transfer coefficient, in W/m^{2}K;
- $h_{re,eli}$ is the external radiative surface heat transfer coefficient, in W/m^{2}K;
- $\alpha_{sol,eli}$ is the solar absorption coefficient at the external surface, in W/m^{2}K;
- $I_{sol,dif,eli,t}$ is the diffuse part (including circumsolar) of the solar irradiance on the element with tilt angle β_{eli} and orientation angle γ_{eli};
- $I_{sol,dir,eli,t}$·is the direct part (excluding circumsolar) of the solar irradiance on the element with tilt angle β_{eli} and orientation angle γ_{eli};
- $F_{sh,obst,eli,t}$ is the shading reduction factor for external obstacles for the element;
- $\theta_{sky,eli,t}$ is the (extra) thermal radiation to the sky, in W/m^2;
- β_{eli} is the tilt angle of the element (from horizonal, measured upwards facing), in degrees;
- γ_{eli} is the orientation angle of the element, in degrees.

References

1. West, J.J.; Smith, S.J.; Silva, R.A.; Naik, V.; Zhang, Y.; Adelman, Z.; Fry, M.M.; Anenberg, S.; Horowitz, L.W.; Lamarque, J.-F. Co-benefits of mitigating global greenhouse gas emissions for future air quality and human health. *Nature Climate Change* **2013**, *3*, 885–889. [CrossRef] [PubMed]
2. Dodman, D. Blaming cities for climate change? An analysis of urban greenhouse gas emissions inventories. *Environ. Urban.* **2009**, *21*, 185–201. [CrossRef]
3. Schimschar, S.; Blok, K.; Boermans, T.; Hermelink, A. Germany's path towards nearly zero-energy buildings—Enabling the greenhouse gas mitigation potential in the building stock. *Energy Policy* **2011**, *39*, 3346–3360. [CrossRef]

4. Chwieduk, D.A. Towards modern options of energy conservation in buildings. *Renew. Energy* **2017**, *101*, 1194–1202. [CrossRef]
5. Aditya, L.; Mahlia, T.M.I.; Rismanchi, B.; Ng, H.M.; Hasan, M.H.; Metselaar, H.S.C.; Muraza, O.; Aditiya, H.B. A review on insulation materials for energy conservation in buildings. *Renew. Sustain. Energy Rev.* **2017**, *73*, 1352–1365. [CrossRef]
6. Paoletti, G.; Pascuas, R.P.; Pernetti, R.; Lollini, R. Nearly Zero Energy Buildings: An Overview of the Main Construction Features across Europe. *Buildings* **2017**, *7*, 43. [CrossRef]
7. Loukaidou, K.; Michopoulos, A.; Zachariadis, T. Nearly-zero Energy Buildings: Cost-optimal Analysis of Building Envelope Characteristics. *Procedia Environ. Sci.* **2017**, *38*, 20–27. [CrossRef]
8. Cao, X.; Dai, X.; Liu, J. Building energy-consumption status worldwide and the state-of-the-art technologies for zero-energy buildings during the past decade. *Energy Build.* **2016**, *128*, 198–213. [CrossRef]
9. Ürge-Vorsatz, D.; Cabeza, L.F.; Serrano, S.; Barreneche, C.; Petrichenko, K. Heating and cooling energy trends and drivers in buildings. *Renew. Sustain. Energy Rev.* **2015**, *41*, 85–98. [CrossRef]
10. Santamouris, M. Cooling the buildings – past, present and future. *Energy Build.* **2016**, *128*, 617–638. [CrossRef]
11. Huang, K.-T.; Hwang, R.-L. Future trends of residential building cooling energy and passive adaptation measures to counteract climate change: The case of Taiwan. *Appl. Energy* **2016**, *184*, 1230–1240. [CrossRef]
12. Ürge-Vorsatz, D.; Petrichenko, K.; Staniec, M.; Eom, J. Energy use in buildings in a long-term perspective. *Curr. Opin. Environ. Sustain.* **2013**, *5*, 141–151. [CrossRef]
13. Luterbacher, J.; Dietrich, D.; Xoplaki, E.; Grosjean, M.; Wanner, H. European seasonal and annual temperature variability, trends, and extremes since 1500. *Science* **2014**, *303*, 1499–1503. [CrossRef] [PubMed]
14. Long, L.; Ye, H. The roles of thermal insulation and heat storage in the energy performance of the wall materials: a simulation study. *Sci. Rep.* **2016**, *6*, 24181. [CrossRef] [PubMed]
15. Csáky, I.; Kalmár, F. Investigation of the relationship between the allowable transparent area, thermal mass and air change rate in buildings. *J. Build. Eng.* **2017**, *12*, 1–7. [CrossRef]
16. Csáky, I.; Kalmár, F. Effects of thermal mass, ventilation and glazing orientation on indoor air temperature in buildings. *J. Build. Phys.* **2015**, *39*, 189–204. [CrossRef]
17. Balaras, C.A. The role of thermal mass on the cooling load of buildings. An overview of computational methods. *Energy Build.* **1996**, *24*, l–10. [CrossRef]
18. Reilly, A.; Kinnane, O. The impact of thermal mass on building energy consumption. *Appl. Energy* **2017**, *198*, 108–121. [CrossRef]
19. Verbeke, S.; Audenaert, A. Thermal inertia in buildings: A review of impacts across climate and building use. *Renew. Sustain. Energy Rev.* **2018**, *82*, 2300–2318. [CrossRef]
20. Aste, N.; Leonforte, F.; Manfren, M.; Mazzon, M. Thermal inertia and energy efficiency – Parametric simulation assessment on a calibrated case study. *Appl. Energy* **2015**, *145*, 111–123. [CrossRef]
21. Di Perna, C.; Stazi, F.; Ursini Casalena, A.; D'Orazio, M. Influence of the internal inertia of the building envelope on summertime comfort in buildings with high internal heat loads. *Energy Build.* **2011**, *43*, 200–206. [CrossRef]
22. Csáky, I.; Kalmár, F. Effects of solar radiation asymmetry on buildings' cooling energy needs. *J. Build. Phys.* **2016**, *40*, 35–54. [CrossRef]
23. Schmidt, D. Low exergy systems for high-performance buildings and communities. *Energy Build.* **2009**, *41*, 331–336. [CrossRef]
24. Zhai, X.Q.; Qu, M.; Li, Y.; Wang, R.Z. A review for research and new design options of solar absorption cooling systems. *Renew. Sustain. Energy Rev.* **2011**, *15*, 4416–4423. [CrossRef]
25. Eicker, U.; Pietruschka, D. Design and performance of solar powered absorption cooling systems in office buildings. *Energy Build.* **2009**, *41*, 81–91. [CrossRef]
26. Sangi, R.; Müller, D. Exergy-based approaches for performance evaluation of building energy systems. *Sustain. Cities Soc.* **2016**, *25*, 25–32. [CrossRef]
27. Hepbasli, A. Low exergy (LowEx) heating and cooling systems for sustainable buildings and societies. *Renew. Sustain. Energy Rev.* **2012**, *16*, 73–104. [CrossRef]
28. Toftum, J. Human response to combined indoor environment exposures. *Energy and Buildings* **2002**, *34*, 601–606. [CrossRef]

29. Schellen, L.; Loomans, M.G.L.C.; de Wit, M.H.; Olesen, B.W.; van Marken Lichtenbelt, W.D. The influence of local effects on thermal sensation under non-uniform environmental conditions—Gender differences in thermophysiology, thermal comfort and productivity during convective and radiant cooling. *Physiol. Behav.* **2012**, *107*, 252–261. [CrossRef] [PubMed]
30. Pallubinsky, H.; Schellen, L.; Rieswijk, T.A.; Breukel, C.M.G.A.M.; Kingma, B.R.M.; van Marken Lichtenbelt, W.D. Local cooling in a warm environment. *Energy Build.* **2016**, *113*, 15–22. [CrossRef]
31. Imanari, T.; Omori, T.; Bogaki, K. Thermal comfort and energy consumption of the radiant ceiling panel system. Comparison with the conventional all-air system. *Energy Build.* **1999**, *30*, 167–175. [CrossRef]
32. Kalmár, F. Interrelation between glazing and summer operative temperature in buildings. *Inter. Rev. Appl. Sci. Eng.* **2016**, *7*, 53–62. [CrossRef]
33. Nardi, I.; de Rubeis, T.; Perilli, S. Ageing effects on the thermal performance of two different well-insulated buildings. *Energy Procedia* **2016**, *101*, 1050–1057. [CrossRef]
34. Karmann, C.; Schiavon, S.; Bauman, F. Thermal comfort in buildings using radiant vs. all-air systems: A critical literature review. *Build. Environ.* **2017**, *111*, 123–131. [CrossRef]
35. Lin, B.; Wang, Z.; Sun, H.; Zhu, Y.; Ouyang, Q. Evaluation and comparison of thermal comfort of convective and radiant heating terminals in office buildings. *Build. Environ.* **2016**, *106*, 91–102. [CrossRef]
36. Li, R.; Yoshidomi, T.; Ooka, R.; Olesen, B.W. Field evaluation of performance of radiant heating/cooling ceiling panel system. *Energy Build.* **2015**, *86*, 58–65. [CrossRef]
37. ISO 13790:2008. *Energy performance of buildings—Calculation of energy use for space heating and cooling*; ISO copyright office: Geneva, Switzerland, 2008.
38. ISO 52016-1:2017, Energy performance of buildings—Energy needs for heating and cooling, internal temperatures and sensible and latent heat loads—Part 1: Calculation procedures. Available online: https://www.iso.org/standard/65696.html (accessed on 12 June 2018).
39. Csáky, I. Energy analysis of buildings' summer heat loads. Doctoral Thesis, University of Debrecen, Hungary, 2015.

energies

MDPI

Article

Phase Balancing Home Energy Management System Using Model Predictive Control

Bharath Varsh Rao [1,*], Friederich Kupzog [1] and Martin Kozek [2]

[1] Electric Energy Systems—Center for Energy, AIT Austrian Institute of Technology, 1210 Vienna, Austria; friederich.kupzog@ait.ac.at

[2] Institute of Mechanics and Mechatronics—Faculty of Mechanical and Industrial Engineering, Vienna University of Technology, 1060 Vienna, Austria; martin.kozek@tuwien.ac.at

* Correspondence: bharath-varsh.rao@ait.ac.at; Tel.: +43-664-88256043

Received: 31 October 2018; Accepted: 25 November 2018; Published: 28 November 2018

Abstract: Most typical distribution networks are unbalanced due to unequal loading on each of the three phases and untransposed lines. In this paper, models and methods which can handle three-phase unbalanced scenarios are developed. The authors present a novel three-phase home energy management system to control both active and reactive power to provide per-phase optimization. Simplified single-phase algorithms are not sufficient to capture all the complexities a three-phase unbalance system poses. Distributed generators such as photo-voltaic systems, wind generators, and loads such as household electric and thermal demand connected to these networks directly depend on external factors such as weather, ambient temperature, and irradiation. They are also time dependent, containing daily, weekly, and seasonal cycles. Economic and phase-balanced operation of such generators and loads is very important to improve energy efficiency and maximize benefit while respecting consumer needs. Since homes and buildings are expected to consume a large share of electrical energy of a country, they are the ideal candidate to help solve these issues. The method developed will include typical distributed generation, loads, and various smart home models which were constructed using realistic models representing typical homes in Austria. A control scheme is provided which uses model predictive control with multi-objective mixed-integer quadratic programming to maximize self-consumption, user comfort and grid support.

Keywords: three-phase unbalance minimization; model predictive control; home energy management system

1. Introduction

The Energy Efficiency Directive of the European Commission provides great emphasis on the need to empower and integrate customers by considering them as key entity towards sustainable and energy efficient future [1]. Evolving systems such as smart meters are on a road map towards increased market integration. With the help of such devices, ICT aspects such as data mining, management, processing, and commutation are gaining lots of traction in smart grid [2].

In recent days, with rigorous funding and investment in renewable energy, large number of distributed energy resources such as photo-voltaic systems, wind generators, and new loads such as electric mobility and storage systems are gaining importance. They pose lots of challenges to the network such as voltage violations and line loading. Most of the typical distribution networks are unbalanced due to unequal loading on each of the three phases and untransposed lines [3]. Additionally, unbalance is further increased with the high penetration of single-phase distributed generators. Three-phase unbalance imposes various degrees of stresses on different components in distribution network. Losses on the lines and distribution transformers increase considerably with

the increase in phase unbalance [3]. Therefore, it is extremely important to consider three-phase models. They have strong dependencies on external factors such as weather, ambient temperature, and irradiation which follows daily, weekly, and seasonal cycles. Photo-voltaic systems inject large amounts of active power into the network, especially when the solar irradiation is high during midday. Voltage violations may occur due to partial stochastic power input. Therefore, it is important to include reactive power in models so that it can be used to performed voltage regulation.

Homes and buildings are projects to consume a large share of total energy production. Therefore, it makes sense to produce strategies to use them to help mitigate the issues discussed above. Most of the homes today are not capable of providing any kind of support to the grid. Certain upgrades need to be made so that they can perform demand response. Loads which can be controlled directly or indirectly to provide demand response is referred to as demand side management (DSM). DSM is also referred to as flexibility. DSM can be used to provide number of grid support functionalities such as shifting the peak load to off-peak hours or curtailing the load to reduce the peak demand [4]. Smart building customers are given the opportunity to schedule the devices on their own to maximize comfort level and based on this initial schedule, the optimizer maximizes economic return which will result in demand which is more leveled over time [5]. Additionally, the optimizer will either minimize payment or maximize comfort based on the consumer needs in which, the user comfort is represented as a group of linear constraints [6].

2. Related Work

To control various devices in smart homes and all the issues associated with it, the authors in paper have presented a control scheme using Model predictive control, which is an ideal candidate to handle dynamic systems with evolving disturbances described in the previous section.

Various implementations of model predictive controller (MPC) in buildings are available in the literature. The core principle or issue being addressed by bodies of research mentioned below is dynamic scheduling of various flexibilities in building. Most of the authors below have addressed this issue using various MPC algorithms, problem formulations and objectives.

After analyzing the large body of work in MPC for buildings, three major categories can be defined. MPC in buildings is mainly used for demand side and flexibility management, building temperature control and optimal usage of energy.

2.1. Demand Side and Flexibility Management

A multi-scale stochastic MPC is implemented to schedule heating, ventilation, air conditioning which is referred to as HVAC systems and controllable loads such as electric vehicles and washer/dryers is implemented in [7]. In [8], the authors have presented an MPC approach to tackle the load shifting problem in households equipped with controllable appliances and electric storage units. This approach used time of day tariff to minimize energy consumption. A decision-making framework for real time control of load serving entity of flexibilities used to provide ancillary services to the market is presented in [9]. This paper provides a generalized framework which includes wide array of flexibilities. An example with electric vehicle charging is provided in detail.

The authors in [10] have proposed a scheme which uses time varying real time pricing to schedule appliances in buildings in smart grid context. Thermal mass of the building is considered with a comfort indicator and a model associated with it is presented. Thermal mass storage is used to hedge against varying prices with a goal to minimize energy costs. Control approach for home energy management system (HEMS) under forecast uncertainty is presented in [11]. The smart home is controlled as a grid connected micro-grid with PV generation, battery systems, critical and controllable loads. Objective of MPC is to maximize the use of renewable energy generation and to minimize operation costs. It includes predictions of PV, load, and market prices. Various scenarios are considered with different forecasting accuracies.

The authors in [12] presented an MPC model for HVAC system in medium sized building with receding horizon control. It is used to provide demand side flexibilities. Objective is to operate the building economically while respecting the comfort of dwellers. MPC scheme provided is a robust one to participate in both reserve and spot markets. Sensitivity of the controller towards economic and technical constraints are evaluated. The National Electricity Market of Singapore (NEMS) is used as a study case for grid building integration studies.

In [13], a non-intrusive identification of components in smart home is provided with a sampling frequency of one hertz. These identified models are used to predict flexibilities. These flexibilities are shifted in time to minimize energy costs. An MPC technique for energy optimization in residential appliance is proposed in [14]. Home cooling and heating system control is proposed to analyze the effect of conventional thermostats. In [15], an MPC EMS system for residential micro grids is furnished. EMS optimally schedules smart appliances, heating systems, PV generators based on consumer preferences. Weather and demand forecasts are integrated in it. Mixed-integer linear programming (MILP) is the core of MPC which minimizes the system costs of this residential micro-grid. At each sample time, the optimization algorithm adjusts itself to account for updated weather dependent PV systems and heating units in a receding fashion. This method is coupled with accurate simulation of micro-grid including energy storage and flexible loads. Emulation of real-world grid conditions on standard network interface is presented. The authors in [16] have provided a method to maximize the use of renewable energy resources in islanded grids. PV systems are used to provide energy to home loads and pico hydro power plant. MPC is used to control the flow valve of hydro plant and to modulate the energy supply to fulfill the deficit during islanded conditions.

An economic MPC is illustrated in [17]. It includes PV combined heat and electrical storage system. Uncertainties from thermal behaviors of the building are quantified, formulated and MPC's capability to handle it is presented in this research work. An MPC scheme to control loads in residential buildings are presented in [18]. It also presents a novel load aggregation method using MPC for distribution networks. This method is tested with 342 bus network with 15,000 buildings. In [19], an MPC controller to perform demand side management is presented. It uses an ON/OFF PID controller and MPC to control air conditioning in rooms in houses. It also includes PV systems. Weekly expenses are calculated for each tariff is compared with control methods.

2.2. Temperature Control

The authors in [20], have presented a method to control temperature in building in a cost-effective manner. It uses linear programming heuristic to minimize the objective function of electricity cost to run air conditioning system. In [21], authors have presented models for Heat Recovery Ventilators connected to single zone building, its potential and nonlinear MPC is implemented to optimize energy consumption. Three distinct time zones are used namely, slow timescale for temperature of structural elements, fast timescale for air temperature and intermediate dynamics for recovery systems. A stochastic optimization technique is provided in [22]. This paper introduces several load classes such as heating, ventilation, air conditioning which is commonly referred to as HVAC systems. A first order thermal dynamic model is used with a mixed-integer MPC to generate load schedules. Real data is coupled with numerical solutions. The authors in [23] have proposed an MPC algorithm to control temperature in single zone building coupled with renewable energy generators such as solar and wind. MPC objective is to control temperature within certain permissible limits and optimal amount of power consumption.

In [24], a temperature control scheme with the consideration of occupants with three comfort indicators namely, strict, mild, loose levels are provided. It also includes window blind position control, illumination, and ambient temperature. Weather data such as solar irradiation, illumination, and ambient temperature is forecasted and used in MPC algorithm. Goal of MPC is to minimize energy consumption and maintain the desired level of comfort for occupants. Paper [25] focuses on analysis of MPC application to domestic appliances to optimize them. Relationship between MPC

weight adjustment and minimization of energy consumption is evaluated. In this context, water heater, room temperature control by air conditioning system and refrigerators are explored.

In [26], a centralized direct control of on/off thermostats is furnished. Device operation temperature, on/off status, more importantly, temperature ramps are calculated and communicated to the central controller. It is observed that, same or better performance can be achieved by communication of temperature ramps which are essential data points. It also reduces the communication needs significantly. Right information exchange is essential for better performance and data flow reduction is the concluding argument of this paper.

An MPC control scheme to provide the best tradeoff between temperature control and energy cost is described in [27]. It also provides a comparison between PID controller and MPC. The weights are modified to obtain the best solution to increase quality of various electrical and thermal models. The authors in [28], have presented an MPC for entire building with a comfort metric to ensure high priority to user comfort for each of the various zones in the building. Simulation results are provided for four months showing large percentage of reduction in electrical and thermal energy consumption.

2.3. Optimal Energy Usage

Paper [29] proposes an MPC control strategy in HEMS to optimize energy usage and optimal operational schedules for input variables. It also provides results which demonstrated revenue from selling power to the utility. In [30], authors have furnished an MPC approach to obtain savings in residential households. Impact of local power generation such as roof top PV systems is determined for off-peak, mid-peak and on-peak periods. Hybrid MPC formulation for buildings is provided in [31]. It describes the interactions between continuous and discrete systems. It involves a two-level computation structure. Individual systems are controlled with upper level discrete commands.

In [32], an approach to minimize energy in home and office building is presented with renewable energy resources such as PV systems. This is done using an MPC technique with mixed-integer programming to handle switching constraints. This method allows for sufficient performance with respect to energy regulation and efficiency. It is shown that with various seasons, an annual savings of about 1.72% can be achieved with this approach. An MPC approach is introduced in [33] which exploits its capacity to reduce energy consumption and improve efficiency to reduce energy bills. MPC was trained for two different weight sets which is compared to thermostat control with three typical household loads.

It is shown that it is necessary to augment control weights to maximize energy cost minimization potential. In [34], an energy scheduling approach for smart home appliances using stochastic MPC is presented. It comprises a combination of genetic algorithm and linear programming. It analyzes the competence of the algorithm proposed with the objective of energy reduction.

An MPC scheme with a sample time of one hour is presented in [35]. It includes hot water usage, electric vehicle, domestic heating and with an actuator with water tank to use it as heat storage. Total power and energy cost is minimized. MPC robustness is evaluated using forecasted load profiles of the household. It is shown that using energy storage, the overall energy consumption of the household can be minimized.

A comprehensive cost optimal design is presented for a building HVAC system which includes MPC to generate cost optimal solution is presented in [36] The controller provides an optimal hourly set point for cooling and heating devices. This method is applied to multi-zone building in Italy. In [37], a study to minimize the cost of electricity for coordinating houses connected a micro-grid. It uses multi-objective optimization for micro-grid control which includes a house and an independent local plant. The control algorithm minimizes losses by power exchanges between the plant and the house.

It can be clearly seen that, three-phase implementation of HEMS is lacking. The papers mentioned above only use simple single-phase flexibility models and appliances are single phased. Additionally, reactive power control is not addressed by any of the research work mentioned above. Since three-phase models are not used, phase unbalance minimization cannot be performed. In this paper, the authors

present a three-phase unbalanced HEMS in which, three objective functions, maximize user comfort, self-consumption and grid support is implemented. It also includes control scheme to manage both active and reactive powers and can handle number of electrical appliances with various configurations.

The contributions in this paper are enlisted below,

1. Various three-phase linear flexibility models are presented in Section 3.
2. Flexibilities are modeled in both active and reactive power.
3. Three objective functions are provided in Section 5 along with three objective weights which are user defined.
4. Control scheme is described in Section 6 for three-phase HEMS with various chronological events.
5. Simulation results for three-phase unbalanced HEMS with active and reactive power control is provided in Section 7.

3. System Models

HEMS is a platform which enables monitoring and control of various energy appliances in the household. It allows the deployment of various control strategies to achieve an objective. Smart home in this paper refers to a home which is fitted with a HEMS. Using this system, various objectives can be achieved. For example, keeping the room temperature within certain comfortable limits.

3.1. Overview

Smart home models can be segregated into two categories. Namely, thermal and electrical models coupled by a heat pump. The main reason to use a thermal model is to characterize indoor temperature due to the thermal inertia of the house, since consumer comfort is paramount. The controller is formulated to give complete control to the user, a user-centric approach. The models are linear in nature so that, simple control strategies can be produced. Figure 1 represents a three-phase HEMS. It contains both single and three-phase components and therefore, it is unbalanced. In this scenario, the heat pump is three phased, inverters for battery and PV are three phased, controllable, and uncontrollable loads are single phased. The control scheme provided in this paper can include variety of configurations such as single-phase—neutral, phase—phase, three-phase star configuration, three-phase star configuration with neutral, and three-phase delta configuration. This can be done using the constraint imposed on the grid connection point described in Section 4.4.

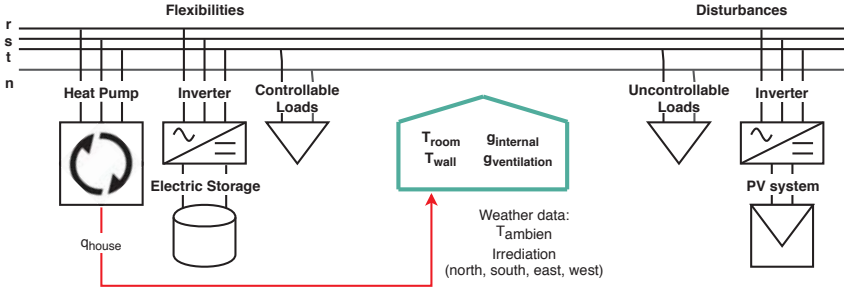

Figure 1. Schematic of three-phase HEMS representing various three-phase interconnections. It can be observed that, heat pump is the only component which connects thermal and electrical models.

3.2. Smart Home Thermal Model

Various linear single zone models representing single family homes with heat pumps and thermal parameters of the building are considered. They are based on nonlinear models which were constructed using data, representing physical behavior of real buildings in Vienna and Salzburg regions in Austria. Due to consumer privacy, more details about these homes cannot be provided. By generalizing these

models, four study cases are derived, and their essential distinguishing features are shown in Table 1. Nonlinear models were created in Dymola [38], which is a modeling and simulation tool, as part of the project iWPP-Flex [39]. They were linearized using the functions within Dymola and were mathematically verified.

Table 1. Building study cases which represent typical households in Austria. During the modeling stage of these houses, they only contained single-phase loads. To perform effective demand response, they had to be upgraded to include various other flexibilities such as single/three-phase heat pumps, controllable loads, electric storage, and PV system with three-phase inverters. Some of the important specifications such as heat demand, control method, and rated capacities which influences the control scheme are provided in this table.

House Hype	Passive House	Low-Energy House	Existing House	Renovated House
Heating demand	15 kWh/(m^{2}a)	45 kWh/(m^{2}a)	100 kWh/(m^{2}a)	75 kWh/(m^{2}a)
Heater	Under floor	Under floor	Radiator	Radiator
Heat exchange medium	Air-water	brine-water	brine-water	air-water
Power control	Variable	On/off	On/off	Variable
Rated capacity (Electrical/thermal)	1 kW/ 3 kW	1.2 kW/5 kW	4 kW/12kW	2.7 kW/7 kW

In the context of smart HEMS, the models of smart homes are recommended to be kept sufficiently simple to maintain generality, so that many building types can be accommodated. Therefore, first order models are implemented. Additionally, the focus of this work is not to use realistic building models but rather the control strategy and to minimize the objective function.

As a result, continuous state space models were generated and are assumed to be ordinary discrete linear time-invariant and is then discretized with a sampling time step of 15 min which can be observed in Equation (1).

$$x_{room}(t+1) = A_{room} \quad x_{room}(t) + B_{room} \quad u_{room}(t) \tag{1}$$

The state variables x_{room} of the building model are the room and wall temperature. The later represents the temperature of wall, floor, and ceiling of the house. A_{room} and B_{room} are the system matrices.

$$x_{room} = \begin{bmatrix} T_{wall} \\ T_{room} \end{bmatrix} \tag{2}$$

Limits on room and wall temperatures are given in Equations (3) and (4)

$$T_{wall}^{min} \leq T_{wall}(t) \leq T_{wall}^{max} \tag{3}$$

$$T_{room}^{min} \leq T_{room}(t) \leq T_{room}^{max} \tag{4}$$

The input quantities for the building are heat flow supplied by the heat pump, ambient temperature, solar irradiation from all directions, internal gains, and ventilation.

$$u_{room} = \begin{bmatrix} q_{room} \\ T_{ambient\ temperature} \\ i_{north} \\ i_{east} \\ i_{south} \\ i_{west} \\ g_{internal\ gain} \\ g_{ventilation} \end{bmatrix} \tag{5}$$

Limits on heat flows into the building are provided in Equation (6)

$$0 \leq q_{room}(t) \leq q_{room}^{max} \tag{6}$$

3.3. Heat Pump in Residential Building

Heat pump is used to provide the heat flow into the home which is the only controllable variable in the home model described in Section 3.2. Heat pump is the only coupling element between electrical and thermal systems as mentioned above.

Equation (7) describes the relationship between heat pump power and heat flows. The model represented below is that of a single-phase heat pump since it is in a modest home. This can be easily extended to three-phase by dividing the right-hand side of Equation (7) by 3 for per-phase balanced active power. Coefficient of performance (cop) is assumed to be constant with respect to time.

$$P_{heat\ pump}(t) = \frac{q_{room}(t)}{cop_{heat\ pump}} \tag{7}$$

Where, $P_{heat\ pump}$ is the active power and $cop_{heat\ pump}$ is the coefficient of performance. Low-energy and existing house contains on-off heat pump. To model this, a binary variable $B_{heat\ pump}$ with 0 for off and 1 for on is used.

$$P_{heat\ pump}(t) = B_{heat\ pump}\ P_{heat\ pump}^{rated} \tag{8}$$

The pump in heat pump consists of an induction motor. This motor is assumed to be lossless and with constant power factor ($pf_{heat\ pump}$) as described in Equation (9), using which reactive power ($Q_{heat\ pump}$) is calculated.

$$Q_{heat\ pump}(t) = tan(cos^{-1}(pf_{heat\ pump}))P_{heat\ pump}(t) \tag{9}$$

Since only heating period is considered, $P_{heat\ pump}$ and $Q_{heat\ pump} \geq 0$. Constraints on heat pump active power limits.

$$0 \leq P_{heat\ pump}(t) \leq P_{heat\ pump}^{max} \tag{10}$$

Constraints on heat pump reactive power limits,

$$0 \leq Q_{heat\ pump}(t) \leq Q_{heat\ pump}^{max} \tag{11}$$

where, $P_{heat\ pump}^{max}$ and $Q_{heat\ pump}^{max}$ are the maximum rated power active and reactive powers of head pump, respectively.

4. Electrical System Constraints

In recent years, lots of smart electrical appliances are becoming popular. It is possible to control the behavior of these appliances. In this paper, the authors have decided to use the following electrical appliances.

4.1. Electric Storage Constraints

For the maximal use of intermittent renewable energy generators and self-consumption, electric batteries are becoming very important in the recent days. Therefore, it is necessary to model and include them in the HEMS systems. In this paper, only linear battery models are used. Equation (12) represents the energy balance of electric storage system, a battery.

$$soc(t+1)\ C_{battery} = soc(t)\ C_{battery} + \Delta t\ \eta_{battery}\ P_{battery}(t) \tag{12}$$

It can be seen in Equation (12) that, $P_{battery}$ takes values both positive and negative. This is a form of linearization because, the battery charging and discharging efficiencies are different and therefore, nonlinear. This nonlinearity can be tackled by solving it as is, using a nonlinear solver or by splitting the $P_{battery}$ into $P_{charging}$ and $P_{discharge}$. The latter is coupled with a binary variable to make it either charge or discharge, leading to MILP. The authors have chosen to use the linear form and the reasons for it are provided in Section 4.2.

Constraints on soc limits are given below,

$$soc^{min} \leq soc(t) \leq soc^{max} \tag{13}$$

Constraints on battery charging and discharging power limits are as follows.

$$P^{min}_{battery} \leq P_{battery}(t) \leq P^{max}_{battery} \tag{14}$$

4.2. Three-Phase Inverter Constraints

The battery described in the previous section is connected to a three-phase inverter. The inverter can control active and reactive power flows on each of the phases. The relationship between battery and inverter is described using simple power balance Equation (15).

$$(P_{battery}(t))^2 = (P_{inverter}(t))^2 + (Q_{inverter}(t))^2 \tag{15}$$

Equation (15) is nonlinear. If on the precious section, a binary variable is defined and $P_{battery}$ is split into $P_{charging}$ and $P_{discharge}$, Equation (15) becomes nonlinear and non-convex. One way to deal with the nonconvexity is to limit the $Q_{inverter}$ with a constant power factor as shown in Equation (16). However, this is still nonlinear.

$$Q^{\rho}_{inverter}(t) = tan(cos^{-1}(pf_{inverter}))P^{\rho}_{inverter}(t) \tag{16}$$

where, ρ is the phase and $\rho \in phases(r, s, t)$. To remedy the nonlinearity, the inverter is only controlled at unity power factor. In other words, the reactive power is zero. This is represented in Equation (17)

$$(P_{battery}(t))^2 = (P_{inverter}(t))^2 \tag{17}$$

Individual phase powers are represented as follows,

$$P_{inverter}(t) = \sum_{\rho} P^{\rho}_{inverter}(t) \tag{18}$$

4.3. Constraints on Controllable Loads

Simple controllable loads are used with constant power factor operation as described in Equation (21). Controllable loads have the following constraints. Equations (19) and (20) are the active and reactive power constraints and Equation (21) is the relationship between them.

$$0 \leq P^{\rho}_{controllable\ load}(t) \leq P^{max}_{controllable\ load} \tag{19}$$

$$0 \leq Q^{\rho}_{controllable\ load}(t) \leq Q^{max}_{controllable\ load} \tag{20}$$

It is assumed that the power factor is constant with time. Typical power factor for household loads is between 0.90 to 0.95.

$$Q^{\rho}_{controllable\ load}(t) = tan(cos^{-1}(pf_{controllable\ load}))P^{\rho}_{controllable\ load}(t) \tag{21}$$

4.4. Constraints on Grid Connection Point

The grid connection point (point of common coupling) is where the smart home is connected to the grid. When excess power is fed into the grid, it is referred to as infeed and when power is drawn, it is referred to as consumption. Since P_{grid} takes both positive and negative values due to battery linearization, both infeed and consumption is represented by P_{grid}. It also represents the energy balance of all the electrical components in the smart home.

Equations (22) and (23) are constraints on limits of active and reactive power at the grid connection point.

$$P^{\rho}_{grid}(t) = P^{\rho}_{inverter}(t) + P^{\rho}_{heat\ pump}(t) + P^{\rho}_{controllable\ load}(t) + P^{\rho}_{uncontrollable\ load} \tag{22}$$

$$Q^{\rho}_{grid}(t) = Q^{\rho}_{heat\ pump}(t) + Q^{\rho}_{controllable\ load}(t) + Q^{\rho}_{uncontrollable\ load} \tag{23}$$

4.5. Various Disturbances Applied to HEMS

Various electrical and thermal disturbances are applied to HEMS during simulation which can be seen in Figure 2.

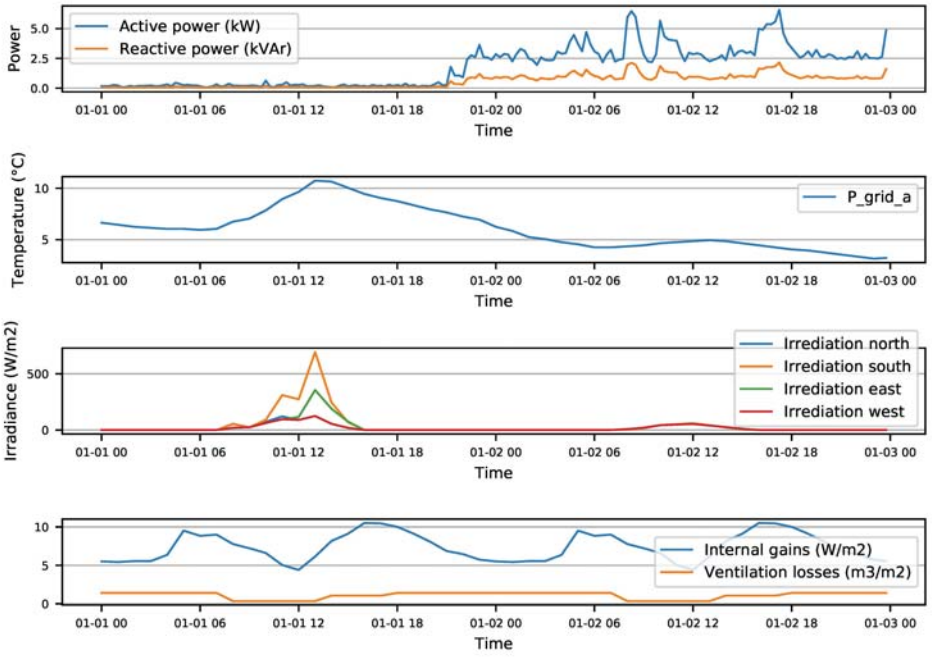

Figure 2. Profiles of disturbances applied to smart HEMS. On the x-axis, data time format is MM-dd HH. Data is from 01-01-2018 00:00:00 to 01-02-2018 00:00:00.

Disturbances are forecasted using a convolutional neural network which is not described in this paper. Uncontrollable loads data is from a smart meter from a real household in Austria. Various thermal disturbances such as ambient temperature and irradiation data is sourced from weather stations in Austria, ventilation, and internal gains from the project iWPP-Flex.

5. Objective Functions

In this paper, three different objectives are considered. These are explained in detail below.

5.1. Improve Self-Consumption

In many countries, with higher share of renewables, it is more economical to self-consume and therefore, the following objective function in Equation (24) is minimized. Since electricity tariffs only depend on active power, reactive power is excluded from the objective.

$$J_{self\ consumption} = \sum_{t}\sum_{p}(P^{\rho}_{grid}(t))^2 \tag{24}$$

On the other hand, in Austria, it is more economical to feed as mush power into the grid as possible since power sale tariff is higher than consumption tariffs. It can be done easily by maximizing equation. It is customary to involve a variable price signal along with P_{grid} which is the electricity tariff provided by the energy retailer. However, this is neglected for the sake of clarity.

5.2. Improve User Comfort

Since user comfort is paramount, this objective is introduced. It minimizes the difference between a reference temperature and actual room temperature in smart home. The limits of these temperature are defined by the user.

$$J_{user\ comfort} = \sum_{t}(T^{reference}_{room}(t) - T_{room}(t))^2 \tag{25}$$

5.3. Improve Grid Support

As mentioned in Section 1, smart homes can provide support to the grid by optimally controlling its renewable generation and consumption. Therefore, objective in Equation (26) is provided. It minimizes the difference between reference and actual active, reactive powers at grid connection point. This reference is generated from a large grid level optimal power flow controller based on a grid level objective function.

$$J_{grid\ support} = \sum_{t}\sum_{p}(P^{\rho}_{grid\ reference}(t) - P^{\rho}_{grid}(t))^2 + (Q^{\rho}_{grid\ reference}(t) - Q^{\rho}_{grid}(t))^2 \tag{26}$$

This paper does not include details or methods to generate this reference profile and instead uses it as is. If the smart home can follow this reference profile, grid level optimization is achieved. The objective on the grid can be loss minimization, line loading minimization, operational efficiency, unit dispatch and so on. In this paper, the reference profiles where generated with an objective to minimize the three-phase unbalance on the grid level. For this to work, multiple buildings connected at various locations in the network must follow its own reference profile provided by the grid controller, simultaneously.

5.4. Complete Objective Function

Complete objective function is provided in Equation (27). Weights $\mathcal{S}$, $\mathcal{U}$ and $\mathcal{G}$ are introduced with self-consumption, user comfort and grid support, respectively. By varying these weights, more importance can be given to the objectives.

$$\text{minimize } J = \mathcal{S}\, J_{self\ consumption} + \mathcal{U}\, J_{user\ comfort} + \mathcal{G}\, J_{grid\ support} \tag{27}$$

These weights can be varied on-line and the controller updates it in the next simulation step. There are the most prominent parameters which the user can determine and can have significant

influence over the controller and ultimately the optimum. Controllable variables are $P_{battery}$, $P_{heat\ pump}$ and $P_{controllable\ load}$.

6. Control Scheme

Due to the high intermittency of renewable energy generators, loading in households along with dependencies on external factors such as weather and solar irradiation, it is extremely important to choose a controller which makes effective use of available predictions.

Therefore, the authors have chosen to use MPC. MPC control used is receding horizon control. Figure 3 describes an MPC and data exchange between various devices in smart home. MPC is responsible to generate optimal set-points to minimize the objective function.

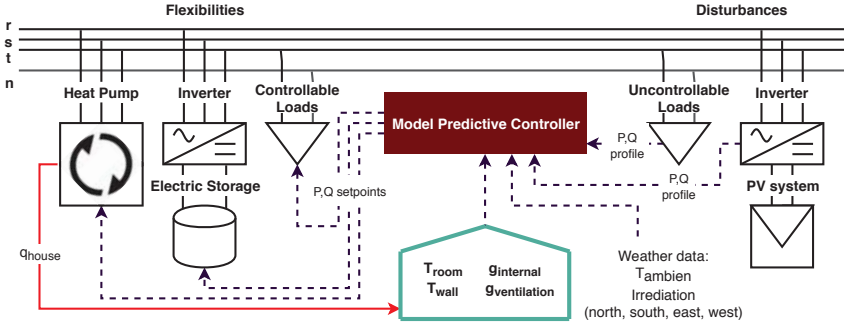

Figure 3. Schematic of three-phase HEMS with model predictive controller. It shows all the interconnections with respect to data exchange.

MPC control scheme is illustrated in Figure 4. It describes various functions which need to be executed within a sample duration.

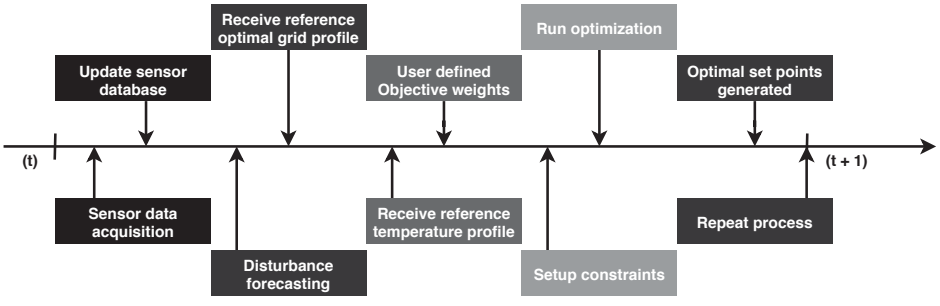

Figure 4. Model predictive control scheme for three-phase HEMS. It describes various functions which are executed for a sample period.

The chronological control functions and events described in Figure 4 are described in detail below.

1. At time *t*, measure thermal disturbances such as irradiation, ambient temperature, ventilation losses and internal gains. Additionally, smart meters measures uncontrollable load and photo-voltaic generation.
2. These sensor data points are acquired by the data acquisition system and sensor database is updated. Figure 5 illustrates the sensor data acquisition system using in this work.

3. Disturbances are forecasted for a given prediction horizon using an appropriate forecasting algorithm. In this paper, using convolutional neural networks.
4. Active and reactive power optimal set-points are received from the grid level controller.
5. Internal temperature reference signals are received.
6. User defined objective weights are received.
7. Objective functions are set up using Equations (24)–(27).
8. Constraints from Equations (1)–(23) are setup.
9. Optimal set-points are generated.
10. The process is repeated for next sample period, $(t+1)$.

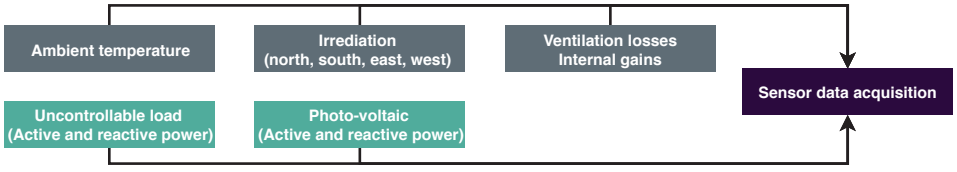

Figure 5. Schematic of a sensor data acquisition system use in three-phase HEMS.

The optimization problem is solved by a suitable quadratic programming for passive, renovated house and mixed-integer quadratic programming for low-energy and existing houses as discussed in Section 3.3.

7. Simulation Results

In this section, simulation setup and results are provided. As mentioned earlier, the objective weights, $\mathcal{S}, \mathcal{U}$ and $\mathcal{G}$ are defined by the user, it is difficult to analyze the controller performance due to large number of combinations of these three variables.

To overcome this, only extreme cases of these weights are considered. This can be observed in Figure 6. The method of choosing weights in such fashion was inspired from [40] in which, mixed-integer quadratic programming is introduced with multi-objective optimization. The simulation is performed for the duration of 48 hours with prediction and control horizon of 24 hours.

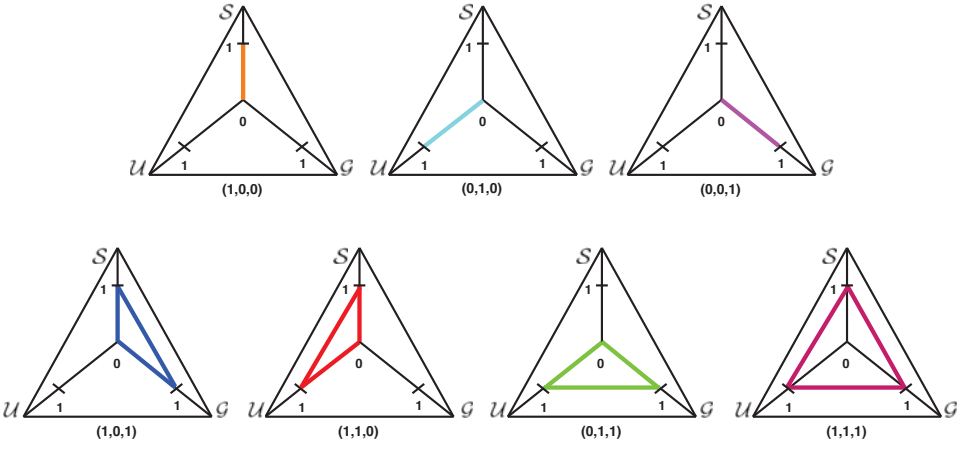

Figure 6. Objective weights, $\mathcal{S}, \mathcal{U}$ and $\mathcal{G}$ for various extreme cases.

Simulation parameters are provided in Table 2.

Table 2. Simulation parameters.

Variable	Value
Simulation parameters	
prediction horizon	24 h
control horizon	24 h
simulation duration	48 h
Building model	
T_{wall}^{min}	10 C
T_{wall}^{max}	40 C
T_{room}^{min}	18 C
T_{room}^{max}	25 C
$T_{initial}$	18 C
$T_{room}^{reference}$	20 C
Controllable load model	
$P_{controllable\ load}^{max}$	2 kW
$pf_{controllable\ load}$	0.95
Electric Storage model	
soc^{min}	0.3
soc^{max}	0.9
$C_{battery}$	20 kWh
$\eta_{battery}$	0.95
$P_{battery}^{min}$	–10 kW
$P_{battery}^{max}$	10 kW
Heat pump model	
cop	3
$pf_{heat\ pump}$	0.90
Passive house: $P_{heat\ pump}^{max}$	1 kW
Low-energy house: $P_{heat\ pump}^{max}$	1.2 kW
Existing house: $P_{heat\ pump}^{max}$	4 kW
Renovated house: $P_{heat\ pump}^{max}$	2.7 kW

7.1. Analysis of Results

Due to the large number of combinations of objective weights and controllable variables, results are analyzed based on the three objective functions. Four scenarios of objective weights are chosen for analysis. $(\mathcal{S}, \mathcal{U}, \mathcal{G}) = (0,0,1)$, $(0,1,0)$, $(1,0,0)$ and $(1,1,1)$. Additionally, to represent powers, only phase r is used. The results are plotted using boxplots. More information about it can be seen in Figure 7.

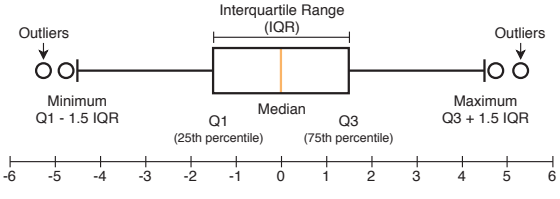

Figure 7. Boxplot is a standardized method to display data.

7.1.1. Improve Self-Consumption

Figure 8 describes the results for the objective function to minimize self-consumption (see, Equation (24)). It illustrates P_{grid} for various home types and for given simulation horizon.

It can be observed that for objective weights $(\mathcal{S}, \mathcal{U}, \mathcal{G}) = (1, 0, 0)$, the controller is trying to get P_{grid} close to zero which can be perceived from the medians which are at zero for all the house types. Same can be observed with objective weights $(\mathcal{S}, \mathcal{U}, \mathcal{G}) = (1, 1, 1)$. Since all three weights are equal, the results are not as effective as the one from before and $\mathcal{S}$ is not dominating other weights.

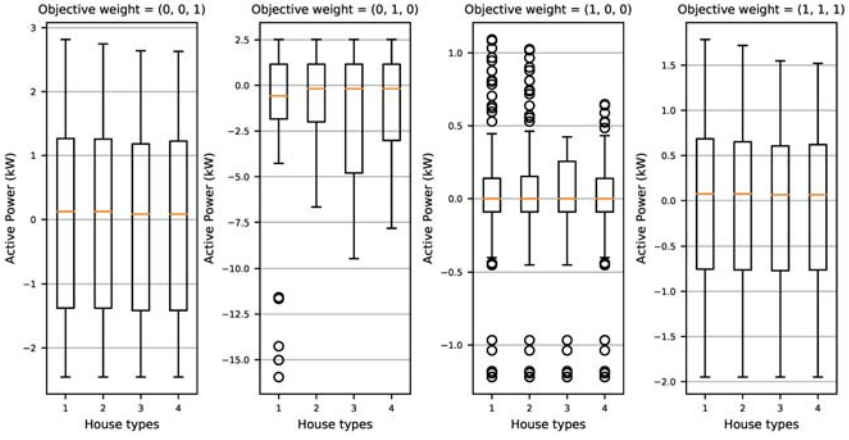

Figure 8. Schematic of Three-Phase HEMS.

7.1.2. Improve User Comfort

Objective terms $abs(T_{room}^{reference} - T_{room})$ is illustrated in Figure 9. Since the objective weight $\mathcal{U}$ is predominant, $(\mathcal{S}, \mathcal{U}, \mathcal{G}) = (0, 1, 0)$, the absolute difference between $T_{room}^{reference}$ and T_{room} is the least. It can be observed that the temperature median is very close to zero. From this, it can be inferred that the objective function to improve user comfort is maximized. However, since the building models are first order, the controller is quiet easily able to achieve similar results with $(\mathcal{S}, \mathcal{U}, \mathcal{G}) = (1, 1, 1)$.

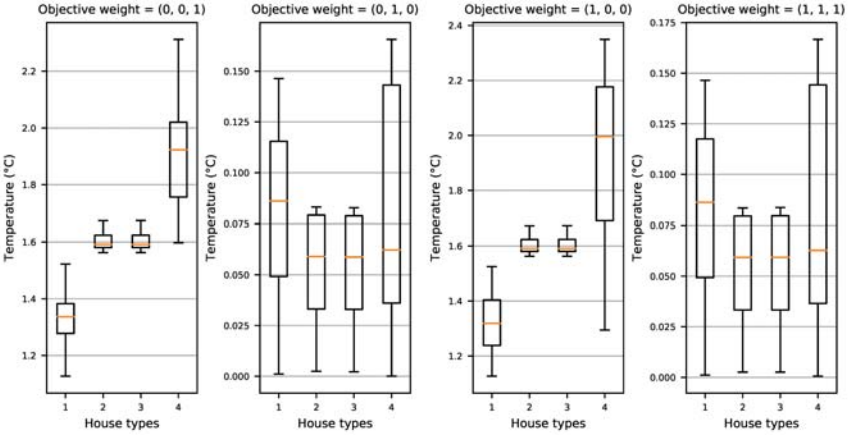

Figure 9. Schematic of Three-Phase HEMS.

7.1.3. Improve Grid Support

Figure 10 illustrates $abs(P_{grid\,reference}(t) - P_{grid})$. With the predominant weight in $(\mathcal{S}, \mathcal{U}, \mathcal{G}) = (0, 0, 1)$ is $\mathcal{G}$. Therefore, similar to previous objectives, it can be observed that the controller is able to minimize the absolute difference between the target profile and the profile at the grid connection

point. This is also illustrated in Figures 11 and 12 where, both active and reactive power profiles are presented for phase *r*.

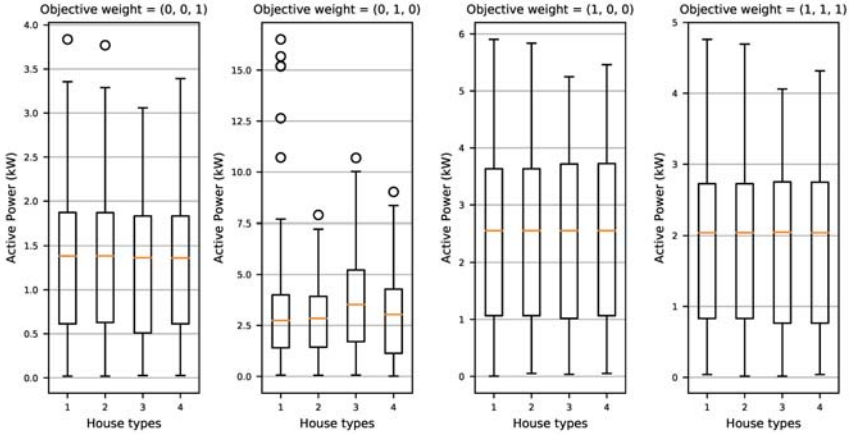

Figure 10. Schematic of Three-Phase HEMS.

Figures 11 and 12 describes all the parameters for passive house with objective weight scenario $(\mathcal{S}, \mathcal{U}, \mathcal{G}) = (0,0,1)$ for both active and reactive power. In Figure 11, since the objective weight scenario is to minimize $abs(P_{grid\,reference}(t) - P_{grid}) + abs(Q_{grid\,reference}(t) - Q_{grid})$, it can be observed that the P_{grid} is trying to closely follow the $P_{grid\,reference}$.

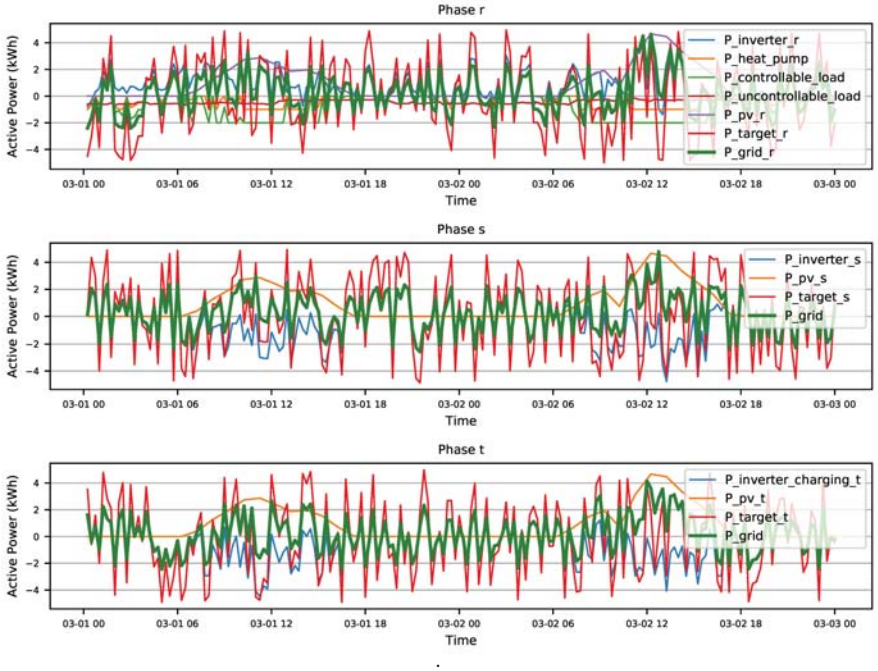

Figure 11. Per-phase active power controllable and disturbance variables for passive house and weight scenario $(\mathcal{S}, \mathcal{U}, \mathcal{G}) = (0,0,1)$

It is evident from Equation (23) that, there are no direct reactive power controllable variables for all the phases. This makes it difficult for the controller to actively tract $Q_{grid\,reference}$ which can be observed in Figure 12. In phase *r*, due to the existing single-phase appliances, better reactive control tracking is possible unlike phase *s* and *t*.

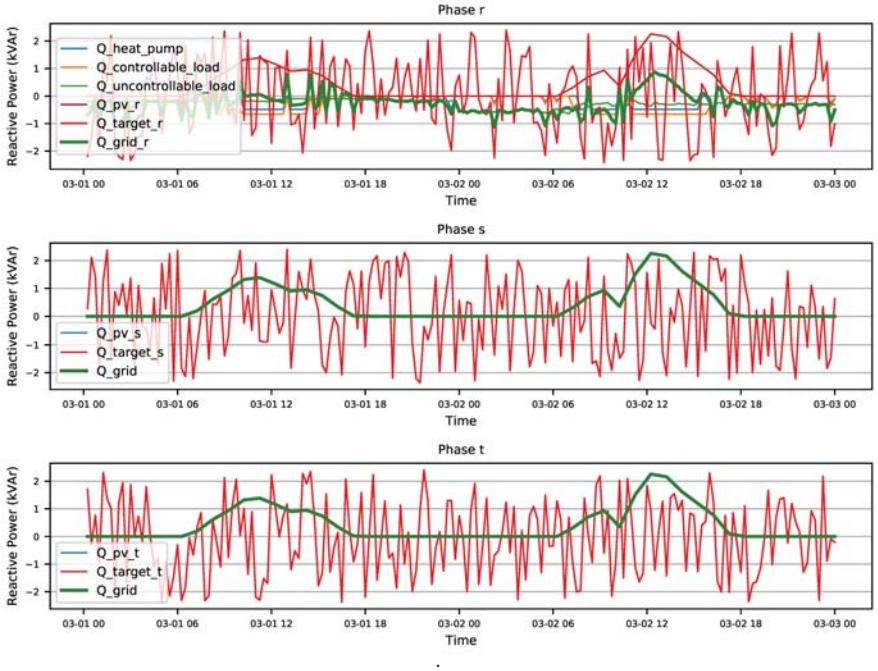

Figure 12. Per-phase reactive power controllable and disturbance variables for passive house and weight scenario $(\mathcal{S}, \mathcal{U}, \mathcal{G}) = (0, 0, 1)$

8. Conclusions and Outlook

In this paper, a novel three-phase balancing HEMS was presented along with control strategies for both active and reactive power. Four linear building models representing typical households in Austria were described. Various linear three-phase flexibility models were presented in detail. Three unique conflicting objective functions with three weights which are user defined is described. Model predictive control scheme was applied to this smart home for various extreme objective weight scenarios. Active and reactive power set-points were generated for all electrical controllable variables. Due to the vast number of combinations of objective weights, four extreme cases were chosen for analysis, $(\mathcal{S}, \mathcal{U}, \mathcal{G}) = (0, 0, 1)$, $(0, 1, 0)$, $(1, 0, 0)$ and $(1, 1, 1)$. Analysis was done based on three objective functions. It was shown that the results reflect the chosen objective weights for each of the three objective functions. In Figures 11 and 12, grid support maximization objective was illustrated for objective weights $(\mathcal{S}, \mathcal{U}, \mathcal{G}) = (0, 0, 1)$. In these figures, it was shown that P_{grid} and Q_{grid} are indeed able to track their reference profiles and implications being, the objectives on the grid level controller (three-phase unbalance minimization) are being met, leading to a grid level optimization.

The models presented in the paper were linear and first order in nature. In reality it makes sense to use higher order nonlinear models to closely match the real behavior of the smart home. Therefore, the model needs to be extended to nonlinear ones. Even though the scheme includes reactive power, it is not given high importance in this paper to keep it linear. Due to high share of renewable generators, it is interesting to be able to control reactive power in this context. The inverter connected to the

battery in this paper only works at unity power factor. However, by including reactive power control, better reactive power tracking can be performed. Additionally, with the power balance equation at the inverter is non-convex in nature. Therefore, the MPC needs to be extended to be able to solve such problems using a non-convex solver.

Author Contributions: Conceptualization, B.V.R. and F.K.; Formal analysis, M.K.; Investigation, B.V.R., F.K. and M.K.; Methodology, B.V.R. and M.K.; Resources, B.V.R. and F.K.; Validation, B.V.R. and M.K.; Visualization, B.V.R. and F.K.

Conflicts of Interest: The authors declare no conflict of interest.

References

1. General, D. Energy Efficiency Directive. Available online: https://ec.europa.eu/energy/en/studies (accessed on 20 August 2018).
2. Barbato, A.; Capone, A.; Barbato, A.; Capone, A. Optimization Models and Methods for Demand-Side Management of Residential Users: A Survey. *Energies* **2014**, *7*, 5787–5824. [CrossRef]
3. Sun, Y.; Li, P.; Li, S.; Zhang, L.; Sun, Y.; Li, P.; Li, S.; Zhang, L. Contribution Determination for Multiple Unbalanced Sources at the Point of Common Coupling. *Energies* **2017**, *10*, 171. [CrossRef]
4. Miceli, R. Energy Management and Smart Grids. *Energies* **2013**, *6*, 2262–2290. [CrossRef]
5. Pedrasa, M.A.A.; Spooner, T.D.; MacGill, I.F. Coordinated Scheduling of Residential Distributed Energy Resources to Optimize Smart Home Energy Services. *IEEE Trans. Smart Grid* **2010**, *1*, 134–143. [CrossRef]
6. Du, P.; Lu, N. Appliance Commitment for Household Load Scheduling. *IEEE Trans. Smart Grid* **2011**, *2*, 411–419. [CrossRef]
7. Jia, L.; Yu, Z.; Murphy-Hoye, M.C.; Pratt, A.; Piccioli, E.G.; Tong, L. Multi-Scale Stochastic Optimization for Home Energy Management. In Proceedings of the 2011 4th IEEE International Workshop on Computational Advances in Multi-Sensor Adaptive Processing (CAMSAP), San Juan, Puerto Rico, 13–16 December 2011; pp. 113–116.
8. Giorgio, A.D.; Pimpinella, L.; Liberati, F. A Model Predictive Control Approach to the Load Shifting Problem in a Household Equipped with an Energy Storage Unit. In Proceedings of the 2012 20th Mediterranean Conference on Control Automation (MED), Barcelona, Spain, 3–6 July 2012; pp. 1491–1498.
9. Alizadeh, M.; Scaglione, A.; Kesidis, G. Scalable Model Predictive Control of Demand for Ancillary Services. In Proceedings of the 2013 IEEE International Conference on Smart Grid Communications (SmartGridComm), Vancouver, BC, Canada, 21–24 October 2013; pp. 684–689.
10. Chen, C.; Wang, J.; Heo, Y.; Kishore, S. MPC-Based Appliance Scheduling for Residential Building Energy Management Controller. *IEEE Trans. Smart Grid* **2013**, *4*, 1401–1410. [CrossRef]
11. Chen, Z.; Zhang, Y.; Zhang, T. An Intelligent Control Approach to Home Energy Management under Forecast Uncertainties. In Proceedings of the 2015 IEEE 5th International Conference on Power Engineering, Energy and Electrical Drives (POWERENG), Riga, Latvia, 11–13 May 2013; pp. 657–662.
12. Hanif, S.; Melo, D.F.R.; Maasoumy, M.; Massier, T.; Hamacher, T.; Reindl, T. Model Predictive Control Scheme for Investigating Demand Side Flexibility in Singapore. In Proceedings of the 2015 50th International Universities Power Engineering Conference (UPEC), Stoke on Trent, UK, 1–4 September 2015; pp. 1–6.
13. Dufour, L.; Genoud, D.; Jara, A.; Treboux, J.; Ladevie, B.; Bezian, J.J. A Non-Intrusive Model to Predict the Exible Energy in a Residential Building. In Proceedings of the 2015 IEEE Wireless Communications and Networking Conference Workshops (WCNCW), New Orleans, LA, USA, 9–12 March 2015; pp. 69–74.
14. Oliveira, D.; Rodrigues, E.M.G.; Mendes, T.D.P.; Catalão, J.P.S.; Pouresmaeil, E. Model Predictive Control Technique for Energy Optimization in Residential Appliances. In Proceedings of the 2015 IEEE International Conference on Smart Energy Grid Engineering (SEGE), Oshawa, ON, Canada, 17–19 August 2015; pp. 1–6.
15. Parisio, A.; Wiezorek, C.; Kyntäjä, T.; Elo, J.; Johansson, K.H. An MPC-Based Energy Management System for Multiple Residential Microgrids. In Proceedings of the 2015 IEEE International Conference on Automation Science and Engineering (CASE), Gothenburg, Sweden, 24–28 August 2015; pp. 7–14.
16. Rofiq, A.; Widyotriatmo, A.; Ekawati, E. Model Predictive Control of Combined Renewable Energy Sources. In Proceedings of the 2015 International Conference on Technology, Informatics, Management, Engineering Environment (TIME-E), Samosir, Indonesia, 7–9 September 2015; pp. 127–132.

17. Hidalgo Rodríguez, D.I.; Myrzik, J.M. Economic Model Predictive Control for Optimal Operation of Home Microgrid with Photovoltaic-Combined Heat and Power Storage Systems. *IFAC-PapersOnLine* **2017**, *50*, 10027–10032. [CrossRef]
18. Mirakhorli, A.; Dong, B. Model Predictive Control for Building Loads Connected with a Residential Distribution Grid. *Appl. Energy* **2018**, *230*, 627–642. [CrossRef]
19. Godina, R.; Rodrigues, E.M.G.; Pouresmaeil, E.; Matias, J.C.O.; Catalão, J.P.S. Model Predictive Control Home Energy Management and Optimization Strategy with Demand Response. *Appl. Sci.* **2018**, *8*, 408. [CrossRef]
20. Arikiez, M.; Grasso, F.; Zito, M. Heuristics for the Cost-Effective Management of a Temperature Controlled Environment. In Proceedings of the 2015 IEEE Innovative Smart Grid Technologies—Asia (ISGT ASIA), Bangkok, Thailand, 3–6 November 2015; pp. 1–6.
21. Touretzky, C.R.; Baldea, M. Model Reduction and Nonlinear MPC for Energy Management in Buildings. In Proceedings of the 2013 American Control Conference, Washington, DC, USA, 17–19 June 2013; pp. 461–466.
22. Yu, Z.; Jia, L.; Murphy-Hoye, M.C.; Pratt, A.; Tong, L. Modeling and Stochastic Control for Home Energy Management. *IEEE Trans. Smart Grid* **2013**, *4*, 2244–2255. [CrossRef]
23. Momoh, J.A.; Zhang, F.; Gao, W. Optimizing Renewable Energy Control for Building Using Model Predictive Control. In Proceedings of the 2014 North American Power Symposium (NAPS), Pullman, WA, USA, 7–9 September 2014; pp. 1–6.
24. Agheb, S.; Tan, X.; Tsang, D.H.K. Model Predictive Control of Integrated Room Automation Considering Occupants Preference. In Proceedings of the 2015 IEEE International Conference on Smart Grid Communications (SmartGridComm), Miami, FL, USA, 2–5 November 2015; pp. 665–670.
25. Oliveira, D.; Rodrigues, E.M.G.; Godina, R.; Mendes, T.D.P.; Catalão, J.P.S.; Pouresmaeil, E. MPC Weights Tunning Role on the Energy Optimization in Residential Appliances. In Proceedings of the 2015 Australasian Universities Power Engineering Conference (AUPEC), Wollongong, NSW, Australia, 27–30 September 2015; pp. 1–6.
26. Vanouni, M.; Lu, N. Improving the Centralized Control of Thermostatically Controlled Appliances by Obtaining the Right Information. *IEEETrans.SmartGrid* **2015**, *6*, 946–948. [CrossRef]
27. Godina, R.; Rodrigues, E.M.; Pouresmaeil, E.; Catalão, J.P. Optimal Residential Model Predictive Control Energy Management Performance with PV Microgeneration. *Comput. Oper. Res.* **2018** *96*, 143–156. [CrossRef]
28. Hilliard, T.; Swan, L.; Qin, Z. Experimental Implementation of Whole Building MPC with Zone Based Thermal Comfort Adjustments. *Build. Environ.* **2017**, *125*, 326–338. [CrossRef]
29. Alrumayh, O.; Bhattacharya, K. Model Predictive Control Based Home Energy Management System in Smart Grid. In Proceedings of the 2015 IEEE Electrical Power and Energy Conference (EPEC), London, ON, Canada, 26–28 October 2015; pp. 152–157.
30. Oliveira, D.; Rodrigues, E.M.G.; Godina, R.; Mendes, T.D.P.; Catalão, J.P.S.; Pouresmaeil, E. Enhancing Home Appliances Energy Optimization with Solar Power Integration. In Proceedings of the IEEE EUROCON 2015—International Conference on Computer as a Tool (EUROCON), Salamanca, Spain, 8–11 September 2015; pp. 1–6.
31. Kozák, .; Pytel, A.; Drahoš, P. Application of Hybrid Predictive Control for Intelligent Buildings. In Proceedings of the 2015 20th International Conference on Process Control, (PC), Strbske Pleso, Slovakia, 9–12 June 2015; pp. 203–208.
32. Zanoli, S.M.; Pepe, C.; Orlietti, L.; Barchiesi, D. A Model Predictive Control Strategy for Energy Saving and User Comfort Features in Building Automation. In Proceedings of the 2015 19th International Conference on System Theory, Control and Computing (ICSTCC), Cheile Gradistei, Romania, 14–16 October 2015; pp. 472–477.
33. Godina, R.; Rodrigues, E.M.G.; Pouresmaeil, E.; Matias, J.C.O.; Catalão, J.P.S. Model Predictive Control Technique for Energy Optimization in Residential Sector. In Proceedings of the 2016 IEEE 16th International Conference on Environment and Electrical Engineering (EEEIC), Florence, Italy, 7–10 June 2016; pp. 1–6.
34. Rahmani-andebili, M.; Shen, H. Energy Scheduling for a Smart Home Applying Stochastic Model Predictive Control. In Proceedings of the 2016 25th International Conference on Computer Communication and Networks (ICCCN), Waikoloa, HI, USA, 1–4 August 2016; pp. 1–6.

35. Sundström, C.; Jung, D.; Blom, A. Analysis of Optimal Energy Management in Smart Homes Using MPC. In Proceedings of the 2016 European Control Conference (ECC), Aalborg, Denmark, 29 June–1 July 2016; pp. 2066–2071.
36. Ascione, F.; Bianco, N.; De Stasio, C.; Mauro, G.M.; Vanoli, G.P. A New Comprehensive Approach for Cost-Optimal Building Design Integrated with the Multi-Objective Model Predictive Control of HVAC Systems. *Sustain. Cities Soc.* **2017**, *31*, 136–150. [CrossRef]
37. Arikiez, M.; Alotaibi, F.; Rehan, S.; Rohouma, W. Minimizing the Electricity Cost of Coordinating Houses on Microgrids. In Proceedings of the 2016 IEEE PES Innovative Smart Grid Technologies Conference Europe (ISGT-Europe), Ljubljana, Slovenia, 9–12 October 2016; pp. 1–6.
38. DYMOLA Systems Engineering. Available online:https://www.3ds.com/products-services/catia/products/dymola/ (accessed on 20 August 2018).
39. Esterl, T.; Leimgruber, L.; Ferhatbegovic, T.; Zottl, A.; Krottenthaler, M.; Weiss, B. Aggregating the flexibility of heat pumps and thermal storage systems in Austria. In Proceedings of the 2016 5th International Conference on Smart Cities and Green ICT Systems (SMARTGREENS), Rome, Italy, 23–25 April 2016; pp. 1–6.
40. Killian, M.; Zauner, M.; Kozek, M. Comprehensive Smart Home Energy Management System Using Mixed-Integer Quadratic-Programming. *Appl. Energy* **2018**, *222*, 662–672. [CrossRef]

energies

MDPI

Article

Simulation and Analysis of Perturbation and Observation-Based Self-Adaptable Step Size Maximum Power Point Tracking Strategy with Low Power Loss for Photovoltaics

Yinxiao Zhu [1], Moon Keun Kim [2,*] and Huiqing Wen [1]

[1] Department of Electrical and Electronic Engineering, Xi'an Jiaotong–Liverpool University, Suzhou 215123, China; Yinxiao.Zhu17@student.xjtlu.edu.cn (Y.Z.); Huiqing.Wen@xjtlu.edu.cn (H.W.)
[2] Department of Architecture, Xi'an Jiaotong–Liverpool University, Suzhou 215123, China
* Correspondence: Moon.Kim@xjtlu.edu.cn or yan1492@gmail.com; Tel.: +86-512-8818-0465

Received: 15 November 2018; Accepted: 24 December 2018; Published: 28 December 2018

Abstract: Photovoltaic (PV) techniques are widely used in daily life. In addition to the material characteristics and environmental conditions, maximum power point tracking (MPPT) techniques are an efficient means to maximize the output power and improve the utilization of solar power. However, the conventional fixed step size perturbation and observation (P&O) algorithm results in perturbations and power loss around the maximum power point in steady-state operation. To reduce the power loss in steady-state operation and improve the response speed of MPPT, this study proposes a self-adaptable step size P&O-based MPPT algorithm with infinitesimal perturbations. This algorithm combines four techniques to upgrade the response speed and reduce the power loss: (1) system operation state determination, (2) perturbation direction decision, (3) adaptable step size, and 4) natural oscillation control. The simulation results validate the proposed algorithm and illustrate its performances in operational procedures.

Keywords: perturbation and observation; adjustable step size; low power loss; maximum power point tracking

1. Introduction

1.1. Background

A direct current (DC) [1] pattern exists in almost all the electrical devices in our daily life. Photovoltaics (PV), as well-known renewable power generation solutions, are a foundational DC source which can supply DC power for DC application directly or drive the alternating current (AC) application after inverting. Owing to the policy support and sharp cost reduction of photovoltaic [2] techniques, solar power, a form of inexhaustible eco-friendly energy, has been widely exploited in daily life in recent years. At the same time, the civilization process enhances the demands of civil space. To increase the utilization of urban space, building-integrated photovoltaic techniques are becoming more widely considered in the research community [3–10].

Building integrated photovoltaics, a significant branch of PV generation, are easily affected by environmental conditions, similar to other PV applications. The output characteristics of the PV panel are mainly influenced by the illumination intensity, temperature, material, and other conditions, especially the received illumination intensity and the surface temperature of the PV panel. For example, increasing the temperature results in a slight increase in the short-circuit current and a significant decrease in the open-circuit voltage, which reduces the maximum output power. However, in any condition, a curve of the output power can be drawn, and the output power has a

maximum output point called the maximum power point (MPP) [7,11–22]. For the PV system operated with higher efficiency, an MPP tracking (MPPT) controller is indispensable; the tracking methodologies are introduced in detail in the MPPT section of this report.

For a PV system with an MPPT controller, the structure can be depicted as consisting of a PV panel, a power converter [7,8,16,19–33], an MPPT controller, and a load (including but not limited to motors, batteries, heaters, energy-storage systems, and other electric appliances). The structure of the PV system is shown in Figure 1.

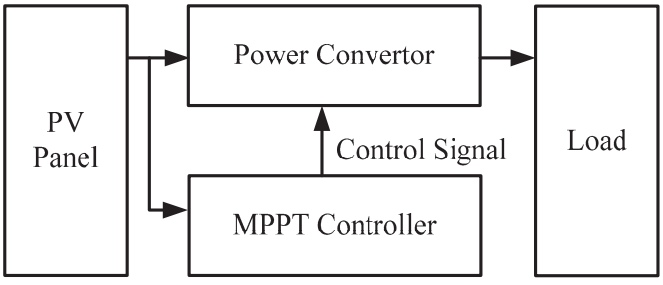

Figure 1. Structure of a photovoltaic (PV) system with a maximum power point tracking (MPPT) controller.

The operating process of the PV system can be simply explained as follows. After absorbing enough radiation, the PV panel supplies electricity to the power converter and the load is driven via the output from the power converter. Simultaneously, the MPPT controller measures specific parameters (such as voltage and current) for controlling the power converter in order to make the system operate at the MPP.

1.2. Aims and Objectives

This study discusses an advanced algorithm to improve the efficiency of the perturbation and observation (P&O)-based MPPT with simulation and numerical analysis tools. Power loss, a common phenomenon in electricity generation, refers to the power consumed during the conversion process; it is unavoidable, but can be reduced. For the conventional P&O-based MPPT controller of a PV system, certain power loss is caused by the ineluctable perturbation of the P&O method. If the power loss can be reduced, the utilization rate of the solar energy can be increased, and more energy can be saved.

To solve the power-loss problem caused by the non-environmental conditions causing oscillation, a P&O-based self-adaptable MPPT algorithm is designed in this study. This algorithm is expected to reduce the power loss and improve the response speed of tracking.

1.3. Model and Characteristics Analysis of PV Panel

The PV cell, also known as a solar cell, is the unit component of the PV panel and is a semiconductor device that can directly convert solar power into electrical energy based on the PV effect [34]. The irradiation directly affects the intensity of photocurrent generation, influencing the photovoltaics.

According to the one diode PV cell structure shown in Figure 2, a PV cell can be considered as the equivalent circuit depicted in Figure 2, consisting of an ideal current source (I_L) with a diode (D), a series resistor (R_S), and a parallel shunt resistor (R_{Sh}).

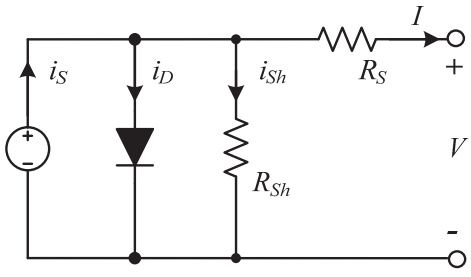

Figure 2. Equivalent circuit of a PV cell.

According to the equivalent circuit shown in Figure 2, the output current of a PV cell can be calculated as follows [6,26,35–39]:

$$I = I_L - I_D - I_{Sh} \tag{1}$$

Here, I is the output current (A), I_L is the photocurrent (A), I_D is the diode current (A), and I_{Sh} is the shunt current (A); I_L, I_D, and I_{Sh} can be expressed as follows [6,26,35–39].

$$I_L = \mu G \tag{2}$$

$$I_D = I_0\left\{\exp\left[\frac{V + IR_S}{n(kq/T)}\right] - 1\right\} \tag{3}$$

$$I_{Sh} = \frac{V + IR_S}{R_{Sh}} \tag{4}$$

Here, μ is a proportional constant (depending on the material and other conditions), G is the illumination intensity, I_0 is the diode reverse saturation current (unit: A), n is the diode ideality factor ($1 < n < 2$, and $n = 1$ for an ideal diode), k is Boltzmann's constant (1.38×10^{-23} J/K), q is the elementary electric charge e (1.6×10^{-19} C), T is the absolute surface temperature of the PV cell (unit: K), V is the output voltage, I is the output current (unit: A), R_S is the series resistor (unit: Ω), and R_{Sh} is the shunt resistor (unit: Ω).

Combining Equations (2)–(4), as well as output current I, Equation (1) yields [6,26,35–39]:

$$I = \mu G - I_0\left\{\exp\left[\frac{q(V + IR_S)}{nkT}\right] - 1\right\} - \frac{V + IR_S}{R_{Sh}} \tag{5}$$

According to Equation (5), the temperature and illumination intensity are the most influential environmental conditions in actual operation, because the other uncertain factors are confirmed upon the completion of the PV cell.

The characteristic current to voltage (I–V) and power to voltage (P–V) curves under different temperature and illumination conditions are shown in Figure 3. Changes in the temperature and illumination can easily affect the MPP, but in different ways. As shown in Figure 3a, under the same illumination (G), the increasing temperature (T) visibly reduces the output voltage of the PV panel, but the decrease in the output current is limited. This is followed by a decrease in the output power. As shown in Figure 3b, at the same surface temperature, as the illumination increases, the output voltage exhibits a slight increase, but the output current increases sharply, followed by an increase in the output power.

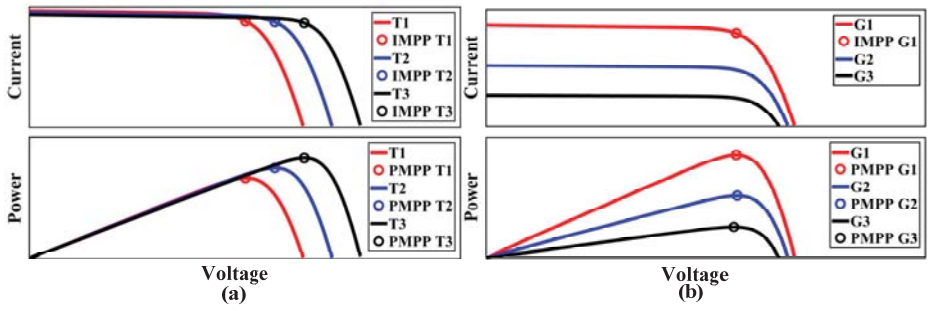

Figure 3. Current to voltage (I–V) and power to voltage (P–V) curves under variable conditions: (**a**) $T_1 > T_2 > T3$; (**b**) $G_1 > G_2 > G_3$.

1.4. Maximum Power Point Tracking (MPPT)

The MPPT technique aims to maintain the maximum output operation of the PV system. MPPs in different environmental conditions are marked in Figure 3.

In most cases, a pulse-width modulation (PWM) wave is the control signal for the power switch of the converter; the duty cycle (*D*) of the PWM wave affects the output voltage, and an MPPT controller controls the duty cycle of the PWM wave [40,41].

In actual operation, the environmental conditions do not change sharply every second; nonetheless, the MPPT controller is needed to achieve the MPP. The core of the MPPT controller is the MPPT algorithm. According to their characteristics, MPPT algorithms can be classified into self-optimization and non-self-optimization algorithms. For example, perturb and observe (P&O) [29,40,42], incremental conductance (InC) [25,43,44], and constant voltage tracking (CVT) [40,45] are three typical self-optimization algorithms. Non-self-optimization algorithms mainly include curve fitting [46] and other methods. Furthermore, there are artificial intelligence techniques, such as fuzzy logic [12,47,48] and particle swarm optimization [12,49–52], that are combined with conventional MPPT methods to achieve a high tracking accuracy.

In the industry, MPPT controllers, mostly self-optimization-based, can help systems track the MPP and automatically maintain steady operation in the maximum-output state. A comparison of three typical methods is shown in Table 1. After the comparison, to simplify the algorithm, the proposed MPPT algorithm is P&O-based [29,42,53], and its differences from the conventional one [13,16,30,36,45,46,53] are introduced in the Methods section of this report.

Table 1. Comparison of constant voltage tracking (CVT), incremental conductance (InC), perturb and observe (P&O), and the proposed maximum power point tracking (MPPT).

MPPT Algorithm	CVT	InC	P&O	This Work
Specific PV Array	Yes	No	No	No
True MPPT	No	Yes	Yes	Yes
Tracking Speed	Adaptable	Medium	Adaptable	Fast
System Complexity	Low	Low	Medium	Medium
Measured Parameters	Voltage	Voltage, Current	Voltage, Current	Voltage, Current

2. Methods

2.1. Principle of the P&O Method

The P&O method is the most widely used self-optimization MPPT algorithm. The basic principle of P&O is as follows. After a certain directional-changing voltage applies perturbation to the output voltage of the PV panel, the MPPT controller compares the output power before and after the perturbation. If the changing direction is positive and the output voltage increases, the MPPT controller

continues the perturbation in this direction; if the output power decreases, the direction reverses in the next perturbation.

Figure 4 shows the characteristic P–V curve, where P_{MPP} is the MPP, P_1 is to the left of the MPP, P_2 is to the right of the MPP, and ΔU_1 and ΔU_2 are the changing ranges of the output voltage. To achieve the MPP, ΔU_1 should be increased in P_1, but ΔU_2 should be decreased in P_2. In this case, ΔU_1 and ΔU_2 differ, and $\Delta U_1 > \Delta U_2$. A greater distance from the MPP yields a greater difference between ΔU_1 and ΔU_2. Owing to the existence of perturbation, it is very difficult for the basic P&O method to eliminate the oscillating phenomenon at the MPP. The step size of the perturbation directly affects the speed and accuracy of the MPPT. All of these factors cause power loss. Figure 5 [40] presents the flowchart of the basic P&O tactic.

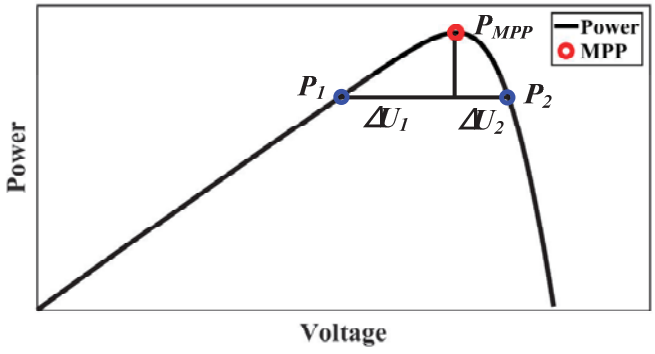

Figure 4. Tracking issues in the P–V curve.

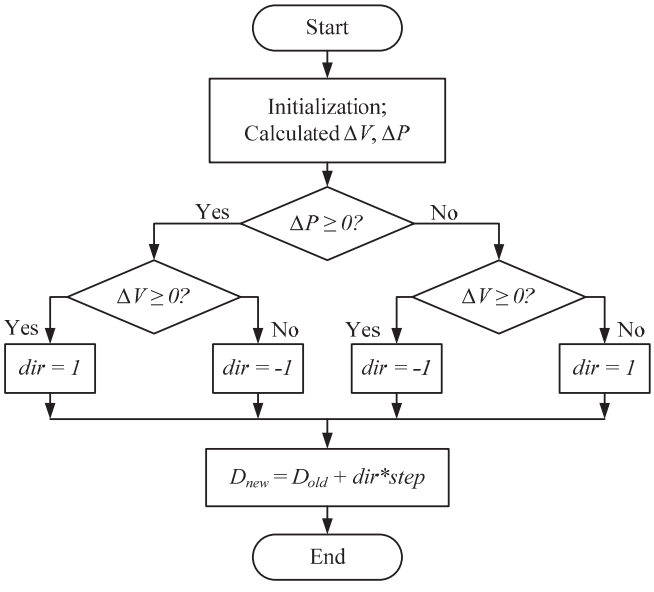

Figure 5. Flowchart of the basic perturb and observe (P&O) tactic.

2.2. P&O-Based Self-Adaptable Step Size MPPT Tactic

In the case of a fixed step size P&O algorithm, opportunely increasing the step size can improve the system response speed, but increase the oscillation region around the MPP and increase the power

loss. A small step size can increase the tracking accuracy and reduce the oscillation, but reduce the response speed. To deal with the contradiction between accuracy and response speed, the variable step size MPPT algorithm is employed. The conventional variable step size MPPT algorithm comprises the optimum gradient method [23,54], the successive approximation optimization method [29,30,42,43,55], and other methods. However, the derivative of the power to the voltage is too large on the right side of the MPP; therefore, the derivative of the power to the voltage is no longer suitable for the parameter of the step size solution. However, the optimal gradient-based variable step size MPPT uses a stationary step size selection equation; this algorithm cannot preferably adapt to changes in the P–V curve.

The tracking tactic of the conventional MPPT algorithm is periodic. For the conventional P&O strategy, the step size is fixed, which means that the ΔU in the operating procedure, shown in Figure 5, cannot change. Owing to the tracking issues presented in Figure 4, a certain oscillation exists. Because of the aforementioned issues, in the steady operation state, although the MPPT controller has tracked the MPP successfully, the output voltage still undergoes perturbation around the MPP and never achieves V_{MPP} (output voltage in the MPP), as shown in Figure 6, and the exiting oscillation around the MPP causes certain power loss. The definition and analysis are introduced in the power-loss analysis and calculation part of this report. To deal with the power loss around the MPP in the steady-state operation as much as possible, an advanced P&O-based MPPT tactic with a self-adaptable step size is proposed. A flowchart of the proposed MPPT tactic is presented in Figure 7.

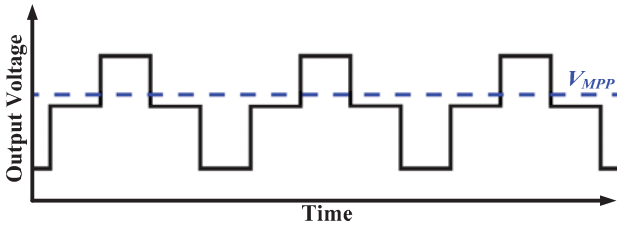

Figure 6. Oscillation in steady-state operation.

Compared with the conventional P&O MPPT [29,30,40,42], the improved procedure of the proposed P&O-based self-adaptable MPPT tactic is based on the following four key aspects: (1) natural oscillation control, (2) system operation state determination, (3) perturbation direction decision, and (4) adaptable step size.

In the natural oscillation control procedure, the proposed tactic can select a suitable tracking loop depending on the oscillation range. In the flowchart, ΔP and *err* detects the output power change in present and previous sample period; E_{TH} is the threshold for error determination. It is used to control the allowable natural oscillation range and as an entry for a continuous module. If $err > E_{TH}$, the program uses the error value and multiplies it by a weight factor (k) as the step size to optimize the tracking speed; otherwise, the program enters the system operation state determination module.

In the system operation state determination module, *Flag* is the identifier of the operation state. If $Flag = 1$, the tracking procedure enters an idle operation loop, and the next perturbation director (*dir*) depends on whether the actual current (I) reaches the threshold for current (I_{TH}), expressed in Equation (7). If $\Delta I > I_{TH}$, *Idle* changes to 0, and the direction (*dir*) is a sine function of ΔI and is the weight of the next perturbation; or, it jumps out of the Idle Mode loop. If $Idle = 0$, the program enters the P&O-based perturbation direction decision procedure.

The procedure of perturbation direction decision is similar to the operation of the basic P&O tactic, but differences exist. The direction for the next perturbation depends on the change in the output power (ΔP). If the output power in this perturbation is increased ($\Delta P > 0$), the perturbation direction is continuous, and the counter is initialized ($Cont = 0$); otherwise, the perturbation direction is changed ($dir = -dir$), and the loop time is counted ($Cont = Cont + 1$). After the conventional P&O procedure, the program determines the change in the output voltage (ΔU) and the number of loop times (*Cont*).

If it loops more than once (*Cont* > *1*) and the change in the output voltage is null ($\Delta U = 0$), the program operates in the *Idle* mode (*Flag* = *1*), provided that the error is within the allowable range.

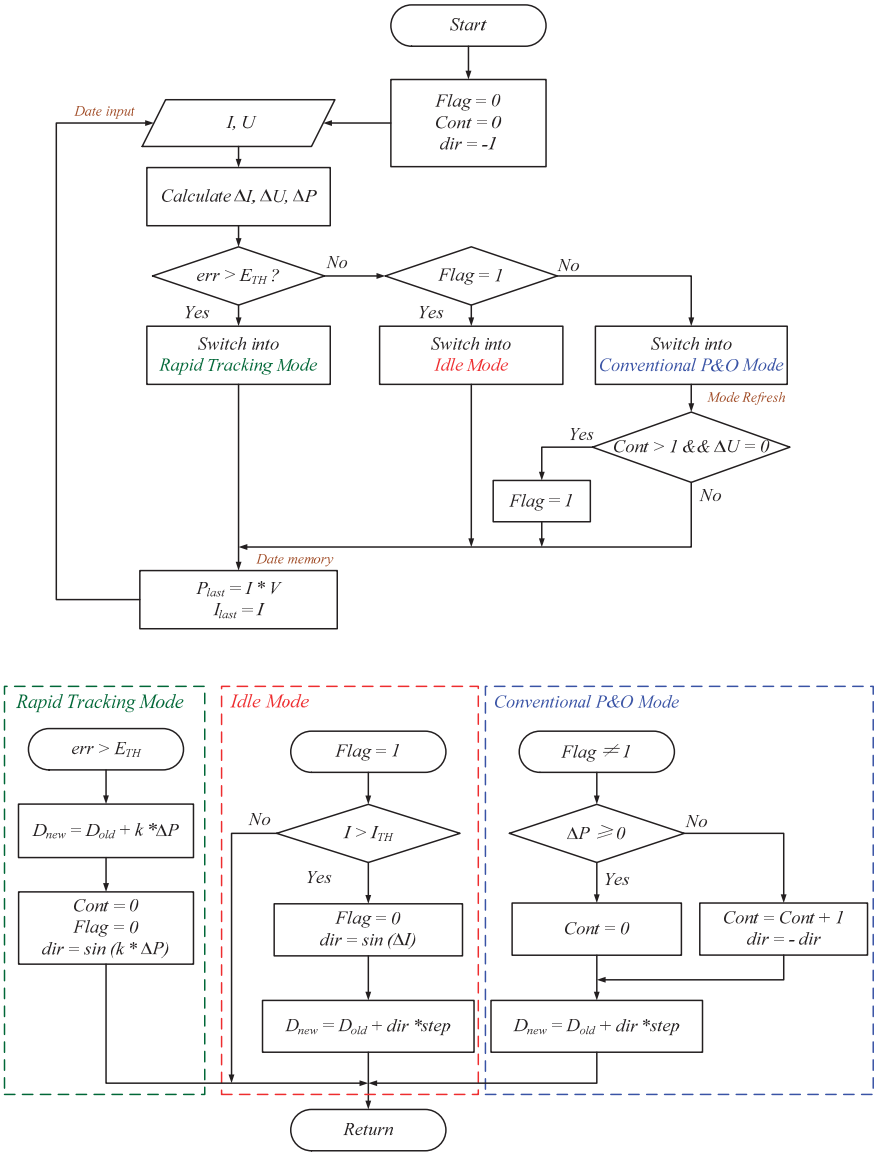

Figure 7. Flowchart of the proposed MPPT tactic.

As shown in Figure 6, the standard P&O tactic gives rise to a certain oscillation around the MPP, and the range of the oscillation depends on the setting of the perturbation step size. The adaptable step size is included in every aspect introduced above. Mainly, the step size depends on the change in the last operation state (*Flag* = *0 or Flag* = *1*) and the range of actual oscillation (*err*). The change in the step size affects the duty cycle of the PWM wave and is displayed as the change in the output

voltage of the boost converter. In this tactic, the step size is identified as *step* and can be measured by determining the output voltage or duty cycle of the PWM wave in actual operation.

The boundary condition chosen is based on the characteristics of selected PV elements as shown in Table 2. During the irradiation change, the change in interface temperature would not be significant. Hence, the consideration of boundary selection is only based on the change in MPP while the irradiation changes.

In the simulation, the boundary condition of E_{TH} is selected by the change in measure power during the no-oscillation state. The value of E_{TH} is selected as 0.03; in other words, the judgement follows the relationship of $|(P\text{-}P\_old)/P\_old| >= 0.03$ (P is the present sampled power and P_old is the value in previous sample time). $|(P\text{-}P\_old)/P\_old|$ is the explaination for *err*. The selection of 0.03 is based on the change in power while the irradiation changes for the PV element MSX-60W, as shown in Figure 8. According to Figure 8, if the change in power is more than 0.03 of the previous MPP point, the change in irradiation could be determined and the Rapid Tracking Model is activated.

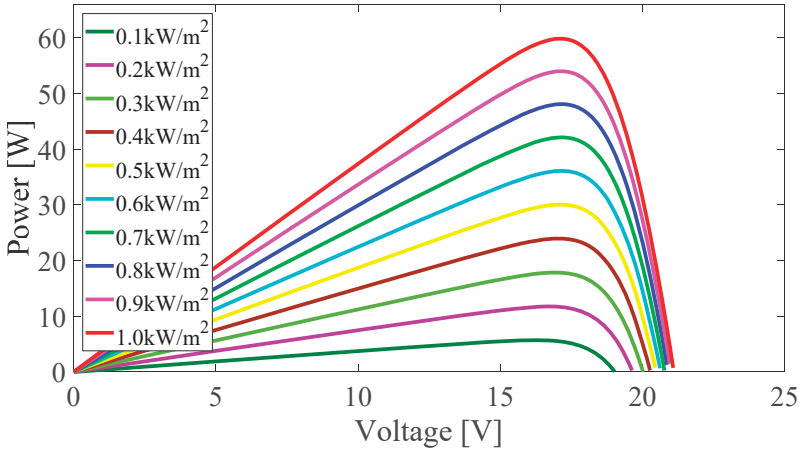

Figure 8. Variation of power while the irradiation changes.

The selected of I_{TH} in the Idle Mode is based on the change of MPP current in the MPP region, as shown in Figure 9. At the MPP, the relational gain *KIsc* between MPP current *Impp* and short-circuit current *Isc* is a constant, and 0.78 < *KIsc* < 0.92 [56]. In this condition, the *Isc* can be estimated using the listing formula in the left of the MPP.

$$Isc = I - \frac{I - I\_old}{V - V\_old} \cdot V \tag{6}$$

KIsc is selected as 0.92 in the simulation.

I_{TH} is expressed as follows:

$$I_{TH} = K_{Isc}\left(I - \frac{I - I\_old}{V - V\_old} \cdot V\right) \tag{7}$$

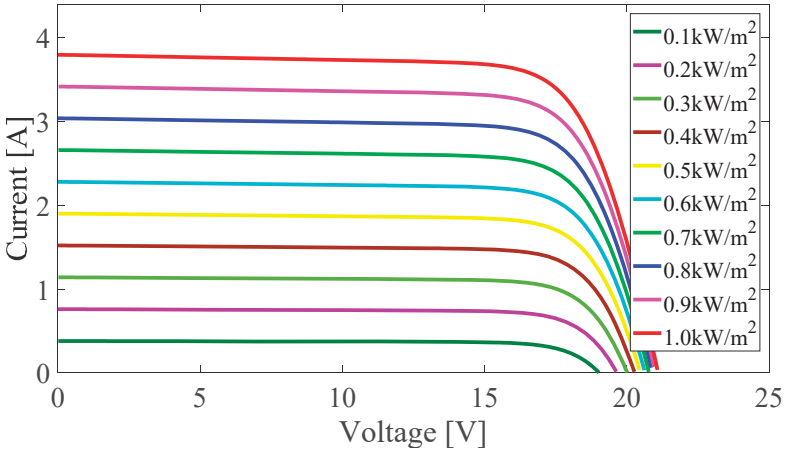

Figure 9. Variation of the MPP current.

2.3. Simulation Modeling and Power-Loss Analysis

In this part, the simulation modeling and the mathematical method for the power-loss analysis are introduced. To verify the proposed MPPT tactic, a MATLAB/Simulink module is used as a platform for simulation. During the simulation, some parameters are changed to simulate the change in the environmental conditions. The power-loss analysis and calculation are expressed by mathematical equations.

2.4. Simulation Modeling

Simulation modeling mainly includes three key aspects: (1) PV module modeling, (2) MPPT controller modeling, and (3) PV system combination. The modeling strategies and parameter settings are presented in the tables and figures.

2.4.1. PV Module Modeling

The modeling of the PV array module is based on the template BP MSX-60W1 from Simulink Library. The symbol and connection are displayed in Figure 10, and the parameters are explained in Table 2.

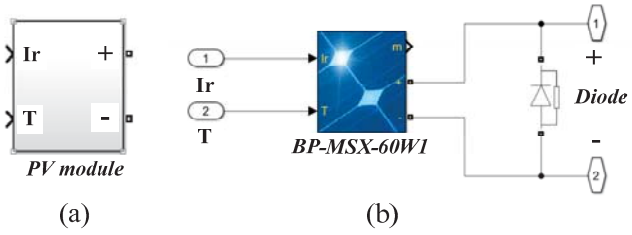

Figure 10. PV array module modeling (**a**) symbol and (**b**) internal connection.

In Figure 10, Ir is the input for the illumination intendancy, T is the input for the temperature, "+" is the positive electrode of the output voltage, and "−" is the negative electrode of the output voltage. The diode in Figure 10b protects the PV panel.

Table 2. Installed characteristic parameters of the PV array module

Parameter	N [cell]	P_{MPP} [W]	V_{OC} [V]	V_{MPP} [V]	I_{SC} [A]	I_{MPP} [A]	C_{VOC} [%/°C]	C_{ISC} [%/°C]
Value	36	59.85	21.1	17.1	3.8	3.5	−0.379	0.065

In Table 2, N is the number of cells per module, P_{MPP} is the maximum power, V_{OC} is the open-circuit voltage, V_{MPP} is the voltage at the MPP, I_{SC} is the short-circuit current, I_{MPP} is the current at the MPP, C_{VOC} is the temperature coefficient of V_{OC}, and C_{ISC} is the temperature coefficient of I_{SC}.

2.4.2. MPPT Controller Module Modeling

To compare the conventional and proposed MPPT tactics, two MPPT controller modules were built. Figure 11 shows the connections of the proposed MPPT control. The codes in the m-functions are based on the flowcharts shown in Figure 7.

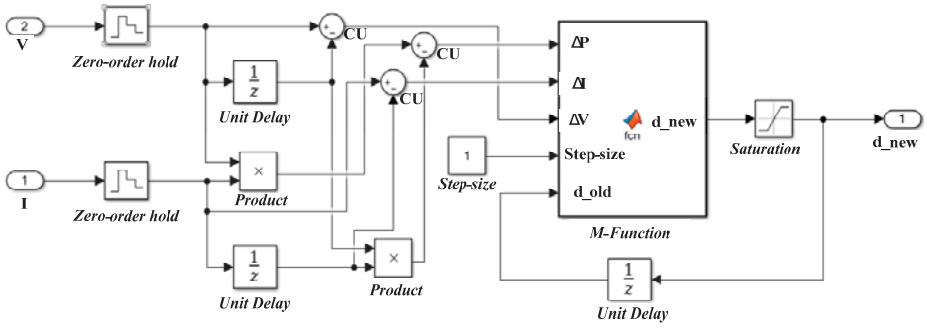

Figure 11. Internal connections of the proposed MPPT tactic.

In Figure 11, V is the input data of voltage, I is the input data of current, "zero-order hold" is for updating and holding data at every sample time, "unit delay" is for memorizing data, "product" is a multiplier, "CU" is the unit for data minus, "step size" is for setting the initial value of the step size, "M-function" is a function builder that employs the m-language (five input ports: three for the change in power, current, and voltage; one for initial step size setting; and one for the old duty cycle), "saturation" is for limiting the upper and lower values of a signal, and "d_new" is the updating duty cycle of the PWM wave.

2.4.3. PV System Combination

According to the basic structure of the PV system displayed in Figure 1, the proposed P&O-based PV system simulation platform is shown in Figure 12.

The PV module is introduced in the PV array modeling section. The proposed MPPT is explained in the Methods section, and the initial connection is shown in Figure 12. The power converter and load include a boost converter and a 30-Ω resistor (as the electrical appliance); Ir is an input port for the illumination, T is an input port for the temperature, the I sensor is for measuring the photocurrent, the V sensor is for measuring the photovoltage, and C is a filter capacitor (47 μF). The repeating sequence and relational operator work together and generate the control signal (PWM wave) for the power converter. The connections are based on the initial characteristics of each component.

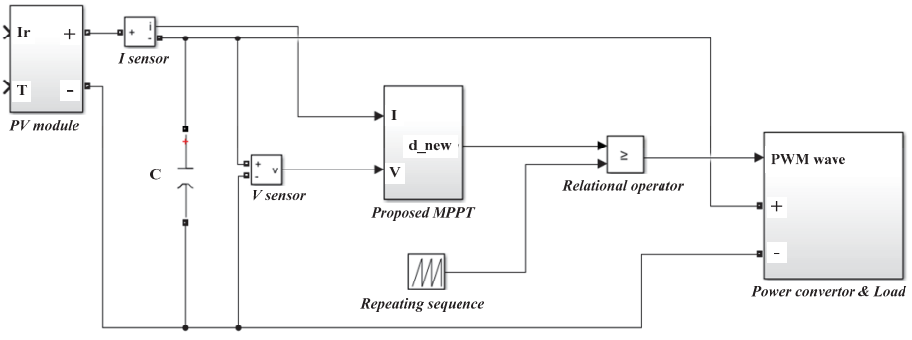

Figure 12. Simulation platform of the proposed MPPT tactic. PWM—pulse-width modulation.

2.5. Power-Loss Analysis and Calculation

The power-loss analysis is an important aspect for defining the tracking efficiency of the MPPT. The artificial oscillation around the MPP of the proposed MPPT strategy is diminished to close to zero and can even be removed in an ideal environment; moreover, the tracking step size can be adapted automatically. A typical operation issue of the conventional P&O MPPT strategy is displayed in Figure 13, and the power-loss analysis and calculation are based on this figure.

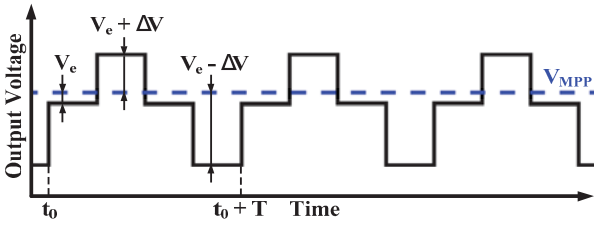

Figure 13. Typical operation issue analysis of ordinary P&O.

The relationship between the power loss (P_L) and the theoretical power (P_{MPP}) is expressed as follows [57]:

$$\frac{P_L}{P_{MPP}} \approx \left(\frac{(\Delta V_{PV})_{RMS}}{V_{MPP}}\right)^2 \left(1 + \frac{V_{cell}}{2nkT/q}\right) \tag{8}$$

Here, V_{MPP} is the theoretical output voltage when the PV panel operates in the MPP, $(\Delta V_{PV})_{RMS}$ is the root-mean-square [58] value of the voltage perturbation, and V_{cell} is the output voltage of every single cell when the PV panel operates in the MPP (mostly around 0.5 V).

According to Figure 13, in one oscillation cycle (T), the function of the change in the output voltage corresponding to time ($\Delta V_{PV}(t)$) is expressed as follows.

$$\Delta V_{PV}(t) = \begin{cases} V_e & (t_0 < t < t_0 + T/4) \\ V_e + V_{step-size} & (t_0 + T/4 < t < t_0 + T/2) \\ V_e & (t_0 + T/2 < t < t_0 + 3T/4) \\ V_e - V_{step-size} & (t_0 + 3T/4 < t < t_0 + T) \end{cases} \tag{9}$$

Here, V_e is the minimum difference between V_{MPP} and the output voltage (V_{PV}) set by the MPPT controller, and $V_{step\ size}$ is due to the step size and is displayed as ΔV in Figure 12. The relationship between V_e and $V_{step\ size}$ can be observed as follows.

$$V_e = \beta V_{step-size} \tag{10}$$

Here, β is a constant. Replacing V_e with Equation (9), Equation (10) can be expressed as follows.

$$\Delta V_{PV}(t) = \begin{cases} \beta V_{step-size} & (t_0 < t < t_0 + T/4) \\ (\beta+1)V_{step-size} & (t_0 + T/4 < t < t_0 + T/2) \\ \beta V_{step-size} & (t_0 + T/2 < t < t_0 + 3T/4) \\ (\beta-1)V_{step-size} & (t_0 + 3T/4 < t < t_0 + T) \end{cases} \tag{11}$$

Therefore, the root-mean-square (RMS) value of the voltage perturbation ($(\Delta V_{PV})_{RMS}$) can be calculated as follows.

$$\begin{aligned} (\Delta V_{PV})_{RMS} &= \sqrt{\frac{1}{T}\int_0^T \Delta V_t{}^2 dt} \\ &= V_{step-size}\sqrt{\frac{1}{4}\left(\beta^2 + (\beta+1)^2 + \beta^2 + (\beta-1)^2\right)} \\ &= V_{step-size}\sqrt{\frac{1}{2} + \beta^2} \end{aligned} \tag{12}$$

By combining Equations (8) and (12), the steady-state power loss can be expressed as follows.

$$\frac{P_L}{P_{MPP}} \approx \left(\frac{1}{2} + \beta^2\right)\left(\frac{V_{step-size}}{V_{MPP}}\right)^2\left(1 + \frac{V_{cell}}{2nkT/q}\right) \tag{13}$$

For the proposed MPPT tactic, the output voltage does not give rise to any artificial oscillation, but differences still exist between V_{PV} and V_{MPP}. The difference between V_{PV} and V_{MPP} in this condition can be expressed as follows.

$$(\Delta V_{PV})_{RMS} = \beta V_{step-size} \tag{14}$$

By substituting Equation (14) into Equation (8), the power loss of the proposed MPPT tactic can be expressed as follows.

$$\left(\frac{P_L}{P_{MPP}}\right)_{proposed} \approx \beta^2\left(\frac{V_{step-size}}{V_{MPP}}\right)^2\left(1 + \frac{V_{cell}}{2nkT/q}\right) \tag{15}$$

3. Results and Discussion

The results are categorized into two parts: (1) the simulation results are displayed, analyzed, and compared with the conventional P&O MPPT tactic to show the improvement; and (2) the power loss is calculated via the statistical method expressed in the Methods and power-loss analysis and calculation parts of this report.

3.1. Simulation Results

To verify the advanced performances of the proposed MPPT controlling tactic, the simulations follow the single-variable principle, and the comparisons are performed under the same parameter settings (excluding the MPPT controller module). The settings of the PV array module and the other basic simulation parameters are shown in Table 3.

Table 3. Global simulation parameters.

Parameter	Temperature [°C]	Step Size [%]	E_{TH} [W]	I_{TH} [A]	k
Value	25	1	0.03	Equation (7)	0.5

The simulation results are divided into three parts: (1) tracking speed comparison under steady environment conditions, (2) reliability under variable environment operation, and (3) improvement of the steady state operation.

3.1.1. Tracking Speed Comparison

The simulation verifies the increasing tracking speed of the proposed MPPT tactic. The other simulation parameter is set to the ideal value (illumination = 1000 W/m^2) to eliminate the effects of environmental conditions.

Figure 14 shows the power–time curves of the proposed MPPT tactic (red line) and the conventional P&O algorithm (green line). According to Figure 14, the time needed for the conventional P&O MPPT tactic is 1.061 s, and that for the proposed MPPT tactic is 0.272 s. The decrease in the tracking time verified the increase in the tracking speed; compared with the conventional P&O tactic, the proposed tactic can reduce the tracking speed by approximately 74.5%.

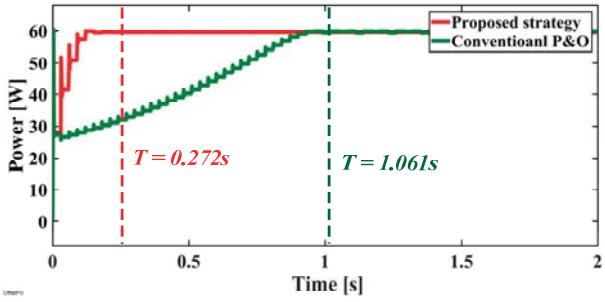

Figure 14. Power–time curves of the conventional and proposed MPPT tactics.

3.1.2. Reliability under Variable Environmental Conditions

In actual operation, the change in temperature is not sharp, and the main influencing factor is the change in illumination because of partial shading; therefore, the reliability of the proposed tactic is defined via simulation in the environment with a variable change in illumination, as shown in Figure 15.

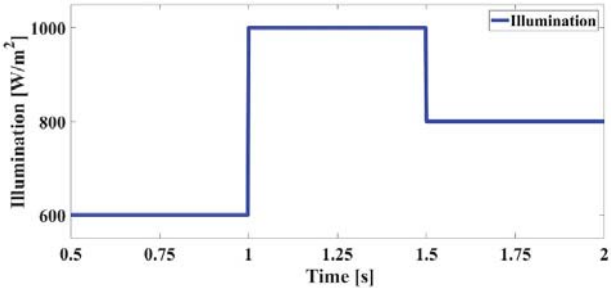

Figure 15. Change curve of the illumination.

In this situation, the simulation results, including the current, voltage, and power curves, are shown in Figures 16–18, respectively. In these figures, short explanations of the existing phenomenon are presented. Each figure includes two parts—one is from the conventional P&O tactic, and the other is from the proposed MPPT tactic. Each sub-figure has a standard line of the theoretical output parameters in MPP operation for verifying the tracking accuracy.

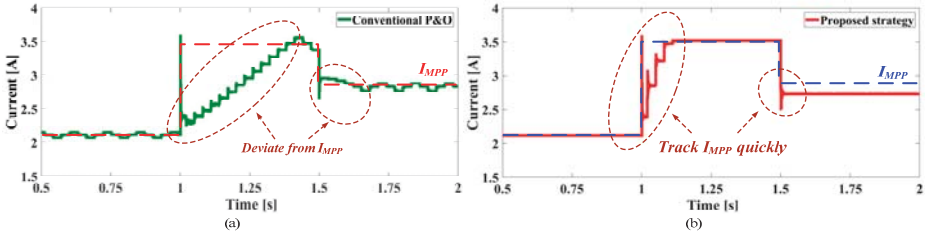

Figure 16. Current curves: (**a**) conventional P&O and (**b**) the proposed MPPT tactic.

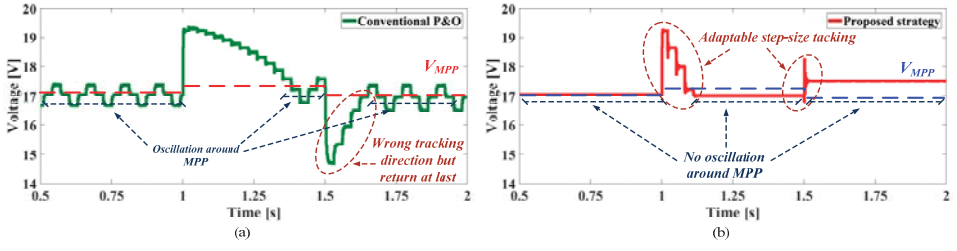

Figure 17. Voltage curves: (**a**) conventional P&O and (**b**) the proposed MPPT tactic.

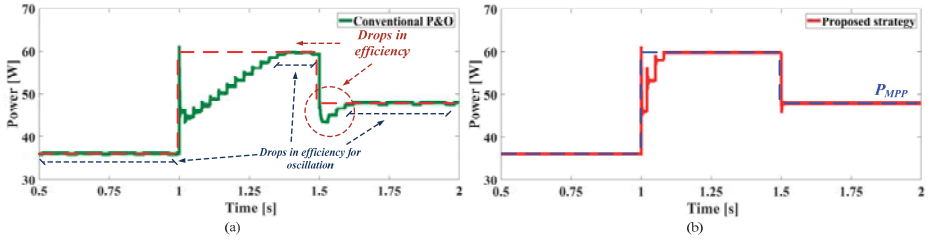

Figure 18. Power curves: (**a**) conventional P&O and (**b**) the proposed MPPT tactic.

Figure 16 shows the curves of the PV array output current (I_{PV}). Figure 16a shows the measured current for the conventional P&O tactic. The results for the tracking during the increase in the illumination show a lack of speed and departures from the standard line (I_{MPP}). As shown in Figure 16b, the proposed tactic does not cause departures and has a high tracking accuracy with the standard.

Figure 17 shows the curves of the PV array output voltage (V_{PV}). The conventional P&O tactic can track the MPP, but a loss of efficiency exists in the illumination increasing procedure. This method tracks in the wrong direction owing to the falling illumination and returns to the right direction when this phenomenon stops. During the increase or decrease in the illumination, the proposed strategy operates in the self-adapted step size model and maintains a limited departure from the theoretical output voltage.

Figure 18 shows the curves of the PV array output power (P_{PV}). According to the tracking mistakes and errors, the conventional tactic results in efficiency drops, as shown in Figure 18a. At the same time, the oscillation around the MPP causes efficiency drops. As shown in Figure 18b, the output–power curve of the proposed tactic almost coincides with the theoretical output of that of a verification of the tracking accuracy and efficiency.

3.1.3. Steady-State Operation Comparison

Figure 19 shows the output–voltage state under steady operation. Compared with the theoretical output value (V_{MPP}), there exist conventional P&O strategy oscillations around the MPP in the steady

state; the proposed tactic experiences deviations from the theoretical output, but can maintain operation without oscillation.

3.2. Power-Loss Analysis Results

According to Figure 19 and the parameters of the PV module shown in Table 2, the power loss can be calculated using the equation expressed in the Methods section of this report.

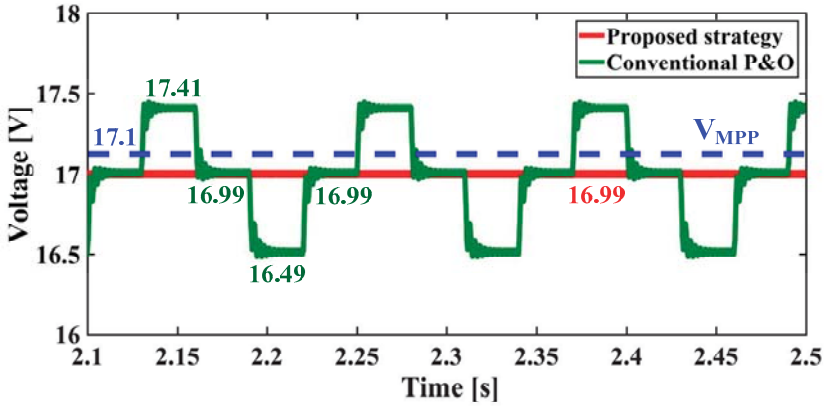

Figure 19. Comparison of the voltage in the steady state.

According to Equations (8) and (11), the steady-state power loss of the conventional P&O tactic is calculated as follows.

$$\left(\frac{P_L}{P_{MPP}}\right)_{conventianl} \approx 0.69\% \tag{16}$$

According to Equations (8) and (13), the steady-state power loss of the conventional P&O tactic is given as follows.

$$\left(\frac{P_L}{P_{MPP}}\right)_{proposed} \approx 0.23\% \tag{17}$$

The efficiency of the power-loss reduction is calculated as follows.

$$\eta_{efficiency} = \left(1 - \frac{0.23\%}{0.69\%}\right) \times 100\% \approx 66.7\% \tag{18}$$

Via the proposed strategy, the power loss in steady-state operation drops to 0.23%; compared with the conventional P&O algorithm, the percentage reduction in the power loss around the MPP is 66.7%.

Assuming the PV element is in the standard test condition (STC) (1000 W/m^2, 25 °C, AM1.5), the simulation in steady-state operation for the conventional P&O MPPT and proposed control is as shown in Figure 20.

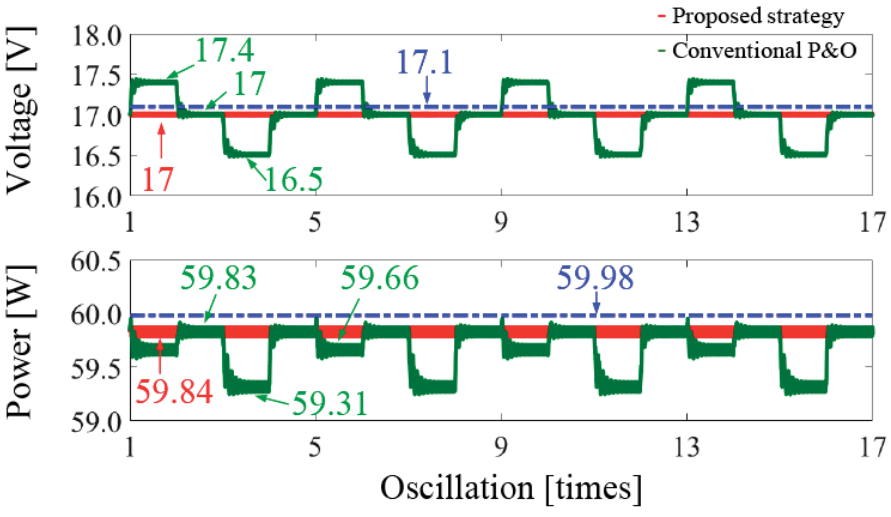

Figure 20. Comparison of the voltage and power in the steady state.

The percentage of power absorbed in every oscillation period for the conventional P&O algorithm can be calculated as follows.

$$\frac{P_{t1}+P_{t2}+P_{t3}+P_{t4}}{P_{theo}}=\frac{59.66\text{W}+59.83\text{W}+59.31\text{W}+59.83\text{W}}{59.98\text{W}\times 4}\times 100\%=99.46\% \tag{19}$$

where P_{ti} is the i^{th} oscillation in a period and P_{theo} is the theoretical output power during the period.

The power absorbed in every oscillation period for the proposed control scheme can be calculated as follows.

$$\frac{P_{t1}+P_{t2}+P_{t3}+P_{t4}}{P_{theo}}=\frac{59.84\times 4}{59.98\text{W}\times 4}\times 100\%=99.77\% \tag{20}$$

The power loss in the P&O algorithm is expressed as 0.54% and 0.23% for the proposed control. The simulation result is close to the calculation in the submitted manuscript. The energy saving for every oscillation period in STC is expressed as follows.

$$\sum_{i=1}^{n=4}P_{proposed,ti}-\sum_{i=1}^{n=4}P_{po,ti}=0.73\text{W} \tag{21}$$

The average energy saving in every oscillation is 0.1825W.

A comparison with the conventional P&O algorithm and the theoretical value reveals that the simulation results are well-matched. As the efficiency improves, as shown in Equation (21), the proposed self-adaptable step size MPPT tactic can uncommonly reduce the power loss during the steady-state operation. According to the response speed and tracking accuracy shown in the simulation results at Figure 16 to Figure 18, this proposed tactic can also reduce the power loss during the tracking procedure. Furthermore, the ungraded installations of this proposed tactic are software-based, which means that every PV system with a processor-based MPPT controller can upgrade without any hardware cost.

4. Conclusions

This research presents an advanced P&O-based self-adaptable step size MPPT tactic. Compared with the conventional P&O algorithm, this advanced MPPT strategy can reduce the power loss by 0.1825W per oscillation at steady state during the MPP operation; at the same time, the response speed

is lower than 0.3 s, and this strategy has a high stability when facing the slope changing illumination condition. These improvement results are given as follows: (1) the activation of idle operating with the achievement of an allowable tracking error; (2) multiple step size selection; (3) avoidance of natural oscillation; and (4) system operation state determination. The overall performance development, including the steady state and changing illumination operation, verified the benefits of the proposed strategy. These results will contribute to the development of PV installation because the proposed version has higher energy efficiency and reduces the tracking speed and power loss compared with conventional algorithms. In addition to the findings of this study, only numerical calculations show limitations to prove the results. Accordingly, in a future study, an experimental test will be carried out for evaluating the proposed control.

Author Contributions: conceptualization, Y.Z., and H.W.; methodology, Y.Z. and M.K.K.; validation, Y.Z.; formal analysis, Y.Z., and H.W.; investigation, Y.Z., and H.W.; resources, Y.Z., and H.W.; Software, Y.Z.; writing original draft preparation, Y.Z. and M.K.K.; writing—review and editing, Y.Z. and M.K.K.; supervision, M.K.K.

Funding: This research received no external funding.

Conflicts of Interest: The authors declare no conflict of interest.

References

1. Aaboud, M.; Aad, G.; Abbott, B.; Abdallah, J.; Abdinov, O.; Abeloos, B.; Abidi, S.H.; AbouZeid, O.S.; Abraham, N.L.; Abramowicz, H.; et al. Measurement of multi-particle azimuthal correlations in pp, p + Pb and low-multiplicity Pb + Pb collisions with the ATLAS detector. *Eur. Phys. J. C Part Fields* **2017**, *77*, 428. [CrossRef] [PubMed]
2. Porayath, C.; Salim, A.; Veedu, A.P.; Babu, P.; Nair, B.; Madhavan, A.; Pal, S. Characterization of the bacteriophages binding to human matrix molecules. *Int. J. Biol. Macromol.* **2018**, *110*, 608–615. [CrossRef] [PubMed]
3. Chatzipanagi, A.; Frontini, F.; Virtuani, A. BIPV-temp: A demonstrative Building Integrated Photovoltaic installation. *Appl. Energy* **2016**, *173*, 1–12. [CrossRef]
4. Luo, Y.; Zhang, L.; Liu, Z.; Wang, Y.; Meng, F.; Wu, J. Thermal performance evaluation of an active building integrated photovoltaic thermoelectric wall system. *Appl. Energy* **2016**, *177*, 25–39. [CrossRef]
5. Gautam, K.R.; Andresen, G.B. Performance comparison of building-integrated combined photovoltaic thermal solar collectors (BiPVT) with other building-integrated solar technologies. *Sol. Energy* **2017**, *155*, 93–102. [CrossRef]
6. Osseweijer, F.J.; Van Den Hurk, L.B.; Teunissen, E.J.; van Sark, W.G. A comparative review of building integrated photovoltaics ecosystems in selected European countries. *Renew. Sustain. Energy Rev.* **2018**, *90*, 1027–1040. [CrossRef]
7. Du, Y.; Yan, K.; Ren, Z.; Xiao, W. Designing Localized MPPT for PV Systems Using Fuzzy-Weighted Extreme Learning Machine. *Energies* **2018**, *11*, 2615. [CrossRef]
8. Farh, H.; Othman, M.; Eltamaly, A.; Al-Saud, M. Maximum Power Extraction from a Partially Shaded PV System Using an Interleaved Boost Converter. *Energies* **2018**, *11*, 2543. [CrossRef]
9. Manuel Godinho Rodrigues, E.; Godina, R.; Marzband, M.; Pouresmaeil, E. Simulation and Comparison of Mathematical Models of PV Cells with Growing Levels of Complexity. *Energies* **2018**, *11*, 2902. [CrossRef]
10. Nižetić, S.; Papadopoulos, A.M.; Tina, G.M.; Rosa-Clot, M. Hybrid energy scenarios-for residential applications based on the heat pump split air-conditioning units for operation in the Mediterranean climate conditions. *Energy Build.* **2017**, *140*, 110–120. [CrossRef]
11. Kaartokallio, T.; Utge, S.; Klemetti, M.M.; Paananen, J.; Pulkki, K.; Romppanen, J.; Tikkanen, I.; Heinonen, S.; Kajantie, E.; Kere, J.; et al. Fetal Microsatellite in the Heme Oxygenase 1 Promoter Is Associated With Severe and Early-Onset Preeclampsia. *Hypertension* **2018**, *71*, 95–102. [CrossRef] [PubMed]
12. Alajmi, B.N.; Ahmed, K.H.; Finney, S.J.; Williams, B.W. A Maximum Power Point Tracking Technique for Partially Shaded Photovoltaic Systems in Microgrids. *IEEE Trans. Ind. Electron.* **2013**, *60*, 1596–1606. [CrossRef]

13. Daraban, S.; Petreus, D.; Morel, C. A novel MPPT (maximum power point tracking) algorithm based on a modified genetic algorithm specialized on tracking the global maximum power point in photovoltaic systems affected by partial shading. *Energy* **2014**, *74*, 374–388. [CrossRef]
14. Dileep, G.; Singh, S.N. Maximum power point tracking of solar photovoltaic system using modified perturbation and observation method. *Renew. Sustain. Energy Rev.* **2015**, *50*, 109–129. [CrossRef]
15. Saravanan, S.; Babu, N.R. Maximum power point tracking algorithms for photovoltaic system—A review. *Renew. Sustain. Energy Rev.* **2016**, *57*, 192–204. [CrossRef]
16. Verma, D.; Nema, S.; Shandilya, A.M.; Dash, S.K. Maximum power point tracking (MPPT) techniques: Recapitulation in solar photovoltaic systems. *Renew. Sustain. Energy Rev.* **2016**, *54*, 1018–1034. [CrossRef]
17. Abu Eldahab, Y.E.; Saad, N.H.; Zekry, A. Enhancing the tracking techniques for the global maximum power point under partial shading conditions. *Renew. Sustain. Energy Rev.* **2017**, *73*, 1173–1183. [CrossRef]
18. Ayop, R.; Tan, C.W. Design of boost converter based on maximum power point resistance for photovoltaic applications. *Sol. Energy* **2018**, *160*, 322–335. [CrossRef]
19. Shen, C.-L.; Tsai, C.-T. Double-Linear Approximation Algorithm to Achieve Maximum-Power-Point Tracking for Photovoltaic Arrays. *Energies* **2012**, *5*, 1982–1997. [CrossRef]
20. Andrean, V.; Chang, P.; Lian, K. A Review and New Problems Discovery of Four Simple Decentralized Maximum Power Point Tracking Algorithms—Perturb and Observe, Incremental Conductance, Golden Section Search, and Newton's Quadratic Interpolation. *Energies* **2018**, *11*, 2966. [CrossRef]
21. Chen, P.-Y.; Chao, K.-H.; Wu, Z.-Y. An Optimal Collocation Strategy for the Key Components of Compact Photovoltaic Power Generation Systems. *Energies* **2018**, *11*, 2523. [CrossRef]
22. Pei, T.; Hao, X.; Gu, Q. A Novel Global Maximum Power Point Tracking Strategy Based on Modified Flower Pollination Algorithm for Photovoltaic Systems under Non-Uniform Irradiation and Temperature Conditions. *Energies* **2018**, *11*, 2708. [CrossRef]
23. Kofinas, P.; Dounis, A.I.; Papadakis, G.; Assimakopoulos, M.N. An Intelligent MPPT controller based on direct neural control for partially shaded PV system. *Energy Build.* **2015**, *90*, 51–64. [CrossRef]
24. Messalti, S.; Harrag, A.; Loukriz, A. A new variable step size neural networks MPPT controller: Review, simulation and hardware implementation. *Renew. Sustain. Energy Rev.* **2017**, *68*, 221–233. [CrossRef]
25. Shahid, H.; Kamran, M.; Mehmood, Z.; Saleem, M.Y.; Mudassar, M.; Haider, K. Implementation of the novel temperature controller and incremental conductance MPPT algorithm for indoor photovoltaic system. *Sol. Energy* **2018**, *163*, 235–242. [CrossRef]
26. Jordehi, A.R. Maximum power point tracking in photovoltaic (PV) systems: A review of different approaches. *Renew. Sustain. Energy Rev.* **2016**, *65*, 1127–1138. [CrossRef]
27. Ishaque, K.; Salam, Z.; Lauss, G. The performance of perturb and observe and incremental conductance maximum power point tracking method under dynamic weather conditions. *Appl. Energy* **2014**, *119*, 228–236. [CrossRef]
28. Bradai, R.; Boukenoui, R.; Kheldoun, A.; Salhi, H.; Ghanes, M.; Barbot, J.P.; Mellit, A. Experimental assessment of new fast MPPT algorithm for PV systems under non-uniform irradiance conditions. *Appl. Energy* **2017**, *199*, 416–429. [CrossRef]
29. Mamarelis, E.; Petrone, G.; Spagnuolo, G. A two-steps algorithm improving the P&O steady state MPPT efficiency. *Appl. Energy* **2014**, *113*, 414–421.
30. Salas, V.; Olias, E.; Lazaro, A.; Barrado, A. Evaluation of a new maximum power point tracker (MPPT) applied to the photovoltaic stand-alone systems. *Sol. Energy Mater. Sol. Cells* **2005**, *87*, 807–815. [CrossRef]
31. Soulatiantork, P. Performance comparison of a two PV module experimental setup using a modified MPPT algorithm under real outdoor conditions. *Sol. Energy* **2018**, *169*, 401–410. [CrossRef]
32. Boico, F.; Lehman, B. Multiple-input Maximum Power Point Tracking algorithm for solar panels with reduced sensing circuitry for portable applications. *Sol. Energy* **2012**, *86*, 463–475. [CrossRef]
33. Yahyaoui, I.; Chaabene, M.; Tadeo, F. Evaluation of Maximum Power Point Tracking algorithm for off-grid photovoltaic pumping. *Sustain. Cities Soc.* **2016**, *25*, 65–73. [CrossRef]
34. Bube, R.H. *Photovoltaic Materials*; Series on Properties of Semiconductor Materials; Distributed by World Scientific. x; Imperial College Press: London, UK; River Edge, NJ, USA, 1998; 281p.

35. Zaki Diab, A.A.; Rezk, H. Global MPPT based on flower pollination and differential evolution algorithms to mitigate partial shading in building integrated PV system. *Sol. Energy* **2017**, *157*, 171–186. [CrossRef]
36. Batarseh, M.G.; Za'ter, M.E. Hybrid maximum power point tracking techniques: A comparative survey, suggested classification and uninvestigated combinations. *Sol. Energy* **2018**, *169*, 535–555. [CrossRef]
37. Belhachat, F.; Larbes, C. A review of global maximum power point tracking techniques of photovoltaic system under partial shading conditions. *Renew. Sustain. Energy Rev.* **2018**, *92*, 513–553. [CrossRef]
38. Danandeh, M.A. Comparative and comprehensive review of maximum power point tracking methods for PV cells. *Renew. Sustain. Energy Rev.* **2018**, *82*, 2743–2767. [CrossRef]
39. Li, X.; Wen, H.; Chu, G.; Hu, Y.; Jiang, L. A novel power-increment based GMPPT algorithm for PV arrays under partial shading conditions. *Sol. Energy* **2018**, *169*, 353–361. [CrossRef]
40. Noguchi, T.; Togashi, S.; Nakamoto, R. Short-current pulse-based maximum-power-point tracking method for multiple photovoltaic-and-converter module system. *IEEE Trans. Ind. Electron.* **2002**, *49*, 217–223. [CrossRef]
41. Labar, H.; Kelaiaia, M.S. Real time partial shading detection and global maximum power point tracking applied to outdoor PV panel boost converter. *Energy Convers. Manag.* **2018**, *171*, 1246–1254. [CrossRef]
42. Alik, R.; Jusoh, A. Modified Perturb and Observe (P&O) with checking algorithm under various solar irradiation. *Sol. Energy* **2017**, *148*, 128–139.
43. Chihchiang, H.; Jongrong, L.; Chihming, S. Implementation of a DSP-controlled photovoltaic system with peak power tracking. *IEEE Trans. Ind. Electron.* **1998**, *45*, 99–107. [CrossRef]
44. Sivakumar, P.; Kader, A.A.; Kaliavaradhan, Y.; Arutchelvi, M. Analysis and enhancement of PV efficiency with incremental conductance MPPT technique under non-linear loading conditions. *Renew. Energy* **2015**, *81*, 543–550. [CrossRef]
45. Lasheen, M.; Rahman, A.K.; Abdel-Salam, M.; Ookawara, S. Performance Enhancement of Constant Voltage Based MPPT for Photovoltaic Applications Using Genetic Algorithm. *Energy Procedia* **2016**, *100*, 217–222. [CrossRef]
46. Kislovski, A.S.; Redl, R. Maximum-power-tracking using positive feedback. In Proceedings of the 25th Annual IEEE Power Electronics Specialists Conference, Taipei, Taiwan, 20–25 June 1994.
47. Kwan, T.H.; Wu, X. Maximum power point tracking using a variable antecedent fuzzy logic controller. *Sol. Energy* **2016**, *137*, 189–200. [CrossRef]
48. Soufi, Y.; Bechouat, M.; Kahla, S. Fuzzy-PSO controller design for maximum power point tracking in photovoltaic system. *Int. J. Hydrogen Energy* **2017**, *42*, 8680–8688. [CrossRef]
49. Ishaque, K.; Salam, Z. A Deterministic Particle Swarm Optimization Maximum Power Point Tracker for Photovoltaic System Under Partial Shading Condition. *IEEE Trans. Ind. Electron.* **2013**, *60*, 3195–3206. [CrossRef]
50. Chao, K.-H.; Lin, Y.-S.; Lai, U.-D. Improved particle swarm optimization for maximum power point tracking in photovoltaic module arrays. *Appl. Energy* **2015**, *158*, 609–618. [CrossRef]
51. Dileep, G.; Singh, S.N. An improved particle swarm optimization based maximum power point tracking algorithm for PV system operating under partial shading conditions. *Sol. Energy* **2017**, *158*, 1006–1015. [CrossRef]
52. Mirhassani, S.M.; Golroodbari, S.Z.; Golroodbari, S.M.; Mekhilef, S. An improved particle swarm optimization based maximum power point tracking strategy with variable sampling time. *Int. J. Electr. Power Energy Syst.* **2015**, *64*, 761–770. [CrossRef]
53. Fathabadi, H. Novel fast dynamic MPPT (maximum power point tracking) technique with the capability of very high accurate power tracking. *Energy* **2016**, *94*, 466–475. [CrossRef]
54. Su, H.C.; Chen, Z.; Liu, J.; Chen, X.F. Photovoltaic System MPPT Control Based on Optimum Gradient Method of Open-circuit Voltage and Short-circuit Current. *Electr. Switch.* **2010**, *48*, 17–20.
55. Chen, X.; Wang, A.; Hu, Y.; Lu, Z.; Nie, X. Research of Maximum Power Point Tracking Algorithms of Photovoltaic Arrays Based on the Improved Disturbance of Observer Method. *Electr. Drive* **2017**, *47*, 66–69.
56. Esram, T.; Chapman, P.L. Comparison of photovoltaic array maximum power point tracking techniques. *IEEE Trans. Energy Convers.* **2007**, *22*, 439–449. [CrossRef]

57. Sullivan, C.R.; Awerbuch, J.J.; Latham, A.M. Decrease in Photovoltaic Power Output from Ripple: Simple General Calculation and the Effect of Partial Shading. *IEEE Trans. Power Electron.* **2013**, *28*, 740–747. [CrossRef]
58. Abbott, B.P.; Abbott, R.; Abbott, T.D.; Acernese, F.; Ackley, K.; Adams, C.; Adams, T.; Addesso, P.; Adhikari, R.X.; Adya, V.B.; Affeldt, C. GW170817: Observation of Gravitational Waves from a Binary Neutron Star Inspiral. *Phys. Rev. Lett.* **2017**, *119*, 161101. [CrossRef]

energies

MDPI

Article

Data-Driven Evaluation of Residential HVAC System Efficiency Using Energy and Environmental Data

Huyen Do [1,2] and Kristen S. Cetin [1,*]

[1] Department of Civil Construction and Environmental Engineering, Iowa State University, Ames, IA 50011, USA; huyendo@iastate.edu

[2] Faculty of Project Management, The University of Danang-University of Science and Technology, Danang 50000, Vietnam

* Correspondence: kcetin@iastate.edu; Tel.: +1-515-294-8180

Received: 2 December 2018; Accepted: 4 January 2019; Published: 8 January 2019

Abstract: In the U.S., the heating, ventilation, and air conditioning (HVAC) system is generally the largest electricity-consuming end-use in a residential building. However, homeowners are less likely to have their HVAC system serviced regularly, thus inefficiencies in operation are also more likely to occur. To address this challenge, this research works towards a non-intrusive data-driven assessment method using building assessors' data, HVAC electricity demand data, and outdoor environmental data. Building assessors' data is first used to estimate the HVAC system size, then estimate the electricity demand curve of the HVAC system. A comparison of the proposed electricity demand curve development method demonstrates strong agreement with physics-based HVAC model results. An HVAC efficiency rating is then proposed, which compares the model-predicted and actual performance data to define whether an HVAC system is operating as expected. As a case study, detailed data for 39 occupied, conditioned residential buildings in Austin, Texas, was used demonstrating the identification of the presence of potential HVAC inefficiencies. The results prove beneficial for utilities to help target residential HVAC systems in need of service or energy efficiency upgrades, as well as for homeowners as a continuous assessment tool for HVAC performance.

Keywords: HVAC demand; prediction; energy efficiency; residential buildings

1. Introduction

Residential building electricity consumption makes up approximately 40% of total electricity use in the U.S. [1,2]. Many factors impact the electricity use in residential buildings, including weather conditions, building size, building characteristics such as window and building envelope properties, air infiltration and ventilation, occupant behavior, and occupant-dependent end-uses, among others [3,4]. However, in the U.S., the heating, ventilation, and air conditioning (HVAC) system is among the largest electricity-consuming end-use in a home [5]; its electricity demand is associated with the amount of heat gains and losses in a building, as well as its size, efficiency, thermostat setpoints, and the local environmental conditions in which it operates.

The completion of a home energy audit or HVAC system tune-up is among the most common methods used to assess residential HVAC system energy efficiency and performance [6] and are often completed by a service technician who comes to the residence in person for an on-site evaluation of HVAC operations. Based on the results, recommendations of how to improve inefficiencies of the HVAC system are then made to the homeowner. This is often done by or in collaboration with programs in many utility companies that provide incentives and rebates for more energy-efficient HVAC systems or other upgraded components [7].

However, the main challenge when achieving efficiency improvements for HVAC systems in residential buildings is the periodic occurrence of inefficiencies, i.e., faults, that still allow the HVAC

system to run, but in a less efficient way. These faults likely go undetected, until either the system is serviced, or the inefficiency is corrected, or until a more catastrophic failure occurs and the system is replaced. However, unlike commercial systems, most homeowners do not have their HVAC system regularly serviced [8,9], and rather, they service their system when something occurs that renders the system non-operational. As a result, survey results indicate that a large number of residential HVAC systems are considered to be operating in a faulty state [9]. This typically impacts both the electricity demand (kW) associated with the operation of the system, as well as the cycle length (minutes) associated with the system's on–off operation. Therefore, to overcome the barrier of requiring a visit from an HVAC technician and homeowner time to assess the efficiency of operation of a system, it is beneficial to have a less intrusive and more frequent method to evaluate the operational efficiency of an HVAC system in a residential building.

The body of literature in fault detection of HVAC systems focuses mostly on commercial buildings, particularly given that a continuous service model is more common for more expensive commercial HVAC systems. However, some previous research efforts have explored the possibilities of fault detection and diagnostics for packaged unitary systems, which include mini split systems for residential buildings, and roof top units (RTUs) for small commercial buildings [10–12]. However, most of the literature has focused on roof top units for light commercial buildings. A limited number have focused specifically on residential heat pumps and mini split systems [10,12,13]. Common faults cited in the literature include high or low refrigerant charge, and airflow restrictions to the condenser/evaporator; others include refrigerant line restrictions, expansion valve failure, the presence of non-condensable, short cycling, and/or sensor failures [10,12,13].

To determine the occurrence of faults, these studies measured a range of variables, including environmental parameters (e.g., indoor and outdoor air temperature, dew point, relative humidity), and HVAC system-dependent parameters (e.g., refrigerant flow rate, pressure, and temperature, power, and air flow rate and pressure). These parameters are measured for use in determining HVAC efficiency and/or capacity. However, the collection of data on these variables requires additional sensors be placed for data collection in a home. Most methods have not considered the use of energy data to assess HVAC performance.

Due to the development and implementation of many state-of-the-art technologies such as smart meters and home energy management systems [14], as well as the now ubiquitous availability of the internet and cloud storage, computing, obtaining, storing, and processing data related to the energy performance of residential systems, while still challenging, has become more accessible in recent years. This availability has also benefited from the wider spread and commercialization of technologies that can reliably collect energy/electricity data [15]. Data can be collected at different frequencies depending on the technology utilized for data collection. Frequencies vary from monthly, hourly, 15-min, or 1-min intervals, with some technologies providing data at the second and sub-second level. Other data to support the evaluation of the operation of an HVAC system, including indoor environmental conditions, is also more easily collected, stored, and accessed from smart thermostats. Smart thermostat and/or energy consumption data, however, while typically available to an individual homeowner, is not typically publicly available for large-scale analysis. Utility companies have access to their customers' energy data, or service providers and/or manufacturers, also have or could be granted access to such data by a homeowner. Weather data continues to be available from various public sources, such as ground-based weather stations (GBWS). Additionally, significant improvements have also been made in availability of satellite-based weather data available in more locations than GWBS (e.g., [16]). Finally, assessors' data which provides basic residential building characteristics, is publicly available information in the U.S.

This research, thus, focuses on the development of a methodology that uses assessor's data, energy data, and weather data to, first, predict residential HVAC electricity demands as a function of environmental conditions. This is ultimately used to assess the efficiency of operation of the HVAC system itself, independent of the influence that occupants may have on HVAC operation.

More specifically, when looking at the information that can be extracted from an electricity use signal of an HVAC system, the electricity demand (kW) when the system is on depends only on the characteristics of the HVAC system itself and the environmental conditions in which it is operating. Runtime values and electricity consumption also depend on the characteristics of the HVAC system, but are also dependent on the interior temperature setpoints set by occupants, and occupant behavior. Therefore, the focus of this work is on electricity demand as a proxy for evaluation of efficiency.

This research works towards an assessment method that can be used to assess in real-time, the energy efficiency of residential split, all-air HVAC systems without the need for more traditional methods such as costlier time intensive, and intrusive energy audits. The focus of this work is on developing a method which requires minimal to no information or engagement from the homeowner, and strictly uses data that can be obtained from energy use data and assessors' data. This is motivated by the needs and interests from utility companies which typically provide incentive programs for motivating energy efficiency upgrades of residential HVAC systems. Feedback received from several utilities has indicated that a methodology to better target residential customers in need of HVAC servicing or efficiency upgrades is needed using easily accessible datasets, thus the development of this methodology. In addition, the proposed method could enhance the economic efficiency with the appropriate HVAC energy efficiency upgrades and energy retrofit strategies [17,18].

This research is organized into three main sections, including the methodology, results and conclusions, limitations and future work. The methodology for estimating residential household level HVAC electricity demand of a large dataset of homes and for evaluation of residential HVAC performance efficiency is proposed. A case study then uses detailed energy and weather data, and building assessor's data for 39 occupied, conditioned residential buildings in Austin, Texas with the proposed method to determine HVAC efficiency ratings, demonstrating the identification of the presence of potential HVAC inefficiencies using the proposed method. The results section then shows the HVAC efficiency rating that compares the model-predicted and actual performance data to define whether an HVAC system is operating as expected. This result will help target HVAC systems in homes in need of service, energy efficiency upgrades, and be a continuous assessment tool for HVAC performance.

2. Methods

To predict the level of efficiency of operation of a dataset of residential building HVAC systems, the following methodology is developed and followed in this work. This includes several overall stages. First (Figure 1) is the utilization of data collected on basic building characteristics to determine the most probable size of the HVAC system. This is among the more challenging features to estimate without detailed system-level data, as HVAC system data is not typically available except through an on-site energy audit or service call. Next is the development of a model to predict the HVAC system electricity demand as a function of environmental conditions. The final stage is the energy efficiency evaluation of the HVAC systems (Figure 2).

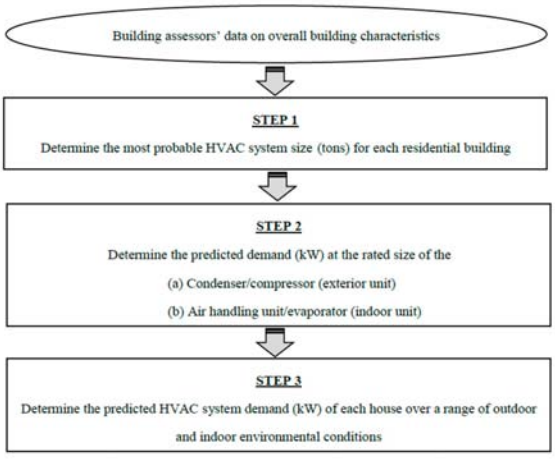

Figure 1. Methodology for estimating residential household level heating, ventilation, and air conditioning (HVAC) system electricity demand of a large dataset of homes.

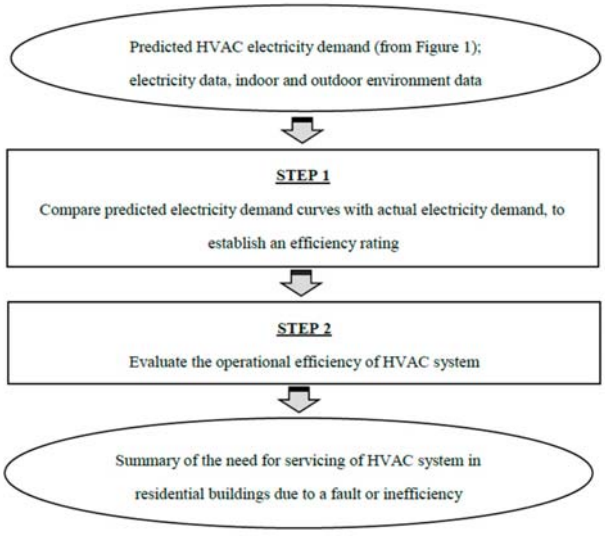

Figure 2. Methodology for evaluation of residential HVAC performance efficiency.

2.1. Prediction of Residential HVAC Demand

2.1.1. Step 1—Determine the Most Probable HVAC System Size

To determine the best estimates of residential heating and cooling loads for the right sizing of HVAC equipment, in the U.S. it is generally recommended to use calculation methods in Manual J from the Air Conditioning Contractors of America (ACCA) [19]. This method utilizes information on many aspects of a building's thermal characteristics such as wall, floor, roof, windows, and door types, basement characteristics, and expected indoor and outdoor environmental conditions, among other details. [19,20]. However, the significant number of inputs and information needed to complete the Manual J calculations are not readily available for a utility company or other party attempting to assess HVAC performance of a large number of homes, without a detailed audit of the building

stock. Assessor's data (e.g., [21,22]) generally includes information such as the age of house, year of occurrence and type of any major improvement, total conditioned area, building style, exterior wall material, number of total rooms, bedrooms, and bathrooms, fuel type, HVAC system type, presence of a basement, etc. In the U.S., generally assessor's data is publicly-available information, since it is used for tax purposes, however the level of availability and ease of accessibility varies by location. Thus, assuming there is only publicly-available assessor's data as a worst-case scenario, this research proposes a method that uses this limited data to determine the most probable HVAC size. It is noted, however, if homeowners can provide the size of the HVAC system installed, or the system sizing can otherwise be determined from other data sources, this step can be skipped.

Assuming this is not the case, several different methods are explored. For the first method, an analysis of the 72 homes in the Austin, TX, area where home area and HVAC size (Figure 3a) is available from the utilized dataset. This indicates that the average size of the HVAC system per square meter of conditioned floor area is approximately 0.016 (tons/m^2). The average size of the HVAC system per conditioned area (ton/m^2) in the other datasets in Cedar Falls, Iowa and (Energy Conservation Audit and Disclosure) ECAD program are close, at 0.017 and 0.020, respectively (Figure 3b,c).

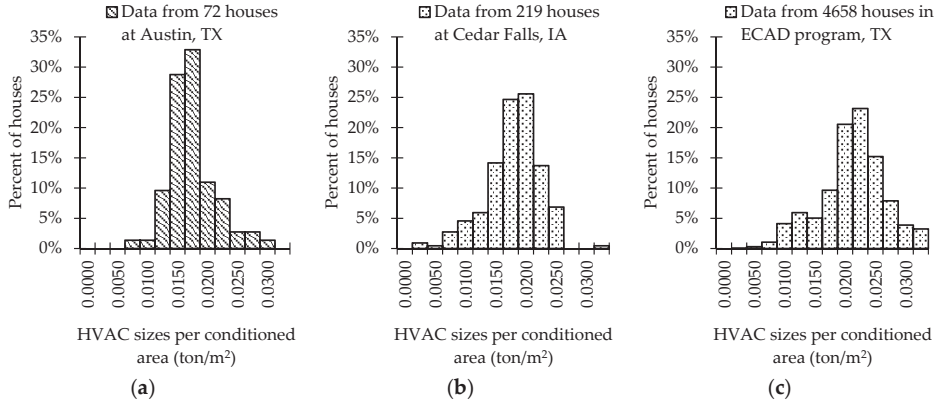

Figure 3. HVAC sizes per conditioned area (m^2) for houses in three locations: (**a**) the utilized Austin, Texas dataset; (**b**) Cedar Falls, Iowa dataset, and (**c**) ECAD program in Texas.

The distribution of HVAC sizes per unit area indicates there is some uncertainty associated with this estimate; however, of the potential predictor variables available in assessor's data, the conditioned area was the most significant (p-value = 0.0007×10^{-5}, $R^2 = 0.678$). The second method considered is an industry rule of thumb, cited in a number of publications (e.g., [23]), where the HVAC size (S, in tons) is approximated as follows (Equation (1)), where A is conditioned area (m^2):

$$S = \frac{A \times 0.093}{400} - 1 \quad (1)$$

The last method depends on the U.S. climate region in which a system is located, based on the Residential Energy Consumption Survey (Figure 4, Table 1) [24,25]. Houses in Austin are in Zone 1.

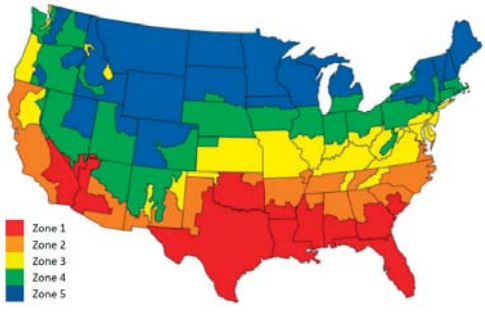

Figure 4. U.S climates zone divisions from the U.S. EIA (Energy Information Administration) Residential Energy Consumption Survey (RECS) [25].

Table 1. Size of HVAC system based on home size (m^2) by RECS climate zone [24].

Size (Tons)	Zone 1	Zone 2	Zone 3	Zone 4	Zone 5
1.5	56–84	56–88	56–93	65–98	65–102
2	84–111	88–116	93–121	98–125	102–130
2.5	112–138	116–144	121–149	126–149	130–153
3	139–167	144–172	149–177	149–186	153–195
3.5	167–195	172–200	177–204	186–209	195–214
4	195–223	200–232	204–242	209–251	214–251
5	223–279	232–288	242–297	251–307	251–307

2.1.2. Step 2—Determine the Predicted HVAC Capacity at the Rated Size

The sizing and efficiency rating of the HVAC system must then be converted to a cooling capacity and power demand at design conditions. The rated capacity of an HVAC system is based on the AHRI (Air-Conditioning, Heating, and Refrigeration Institute) design conditions (Table 2) [26]. While there are a range of rating conditions used to evaluate parameters such as energy efficiency ratio (EER) and coefficient of performance (COP), which are then used to calculate the seasonal energy efficiency ratio (SEER) and/or heating seasonal performance factor (HSPF), of these conditions, two standard rating conditions are generally accepted by industry to be used for evaluating HVAC capacity. For the cooling season, this rated value is associated with an outdoor drybulb temperature of 35 °C; and for the heating season, the outdoor drybulb temperature of 8.3 °C is used.

Table 2. Air-Conditioning, Heating, and Refrigeration Institute (AHRI) design conditions for a residential HVAC system [26].

AHRI Design Conditions	Air Entering Indoor Units		Air Entering Outdoor Units (°C)	
	Drybulb (°C)	Wetbulb (°C)	Drybulb (°C)	Wetbulb (°C)
Cooling	26.7	19.4	35.0	23.9
Heating	21.1	15.6	8.3	6.1

A SEER value must also be determined or assumed. If available, the HVAC system model numbers can provide information on the efficiency of the system [27]. However, this data is not always available, particularly in assessor's data. While there are efforts to require energy benchmarking and/or energy audits to be performed for the residential building stock, such as the ECAD program in Austin, TX [28], there are very few locations in the U.S. that require such information to be gathered for residential buildings. The U.S. Department of Energy currently requires a minimum efficiency of SEER 13 or 14 for residential systems, depending on the location and climate zone where the system is installed [29]. However, this does not mean that the HVAC system being evaluated using this method

will be at this level of efficiency. Previously, lower SEER ratings have been required, thus it is likely that older systems will also have a lower SEER value. For the purpose of development of the proposed methodology, in the development of the predicted HVAC electricity demand curve, it can be assumed that the SEER value is the current code-required value, as the purpose of the results of this analysis method is to determine if a system is less efficient than is code minimum (i.e., code-required, properly functioning system). The implications of this are, if the system under evaluation is less than a SEER 13/14, the results of the use of the developed method will indicate the system is less efficient than predicted, regardless of if an operational inefficiency or fault exists. This aligns with the purpose of the proposed method to identify if the system is less efficient than desired, to indicate that there are opportunities for improvement as compared to code minimum.

Using the determined size (S, tons) from the previous step and SEER value, the HVAC capacity ($\dot{Q}_{total,rated}$, kW) is estimated in Equation (2), based on the relationship between SEER and EER established by Wassmer [30] and widely used, including in residential building energy simulation protocols [31]:

$$\dot{Q}_{total,rated} = S\frac{12}{(1.12 \times SEER - 0.02 \times SEER^2)} \quad (2)$$

In addition, the fan's electricity demand must also be predicted. The indoor fan power demand ($\dot{P}_{fan}$, kW) is determined using 0.773 kW per m^3/s with the flow rate of 0.189 m^3/s per ton [32]. The 0.773 kW per m^3/s is the AHRI default value for fan efficiency if the information about the indoor fan is unknown in ANSI (American National Standards Institute)/AHRI (Air Conditioning, Heating, and Refrigeration Institute) Standard 210/240 [32]. The fan is assumed to be a single stage fan. The rated energy input ratio (EIR) must also be determined and is defined as the inverse of the COP.

2.1.3. Step 3—Determine the Predicted HVAC System Power Demand (kW) Over a Range of Outdoor and Indoor Weather Conditions

Using these design conditions, a set of empirical equations are used to relate the estimated capacity at design conditions to an estimated electric power demand over a range of environmental conditions. These equations follow the format of the direct expansion (DX) model utilized in EnergyPlus 9.0.1 [33] to simulate DX equipment. This includes several biquadratic functions, with the values of the dependent variables being the design conditions listed in Table 2, where T_{ewb} and T_{odb} are the entering wet bulb temperature and outdoor drybulb temperature, respectively. These equations take the following form (Equation (3)):

$$y = a + b \times T_{ewb} + c \times T_{ewb}^2 + d \times T_{odb} + e \times T_{odb}^2 + f \times T_{odb} \times T_{ewb} \quad (3)$$

The gross power demand ($\dot{P}_{gross}$, kW) is calculated as a function of the energy input ratio *(EIR)* and the total cooling and/or heating capacity ($\dot{Q}_{total}$, kW) (Equation (4)) [24]. By combining the gross power demand ($\dot{P}_{gross}$, *kW*) and the calculated indoor fan capacity ($\dot{P}_{fan}$, kW), the net power demand, i.e., the predicted HVAC system demand, ($\dot{P}_{net}$, kW) is determined. The values of *EIR* and $\dot{Q}_{total}$ are calculated using Equations (5) and (6), where $EIR_{f(T)}$ and $\dot{Q}_{f(T)}$ are the normalized energy input ratio curve and the normalized total cooling and/or heating capacity curve that are calculated as a function of T_{ewb} and T_{odb} in the form of Equation (3). These curves allow for temperature-based adjustments to the final calculated *EIR* and $\dot{Q}_{total}$ values from the rated values. The flow fraction and runtime fraction are assumed to be 1.

$$\dot{P}_{net} = \left(EIR \times \dot{Q}_{total}\right)_{gross} + \dot{P}_{fan} \quad (4)$$

$$EIR = EIR_{rated} \times EIR_{f(T)} \quad (5)$$

$$\dot{Q}_{total} = \dot{Q}_{total,rated} \times \dot{Q}_{f(T)} \quad (6)$$

The values of the coefficients (a through f) in the equations for $EIR_{f(T)}$ and $\dot{Q}_{f(T)}$ are determined based on laboratory-collected data from the testing of a range of residential HVAC systems, and are summarized in Table 3. These values assume the HVAC system is a single-stage, single-zone air conditioning or heat pump system.

Table 3. Curve coefficients of the energy input ratio ($EIR_{f(T)}$) and total capacity ($\dot{Q}_{f(T)}$) [26].

Coefficients	Air Conditioner (Cooling)		Heat Pump (Cooling)		Heat Pump (Heating)	
	Energy Input Ratio	Total Capacity	Energy Input Ratio	Total Capacity	Energy Input Ratio	Total Capacity
a	−3.10715	4.77794	−3.13275	4.78154	−2.53999	4.40420
b	0.20088	−0.16405	0.19920	−0.16377	−0.01249	−0.00030
c	−0.00190	0.00172	−0.00189	0.00172	0.00026	−0.00002
d	−0.03095	0.00333	−0.02442	0.00244	−0.02163	0.00596
e	0.00039	−0.00003	0.00033	−0.00002	0.00025	0.00009
f	−0.00026	−0.00024	−0.00026	−0.00024	−0.00039	−0.00001

2.2. Evaluation of Residential HVAC Efficiency

2.2.1. Step 1—Compare Predicted Electricity Demand with Actual Electricity Demand, to Establish an Efficiency Rating

To evaluate the efficiency of a particular system, the final predicted and actual (measured) demand of HVAC system are compared. An efficiency rating of an HVAC system is determined, represented as the ratio between actual (kW) and predicted (kW) values (Equation (7)). Using this ratio, if the actual demand is higher than predicted, the rating will be greater than 1; if the actual demand is lower than predicted, the rating will be less than one.

$$\text{HVAC efficiency rating} = \frac{\text{HVAC Demand}_{\text{ actual}}}{\text{HVAC Demand}_{\text{ predicted}}} \quad (7)$$

2.2.2. Step 2—Evaluate the Operational Efficiency of the HVAC System

When comparing actual and predicted values, two methods of comparison may be used. The actual performance may be compared to the expected performance based on the age of the home, expected age of the HVAC system and corresponding minimum efficiency of the required HVAC system at the time of construction. This comparison's results would be a reflection on what the system operational characteristics should look like at a minimum, based on the code minimum performance specifications. Second, the actual performance could be compared to the predicted performance based on the rated size and SEER value of the system. This comparison would be a reflection of the overall system health and whether or not it needs to be serviced due to a fault or inefficiency.

If the HVAC system under consideration is operating as expected, then the electricity demand of the system should be similar to that of the predicted value. If the system is not functioning properly or the system is less (or more) efficient than expected, then the system will have a higher or lower electricity demand for a given set of environmental conditions, depending on the type of fault or inefficiency present. The thresholds above and below what is deemed to be acceptable performance are next determined based on the sensitivity of the curve development to faults and inefficiencies.

3. Results and Discussion

To assess the ability of the proposed methodology to identify the relative efficiency or inefficiency of an HVAC system, first a detailed HVAC modeling program air conditioning/heat pump (ACHP) [34], is used to predict the electricity demand of a residential HVAC system of a real home, which is

then compared to the proposed method-predicted values. The home is a 10-year-old single-family house (111 m^2) serviced by a SEER 13, 2.5 ton residential HVAC heat pump split-system with 410 A refrigerant [34]. The system electricity demand is modeled under a range of outdoor temperature conditions (18.3 °C to 40.5 °C). In Figure 5, the black line represents the HVAC model-predicted demand from ACHP (black line), which is compared to the predicted demand curve using the proposed method (blue-dashed line). The model-predicted values and the theoretical demand values are nearly identical across the range of environmental conditions considered. Based on this analysis, the proposed method provides a generally good agreement with physics-based model predictions of demand.

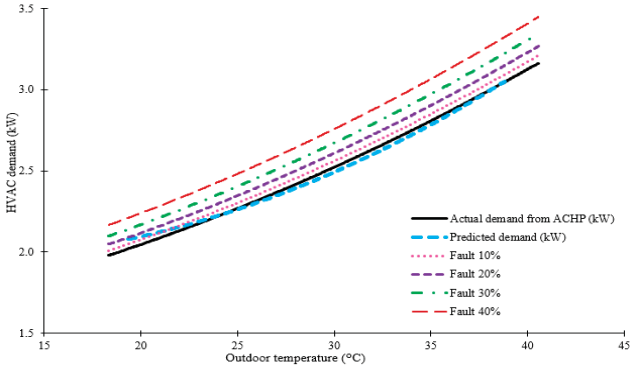

Figure 5. HVAC demand curves using the air conditioning/heat pump (ACHP) model and predicted data for a properly functioning, and faulty HVAC system (Note: The fault indicated is due to reduced HVAC condenser airflow).

To determine the threshold efficiency ratio above and below which an HVAC system should evaluated to be inefficient or faulty, the impact of faults and inefficiencies is evaluated using ACHP. For faults, condenser airflow rate reduction, a common inefficiency, is modeled in ACHP, at a range of 10% to 40% airflow reduction. As shown in Figure 5, the more condenser airflow reduction, the higher HVAC demand, which is consistent with other research findings. The HVAC system efficiency rating in these cases are 1.02, 1.03, 1.09, and 1.12, respectively, for the faults of 10%, 20%, 30%, and 40%. Other literature has demonstrated that other common faults such as high- and low-refrigerant charge, also increase or decrease HVAC demand at similar levels [9,35]. Considering such fault types, electricity demand values that are both higher and lower than the predicted temperature–electricity demand curve values may be due to a fault or an inefficiency. Based on these results, and accounting for inherent uncertainties, lower and upper thresholds of 0.9 and 1.1 were chosen to be the threshold values between which an acceptable system operation is defined. Within this range, a system is considered to be within normal operational range. Outside this range could indicate either a less efficient system or a fault in the system, either of which could be interpreted as in need of attention of a utility company that is hoping to target customers who would benefit in terms of efficiency from an HVAC system upgrade or service.

Next, to mimic how a utility or service provider might use this method to identify homes with inefficient systems, this method is then used with a dataset of HVAC electricity demand of real homes, to understand if faults and inefficiencies appear to be present and detectable using the proposed method with real data. Electricity demand data for 39 residential HVAC systems was collected from Austin, Texas from January to December of 2015 [27]. Overall, the buildings studied were 28 years old on average, with a significant range of ages, from over 80 to less than 5 years old. The conditioned areas of the buildings also varied substantially, with an average size of 210 m^2. These residential buildings can be divided into 15 main groups based on size (tons) and SEER value (Table 4), including sizes of 1.5 to 5 tons, and SEER values of 9 to 16. To develop the demand curves and assess overall efficiency of the

HVAC systems, energy audit data was used, which included the HVAC system characteristics; this is compared to the high frequency 1-min level HVAC energy data available over the observation period.

Table 4. Characteristics of grounds of residential buildings and their HVAC systems.

Group	# of Houses	Average Area (m^2)	Size (Tons)	SEER
1	1	140	3	9
2	2	104	2.5	10
3	1	367	2	12
4	2	226	2.5	13
5	1	287	3	13
6	6	165	2.5	14
7	7	190	3	14
8	5	220	3.5	14
9	5	274	4	14
10	2	159	2.5	15
11	1	166	3	15
12	2	145	3	16
13	1	221	3.5	16
14	1	200	4	17
15	2	199	3	19

To compare the average actual HVAC demands in each group, two cases are considered: first, the same size but different SEER values, and second, the same SEER value but different sizes (Figure 6a,b). In these figures, the actual HVAC demands associated with the data collected from the systems are classified into each category (as Table 4), then average values of actual HVAC demand in each group were calculated, and the trend lines as non-linear curves were created from these average values. With the same size (3 tons) system, when the SEER values increased from 13 to 16, the HVAC demand decreased approximately from 3.6 kW to 2.5 kW at design conditions. Thus, as expected, the higher SEER values had lower HVAC demands; this is consistent with the modeled data in Figure 5. The increase in size of HVAC systems from 2.5 tons to 4 tons also increased the HVAC demand, also as expected. Using this same data, the predicted curve of the HVAC system demand was developed. Some examples of predicted and actual demands of HVAC systems are represented in Figure 7. In these figures, the actual HVAC demands were created from the actual data points of 1-min interval electricity data (kW).

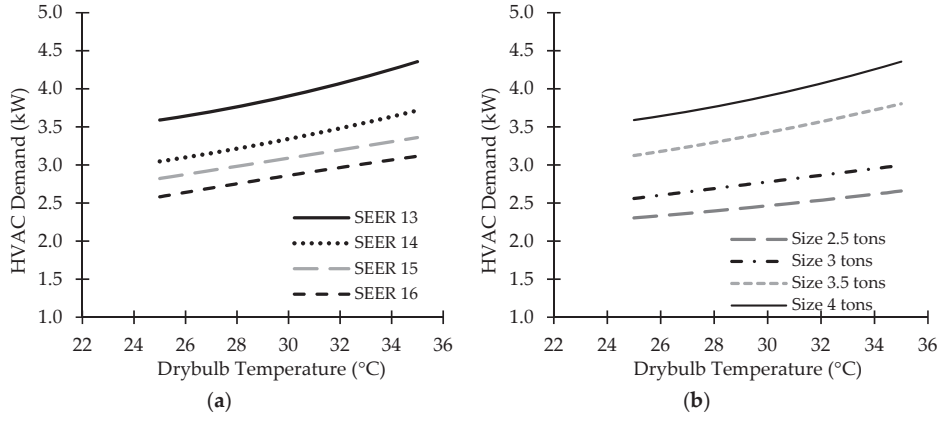

Figure 6. Comparison of two cases of HVAC demand: (**a**) same size (size 3 tons) but different seasonal energy efficiency ratio (SEER) values, and (**b**) same SEER value (SEER 14) but different sizes.

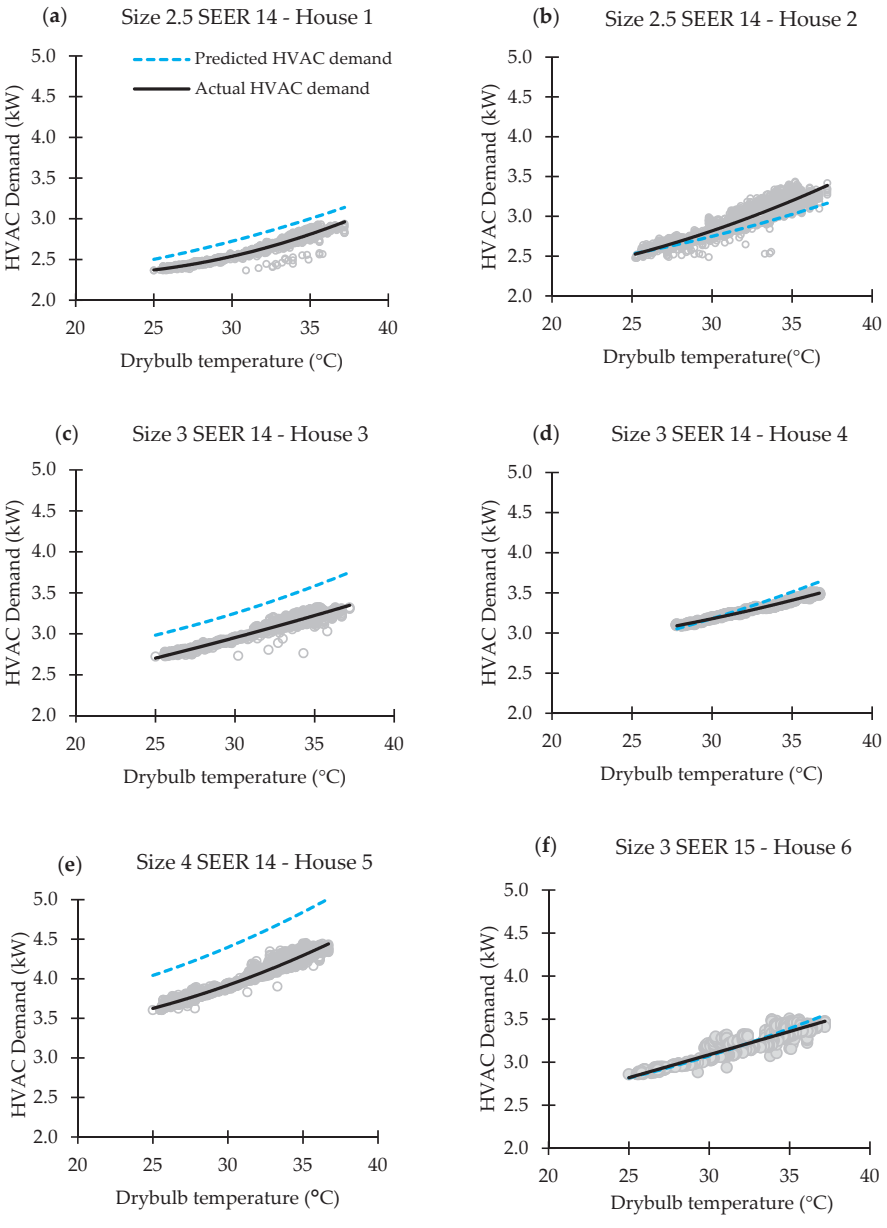

Figure 7. Examples of predicted and measured demands of residential HVAC systems by size.

The observed data in Figure 7 is shown as grey data points; the black solid lines represent a curve fit to the data. The blue-dashed lines represent the predicted demand based on the method proposed in this work. In these examples, the differences between the blue and black line likely represent a fault in the HVAC systems rather than a lower than required efficiency system, given that all systems in the figure are of a SEER 14 or above. Several trends are noted. In Figure 7a,c,e the measured energy consumption is lower than the predicted values. As this difference is not due to a difference in SEER

value, and literature on the impact of various HVAC faults on power demand, this may be due to low refrigerant charge. Each of these homes would have an efficiency rating of 0.89, 0.86, and 0.81, respectively, if measured at the rated temperature, thus in all cases, using the proposed thresholds for faults, these systems would be considered inefficient. In addition, it is observed that the difference between the predicted and actual measure data is consistent across the data collected over a range of outdoor temperatures. Figure 7f shows nearly identical agreement between the measured and actual data. Figure 7b,d shows strong agreement for lower outdoor temperature conditions; however, at higher temperatures there is more of a difference between measured and predicted data. This points to the importance of, for the efficiency rating evaluation proposed, determining at what specific conditions this is evaluated.

Summarizing the results of the 39 homes of observed data, a histogram was created to understand the distribution of efficiency ratings. For this data, all ratings indicate HVAC faults rather than the presence of an inefficient HVAC system, as all SEER ratings for the HVAC systems considered are at or above the code-required values. Using the values of predicted and actual HVAC demands in the HVAC system rating Equation (Equation (7)), the resulting distribution of HVAC system ratings is shown in Figure 8. Most of the houses (85%) have the HVAC system rating ranging from 0.9 to 1.1.

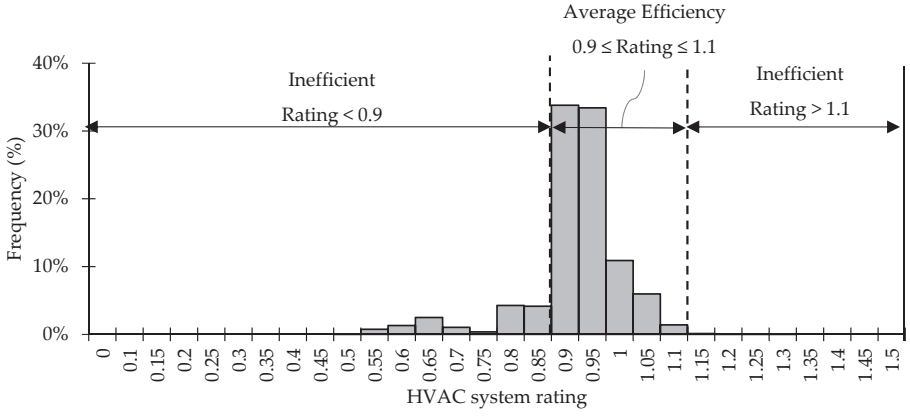

Figure 8. HVAC efficiency evaluation based on the distribution of HVAC system efficiency rating.

4. Conclusions

To evaluate the energy efficiency in residential HVAC systems, a methodology was developed which uses limited building and HVAC data, similar to the data that would be available to a utility company on the building stock from assessor's data, to predict a HVAC electricity demand curve. When compared to the demand prediction from a detailed HVAC system model ACHP, the proposed prediction method was found to have strong agreement. This methodology was then used to compare to the actual measured electricity demand of HVAC systems to assess the efficiency of operation. Based on analysis of 39 homes in the Austin area, using a proposed set of thresholds of 0.9 to 1.1, it was found that approximately 85% of total houses were evaluated as having average HVAC energy efficiency. If the value of HVAC rating is under 0.9 or higher than 1.1, the HVAC system in this house is evaluated as faulty or inefficient and would benefit from servicing or replacement. As HVAC systems continue to become more efficient, and as efficiency standards require higher efficiency residential HVAC systems, these values can be updated with results from new data and information.

One limitation of this effort is that a smaller subset of residential buildings in Texas was studied. While HVAC systems are typically similar in type and characteristics throughout the U.S., climate conditions can vary by location, thus it would be beneficial to further study buildings and their HVAC systems located in different climate zones. In addition, more HVAC systems with a broader range

of SEER values would be beneficial to include in future studies. This will help to further assess the method's applicability for the evaluation of HVAC efficiency. In addition, other fault types should be investigated to understand the impact on HVAC electricity demand, and what level of detection of such faults can be achieved through the proposed methods. Another potential limitation is the weather data. This effort uses airport-based weather data which is not necessarily representative of the building microclimate in which the HVAC system operates. This may be a source of error from the input data which could impact the ability of the model to predict electricity demands. However, as building microclimate data was not measured at each home considered, this was not a factor that could be considered in this work. In addition, further study is needed to assess the economics associated with the collection and analysis of data to achieve early detection of faults and/or system inefficiencies, and act on these issues with corrective actions or system replacement earlier than otherwise is likely to occur.

The findings of this study have significance, in particular for the residential building systems, energy efficiency, and HVAC areas of research. The ability to predict demand and rate efficiency of an HVAC system without the additional collection of detailed data on the HVAC system characteristics is highly beneficial in the case where evaluating the efficiency of a system is desired, yet there is limited availability of energy and weather data. Such would be the case, for example, if a utility company is seeking to determine which homes in their service area to target for HVAC energy efficiency upgrades. Traditionally such evaluation would require more costly and intrusive energy audits and require the collaboration with homeowners. The proposed methods developed as part of this investigation can overcome such barriers to identify potential opportunities for efficiency improvements without the need for significant time or homeowner engagement. The continuous monitoring of the HVAC system demand data and reevaluation of the efficiency over time would also enable ongoing evaluation of performance, thus also enabling the identification of issues with HVAC systems earlier on, before failure occurs.

The application of this research has benefits for homeowners and/or occupants of residential buildings and the utility companies that supply energy to these homes. The feedback provided to homeowners using the HVAC efficiency evaluation can raise awareness of the homeowners and/or occupants in energy savings in their residential buildings, and in particular, know the efficiency status of HVAC system and be notified of abnormal energy consumption. For utilities, the information resulting from the proposed models can be used to target those customers that would most benefit from efficiency upgrades and other commonly implemented rebate programs.

Author Contributions: Conceptualization, K.S.C.; Methodology, K.S.C., H.D.; Software, H.D.; Formal Analysis, H.D.; Data Curation, H.D.; Writing—Original Draft Preparation, H.D.; Writing—Review & Editing, K.S.C.; Visualization, H.D.; Supervision, K.S.C.

Funding: This research was funded, in part, by the Vietnam Ministry of Education and Training.

Acknowledgments: The HVAC energy data is from the Pecan Street Research Institute. This research was conducted in collaboration with Whisker Labs. However, any opinions, results, and conclusions from this paper do not reflect the views of these organizations.

Conflicts of Interest: The authors declare no conflict of interest. The funders had no role in the design of the study, in the collection, analyses, or interpretation of data, in the writing of the manuscript, or in the decision to publish the results.

References

1. United Nations Environment Program (UNEP). Sustainable Building and Climate Initiative. Available online: http://staging.unep.org/sbci/AboutSBCI/Background.asp (accessed on 12 October 2018).
2. United States Energy Information Administration (US EIA). How much Energy Is Consumed in Residential and Commercial Buildings in the United States? Available online: https://www.eia.gov/tools/faqs/faq.php?id=86&t=1 (accessed on 12 October 2018).

3. Swan, L.G.; Ugursal, V.I. Modeling of end-use energy consumption in the residential sector: A review of modeling techniques. *Renew. Sustain. Energy Rev.* **2009**, *13*, 1819–1835. [CrossRef]
4. Pérez-Lombard, L.; Ortiz, J.; Pout, C. A review on buildings energy consumption information. *Energy Build.* **2008**, *40*, 394–398. [CrossRef]
5. United States Energy Information Administration (US EIA). Residential Energy Consumption Survey (RECS). 2015 RECS Survey Data. Available online: https://www.eia.gov/consumption/residential/data/2015/ (accessed on 12 October 2018).
6. U.S. Department of Energy. Home Energy Audits. Available online: https://energy.gov/public-services/homes/home-weatherization/home-energy-audits (accessed on 12 October 2018).
7. Database of State Incentives for Renewables & Efficiency (DSIRE). NC Clean Energy Technology Center. Available online: http://www.dsireusa.org/ (accessed on 12 October 2018).
8. Cetin, K.S.; Novoselac, A. Single and multi-family residential central all-air HVAC system operational characteristics in cooling-dominated climate. *Energy Build.* **2015**, *96*, 210–220. [CrossRef]
9. Cetin, K.S. Smart Technology Enabled Residential Building Energy Use and Peak Load Reduction and Their Effects on Occupant Thermal Comfort. Ph.D. Thesis, The University of Texas at Austin, Austin, TX, USA, 2015.
10. Kim, M.; Payne, W.V.; Domanski, P.A.; Yoon, S.H.; Hermes, C.J. Performance of a residential heat pump operating in the cooling mode with single faults imposed. *Appl. Therm. Eng.* **2009**, *29*, 770–778. [CrossRef]
11. Palmiter, L.; Kim, J.H.; Larson, B.; Francisco, P.W.; Groll, E.A.; Braun, J.E. Measured effect of airflow and refrigerant charge on the seasonal performance of an air-source heat pump using R-410A. *Energy Build.* **2011**, *43*, 1802–1810. [CrossRef]
12. Yoon, S.H.; Payne, W.V.; Domanski, P.A. Residential heat pump heating performance with single faults imposed. *Appl. Therm. Eng.* **2011**, *31*, 765–771. [CrossRef]
13. Southern California Edison (SCE). Laboratory Assessment of a Retrofit Fault Detection and Diagnostics Tool on a Residential Split System. HT.11.SCE.005 Report. 2013. Available online: https://www.etcc-ca.com/reports/laboratory-assessment-retrofit-fault-detection-and-diagnostics-tool-residential-split-system (accessed on 12 October 2018).
14. Cooper, A. *Electric Company Smart Meter Deployments: Foundation for a Smart Grid*; IEI Report; The Edison Foundation, Institute for Electrical Innovation: Washington, DC, USA, 2016.
15. Cetin, K.S.; O'Neill, Z. Smart meters and smart devices in buildings: A review of recent progress and influence on electricity use and peak demand. *Curr. Sustain. Renew. Energy Rep.* **2017**, *1*, 1–7. [CrossRef]
16. National Aeronautics and Space Administration (NASA). Modern-Era Retrospective Analysis for Research and Applications, Version 2. Goddard Space Flight Center. Available online: https://gmao.gsfc.nasa.gov/reanalysis/MERRA-2/data_access/ (accessed on 12 October 2018).
17. Valdiserri, P.; Biserni, C. Energy performance of an existing office building in the northern part of Italy: Retrofitting actions and economic assessment. *Sustain. Cities Soc.* **2016**, *27*, 65–72. [CrossRef]
18. Biserni, C.; Valdiserri, P.; D'Orazio, D.; Garai, M. Energy Retrofitting Strategies and Economic Assessments: The Case Study of a Residential Complex Using Utility Bills. *Energies* **2018**, *11*, 2055. [CrossRef]
19. Air Conditioning Contractors of America. Speed-Sheet for ACCA Manual J. 2015. Available online: https://www.acca.org/communities/community-home/librarydocuments/viewdocument?DocumentKey=0bc73e80-6c3c-43cb-bdb2-43316a380fa4 (accessed on 12 October 2018).
20. Proud Green Home. Can You Do a Manual J HVAC Calculation in Less than 60 Seconds? Available online: https://www.proudgreenhome.com/news/can-you-do-a-manual-j-hvac-calculation-in-less-than-60-seconds/ (accessed on 12 October 2018).
21. New York State Office of Real Property Services. Assessor's Manual. Data Collection—Residential/Farm/Vacant Land. Available online: https://www.tax.ny.gov/pdf/publications/orpts/manuals/rfv_manual_published.pdf (accessed on 12 October 2018).
22. Jon, S.; Nancy, M. Collecting Parcel Data from Assessors. The U.S. Department of Housing and Urban Development (HUD). Office of Policy Development and Research (PD&R). Available online: https://www.iaao.org/uploads/FE_April_Parcel_Data.pdf (accessed on 12 October 2018).
23. Bell, A.A., Jr. *HVAC: Equations, Data, and Rules of Thumb*; McGraw-Hill: New York, NY, USA, 2008; ISBN 9780071482424.

24. Tim, K.; What Size Central Air Conditioner Do I Need for My House? A Short Consumer's Guide from ASM. All System Mechanical (ASM). Available online: https://asm-air.com/airconditioning/what-size-central-air-conditioner-for-my-house/ (accessed on 12 October 2018).
25. United States Energy Information Administration (US EIA). Residential Energy Consumption Survey (RECS). Maps. Available online: https://www.eia.gov/consumption/residential/maps.php (accessed on 12 October 2018).
26. Cutler, D.; Cutler, J.; Kruis, N.; Christensen, C.; Brandemuehl, M. *Improved Modeling of Residential Air Conditioners and Heat Pumps for Energy Calculations*; Technical Report; NREL/TP-5500-56354; National Renewable Energy Laboratory (NREL): Golden, CO, USA, 2013.
27. The Pecan Street Research Institute, The University of Texas at Austin. The Dataport Database. Available online: http://www.pecanstreet.org/category/dataport/ (accessed on 12 October 2018).
28. Austin Energy. Energy Conservation Audit and Disclosure (ECAD) Ordinance. The City of Austin. Available online: https://austinenergy.com/ae/energy-efficiency/ecad-ordinance/energy-conservation-audit-and-disclosure-ordinance (accessed on 12 October 2018).
29. U.S. Department of Energy. Appliance and Equipment Standards Rulemakings and Notices. Available online: https://www1.eere.energy.gov/buildings/appliance_standards/standards.aspx?productid=48&action=viewlive#current_standards (accessed on 12 October 2018).
30. Wassmer, M. A Component-Based Model for Residential Air Conditioner and Heat Pump Energy Calculations. Master's Thesis, University of Colorado at Boulder, Boulder, CO, USA, 2003.
31. Hendron, R.; Engebrecht, C. Building America House Simulation Protocols. Available online: https://www.nrel.gov/docs/fy11osti/49246.pdf (accessed on 12 October 2018).
32. Air Conditioning, Heating, and Refrigeration Institute (AHRI). Standard 210/240—2017 Standard for Performance Rating of Unitary Air-conditioning & Air-source Heat Pump Equipment. 2017. (ANSI/AHRI 2017). Available online: http://www.ahrinet.org/App_Content/ahri/files/STANDARDS/AHRI/AHRI_Standard_210-240_2017.pdf (accessed on 12 October 2018).
33. United States Department of Energy. Energy Plus. Engineering Reference. Washington, DC, USA. Available online: https://energyplus.net/ (accessed on 12 October 2018).
34. Ian, B. Air Conditioning/Heat Pump (ACHP). Purdue University. Available online: http://achp.sourceforge.net/ (accessed on 12 October 2018).
35. Cetin, K.S.; Kallus, C. Data-driven methodology for energy and peak load reduction of residential HVAC systems. *Procedia Eng.* **2016**, *145*, 852–859. [CrossRef]

energies

MDPI

Article

Using Edible Plant and Lightweight Expanded Clay Aggregate (LECA) to Strengthen the Thermal Performance of Extensive Green Roofs in Subtropical Urban Areas

Yi-Yu Huang * and Tien-Jih Ma

Department of Landscape Architecture, Tunghai University, 40704 Taichung, Taiwan; jackie82430@gmail.com
* Correspondence: yyhuang@thu.edu.tw

Received: 17 December 2018; Accepted: 25 January 2019; Published: 29 January 2019

Abstract: Gazing at natural landscapes and participating in agricultural activities can elicit psychophysiological restoration. However, most buildings are constructed merely to meet the minimum legal requirements for structure weight load. Extensive green roofs consisting of vegetables and a lightweight growth medium can be designed to provide not only passive-cooling effects on bare rooftops, but also to convert idle rooftops into temporary retreats for stressed individuals. The purpose of this study is to both measure the surface temperature reduction and heat amplitude reduction of a bare rooftop using the extensive green roofs containing a lightweight expanded clay aggregate (LECA) and *Ipomoea batata* as well as conduct a weight-reduction-and-cost analysis to measure the weight loss of the extensive green roofs incurred through LECA replacement. A four-stage field experiment was performed on the flat rooftop of a dormitory in a subtropical climate during summer. The results indicated that roofs with *Ipomoea batata* had a significantly higher passive-cooling effect than did roofs without *Ipomoea batata*. The roofs with 10%–40% LECA exhibited a slightly higher passive-cooling effect than did roofs with conventional garden soil. At a slightly different average air temperature (0.56 °C; i.e., 32.04 °C minus 31.48 °C), the combined effects of LECA and *Ipomoea batata* helped to significantly reduce the average temperature of the bare rooftop by an additional 10.19 °C, namely, temperature reduction of the bare rooftop increased from 9.54 °C under a roof with 0% LECA and without plants in the second stage to 19.73 °C under a roof with 10% LECA and with plants in the fourth stage.

Keywords: *Ipomoea batatas*; lightweight expanded clay aggregate (LECA), thermal performance; extensive green roof; subtropical climate

1. Introduction

In modern urban societies, stressful lifestyles have increasingly driven humans to seek temporary stress relief, and stressful lifestyles are well known as the major causes for many physical and psychological illnesses [1], including anxiety, depression, insomnia, burnout syndrome, as well as gastroenterological, cardiovascular, neurological, and immunological diseases [2,3]. Consequently, stress management should receive significant research attention in the interests of public health.

Compared with urban environments, natural environments are generally associated with positive health effects [4,5]. When city dwellers have insufficient time to relax in a city park, a rooftop garden may be an ideal alternative site for a temporary daily retreat. More than three decades ago, Kaplan [4] and Ulrich [5] emphasized the importance of natural environment and landscapes in reducing stress. More recent findings have demonstrated that even short visual encounters with natural settings can elicit significant psychophysiological restoration within 3–5 min at most or as

quickly as 20 s [6–8]. Furthermore, with the exception of passive gazing, more benefits could be elicited from actively participating in horticultural activities because they invoke reminiscence of meaningful past experiences, spiritual healing, and stimulation of five senses [9].

Consequently, rather than sedum or crassulacean acid metabolisum (CAM) plants [10], which have frequently been used in studies to assess the thermal performance of extensive green roofs because of their endurance in arid and windy rooftop environment, we decided to use vegetables for our extensive green roofs. The advantages of using vegetables rather than sedum or CAM plants, which usually have low leaf-area indexes (LAIs), for extensive green roofs include high LAI, edibility, low carbon dioxide emissions, and provision of horticultural activity.

LAI, measured as a ratio of total one-sided area of photosynthetic tissue to the ground-surface area below them, represents the area of leaf coverage and defines the latent heat loss of an extensive green roof [11]. The higher the LAI, the greater the effects of shading, insulation, and evapotranspiration of the extensive green-roof plant layer, which contribute to significant reduction in rooftop surface temperature [11]. Moreover, the use of edible plants can be considered an implementation of the *Edible Landscape Initiatives*, which reintroduce food into urban and rural landscapes to increase local food security. If numerous empty and idle rooftops [12] can be converted into city farms, then these farms can be expected to significantly reduce carbon dioxide emissions because less food would require transportation from rural areas to cities, and our neighborhood microclimate and human thermal comfort can also be improved [13].

Vegetables suitable for rooftop planting in subtropical climates in Taiwan include *Rosmarinus officinalis*, *Abelmoschus esculentus*, *Ipomoea batatas*, *Gynura bicolor*, *Perilla frutescens*, *Capsicum annuum*, *Ocimum basilicum*, *Solanum melongena*, *Phaseolus vulgaris*, and *Luffa cylindrical* [14]. After careful consideration, *Ipomoea batatas* was selected because of its resistant to wind, sun, and drought as well as its low maintenance, high LAI, easy obtainment of 100% plant-bed coverage, year-round harvesting, high nutrition, and popularity.

To reduce construction costs, the structural loads of most buildings in Taiwan frequently only barely meet minimum requirements. According to architectural regulations, the live load of a building—that is, the static and constant forces to which a building is subjected for an extended time period—is 200.00 kg/m^2 [15]. Thus, lightweight green-roof systems are recommended in Taiwan. Quality growth medium for extensive green roofs should drain well, demonstrate excellent water-holding and nutrition-holding capabilities, provide sufficient support for plant roots in shallow soil depths of 10–20 cm, and be lightweight. A common growth medium utilized for extensive green roofs is a mixture of sandy loam, organic matter, and a lightweight growth medium. The most common organic matters are compost and peat, and the most common lightweight growth medium are perlite, zeolite, pumice and lightweight expanded clay aggregate (LECA) [16–21]. A common formula used for lightweight growth medium is 15–30% sandy loam, 20–30% organic matter, and 50–70% lightweight growth medium [16–21].

According to field measurements, LECA has a potentially superb thermal reduction performance. Lin and Lin [22] compared the thermal reduction performance of four different types of growth mediums: sand; sand and white-charcoal debris (5:1); peat moss, vermiculite, and burned clay (1:1:1); and burned reservoir sludge mixed with rice hull, baked at 900 °C (which is similar to LECA). They compared the performance of these mediums with four CAM plants in the tropical climate of Taiwan and discovered that the burned reservoir sludge exhibited the greatest reduction in heat amplitude (88.8%) and exhibited the second best bare-rooftop temperature reduction. Although sand was the optimal growth medium for bare-rooftop temperature reduction, its weight poses potential problems for the weight load of building structures, and sand mining causes numerous environmental problems, including land erosion and habitat destruction [22]. Burned reservoir sludge, an efficient tool for clearing mud build-up at the bottom of reservoirs to prolong reservoir lifespans, also demonstrated an excellent temperature-reduction performance on the bare rooftop because of its ability to hold water and air as a mesoporous material. Because water content can effectively slow the rise in temperature

of growth mediums during the daytime, and air content can increase the heat insulation of growth mediums, porous growth mediums can produce superior temperature-reduction effects. Further, great porosity can also invigorate plant roots by increasing air content. By comparing porous (pebbles and silica sand) and nonporous (volcanic ash and siliceous shale) materials of various particle sizes, Wanphen and Nagano [23] demonstrated that porous materials can more effectively lower the surface temperature of bare rooftops than can nonporous materials. The reason for this is that mesoporous materials contain a high volume of pores of an appropriate size to hold water during the night and release substantial vapor during the day, resulting in the release of considerable latent heat and more effective rooftop surface temperature reduction. Sutcu reported that the thermal conductivity of porous brick containing 10% expanded vermiculite was 32% lower than that of conventional brick (a reduction from 0.96 to 0.65 W/m^2K) and thus could be used as an effective insulating material for combating the high ambient temperature [24]. Consequently, we selected LECA as the lightweight growth medium because, as a mesoporous material, its porosity enables it to hold water, air, and nutrients while also draining effectively; furthermore, LECA does not rot, which means that it provides excellent support to plants in shallow depths, and it is inexpensive, widely available in Taiwan, and environmentally friendly.

The present study aimed to fulfill the following objectives by conducting a four-stage experiment during the hottest months in a subtropical climate:

1. Investigate the depth of the growth medium;
2. Investigate the proportion of LECA in the growth medium;
3. Investigate the placement of LECA in the growth medium;
4. Investigate how adding *Ipomoea batatas* affects the thermal performance of extensive green roofs.
5. Conduct a weight-reduction-and-cost analysis of extensive LECA roofs.

2. Materials and Methods

2.1. Experiment Site

Field measurements were conducted on the rooftop of a multistory student dormitory in a university (24°10′54.0″ N 120°36′04.3″ E) located in the metropolitan area of Taichung, the third largest city in Taiwan. According to the East Asia map of the Koppen climate classification, the site is located in a warm oceanic climate/humid subtropical climate (Cfa) zone with the lowest monthly average temperature of 16.8 °C in January and highest temperature of 30.1 °C in July for the years 2014–2016; additionally, the lowest monthly relative humidity is 76.0% in January, and the highest relative humidity is 83.7% in May (Figure 1) [25]. Figure 2 shows the floor plans of the fourth and fifth floors (experiment site) and the experimental setup.

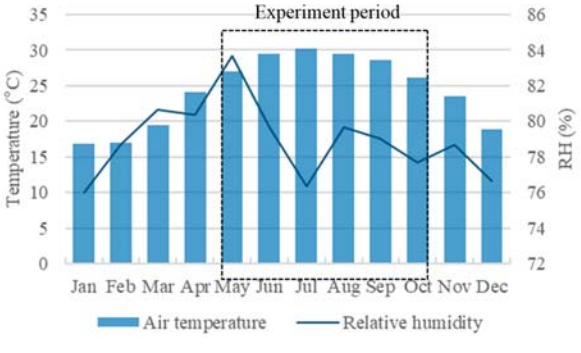

Figure 1. Average temperature and relative humidity observed at the nearest weather station (Long-Jing station), Taichung, 2014–2016.

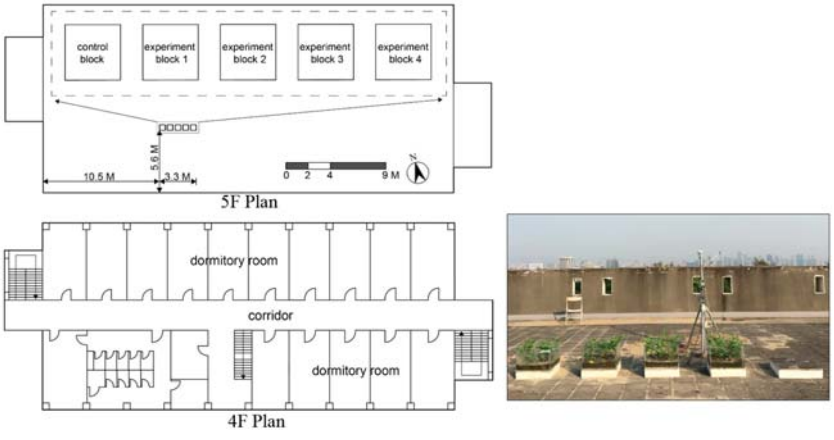

Figure 2. Floor plans of the fourth (**lower left**) and fifth (**upper left**) floors. Five blocks on the fifth floor served as experimental blocks (**upper left**). Experiment site and experimental setup (**right**).

2.2. Description of Plant Material and Growth Medium

To obtain favorable thermal benefits of the extensive green roof and to yield a year-round food supply, *Ipomoea batatas* (sweet potato) (Figure 3) was selected as our plant material. *Ipomoea batatas* thrives in warm weather. *Ipomoea batatas* leaves are heart-shaped and tend to grow on slender and lengthy stems; the herbaceous perennial vine grows vigorously and easily achieve 100% coverage, which helps lower the surface temperature and heat amplitude of a bare rooftop. *Ipomoea batatas* leaves can be harvested throughout the year. A few species of *Ipomoea batatas* can be used as ornamental ground cover owing to their attractive leaves. *Ipomoea batatas* can grow abundantly in poor soil. It has a mild and lightly sweet flavor. It is beneficial to the digestive system because of its high dietary fiber content. It helps reduce blood sugar and cholesterol levels, prevent infections, boosts the immune system, and provides a number of benefits to the eyes.

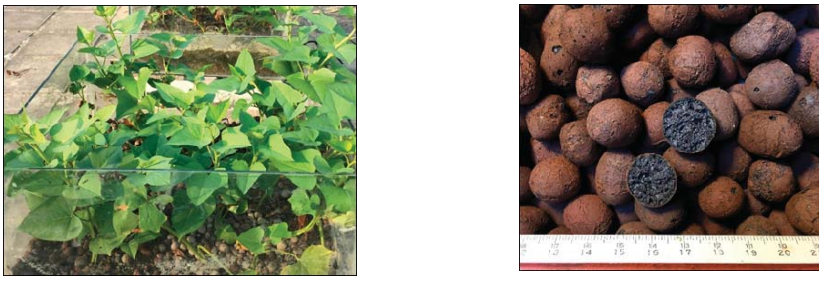

Figure 3. *Ipomoea batatas* (sweet potato) (**left**) and LECA (**right**). Ruler in centimeters (**right**).

LECA (Figure 3) was selected for mixing with the conventional garden soil, composed of sandy loam:compost = 3:1, to reduce the weight load of the building structure [26] and the thermal conductivity of the growth medium, which, in turn, would lead to temperature reduction of the underlying bare rooftop [23,24]. Sandy loam is capable of quickly draining excess water, however, it cannot hold significant amount of water and nutrients for plants. The addition of the compost would help increase the the water-holding and nutrient-holding capacity of the soil for plants. The designed conventional garden soil supports the growth of various plants, including vegetables. LECA is a lightweight aggregate produced by baking a mixture of clay powder and saw dust for 7 h at 1000 °C [27]. It has a hard ceramic shell, a porous core, and a porous surface [27,28]. LECA is durable,

stable, and nontoxic [27,28]. It can be used to increase the breathability of plant roots, support plants, and prevent soil hardening when it is thoroughly mixed with conventional garden soil or laid at the bottom of the tank [26]. When mixed with cement, LECA can be used to lighten the structure weight load and for thermal insulation and acoustic insulation in buildings [29,30].

2.3. Experimental Design

In summer 2017, five 50 × 50 × 10 cm^3 (length [L] × width [W] × height [H]) cement boards capped with ceramic tiles were placed on a flat rooftop to simulate a flat bare roof (Figure 2). Five 50 × 50 × 4 cm^3 (L × W × H) Styrofoam boards were placed under the cement boards to block heat conduction from the surrounding bare rooftop. All cement boards were placed close to the middle left of the bare rooftop. They were exposed to direct sunlight at all times, without any shadow interference from surrounding building walls or parapet walls. Four 50 × 50 × 30 cm^3 (L × W × H) glass tanks were placed on top of four cement boards. The glass tanks helped avoid shadow interference from neighboring tanks. One cement board without any tank was exposed directly to the sunlight to simulate a bare rooftop as a control (Figure 2). The experiment tanks were approximately the same size as those used in the studies of Song et al. [31], and Huang et al. [32]. Fifteen dormitory rooms were located directly under the bare rooftop. An extensive green roof system on the bare rooftop would help reduce the temperature of the bedrooms below and hence increase the students' living comfort [33,34]. Because heat always flows out of a room and a green roof would act as a heat sink in a green-roofed building during daytime in sunny days, the indoor temperature of a room underneath a green roof is lower than that of a room underneath a common roof during daytime [33]. Based on field measurements, the indoor temperature underneath a green roof was 2°C lower than that under a common roof at noon with strong solar radiation [33,34].

The experiment consisted of four stages. The first stage (Figure 4) involved comparing the thermal performance of the extensive roofs when four different depths of the conventional garden soil (0% LECA) were employed: 10, 15, 20, and 25 cm. The marginal temperature reduction, determined as the ratio of additional temperature reduction to incremental increase in the depth of the growth medium, was calculated to determine the most efficient depth of growth medium in the second, third, and fourth stages. The second stage (Figure 8) involved comparing the thermal performance when different proportions of LECA—0% (conventional garden soil), 10%, 40%, 70%—were laid at the bottom of the tanks. The third stage (Figure 12) involved investigating which combination (proportion of LECA × LECA placement) yielded the highest thermal performance without the introduction of *Ipomoea batatas*. The fourth stage (Figure 16) involved investigating the additional thermal performance after the introduction of *Ipomoea batatas* have achieved 100% coverage.

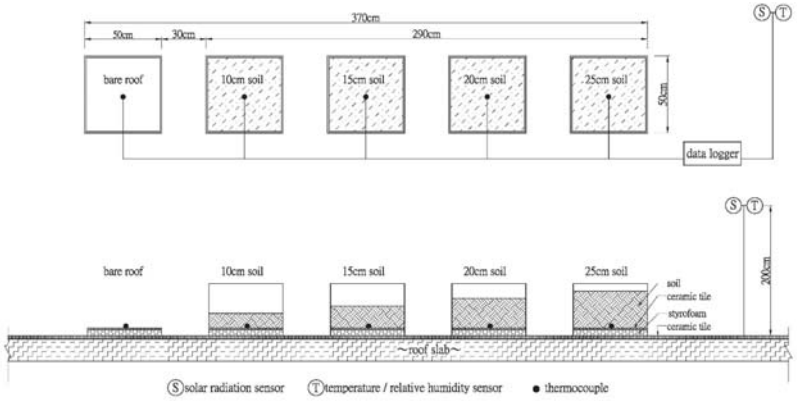

Figure 4. Experimental setup for the first stage. The plan (**top**) and the elevation (**bottom**).

2.4. Instrument Settings and Measurement Data

Five measurement points were placed at the bottom center of the extensive roof and at the center of the simulated bare roof. Thermocouples (Onset Computer Corporation) were placed horizontally in close contact with the surface to measure the temperature accurately. Air temperature, relative humidity, and solar radiation were measured at a point 2 m above the rooftop surface [35,36] and 5.6 m (shortest distance) away from the parapet walls to prevent any reflective interference from the bare rooftop and parapet walls. A thermal monitoring system comprising three HOBO micro station data loggers (Onset Computer Corporation) was employed to record all measurements at intervals of 10 min. The experiment was conducted in the following four periods: 13–23 May 2017, 14–26 July 2017, 20–27 September 2017 and 28 September–13 October 2017. Please refer to Table 1 for the equipment list.

Table 1. Equipment list.

Parameters	Equipment Used	Type	Measurement Range	Accuracy
Solar radiation	Solar radiation smart sensor (Silicon Pyranometer)	S-LIB-M003	−40 to 75 °C	±10 W/m^2 or ±5%, whichever is greater in sunlight. Additional temperature induced error ±0.38 W/m^2/°C from 25 °C
Air temperature & Relative humidity	12-bit Temperature/Relative humidity smart sensor	S-THB-M002	Temp: −40 to 75 °C, RH: 0% to 100% at −40 to 75 °C	Temp: +/− 0.21 °C from 0 to 50 °C; RH: +/− 2.5% from 10% to 90% RH (typical), to a maximum of +/− 3.5% including hysteresis at 25 °C; below 10% and above 90% ±5% typical
Temperature	12-bit Temperature smart sensor	S-TMB-M002, S-TMB-M006	−40 to 75 °C, sensor tip	< ±0.2 °C from 0 to 50 °C
–	Hobo micro station data logger	H21-002	−20 to 50 °C with alkaline batteries, −40 to 70 °C with lithium batteries	0 to 2 seconds for the first data point and ±5 seconds per week at 25 °C

3. Results and Discussion

3.1. Marginal Temperature Reduction When 10, 15, 20, and 25 cm Conventional Garden Soil and No Plants Were Used

The first stage (Figure 4) involved comparing the thermal performance of extensive roofs with four different depths of conventional garden soil: 10, 15, 20, and 25 cm. Table 2 shows that the mean air temperature and mean rooftop temperature were 25.15 and 28.44°C, respectively; the ranges of air temperature and rooftop temperature were 19.37–33.29 °C and 18.82–52.67 °C, respectively; the maximum solar radiation was 1170.60 W/m^2; the mean relative humidity was 85.54%. A period of 24 h was selected for further analysis based on the following criteria: high temperature at noon, relatively stable air temperature progression over 24 h, and ample solar radiation with relatively little cloud interference. The date selected was 14–15 May 2017 (Figure 5). The time frame 07:00–14:00 was further selected to compute the passive cooling effects among all extensive roofs for comparisons within and between different stages, because this is the single maximum period of time frame when the passive cooling effects were concurrent across four different stages. According to the experiment results, the passive cooling effects occurred over time frame 07:00–16:00, 07:00–14:00, 07:00–16:00, and 07:00–17:00 for the fist (5 July), second (25 July), third (24 September), and fourth (1 October) stages, respectively.

Table 2. Weather data for the first stage (13 May 2017 05:59:44 to 23 May 2017 05:49:44).

First Stage	Value
Period of measurement	13–23 May 2017
Range of air temperature	19.37–33.29 °C
Mean air temperature	25.15 °C
Range of rooftop temperature	18.82–52.67 °C
Mean rooftop temperature	28.44 °C
Maximum solar radiation	1170.60 W/m^2
Mean relative humidity	85.54%
Date selected for further analysis (marked with dotted box)	14–15 May 2017

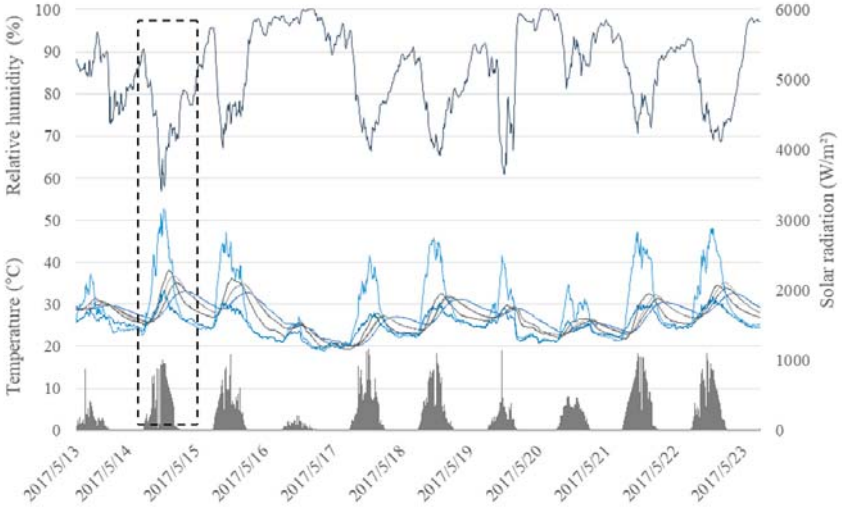

Figure 5. Temperatures, solar radiation, and relative humidity in the cases of 10, 15, 20, and 25 cm conventional garden-soil roofs without plants (13 May 2017 05:59:44 to 23 May 2017 05:49:44).

Because roofs with different depths of conventional garden soil resulted in the insulation, absorption, and evaporation effects, the thicker the growth medium, the greater the temperature reduction of the bare rooftop. On 14 May from 07:00 to 14:00, when the average air and rooftop temperatures were 29.18 and 41.72 °C, respectively, the average temperatures at the bottom of the roofs with the conventional garden soil (0% LECA) at depths of 10, 15, 20, and 25 cm were 30.28, 28.91, 27.54, and 27.26 °C, respectively (Figures 6 and 7, Table 3). Consequently, the marginal temperature reduction achieved by the roofs with conventional garden-soil depths of 10, 15, 20, and 25 cm, determined as the ratio of the additional temperature reduction to the incremental increase in garden-soil depth (in other words, the additional temperature reduction of the bare rooftop as a result of a 1-cm increase in garden soil depth), were 1.15 °C for 10 cm, 0.27 °C for 15 cm, 0.27 °C for 20 cm, and 0.06 °C for 25 cm (Table 4). These results indicated a decline in the marginal temperature reduction with increasing garden-soil depth, suggesting that the roof with 10-cm deep garden soil was the most efficient in reducing the temperature of the bare rooftop. We did not test the garden soil less than 10 cm because it is too shallow to grow healthy plants. Consequently, a 10 cm depth of growth medium was selected for the second, third and fourth stages. Noted that the reason for choosing the time frame of 07:00–14:00 to average the temperature reduction values was because this is the common and maximum lengthen of time frame for passive cooling effects to occur for four stages.

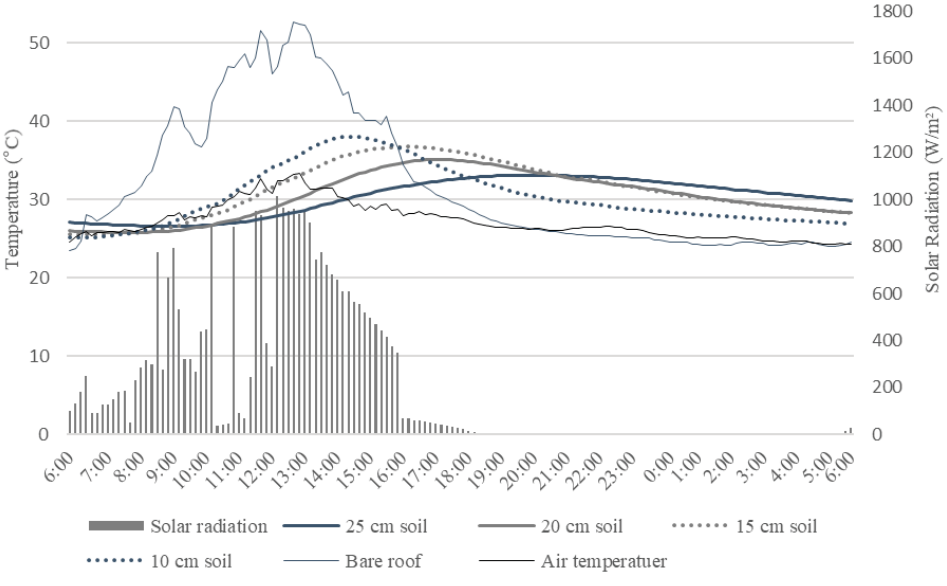

Figure 6. Temperatures and solar radiation in the cases of 10, 15, 20, and 25 cm conventional garden-soil roofs without plants (14 May 2017 05:59:44 to 15 May 05:49:44).

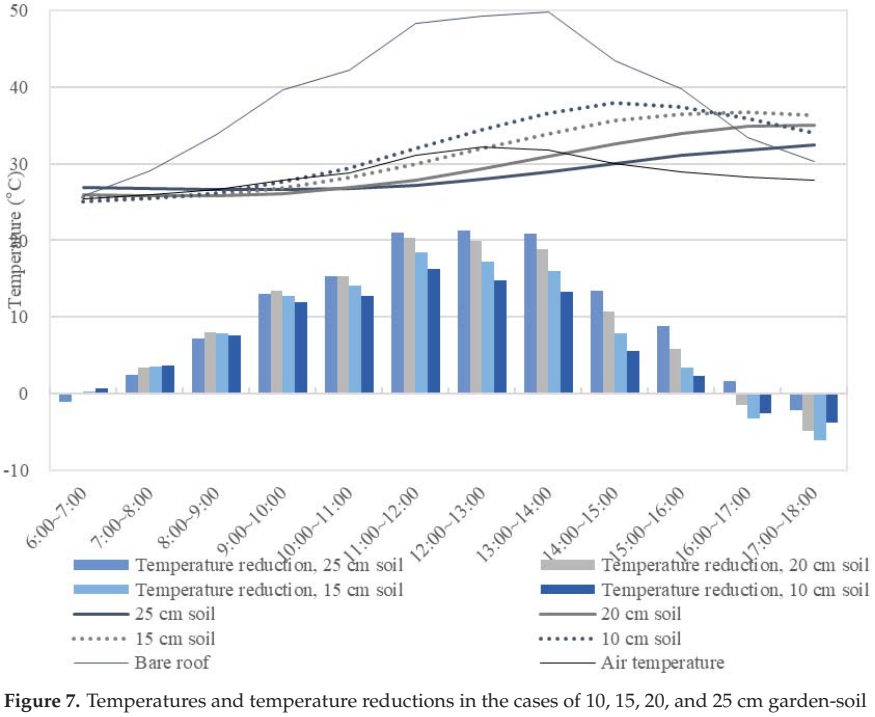

Figure 7. Temperatures and temperature reductions in the cases of 10, 15, 20, and 25 cm garden-soil roofs without plants (14 May 2017 05:59:44 to 14 May 2017 17:49:44).

Table 3. Temperature at the bottom of the roofs and temperature reductions in the cases of 10, 15, 20, and 25 cm conventional garden-soil roofs without plants (14 May 2017 05:59:44 to 14 May 2017 17:49:44).

Thermocouple Position		06:00–07:00 (°C)	07:00–08:00 (°C)	08:00–09:00 (°C)	09:00–10:00 (°C)	10:00–11:00 (°C)	11:00–12:00 (°C)	12:00–13:00 (°C)	13:00–14:00 (°C)	14:00–15:00 (°C)	15:00–16:00 (°C)	16:00–17:00 (°C)	17:00–18:00 (°C)
In the air		25.43	25.90	26.57	27.85	28.86	31.14	32.14	31.81	30.07	28.96	28.25	27.85
Bare rooftop surface		25.85	29.12	33.82	39.59	42.16	48.26	49.27	49.85	43.40	39.79	33.39	30.23
At the bottom	10 cm soil, no plants	25.13	25.46	26.18	27.72	29.48	32.02	34.49	36.60	37.91	37.45	35.91	34.00
	15 cm soil, no plants	25.55	25.63	25.95	26.83	28.13	29.90	32.02	33.89	35.59	36.47	36.70	36.32
	20 cm soil, no plants	25.92	25.81	25.83	26.15	26.85	27.88	29.31	30.96	32.65	34.00	34.84	35.07
	25 cm soil, no plants	26.96	26.76	26.59	26.57	26.80	27.24	27.97	28.92	30.04	31.04	31.82	32.41
Temperature Reduction	10 cm soil, no plants	0.73	3.66	7.64	11.87	12.68	16.24	14.79	13.25	5.49	2.35	−2.52	−3.77
	15 cm soil, no plants	0.30	3.49	7.87	12.76	14.03	18.36	17.26	15.97	7.81	3.33	−3.31	−6.09
	20 cm soil, no plants	−0.07	3.32	7.99	13.44	15.32	20.38	19.97	18.90	10.75	5.79	−1.45	−4.83
	25 cm soil, no plants	−1.11	2.37	7.23	13.02	15.36	21.02	21.30	20.93	13.36	8.75	1.57	−2.18

Table 4. Temperature reductions in the cases of 10, 15, 20, and 25 cm conventional garden-soil roofs without plants (14 May 2017 07:00–14:00).

Thermocouple Position		Average Temperature (°C)	Average Temperature Reduction (°C)	Additional Temperature Reduction due to Increased Soil Depth (°C)	Incremental Increase in Soil Depth (cm)	Marginal Temperature Reduction (°C)
Air temperature		29.18	-	-	-	-
Bare rooftop surface		41.72	-	-	-	-
At the bottom	10 cm soil, no plants	30.28	11.45	11.45	10	1.15
	15 cm soil, no plants	28.91	12.82	1.37	5	0.27
	20 cm soil, no plants	27.54	14.19	1.37	5	0.27
	25 cm soil, no plants	27.26	14.46	0.28	5	0.06

Note: Marginal temperature reduction is determined as the ratio of additional temperature reduction to the incremental increase in conventional garden soil depth.

3.2. Temperature Reduction When 0%, 10%, 40%, and 70% LECA Were Laid at the Bottom and No Plants Were Used

The second stage (Figure 8) involved investigating the reductions in average temperature and heat amplitude owing to the extensive roof when different proportions of LECA were laid at the bottom of the tanks. The roofs with 0%, 10%, 40% and 70% LECA have 0, 1, 4, 7 cm of LECA laid at the bottom of the tank, and 10, 9, 6, 3 cm of conventional garden soil laid at the top of the tanks, respectively. Table 5 shows that the mean air and rooftop temperatures were 29.15 and 33.96 °C, respectively; the ranges of air and rooftop temperatures were 25.53–33.94 °C and 25.45–52.24 °C, respectively; the maximum solar radiation was 1138.10 W/m^2; and the mean relative humidity was 80.88%. A period of 24 h was selected for further analysis based on the aforementioned criteria. The date selected was 25–26 July 2017 (Figure 9).

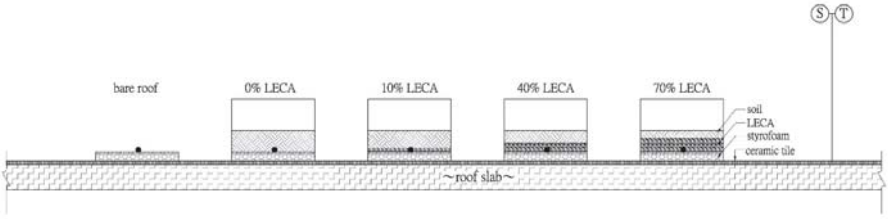

Figure 8. Experimental setup for the second stage.

Table 5. Weather data for the second stage (14 July 2017 06:00:09 to 26 July 2017).

Second Stage	Value
Period of measurement	14–26 July 2017
Range of air temperature	25.53–33.94 °C
Mean air temperature	29.15 °C
Range of rooftop temperature	25.45–52.24 °C
Mean rooftop temperature	33.96 °C
Maximum solar radiation	1138.10 W/m^2
Mean relative humidity	80.88%
Date selected for further analysis (marked with dotted box)	25–26 July 2017

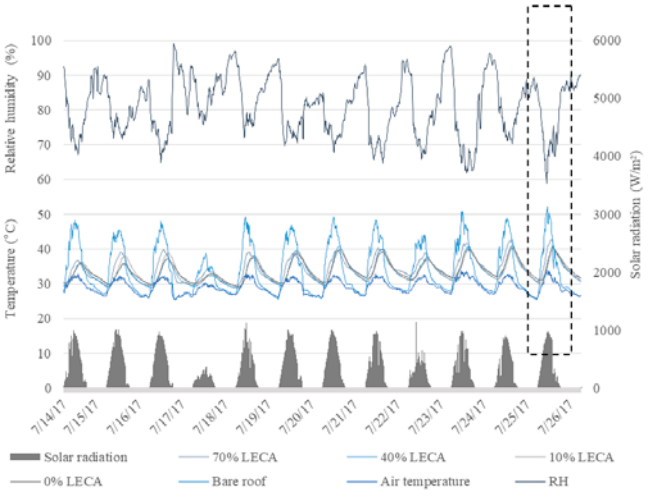

Figure 9. Temperatures, solar radiation, and relative humidity in the cases of 0%, 10%, 40%, and 70% LECA laid at the bottom without plants (14 July 2017 06:00:09 to 26 July 2017 05:50:09).

Roofs with various proportions of LECA exhibited different insulation, absorption, and evaporation effects in the garden-soil layer and additional insulation, absorption, and evaporation effects in the LECA layer. Consequently, the roofs with 10% and 40% LECA were not only lighter than the 0% LECA (conventional garden-soil) roof but also exhibited a lower average temperature in the bare rooftop than in the 0% LECA roof. On 25 July from 07:00–14:00 (Table 6, Figure 10), when the average air temperature was 31.48 °C and the average rooftop temperature was 44.28 °C, the average bottom temperatures of the roofs with 10% and 40% LECA were 33.71 and 34.34 °C, respectively, whereas the average bottom temperature of the roof with 0% LECA was 34.74 °C. These results indicated that roofs with 10% and 40% LECA reduced the average rooftop temperature by an additional 1.03 and 0.4 °C, respectively. The roof with 70% LECA (37.44 °C) exhibited inferior temperature-reduction performance than the 0% LECA roof (34.74 °C) by a difference of 2.70 °C. Consequently, the proportions of 10% and 40% LECA were selected for the third and fourth stages.

Furthermore, all four extensive roofs containing different LECA proportions also contributed to stabilizing the rooftop temperature, which in turn mitigate the fluctuation of indoor temperature. Our experimental results revealed that the reduction of heat amplitude decreased as the proportion of LECA was increased. On July 25–26 (Table 7, Figure 11), the roof with 0% LECA and without plants reduced the heat amplitude of the bare rooftop by a significant 63.03%, whereas the roofs with 10%, 40%, 70% LECA and without plants reduced the heat amplitude of the bare rooftop by 61.91%, 58.47%, and 53.40%, respectively. The reduction in heat amplitude was calculated as 1 minus the ratio of fluctuation in the experimental temperature to fluctuation in the bare rooftop temperature. Compared with the roof with 70% LECA and without plants, the roof with 0% LECA and without plants provided an additional 9.63% reduction in the heat amplitude of the bare rooftop. In summary, although the roof with 10% LECA and without plants yielded the largest reduction in the temperature of the bare rooftop, it is the roof with 0% LECA and without plants offered the largest reduction in heat amplitude of the bare rooftop.

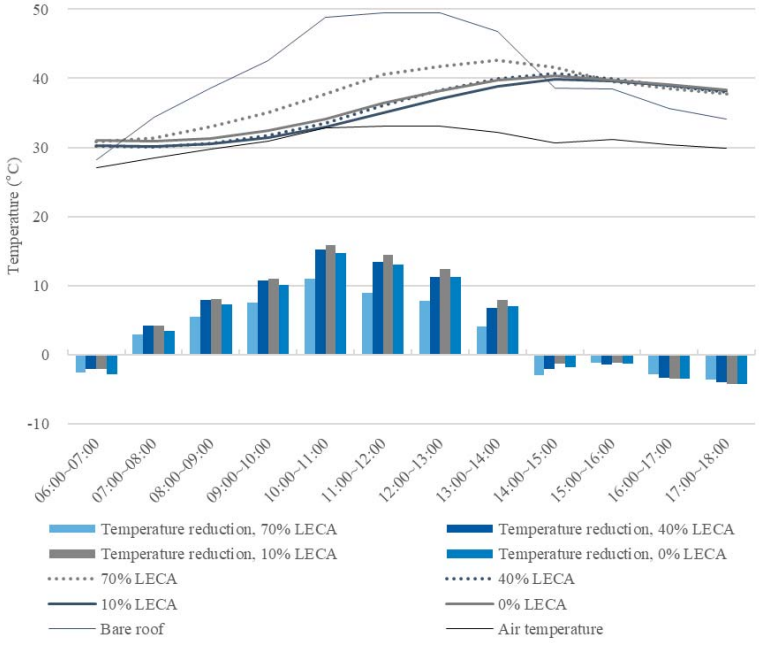

Figure 10. Temperatures and temperature reductions in the cases of the roofs with 0%, 10%, 40%, and 70% LECA laid at the bottom without plants (25 July 2017 06:00:09 to 25 July 2017 17:50:09).

Table 6. Temperature at the bottom of the extensive roofs and temperature reductions in the cases of the extensive roofs with 0%, 10%, 40%, and 70% LECA laid at the bottom without plants (25 July 2017 06:00:09 to 25 July 2017 17:50:09).

Thermocouple Position		06:00–07:00 (°C)	07:00–08:00 (°C)	08:00–09:00 (°C)	09:00–10:00 (°C)	10:00–11:00 (°C)	11:00–12:00 (°C)	12:00–13:00 (°C)	13:00–14:00 (°C)	14:00–15:00 (°C)	15:00–16:00 (°C)	16:00–17:00 (°C)	17:00–18:00 (°C)
In the air		27.04	28.49	29.73	30.93	32.87	33.15	33.06	32.16	30.70	31.20	30.37	29.90
Bare rooftop surface		28.20	34.32	38.59	42.53	48.78	49.47	49.51	46.73	38.59	38.41	35.64	34.09
At the bottom	0% LECA, no plants	31.05	30.93	31.32	32.40	34.08	36.42	38.26	39.74	40.37	39.74	39.04	38.28
	10% LECA, no plants	30.30	30.13	30.53	31.47	32.91	35.02	37.08	38.80	39.83	39.62	39.04	38.26
	40% LECA, no plants	30.20	30.11	30.64	31.80	33.57	36.07	38.21	39.96	40.68	39.87	38.97	38.01
	70% LECA, no plants	30.80	31.35	33.06	35.01	37.77	40.54	41.74	42.60	41.60	39.55	38.51	37.72
Temperature Reduction	0% LECA, no plants	−2.85	3.39	7.27	10.13	14.70	13.05	11.25	6.98	−1.78	−1.33	−3.40	−4.19
	10% LECA, no plants	−2.10	4.19	8.07	11.06	15.87	14.46	12.43	7.93	−1.24	−1.21	−3.40	−4.17
	40% LECA, no plants	−2.00	4.21	7.96	10.73	15.21	13.40	11.30	6.77	−2.09	−1.46	−3.33	−3.92
	70% LECA, no plants	−2.60	2.96	5.54	7.52	11.01	8.93	7.77	4.12	−3.01	−1.14	−2.88	−3.64

Table 7. Reductions in heat amplitude in the cases of the roofs with 0%, 10%, 40%, and 70% LECA laid at the bottom without plants (25 July 2017 06:00:09 to 26 July 2017 05:50:09).

Thermocouple Position		Average Temperature (°C)	Range of Temperature (°C)	Difference in Temperature (°C)	Heat Amplitude Reduction
In the air		29.13	26.33–33.94	7.61	-
Bare rooftop surface		34.35	26.38–52.24	25.86	-
At the bottom	0% LECA, no plants	35.13	30.90–40.46	9.56	63.03%
	10% LECA, no plants	34.46	30.09–39.94	9.85	61.91%
	40% LECA, no plants	34.55	30.04–40.78	10.74	58.47%
	70% LECA, no plants	35.56	30.72–42.77	12.05	53.40%

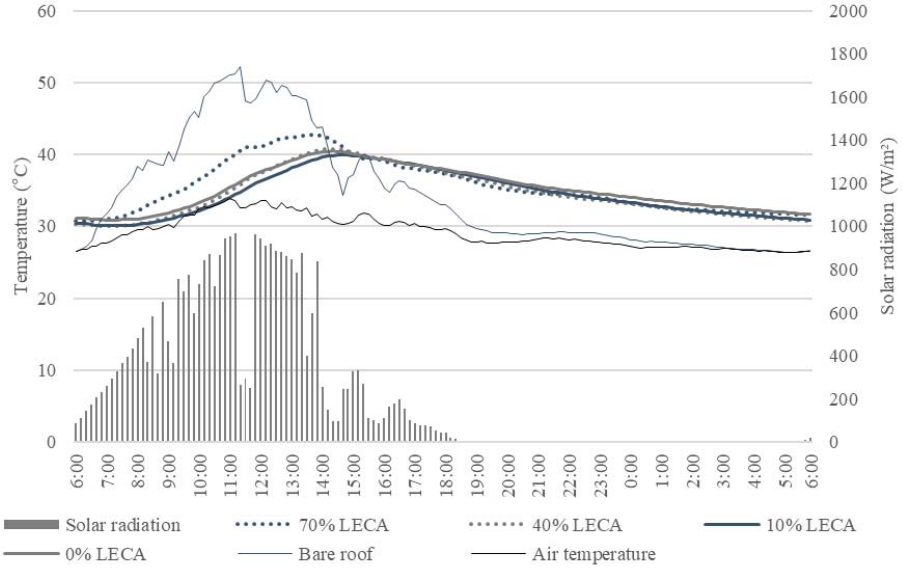

Figure 11. Temperatures and solar radiation in the cases of roofs with 0%, 10%, 40%, and 70% LECA laid at the bottom without plants (25 July 2017 06:00:09 to 26 July 2017 05:50:09).

3.3. Temperature Reduction When 10% and 40% LECA Were Laid at the Bottom without Plants and When 10% and 40% LECA Were Mixed with the Soil without Plants

The third stage (Figure 12) involved investigating the reductions in temperature and heat amplitude of the bare rooftop owing to the extensive roofs with 10% and 40% LECA laid at the bottom or mixed with the conventional garden soil without plants. Table 8 shows that the mean air and rooftop temperatures were 29.29 and 35.42 °C, respectively; the ranges of air and rooftop temperatures were 25.74–34.76 °C and 23.55–61.49 °C, respectively; the maximum solar radiation was 873.10 W/m^2; and the mean relative humidity was 80.93%. A period of 24 h was selected for further analysis based on the aforementioned criteria. The date selected was 24–25 September 2017 (Figure 13).

Because roofs with various proportions and placements of LECA without plants resulted in the insulation, absorption, and evaporation effects of the soil layer and the LECA layer, the roofs with 10% LECA and without plants exhibited a greater temperature reduction on the bare rooftop than did the roofs with 40% LECA and without plants. On 24 September from 07:00–14:00 (Table 9, Figure 14), when the average air and rooftop temperatures were 32.08 °C and 50.14 °C, respectively, the average bottom temperatures of the roofs with 10% and 40% LECA laid at the bottom and without plants were 36.32 and 37.26 °C, respectively; the average bottom temperatures of the roofs with 10% and 40% LECA

mixed with the soil and without plants were 36.22 and 38.63 °C, respectively. These results indicated that the roofs with 10% LECA laid at the bottom and mixed with the soil (both without plants) can reduce the average bare rooftop temperature by an additional 0.94 and 2.41 °C, respectively, than their counterparts with 40% LECA laid at the bottom and mixed with the soil (both without plants). If brief, the extensive roofs with 10% LECA and without plants demonstrated superior passive cooling performance compared with the extensive roofs with 40% LECA and without plants.

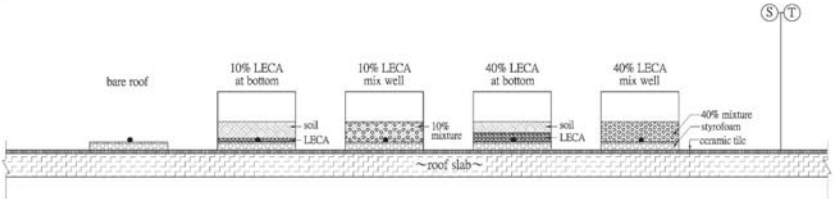

Figure 12. Experimental setup for the third stage.

Table 8. Weather data for the third stage (2017/09/20 06:08:41 to 2017/09/27 05:58:41).

Third Stage	Value
Period of measurement	20–27 September 2017
Range of air temperature	25.74–34.76 °C
Mean air temperature	29.29 °C
Range of rooftop temperature	23.55–61.49 °C
Mean rooftop temperature	35.42 °C
Maximum solar radiation	873.10 W/m^2
Mean relative humidity	80.93%
Date selected for further analysis (marked with dotted box)	24–25 September 2017

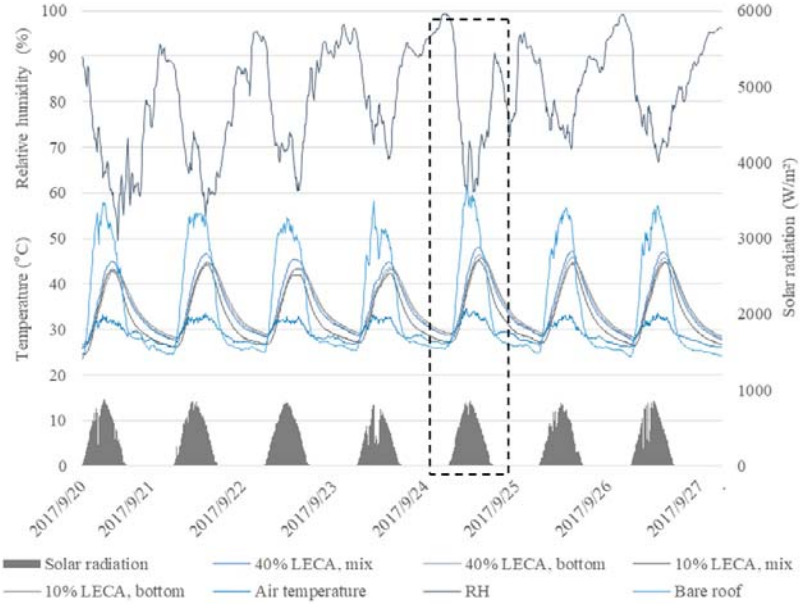

Figure 13. Temperatures, solar radiation, and relative humidity in the cases of roofs with 10% and 40% LECA laid at the bottom without plants, and of 10% and 40% LECA mixed with the soil without plants (20 September 2017 06:08:41 to 27 September 2017 05:58:41).

Table 9. Temperatures at the bottom of the roofs and temperature reductions in the cases of roofs with 10% and 40% LECA laid at the bottom without plants, and of 10% and 40% LECA mixed with the soil without plants (24 September 2017 06:08:41 to 24 September 2017 17:58:41).

Thermocouple Position		06:00–07:00 (°C)	07:00–08:00 (°C)	08:00–09:00 (°C)	09:00–10:00 (°C)	10:00–11:00 (°C)	11:00–12:00 (°C)	12:00–13:00 (°C)	13:00–14:00 (°C)	14:00–15:00 (°C)	15:00–16:00 (°C)	16:00–17:00 (°C)	17:00–18:00 (°C)
In the air		27.19	28.44	30.40	31.80	33.76	33.23	33.60	33.35	32.42	32.19	31.21	29.67
Bare rooftop surface		26.90	30.75	40.10	48.77	58.08	59.11	58.38	55.77	50.42	45.67	39.95	32.81
At the bottom	10% LECA, bottom, no plants	29.13	29.32	30.40	32.59	35.90	39.38	42.26	44.42	45.51	45.29	44.39	42.55
	10% LECA, mix, no plants	27.26	27.62	29.14	32.11	36.24	40.46	43.19	44.80	45.00	43.79	41.50	38.36
	40% LECA, bottom, no plants	28.74	29.12	30.60	33.28	37.26	41.06	43.78	45.74	46.24	45.27	43.93	41.80
	40% LECA, mix, no plants	28.78	29.34	31.19	34.31	38.88	42.99	45.96	47.72	47.84	46.23	44.21	41.36
Temperature reduction	10% LECA, bottom, no plants	−2.22	1.44	9.70	16.18	22.18	19.74	16.12	11.36	4.91	0.38	−4.44	−9.75
	10% LECA, mix, no plants	−0.36	3.14	10.96	16.66	21.84	18.65	15.19	10.97	5.42	1.88	−1.55	−5.55
	40% LECA, bottom, no plants	−1.83	1.64	9.50	15.49	20.83	18.06	14.60	10.04	4.18	0.40	−3.98	−9.00
	40% LECA, mix, no plants	−1.88	1.41	8.91	14.47	19.21	16.12	12.42	8.06	2.58	−0.56	−4.26	−8.55

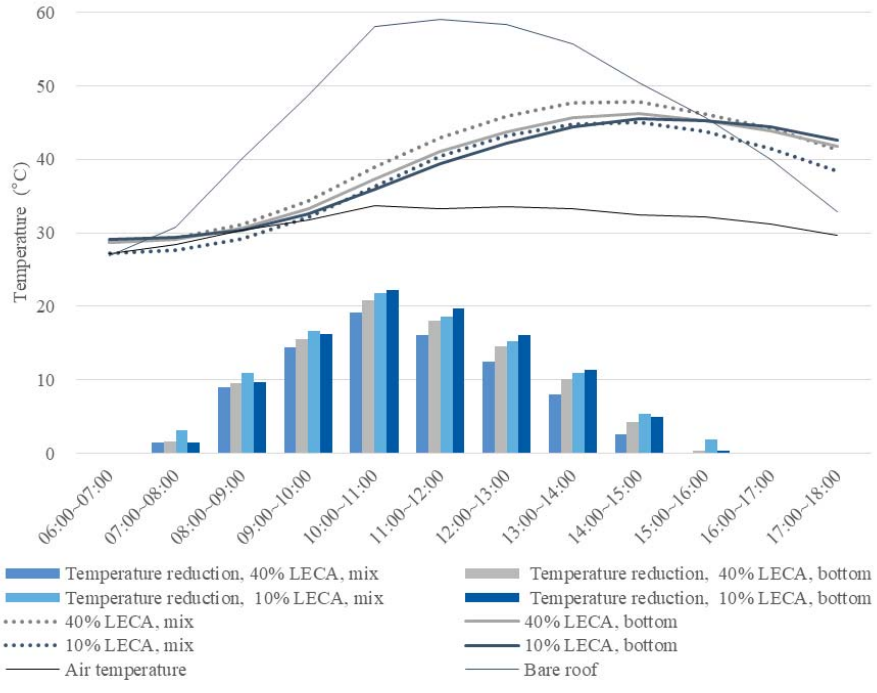

Figure 14. Temperatures and temperature reductions in the cases of the roofs with 10% and 40% LECA laid at the bottom without plants, and of 10% and 40% LECA mixed with the soil without plants (24 September 2017 06:08:41 to 24 September 2017 17:58:41).

All four extensive roofs containing different proportions and placements of LECA contributed to stabilizing the temperature of bare rooftop, which in turn mitigate the fluctuation of indoor temperatures and hence increased comfort level in the rooms underneath the roofs. Our experimental results revealed that the roofs with 10% LECA and without plants yielded a larger reduction in the heat amplitude of the bare rooftop than did the roof with 40% LECA and without plants. On 24–25 September (Table 10, Figure 15) when the average air and rooftop temperatures were 29.86 and 36.11°C, respectively, the roof with 10% LECA laid at the bottom and without plants (54.98%) reduced the heat amplitude of the bare rooftop by a further 3.10% more than the roof with 40% LECA laid at the bottom without plants (51.88%); the roof with 10% LECA mixed with the soil and without plants (50.98%) further reduced the heat amplitude of the bare rooftop by 3.68% more than the roof with 40% LECA mixed with the soil without plants (47.30%).

Table 10. Reduction in the heat amplitude in the cases of the roofs with 10% and 40% LECA laid at the bottom without plants, and of 10% and 40% LECA mixed with the soil without plants (24 September 2017 06:08:41 to 25 September 2017 05:58:41).

Thermocouple Position		Average Temperature (°C)	Range of Temperature (°C)	Difference inTemperature (°C)	Heat Amplitude Reduction
In the air		29.86	26.50–34.76	8.26	-
Bare rooftop surface		36.11	24.77–61.49	36.72	-
At the bottom	10% LECA, bottom, no plants	35.79	29.09–45.62	16.53	54.98%
	10% LECA, mix, no plants	33.89	27.19–45.19	18.00	50.98%
	40% LECA, bottom, no plants	35.96	28.72–46.39	17.67	51.88%
	40% LECA, mix, no plants	36.23	28.72–48.07	19.35	47.30%

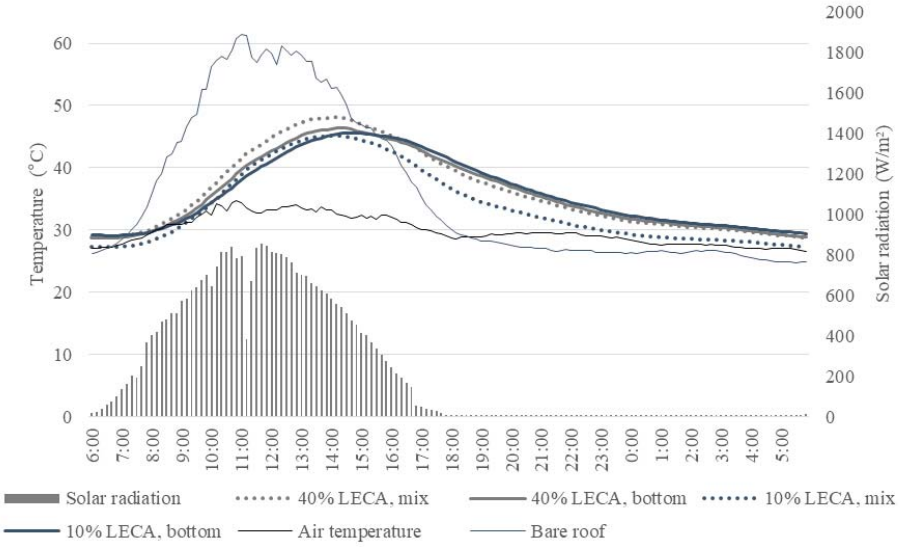

Figure 15. Temperatures and solar radiation in the cases of roofs with 10% and 40% LECA laid at the bottom without plants, and of 10% and 40% LECA mixed with the soil without plants (24 September 2017 06:08:41 to 25 September 2017 05:58:41).

3.4. Temperature Reduction When 10% and 40% LECA Were Laid at the Bottom with Plants and When 10% and 40% LECA Were Mixed with the Soil with Plants

The fourth stage (Figure 16) involved investigating the reductions in temperature and heat amplitude of the bare rooftop owing to the extensive roofs with 10% and 40% LECA laid at the bottom or mixed with the soil and with plants. Table 11 shows that the mean air and rooftop temperatures were 28.80 and 33.80 °C, respectively; the ranges of air temperature and rooftop temperature were 24.12–35.72 °C and 23.04–61.90 °C, respectively; the maximum solar radiation was 921.90 W/m^2; and the mean relative humidity was 82.15%. A period of 24 h was selected for further analysis based on the aforementioned criteria. The date selected was 1–2 October 2017 (Figure 17).

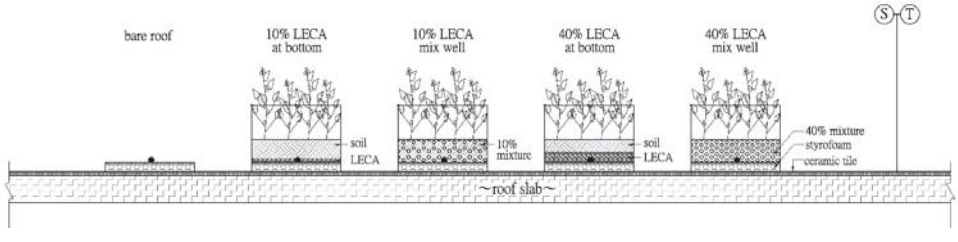

Figure 16. Experimental setup for the fourth stage.

Table 11. Weather data for the fourth stage (28 September 2017 06:07:57 to 13 October 2017 05:57:57).

Fourth Stage	Value
Period of measurement	28 September 2017–13 October 2017
Range of air temperature	24.12–35.72 °C
Mean air temperature	28.80 °C
Range of rooftop temperature	23.04–61.90 °C
Mean rooftop temperature	33.80 °C
Maximum solar radiation	921.90 W/m^2
Mean relative humidity	82.15%
Date selected for further analysis (marked with dotted box)	1–2 October 2017

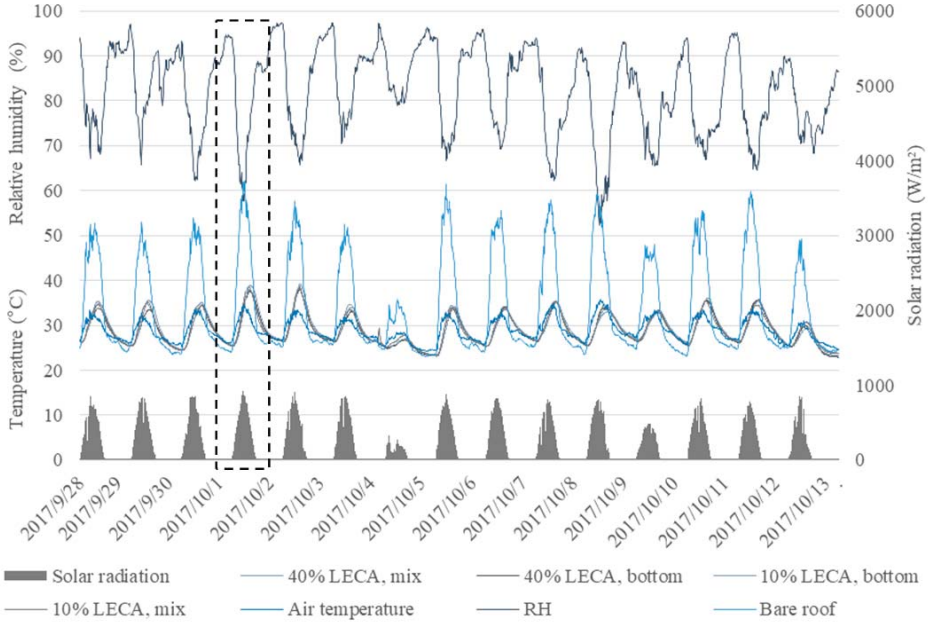

Figure 17. Temperatures, solar radiation, and relative humidity in the cases of roofs with 10% and 40% LECA laid at the bottom with *Ipomoea batatas*, and of 10% and 40% LECA mixed with soil with *Ipomoea batatas* (28 September 2017 06:07:57 to 13 October 2017 05:57:57).

Because roofs with various proportions and placements of LECA with plants resulted in the insulation, absorption, and evaporation effects of the soil and LECA layers as well as demonstrated additional reflective, photosynthetic, shielding, shading, and evapotranspiration effects on the *Ipomoea batata* layer, the roofs with 10% LECA with plants yielded a greater reduction in the bare rooftop surface temperature than roofs with 40% LECA with plants. On October 1 from 07:00–14:00 (Table 12, Figure 18), when the average air and rooftop temperatures were 32.04 °C and 50.53 °C, respectively, the average bottom temperatures of the roofs with 10% and 40% LECA laid at the bottom and with plants were 30.80 and 31.17 °C, respectively; the average bottom temperatures of the roofs with 10% and 40% LECA mixed with the soil and with plants were 31.80 and 32.09 °C, respectively. These results indicated that roofs with 10% LECA laid at the bottom and mixed with the soil (both with plants) can reduced the average rooftop temperature by an additional 0.36 and 0.29 °C more than their counterparts with 40% LECA laid at the bottom and mixed with the soil (both with plants), respectively. In brief, the extensive roof with 10% LECA and with plants demonstrated a slightly greater passive-cooling performance compared with the extensive roofs with 40% LECA and with plants.

Table 12. Temperatures at the bottom of the roofs and temperature reductions in the cases of the roofs with 10% and 40% LECA laid at the bottom with *Ipomoea batatas*, and of 10% and 40% LECA mixed with the soil with *Ipomoea batatas* (1 October 2017 06:07:57 to 1 October 2017 17:57:57).

Thermocouple Position		06:00–07:00 (°C)	07:00–08:00 (°C)	08:00–09:00 (°C)	09:00–10:00 (°C)	10:00–11:00 (°C)	11:00–12:00 (°C)	12:00–13:00 (°C)	13:00–14:00 (°C)	14:00–15:00 (°C)	15:00–16:00 (°C)	16:00–17:00 (°C)	17:00–18:00 (°C)
In the air		26.86	28.18	30.21	31.65	33.00	34.12	34.03	33.08	32.32	31.07	29.74	28.70
Bare rooftop surface		25.43	31.57	41.23	49.19	56.61	60.32	58.98	55.83	50.96	44.17	38.07	31.28
At the bottom	10% LECA, bottom, with plants	25.50	25.68	26.53	28.04	30.14	32.60	35.28	37.33	38.69	38.72	37.91	36.40
	10% LECA, mix, with plants	25.37	25.80	27.24	29.25	31.70	34.46	36.68	37.49	37.84	37.25	35.61	33.61
	40% LECA, bottom, with plants	25.31	25.74	26.99	28.73	31.13	33.45	35.51	36.62	37.55	37.31	36.44	34.97
	40% LECA, mix, with plants	25.57	25.98	27.17	29.28	32.19	34.69	37.09	38.24	38.46	37.35	36.02	34.46
Temperature reduction	10% LECA, bottom, with plants	−0.07	5.90	14.70	21.15	26.47	27.73	23.70	18.50	12.27	5.45	0.16	−5.13
	10% LECA, mix, with plants	0.06	5.77	13.99	19.95	24.90	25.87	22.31	18.35	13.12	6.93	2.46	−2.33
	40% LECA, bottom, with plants	0.12	5.84	14.24	20.46	25.47	26.87	23.47	19.22	13.41	6.86	1.64	−3.69
	40% LECA, mix, with plants	-0.14	5.59	14.06	19.91	24.42	25.64	21.89	17.60	12.50	6.82	2.06	−3.18

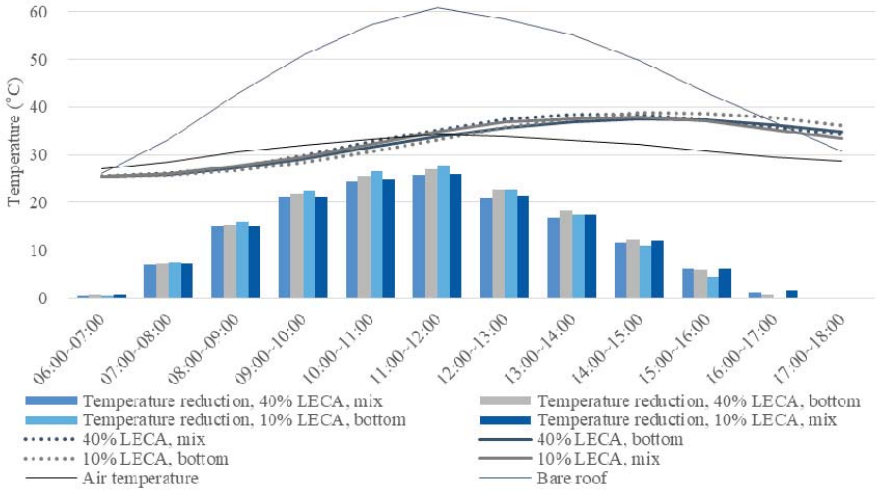

Figure 18. Temperatures and temperature reductions in the cases of the roofs with 10% and 40% LECA laid at the bottom with *Ipomoea batatas*, and of 10% and 40% LECA mixed with the soil with *Ipomoea batatas* (1 October 2017 06:07:57–1 October 2017 17:57:57).

The addition of the *Ipomoea batatas* layer caused additional evaporation and absorption effects on the growth medium layer as well as reflective, photosynthetic, shielding, shading, and evapotranspiration effects on the *Ipomoea batatas* layer as a result of irrigation. Our findings demonstrated that the planting of *Ipomoea batatas* contributed to additional and significant reductions in the rooftop surface temperature by 5–7 °C when results from the third and fourth stages were compared under slightly different average ambient temperatures (32.08°C in the third stage and 32.04 °C in the fourth stage). The roof with 10% LECA laid at the bottom and with plants (1 October 2017 07:00–14:00, 19.73 °C average temperature reduction of the bare rooftop) helped to reduce the average temperature of the bare rooftop by an additional 5.91°C than the roof with 10% LECA laid at the bottom and without plants (24 September 2017 07:00–14:00, 13.82 °C); the roof with 10% LECA mixed with the soil and with plants (same period, 18.73 °C) helped to reduce the average temperature of the bare rooftop by an additional 4.81 °C more than the roof with 10% LECA mixed with the soil and without plants (same period, 13.92 °C); the roof with 40% LECA laid at the bottom and with plants (same period, 19.37 °C) helped to reduce the average temperature of the bare rooftop by an additional 6.49 °C more than the roof with 40% LECA laid at the bottom and without plants (same period, 12.88 °C); the roof with 40% LECA mixed with the soil and with plants (same period, 18.44 °C) helped to reduce the average temperature of the bare rooftop by an additional 6.93 °C more than the roof with 40% LECA mixed with the soil and without plants (same period, 11.51 °C). In brief, the roofs with plants could elicit higher passive-cooling effects than roofs without plants.

All four extensive roofs containing different proportions and placements of LECA and plants contributed to stabilizing the temperature of bare rooftop, which in turn mitigate the fluctuation of indoor temperatures and hence increased comfort level in the rooms underneath the roofs. Generally speaking, our experimental results revealed that the roofs with 10% and 40% LECA with plants yielded similar reduction in the heat amplitude of the bare rooftop (64.32%–67.11%) (Table 13, Figure 19). Furthermore, our findings demonstrated that the planting of *Ipomoea batatas* contributed to additional reduction in the heat amplitude of the bare rooftop by 9.34% to 17.90% when the results from the third and fourth stages were compared under slightly different average ambient temperatures (32.08 °C in the third stage and 32.04 °C in the fourth stage). In brief, the planting contributed to significant reduction in the heat amplitude of bare rooftop.

Table 13. Reduction in heat amplitude in the cases of the roofs with 10% and 40% LECA laid at the bottom with *Ipomoea batata*, and of 10% and 40% LECA mixed with the soil with *Ipomoea batatas* (1 October 2017 06:07:57 to 2 October 2017 05:57:57).

Thermocouple Position		Average Temperature (°C)	Range of Temperature (°C)	Difference in Temperature (°C)	Heat Amplitude Reduction
In the air		29.30	26.26–34.41	8.15	-
Bare rooftop surface		35.77	24.29–61.90	37.61	-
At the bottom	10% LECA, bottom, with plants	30.89	25.48–38.90	13.42	64.32%
	10% LECA, mix, with plants	30.36	25.36–37.87	12.51	66.74%
	40% LECA, bottom, with plants	30.51	25.28–37.65	12.37	67.11%
	40% LECA, mix, with plants	30.81	25.55–38.64	13.09	65.20%

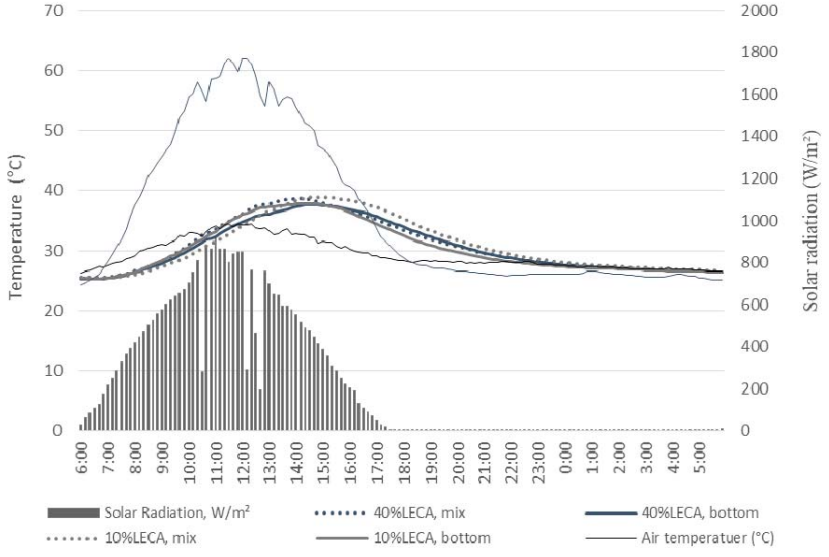

Figure 19. Temperatures and solar radiation in the cases of roofs with 10% and 40% LECA laid at the bottom with *Ipomoea batata*, and of 10% and 40% LECA mixed with the soil with *Ipomoea batatas* (1 October 2017 06:07:57 to 2 October 2017 05:57:57).

Table 14 presents the information we collected regarding treatments, average air temperatures, and average rooftop temperature reductions for the purpose of conveniently comparing four stages to draw the most important conclusions from the details in each stage. In summary, the findings from the four stages demonstrated that, first, under slightly different average air temperature (0.56 °C; i.e., 32.04 °C minus 31.48 °C), the combined effects of LECA and *Ipomoea batata* significantly reduced the average temperature of the bare rooftop by an additional 10.19 °C, or 106.81%, as can be seen by the additional bare-rooftop temperature reduction from 9.54 °C (0% LECA without plants in the second stage) to 19.73 °C (10% LECA with plants in the fourth stage). Second, at slightly different air temperatures, *Ipomoea batata* further reduced the average temperature of the bare rooftop from 4.81 to 6.93 °C (based on the results from the third and fourth stages), whereas the 10%–40% LECA could only further reduce the average temperature of the bare rooftop from 0.4 to 1.03 °C (based on the results from the second stage). Nevertheless, because the unit weight of the roof with 0% LECA (conventional garden soil) after irrigation would have reached 135.95 kg/m^2 (Table 15), which would exceed the designed live load of 200 kg/m^2 if an adult with a normal weight (60 kg) was introduced, using LECA to partly replace the conventional garden soil is highly recommended.

Table 14. Comparisons of the passive-cooling effects for four stages.

Stage	Treatment	Average Air Temperature (°C)	Average Rooftop Temperature Reduction (°C)	Conclusions
First stage	0% LECA, 10 cm	29.18	11.45	• Although the 0% LECA roof with the growth-medium depth of 25 cm demonstrated the greatest passive-cooling effect, the 0% LECA roof with a growth-medium depth of 10 cm, in yielding the highest marginal temperature reduction, demonstrated the most efficient passive-cooling effect.
	0% LECA, 15 cm		12.82	
	0% LECA, 20 cm		14.19	
	0% LECA, 25 cm		14.46	
Second stage	0% LECA, 10 cm, bottom, no plant	31.48	9.54	• The roofs with 10% and 40% LECA had slightly greater passive-cooling effects (by 0.4–1.03 °C) than did the roof with 0% LECA. • The roof with 10% LECA had a slightly greater passive-cooling effect (by 0.63°C) than did the roof with 40% LECA.
	10% LECA, 10 cm, bottom, no plant		10.57	
	40% LECA, 10 cm, bottom, no plant		9.94	
	70% LECA, 10 cm, bottom, no plant		6.84	
Third stage	10% LECA, 10 cm, bottom, no plant	32.08	13.82	• Comparing the results for the second, third and fourth stages, the roofs with 10% LECA, regardless of whether the LECA was laid at the bottom or mixed with the soil, demonstrated slightly greater passive-cooling effects than did roofs with 40% LECA. • Without plants (second and third stages), the roofs with 10% LECA slightly reduced the average temperature of the bare rooftop by an additional 0.63–2.41 °C more than roofs with 40% LECA. • With plants (fourth stage), the roofs with 10% LECA slightly reduce the average temperature of the bare rooftop by an additional 0.31–0.35 °C more than roofs with 40% LECA.
	10% LECA, 10 cm, mixed, no plant		13.92	
	40% LECA, 10 cm, bottom, no plant		12.88	
	40% LECA, 10 cm, mixed, no plant		11.51	
Fourth stage	10% LECA, 10 cm, bottom, with plants	32.04	19.73	• At slightly different average air temperatures (0.04 °C), 32.08 °C in the third stage versus 32.04 °C in the fourth stage, planting helped to significantly reduce the average temperature of the bare rooftop by an additional 4.81–6.93 °C. • At slightly different average air temperatures (0.56 °C), 31.48 °C in the second stage versus 32.04 °C in the fourth stage, the combined effects of 10% LECA and plants helped to significantly reduce the average temperature of the bare rooftop by an additional 10.19°C (19.73 °C minus 9.54 °C).
	10% LECA, 10 cm, mixed, with plants		18.73	
	40% LECA, 10 cm, bottom, with plants		19.37	
	40% LECA, 10 cm, mixed, with plants		18.44	

Note: The dates selected for the first, second, third, and fourth stages were 14 May 2017, 25 July 2017, 24 September 2017 and 1 October 2017, respectively. To standardize the temperature calculations for comparison across stages, the time slot selected for calculating the "average air temperature" and the "average rooftop temperature reduction" was from 07:00 to 14:00 on the same day for all four stages. The depth of the growth medium was 10 cm for the second, third, and fourth stages.

Table 15. Cost–benefit analysis of the LECA extensive roofs.

The Roofs with LECA Laid at the Bottom and Without Plants (Decision)	Unit Weight of Growth Medium Before Irrigation (kg/m^2)	Unit Weight of Growth Medium after Irrigation (kg/m^2)	Saturated Water Weight (kg)	Estimated Unit Cost ($US Dollars/$m^2$)	Total Weight before Irrigation (kg) (per Unit Building, Green Roof Area 42 m^2 or 452 ft^2)	Total Weight after Irrigation (kg) (per Unit Building, Green Roof Area 42 m^2 or 452 ft^2)	Estimated Total Cost of Growth Medium per Unit Building ($US dollar)	Average Rooftop Temperature Reduction (°C)	Heat Amplitude Reduction (%)
0% LECA roof, (benchmark)	81.27	135.95	54.68	21.67	3413.34	5709.90	910.14	9.54	63.03
10% LECA roof (preferred)	76.71	126.38	49.67	23.07	3221.82 (cut by 191.52 kg, 5.6%, 3 adults)	5307.96 (cut by 401.94 kg, 7.0%, 7 adults)	968.94 (US$58.8 more)	10.57	61.91
40% LECA roof (preferred)	63.02	97.69	34.67	27.26	2646.84 (cut by 766.50 kg, 22.5%, 13 adults)	4102.98 (cut by 1606.92 kg, 28.1%, 27 adults)	1144.92 (US$234.8 more)	9.94	58.47
70% LECA roof (not preferred)	49.32	69.00	19.68	31.44	2071.44	2898.00	1320.48	6.84	53.40

Note: Because soil costs New Taiwan (NT) $200 (US$6.67) per bag (25.0 kg or 55.1 lbs.), soil costs NT$0.008/g. Because LECA costs NT$360 (US$12) per bag (12 kg or 26.5 lbs.), LECA costs NT$0.03/g. The average rooftop area of a residential townhouse in Taiwan is approximately 60.0 m^2 (L × W =15 m × 4 m) or 645.5 ft^2. Given that the average surface area of a set of stairs is approximately 9 m^2 or 96.8 ft^2 and the average surface area of a path on a bare rooftop is approximately 9 m^2 (L × W =15 m × 0.6 m), the surface area of a green-roof system is approximately 42 m^2 (60 m^2 −9 m^2–9 m^2) or 452 ft^2 per unit building. NT$ to US$ = 30:1. m^2 to ft^2 = 1:10.758. kg to lbs = 1:2.205. The time slot selected to calculate the "average rooftop temperature reduction" was from 07:00 to 14:00 of the same day.

3.5. Weight-Reduction-and-Cost Analysis of the Extensive Roofs Containing LECA

According to the results of the weight-reduction-and-cost analysis (Table 15), the growth medium alone constantly yields a weight load of 135.95 kg/m^2 on the rooftop structure when the roof with 0% LECA (conventional garden soil) is applied after irrigation in 100% saturation. By further including the weight loads of other supplementary structures—the filter fabric, the drainage layer, the root barrier, and the supporting racks, for example—of the extensive roof system, the total weight load can easily exceed the designed live load of 200 kg/m^2 if *an* adult is introduced. As a result, an extensive roof system with lightweight growth medium is preferred and needed. Based on the results obtained in the second stage, the roofs designed with 10% or 40% LECA were revealed to be not only lighter than those without LECA but also to provide a slightly additional passive-cooling effect for the bare rooftop. Compared with the roof with 0% LECA, the roof with 10% LECA laid at the bottom—despite costing an additional US$58.8 dollars per unit building—can slightly reduce the average temperature of the bare rooftop by additional 1.03 °C (from 9.54 to 10.57 °C) and alleviate the weight load on the building structure by 191.52 kg or 422.30 lbs. (equivalent to 3 adults, assumed 1 adult equaling 60.00 kg or 132.30 lbs.) and 401.94 kg or 886.28 lbs. (7 adults) before and after irrigation, respectively. Compared with the roof with 0% LECA, the roof with 40% LECA—despite costing an additional US$234.8 dollars per unit building—can slightly reduce the temperature of the bare rooftop by additional 0.40 °C (from 9.54 to 9.94 °C) and significantly reduce the weight load on the building structure by 766.50 kg or 1690.13 lbs. (13 adults) and 1606.92 kg or 3543.26 lbs. (27 adults) before and after irrigation, respectively. If brief, although the additional thermal reduction in the bare rooftop in the roofs with 10%–40% LECA was not as high as one might expect, the greatest contribution of the LECA roofs was the increase in building safety resulting from the alleviation of the constant weight load to which the building structure is subjected.

4. Conclusions

Stressful lifestyles compel humans to seek temporary retreats. Both gazing at natural landscapes and participating in agricultural activities can help to reduce stress, promote positive mood and psychophysiological restoration, and improve mental health. Because most buildings, in an effort to reduce construction costs, are designed only to meet minimum legal requirements for structural live load, the development of lightweight growth mediums for the extensive green-roof systems is needed. Whether lighter green roof systems can be developed to yield superior thermal performance and to serve as food sources for a city lacking agricultural sites and temporary retreat sites is a question of interest. In this paper, we demonstrated that, at a slightly different average air temperature (0.56 °C), the combined effects of LECA and the planting of *Ipomoea batatas* helped to significantly reduce the average temperature of the bare rooftop by an additional 10.19 °C (from 9.54 °C to 19.73 °C) compared with the temperature of the roof with conventional garden soil of the same depth (10 cm) and without plants. Our key conclusions are as follows:

- Because of the evapotranspiration, shading, shielding, reflective, and photosynthetic effects of the vegetation layer, the roofs with *Ipomoea batata* exhibited significantly higher passive-cooling effects than did the roofs without *Ipomoea batata*.
- Because of the air pockets inside and between particles in LECA, the roofs with 10% and 40% LECA had slightly greater passive-cooling effects than did the roofs with 0% LECA (conventional garden soil).
- At a slightly different average air temperature (0.56 °C; i.e., 32.04 °C minus 31.48 °C), the combined effects of LECA and *Ipomoea batata* helped to significantly reduce the average temperature of the bare rooftop by an additional 10.19 °C, or by 106.81% (temperature reduction of the bare rooftop increased from 9.54 °C in 0% LECA without plants in the second stage to 19.73 °C in 10% LECA with plants in the fourth stage).

- LECA reduces the effect of heat-amplitude reduction, whereas *Ipomoea batata* helps to strengthen this effect. The roofs with 10–40% LECA and *Ipomoea batata* helped to reduce the heat amplitude of the bare rooftop by approximately 65%.
- Although the 40% and 10% LECA roofs in the second stage demonstrated a similar performance in reducing the temperature of the bare rooftop (only different by 0.63 °C), after irrigation, the roofs with 40% and 10% LECA were able to reduce the weight load by 1606.92 kg (3543.26 lbs, 27 adults) and 401.94 kg (886.28 lbs, 7 adults) per unit building, respectively.

In summary, compared with the use of roofs with the conventional garden soil and containing no LECA and no plants of the same depth (10 cm), we recommend the use of roofs with 40% LECA and *Ipomoea batata* to achieve significant temperature reductions in bare rooftop, alleviating the weight load of building structures and providing a nutritious, low-maintenance, and year-round food supply. In the future, we suggest comparing thermal performance in absolute terms by simultaneously arranging the experimental blocks with and without plants when more equipment becomes available. Second, because it was the plant material rather than LECA that helped to elicit significant passive-cooling effects in the bare rooftops and reduce the carbon dioxide emissions resulting from transporting food from farm to table, we suggest that in the future more species of vegetables be explored for their adaptability on rooftops and passive-cooling performances in extensive green-roof systems. Third, we also suggest other lightweight growth mediums be explored for their potential thermal performance in reducing the temperature and heat amplitude of the bare rooftops.

Author Contributions: Conceptualization, Y.-Y.H.; Methodology, Y.-Y.H.; Software, T.-J.M.; Validation, Y.-Y.H.; Formal Analysis, Y.-Y.H.; Investigation, T.-J.M.; Resources, Y.-Y.H.; Data Curation, Y.-Y.H.; Writing-Original Draft Preparation, Y.-Y.H.; Writing-Review & Editing, Y.-Y.H.; Visualization, T.-J.M.; Supervision, Y.-Y.H.; Project Administration, Y.-Y.H.; Funding Acquisition, Y.-Y.H.

Funding: This research received no external funding.

Acknowledgments: The authors express their sincere thanks to Yen-Chi Tsai for preparing Figure 4, Figure 8, Figure 12, and Figure 16. The authors also thanks Department of Landscape Architecture and Wen-Tsan Liu for providing experiment equipment.

Conflicts of Interest: The authors declare no conflict of interest.

References

1. Frumkin, H. Beyond toxicity: Human health and the natural environment. *Am. J. Prev. Med.* **2001**, *20*, 234–240. [CrossRef]
2. McEwen, B.S. Protective and damaging effects of stress mediators. *N. Engl. J. Med.* **1998**, *338*, 171–179. [CrossRef] [PubMed]
3. Sluiter, J.K.; Frings-Dresen, M.H.W.; Meijman, T.F.; van der Beek, A.J. Reactivity and recovery from different types of work measured by catechol amines and cortisol: A systematic literature overview. *J. Occup. Environ. Med.* **2000**, *57*, 298–315. [CrossRef]
4. Kaplan, R. Some psychological benefits of gardening. *Environ. Behav.* **1973**, *5*, 145–162. [CrossRef]
5. Ulrich, R.S. Visual landscapes and psychological well-being. *Landsc. Res.* **1979**, *4*, 17–23. [CrossRef]
6. Hartig, T.; Book, A.; Garvill, J.; Olsson, T.; Garlilng, T. Environmental influences on psychological restoration. *Scand. J. Psychol.* **1995**, *37*, 378–393. [CrossRef]
7. Ulrich, R.S.; Simons, R.F.; Losito, B.D.; Fiorito, E.; Miles, M.A.; Zelson, M. Stress recovery during exposure to natural and urban environments. *J. Environ. Psychol.* **1991**, *11*, 201–230. [CrossRef]
8. Van den Berg, A.; Koole, S.L.; Van der Wulp, N.Y. Environmental preference and restoration: (How) are they related? *J. Environ. Psychol.* **2003**, *23*, 135–146. [CrossRef]
9. Heliker, D.; Chadwick, A.; O'Connell, T. The meaning of gardening and the effects on perceived well being of a gardening project on diverse populations of elders. *Act. Adapt. Aging* **2000**, *24*, 35–56. [CrossRef]
10. Liu, T.C.; Shyu, G.S.; Fang, W.T.; Liu, S.Y.; Cheng, B.Y. Drought tolerance and thermal effect measurements for plants suitable for extensive green roof planting in humid subtropical climates. *Energy Build.* **2012**, *47*, 180–188. [CrossRef]

11. Karachaliou, P.; Santamouris, M.; Pangalou, H. Experimental and numerical analysis of the energy performance of a large scale intensive green roof system installed on an office building in Athens. *Energy Build.* **2016**, *114*, 256–264. [CrossRef]
12. Peng, L.L.H.; Jim, C.Y. Green-roof effects on neighborhood microclimate and human thermal sensation. *Energies* **2013**, *6*, 589–618. [CrossRef]
13. Abuseif, M.; Gou, Z. A review of roofing methods: Construction, features, heat reduction, payback period and climatic responsiveness. *Energies* **2018**, *11*, 3196. [CrossRef]
14. My Garden. *Family Farm*; My House Publishing: Taipei, Taiwan, 2011.
15. Construction and Planning Agency. Ministry of the Interior, Architectural Regulations: Weight Load Section. Available online: http://w3.cpami.gov.tw/law/law/lawe-2/b-rule.htm/ (accessed on 14 October 2017).
16. Dunnett, N.; Nolan, A. The effect of substrate depth and supplementary watering on the growth of nine herbaceous perennials in a semi-extensive green roof. *Acta Hortic.* **2004**, *643*, 305–309. [CrossRef]
17. Papafotiou, M.; Pergialioti, N.; Tassoula, L. Growth of native Aromatic Xerophytes in an extensive Mediterranean green roof as affected by substrate type and depth and irrigation frequency. *HortScience* **2013**, *48*, 1327–1333.
18. Kotsiris, G.; Nektarios, P.A.; Paraskevopoulou, A.T. Lavandula angustisfolia growth and physiology is affected by substrate type and depth when grown under Mediterranean semi-intensive green roof conditions. *HortScience* **2012**, *47*, 311–317.
19. Nektarios, P.A.; Amountzias, L.; Kokkinou, I.; Ntoulas, N. Green roof substrate type and depth affect the growth of the native species Dianthus fruticosus under reduced irrigation regimens. *HortScience* **2011**, *46*, 1208–1216.
20. Ntoulas, N.; Kektarios, P.A.; Spaneas, K.; Kadoglou, N. Semi-extensive green roof substrate type and depth effects on Zoysia matrella "Zeon" growth and drought tolerance under different irrigation regimes. *Acta Agric. Scand. Sect. B—Soil Plant Sci.* **2012**, *62* (Suppl. 1), 165–173. [CrossRef]
21. Kotsirisa, G.; Nektariosa, P.A.; Ntoulasa, N.; Kargasb, G. An adaptive approach to intensive green roofs in the Mediterranean climate region. *Urban Urban Gree* **2013**, *12*, 380–392. [CrossRef]
22. Lin, Y.J.; Lin, H.T. Thermal performance of different planting substrates and irrigation frequencies in extensive tropical rooftop greeneries. *Build. Environ.* **2011**, *46*, 345–355. [CrossRef]
23. Wanphen, S.; Nagano, K. Experimental study of the performance of porous materials to moderate the roof surface temperature by its evaporative cooling effect. *Build. Environ.* **2009**, *44*, 338–351. [CrossRef]
24. Sutcu, M. Influence of expanded vermiculite on physical properties and thermal conductivity of clay bricks. *Ceram. Int.* **2015**, *41*, 2819–2827. [CrossRef]
25. Central Weather Bureau. Climate Statistics for Temperature. Available online: http://e-service.cwb.gov.tw/HistoryDataQuery/index.jsp/ (accessed on 31 October 2017).
26. Boudaghpour, S.; Hashemi, S. A study on light expended clay aggregate (LECA) in a Geotechnical view and its application on greenhouse and greenroof cultivation. *Int. J. Geol.* **2008**, *4*, 59–63.
27. Mun, K.J. Development and tests of lightweight aggregate using sewage sludge for nonstructural concrete. *Constr. Build. Mater.* **2007**, *21*, 1583–1588. [CrossRef]
28. Arioz, O.; Kilinc, K.; Karasu, B.; Kaya, G.; Arslan, G.; Tuncan, M.; Tuncan, A.; Korkut, M.; Kivrak, S. A preliminary research on the properties of lightweight expanded clay aggregate. *J. Aust. Ceram. Soc.* **2008**, *44*, 23–30.
29. Sales, A.; Souza, F.R.; Santos, W.N.; Zimer, A.M.; Almeida, F.C.R. Lightweight composite concrete produced with water treatment sludge and sawdust: Thermal properties and potential application. *Constr. Build. Mater.* **2010**, *24*, 2446–2453. [CrossRef]
30. Zhang, B.; Poon, C.S. Use of furnace ash for producing lightweight aggregate concrete with thermal insulation properties. *J. Clean. Prod.* **2015**, *99*, 94–100. [CrossRef]
31. Song, U.; Kim, E.; Bang, J.H.; Son, D.J.; Waldman, B.; Lee, E.L. Wetlands are an effective green roof system. *Build. Environ.* **2013**, *66*, 141–147. [CrossRef]
32. Huang, Y.Y.; Chen, C.T.; Tsai, Y.C. Reduction of temperatures and temperature fluctuations by hydroponic green roofs in a subtropical urban climate. *Energy Build.* **2016**, *129*, 174–185. [CrossRef]
33. He, Y.; Yu, H.; Dong, N.; Ye, H. Thermal and energy performance assessment of extensive green roof in summer: A case study of a lightweight building in Shanghai. *Energy Build.* **2016**, *127*, 762–773. [CrossRef]
34. Jaffal, I.; Ouldboukhitine, S.E.; Belarbi, R. A comprehensive study of the impact of green roofs on building energy performance. *Renew. Energy* **2012**, *43*, 157–164. [CrossRef]

35. Jim, C.Y.; Peng, L.L.H. Weather effect on thermal and energy performance of an extensive tropical green roof. *Urban Urban Gree* **2012**, *11*, 73–85. [CrossRef]
36. Wong, N.H.; Tan, P.Y.; Chen, Y. Study of thermal performance of extensive rooftop greenery systems in the tropical climate. *Build. Environ.* **2007**, *42*, 25–54. [CrossRef]

energies

MDPI

Article

Prediction Model Based on an Artificial Neural Network for User-Based Building Energy Consumption in South Korea

Seunghui Lee [1], Sungwon Jung [1,*] and Jaewook Lee [2]

[1] Department of Architecture, Sejong University, Seoul 05006, Korea; softbutter25@sju.ac.kr
[2] Department of Architectural Engineering, Sejong University, Seoul 05006, Korea; jaewook@sejong.ac.kr
* Correspondence: swjung@sejong.ac.kr; Tel.: +82-02-3408-3289

Received: 20 January 2019; Accepted: 13 February 2019; Published: 15 February 2019

Abstract: The evaluation of building energy consumption is heavily based on building characteristics and thus often deviates from the true consumption. Consequently, user-based estimation of building energy consumption is necessary because the actual consumption is greatly affected by user characteristics and activities. This work aims to examine the variation in energy consumption as a function of user activities within the same building, and to employ an artificial neural network (ANN) to predict user-based energy consumption. The study exploited the actual 24-h schedules of 5240 single-person households and computed the respective energy consumption using EnergyPlus V 8.8.0 software. The calculated values were clustered according to gender, age, occupation, income, educational level, and occupancy period and the difference among them was analyzed. The simulation results showed that for single-person households in Korea, females used more energy than males did, and the difference increased with age. Furthermore, unemployed and low-income individuals consumed more energy whereas consumption was inversely proportional to the educational level. Energy consumption increased with the occupancy period. Based on the simulation results and six user characteristics, the ANN model indicated a correlation between user characteristics and energy usage. This study analyzed the differences in energy usage depending on user activity and characteristics that affect building energy consumption.

Keywords: artificial neural network; big data; energy-performance gap; building energy prediction; building user activity; single-person household; Korean household energy consumption

1. Introduction

Buildings are responsible for a high percentage of CO_2 emissions in cities as well as 40% of the total energy consumption worldwide [1]. Many countries have passed environmental laws and policies to increase the energy efficiency of new buildings and to promote green remodeling of existing buildings for improved efficiency. Subsequently, building energy performance assessments are conducted according to national standards and performance ratings must be disclosed during real estate transactions. In Europe, for instance, all countries registered in Energy Performance of Building Directives (EPBD) since 2009 are required to disclose the building energy performance rating to the market. A similar policy has been adopted by the city of Seoul, Korea since 2013 and is gradually expanding to other cities to raise awareness and encourage the development of energy-efficient buildings, green remodeling revitalization.

The conventional approach to the evaluation of energy consumption often yields inaccurate estimates. Majcen et al. observed that the total amount of energy used by the occupants of buildings with a high energy performance rating was higher than the estimated value [2]. Researchers refer to this discrepancy between actual and predicted energy usage as the "energy–performance gap" [3].

The fact that current building energy performance assessments are based heavily on the physical building characteristics rather than the actual characteristics and activities of building occupants is responsible for introducing the energy–performance gap. According to Al-Zubaidy and Kaddory, building energy consumption may vary by factors of 0.5–2.8, depending on the user [4].

The building energy performance rating is publicly disclosed in an effort to promote the voluntary revitalization of the energy performance of buildings. Nonetheless, the provision of accurate building information to users is challenging because of the "Energy-performance Gap." Moreover, even though the building performance enhancement before and after green remodeling can be assessed objectively, the energy consumption variation between two or more occupants is difficult to evaluate. However, occupant characteristics and activities must be considered along with building characteristics when predicting the energy consumption to enhance the accuracy of energy information provided to buyers and residents.

This study analyzes the influence of users on the energy usage of buildings and proposes the possibility of predicting energy usage considering users' characteristics and activities. This study combines energy simulations and an artificial neural network (ANN) to examine the variation in building energy consumption with respect to user activities and characteristics within the same building. A model for energy consumption forecasting is then constructed based on the analysis.

2. Literature Review

2.1. Effects of Occupant Characteristics on Energy Consumption

Various researchers have demonstrated that occupants affect the building energy consumption the most, and they are also the primary cause of the "Energy-performance Gap" [5–8]. Several previous studies have investigated the variation in energy consumption as a function of the actual occupant characteristics and activities. For example, Van den Brom et al. analyzed information from 1.4 million households and observed a variation in energy consumption according to income and age [3], whereas Guerra-Santin showed energy usage to be directly proportional to education level [9]. Schipper et al. and Noh demonstrated variation in energy consumption as a function of the occupancy period because of different lifestyles [10,11], whereas Räty observed that the energy consumption varied with respect to the gender of the occupant [12]. Jones et al. reported that population socioeconomic characteristics affect the use of indoor electrical energy [13].

The differences in the aforementioned demographic, social, and economic characteristics of the occupants give rise to distinct daily activities. These activities determine user-dependent indoor energy usage in terms of cooling, heating, lighting, the use of appliances which eventually results in various energy consumption profiles. In this work, the energy usage is computed as a function of the activities of the occupant, and its correlation with the demographic, social, and economic characteristics of the occupants is examined to study the variations in user-based energy consumption.

2.2. Building Energy Performance Assessment Methods

Two building energy performance assessment methods exist. The asset rating (AR) method computes energy consumption by taking into account the physical characteristics of buildings whereas the operational rating (OR) method is based on the actual energy usage of a building [14].

The AR method determines the energy consumption with simulation tools that consider the floor plan, installation, and construction materials of a building when evaluating the energy performance of a building. Although the AR method allows for objective performance assessment based on building characteristics, the variation in consumption as a function of occupant activities cannot be easily examined. A number of tools are available to evaluate the dynamic building load by taking into account the standard building schedule and the number of occupants, but they cannot consider the indoor energy usage and usage hours accurately. The ECO2 software, which is used widely in

Korea for building performance assessment, cannot take the operational schedule of the building into account [15].

The OR method evaluates energy consumption by importing the actual data pertaining to building energy usage over a time period from utility bills or companies. However, consistent building use over a significant time period is necessary because the evaluation is based on actual measurements. Patterns must be identified from large data sets or probabilistic forecasting is necessary to analyze the correlation between the energy consumption of a particular building and user activities and characteristics. Data collection, however, typically requires a prolonged measurement period and the prediction of random user activities poses clear limitations [14,15].

Both of the aforementioned methods are restrictive in terms of obtaining variations in user-based energy consumption. This work exploits the AR method, which takes the detailed building characteristics into account for simulations, to complement the drawbacks of the OR method, which takes the actual user activities into consideration. The simulations that were conducted as part of the present study used EnergyPlus V 8.8.0, which is a dynamic simulation tool capable of reflecting the indoor energy usage and occupant characteristics with sufficient accuracy. In addition, we controlled the physical variables in the same building and studied the changes in user-based energy consumption using actual activity data from 5240 residents. This work contributes to the ultimate reduction in building energy consumption by making it easier to identify and predict user-based building energy consumption for the purpose of real estate transactions or building remodeling.

3. Materials and Methods

3.1. Research Method and Procedure

The present study utilizes data from the "Korean Time Using Survey" provided by Statistics Korea. The data relate to the activities and characteristics of 5240 users and were used to investigate variations in user-based energy consumption [16]. In addition, EnergyPlus V 8.8.0 software and ANN, a multi-variate machine-learning method, were employed to construct a prediction model encompassing both user activities and characteristics. The study was conducted as illustrated in Figure 1.

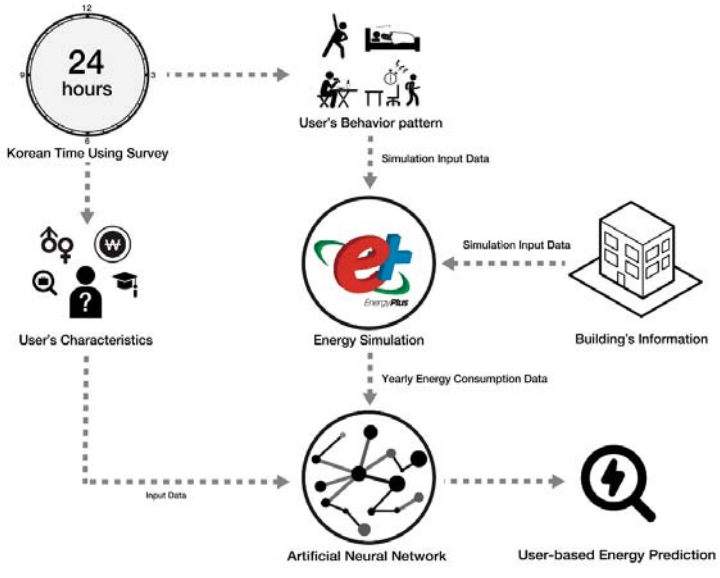

Figure 1. Flow chart depicting research process.

EnergyPlus is a dynamic simulation program that is used to compute energy consumption as a function of user activities in the same building. The data referenced in the simulation were the daily activity schedules of 5240 single-person households in Korea from the "2014 Korean Time Using Survey" compiled by Statistics Korea. The annual energy consumption was calculated based on user activity schedules and was then clustered according to the following user characteristics: income, age, level of education, occupancy time, gender, and occupation. This approach enabled us to examine variations in the energy consumption with respect to these six distinct characteristics. Subsequently, the validated user characteristics and simulated annual energy consumption were used to devise a model for energy consumption forecasting based on an ANN machine-learning approach as a function of the six user characteristics.

3.2. 2014 Korean Time Using Survey

This work utilized single-person household data from "2014 Korean Time Using Survey" conducted by Statistics Korea [16]. The number of single-person households is increasing rapidly worldwide due to aging, changes in perception. Therefore, governments must perceive single-person households as a major type of household and devise concrete policies and energy reduction plans accordingly. Hence, this study focused on single-person households and analyzed the energy consumption according to their characteristics and activities.

The survey data included approximately 12,000 Korean households with members of age 10 or older and can be divided largely into two sets. Table 1 lists the gender, age, occupation, income, educational level. as the characteristics of each household member and Table 2 presents the 24-h activity log of each household member recorded at 10-min intervals. The single-person household data comprised 5240 people across 800 cities in the Republic of Korea.

Table 1. Household information of the Korean Time-Using Survey [16].

Classification	Details	Literature Review
Number	Household ID	
Gender		Räty (2010)
Age		Van den Brom et al. (2018)
Job	Job status	Noh (2013)
Educational Level		Guerra-Santin (2010)
Income Level		Paula et al. (2018)
Marital Status		
Care	Senior, Handicapped	
Resident	Kind, Area, Ownership	

The daily activity log was categorized according to the codes in Table 2. Nine activity categories were used and subcodes were assigned to identify particular activities. A total of 144 activity codes were recorded by dividing 1440 min in 10 min intervals. Activity codes can be referenced to determine the occupancy period, the use of appliances pertaining to particular activities.

Table 2. Behavior codes of the Korean Time-Using Survey [16].

	Activity	Details
A	Personal	Sleep, Eat, Individual Hygiene
B	Work	
C	Learning	School, Internet Lectures, Private Educational
D	Home Management	Cleaning, Washing, Shopping, Public Office
E	Family Care	
F	Meeting	Religion, Volunteer Work
G	Social & Leisure	Date, Media, Exercise, Rest
H	Move	Commute, Personal
Z	Other	Unclassified Act

4. Simulation Modeling of the Typical Living Environment in Korea

EnergyPlus is a building user-based simulation tool developed by the U.S. Department of Energy and was employed for the present study. EnergyPlus not only accounts for the physical characteristics of a building, but it also considers user schedules to estimate the energy consumption of respective buildings. Numerous previous studies employed EnergyPlus to perform building user-based energy simulations and the tool has been demonstrated to yield highly accurate simulation results based on user activities.

With the rapid industrialization and urbanization of Korea and the growing housing shortage in cities, construction of apartments has increased rapidly. As a result, typical apartments are currently of the residential type in Korea [17]. This work considered a representative Korean residential building type. According to the "2016 Korean Housing Survey," the average gross floor area of a typical single-person household in Korea is 48.5 m^2; hence, a household with an effective living area of 41.39 m^2 was considered in this study. Figure 2 depicts the considered building, Happy House, promoted by the Korea Land and Housing Corporation [18].

(a) (b)

Figure 2. (**a**) Typical housing in the Republic of Korea [18]; (**b**) Typical housing layout for a one-person household [18].

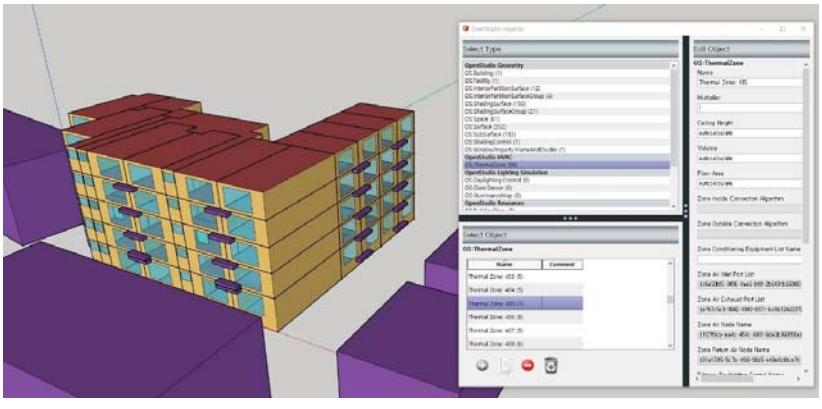

Figure 3. Building modeling for simulation.

Open Studio, which is provided as a Google Sketch-up plugin, was used to model the building [19]. The open studio version used in this study was 2.4.0, sketch-up version 2017. The building was modeled and entered as Figure 3. The entire building was modeled to account for thermal loads between households and a household located on a middle floor was analyzed herein. The input

parameters were the spatial properties and those of the building materials that were obtained from the floor plan and energy-savings plan in addition to the installation capacity.

Geographical conditions of the simulation were focused on those of Seoul, the capital of Korea. As shown in Figure 4, we used "Seoul's standard weather data" from the National Weather Service [20]. Seoul is geographically located in a mid-latitude temperate climate with four clear seasons. It is cold and dry in the winter while, in the summer, there is sultry weather. The average annual temperature in Seoul is 10–15 °C; it is above 30 °C in July–August, which is the warmest period, and temperatures below freezing occur in December–January, which is the coldest period. Approximately 61% of precipitation is distributed in the summer. The weather data for Seoul were converted into an EPW file and imported accordingly [20].

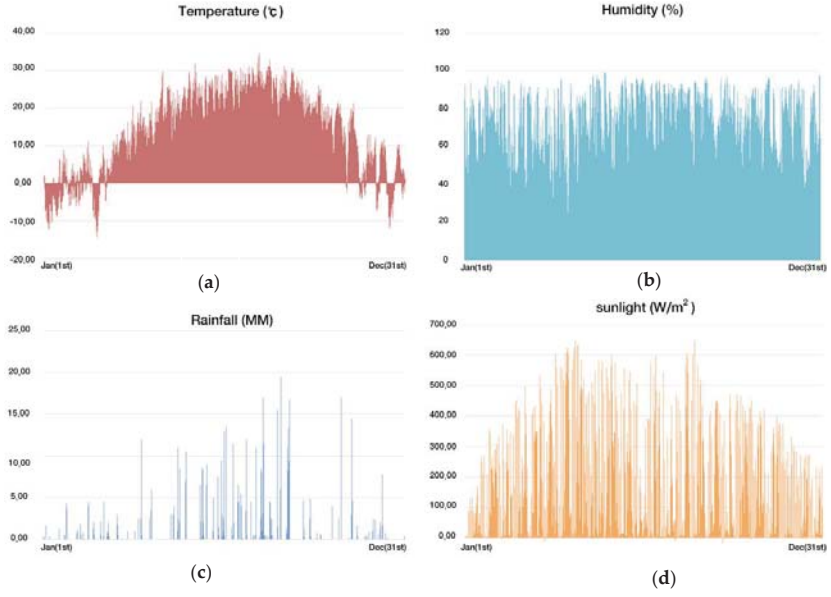

Figure 4. Standard Weather Data in Seoul, Korea [20]: annual values in Seoul for (**a**) temperature; (**b**) humidity; (**c**) rainfall; (**d**) sunlight.

The Korean population traditionally lives a comfortable life using floor heating systems called "Ondol." In modern Korean common housing, hot water piping is installed throughout the floor, and a heating system using a boiler is typical. Penetration of air-conditioning systems is substantial and in single households, wall-mounted air conditioners are often used [21]. Because the actual installation details, particularly those of the HVAC system, were not available, the Korean "Energy Saving Design Standards" were referenced to set December–March and June–September as the heating and cooling periods, respectively, and the indoor temperature was set between 20–26 °C [22]. Furthermore, the cooling system was modeled as a 2300 W wall-mounted "Ductless Air-conditioner" considering the typical HVAC requirements for a single-person household in Korea and the available installation area. On the other hand, the "Low Temperature Radiant Variable Flow" in EnergyPlus was used to model the heating system in the simulation because boilers are used for floor heating in Korea [23,24]. Information about the simulated building is summarized in Table 3.

Table 3. Simulation conditions.

Control Variables	Details
Total Area	2401.53 m^2
Simulation Area	41.39 m^2
Indoor Design Temperature	Set point: 20–26 °C
Heating System	Air Loop HVAC - Ductless Air-conditioner
Cooling System	Low-temperature Radiant Variable Flow
Weather Data	Seoul, Republic of Korea

The EnergyPlus software can estimate the energy consumption as a function of the activities of occupants by importing occupants' schedules as well as the indoor appliance capacity and usage profile. Occupant schedules were employed in the simulation to reflect the variation in energy consumption with respect to occupant activities by referencing the "2014 Korea Time Using Survey" activity codes. Indoor energy consumption was estimated based on the occupancy period and indoor activities, and the total energy used by home appliances and their operating periods were then obtained accordingly. The power consumption of home appliances was obtained from Statistics Korea's "2013 Home Appliance Power Consumption Survey" as listed in Table 4 [25]. Among the listed appliances, the refrigerator was considered to operate continuously for 365 days whereas 25 W light bulbs were considered to be installed in each room with a total power consumption of 100 W.

Table 4. Household appliances and their energy consumption [25].

Appliances	Power Consumption (W)
TV	130.6
Computer	255.9
Washer	242.8
Refrigerator	40.6
Lighting	100
Air conditioner	1200

The occupancy and operating period of each home appliance were interpreted using the activity codes and imported as in Table 5. The light was always on except when the occupant was asleep. The operating periods of other appliances were also estimated accordingly.

Table 5. Sample of daily energy schedule of household on 28th Aug 2014

Time	In & Out	TV	Computer	Lighting	Fridge	Hot Water	Cooking Stove
00:00	0	0	0	0	1	0	0
00:10	0	0	0	0	1	0	0
00:20	0	0	0	0	1	0	0
00:30	0	0	0	0	1	0	0
00:40	1	1	1	1	1	0	0
00:50	1	1	1	1	1	0	0
01:00	1	1	1	1	1	0	0
01:10	1	1	0	1	1	1	0
01:20	1	1	0	1	1	1	0
01:30	1	1	0	1	1	1	0
01:40	1	0	0	0	1	1	0
01:50	1	0	0	0	1	1	0
02:00	1	0	0	0	1	1	0
...	...	...	...	...	...	...	...
24:00	1	0	0	0	1	0	0

5. Modeling of an Artificial Neural Network (ANN) Based on User Information

The algorithm underlying the ANN is a machine-learning algorithm that mimics the human neural network and is used for prediction, clustering, and pattern recognition based on past and present training data. ANNs were first proposed by McCulloch and Pitts, but did not gain popularity in the early days because of the prohibitive amount of time required for training as the complexity of the model increased and as clear correlation between inputs and outputs was lacking [26]. However, Rumelhart et al. proposed the backpropagation algorithm and solved the optimal weight and bias for multi-layers with multiple nodes [27]. Methods for solving the phenomenon of information blurring, such as the ReLu function, have since been suggested, and ANN research has been revivified due to improvements in computer performance. Subsequently, the problem associated with the ANN technique has been solved and improved results can be obtained by increasing the number of hidden layers existing between the input and output layers of ANN. In general, when two or more hidden layers are used, it is known as a Deep Neural Network (DNN) or Deep Learning. A DNN can classify high-level data by using iterative learning to process large amounts of data. ANNs allow the inclusion of a large number of variables, and different weights can be assigned to each variable to yield outputs that closely approximate measurements [28].

An ANN has the general structure shown in Figure 5 and is expressed as Equation (1).

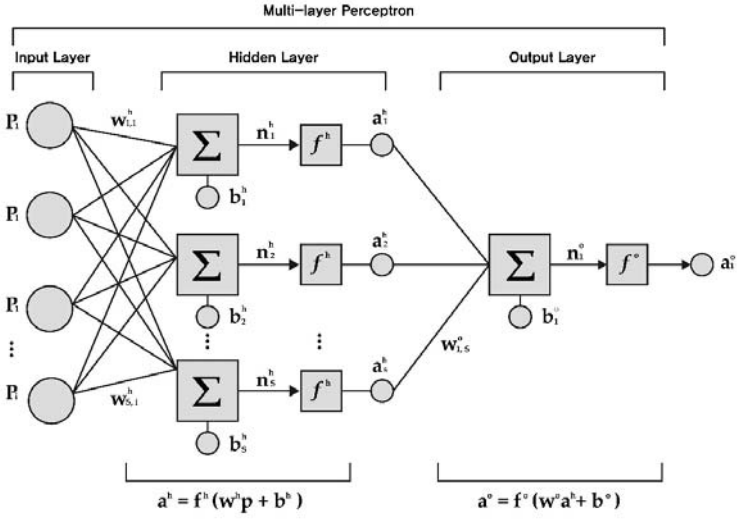

Figure 5. Structure of ANN model.

$$n_k^h = \sum_{j=1}^{R} w_{k_j}^h p_j + b_h^k,\ k = 1\ to\ S. \tag{1}$$

where R is the number of input variables and S is the number of hidden neurons. Further, p is the input variable, b^h is the bias of the hidden layer, and w^h is the weight. The calculated value is used as input for an activation function. The input to the ANN is processed to obtain the output by modifying the weight sum of the values from the previous layer by using the activation function. In general, previous studies used the sigmoid function as an activation function. However, the function exhibits the gradient vanishing phenomenon in which existing information converges to zero as the neural network expands. In addition, the sigmoid function requires additional computing time being an exponential function. In an effort to address this challenge, the nonlinear ReLU function was proposed. Figure 6 shows the sigmoid function and Relu function [29]. This function does not lose information

because it outputs the input value without any modification when it exceeds the threshold value, and the calculation speed is fast with a simple gradient value of 0 or 1. As a result, the performance of ANN increases remarkably with the ReLU function, and this approach was employed in numerous studies and is also used in the present work [30].

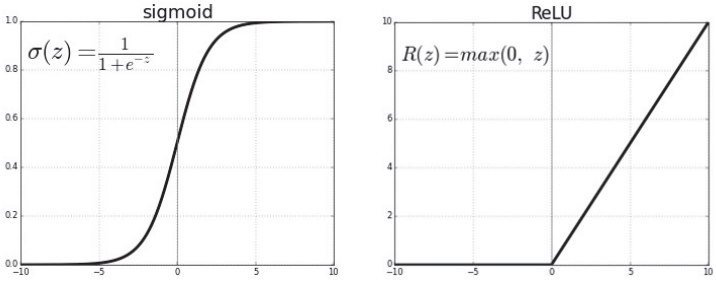

Figure 6. Comparison of two commonly used activation functions [29]: (**a**) Sigmoid; (**b**) ReLU.

In civil engineering and construction, ANN has been used consistently to predict the performance of structures. Yeh predicted the strength of concrete using the components of concrete [31]. Mata predicted the condition of a concrete dam by using environmental factors [32]. In addition, Cascardi predicted the strength of a concrete column, and proceeded to the wall shear strength [33,34]. Abambres et al. carried out the load prediction of an I-Section steel beam [35]. ANNs have been employed extensively in recent building load prediction studies owing to their advantages and improved algorithm. Factors related to building loads were typically given as inputs to forecast the actual load. Dong et al. performed energy prediction using the material properties of a wood office as data [36], whereas Kang forecasted the cooling load as a function of ambient and indoor temperatures [37]. Azadeh et al. considered environmental and economic factors to predict building energy consumption [38]. Martellotta et al. performed energy estimation with high accuracy with EnergyPlus and ANN using a user's representative schedule [39].

Previous studies employed ANNs to predict the building load based on the physical characteristics, environmental factors, or building use schedule. Sena et al. proposed that the behavior and characteristics of users and physical elements of buildings should be predicted through ANN but their approach could not be implemented [40]. The present study employed the demographic, social, and economic characteristics of building residents in an ANN to predict user-based energy consumption.

The user activity-based energy simulation results and user characteristics were used to construct a model to forecast user-based energy consumption. In this study, the ANN was implemented using NN Toolbox in MATLAB R2018b. Among the available user information, demographic, social, and economic characteristics such as age, income, gender, level of education, occupation, and occupancy period were provided as inputs and the energy consumption was obtained as the simulation output. The model was formulated as illustrated in Figure 7 and accepted a total of six inputs and yielded energy consumption as the sole output.

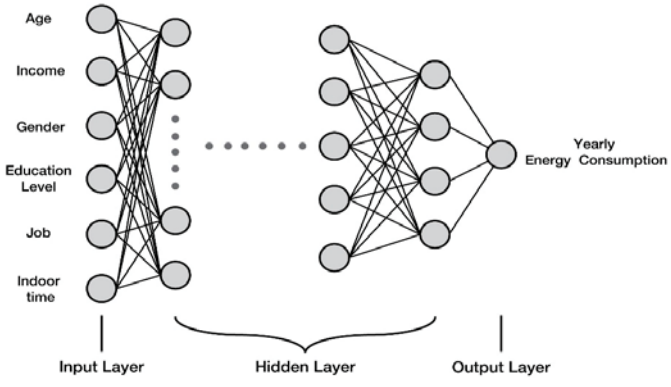

Figure 7. Model structure of the yearly energy prediction model

When using an ANN, there is no clear criterion for determining the number of hidden nodes and layers. The appropriate number of hidden nodes and layers is typically selected by varying the number of hidden nodes in the course of learning, and the optimal number of hidden nodes and layers is determined based on the best prediction performance. Huang and Foo found that it is desirable to determine the number of concealed neurons within 2n + 1 when the number of input variables is n. In this study, six user characteristics are used as input variables. Among them, Job has 10 nominal variables and has 14 inputs in total. Therefore, in this study it is necessary to determine the number of nodes within a total of 29 [41]. In this study, 6 different conditions were set, as listed in Table 6, and were used to construct 6 models with distinct learning rates, number of hidden layers, and nodes. The Levenberg-Marquardt backpropagation algorithm was used as a network training function for learning ANN parameters [42].

Table 6. Running conditions for the ANN

No.	Activation Function	Learning Rate	Number of Layer	Number of Neuron in Layer
Network 1	ReLU	0.01	1	18
Network 2	ReLU	0.01	1	29
Network 3	ReLU	0.01	2	10–19
Network 4	ReLU	0.01	2	14–15
Network 5	ReLU	0.01	3	9–10–10
Network 6	ReLU	0.01	4	5–7–9–8

The ANN model uses given data for training and is then cross-validated with a new set of data. In this study, 70% of the energy simulation results were used for learning, 15% for model validation and 15% for model testing. The number of learning repetitions was set to 200, and training terminated when the number of epochs reached the maximum number or the mean squared error (MSE) continuously increased up to six times.

6. Results and Discussion

6.1. Simulation Result

Simulation was performed based on information of 5240 single-person Korean households to estimate the annual building energy consumption. A total of 48 households with a zero occupancy period were excluded from the simulation and thus the energy consumption for a total of 5192 residents was obtained as summarized in Table 7. The results varied by approximately 20 times from 46.27 kWh/m^2·year to 926.38 kWh/m^2·year depending on the building users.

Table 7. Simulation results

Item	Value
Total	5240
Outlier	48
Extraction	5192
Min	46.27 (kWh/m^2·year)
Max	926.38 (kWh/m^2·year)
Mean	314.62 (kWh/m^2·year)
Median	292.919 (kWh/m^2·year)

6.2. Energy Consumption by Sex and Age

The building energy consumption varies depending on user gender and age. As shown in Figure 8, women feature a wider distribution than men and exhibit higher relative energy usage. The median, i.e., the usage at which 50% of the total population resides, is 274.66 kWh/m^2·year for males and 341.01 kWh/m^2·year for females. Figure 9 depicts the energy consumption by age and shows that consumption increases with age. The maximum value is found in the bin containing people in their 70s, and the lowest value was observed for those in their 30s. The average occupancy period for residents in their 30s is 13.33 h, which is the lowest of all age groups, whereas those in their 70s featured the longest average occupancy period of 18.34 h. Because the difference in occupancy period depends on the extent of economic activity, the younger the occupant, the less energy is used in the house. On the other hand, elderly individuals tend to spend more time at home because of retirement or aging and thus higher energy consumption is observed within this age group.

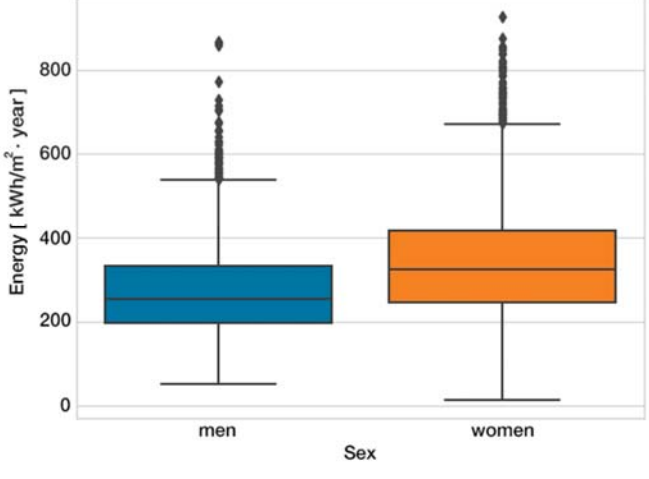

Figure 8. Comparison of energy consumption by sex.

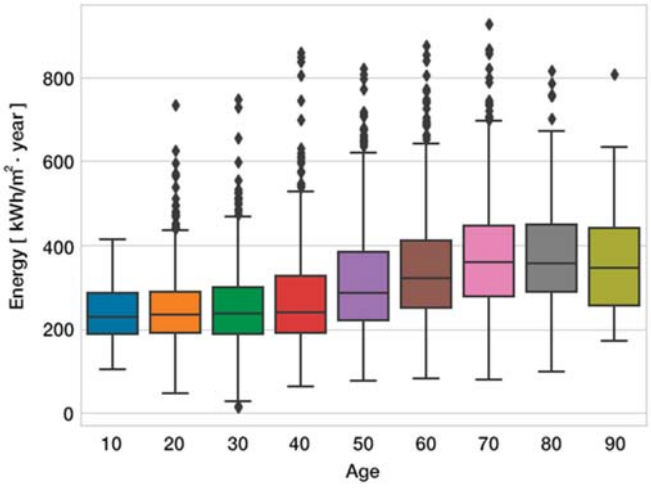

Figure 9. Comparison of energy consumption by age

6.3. Energy Consumption by Occupation and Income

Figure 10 shows That the group with analysis of the energy consumption by occupational status.

The analysis of the energy consumption by occupation revealed that the unemployed group showed the highest energy usage because students were also included in this group and more frequently engage in indoor activities. The distribution of energy consumption was high for simple manual labor and service work, and the lowest distribution was determined for occupants working in management. Although the distribution in energy usage varies slightly depending on the occupation, all except for the unemployed group showed a distribution between 200 and 300 kWh/m^2·year.

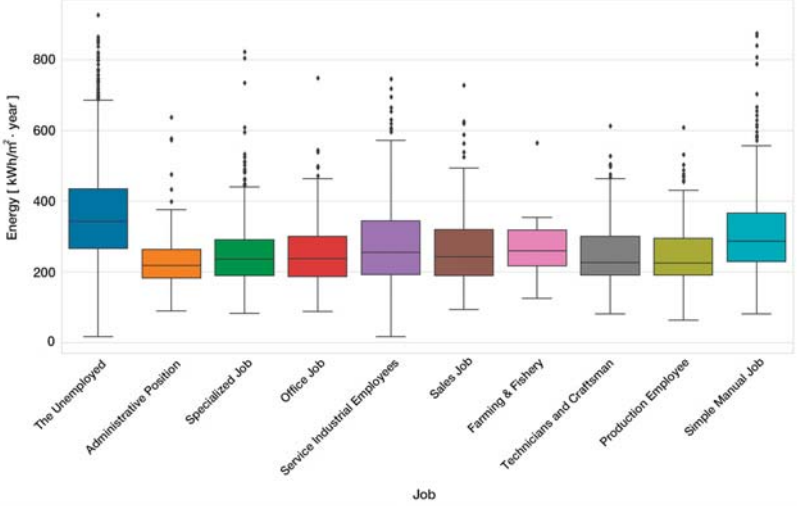

Figure 10. Comparison of energy consumption according to occupational status

Figure 11 shows that the group with a monthly average income of 0–1 million won consumes the most energy. This corresponds to the results in Figure 9. In the case of the unemployed, the number of elderly and retired people aged 60 or over accounted for 1605 out of 2135 or 75.17%. As a result,

elderly individuals without an occupation because of aging or retirement constitute a large portion of the low-income class. Energy consumption also varied as a function of the level of education.

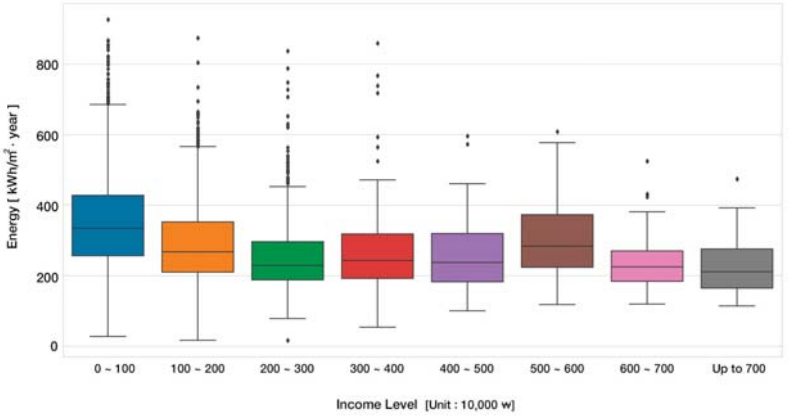

Figure 11. Comparison of energy consumption as a function of income

6.4. Energy Consumption According to the Educational Level

According to the results in Figure 12, the energy consumption decreases as the educational level increases. The group of elementary school graduates features the largest distribution in energy consumption with a median of 366.12 kWh/m^2·year whereas individuals with a Master's degree exhibit the smallest distribution with a median of 258.04 kWh/m^2·year. The group of elementary school graduates achieved peak energy consumption whereas that of associate and four-year college graduates was the lowest. The differences in energy consumption among the considered groups became insignificant above college level.

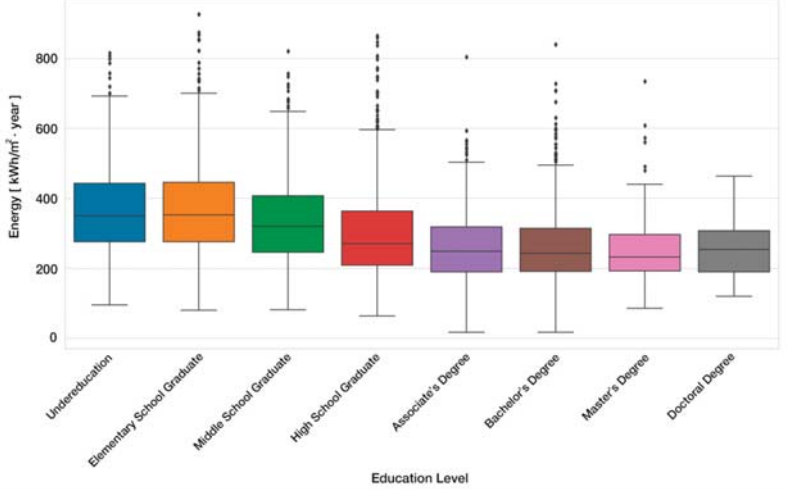

Figure 12. Comparison of energy consumption according to level of education

6.5. Energy Consumption According to the Occupancy Period

The energy consumption is directly proportional to the occupancy period. As shown in Figure 13, the longer the occupancy period, the higher the energy consumption is. This is attributed to the

high usage rates of indoor heating, cooling, lighting, and equipment as the occupancy time increases. The energy consumption is observed to be high within a period of 360 min (6 h) or less because many of the 52 users with an occupancy period of 6 h or less used home appliances such as computers and TV within that time frame. The indoor energy consumption increases in proportion to the occupancy period, but the indoor energy consumption may be higher per occupancy period depending on the user's activity pattern.

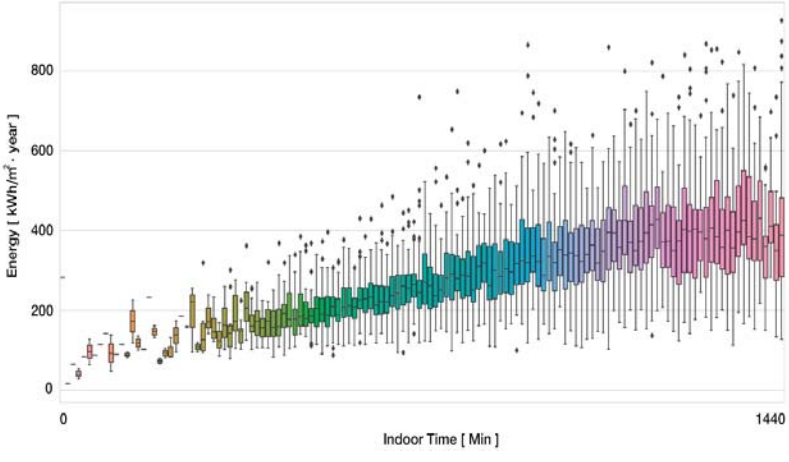

Figure 13. Comparison of energy consumption according to time spent indoors

6.6. Energy Consumption Prediction

Through simulation results, we analyzed the differences in energy usage according to six user characteristics. The ANN energy prediction model was implemented with simulation results and six user characteristics by the method presented in Section 5. Table 8 shows the datasets used in ANN, which should use continuous data as input data. Of the six user characteristics, Job has 10 nominal variables. Jobs are coded 1 and 0 for use as input data. Traditional metrics such as MSE and regression coefficient R were used to evaluate ANN performance. To show the evaluation result of ANN performance, 10 samples are extracted and the predicted value and the error rate are presented here.

Table 8. Sample of data set

Input Data												Output Data	
Age	**Income**	**Gender**	**Education Level**	**Job**								**Indoor Time**	**Energy Consumption**
42	450	0	6	1	0	0	0	0	0	0	0	57	182.0869
83	50	0	1	0	0	0	0	0	0	0	0	123	395.9636
33	350	1	3	0	1	0	0	0	0	0	0	65	232.7648
29	250	1	5	0	1	0	0	0	0	0	0	51	149.0521
30	250	1	5	0	1	0	0	0	0	0	0	62	103.771
47	50	0	3	0	0	0	0	0	1	0	0	144	185.6166
56	150	0	2	0	0	0	0	0	0	0	1	63	334.8878
28	250	1	2	0	0	0	1	0	0	0	0	68	188.5984
70	150	0	1	0	0	0	0	0	0	0	1	82	239.1679

Table 9 shows the results of the ANN model executed under five conditions. Network 4 showed the best results, and the R-value of training was the highest for Network 1. However, the values of Validation and Test were low. The results of the five networks were the poorest for Network 6.

Table 9. The performances of the ANNs with different condition in hidden layer.

No.	R Value of Training	R Value of Validation	R Value of Test	MSE	Terminated Epoch
Network 1	0.64739	0.5805	0.6463	$10^4 \times 1.0513$	9th
Network 2	0.63229	0.59547	0.6153	$10^4 \times 1.0429$	5th
Network 3	0.63544	0.60723	0.60865	$10^4 \times 1.0637$	6th
Network 4	0.64312	0.62886	0.63089	$10^4 \times 1.0356$	13th
Network 5	0.63775	0.63885	0.59859	$10^4 \times 1.0855$	7th
Network 6	0.6155	0.62816	0.61952	$10^4 \times 1.0929$	10th

The performance of Network 4's energy prediction model is shown in Figure 14. The regression R-values of the training, validation, and test data were 0.64312, 0.62886, and 0.63089, respectively. The correlation coefficient shows that the energy usage and the six user characteristics were strongly positively correlated. The MSE was 1.0356×10^4, and the error distribution shows that more than 70% of the total data had a value between −100 and 100. As a result, the conditions of Network 4 of two hidden layers, node configuration 14–15, and learning rate 0.01 were most appropriate among the networks with five different conditions.

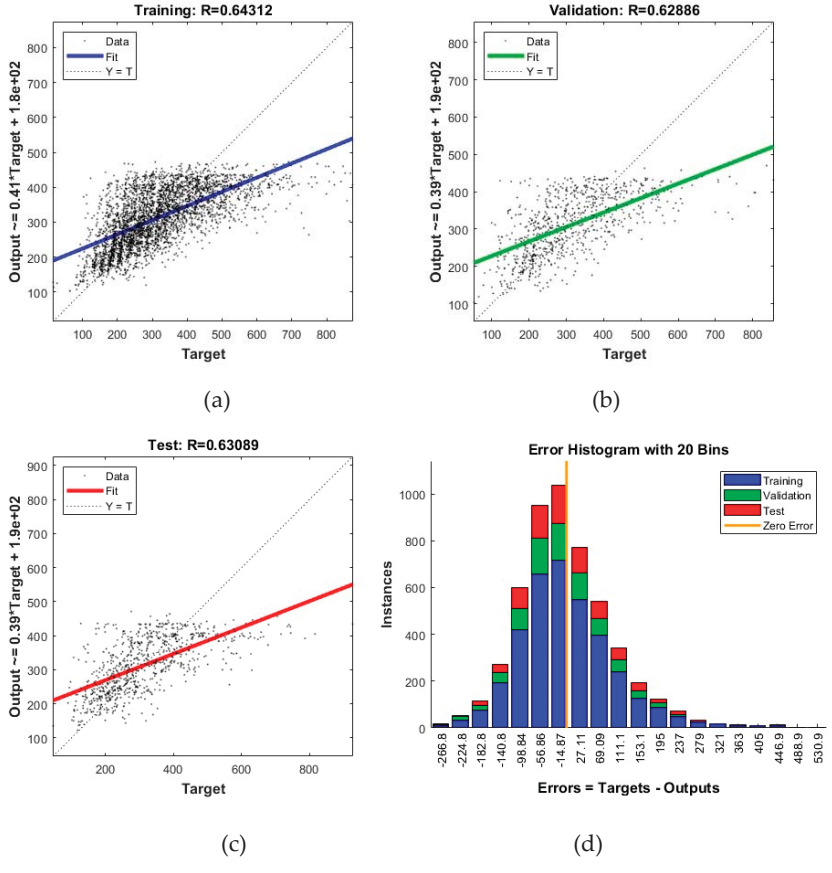

Figure 14. Training result of Network 4: (**a**) regression result from training data; (**b**) regression result from validation data; (**c**) regression result from test data; (**d**) histogram of the distribution of absolute errors.

7. Conclusions

In Korea, previous work on energy prediction using an ANN relied on building characteristics or environmental conditions whereas the present work was based on different user activities in a particular building as well as demographic, social, and economic characteristics. In this study, we tried to improve the accuracy by utilizing actual user activity and characteristic data and we drew six major user variables through simulation analysis.

This study involved the estimation and analysis of the user-based energy consumption in a building according to six user characteristics, namely gender, age, occupation, income, level of education, and occupancy period. The demographic, social, and economic characteristics and actual activity data of 5192 single-person households in Korea were used. In this study, the degree of differences in the influence of user characteristics could be more accurately compared because simulations were conducted by considering user activity within the same building, i.e., within a controlled physical environment. The six user characteristics were used as input to train the ANN model, which produced the simulated annual energy consumption of each individual as the output. As a result, the six user characteristics and energy usage were correlated with an R-value of 0.6 or more, and the model with an MSE of 1.0203×10^4 showed the best result.

The simulation results indicated that our approach enabled us to successfully analyze the difference in energy usage according to six user characteristics. However, the predictive performance of the Neural Network Predictive Model, which is based on six characteristics, is somewhat lower than that of the previous studies based on physical characteristics. The reason for the low prediction rate is that some parts of the model depend on the number of layers and neurons in the neural network, but the energy usage is considered to be a result of the physical and environmental factors of the building in addition to the user characteristics. The results of the study show that predicting the energy usage by only considering the user characteristics may have an influence on the energy consumption although the prediction rate is limited. However, the limitations are that the data used for ANN learning are simulation-based. If large amounts of energy information and user variable data were constructed for previous users in new or currently used buildings, the proposed study method using actual samples would allow users to compare energy use in a more sophisticated manner.

The process and results of this study can help to achieve a more accurate energy performance evaluation by considering all the users together when predicting the energy consumption of a building and it can serve as a basis to facilitate the transmission of energy information to users in energy management.

Author Contributions: S.L. proposed the main idea and performed the modeling, simulation, and data analysis and wrote the original draft; J.L. reviewed and edited the papers; S.J. reviewed the papers and oversaw the study. All authors contributed via discussions and participated in writing the manuscript.

Funding: This research was funded by the Ministry of Land, Infrastructure and Transport of the Korean government.

Acknowledgments: This work is supported by the Korea Agency for Infrastructure Technology Advancement (KAIA) grant funded by the Ministry of Land, Infrastructure and Transport (Grant 18CTAP-C133446-02).

Conflicts of Interest: The authors declare no conflict of interest.

Abbreviations

The following abbreviations are used in this manuscript:

EPBD	Energy Performance of Building Directives
ReLU	Rectified Linear Unit
MSE	Mean Square Error

References

1. International Energy Agency. *Energy, Climate Change and Environment 2014*; IEA Publications: Paris, France, 2015.
2. Majcen, D.; Itard, L.; Visscher, H. Actual and theoretical gas consumption in Dutch dwellings: What causes the differences? *Energy Policy* **2013**, *61*, 460–471. [CrossRef]
3. Van den Brom, P.; Meijer, A.; Visscher, H. Performance gaps in energy consumption: Household groups and building characteristics. *Build. Res. Inf.* **2017**, *46*, 54–70. [CrossRef]
4. Kaddory Al-Zubaidy, M.S. A literature evaluation of the energy efficiency of leadership in energy and environmental design (LEED)-certified buildings. *Am. J. Civ. Eng. Archit.* **2015**, *3*, 1–7. [CrossRef]
5. Gram-Hanssen, K. Efficient technologies or user behaviour, which is the more important when reducing households' energy consumption? *Energy Effic.* **2012**, *6*, 447–457. [CrossRef]
6. Porcar, B.; Soutullo, S.; Enríquez, R.; Jiménez, M.J. Quantification of the uncertainties produced in the construction process of a building through simulation tools: A case study. *J. Build. Eng.* **2018**, *20*, 377–386. [CrossRef]
7. Tronchin, L.; Fabbri, K. Energy performance building evaluation in Mediterranean countries: Comparison between software simulations and operating rating simulation. *Energy Build.* **2008**, *40*, 1176–1187. [CrossRef]
8. Tronchin, L.; Manfren, M.; James, P.A.B. Linking design and operation performance analysis through model calibration: Parametric assessment on a Passive House building. *Energy* **2018**, *165*, 26–40. [CrossRef]
9. Guerra-Santin, O.; Itard, L. Occupants' behaviour: Determinants and effects on residential heating consumption. *Build. Res. Inf.* **2010**, *38*, 318–338. [CrossRef]
10. Jung, J.; Yi, C.; Lee, S. An integrative analysis of the factors affecting the household energy consumption in Seoul. *J. Korea Plann. Assoc.* **2015**, *50*, 75. [CrossRef]
11. Schipper, L.; Bartlett, S.; Hawk, D.; Vine, E. Linking life-styles and energy use: A matter of time? *Annu. Rev. Energy* **1989**, *14*, 273–320. [CrossRef]
12. Räty, R.; Carlsson-Kanyama, A. Energy consumption by gender in some European countries. *Energy Policy* **2010**, *38*, 646–649. [CrossRef]
13. Jones, R.V.; Fuertes, A.; Lomas, K.J. The socio-economic, dwelling and appliance related factors affecting electricity consumption in domestic buildings. *Renew. Sustain. Energy Rev.* **2015**, *43*, 901–917. [CrossRef]
14. Pérez-Lombard, L.; Ortiz, J.; González, R.; Maestre, I.R. A review of benchmarking, rating and labelling concepts within the framework of building energy certification schemes. *Energy Build.* **2009**, *41*, 272–278. [CrossRef]
15. Lee, M.-J.; Kim, J.-U. A study of domestic and foreign system and evaluate tools relative to building energy performance analysis and improvement plan for zero energy building design. *J. Archit. Inst. Korea Plan. Des.* **2015**, *31*, 45–52. [CrossRef]
16. Statistics Korea. *2014 Korea Time Use Survey*; Statistics Korea, Ed.; Micro Integrated Service: Seoul, Korea, 2015.
17. Kim, M.-K.; Yoon, C.-S. A study on statistical characteristics of space dimension of 60 m^2, 85 m^2 size apartment plan types in Seoul. *J. Korean Hous. Assoc.* **2010**, *21*, 53–65. [CrossRef]
18. Korea Land & Housing. Available online: http://www.apply.lh.or.kr (accessed on 10 October 2018).
19. Open Studio. Available online: http://www.openstudio.net/ (accessed on 10 October 2018).
20. National Climate Data Service System. Available online: http://sts.kma.go.kr (accessed on 10 October 2018).
21. Ju, J.-H.; Park, J.-C.; Jeon, Y.-H.; Kim, D.-Y. A study on the usage status and satisfaction of the ventilation system installed in apartment houses. *J. Archit. Inst. Korea Plan. Des.* **2015**, *31*, 185–192. [CrossRef]
22. Go, G.-H.; Lee, S.-R.; Yoon, S.; Kim, M.-J. Optimum design of horizontal ground-coupled heat pump systems using spiral-coil-loop heat exchangers. *Appl. Energy* **2016**, *162*, 330–345. [CrossRef]
23. US DOE. *Engineering Reference with Energy Plus*; US Department of Energy: Washington, DC, USA, 2009.
24. US DOE. *Input Output Reference with Energy Plus*; US Department of Energy: Washington, DC, USA, 2009.
25. Lee, W.H.; Oh, H.S. Distribution characteristics of neophyten in Seongnagwon of scenic site no. 35. *J. Korea Soc. Plants People Environ.* **2013**, *16*, 181–185. [CrossRef]
26. McCulloch, W.S.; Pitts, W. A logical calculus of the ideas immanent in nervous activity. *Bull. Math. Biophys.* **1943**, *5*, 115–133. [CrossRef]

27. Rumelhart, D.E.; Hinton, G.E.; Williams, R.J. Learning representations by back-propagating errors. *Nature* **1986**, *323*, 533–536. [CrossRef]
28. Salakhutdinov, R.; Mnih, A.; Hinton, G. Restricted Boltzmann machines for collaborative filtering. In Proceedings of the 24th International Conference on Machine Learning, Corvalis, OR, USA, 20–24 June 2007; pp. 791–798.
29. Towards Data Science. Available online: https://towardsdatascience.com (accessed on 10 October 2018).
30. Nair, V.; Hinton, G.E. Rectified linear units improve restricted Boltzmann machines. In Proceedings of the 27th International Conference on Machine Learning (ICML-10), Haifa, Israel, 21–24 June 2010; pp. 807–814.
31. Yeh, I.-C. Modeling of strength of high-performance concrete using artificial neural networks. *Cem. Concr. Res.* **1998**, *28*, 1797–1808. [CrossRef]
32. Mata, J. Interpretation of concrete dam behaviour with artificial neural network and multiple linear regression models. *Eng. Struct.* **2011**, *33*, 903–910. [CrossRef]
33. Cascardi, A.; Micelli, F.; Aiello, M.A. Analytical model based on artificial neural network for masonry shear walls strengthened with FRM systems. *Compos. Part B Eng.* **2016**, *95*, 252–263. [CrossRef]
34. Cascardi, A.; Micelli, F.; Aiello, M.A. An Artificial Neural Networks model for the prediction of the compressive strength of FRP-confined concrete circular columns. *Eng. Struct.* **2017**, *140*, 199–208. [CrossRef]
35. Abambres, M.; Rajana, K.; Tsavdaridis, K.; Ribeiro, T. Neural Network-based formula for the buckling load prediction of I-section cellular steel beams. *Computers* **2019**, *8*, 2. [CrossRef]
36. Dong, Q.; Xing, K.; Zhang, H. Artificial neural network for assessment of energy consumption and cost for cross laminated timber office building in severe cold regions. *Sustainability* **2017**, *10*, 84. [CrossRef]
37. Kang, I.; Lee, K.; Lee, J.; Moon, J. Artificial neural network-based control of a variable refrigerant flow system in the cooling season. *Energies* **2018**, *11*, 1643. [CrossRef]
38. Azadeh, A.; Saberi, M.; Anvari, M.; Mohamadi, M. An integrated artificial neural network-genetic algorithm clustering ensemble for performance assessment of decision making units. *J. Intell. Manuf.* **2009**, *22*, 229–245. [CrossRef]
39. Martellotta, F.; Ayr, U.; Stefanizzi, P.; Sacchetti, A.; Riganti, G. On the use of artificial neural networks to model household energy consumptions. *Energy Procedia* **2017**, *126*, 250–257. [CrossRef]
40. Sena, B.; Zaki, S.A.; Yakub, F.; Yusoff, N.M.; Ridwan, M.K. Conceptual framework of modelling for Malaysian household electrical energy consumption using artificial neural network based on techno-socio economic approach. *Int. J. Electr. Comput. Eng.* **2018**, *8*, 1844–1853. [CrossRef]
41. Huang, W.; Foo, S. Neural network modeling of salinity variation in Apalachicola River. *Water Res.* **2002**, *36*, 356–362. [CrossRef]
42. Marquardt, D.W. An algorithm for least-squares estimation of nonlinear parameters. *J. Soc. Ind. Appl. Math.* **1963**, *11*, 431–441. [CrossRef]

energies

MDPI

Article

What Affects the Progress and Transformation of New Residential Building Energy Efficiency Promotion in China: Stakeholders' Perceptions

Yinan Li [1,*], Neng Zhu [1] and Beibei Qin [2]

[1] School of Environmental Science and Engineering, Tianjin University, Tianjin 300350, China; nzhu@tju.edu.cn
[2] School of Built Environment, University of Reading, Reading RG6 6AW, UK; b.qin@pgr.reading.ac.uk
* Correspondence: lyn.tju@live.com; Tel.: +86-1381-124-0163

Received: 16 February 2019; Accepted: 12 March 2019; Published: 16 March 2019

Abstract: Nationwide energy efficiency (EE) promotion of new residential buildings is affected by multiple factors regarding policies, markets, technologies, capacities, and economics. The perceived influences of these factors by stakeholders are crucial to the effectiveness evaluation of current policies and the selection of policy instruments. However, they are normally assumed or taken for granted. The knowledge gap between stakeholders' perceptions and research assumptions may lead to researchers' recognition bias. Correspondingly, this paper aims to identify the significant factors, perceived by frontline stakeholders, influencing nationwide EE promotion of new residential buildings before 2020 and 2030. Factors were collected through literature review and their influence were evaluated via Analytical Hierarchy Process based on the data collected in the questionnaires distributed to 32 institutes. The theory of Nested Policy Design Framework and Policy Environment was used to structure the hierarchy and generate policy implications. Results indicate that (1) policy factors are of the greatest influence before 2020 and market perfection factors will have great influences from 2020 to 2030, indicating the transformation of governance arrangement to "market-based" and "network-based" from the current legal-based system; and (2) factors regarding market needs are of significant influence in both terms, revealing the way the transformation should be accomplished.

Keywords: analytical hierarchy process; energy efficiency promotion; influencing factors; residential buildings; policy design

1. Introduction

China's unprecedented socio-economic development and fast urbanization (see Figure 1) has driven great expansion of residential buildings. As indicated in Figure 1, the urbanization rate has been increasing steadily and rapidly from 36.22% in 2000 to 58.52% in 2017. The total Gross Domestic Production increased by approximately 7 times from 10.02 trillion Yuan in 2000 to 82.71 trillion Yuan in 2017. In accordance with the fast development of Gross Domestic Production (GDP) and urbanization rate, the area of residential buildings also increased dramatically. According to the data from the Nation Bureau of Statistics of China [1], the area of new residential buildings under construction per year has been increasing by 17% per year on average, compared to the year 2000 level, and reached 12.50 billion square meters in 2014 (see Figure 2). The area of new residential buildings under construction and constructed, after 2014, are leveling out around 12.5 billion square meters and 4.2 square meters, respectively. Along with the gradual improvement of living quality, fast increase of building area, and rapid urbanization, the energy consumption of residential buildings has also been increasing dramatically [2,3]. According to the data from Tsinghua University Building Energy Research Center, as indicated in Figure 3, building energy consumption has increased by more than

two times and reached 814 million tons of standard coal in 2014 whilst it was only 300 million tons of standard coal in 2000. During the same period, energy consumed by residential building rose to 301 million tons of standard coal in 2014 from 131 million tons of standard coal in 2000 [4]. In 2015, energy consumed by residential buildings accounted for 19.10% of total energy consumption (see Figure 4) [5]. Excluding urban centralized heating in Northern China, the energy consumption in residential buildings increased to 199 million tons of standard coal in 2015, which is approximately three times the amount in 2001. Currently, the energy consumption of residential buildings is still growing rapidly. The World Bank predicts that the Chinese urbanization rate will be 70% by 2030 [6]. Experience from developed countries shows that the building industry will account for 30% of annual global CO_2 emissions and 40% of total energy consumption in 2030 [7].

Figure 1. Gross Domestic Production (GDP) and urbanization rate from 2000 to 2017.

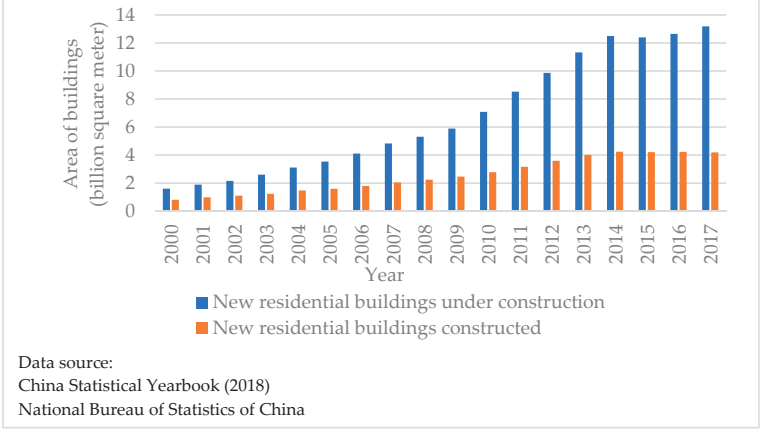

Figure 2. New residential building area from 2000 to 2017.

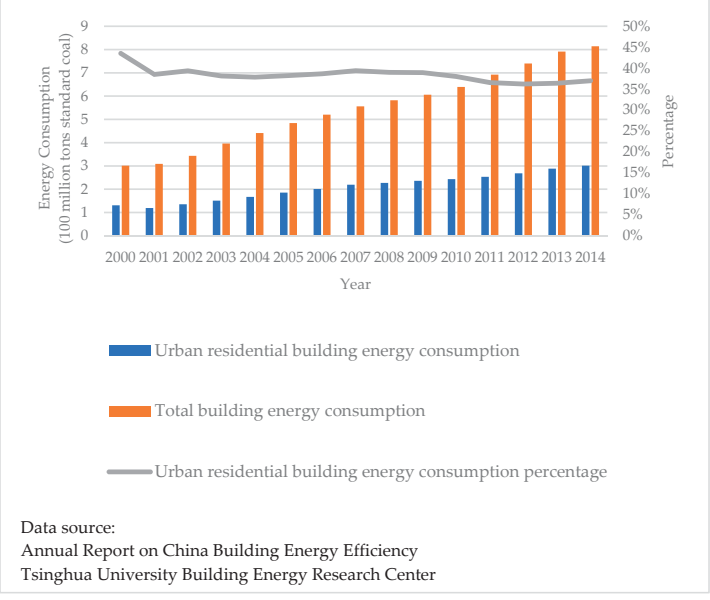

Figure 3. Building energy consumption from 2000 to 2014.

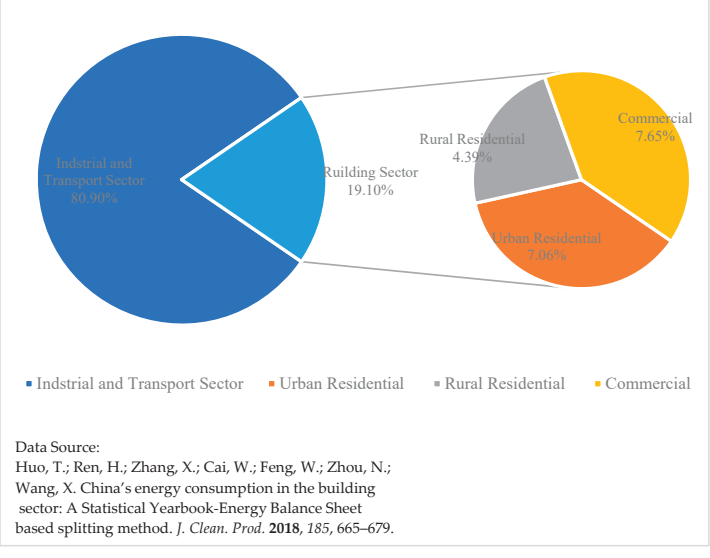

Figure 4. Breakout of China building energy consumption by sector in 2015.

The fast increase of energy consumption has not gone unnoticed and translates into the serious risk of China locking itself in with a large and energy-inefficient housing stock [8]. According to the "13th-Five Year Plan of Building Energy Conservation and Green Building Development" (PLAN) published by China's central government in 2016, all new residential buildings should be built to a standard of 72% energy efficiency (EE) level, compared with the 1980s level, and some advanced provinces have increased this requirement to 75%. Additional policy measures to ensure the realization

of the targets have also been proposed by central and local governments, by eliminating the known barriers in the current policy system, stimulating market-based innovations, improving the capacity of stakeholders developing, and constructing high-performance projects (also known as "Capacity Building" in the China case), as well as accelerating the technology evolvement and its penetration into market. Notably, the EE promotion of new residential buildings is a complex socio-technical system [9]. In addition to the homebuyers, the system involves a large variety of stakeholders concerned with policymaking, marketing, and technology, and it could be influenced by factors that include real estate, construction, buildings, and industry [10–12]. The complexity of the system leads to a difficult question to answer—"**perceived by frontline stakeholders, what on earth has significant influence on the development of the EE promotion of new residential buildings?**", or in other words, whether these policy packages (or factors included in the policy packages) could affect the industry as expected or if the stakeholders within the industry would respond as assumed.

As for identifying the influencing factors, the existing literature have provided deep insights from both technology and management (policy, market, etc.,) perspectives [11–14]. The results in existing literature has provided abundant data for factor identification for the study, but they are discussed independently in different domains. A panoramic view and a systematic analysis of the new residential building energy efficiency promotion should take all the factors in all the domains into consideration. According to a review by De Boeck, research has tended to focus on the following domains: (1) Area of application and design variables, (2) objective and performance measures, (3) type of analysis [15–17], (4) solution methodology, (5) software tools, (6) case study location, and (7) type of building [18]. Regarding factors influencing the EE promotion of new residential buildings, domain 1 provides a classification of technology factors based on which EE promotion measure is applied and in which part the dwelling it is implemented. Five major groups of technology measures application and corresponding design variables are identified, namely the whole building, the construction parts of the envelope (roof, wall, ceiling, and floor), windows and shading, HVAC systems, and finally, appliance and lightning. Domain 2 and 4 stress the popularity of life cycle studies and indicate the importance of factor identification from life-cycle perspective. Chau et al. summarized the similarities and differences of three streams of life-cycle studies and briefly identified major influencing factors in the construction phase, operational phase, and dismantle/renovation phase [19]. More detailed research regarding factor identification in these phases could be classified into two categories: Practice-based and evaluation system-based. The former focuses on factors of significant impacts in reality [20,21], while the latter pays attention to the factors included in various green building evaluation system, such as LEED (Leadership in Energy and Environmental Design), BREEAM (Building Research Establishment Environmental Assessment Method), or DGNB (German Sustainable Building Concil) [22–24]. In addition, economic factors are often discussed with technology factors [25]. For example, Shi et al. [26] proposed a detailed influencing factors list concerning cost optimization, such as technology R&D cost, marketization cost, and labor cost, according to different stages of construction [17].

From the management perspective, in addition to policy review [27] and status quo [28], research tends to focus on policy instrument evaluation and selection [29], barriers analysis [30,31], and theoretical interacting mechanisms among stakeholders from the perspectives of governments and market. The policy instruments, barriers, and interaction mechanism between policy and markets all could be considered as influencing factors which should be collected in this paper, because they would affect the development of the EE promotion. Representatively, Shen et al. [32] identified major policy instrument for building EE promotion and evaluated their influence based on the comparison of practice in seven countries and regions. Li et al. [28] further analyzed the strengths and weaknesses of current policy instruments. As of barriers, Zhang et al. [33] summarized those major ones and argued that deficiency existed in both policy system and market mechanism field. In addition to mandatory policies, economic incentives are also of great influence yet it is still lacking in current policy system [34]. Market failures, mainly caused by information asymmetries and externalities of

the industry, are identified as the major barriers causing the market to systematically underproduce green buildings [35]. Compared with the relatively independent researches, Zou [36] employed the system dynamics methodology to identify and analyze the risks that could affect building EE promotion market. Risks in six subsystems are involved, namely the laws and regulations, standards and specifications, economy, technology, policy, and education.

As for evaluating the significances of the identified factors, six techniques are of great popularity, namely the economic analysis, the sensitivity analysis, the scenario analysis, single objective optimization analysis, multi-objective optimization analysis, and statistical analysis [18]. The economic analysis is always widely used for the evaluation of a certain technology [15], and for analyzing the propagation of high-performance building technologies [16]. The sensitivity analysis or the scenario analysis is always combined with other types of analysis [37]. The selection between single-objective analysis and multi-objective analysis is normally based on the number of the factors to be discussed. The multi-objective optimization analysis helps identify those factors of significant influence in a complicated system and deals with the optimized choices for multiple objectives [38], which is in line with the focus of this paper. Among the approaches to multi-objective optimization, the analytical hierarchy process (AHP) is widely used in the research regarding building EE promotion [12,39]. For example, Roberti et al. utilized the AHP process to determine the portfolio of optimal retrofits of historic building, by quantifying the intrinsically qualitative conservation compatibility of energy retrofits so that it could be analyzed along with the quantitively expressed energy savings and thermal comfort. This is also what the AHP is good at and the reason why it is adopted in this paper—the AHP provides a comprehensive and rational framework for structuring a decision problem, representing and quantifying its elements, relating those elements to overall goals, and evaluating alternative solutions [40]. The specialty of AHP is its flexibility to be integrated with different techniques like linear programming, quality function deployment, fuzzy logic, and so forth. This enables the user to extract benefits from all the combined methods, and hence, achieve the desired goal in a better way [41]. The AHP approach also has the flexibility to combine quantitative and qualitative factors, to handle different groups of actors, to combine the opinions expressed by many experts, and can help in stakeholder analysis [42].

Notably, most current literature draw conclusions based on international experience [43,44], theoretical analysis [36], or the development history [33]. Despite the great contributions of existing literature, the actual perceptions by stakeholders to the influence of these factors remain insufficiently investigated and analyzed. The identification and the understanding of stakeholders' requirements, expectations, and attitudes towards the influence of these factors are fundamental to the successful implementation of strategies to achieve a higher EE level [45,46]. Making decisions without considering stakeholders' voices may lead to confrontation, dispute, disruption, boycott, distrust, and public dissatisfaction [47]. The neglect, or insufficient consideration of stakeholders' perceptions can lead to the cognitive bias of researchers and decisionmakers [48], and further result in an unsatisfied policy implementation outcome [49]. Defined by Von Winterfeldt and Edwards [50], the cognitive bias is a systematic discrepancy between the "correct" answer in a judgmental task, given by a forma normative rule, and the decisionmaker's or expert's actual answer to such a task. When the biased information/perceptions are used for analysis or decision-making, the quality of modeling and resulting analysis will be seriously reduced. Accordingly, the perceived influences of various factors by frontline stakeholders contribute explanations to the gaps between the expected outcome of policy settings ("the 'correct' answer") and the actual responses from stakeholders ("the 'actual' answer"), by presenting the responsive sensitivity of various stakeholders within the industry confronted with different settings of policy systems.

Contributing to the knowledge gap of the disaccord of perceptions of influencing factor between frontline stakeholders and researchers' recognitions and the lack of stakeholders' perceptions to the influence of factors, this paper aims to identify the factors of significant influence to the nationwide EE promotion of new residential buildings based on the lived experience perceived by relevant

frontline stakeholders. Factors are collected through experts' brainstorming and a literature review and are organized into three hierarchic levels according to the PLAN and the "Nested Policy Design Framework" proposed by Howlett [51]. The short-term (until 2020) and long-term (from 2020 to 2030) significances of each factor are evaluated separately because 2020 is the final year of the 13th five-year plan and most international agreements that China has signed are effective till 2030. The corresponding evaluation process is accomplished by institutional questionnaires distributed nationwide to 32 institutes representing different interests. The final quantitative value of significance of each factor is determined by the results of the analytical hierarchy process (AHP). The corresponding results in each hierarchic level give a stereo and panoramic view of factors, perceived by frontline stakeholders, influencing the EE promotion of new residential buildings in China from the perspective of governance arrangement, policy regime logic, and policy instrument selection for a better policy design and the corresponding implementation outcome.

Specifically, this paper contributes to the literature by answering the following three questions:

(1) *What do stakeholders think in general?* This was asked to elicit detailed descriptions of nationwide investigated stakeholders' opinions regarding the identified factors (described in Section 4.1);

(2) *What significantly affects the progress of the EE promotion of new residential buildings?* This was asked to provide a thorough identification and to prioritize the influencing factors of the EE promotion of new residential buildings in China on the governance arrangement level, policy regime logic level, and policy instrument selection level on the basis of the AHP method (described in Sections 4.2 and 4.3); compared with the existing literature regarding barriers, this question aims to explore factors both of positive and negative effects.

(3) *What will significantly affect the transformation of the EE promotion of new residential buildings in the future?* This was asked to determine the factors of significant influence in both the short term and long term (described in Section 4.4).

The complete structure and corresponding logic flow of this article is illustrated in Figure 5. The remainder of this paper is organized as follows. Section 2 introduces the novelty of this paper and the theoretical foundation for hierarchy construction, which are based on the nested policy design framework and the policy environment theory. Section 3 presents the detailed process of factor collection, classification, and evaluation. Section 4 summarizes the results of the data processing; discusses the weights and ranking of each criteria, sub-criteria, and factors to provide additional details on how the progress of the EE promotion in new residential buildings is affected; discusses the expectations regarding the situation in the long term; and discusses the achievements and limitations of this study. Section 5 presents the conclusions and corresponding policy implications. By investigating frontline stakeholders, this paper depicts a panoramic and authentic picture of how the nationwide EE promotion of new residential buildings is affected and stimulated. The result helps eliminate the perception disaccord between researchers, policymakers, and frontline stakeholders, and further help them better understand the current situation and the transformation of the EE promotion of new residential buildings from stakeholders' perspectives.

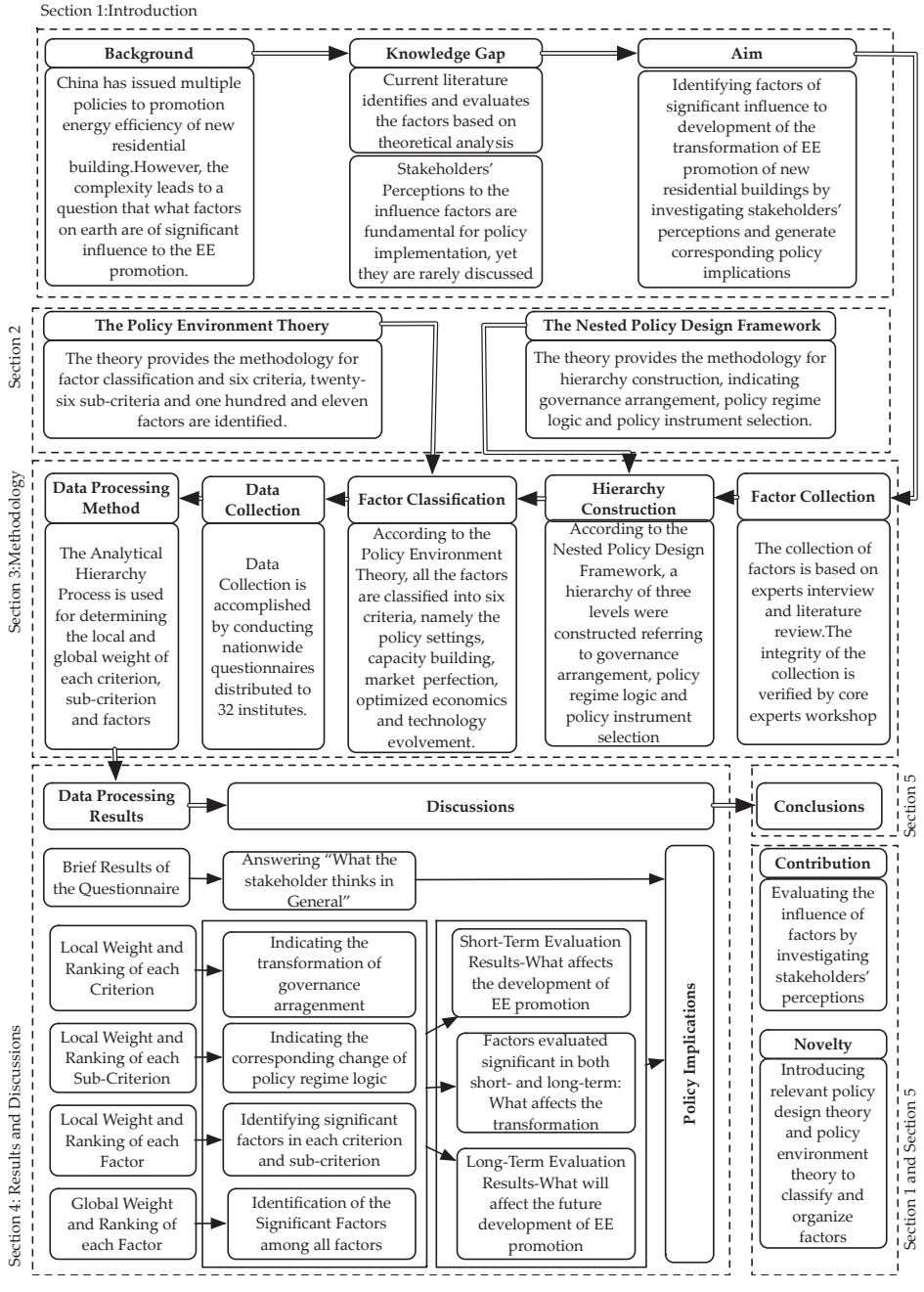

Figure 5. Complete structure and logic flow of the article.

2. The Nested Policy Design Framework and the Policy Environment

The nested policy design framework, proposed by Howlett [51], is a level-based policymaking approach concerning governance arrangement, policy regime, and policy instrument selection

(see Figure 6). Governance comprises actors from all segments of society working together to pursue collective goals [52]. The general category of governance arrangements is legal-based, corporatist-based, market-based, or network-based. Governance arrangement can also be understood from the political (actor constellations), polity (policy regime logic/institutional property), and policy (policy instruments) [53] dimensions. Types of governance arrangements result in different preferences of policy regime logic and policy instrument selection (see Table A2).

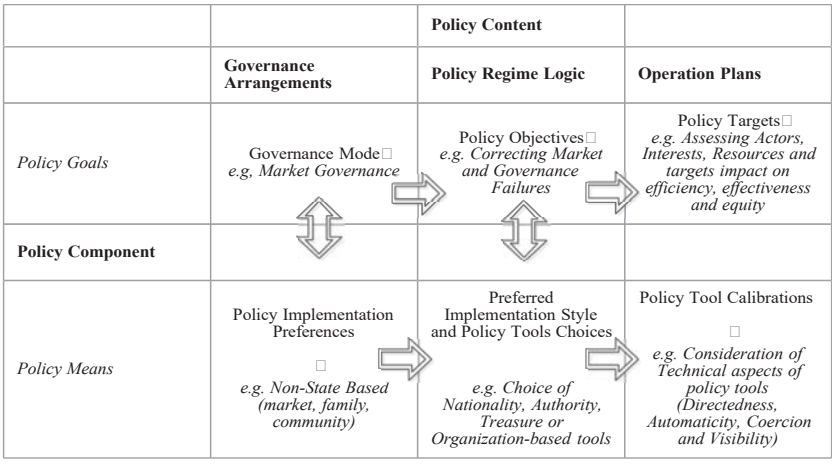

Figure 6. Three-level nested framework for policy design.

In the case of China, Zhang, Zhou et al. [52] conducted a detailed governance analysis based on the policy cycle theory raised by Howlett and Ramesh [54] and argued that the legal-based governance continues to dominate in China, although there are elements of market-based governance. This conclusion was also supported by the research conducted by He, Zhang et al. [55], who summarized, classified, and evaluated all the policy instruments used to promote energy efficiency of buildings from 1986 to 2015. The application and impact differences among the administrative, information-based policy instrument and the voluntary agreement were also analyzed in this research. A more detailed analysis was conducted by Shen, He et al., based on a comparison of policy data from seven typical countries [32]. By taking policy resources into consideration in the selection process of a policy instrument, the research further explored the feasibility of each instrument based on international experience and common application strategy of the seven countries.

The policy environment theory is used to identify and classify those factors beyond the full control of the government. In addition to the policy settings, four key fields of factors are proposed: technology progress, optimized economics, market perfection, and capacity building. Technology is the foundation of the EE improvement in housings. The evolvement of technology decides the pace of EE improvement of buildings. Factors of optimized economics affect the massive adoption of energy efficient technologies. The level of capabilities of relevant stakeholders decides the feasibility regarding the implementation of techniques and policies. Factors of market perfection focus on the relationship of various stakeholders. The target of market perfection is to help energy-efficient technologies, products, and applications win in market competition. Above all, drivers in these fields focus on improving the EE level of technologies, industries, housing, and the massive application of energy efficient technology from technical and social perspective.

3. Methodology

The whole methodology comprises three major parts: (1) Factor collection and hierarchy construction, (2) investigation and data collection, and (3) evaluation based on the AHP. The boundaries for factor collection are set at first. Factors were collected according to the literature from the technology and policy perspectives. The classification of the factors was based on the policy environment theory. The structure of the hierarchy was built based on the nested policy design framework. Nationwide institutes' questionnaires were conducted to collect judgements on the influence of these factors. The target group comprised institutes from different climate zones and of different interests. Collected data was processed using the AHP approach. Corresponding conclusions and policy implications were provided based on the calculated weights and rankings. The structure of the methodology and its implementation process are detailed in Figure 7.

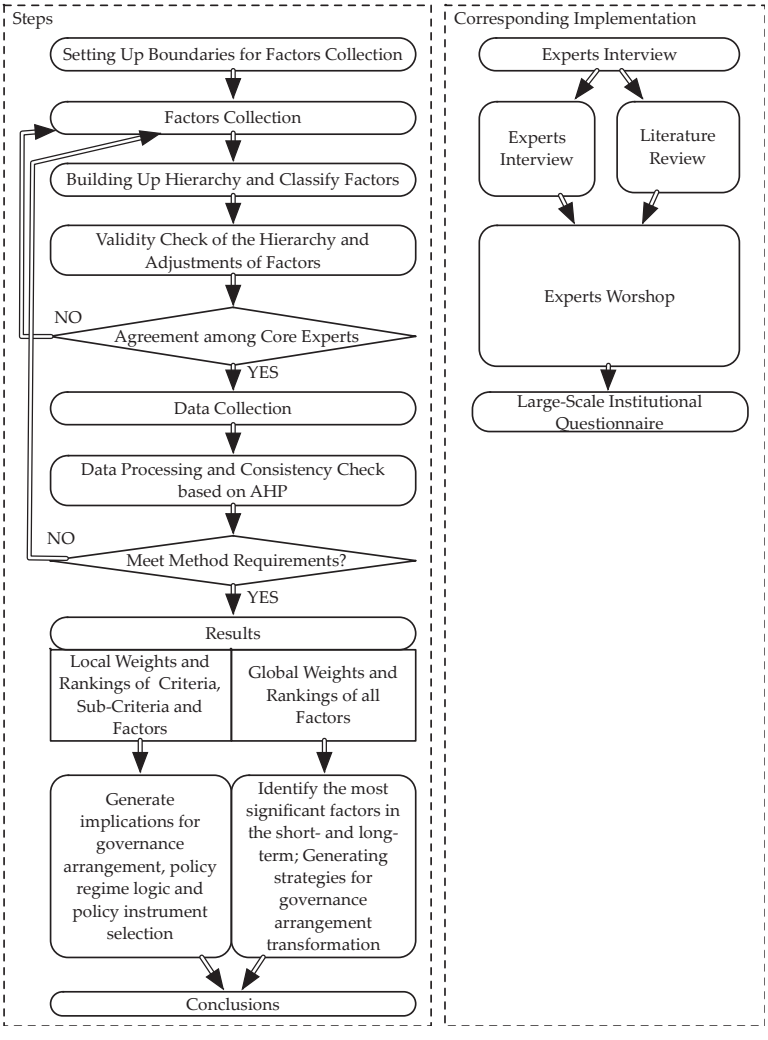

Figure 7. Implementation process.

The AHP method is fundamentally based on pairwise comparisons to generate conclusions. Two elements being compared at a given time un-repeatedly reduces the conceptual complexity of an analysis greatly. This simplification involves reasonable assumptions proposed by Satty [56] and the others [57,58]. Given a pairwise comparison, the analysis involves three tasks: (1) Developing a comparison matrix at each level of the hierarchy starting from the second level and working down, (2) computing the relative weights for each element of the hierarchy, and (3) estimating the consistency ratio to check the consistency of the judgment [59].

The AHP method is selected for the following reasons. (1) The AHP converts these evaluations to numerical values that can be processed and compared over the entire range of the problem. A numerical weight or priority is derived for each element of the hierarchy, allowing diverse and often incommensurable elements to be compared in a rational and consistent manner. This specialty helps evaluate those factors quantitively and makes inter-category comparison possible among the factors. (2) Pairwise comparisons and judgements are made by experts. Through a proper selection of experts, this method enables various stakeholders to participate in the evaluation of factors, revealing their effectiveness from an empirical perspective. (3) The AHP method requires a hierarchy and classification of all the factors. If designed properly, the priority ranking of criteria, sub-criteria, and factors (i.e., local and global) can reveal the truth regarding respondents' opinions.

3.1. Factor Collection and Hierarchy Construction

As a complex socio-technical industry, the EE promotion of new residential buildings can be affected by a large quantity of factors from multiple aspects, from the macro economy to technology (Section 2). Therefore, the following principles were applied to limit the range of factors before the identification of specific factors: (1) Factors should influence, or be influenced by, the policies issued by the Ministry of Housing and Urban-Rural Development (MOHURD) in China because it oversees promoting the EE of buildings in urban areas, policymaking, implementation, supervision, and conducting major projects concerning the EE promotion of new residential buildings; (2) factors directly relevant to building EE promotion in single and district scales and extended construction value chains are considered; and (3) factors could influence the interactions between the policy system and market mechanism to eliminate market failure. The first principle defines the boundary from a policymaking perspective, the second principle is from a policy-environment perspective, and the third principle stresses the interaction between policy factors and factors from the policy environment. Based on the literature review, 111 factors were identified and are listed in the Table A1.

With the help of the nested policy design framework, a hierarchy of three levels were designed as follows: Level 1—criteria level-preference of governance arrangement. These criteria concentrate on only the fields and sectors (e.g., market and technology)—that is, "what type of governance arrangement does, or will China have, and what type of policy instruments should be preferred?" is analyzed or answered on this level. Level 2—sub-criteria level-preference of policy regime logic. These sub-criteria concentrate on the subsectors of the EE promotion of new residential buildings— that is, they are trying to build up the foundation for answering the question "which type of instruments should be selected or preferred?" on this level. Level 3: factor-preference of operational plans (technical policy instrument selection). These factors provide the empirical statistics and evidence of parameter configuration of policy instruments for implementation and collaboration among instruments. Figure 8 gives a detailed graphical presentation of the structure of the constructed hierarchy and its components. The correspondence between the different hierarchic levels and the nested policy design framework is also illustrated.

Regarding the design of criteria and sub-criteria, the policy settings (C5), as a major contributor to the improvement of EE level, was first identified. All the policies can be categorized into three types in China: macro policy (C51), operable policy, and technical policy (C54). Plans, decisions, and other supporting industry policies are classified into the macro level because they are not operable; however, they are sometimes directly associated with the building EE promotion industry. Operable policies

can be divided into two sub-categories, namely, monetary policies (C52) and administrative policies (institutions) (C53), because of the different types of policy resources they require.

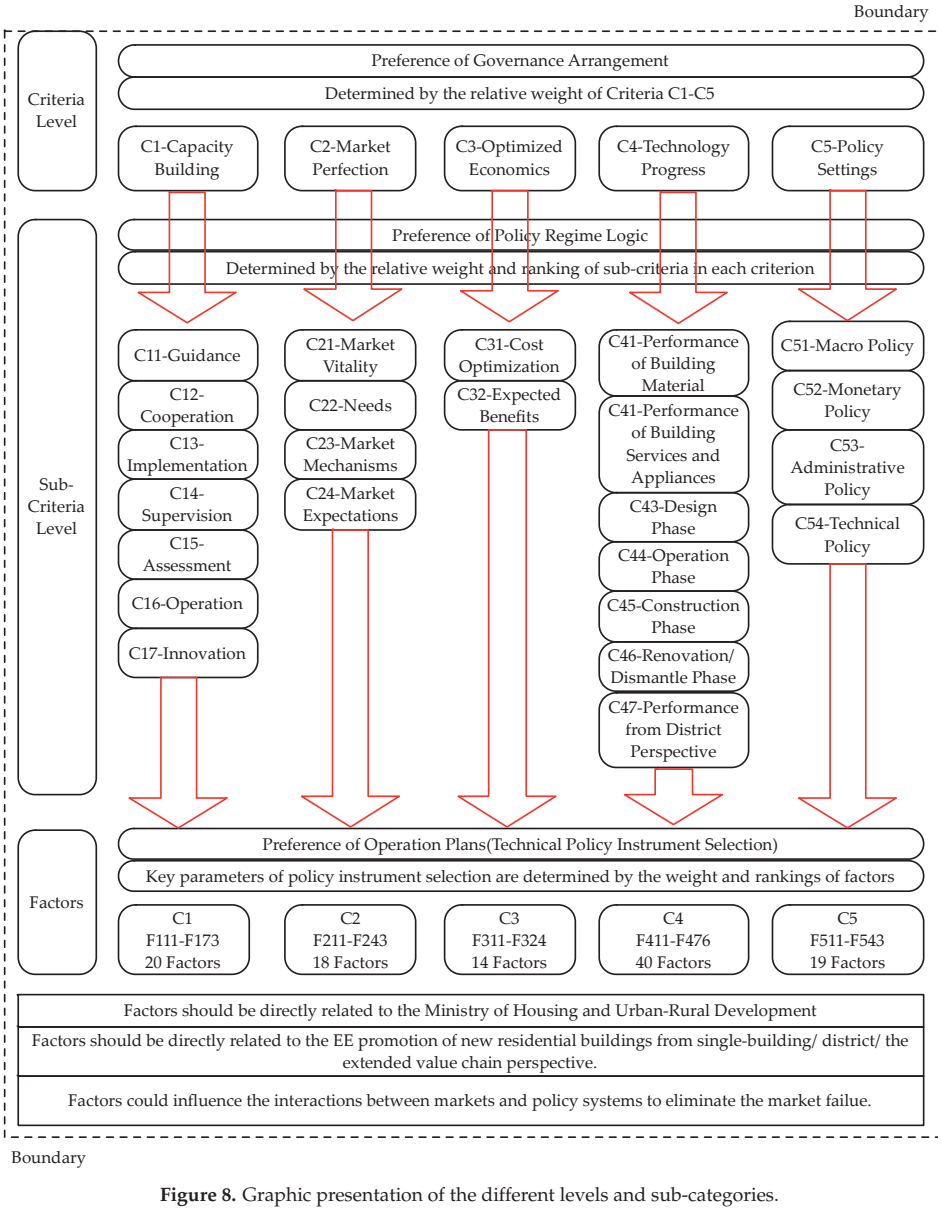

Figure 8. Graphic presentation of the different levels and sub-categories.

In addition to policy settings (C5), the policy environment theory was introduced for criteria and sub-criteria identification. Influencing factors from a policy environment were classified into four categories according to the literature—technology progress (C4), optimized economics (C3), market perfection (C2), and capacity building (C1). The technology progress (C4) focuses on technical factors, which can be classified into six sub-criteria based on the fundamental theory of heating, ventilation, and

air-conditioning from life-cycle perspective (C41 to C46). In addition, factors associated with promoting EE level and efficient use of resources, such as water recycling, distributed energy, and micro-grids were considered because building EE promotion from the district level is a future development trend (C47). The criteria of optimized economics (C3) focuses on costs (C31) and benefits (C32) from technology innovation, the massive application perspective, and the perspective of operation of enterprises in the industry. The criteria of market perfection (C2) attempts to solve the market failure in the EE promotion of new residential buildings industry [40]. The needs (C22) (from all the market stakeholders and governments), as one of the drivers of market development, was a primary consideration. Additionally, according to the requirements of boundary, other factors influencing the interaction between market and policy systems were considered, such as market vitality (C21) (same as market activity) [41], market expectations (C24), and market mechanisms (C23). The capacity building (C1), defined by Robert B. Hawkins from the perspective of political management, is "a concept that encompasses a broad range of activities that are aimed at increase the abilities of citizens and their governments to produce more responsive and efficient public goods. At its core capacity building is concerned with the selection and development of institutional arrangements; both political and administrative" [60]. Seven capacities were identified based on different actors as follows: guidance (C11) and cooperation (C12), referring to central and local government; implementation (C13), referring to planning, designing, and construction enterprises in the industry value chain; supervision (C14), referring to government and third-party institutes; assessment (C15), referring to third-party institutes; operation (C16), referring to institutions involved in the operation stage of buildings like ESCOs(Energy Service Companies) and facility management enterprises; and innovation (C17), referring to all stakeholders in the industry.

3.2. Questionnaire Design and Data Collection Method

In accordance with the principles of questionnaire design [61], the design of the institutional questionnaire are simple, specific, and easy to understand. However, if strictly following the requirements of the AHP methods, the evaluation of 111 factors in three hierarchic levels will lead to 322 times of pairwise comparisons, which is almost impossible for an expert to finish patiently and effectively. Therefore, the Likert 5-Scale was introduced to evaluate the perceived influence of the criteria, sub-criteria, and factors by the investigated institutes independently—1 is for the least importance and 5 is for the greatest importance. To provide additional details on the future situation, the experts in the target group were required to provide their judgements on the short-term and long-term influence of all the factors.

Nationwide institutional questionnaires were used to collect opinions from various frontline stakeholders. Thirty-two institutions from different types of stakeholders, climate zones, and development levels from the national perspective were asked to fill out the questionnaire. The systematic sampling method was used to select these institutes. Additionally, to further improve the stability and amplify the representation of questionnaires, additional requirements were added depending on the property of the institutes when conducting the institutional questionnaires. These requirements are as follows. For government departments, advice from same-level departments, for example, financial departments, industrialization departments, and quality supervision departments, should also be collected when accomplishing the questionnaire. For other institutions, opinions reflected in the questionnaire should be a combination of opinions from high-level decision-makers, frontline workers, and other individuals involved in the industry. The result of institution selection is in Figure 9.

New residential buildings constructed in different climate zones achieve the same level of EE at different rates. Climate differences also lead to different technical strategies and solutions for achieving the same EE level. As indicated in Figure 9, the selected institutes cover all the three major climate zones in China, namely the cold and severe-cold climate zone, the summer-hot&winter-cold climate zone and the summer-hot&winter-warm climate zone. In addition, three national level institutes were also selected to generate more comprehensive opinions.

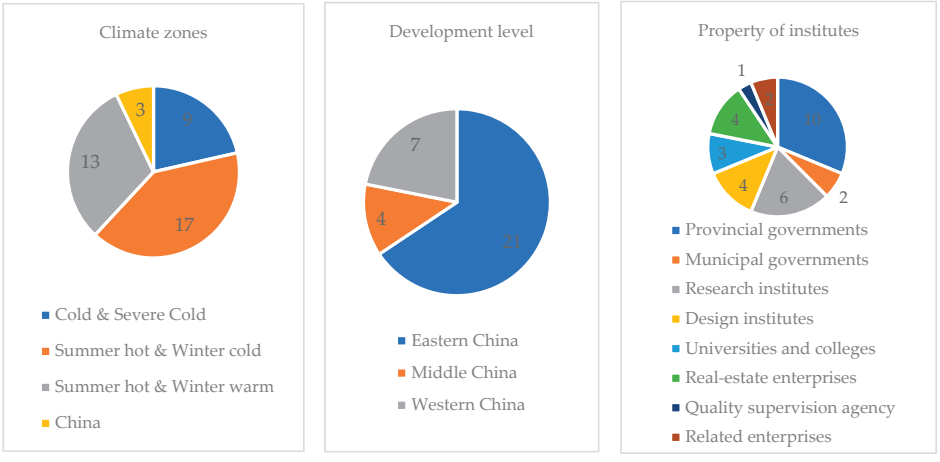

Figure 9. Results of institution selection.

From the development-level perspective, cities in eastern China started their career of EE promotion in buildings also in the 1980s and until now, policy systems and relevant technologies have been well-developed, meaning that they have more successful experience than the other two districts. As for western China, affected by "the grand western development program", its industry of building EE promotion develops at an unprecedented pace. Cities/provinces like Chongqing, Yunnan have already formed their own effective policy systems and technological systems which can also provide useful experience. And in middle China, owing to a lack of supporting policy package on the overall level and diversity of climate within the province, much effort was spent on exploring how to coordinate different policies to promote the EE of buildings in one province as a whole.

Additionally, the consideration of institutes' properties was mainly based on the role which various institutes play in the industry. For example, the externality of new residential EE promotion makes it hard for developers to profit from developing new residential buildings of high energy performance. However, it is strongly favored by provincial and municipal authorities due to policy influence and potential benefit, such as increasing job opportunities.

3.3. Data Processing

Before applying the AHP method to the collected data, efforts were taken to transform the independent evaluation based on the Likert 5-Scale into a pairwise 9-scale comparison. The process is as follows:

Step 1: Calculate the mean value (mv_{ik}) of each element in each level. Let v_{ijk} represent the element k's value in the level i from No. j institutions, in which $1 \leq i \leq 3; 1 \leq j \leq 32$

$$mv_{ik} = \sum_{j=1}^{32} v_{ijk}/32. \tag{1}$$

Step 2: Calculate the maximum and minimum value of elements in each level of the hierarchy. Let

$$mv_i^{max} = \max\{mv_{ik}, 1 \leq i \leq 3\} \tag{2}$$

$$mv_i^{min} = \min\{mv_{ik}, 1 \leq i \leq 3\}. \tag{3}$$

Step 3: Normalize each element into 9-scale pairwise comparisons. For the random two elements mv_{im}, mv_{in} in the criteria, assuming that $mv_{im} \geq mv_{in}$, then

$$a_{mn} = round\left[1 + \frac{mv_{im} - mv_{in}}{mv_i^{max} - mv_i^{min}} \times 8\right] \tag{4}$$

$$a_{nm} = 1/a_{mn}. \tag{5}$$

With the aforementioned adjustment, the judgement matrix A is formed, filled by the elements calculated in Step 3. The following data processing follows the requirement of the AHP method as follows:

Step 4: Determining of the weight vector. The weight factor is the row factor through ensemble average calculation and normalization of the judgement matrix. Assume that the largest eigenvalue of the judgement matrix is λ_m and the corresponding eigenvector is W_m, the following equation will be achieved:

$$\mathrm{A}Wm = \lambda mWm\ \mathrm{A}W_m = \lambda_m W_m \tag{6}$$

The complete process to calculate the weight factor is as follows:

Sub-Step 1: Calculation of the product of all elements (P_i) in each row

$$Pi = j = 1naijP_i = \prod_{j=1}^{n} a_{ij}. \tag{7}$$

Sub-Step 2: Calculation of n times squaring root of P achieved in Sub-Step 1

$$W_i = \sqrt[n]{P_i}. \tag{8}$$

Sub-Step 3: Calculation of weight factor by normalization of the vector W

$$w_i = W_i \div \sum_{i=1}^{n} W_i. \tag{9}$$

Sub-Step 4: Calculation of largest eigenvalue

$$\lambda_m = \frac{1}{n} \times \sum_{i=1}^{n} \frac{(AW)_i}{w_i}. \tag{10}$$

Until this point in this study, the value of w_i represents the weight of each factor and the sum of the weights is 1.

Step 5: Consistency check. The purpose of the consistency check is to verify the reliability of the weight ranking. The larger the difference between the greatest eigenvalue and the number of the elements, the larger the inconsistency. The larger inconsistency can also cause large judgement bias. Thus, the consistency index (CI) is introduced to quantitively measure the inconsistency as follows:

$$\mathrm{CI} = \frac{\lambda - n}{n - 1} \tag{11}$$

when the CI approaches 0, the judgement matrix has an increasing consistency, and vice versa. To measure the CI quantitively, the random consistency index (RI) is introduced. Based on the research result from Saaty, the distribution of RI is as follows in Table 1:

Table 1. Distribution of RI.

N	1	2	3	4	5	6	7	8	9	10	11	12	13	14	15
RI	0	0	0.52	0.89	1.12	1.26	1.36	1.41	1.46	1.49	1.52	1.54	1.56	1.58	1.59

The corresponding consistency ratio (CR) is defined as follows:

$$\mathrm{CR} = \frac{CI}{RI} \tag{12}$$

The judgement matrix is believed to have a satisfying consistency when CR < 0.1. The corresponding normalized eigenvector can be used as the weight vector. Otherwise the judgement matrix shall be re-built and adjustments to the element shall be made.

Because the Likert 5-Scale was introduced to collect the opinions of stakeholders, whereas the AHP method was used for data processing, the results and discussions are correspondingly two-fold. The results based on the Likert 5-Scale reveals the influence of each factor quantitively. The change of average value between the short term and long term indicates the perceived judgements on each factor independently. However, the other results based on the AHP methods provides more information on the weight and ranking of one factor's influence on the rest—locally and globally—according to the methodology. Therefore, both results are considered when analyzing the collected data.

On the one hand, results based on the Likert 5-Scale are analyzed based on the differences in the interests of the stakeholders. The average scoring of each type of stakeholders and variance (the percentage of maximum difference of average value among stakeholders to the overall average value) between actors are calculated. If the variance is less than 20%, the average value could be considered an agreement among various stakeholders. If the variance is equal to or greater than 20%, it is considered that disagreements among stakeholders are sufficiently significant and require extra consideration.

On the other hand, the results based on the AHP are analyzed based on the calculated weight and ranking of each factor in the three levels. The local priority ranking of all the criteria and sub-criteria indicates the stakeholders' judgements regarding the government arrangement and policy regime logic, respectively. The higher ranking of a certain system is equal to the greater effect of the corresponding factors. The weight and ranking changes on the criteria level indicate the changes that will occur to the governance arrangement in China and suggest what type of policy instruments are preferred under the context of governance arrangement transformation. The weight and ranking of each factor indicate its significance to the sub-criteria level from a stakeholder's perspective. The results also provide suggestions regarding the details of how the preferred policy instrument should be configured. The factor with a higher weight is considered more effective in realizing the expected outcome of a policy instrument. Those factors of higher ranking should be given priority and considered.

4. Results and Discussions

4.1. Brief Results of Investigation

The average opinions of judgements from different stakeholders are summarized in Table 2. All the experts agree on the judgements of the influence of policy settings (C5), market optimization (C2), capacity building (C1), and technology progress (C4) in both terms. The overall opinions (M values in Table 2) indicate that policy settings (C5) have the greatest influence in the short term and the second least influence in the long term. The influence of technology progress (C4) and market optimization (C2) will slightly increase, and market optimization (C2) will result in the greatest impacts in the long term. The changes of C2 and C5 between terms indicate strategic change of the development of EE promotion of new residential buildings in China—that is, a more "marketized" policy environment should be formed. The M increase of C4 stresses the necessity of technology—no matter what type of development pattern should occur; technological progress remains the influence of the same level.

Table 2. Average opinions of judgements from different stakeholders.

		2016–2020					2020–2030				
		E	**G**	**RI**	**M**	**V**	**E**	**G**	**RI**	**M**	**V**
Criteria Level	Capacity(C1)	4.250	3.889	4.375	4.160	11.7%	4.250	3.889	4.500	4.200	14.6%
	Market(C2)	4.250	4.182	4.500	4.296	7.4%	4.625	4.182	4.500	4.407	10.1%
	Economy(C3)	4.500	3.800	4.250	4.154	16.9%	**4.500**	**3.455**	**4.250**	**4.000**	**26.1%**
	Technology(C4)	4.125	4.091	4.250	4.148	3.8%	*4.125*	*4.364*	*4.250*	*4.259*	*5.6%*
	Policy(C5)	4.500	4.273	4.375	4.370	5.2%	4.500	4.000	4.111	4.179	12.0%
	Mean	4.325	4.047	4.350	4.226	7.2%	4.400	3.978	4.322	4.209	10.0%
Capacity	C11	**5.000**	**3.889**	**5.000**	**4.444**	**25.0%**	**4.750**	**3.889**	**4.600**	**4.278**	**20.1%**
	C12	**4.250**	**3.111**	**4.400**	**3.722**	**34.6%**	**4.000**	**3.111**	**4.400**	**3.667**	**35.2%**
	C13	4.500	3.778	4.400	4.111	17.6%	4.000	3.889	4.600	4.111	17.3%
	C14	4.500	3.778	4.400	4.111	17.6%	4.000	4.222	4.600	4.278	14.0%
	C15	**4.250**	**3.556**	**4.400**	**3.944**	**21.4%**	**4.250**	**3.667**	**5.000**	**4.167**	**32.0%**
	C16	**4.000**	**3.778**	**4.600**	**4.056**	**20.3%**	**4.000**	**3.889**	**5.000**	**4.222**	**26.3%**
	C17	4.750	4.111	4.400	4.333	14.7%	4.750	4.222	4.400	4.389	12.0%
	M	4.464	3.714	4.514	4.103	19.5%	4.250	3.841	4.657	4.149	19.6%
Market	C21	3.800	3.556	4.200	3.789	17.0%	4.400	3.778	4.200	4.053	15.4%
	C22	*4.000*	*4.333*	*4.600*	*4.316*	*13.9%*	4.400	4.333	4.800	4.474	10.4%
	C23	3.800	3.444	3.800	3.632	9.8%	4.200	3.778	4.400	4.053	15.4%
	C24	4.000	3.556	4.200	3.842	16.8%	4.200	3.875	4.400	4.111	12.8%
	M	3.900	3.722	4.200	3.895	12.3%	4.300	3.941	4.450	4.173	12.2%
Economy	C31	*4.000*	*4.111*	*4.600*	*4.222*	*14.2%*	**4.500**	**4.000**	**5.000**	**4.389**	**22.8%**
	C32	*4.000*	*4.111*	*4.600*	*4.222*	*14.2%*	4.250	4.000	4.800	4.278	18.7%
	M	4.000	4.111	4.600	4.222	14.2%	4.375	4.000	4.900	4.333	20.8%
Technology	C41	*4.500*	*4.333*	*4.200*	*4.350*	*6.9%*	**3.500**	**3.889**	**4.600**	**3.950**	**27.8%**
	C42	3.833	4.000	4.200	4.000	9.2%	3.667	4.000	4.200	3.950	13.5%
	C43	4.500	4.444	4.800	4.550	7.8%	4.667	4.667	5.000	4.750	7.0%
	C44	*3.667*	*3.667*	*4.400*	*3.850*	*19.0%*	**3.500**	**4.111**	**5.000**	**4.150**	**36.1%**
	C45	3.833	3.667	3.800	3.750	4.4%	4.000	4.111	4.800	4.250	18.8%
	C46	3.500	3.444	4.000	3.600	15.4%	4.167	3.889	4.600	4.150	17.1%
	C47	3.667	3.333	3.800	3.550	13.1%	4.000	3.889	4.600	4.100	17.3%
	M	3.929	3.841	4.171	3.950	8.4%	3.929	4.079	4.686	4.186	18.1%
Policy	C51	*4.000*	*4.333*	*4.400*	*4.278*	*9.4%*	4.250	4.000	4.800	4.278	18.7%
	C52	4.750	4.333	4.600	4.500	9.3%	4.750	4.000	4.600	4.333	17.3%
	C53	4.500	4.222	4.600	4.389	8.6%	4.500	4.500	4.600	4.529	2.2%
	C54	4.500	4.000	4.200	4.167	12.0%	4.500	4.125	4.500	4.313	8.7%
	M	4.438	4.222	4.450	4.333	5.3%	4.500	4.156	4.625	4.363	16.7%

Notes: E—Enterprises; G—Governments; RI—Research Institute; M—Mean; V—Variance.

In addition to the agreements achieved among various stakeholders, there are still attitude preferences caused by the information asymmetry existing in the EE promotion industry. Different stakeholders hold different opinions about the influence of in each criterial and sub-criterial level. Generally, governments tended to be the most conservative stakeholders about the influence of the identified criteria and sub-criteria. Exceptions are marked as italic in Table 2. Research institutes, overall, gave higher evaluation scorings than the responses from enterprises. The corresponding exceptions are marked as underlined.

As to stakeholders' attitudes towards the influence of each criteria, Figure 10 depicts the corresponding results. In the short term, enterprises believe that the influence of economic factors (C3) is greatest and is in line with the influence of policy settings (C5), whereas governments believe that economic factors (C3) is of the least influence. Research institutes believe that factors regarding market (C2) are of the great influence. In the long term, all the stakeholders believe that the factors regarding market (C2) are of the most significant influence. In addition, research institutes also believe that the capacity building (C1) is of the same influence as the factors in market system (C2). Enterprises hold the opinions that factors regarding economy (C3) are as influential as the factors regarding policy settings (C5). Research institutes believe the economy factors (C3) are of greater influence than policy settings (C5), while governments hold the opposite judgements.

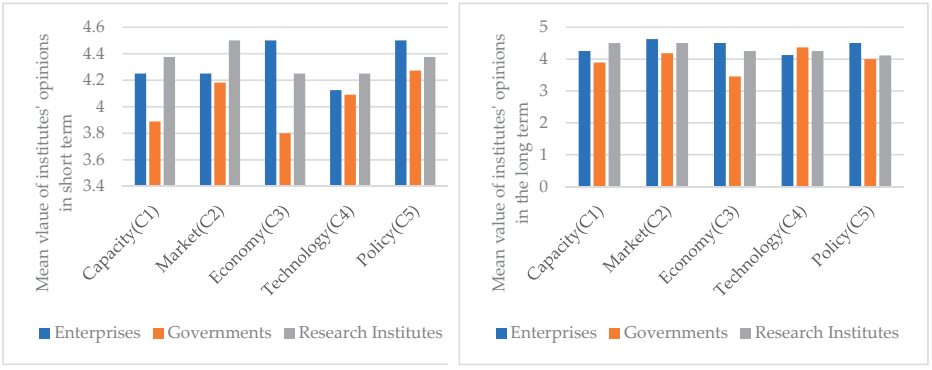

(**a**) (**b**)

Figure 10. Stakeholders' average opinions on each criterion. (**a**) Depicts their opinions regarding the short-term influence of each criteria and (**b**) depicts the opinions regarding the long-term influence.

However, according to the methodology in Section 3.3, agreements on the importance of these criteria are still considered to be reached because the variance of stakeholders' judgements are smaller than 20%. Under this circumstance, it is considered by the author that whichever stakeholders' opinions differ, they are not significant enough to change the agreements among all the stakeholders.

Notably, significant disagreements are still observed among stakeholders on the criteria and sub-criteria levels, in addition to the attitude's preference. These disagreements are marked as bold in Table 2. Experts representing enterprises and research institutes believe economic factors in C2 have substantial impacts, whereas experts from governments do not. The author asserts that this disagreement is the symbol of information asymmetry in the EE promotion of new residential building industry and the proof of the externalities as described by Reference [35]. The judgements provided by enterprises reveal their eagerness for profits due to externalities, whereas governments believe that economic factors could not influence the EE promotion as effectively as policies (see C5) and the perfection of market mechanisms (see C2). In the long term, this disagreement is further enlarged. Governments' judgements on economic factors' influence have further decreased, and the remaining stakeholders keep the same.

Regarding the sub-criteria level, disagreements are also observed and are mostly in the capacity field (see C11–C17). Enterprises and research institutes believe the capacity of guidance (C11), cooperation (C12), assessment (C15), and operation (C16) will significantly influence the improvement in capacity in both terms, whereas governments do not. These disagreements further support the information asymmetry between governments and markets as mentioned in a previous section. In addition, these disagreements stressed the need for more capable and effective governments from the market's perspective because the sub-criteria C11, C12, and C15 mainly refer to governments. This judgement is further proven by the judgements from research institutes.

As for the disagreement identified in the economy system (see C31–C32), the debate concentrates on whether costs should have great significance or super significance. Consensus could therefore be considered achieved. The disagreements in technology aspects (see C41–C47) focus on the efficiency of building materials (C41) and building operation (C44), which are in consensus in the short term. This result is partly because, currently, China is realizing the EE target of a building by increasing the thickness of insulation, which causes many safety problems regarding structural strength of the envelop and inflammability. A small step in improving the efficiency of building materials could lead to a giant leap in the overall energy efficiency promotion. As for operation, technology measures cannot significantly reduce the energy consumption of residential buildings due to the complexities, such as property rights, residential patterns, and various lifestyles.

4.2. Weights and Rankings of Criteria and Sub-Criteria

The weights and rankings of criteria and sub-criteria are summarized in Table 3. The weights and rankings of all the criteria indicate what governance arrangement dominates at the current stage and should occur in the long term, while those of all the sub-criteria prove the governance arrangement transformation and further indicate how should the transformation be realized.

Table 3. Results of the analytical hierarchy process (AHP) on criteria and sub-criteria levels.

Criteria	2016–2020		2020–2030		Sub-Criteria		2016–2020		2020–2030		Weight Change
	W	*R*	W	*R*			W	*R*	W	*R*	
Capacity Building	0.053	3	0.085	3	Guidance	C11	0.358	1	0.188	3	−0.170
					Cooperation	C12	0.055	6	0.033	7	−0.022
					Implementation	C13	0.097	3	0.067	6	−0.030
					Supervision	C14	0.097	3	0.188	3	0.091
					Assessment	C15	0.055	6	0.099	5	0.044
					Operation	C16	0.097	3	0.121	2	0.024
					Innovation	C17	0.243	2	0.304	1	0.061
Market Perfection	0.261	2	0.623	1	Market Vitality	C21	0.142	3	0.106	3	−0.036
					Needs	C22	0.627	1	0.598	1	−0.029
					Market Mechanism	C23	0.073	4	0.106	3	0.033
					Market Expectation	C24	0.158	2	0.189	2	0.031
Optimized Economics	0.053	3	0.045	5	Cost	C31	0.5	1	0.667	1	0.167
					Benefit	C32	0.5	1	0.333	2	−0.167
Technology Evolvement	0.053	3	0.185	2	Building Materials	C41	0.265	2	0.039	6	−0.226
					Building Services and Appliance	C42	0.116	3	0.039	6	−0.077
					Design Phase	C43	0.432	1	0.515	1	0.083
					Operation Phase	C44	0.074	4	0.09	3	0.016
					Construction Phase	C45	0.053	5	0.148	2	0.095
					Dismantle/Renovation Phase	C46	0.032	6	0.09	3	0.058
					District Perspective	C47	0.029	7	0.08	5	0.051
Policy Settings	0.58	1	0.061	4	Macro Policy	C51	0.16	3	0.239	2	0.079
					Monetary Policy	C52	0.467	1	0.433	1	−0.034
					Policy Mechanism Design	C53	0.278	2	0.239	2	−0.039
					Technology Policy	C54	0.095	4	0.088	4	−0.007

Notes: W—Weight; R—Rank.

4.2.1. Weights and Rankings of Criteria

At the criteria level, policy settings (C5) and market optimization (C2) are of the greatest importance in the short term. The summation of the weights of these two criteria accounts for over 80% of the total weight of the five criteria. This result is in accordance with the fact that the combination of "legal-based governance" and "corporatist-based governance" dominates in the field of the EE promotion of new residential buildings at the current stage, as reviewed in Section 2 and discussed in Section 4.1. The ranking of C2 in second place in the short term also indicates that the market for EE promotion of new residential buildings is still not mature. In addition to market failure, many problems must be solved by policy settings based on a mandatory method such as administrative licensing [62–64]. In the long term, the influence of policy settings (C5) will be significantly reduced by almost 90% and will rank fourth in the long term, and the ranking of market optimization (C2) rises to first. The ranking shift implies that the current developing mode will be substituted by the new mode "guided by government, predominated by market entities" in the long term, and the governance arrangement will shift toward "market governance" and "network governance."

The criteria of capacity building (C1), optimized economics (C3), and technology evolvement (C4) have an identical ranking in the short term, which reveals their equal importance to the EE promotion under current governance arrangement. In the long term, the ranking of C4 rises to second while that of C3 decreases to fifth. The ranking change of C4 between terms shows the importance of technology

factors. Under the background of stable and effective market mechanisms and policy settings, the continuous development and popularization of technology will become a strong support for the industry. As for C3, the author asserts that, the identical rankings in both terms are determined by market stakeholders' continuous eagerness of benefits. This argument is also proved in Table 2—that C3, evaluated by enterprises, is of the same importance in both terms. In addition, the weight increase implies that economy will play a more important role in the long term.

4.2.2. Weights and Rankings of Sub-criteria

The forecasted governance arrangement transformation does not lead to substantial ranking changes of most sub-criteria (except C23 and C51) in C2 and C5, as indicated in Figure 11. It is asserted by the author that the consistency of these criteria between terms are determined by the role that each sub-criterion plays in the EE promotion process. As for the sub-criteria in policy setting (C5), the monetary policy (C52) and policy mechanism design (C53) rank stably front due to their effectiveness in satisfying market stakeholders' eagerness for profit (C31, C32). Technology policy (C54) ranks last since it has no incentives for stakeholders. Regarding market perfection (C2), market needs (C22), as the source power of market development, stably rank first in both terms. Market expectations (C24), depicting stakeholders' willingness participating in the building EE promotion market, ranks second in both terms. Market vitality (C21), as the sub-criterion describing the real activeness of the market, ranks third in both terms with a decreased weight.

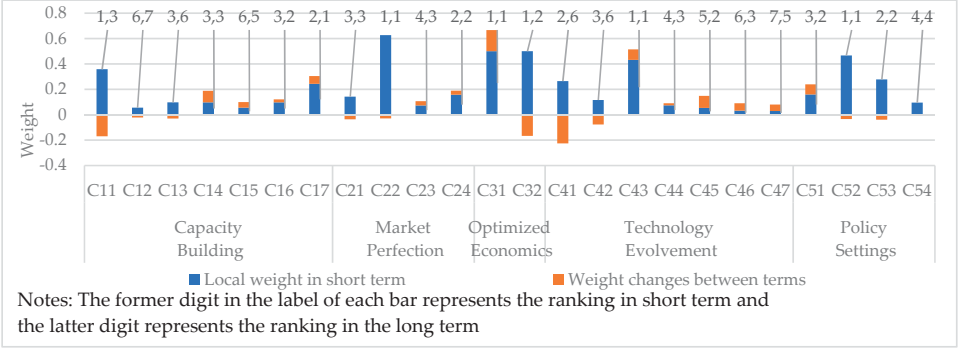

Figure 11. Weights and rankings of each sub-criterion.

However, the weight change of each sub-criterion still reveals how the policy setting will change and how the market should be perfected. For example, the weight decrease in policy mechanism design (C53), along with the weight increase in market mechanisms (C23), stress the long-term market perfection through improved policy settings (C52) in the short term. The weight and ranking increases in macro policy (C51) also indicate the importance of market expectations (C24).

The substantial ranking changes in capacity building (C1) criteria depict the importance of various kinds of capacities regarding difference stakeholders. In the forecasted market-based/network-based governance arrangement, governments play a role in eliminating market failures. The opinions and perceptions of market stakeholders are expected to dominate, and guidance from governments is not a necessity. Therefore, the government's capacity of guiding (C11) will not be as important as they are now. The capacity for supervision (C14), as a policy instrument adjusting market activities, remains of great importance in both terms. The corresponding weight increase indicates its increasing importance in eliminating market failures with the change to the new governance arrangement. The capacity of assessment (C15), defined as the capability to evaluate the quality and the amount of building EE promotion, will be of great influence and a prioritized ranking because it is the foundation for the development of "energy efficiency-oriented market mechanisms." The capacity of innovation (C17)

ranks second and further rises to first place in the long term. The author asserts that this ranking is caused by the specialty of China situation—the specialty of overall governance arrangement and the residence pattern lead stakeholders to little advanced experience that can be referred to. The encountered barriers and problems need to be solved innovatively according to specific situation.

The ranking changes of technology evolvement (C4) also indicate the technology strategy change for a higher efficiency in the new residential building sector. In the short term, the EE level in the design phase (also known as energy efficient design) accounts for the biggest weight. This ranking shows the importance of energy efficient design and reveals that, in the current stage, the throttle of EE promotion before construction is the building materials. The ranking of appliances and operation implies that space remains for the reduction of energy consumption by renovations at a low cost or the behavior of residents. In the long term, this priority ranking becomes EE promotion in the design phase > construction phase > operation phase = dismantle/renovation phase > building materials = building services and appliance. The new ranking stresses the importance of construction and shows that the influence of the EE performance of building materials and appliances will significantly decrease.

4.3. Independent Analysis of Factors

The calculation results of all the factors are listed in Table A3. The weight and ranking of each factor indicate their importance and relative priority in a sub-criterion perceived by experts. Instead of simply describing the meanings of weight and ranking of each factor, this section concentrates on the factors with significant influence, the corresponding empirical proofs, and the relations between these factors. Those factors with a higher weight than the average, in either term, in a cluster are identified as significant. The results are summarized in Figures 12–16.

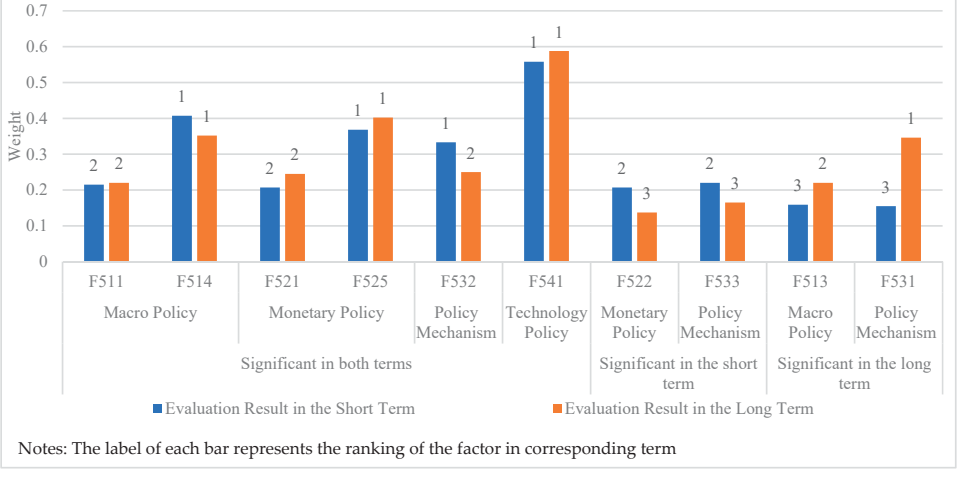

Figure 12. Evaluation results of significant factors in policy settings criteria.

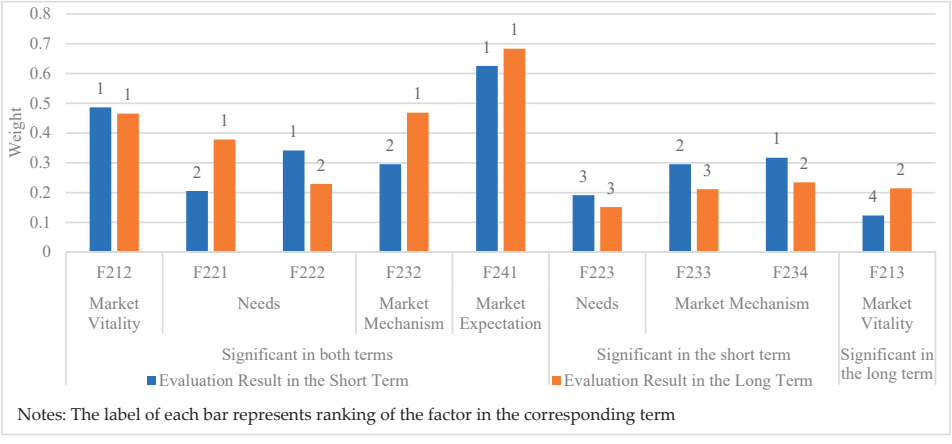

Notes: The label of each bar represents ranking of the factor in the corresponding term

Figure 13. Evaluation results of significant factors in market perfection criteria.

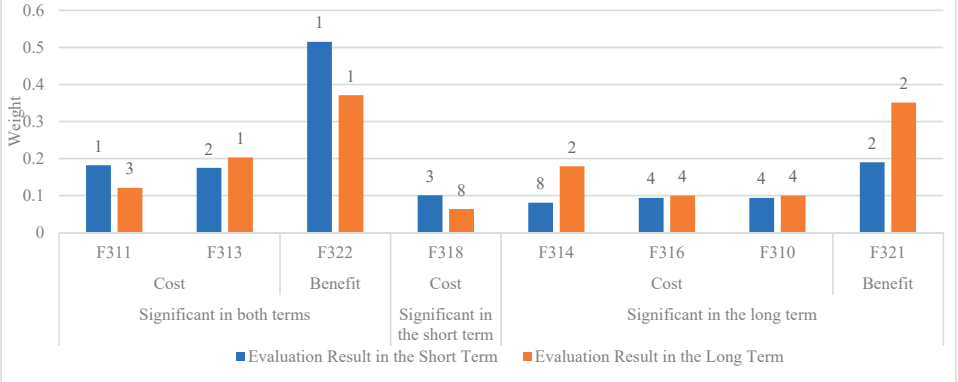

Notes: The lable of each bar represents the ranking of the factor in the corresponding term

Figure 14. Evaluation results of significant factors in optimized economics criteria.

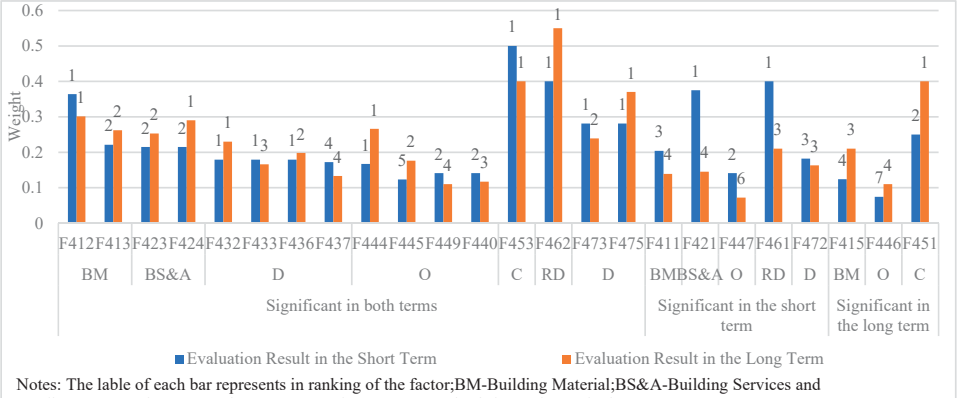

Notes: The lable of each bar represents in ranking of the factor;BM-Building Material;BS&A-Building Services and Appliance;D-Desgin;O-Operation;C-Construction;RD:Renovation/Dismantle;D-District

Figure 15. Evaluation results of significant factors in technology evolvement criteria.

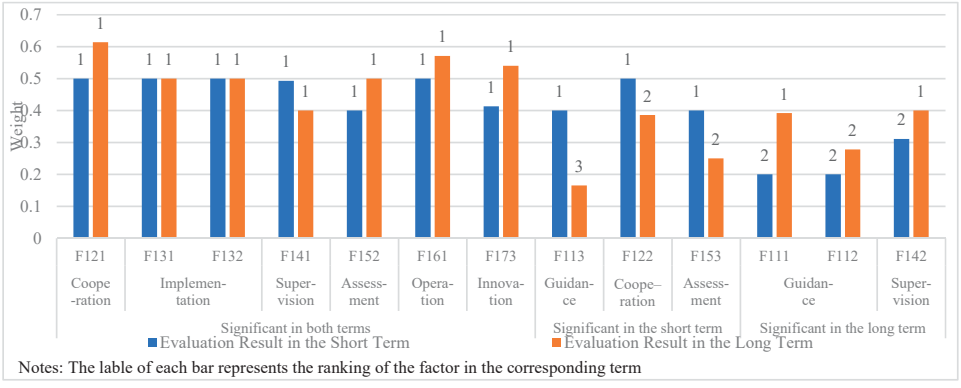

Figure 16. Evaluation results of significant factors in capacity building criteria.

The following discussions will start from the significant factors in the policy system (C5) as it ranks first in the short term on criteria level, followed by market system (C2) as it ranks second in the short term and has the greatest weight in the long term. The factors in economic criteria (C3), as a connection between market and technology, will be discussed afterward. Factors in technology criteria (C4) will be analyzed relatively independently to find the routine for future development. Finally, the factors in capacity building criteria (C1) will be discussed in association with the aforementioned criteria as it involves all the stakeholders in the construction value chain.

Policy Settings (see Figure 12): National mid-/long-term development plan (F511) is of significant importance in both terms since it plays an important role in establishing market expectations (see F241). The significance of industry-supporting policy (F514) is determined by the complexity of the EE promotion industry as a crossover industry among production, construction, and operation. The industry-supporting policies focus the whole construction value chain instead of one key link. Correspondingly, the factor "floor-area ratio reward" (F525) is evaluated as the most effective policy instrument by experts because it is normally awarded to the developers. By increasing the profit of the developers who are in the font stage of the value chain, the value will be further conducted to the downstream industry [65,66]. Additionally, the high housing price makes it easier for developers and downstream stakeholders to attain more profit than other current monetary policies in China.

The factor "local government assessment system" (F532) is evaluated as significant in both terms due to its effectiveness in stimulating local governments' willingness to participate in the EE promotion of new residential buildings. The assessment result will directly influence the human source allocation of local governments and the total amount of subsidy from central governments.

For technology policy (see C54), the revision of codes and standards (F541) is significant because codes and standards draw the EE baseline of design and construction of high-performance buildings, and their renovation speeds determine the pace of technology evolvement of the whole industry. The diversity of methods realizing the requirements of the standards determines that the renovation of atlas is not such a profound influence as the renovation of codes. Additionally, because of the property of compulsion, the renovation of codes, standards, and atlas have greater influence than the recommended list.

Market Perfection (see Figure 13): Regarding the specific factors in the "needs" field, the needs of governments and homebuyers (see F221, F222 in Figure 13) dominate. In the short term, the building EE promotion market is driven by the need of governments to simply fulfill their responsibility, while in the long term, homebuyers will play the most significant role in the process. The ranking change of these two factors is also the proof of the governance arrangement transformation.

The weights and rankings of factors in the other three sub-criteria depict the details regarding how they interact with each other. The stability and continuity of policies (F241) will significantly

increase the market expectations of various stakeholders [67]. After the ignition of market entities' willingness, a good policy environment (see F212) can be a powerful support for stakeholders to develop continuously in this field. Governments shall also take actions to establish effective business modes (F233) and financing channels (F232) for the enterprises in the short term. In accordance with the governance arrangement transformation discussed in Section 4.1, the influence of factors introducing market investment (an identical ranking change of F213 and F233) will also increase in the long term. The availability of financing products, services, and channels (F213) will become of great significance and affect the stakeholders' active participation in the market. Additionally, the buildup of an effective market mechanism should start with taking advantage of energy efficiency trading (F234) because successful pilot projects have already been observed in Shenzhen.

Optimized Economics (see Figure 14): In the cost field, the cost of technology R&D (F311) plays the most important role in the short term. In accordance with the conclusions and speculations on the analysis of the market system and capacity system (F173), this ranking indicates that the promotion of technology shall be conducted, and an upgrade of the technology system is a necessity. In the long term, the level of marketization of technology and products (F314) becomes primary in the cost sub-criteria, which is logically in line with the theory of the technology life-cycle [68]. The payback period (F322) in the benefit part remains significant in both terms. On the one hand, the significance of F322 is in accordance with the ranking of the cost because technology R&D and marketization are tightly associated with the calculation of the payback period; on the other hand, in China's residential building sector, despite the amount of EE promotion, a relatively low energy price [69] leads to a longer payback period for enterprises, concerning facility management or energy management.

Technology Evolvement (see Figure 15): The design phase, as an early stage of the building's life-cycle, plays a critical role in determining the EE level of the architecture in both terms. Factors regarding thermal performance of windows (F413, F432, F433) rank front, followed by the direction the building faces (F437) and natural ventilation (F436) in both terms. In accordance with the factors' evaluation in the building material field (F411), the strategy of energy efficient design can be described as follows. "For the non-transparent part, the EE improvement should focus on the thermal performance of insulation, instead of simply increasing the thickness. For the transparent part of a building (see F412), its design should comprehensively take the layout of the buildings, certain room and the thermal performance of materials into consideration."

For the other technology aspects of newly constructed buildings, the concept of "clean and renewable energy/resources utilization" (F444, F449, F473, F475, F447) dominates in the short term, and the concept of "energy/resources recycling" (F445, F440, F462) dominates in the long term. This ranking of factors in the construction (see C45), operation (see C44), and renovation (see C46) fields means that, despite the energy and resource shortage in China, sufficient no-fossil energy/high-grade energy remains for the consumption of residential buildings in the short term. The comprehensive use of various types of energy and resources will increase the EE level because the evaluation is normally fossil-energy/non-renewable resources-based. However, the exacerbation of energy and resources will finally affect the energy consumption of housing in the long term. The strategy will then shift to "recycling" rather than "comprehensive utilization."

Capacity Building (see Figure 16): Governments always play an important role in both terms. In the short term, the governments' ability to establish the implementation standards (F113) ranks first. The implementation standard, under this context, refers to instructing market entities regarding how to realize the EE target by setting up a conditional incentive system and technological specifications. The more detailed the implementation standard, the more extensively the government dominates. In the long term, a government's ability to guide the energy-saving consciousness (F111) ranks first. Along with the decrease in the influence of the cooperation ability between governments (F122), the ability to guide cooperation market entities (F121) is of more significance in the long term. The shift of this ranking also shows that "market governance" and "network governance" will gradually form. In addition to the enforcement of the energy-saving consciousness of stakeholders (see F111), the

building up of a stable cooperation relationship among market entities (see F112, F121, F122) is also important.

Regarding the stakeholders in the construction value chain, the ability of the design construction (F131, F132) of the same importance are observed in both terms. The weight of the factor "capacity of facility management" (F161) ranks first in the management field and increases to approximately 15%. Due to the application of various energy-saving technologies, the operation quality of these pieces of equipment directly affect the energy consumption of a certain building.

With respect to the relevant third-party institutes, Figure 16 presents the details of the capacity building of supervision and assessment. The construction quality (F141), as a basic and mandatory requirement of a building, remains of significant importance in both terms. The capacity of credit supervision (F142) is also evaluated as significant since market stakeholders will dominate the EE promotion process in the long term. The capacity of assessing energy saving (F152) is evaluated as significant in both terms since the quantified evaluation of energy saving is the foundation for the design of incentives. Additionally, that the innovation ability (C17) ranks second indicates its importance in promoting the EE level of buildings. In accordance with the ranking change of a technology system on a criteria level, the ability of technology innovation (F173) ranks first. Technology, as the foundation of the EE improvement, directly determined the highest level of the promotion.

4.4. Comprehensive Analysis of All the Factors

Other sections have discussed the weights, rankings, and corresponding implications of each factor in a separate sub-criteria system. However, chances remain that one factor in a certain system of minor influence may have a great global influence. Additionally, the continuity of one factor having a significant impact in both terms will help the policymakers improve their understanding of the building EE promotion process in China. Thus, all the factors are analyzed in this section. Weight and the corresponding global ranking of each factor is calculated, neglecting its belonging field. Figure 17 is a plot of all the factors based on their rankings in both terms.

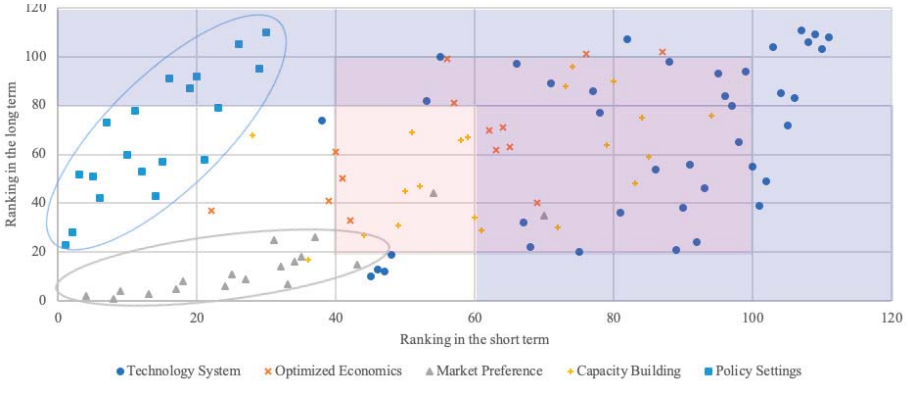

Figure 17. Distribution of all the factors.

As shown in Figure 17, factors in the "market perfection system" (C2) and "policy settings system" (C5) tend to cluster (as indicated in the blue and gray circles), whereas the distribution of the factors in the remainder of the systems is decentralized. Factors in the policy settings criteria (C5) have a higher ranking in the short term, and the factors regarding market perfection (C2) have a higher ranking in the long term. Factors in the optimized economics system (C3) and capacity building system (C1) are generally located within a range of 40–100 in the short term and 20–100 in the long term, as indicated by the color orange in Figure 17. Most of the factors in the technology system (C4) have even lower

rankings between 60 and 120 in the short term or between 80 and 120 in the long term (blue area in Figure 17).

As shown in Figure 18, few factors are of great weight, and most factors have weights less than 0.020. To focus on the factors of relatively great influence and to cover at least 80% of the weight of the total, the accumulative weight based on the top-down ranking was calculated. Correspondingly, the value at which the accumulative weight exceeds 0.8 for the first time was taken as the baseline for factor selection. Now, 53 factors (i.e., 16 from short term specifically, 25 from long term specifically, and 12 overlaps in both terms) remain on the list. The calculation results of effective factors are listed in Figure 19.

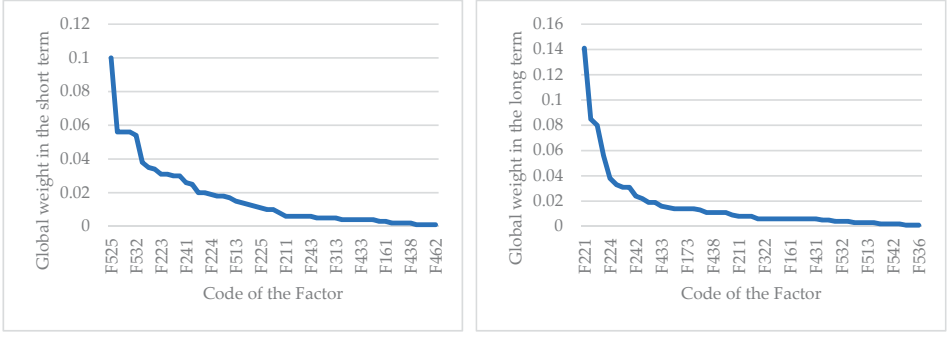

(**a**) (**b**)

Figure 18. Top-down ranking of factors in the short and long term; (**a**) presents the ranking in the short term and (**b**) presents the ranking in the long term.

Most factors specific in the short term belong to the policy setting system (C1). The corresponding range covers all the fields of the policy settings. The only exception in this category, the factor of setting up an implementation standard (F113), is also "government relevant." The distribution of these factors indicates the importance of government and policies in the short term.

As to factors in the long term, the span covers the systems of capacity building, optimized economics, market preference, and technology. The diversification of these factors implies that more stakeholders will take part in the promotion process under the framework of market governance or network-based governance. Instead of the diminished influence of factors regarding policy settings, factors concerning market optimization (C2) are of great importance in the long term. Additionally, other long-term factors, except those regarding the technology field (C4), are also market-relevant.

Moreover, a total of 12 factors overlap in both terms, covering the fields of policy setting (C1), optimized economic system (C3), and market system (C2). As a bridge between the current stage and the future, these factors, significant in both terms, will play a continuous role in the next 15 years in the process of building EE promotion. The high significances of these factors also provide a solid foundation and continuity for the transformation and the development of the Chinese market. Furthermore, most of the market factors belong to the "needs" sector. As one of the drivers of building EE promotion, this need for EE promotion of new residential buildings will continue to be in an increasing and transforming process, and the EE level in the residential sector must be promoted for, at least, the next 15 years. The increase in the number of factors that remain on the list in market and economics and the decrease in policy systems prove that China is shifting its development pattern into a "market-dominated" mode. The increase in the number of factors of capacity building systems proves that this pattern shift, and future building EE promotion development, should be led and cultivated by the government, which is quoted in Section 5 as "guided by governments."

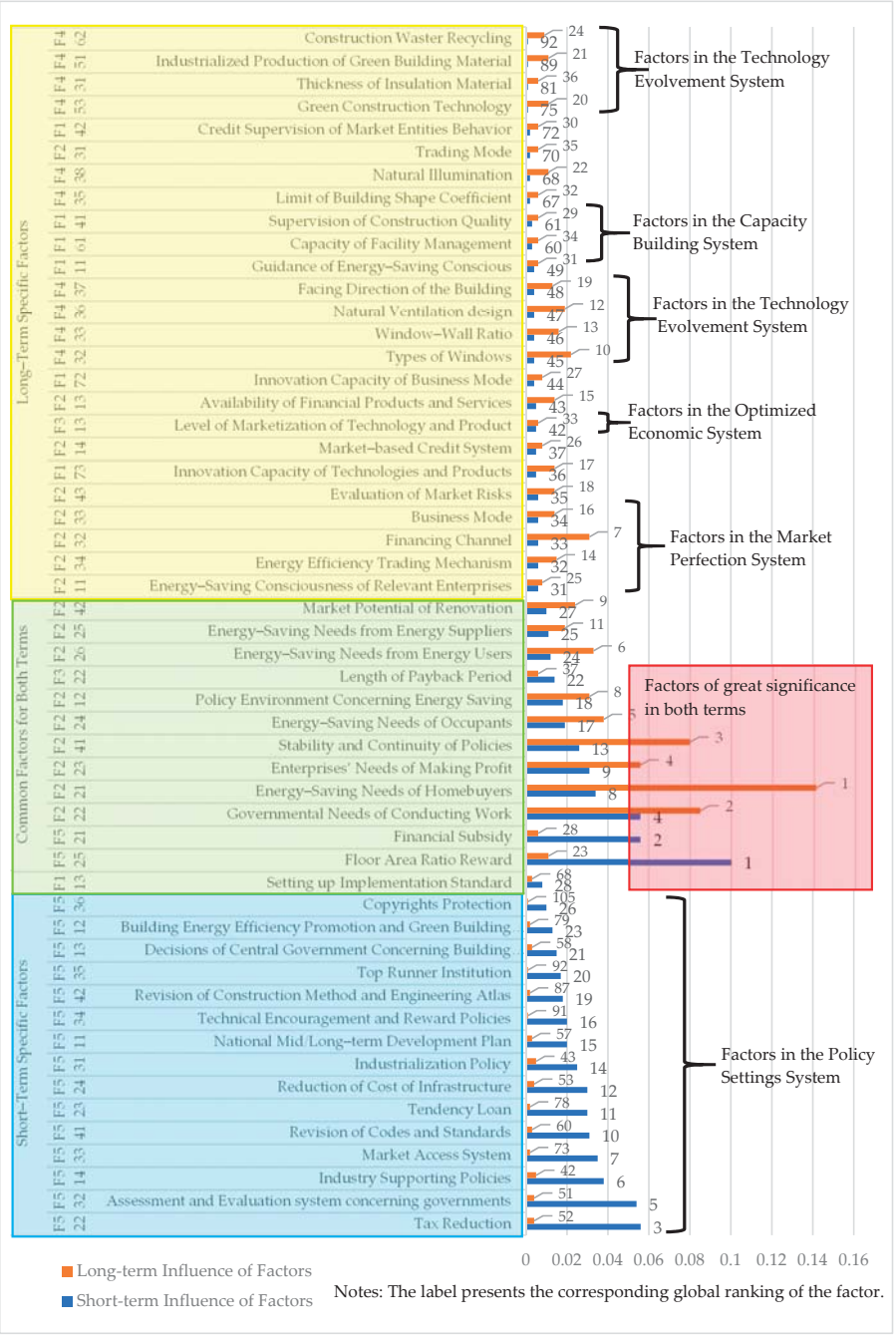

Figure 19. Factor selection results of significant influence.

4.5. Future Study and Practical Implications of the Study

4.5.1. Limitations and Future Study

By investigating frontline stakeholders involved in the industry of EE promotion of new residential buildings, this paper collected and reported stakeholders' perceptions of the factors influencing the EE promotion of new residential buildings in the case of China. By adopting the "nested policy design framework" and the "policy environment" theory, this paper constructed a structure for classifying and organizing the collected influencing factors. The perceived influence of each factor was evaluated by frontline institutes via Likert 5-Scale, and the corresponding weight and ranking was further determined through the AHP process. The investigation and data processing results were validated based on the history of the development, and the corresponding policy implications are further derived.

However, due to the complexity of the industry, the data collected from 32 institutes are still not sufficient for a detailed analysis from each stakeholders' perspective. This paper listed eight categories of stakeholders in Figure 9 but classified them into three categories—government departments, enterprises, and research institutes in the following analysis. The corresponding implication also limit its range within the interactions policy settings and the response from the frontlines. It is considered by the author that too few institutes' voices cannot represent the overall attitudes of the same kind of stakeholders. More and carefully selected institutions involved in the study will provide more useful and authentic information about the perceived influence of factors by different stakeholders. Correspondingly, the question "what stakeholder thinks in detail rather than in general?" can be answered, by taking relevant theories, such as the gaming theory, into consideration. The results can thus help researchers and decisionmakers better understand the difference of response from different stakeholders confronted with the same policy system.

Despite the aforementioned limitations, the current results can still be considered as effective due to current governance arrangement in the investigated institutes in China. Once the questionnaire is delivered to a certain institute, managers (college deputies and heads of other government departments and public institutions) will break it down and send them to different departments. Experts in each department will first fill in the questionnaire based on their perceived experiences and their majors. A follow-up workshop, where all the responses from experts and corresponding reasons are stated and discussed, will be conducted to find the most agreed-upon EE level. When approved by the manager of the institute, the most agreed-upon EE level will be the formal response. Therefore, a formal response could be seen as the result of negotiations among experts of different research domains and professional ranks.

4.5.2. Practical Policy Implications

In the following 15 years, the current governance regarding new residential building EE promotion in China will shift to "market-based" and "network-based" from a "legal-based" governance. The industry will correspondingly be guided by governments and dominated by market stakeholders. This transformation also indicates that the building EE promotion process will be more sensitive to diversified factors regarding marketization, namely, market perfection, technology, economy, and capacity building.

With respect to the preference of policy instrument selection, marketization is one of the future trends under the changed framework of governance arrangement. Despite the decreasing influence of a policy system, the monetary policy and policy mechanism remain of great influence because they are effective policy instruments for the ignition of market development and building up market expectation, as perceived by stakeholders within the industry. "Needs", as a basic driver for market development, are the most significant influence on the promotion. Factors of market expectation decide the willingness to participate in the promotion process. Due to the increasing awareness of the externality, market entities are less sensitive to benefit, but remain sensitive to the cost of various types. Regarding the ability to fulfill the corresponding duties of respective stakeholders, the capacity

of governments is of great importance in the short term, and the innovation ability of stakeholders becomes more important because it is one of the core competences of enterprises in the market.

The weight of each factor further indicates the importance of various types of policy instrument selection and specifications. In the short term, governments play a critical role in guiding and cultivating the development of the EE promotion of new residential buildings. With abundant policy resources [70] such as legislation and tax-collecting rights, the government can compensate market failure and adjust industry development along an approach toward higher efficiency under the situation that policy instruments can be selected and designed into a policy package correctly. In addition, evaluation results of factors in the market system indicate that policies should first encourage more enterprises to participate in the EE promotion process by igniting the home buyers' need and satisfying enterprises needs for profits on overall level. When there are more entities participating in the market, it is important to build up a perfect mechanism to further promote the development of the market. In the economy part, factors' weights concerning cost became larger than that of benefits. Current policy should solve the question of the long payback period for incremental cost caused by EE promotion. Regarding the technology system, the strategy of construction can be described as follows: "For the non-transparent part, the EE improvement should focus on the thermal performance of insulation, instead of simply increasing the thickness.; for the transparent part of a building, its design should comprehensively take the layout of the buildings and certain room and the thermal performance of materials into consideration." Additionally, the results of technology evolvement factors imply that the concept of life cycle is becoming mainstream and all the components of building EE promotion tend toward the same importance. Correspondingly, greater attention should be paid to a regulated design, construction, operation, and life-cycle energy saving of buildings (single and district). With respect to capability building system, factors of innovation capacity and supervision capacity concerning regulating and exciting the market show great significance in the long term, implying that building EE promotion should be market-based and market-dominated.

5. Conclusions

Contributing to the gap of the disaccord between stakeholders' perceptions and research assumptions, this paper identified the factors of significant influence to the nationwide EE promotion of new residential buildings before 2020 and 2030 based on the lived experiences of the first-front workers and institutes. Factors were collected through literature review. Questionnaires distributed to over 30 institutes were used to evaluate the influences of all the factors quantitatively and the result was generated from the AHP process. The nested policy design framework and policy environment theory was used to structure the hierarchy and generate policy implications. The corresponding conclusions summarized by answering the following three questions. The stakeholder's attitudes towards various factors regarding EE promotion of new residential buildings presented in this paper helps policymakers, decisionmakers, and researchers better understand the current situation and the future development in China. More internationally, the correspondence between governance arrangement, policy regime logic, and preference of policy instrument selection analyzed in this article helps researchers to understand how the importance of factors will change under different context. The questions are as follows:

- What do stakeholders think in general?

Due to the information asymmetry and the different interests that various stakeholders stand for, the perception difference lies not only the general level, but also specifically on the judgements to criteria, sub-criteria, and factors.

Generally, government departments tend to be conservative in evaluating factor importance. The only exception found, on the criteria level, is the importance of technology evolvement in the long term. This stresses governments' attention on the technology evolvement. According to their perceptions, technology evolvement is the foundation of, and decides the pace of, the EE promotion

of new residential buildings. In addition, there was no consistent relationship be found between the judgements from enterprises and those from research institutes. On the criteria level, enterprises believe the factors regarding policy settings (C5) and the economy (C3) are of more significant importance, in both the short term and long term, than the research institutes expect. Regarding the judgements on the market criterion (C2), research institutes hold more ambitious opinions about the short-term importance of C2 while enterprises are more ambitious in the long term. Regarding factors on the sub-criteria level, the responses from enterprises are overall more conservative than those from research institutes, although there are six and four exceptions in the short and long term, respectively.

In addition to the attitude preference, significant disagreements can also be observed. These disagreements are further enlarged in evaluating the importance of all the criteria and sub-criteria in the long term. It is considered by the author that these disagreements are caused, not only by the information asymmetry and the externality of the industry, but also by the interests that various stakeholders stand for and the corresponding expectations. The major two significant disagreements are relative to the influence of economic factors and governments' capacity. Enterprises are calling for more profits and they believe governments can effectively affect the development of EE promotion by issuing policies. However, governments believe that the economic factors should have the least influence. Besides, both research institutes and enterprises expect that current governments should increase their ability to regulate the market, thus realizing a better market environment. However, government departments do not believe their capacity are not of such significant influence, as expected.

Despite the attitude preference and the significant disagreements, the agreement on the importance of most criteria, sub-criteria, and factors are still reached. The results of consensus are as follows:

- What significantly affects the progress of the EE promotion of new residential buildings?

Indicated by the weights and rankings of policy settings (C2) and market optimization (C5) in the short term, the "legal-based governance" and the "corporatist-based governance" dominate in the field of EE promotion of new residential buildings. Correspondingly, factors regarding policy settings (C5) have the greatest influence in the short term. The monetary policy (C52) ranks front due to its effectiveness in satisfying market stakeholders' eagerness for profit (C31, C32). The policy mechanism design (C53) has the second greatest importance in regulating market activities and setting up mechanisms for sustainable developments. Technology policy (C54) ranks last since it has no incentives for stakeholders. As for specific factors, those of significant short-term influence are listed in Figure 19 (factors with blue and green cover). The floor-area ratio reward (F525) is of the greatest significant as it stimulates the developers—the stakeholder locating front of the value chain.

It is argued by the author that governments play the most important role in promoting the EE of new residential buildings. With abundant policy resources, they can effectively affect the development of the industry by issuing mandatory policies, setting up implementation standards, and stimulating the activeness of market stakeholders through incentives such as financial subsidies. In addition, it shall be noted that, for local governments, they are stimulated by the requirements from central governments.

- What will significantly affect the transformation of the EE promotions of new residential buildings in the future?

Indicated by the weight and ranking changes of all the five criteria, the current "legal-based" and "corporatist-based" governance arrangements in China in the EE promotion field of new residential buildings will transform into "market-based" and "network-based" governance arrangements. However, this transformation cannot be accomplished suddenly at a specific time. How the transformation should be accomplished or affected, perceived by frontline stakeholder, are illustrated in Figure 19 (factors with green cover).

Generally, the transformation process is affected both by monetary factors and market-related factors. At the beginning, monetary policies (C52) are still of great importance in stimulating the market, as they can directly reduce the incremental cost and increase the benefits of enterprises. However, stakeholders involved in the market activities are calling for a more "stable" market environment. This is also the reason that governments' needs of conducting work (F222), homebuyers' need (F221), and the stability and continuity of policies (F241) are of extreme significant importance in the long term.

Along with the transformation of governance arrangements, factors in more criteria can have significant influence on the future development of EE promotion. Market mechanisms (C23), referring to well-organized competition among stakeholders, are of the greatest importance. The level of marketization of energy efficient building materials and products (F313) determines stakeholder's access to the technology solutions with limited incremental cost. The capacity building of governments (F111, F114, F116) decides how effectively the governments can regulate the market and eliminate market failures. The technology evolvements (F431, F432, F433, F436, F437, F451, F453, F462) indicates how the EE level of technology should be further promoted.

By introducing the nested policy design framework and the policy environment theory, this paper shed further light on the correspondence between governance arrangement, policy regime logic, and the preference of policy instrument selection. The "legal-based" and "corporatist-based" governance arrangement is in accordance with the "government-dominated" development of EE promotion of new residential buildings. Correspondingly, policies issued by governments are of significant importance in stimulating the market. Taking enterprises' eagerness for benefit into consideration, the preferred policy instruments are those monetary ones such as financial subsidy or the floor-area ratio reward. On the contrary, the "market-based" and "network-based" governance involves more stakeholders as the "decisionmakers" in promoting EE of new residential buildings. The development is correspondingly "market-oriented stakeholders-dominated" and governments play a role as a pioneer, a supervisor, and a regulator of the market. Under this circumstance, the EE promotion of new residential buildings can be affected by factors from more aspects than the development mode under "legal-based "and "corporatist-based" governance.

Author Contributions: Conceptualization, Y.L. and N.Z.; data curation, Y.L. and B.Q.; formal analysis, Y.L., N.Z., and B.Q.; funding acquisition, N.Z.; investigation, Y.L. and B.Q.; methodology, Y.L. and N.Z.; project administration, N.Z.; resources, Y.L. and B.Q.; supervision, N.Z.; validation, Y.L. and B.Q.; visualization, B.Q.; writing—original draft, Y.L. and B.Q.; writing—review and editing, N.Z.

Funding: This research was funded by Energy Foundation, grant number G-1402-19981.

Conflicts of Interest: The authors declare no conflict of interest.

Appendix A

Table A1. Hierarchy and details of assessing factors' weight.

Criteria	Sub-Criteria	Factors	No.
Promotion by Technology Progress-C4	Building Materials Efficiency-C41	Insulation Performance of Non-Transparent Envelope	F411
		Insulation Performance of Transparent Envelope	F412
		Airtightness of Windows	F413
		New type of wall structure	F414
		Solar Shading Devices	F415
	Building Services and Appliance Energy Efficiency-C42	Appliances of higher energy efficiency	F421
		Choice of Different types of Energy	F422
		Optimized Parameter Settings of Devices	F423
		High Efficiency Component of HVAC system	F424
		High Efficiency Lighting system	F425
	Design Phase-C43	Thickness of Insulation Material	F431
		Types of Windows	F432
		Window-Wall Ratio	F433
		Design of Solar Shading System	F434
		Limit of Building Shape Coefficient	F435
		Natural Ventilation design	F436
		Facing Direction of the Building	F437
		Natural Illumination	F438
	Operation Phase-C44	Human Behavior Sensors Installations	F441
		Indoor Temperature/Humidity Control	F442
		Indoor Heating/Cooling Energy Consumption Supervision	F443
		Renewable Energy Application on Buildings	F444
		Energy Recycling	F445
		Distributed Energy Utilization	F446
		New Heating/Cooling sources Utilization	F447
		Building Energy Consumption Supervision	F448
		Comprehensive Utilization of Resources	F449
		Water Saving and Recycling	F440
	Construction Phase-C45	Industrialized Production of Green Building Material	F451
		Construction Process Requirement	F452
		Green Construction Technology	F453

Table A1. *Cont.*

Criteria	Sub-Criteria	Factors	No.
	Dismantle/Renovation Phase-C46	Construction Waste Reduction	F461
		Construction Waster Recycling	F462
		R&D of Construction Waster Utilization	F463
	From District Perspective-C47	Reclaimed Water Utilization	F471
		Rian Water Collection and Utilization	F472
		Underground Space Utilization	F473
		Heat Island Effect Reduction	F474
		District Energy Utilization Plan	F475
		Distributed Energy Utilization	F476
Promotion by Optimized Economics-C3	Cost Optimization-C31	Technology R&D Cost	F311
		Labor Cost	F312
		Level of Marketization of Technology and Product	F313
		Level of Massive Development of Technology and Product	F314
		Financing Cost	F315
		Promotion of Comprehensive Design Capacity Requirement	F316
		Promotion of Construction Requirement	F317
		Technology Application Cost	F318
		Technology Designing Cost	F319
		Technology Maintenance Cost	F310
	Expected Benefits-C32	Reduction of Energy Consumption	F321
		Length of Payback Period	F322
		Promotion of Building's Value	F323
		Energy-Saving Consciousness of Occupants	F324
Promotion by Market Perfection-C2	Market Vitality-C21	Energy-Saving Consciousness of Relevant Enterprises	F211
		Policy Environment Concerning Energy Saving	F212
		Availability of Financial Products and Services	F213
		Market-based Credit System	F214
		Third-party institutions Development Concerning Energy Services	F215
	Needs-C22	Energy-Saving Needs of Homebuyers	F221
		Governmental Needs of Conducting Work	F222
		Enterprises' Needs of Making Profit	F223
		Energy-Saving Needs of Occupants	F224
		Energy-Saving Needs from Energy Suppliers	F225
		Energy-Saving Needs from Energy Users	F226

Table A1. *Cont.*

Criteria	Sub-Criteria	Factors	No.
	Market Mechanisms-C23	Trading Mode	F231
		Financing Channel	F232
		Business Mode	F233
		Energy Efficiency Trading Mechanism	F234
	Market Expectations-C24	Stability and Continuity of Policies	F241
		Market Potential of Renovation	F242
		Evaluation of Market Risks	F243
Promotion by Capacity Building-C1	Guidance-C11	Guidance of Energy-Saving Conscious	F111
		Cultivation of Market Development	F112
		Setting up Implementation Standard	F113
		Guidance of Value Chain Perfection	F114
	Cooperation-C12	Cooperation among market entities adjusted by governments	F121
		Cooperation between Governmental Departments	F122
	Implementation-C13	Capacity of Planning and Design	F131
		Capacity of Construction	F132
	Supervision-C14	Supervision of Construction Quality	F141
		Credit Supervision of Market Entities Behavior	F142
		Behavior Criterion for Market Entities	F143
	Assessment-C15	Capacity of Assessing Construction Quality	F151
		Capacity of Assessing Energy Saving	F152
		Capacity of Energy Efficiency MRV	F153
	Operation-C16	Capacity of Facility Management	F161
		Technical Capacity of ESCOs	F162
		Maintenance Capacity of Energy Supply Enterprises	F163
	Innovation-C17	Innovation of Cooperation Mode promoted by governments	F171
		Innovation Capacity of Business Mode	F172
		Innovation Capacity of Technologies and Products	F173

Table A1. *Cont.*

Criteria	Sub-Criteria	Factors	No.
Efficiency Promotion Caused by Policy Settings-C5	Macro Policy-C51	National Mid/Long-term Development Plan	F511
		Building Energy Efficiency Promotion and Green Building Development Plan	F512
		Decisions of Central Government Concerning Building Energy Efficiency Promotion	F513
		Industry Supporting Policies	F514
		Developing trend of Building Energy Efficiency on Domestic/International Level	F515
	Monetary Policy-C52	Financial Subsidy	F521
		Tax Reduction	F522
		Tendency Loan	F523
		Reduction of Cost of Infrastructure	F524
		Floor Area Ratio Reward	F525
	Policy Mechanism Design-C53	Industrialization Policy	F531
		Assessment and Evaluation system concerning governments	F532
		Market Access System	F533
		Technical Encouragement and Reward Policies	F534
		Top Runner Institution	F535
		Copyrights Protection	F536
	Technology Policy-C54	Revision of Codes and Standards	F541
		Revision of Construction Method and Engineering Atlas	F542
		List of Recommended Products and Technologies	F543

Table A2. Modes of governances and its implementation preference.

Mode of Governance	Overall Governance Aim	Implementation Preference
Legal governance	Legitimacy and compliance through the promotion of law and order in social relationships	Legal system: legislation, law, and rules and regulations
Corporatist governance	Controlled and balanced rates of socioeconomic development through the management of major organized social actors	State system: plans and macro-level bargaining
Market governance	Resource/cost efficiency and control through the promotion of small- and medium-sized enterprises and competition	Market system: auctions, contracts, subsidies, and tax incentives and penalties
Network governance	Co-operation of dissent and self-organization of social actors through the promotion of inter-actor organizational activity	Network system: collaboration and voluntary associational activity and service delivery

Table A3. Local weights and rankings of factors.

Sub-Criteria	No.	Factors	Local Weight		Ranking	
			ST	LT	ST	LT
Macro Policy	F511	National Mid/Long-term Development Plan	0.215	0.22	2	2
	F512	Building Energy Efficiency Promotion and Green Building Development Plan	0.139	0.134	4	4
	F513	Decisions of Central Government Concerning Building Energy Efficiency Promotion	0.159	0.22	3	2
	F514	Industry-Supporting Policies	0.407	0.352	1	1
	F515	Developing trend of Building Energy Efficiency on Domestic/International Level	0.08	0.075	5	5
Monetary Policy	F521	Financial Subsidy	0.207	0.245	2	2
	F522	Tax Reduction	0.207	0.137	2	3
	F523	Tendency Loan	0.109	0.079	4	5
	F524	Reduction of Cost of Infrastructure	0.109	0.137	4	3
	F525	Floor-Area Ratio Reward	0.368	0.402	1	1
Policy Mechanism Design	F531	Industrialization Policy	0.155	0.346	3	1
	F532	Assessment and Evaluation system concerning governments	0.333	0.25	1	2
	F533	Market Access System	0.22	0.165	2	3
	F534	Technical Encouragement and Reward Policies	0.121	0.091	4	4
	F535	Top Runner Institution	0.108	0.091	5	4
	F536	Copyrights Protection	0.063	0.057	6	6
Technology Policy	F541	Revision of Codes and Standards	0.558	0.588	1	1
	F542	Revision of Construction Method and Engineering Atlas	0.32	0.323	2	2
	F543	List of Recommended Products and Technologies	0.122	0.089	3	3
Market Vitality	F211	Energy-Saving Consciousness of Relevant Enterprises	0.172	0.123	2	3
	F212	Policy Environment Concerning Energy Saving	0.486	0.465	1	1
	F213	Availability of Financial Products and Services	0.123	0.214	4	2
	F214	Market-based Credit System	0.141	0.123	3	3
	F215	Third-party institutions Development Concerning Energy Services	0.078	0.075	5	5
Needs	F221	Energy-Saving Needs of Homebuyers	0.205	0.378	2	1
	F222	Governmental Needs of Conducting Work	0.341	0.229	1	2
	F223	Enterprises' Needs of Making Profit	0.191	0.151	3	3
	F224	Energy-Saving Needs of Occupants	0.118	0.102	4	4
	F225	Energy-Saving Needs from Energy Suppliers	0.07	0.051	6	6
	F226	Energy-Saving Needs from Energy Users	0.075	0.089	5	5
Market Mechanism	F231	Trading Mode	0.092	0.086	4	4
	F232	Financing Channel	0.295	0.468	2	1
	F233	Business Mode	0.295	0.211	2	3
	F234	Energy Efficiency Trading Mechanism	0.317	0.234	1	2
Market Expectation	F241	Stability and Continuity of Policies	0.625	0.683	1	1
	F242	Market Potential of Renovation	0.238	0.2	2	2
	F243	Evaluation of Market Risks	0.136	0.117	3	3

Table A3. *Cont.*

Sub-Criteria	No.	Factors	Local Weight		Ranking	
			ST	LT	ST	LT
Cost	F311	Technology R&D Cost	0.182	0.121	1	3
	F312	Labor Cost	0.034	0.033	10	9
	F313	Level of Marketization of Technology and Product	0.175	0.203	2	1
	F314	Level of Massive Development of Technology and Product	0.081	0.179	8	2
	F315	Financing Cost	0.094	0.083	4	6
	F316	Promotion of Comprehensive Design Capacity Requirement	0.094	0.1	4	4
	F317	Promotion of Construction Requirement	0.094	0.083	4	6
	F318	Technology Application Cost	0.101	0.064	3	8
	F319	Technology Designing Cost	0.051	0.033	9	9
	F310	Technology Maintenance Cost	0.094	0.1	4	4
Benefit	F321	Reduction of Energy Consumption	0.19	0.351	2	2
	F322	Length of Payback Period	0.515	0.371	1	1
	F323	Promotion of Building's Value	0.19	0.209	2	3
	F324	Energy-Saving Consciousness of Occupants	0.105	0.07	4	4
Building Material	F411	Insulation Performance of Non-Transparent Envelope	0.204	0.139	3	4
	F412	Insulation Performance of Transparent Envelope	0.364	0.301	1	1
	F413	Airtightness of Windows	0.221	0.262	2	2
	F414	New type of wall structure	0.087	0.089	5	5
	F415	Solar Shading Devices	0.124	0.21	4	3
Building Services and Appliance	F421	Appliances of higher energy efficiency	0.375	0.145	1	4
	F422	Choice of Different types of Energy	0.073	0.167	5	3
	F423	Optimized Parameter Settings of Devices	0.215	0.253	2	2
	F424	High Efficiency Component of HVAC system	0.215	0.29	2	1
	F425	High Efficiency Lighting system	0.121	0.145	4	4
Design	F431	Thickness of Insulation Material	0.053	0.059	7	7
	F432	Types of Windows	0.179	0.23	1	1
	F433	Window–Wall Ratio	0.179	0.166	1	3
	F434	Design of Solar Shading System	0.043	0.038	8	8
	F435	Limit of Building Shape Coefficient	0.097	0.065	5	6
	F436	Natural Ventilation Design	0.179	0.198	1	2
	F437	Facing Direction of the Building	0.172	0.133	4	4
	F438	Natural Illumination	0.097	0.112	5	5
Operation	F441	Human Behavior Sensors Installations	0.043	0.046	9	8
	F442	Indoor Temperature/Humidity Control	0.041	0.03	10	9
	F443	Indoor Heating/Cooling Energy Consumption Supervision	0.044	0.023	8	10
	F444	Renewable Energy Application on Buildings	0.167	0.266	1	1
	F445	Energy Recycling	0.123	0.176	5	2
	F446	Distributed Energy Utilization	0.074	0.11	7	4
	F447	New Heating/Cooling sources Utilization	0.141	0.072	2	6

Table A3. *Cont.*

Sub-Criteria	No.	Factors	Local Weight		Ranking	
			ST	LT	ST	LT
	F448	Building Energy Consumption Supervision	0.086	0.051	6	7
	F449	Comprehensive Utilization of Resources	0.141	0.11	2	4
	F440	Water Saving and Recycling	0.141	0.117	2	3
Construction	F451	Industrialized Production of Green Building Material	0.25	0.4	2	1
	F452	Construction Process Requirement	0.25	0.2	2	2
	F453	Green Construction Technology	0.5	0.4	1	1
Renovation/Dismantle	F461	Construction Waste Reduction	0.4	0.21	1	3
	F462	Construction Waste Recycling	0.4	0.55	1	1
	F463	Technology R&D of Construction	0.2	0.24	2	2
District	F471	Reclaimed Water Utilization	0.044	0.043	6	6
	F472	Rain Water Collection and Utilization	0.182	0.163	3	3
	F473	Underground Space Utilization	0.281	0.239	1	2
	F474	Heat Island Effect Reduction	0.066	0.061	5	5
	F475	District Energy Utilization Plan	0.281	0.37	1	1
	F476	Distributed Energy Utilization	0.145	0.123	4	4
Guidance	F111	Guidance of Energy-Saving Conscious	0.2	0.392	2	1
	F112	Cultivation of Market Development	0.2	0.278	2	2
	F113	Setting up Implementation Standard	0.4	0.165	1	3
	F114	Guidance of Value Chain Perfection	0.2	0.165	2	3
Cooperation	F121	Cooperation among market entities adjusted by governments	0.5	0.614	1	1
	F122	Cooperation between Governmental Departments	0.5	0.386	1	2
Implementation	F131	Capacity of Planning and Design	0.5	0.5	1	1
	F132	Capacity of Construction	0.5	0.5	1	1
Supervision	F141	Supervision of Construction Quality	0.493	0.4	1	1
	F142	Credit Supervision of Market Entities Behavior	0.311	0.4	2	1
	F143	Behavior Criterion for Market Entities	0.196	0.2	3	2
Assessment	F151	Capacity of Assessing Construction Quality	0.2	0.25	2	2
	F152	Capacity of Assessing Energy Saving	0.4	0.5	1	1
	F153	Capacity of Energy Efficiency MRV	0.4	0.25	1	2
Operation	F161	Capacity of Facility Management	0.5	0.571	1	1
	F162	Technical Capacity of ESCOs	0.25	0.286	2	2
	F163	Maintenance Capacity of Energy Supply Enterprises	0.25	0.143	2	3
Innovation	F171	Innovation of Cooperation Mode Promoted by Governments	0.26	0.163	3	3
	F172	Innovation Capacity of Business Mode	0.327	0.297	2	2
	F173	Innovation Capacity of Technologies and Products	0.413	0.54	1	1

Notes: ST—Short Term; LT—Long Term.

References

1. National Bureau of Statistics of China. *China Statistical Yearbook*; China Statistics Press: Beijing, China, 2018; ISBN 978-7-5037-8587-0. (In Chinese)
2. U.S. Energy Information Administration. International Energy Outlook 2014. Available online: https://www.eia.gov/outlooks/archive/ieo14/pdf/0484(2014).pdf (accessed on 10 February 2019).
3. Capros, P.; De Vita, A.; Tasios, N.; Papadopoulos, D.; Siskos, P.; Apostolaki, E.; Zampara, M.; Paroussos, L.; Fragiadakis, K.; Kouvaritakis, N. *EU Energy, Transport and GHG Emissions: Trends to 2050, Reference Scenario 2013*; European Commission: Luxembourg, 2013; ISBN 92-79-33728-9.
4. Tsinghua University Building Energy Research Center. *2017 Annual Report on China Building Energy Efficiency*; China Architecture and Building Press: Beijing, China, 2017; ISBN 978-7-112-20573-8. (In Chinese)
5. Huo, T.; Ren, H.; Zhang, X.; Cai, W.; Feng, W.; Zhou, N.; Wang, X. China's energy consumption in the building sector: A Statistical Yearbook-Energy Balance Sheet based splitting method. *J. Clean. Prod.* **2018**, *185*, 665–679. [CrossRef]
6. Development Research Center of the State Concil, World Bank. *Urban China: Toward Efficient, Inclusive, and Sustainable Urbanization*; World Bank Publications: Washington, DC, USA, 2014; pp. 1–583.
7. United Nations Environmental Programme, Sustainable Buildings and Climate Initiative. *Buildings and Climate Change Summary for Decision-Makers*; United Nations Environmental Programme, Sustainable Buildings and Climate Initiative: Paris, France, 2009.
8. Zhang, M.; Wang, M.; Jin, W.; Xia-Bauer, C. Managing energy efficiency of buildings in China: A survey of energy performance contracting (EPC) in building sector. *Energy Policy* **2018**, *114*, 13–21. [CrossRef]
9. Annunziata, E. *Energy Efficiency Governance in Buildings: A Multi-Level Perspective*; Scuola Superiore Sant'Anna: Pisa, Italy, 2013. Available online: http://www.phdmanagement.sssup.it/documenti/awarded/Annunziata_Thesis.pdf (accessed on 15 January 2019).
10. Ren, S.M.; Guo, H.D.; Xu, Z.-Y. Externality Feature Analysis of Building Energy Efficiency Market and Incentive Policies in China. *Constr. Conserv. Energy* **2009**, *1*, 75–78.
11. Zhan, S.L.; Han, Q.M.; Liu, C.B. Analysis of Demanding Factors about Building Energy-Efficiency Market based on Theory of Behavioral Choice. *J. Beijing Jiaotong Univ.* **2009**, *8*, 65.
12. He, Z.K.; She, L.Z. Evaluation research on the influencing factors of building energy efficiency promotion based on AHP. *J. Guangzhou Univ.* **2013**, *12*, 76–80. (In Chinese)
13. Qu, Y.; Chen, Z.; Darkwa, J. Statistical Analysis of Influence Factors on Building Energy Consumption in China by Literature Overview. *Appl. Mech. Mater.* **2012**, *178–181*, 70–75. [CrossRef]
14. Feng, F.; Li, Z.; Ruan, Y.; Xu, P. An Empirical Study of Influencing Factors on Residential Building Energy Consumption in Qingdao City, China. *Energy Procedia* **2016**, *104*, 245–250. [CrossRef]
15. Stephan, A.; Stephan, L. Life cycle energy and cost analysis of embodied, operational and user-transport energy reduction measures for residential buildings. *Appl. Energy* **2016**, *161*, 445–464. [CrossRef]
16. Liu, Y.; Guo, X.; Hu, F. Cost-benefit analysis on green building energy efficiency technology application: A case in China. *Energy Build.* **2014**, *82*, 37–46. [CrossRef]
17. Zhao, X.; Hwang, B.-G.; Tan, L.L.G. Green building projects: Schedule performance, influential factors and solutions. *Eng. Constr. Archit. Manag.* **2015**, *22*, 327–346.
18. De Boeck, L.; Verbeke, S.; Audenaert, A.; De Mesmaeker, L. Improving the energy performance of residential buildings: A literature review. *Renew. Sustain. Energy Rev.* **2015**, *52*, 960–975. [CrossRef]
19. Chau, C.K.; Leung, T.M.; Ng, W.Y. A review on Life Cycle Assessment, Life Cycle Energy Assessment and Life Cycle Carbon Emissions Assessment on buildings. *Appl. Energy* **2015**, *143*, 395–413. [CrossRef]
20. Wen, T.J.; Siong, H.C.; Noor, Z.Z. Assessment of embodied energy and global warming potential of building construction using life cycle analysis approach: Case studies of residential buildings in Iskandar Malaysia. *Energy Build.* **2015**, *93*, 295–302. [CrossRef]
21. Mao, G.; Chen, H.; Du, H.; Zuo, J.; Pullen, S.; Wang, Y. Energy consumption, environmental impacts and effective measures of green office buildings: A life cycle approach. *J. Green Build.* **2015**, *10*, 161–177. [CrossRef]
22. Doan, D.T.; Ghaffarianhoseini, A.; Naismith, N.; Zhang, T.; Ghaffarianhoseini, A.; Tookey, J. A critical comparison of green building rating systems. *Build. Environ.* **2017**, *123*, 243–260. [CrossRef]

23. Nilashi, M.; Zakaria, R.; Ibrahim, O.; Majid, M.Z.A.; Zin, R.M.; Chugtai, M.W.; Abidin, N.I.Z.; Sahamir, S.R.; Yakubu, D.A. A knowledge-based expert system for assessing the performance level of green buildings. *Knowl.-Based Syst.* **2015**, *86*, 194–209. [CrossRef]
24. Wu, Z.; Shen, L.; Ann, T.; Zhang, X. A comparative analysis of waste management requirements between five green building rating systems for new residential buildings. *J. Clean. Prod.* **2016**, *112*, 895–902. [CrossRef]
25. Zuo, J.; Zhao, Z.-Y. Green building research–current status and future agenda: A review. *Renew. Sustain. Energy Rev.* **2014**, *30*, 271–281. [CrossRef]
26. Shi, Q.; Yan, Y.; Zuo, J.; Yu, T. Objective conflicts in green buildings projects: A critical analysis. *Build. Environ.* **2016**, *96*, 107–117. [CrossRef]
27. Kong, X.; Lu, S.; Yong, W. A review of building energy efficiency in China during "Eleventh Five-Year Plan" period. *Energy Policy* **2012**, *41*, 624–635. [CrossRef]
28. Li, J.; Shui, B. A comprehensive analysis of building energy efficiency policies in China: Status quo and development perspective. *J. Clean. Prod.* **2015**, *90*, 326–344. [CrossRef]
29. Xu, X.; Anadon, L.D.; Lee, H. Increasing Residential Building Energy Efficiency in China: An Evaluation of Policy Instruments. 2016. Available online: https://www.belfercenter.org/sites/default/files/legacy/files/policy-instruments-residential-building-energy-china-3.pdf (accessed on 5 January 2019).
30. U.S. National Renewable Energy Laboratory. *Summary of Gaps and Barriers for Implementing Residential Building Energy Efficiency Strategies*; U.S. Deparment of Commerce: Springfield, VA, USA, 2010. Available online: https://www.nrel.gov/docs/fy10osti/49162.pdf (accessed on 5 January 2019).
31. Zhang, Y.; Wang, Y. Barriers' and policies' analysis of China's building energy efficiency. *Energy Policy* **2013**, *62*, 768–773. [CrossRef]
32. Shen, L.; He, B.; Jiao, L.; Song, X.; Zhang, X. Research on the development of main policy instruments for improving building energy-efficiency. *J. Clean. Prod.* **2016**, *112*, 1789–1803. [CrossRef]
33. Yuan, X.; Zhang, X.; Liang, J.; Wang, Q.; Zuo, J. The Development of Building Energy Conservation in China: A Review and Critical Assessment from the Perspective of Policy and Institutional System. *Sustainability* **2017**, *9*, 1654. [CrossRef]
34. Shen, L.; Zhang, Z.; Long, Z. Significant barriers to green procurement in real estate development. *Resour. Conserv. Recycl.* **2017**, *116*, 160–168. [CrossRef]
35. Matisoff, D.C.; Noonan, D.S.; Flowers, M.E. Policy Monitor—Green Buildings: Economics and Policies. *Rev. Environ. Econ. Policy* **2016**, *10*, 329–346. [CrossRef]
36. Zou, P.X.W. Risk factor analysis of the Chinese building energy efficiency market using system dynamics methodology. *Int. J. Proj. Organ. Manag.* **2014**, *3*, 352–373. [CrossRef]
37. Marszal, A.J.; Heiselberg, P. Life cycle cost analysis of a multi-storey residential Net Zero Energy Building in Denmark. *Energy* **2011**, *36*, 5600–5609. [CrossRef]
38. Deb, K.; Deb, K. Multi-objective Optimization. In *Search Methodologies: Introductory Tutorials in Optimization and Decision Support Techniques*; Burke, E.K., Kendall, G., Eds.; Springer: Boston, MA, USA, 2014; pp. 403–449. ISBN 978-1-4614-6940-7.
39. Roberti, F.; Oberegger, U.F.; Lucchi, E.; Troi, A. Energy retrofit and conservation of a historic building using multi-objective optimization and an analytic hierarchy process. *Energy Build.* **2017**, *138*, 1–10. [CrossRef]
40. Saaty, T.L. Fundamentals of the Analytic Hierarchy Process. In *Analytic Hierarchy Process in Natural Resource and Environmental Decision Making*; Schmoldt, D.L., Kangas, J., Mendoza, G.A., Pesonen, M., Eds.; Managing Forest Ecosystems; Springer Netherlands: Dordrecht, The Netherlands, 2001; pp. 15–35. ISBN 978-94-015-9799-9.
41. Vaidya, O.S.; Kumar, S. Analytic hierarchy process: An overview of applications. *Eur. J. Oper. Res.* **2006**, *169*, 1–29. [CrossRef]
42. Ramanathan, R. A note on the use of the analytic hierarchy process for environmental impact assessment. *J. Environ. Manag.* **2001**, *63*, 27–35. [CrossRef] [PubMed]
43. Berardi, U. A cross-country comparison of the building energy consumptions and their trends. *Resour. Conserv. Recycl.* **2017**, *123*, 230–241. [CrossRef]
44. Nejat, P.; Jomehzadeh, F.; Taheri, M.M.; Gohari, M.; Abd Majid, M.Z. A global review of energy consumption, CO_2 emissions and policy in the residential sector (with an overview of the top ten CO_2 emitting countries). *Renew. Sustain. Energy Rev.* **2015**, *43*, 843–862. [CrossRef]

45. Adinyira, E.; Kwofie, T.E.; Quarcoo, F. Stakeholder requirements for building energy efficiency in mass housing delivery: The House of Quality approach. *Environ. Dev. Sustain.* **2018**, *20*, 1–17. [CrossRef]
46. Mlecnik, E.; Visscher, H.; van Hal, A. Barriers and opportunities for labels for highly energy-efficient houses. *Energy Policy* **2010**, *38*, 4592–4603. [CrossRef]
47. Rowe, G.; Frewer, L.J. A Typology of Public Engagement Mechanisms. *Sci. Technol. Hum. Values* **2005**, *30*, 251–290. [CrossRef]
48. Weber, E.U. Breaking cognitive barriers to a sustainable future. *Nat. Hum. Behav.* **2017**, *1*, 0013. [CrossRef]
49. Montibeller, G.; von Winterfeldt, D. Cognitive and Motivational Biases in Decision and Risk Analysis. *Risk Anal.* **2015**, *35*, 1230–1251. [CrossRef]
50. Von Winterfeldt, D.; Edwards, W. Decision Analysis and Behavioral Research. 1993. Available online: http://agris.fao.org/agris-search/search.do?request_locale=en&recordID=XF2015037843&sourceQuery=&query=&sortField=&sortOrder=&agrovocString=&advQuery=&centerString=&enableField=&aggregatorField= (accessed on 14 March 2019).
51. Howlett, M. Governance modes, policy regimes and operational plans: A multi-level nested model of policy instrument choice and policy design. *Policy Sci.* **2009**, *42*, 73–89. [CrossRef]
52. Zhang, J.; Zhou, N.; Hinge, A.; Feng, W.; Zhang, S. Governance strategies to achieve zero-energy buildings in China. *Build. Res. Inf.* **2016**, *44*, 1–15. [CrossRef]
53. Treib, O.; Bähr, H.; Falkner, G. Modes of Governance: A Note Towards Conceptual Clarification. *J. Eur. Public Policy* **2005**, *14*, 1–20. [CrossRef]
54. Howlett, M.; Ramesh, M. Studying Public Policy: Policy Cycles and Policy Subsystems. *Am. Political Sci. Assoc.* **2009**, *91*, 548–580.
55. He, B.; Zhang, X.L.; Jiao, L.D.; Shen, L.Y. China's Ongoing Policy Instrument for Building Energy Efficiency: Drives, Approaches and Prospects. In Proceedings of the 21st International Symposium on Advancement of Construction Management and Real Estate; Springer: Singapore, 2018.
56. Saaty, T.L. What is the Analytic Hierarchy Process? In *Mathematical Models for Decision Support*; Mitra, G., Greenberg, H.J., Lootsma, F.A., Rijkaert, M.J., Zimmermann, H.J., Eds.; Springer: Berlin/Heidelberg, Germany, 1988; pp. 109–121.
57. Partovi, F.Y.; Burton, J. An analytical hierarchy approach to facility layout. *Comput. Ind. Eng.* **1992**, *22*, 447–457. [CrossRef]
58. Muralidhar, K.; Santhanam, R.; Wilson, R.L. Using the Analytic Hierarchy Process for Information System Project Selection. *Inf. Manag.* **1990**, *18*, 87–95. [CrossRef]
59. Chen, C.F. Applying the analytical hierarchy process (AHP) approach to convention site selection. *J. Travel Res.* **2006**, *45*, 167–174. [CrossRef]
60. Honadle, B.W. A Capacity-Building Framework: A Search for Concept and Purpose. *Public Adm. Rev.* **1981**, *41*, 575–580. [CrossRef]
61. Greatorex, M. *Questionnaire Design*; John Wiley & Sons, Ltd.: Hoboken, NJ, USA, 2015.
62. Zhou, C.; Yu, L. Legislation Experience of Developed Countries. *Shanghai Real Estate* **2010**, *1*, 50–52. (In Chinese)
63. Zhu, D. *Research Evaluation of Building Energy Conservation Policies*; Beijing Communication University: Beijing, China, 2014. (In Chinese)
64. Li, S. *Role of Government and Its Function in Building Energy Promonion*; Qingdao University: Qingdao, China, 2008. (In Chinese)
65. Energy World. *Analysis of Green Building Development in 2013*. 2014. Available online: http://www.chinagb.net/news/waynews/20140117/103758.shtml (accessed on 12 February 2019). (In Chinese)
66. Zhao, Z.Y.; Chang, R.D.; Zillante, G. Challenges for China's energy conservation and emission reduction. *Energy Policy* **2014**, *74*, 709–713. [CrossRef]
67. Yanbing, K.Y. Obstacles and related policy recommendations for promoting building energy efficiency in China. *Heat. Vent. Air Cond.* **2006**, *36*, 33–36.
68. Gao, L.; Porter, A.L.; Wang, J.; Fang, S.; Zhang, X.; Ma, T.; Wang, W.; Huang, L. Technology life cycle analysis method based on patent documents. *Technol. Forecast. Soc. Chang.* **2013**, *80*, 398–407. [CrossRef]

69. Luo, L.; Zhu, S.; Fu, S.; Zang, Y.; Economics, S.O. Impact of Low Carbon Development on China's Energy Price Reform. *Teach. Res.* **2015**, *5*, 14–23.
70. Kagan, R.A.; Axelrad, L. Adversarial legalism: An international perspective. In *Comparative Disadvantages? Social Regulations and the Global Economy*; Brookings Institution Press: Washington, DC, USA, 1997; pp. 146–202.

energies

MDPI

Article

Development of a Passive and Active Technology Package Standard and Database for Application to Zero Energy Buildings in South Korea

Uk-Joo Sung [1] and Seok-Hyun Kim [2,*]

[1] Center for Climatic Environment Real-scale Testing, Korea Conformity Laboratories, Jincheon 27872, Korea; suj21c@kcl.re.kr
[2] Energy ICT·ESS Laboratory, Korea Institute of Energy Research, Daejeon 34101, Korea
* Correspondence: ksh7000@kier.re.kr

Received: 19 March 2019; Accepted: 30 April 2019; Published: 5 May 2019

Abstract: There is much research on zero energy buildings. In this paper, technologies and policies to improve the building energy efficiency of zero energy buildings are presented. The zero energy building certification system in Korea is introduced, and the evaluation is carried out based on the energy self-reliance rate that enables zero energy buildings. Zero energy buildings are able to minimize energy consumption due to the application of highly efficient building materials and equipment technology. In this research, to increase the prevalence of zero energy buildings in Korea, the authors propose a zero energy building technology package. Using a passive and active technology package, we confirmed the necessity and detailed requirements of each technology parameter. We analyze and classify Korean building material testing methods and performance standards, and propose passive and active technology packages, modules, material performance testing methods and minimum requirement performance standards. Finally, this study proposed a table presenting the test methods, standard and minimum value of performance. By these results, the authors confirmed the effectiveness and availability of passive and active technical packages.

Keywords: building energy; passive architecture; test method; energy performance standard; zero energy building; technology package

1. Introduction

The demand for zero energy buildings is increasing in order to reduce the energy consumption of buildings, Technologies and policies to improve building energy efficiency for zero energy buildings are presented, and there is much research on zero energy buildings. As part of this trend, the zero energy building certification system in Korea is introduced, and the evaluation is carried out based on the energy self-reliance rate that enables zero energy buildings. The mean of self-reliance is the ratio of the amount of energy generation through the renewable energy system in a building to the building's energy consumption. A "zero energy building certification system" is executed in Korea. Zero energy buildings apply thermal insulation, double-glazed windows, etc., to minimize the amount of energy lost to the outside through the building's outer skin, utilizing renewable energy such as sunlight and geothermal heat, etc. It refers to a building that minimizes energy consumption by tailoring it to the energy used. In Europe, it is defined as a building with extremely high energy performance in terms of the building and equipment. This performance concerns zero energy building heating, cooling, hot water supply, lighting, ventilation and the like. At this time, the meaning of zero energy incorporates renewable energy produced in or on the ground. Zero energy buildings in Japan use the energy consumption (including CO_2 emissions) of buildings to improve the energy-saving performance of buildings/facilities and utilizes renewable energy in the premises to reduce annual energy consumption

(CO2 emissions); "0" is when the building is closed. A zero energy building in the United States is defined as an "energy-neutral building" that supplies energy to the building's energy supply network. This refers to buildings' yearly energy consumption and energy sources produced [1–3].

In Korea, authors focused on zero energy buildings have studied passive houses. Shim confirmed the economic feasibility of passive houses in Korea [4]. Authors who have proposed passive house alternatives show a short payback period and positive life cycle cost (LCC) results compared to the reference building's life cycle period. Passive houses are acceptable and the possibility of their implementation is high, considering the willingness to pay (WTP) of Korean investors or end users. The term passive house generally refers to a type of low-energy house [5,6]. Kim et al. [7] calculated the energy requirements that satisfied the insulation standards of the Building Energy Conservation Standard (BECS) for building parts by region according to regional climate conditions using the methodology of ISO 13790 and presented the insulation standards that satisfied the passive building standards for each of the regional climate conditions. Oh et al. [8] carried out a state-of-the-art review on the recent studies regarding the implementation strategies of nearly zero energy buildings (nZEBs). As a result, papers related to nZEB can be classified into two categories: passive strategies and active strategies. Based on the results of a case study in Spain, the nZEB definition by Collaboration for nearly zero-energy housing renovation (COHERENO) was adopted to evaluate several energy renovation packages in a given building, which is also representative of the Spanish building stock [9].

Zero Energy Building is able to minimize energy consumption due to the application of highly efficient building materials and equipment technology. In addition, since zero energy is achieved by producing and supplying renewable energy, it is difficult to disseminate zero energy buildings due to an increase in construction costs compared with general buildings as a result of the materials and facilities added. However, since there is a high necessity for various aspects such as a reduction in energy consumption costs at the maintenance and operation stage and national greenhouse gas reduction, much effort has been made by many researchers to construct a zero energy building there.

When implementing a zero energy building, the designer's performance prediction tool is utilized in the design phase. However, in Korea, the performance prediction is managed at the institutional level by evaluating the energy efficiency of the building, and the designer predicts the energy requirement amount and the primary energy requirement by utilizing the certification program ECO 2 (v20170122, Korea energy Agency, Korea) in other parts written as ECO2–us a consistent style. Since these design programs can derive different results according to the input level of the user, the program generates a difference in the analysis result if there is no same input value by the same user. Due to the difference in analysis results, problems arise in the reliability of the program. Even with the same input value, when the performance numerical value input is not the performance measured in the same test environment, the result of the program will be different. When applying the program results to buildings, there are various difficulties, for example, sometimes the results differ from the expected results. In order to solve this, highly reliable guidelines constructed with proven materials and facilities are required, and it is necessary to unify the performance test method and the test environment so that the performance can be compared. The manufacturing process of existing building materials is commercialized by combining materials according to the purpose. Since the connection (or parameter) material is necessary for bonding between the products, there is a problem of compatibility between each product as well as a reduction in production efficiency of the building material. Therefore, it is necessary to consider the parameters required for coupling between the materials and equipment that constitute the zero energy building.

This research, which proposes a zero energy building technology package, will contribute to increasing the prevalence of zero energy buildings in Korea. In addition, the technical package proposed in this research was divided into a passive technology package and an active technology package, and a database (DB) configuration is proposed. Finally, we present the minimum performance standards that must satisfy the packages and constituent materials of the technology used for zero

energy buildings according to the circumstances of Korea. So, the results of this research can be utilized to build an actual zero energy building.

2. Zero Energy Building in Korea

2.1. Current Status of Zero Energy Building in Korea

A zero energy building uses thermal insulation, double-glazed windows, etc., to minimize the amount of energy lost to the outside through the building envelope. Utilizing renewable energy such as sunlight and geothermal power, it covers the energy used for heating and cooling buildings to minimize energy consumption. Unlike general buildings, zero energy buildings will enhance the efficiency of the facilities necessary for the operation of buildings and energy production facilities, in addition to the outer skin composition using energy-efficient building materials. This minimizes the energy consumption of zero-energy buildings, and the energy produced through renewable energy facilities is the greatest. It also aims to distribute and operate the appropriate renewable energy production and to maintain the comfort of residents with the unique production energy of the building without requiring external energy. These zero-energy buildings are relatively difficult to disseminate, as construction costs are set relatively high compared to general buildings, and the installation costs of facilities also increase. Integrated design is not achieved through a specification-oriented design using a simple combination of high-performance elemental technologies. It is necessary to consider compatibility between elemental technologies at the planning stages, and between elemental technologies considering organic collaboration combination. In the case of South Korea, the industrial technology market for improving building energy efficiency, renewable energy, maintenance and management is valued at about 750 million dollars. In Korea, Zero Energy Building Certification has been carried out by the Green Building Composition Support Law. Zero Energy Building Certification subjects are new buildings and existing buildings for all uses, which are the same as those of the building's efficiency evaluation, so we request a building energy efficiency grade of 1++ or higher through the existing energy performance evaluation. According to the energy independence rate, it is classified into five grades from grade 1 to grade 5. In response to the activation of the certification system, various technological developments are being conducted in order to revitalize the dissemination of zero energy buildings. The energy independence rate is similar to the self-reliance rate. It is determined based on the percentage of energy consumed and produced in a building in the absence of an external energy supply. Grade 1 is 100% of the energy independence rate. The zero energy building certification system grants grade 2 if the percentage of the energy independence rate is 80% or more, grade 3 if it is 60% or more, grade 4 if it is 40% or more, and grade 5 if it is above 20%. The amount of energy consumption and production was based on annual primary energy obtained by the simulation results of ECO2. However, compared to the level of building materials that can be actually applied and the development level of high efficiency equipment, development of the parameters that apply this is limited. Furthermore, performance prediction through application between technologies is lacking. Compatibility and organic collaboration with technology to solve these problems has become important, and the technologies reflecting this have received a lot of attention.

2.2. Database for Implementing Zero Energy Building

The database of existing building materials is constructed according to the development of Building Information Modeling (BIM). The zero energy building database can be constructed in the same way as the BIM database. Especially in the BIM field, despite vast research on the composition of DB, the spread of BIM technology is insufficient in the Korean construction industry. The spread of BIM is insufficient because it is difficult to apply to in construction practice due to a lack of a library DB at the time of basic design and the use of BIM in the basic design. In the case of building materials necessary for building construction, foreign libraries are transformed and used. DB and libraries are greatly required for materials actually applied to construction work in Korea. In addition, individual

technologies at the stage of the project are applied, and based on the fact that other libraries are constructed according to the purpose, there is a situation in which compatibility between each library is insufficient. As a result, much research into unifying the file format of the DB is underway, and there are increasing cases of studying BIM libraries (or databases) in consideration of business models based on building materials and information systems. Because this is based on the basic objective for constructing BIM, it is difficult to confirm the effect of combining materials, because it is composed of classification by construction and classification by material. In particular, the means of confirming the performance (or test method), which should ensure the reliability of the performance required for energy analysis, is not immediately applied as the energy analysis and construction cost estimates are configured at the same time, so a difference in performance can occur.

2.3. Energy Performance Evaluation Tool of Zero Energy Building

When designing a zero energy building, we use not only a method of calculating room cooling and heating loads through indoor and outdoor temperature differences and internal heat gains but also use an energy performance evaluation tool (ECO2, EnergyPlus, etc.) for heating and cooling energy consumption due to a change in the indoor and outdoor environment. Additionally, the designer must consider the supply of energy from renewable energy sources to the heating and cooling system in the building. The energy performance calculation tool has to consider the heat flow based on the temperature and weather data from the area where the building is located. So, this calculation method algorithm must be authorized through international standard organization (ISO). Based on the evaluation results, we estimate the building's energy consumption and present various options to reduce it. These options consist of the application of building materials and technology. In this chapter, we apply each technology package of the energy performance analysis tool and confirm the energy saving effect. Additionally, to determine the energy consumption of the building, performance evaluation tools were compared and analyzed based on the ECO2 program. Moreover, the same energy performance evaluation tool was used to confirm the areas of improvement through comparative analysis.

In Korea, when designing a new building, the designer must calculate the energy consumption of the building using ECO 2. ECO 2 uses the ISO 13790 and DIN V 18599 as tools to evaluate the energy efficiency of buildings, and based on the monthly average weather data, the monthly energy demand of the building according to the performance of the system forecast quantity. Additionally, the evaluation is based on the primary energy requirement (kWh/m^2·year) per unit area per year. Energy requirements are classified into heating, cooling, hot water supply, lighting and ventilation energy. System performance inputs are classified into conditioning processing, heating equipment, heating supply system, heating distribution system, cooling equipment, and cooling distribution system regeneration equipment. Based on this, the ECO 2 program calculates the primary energy requirement per unit area using five items: heating, cooling, lighting, hot water supply, and ventilation system.

As with ECO 2, the Passive House Planning Package (PHPP) is a spreadsheet-based Excel program based on the ISO 13790 standards. Detailed criteria are based on the DIN V 18599 and DIN 4108 standards, as well as on many other DIN regulations and EN regulations. According to the input value of the user, PHPP applies the item, the value of the climate data utilizes the international weather measurement data of Switzerland, and 82 climate data values are registered in Korea. In Korea, in order to enhance the thermal insulation performance of buildings, the thermal insulation performance notation is unified and used as the heat transmission coefficient (U-value). The heat transmission coefficient value of the structure constituting the outer skin of the building such as the roof, the wall, the floor, etc., is calculated, and the indoor and external surface heat transfer resistance value follows the international standard EN ISO 6946. The heat loss of the structure is directly divided into the outside air and the floor directly adjacent to the boundary of the generation. Each zoning adopts the defense coefficient, etc., of the solar radiation absorption coefficient and the reflectance according to the finish. The cooling and heating areas of buildings in PHPP are calculated based on the inside

dimension, considering the heat exchange at the joint of the structure and the heat exchange where the insulation is cut or connected. The design of passive houses using PHPP is done in the following order: the energy demands of buildings can be calculated through the selection of climate data, setting the heat transfer coefficient by site, design of hulls, heat exchange analysis, design of foundations and basement, windows (solar control device), design of ventilation and design of the equipment system. The aim is to verify that the final primary energy requirement is less than 120 kWh/m^2 years. The heat exchange calculation takes into consideration the linear heat transmission coefficient according to the external reference dimension, and utilizes the length of the heat exchange part, the linear heat transmission coefficient, the temperature reduction coefficient, the heating city and is included in the heat loss of the structure. The linear heat transmission coefficient is calculated based on the ISO 10211-1 standard by using another 2D heat flow calculation program. The thermal bridge installation takes advantage of 2D heat flow calculations and uses the specified certificate.

EnergyPlus (v9.1.0, U.S. Department of Energy's, USA) is a tool developed by integrating the advantages of conventional interpretation tools DOE-2, BLAST, and COMIS. In this program, incomplete room temperature prediction is possible with the existing analysis tool using the calculation algorithm of wall heat transfer. By choosing the transfer function method and the finite difference method, the program can calculate the heat transfer of the building and calculate energy usage via feedback between buildings, systems and plants. The modular structure is flexible, and its Open Source format has an extendable interface. However, in order for the user to use the interpretation tool, basic knowledge is necessary for building energy analysis. Additionally, the user needs expert knowledge of each input variable. The user interface of EnergyPlus is relatively complicated. Therefore, there is a problem that interpretation of the result differs depending on the user's level of knowledge. The construction of the walls and the arrangement of the walls by zone can be input and arranged by layer structure of building materials like ECO 2, and facilities can be placed and divided by zone. Considering the air infiltration by zone, it is possible to calculate the detailed load, and set in detail the indoor occupancy situation according to the schedule and the operating condition of the equipment. As recently as 3D modeling through Openstudio plug-in, Sketch up plug-in, etc., additional plug-in is introduced for the user's convenience. Table 1 shows the features of ECO 2, PHPP and EnergyPlus which are energy analysis tools.

Table 1. Features of ECO 2, PHPP and EnergyPlus.

Category	ECO2	PHPP	EnergyPlus
Weather data	Monthly (Non modification)	Hourly (Modification)	Hourly (Modification)
Insulation thermal bridge	Non user input	Detail calculation	Non user input
Window thermal bridge	Non user input	Detail calculation	Non user input
Infiltration	Fix	Detail calculation	Detail calculation
Human	Sensible heat	Simple input	Detail calculation
Equipment	Sensible heat	Simple input	Detail calculation
Input level	Simple input and default input	Simple input	Detailed user input
Usability	User-friendly	User-friendly	Complex user interface

2.4. Technology Packaging for Zero Energy Building

The technology package for the implementation of zero energy building consists of a combination of modules consisting of a combination of building materials. The technology package can also be constructed with building materials, equipment and technical elements, etc., so that it can be provided in packages adapted to meet the objectives. Technical packages ensure the reliability of information through DB conversion of materials and facilities, and enable users to update information. Therefore, in order to achieve a zero energy building, technology packages need to be distinguished, in order

to study the compatibility between the technology as well as the thermal performance estimate of the building. In this research, it consists of passive technology packages constituting the form of building based on building materials and an active technology package which constitutes a facility system concerning the air conditioning and lighting, etc., of buildings. In addition, we proposed the composition concept of each technology package. Figure 1 shows the application package of the technical package and a conceptual diagram of the packaging structure of the whole technology. The Zero Energy Building Technology package is composed of material-module-package. Modules of combined forms of high performance/high efficiency building materials and equipment constitute each part of the building. Each module is integrated into a wall-like technology package using connection technology for coupling between the modules to maintain performance and construct the building with multiple technology packages. At this time, the equipment technology package is composed of a combination of the respective equipment modules and is applied according to the needs of the building.

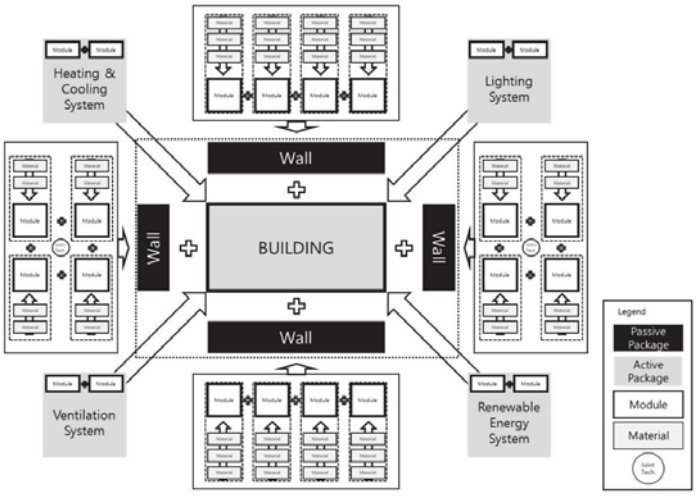

Figure 1. Technical package composition in the building.

2.5. Performance Test Method of Building Materials and Equipment for the Construction of the Zero Energy Building Technology Package

Due to the construction of the Zero Energy Building Technology Package, the performance of building materials and equipment of the Zero Energy Building Technology Package is composed of various materials and equipment. The components and equipment of the technology package therefore require selection criteria. Therefore, in this research, we propose a performance measurement method and performance criteria based on the performance measurement method of the test which is currently utilized in Korea. Korean Industrial Standards (KS) is the government standard according to the law for industrial standardization of Korea. This standard is announced by the chief of the Korean Agency for Technology and Standards. Based on the World Trade Organization (WTO)/Technical Barriers to Trade (TBT) Agreement and the recommendation by Asia Pacific Economic Cooperation (APEC)/Sub-Committee on Standards and Conformance (SCSC), the standard corresponding to the international standard operates in conformity. KS consists of 21 areas from basic section (A) to information section (X). This is divided into three parts. First is the standard of product (shape, size, quality); second is the standard of method (test, analysis, examine, operation standard); last is the standard of transmission (term, technique, unit). The Korean government has undertaken three energy efficiency management programs to increase the energy efficiency of appliances: energy standards and labeling, high-efficiency equipment certification, and e-Standby [10]. Having been implemented

since 1992, the energy standards and labeling program mandates all manufacturers to attach an energy efficiency label with a rank from 1 to 5 to their energy-intensive and highly disseminated appliances. Appliances failing to meet the minimum energy performance standards (MEPS) will be terminated from production and sales. The program targets 37 appliances including home appliances, lighting products, vehicles and tires. In addition to these domestic standards, we examined the international standard (ISO), the international standard (ASTM), and the passive house standard (PHI), which is the building-related standard. In this research, we selected the necessary performance measurement method and performance standard.

3. Proposed Technology Package Composition

3.1. Structure of the Passive Technology Package

The passive technology package for zero energy building installation considers the thermal insulation performance to reduce the load of cooling and heating energy of buildings based on the ability to resist the external environment through the building envelope. In Korea, after the legalization of the criteria for the application of thermal insulating materials for the outer skin of buildings since the 1970s, the thermal insulation standards of the insulation materials and the outer walls have been steadily strengthened, and insulation equipment such as windows, doors, etc., has been refined. Recent building materials also consider insulation performance according to the temperature difference between the inside and outside of the room and the solar heat gain coefficient, which is the amount of the solar heat gain from windows. Therefore, when building materials are combined, in addition to the building envelope composition having high heat insulating performance, a combination of building materials capable of exhibiting various levels of performance is required. In the case of building walls with high thermal insulation performance, it is possible to effectively block the heat exchange phenomenon generated by the connection with the dysentery material, and the insulation organize method is used. In the case of using the internal insulation, constructors use high performance materials such as vacuum insulation materials with low thermal conductivity while reducing the insulation material thickness when using the insulation organize method. In other words, it is a method of improving the heat insulating performance while making it easy to secure a large internal space. In the case of using high performance materials (e.g., low value of U-value) or using materials that prevent heat exchange (e.g., using thermal breaks), it is necessary to consider the accessory materials necessary for bonding between materials. Additionally, due to the difference in construction method, it is necessary to set it according to the package. The packages of these technologies can be composed of modules such as walls and windows via a step-by-step combination between building materials. In addition, when systemized (or packaged) via coupling between modules, it is possible to ensure performance according to the requirement of building energy performance.

Additionally, we can be satisfied with the expected performance at the design stage even after construction. The proposed configuration of the packages of these technologies is the same concept as the "application of material performance-construction of building structure-part of building" procedure used in the energy analysis tool. Based on these results, an integrated module of building materials becomes possible. Integration module means the combination of different building materials depending on the standards and sizes between various building materials and design standards. Further, it is possible to improve construction efficiency by modularization. A passive technology package can be configured as follows.

We construct a module through a combination of building materials and apply a joint technology for joining modules to construct a package. Finally, buildings can be constructed by coupling packages. Figure 2 shows the overall configuration of the passive technology package.

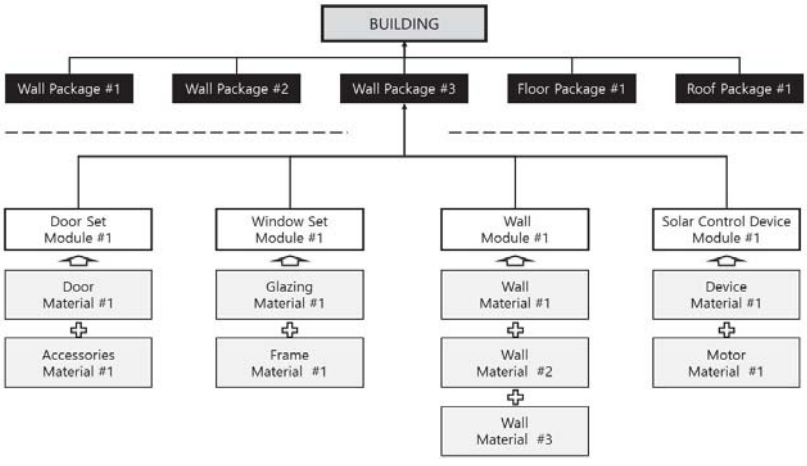

Figure 2. Passive package composition.

3.2. Structure of the Passive Technology Package Module

The modules of the passive technology package can be composed of a wall, a window, a door and a solar control device, respectively. The wall module contains information on multiple layers such as the insulation, structure, exterior material and interior material of a building material constituting the outer skin of the building. In addition to performance information including confidential performance, etc., obtained by checking the thermal resistance (or heat transmission coefficient) of the wall, the wall module also needs to include basic material information including durability and strength. The window module was constructed based on a window set consisting of a glazing and a window frame. For the window module, the product that is applied at the site installation is the standard. The window frame is made of an aluminum alloy material, a steel material, a synthetic resin material, wood, etc. Glazing is composed of multiple layers such as single glass and double glass. The door module was constructed based on a door set consisting of a door frame and a door. For the door module, the product that is applied at the site installation is the standard. The door set comprises hinged and sliding doors that are used internally and externally. Depending on the material of the main part of the door, it is divided into aluminum alloy material, wood, steel material, synthetic resin and stainless steel. The constituent materials of the inquiry are classified into a core material, a finishing material and an accessory. The solar control device module includes all devices capable of adjusting the functions of sunshade and solar introduction. Depending on the installation location, it can be distinguished between inside, outside, and glass. In addition, this module can be classified into a fixed type and a variable type according to the presence or absence of movement. Therefore, the solar control device module can be distinguished from the constituent material such as the slat, the louver and the drive motor.

3.3. Structure of the Active Technology Package

The air conditioning equipment consumes energy for the operation of buildings connected to the renewable equipment to achieve zero energy consumption of the building. Additionally, designers need to consider the compatibility between facility size setting and facilities. For proper design, it is necessary to calculate the capacity of equipment and the structure of the system. Cooperation between different systems can be performed using thermal-based technology (heat storage) and power-based ESS. The BEMS can be maintained and operate efficiently in order to conform to the load considered at the design phase. The heat source package of renewable energy is created by combining the heat source equipment package and the renewable energy heat source equipment element, which is performed

by coupling the elements constituting the heat source equipment. Additionally, parameters that can cooperate with each other are applied. As a result, it is possible to derive an alternative system suitable for the purpose and type of each facility. It is possible to improve the energy independence rate and quality of living environment at the operation stage through BEMS. Providing continuous technology updates and appropriate solutions to problems, it is possible to control the energy consumption of the building through cooperation with the passive technology package. Figure 3 shows the overall configuration of the active technology package.

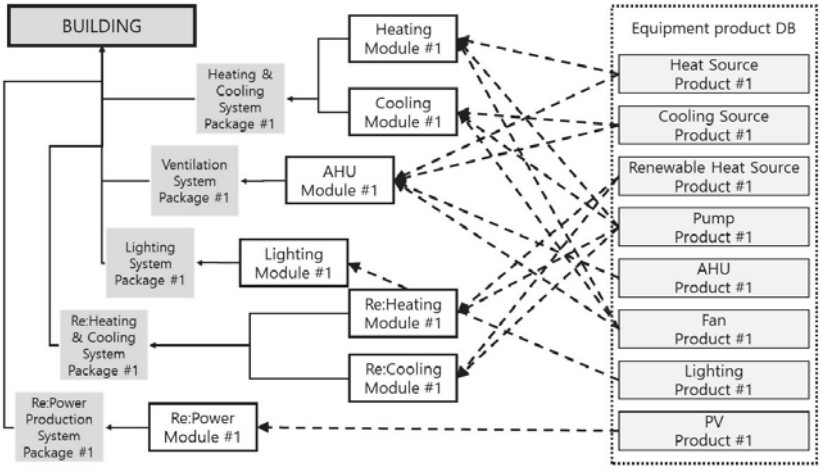

Figure 3. Active package composition.

3.4. Structure of the Active Technology Package Module

Active technology package modules can be distinguished as heating, cooling, air conditioning, ventilation, lighting, heat source of renewable energy, and power of renewable energy. Unlike the modular configuration of the passive technology package, the active technology package module can be constructed based on the building's air conditioning equipment plan. As shown in Figure 4, it is possible to add or delete constituent facilities depending on the configuration order of modules and the nature of modules. After calculating the capacity according to the initial load calculation and choosing the cooling and heating method, the application system of renewable energy is selected according to the final setting of the cooling and heating system and the lighting method. Then, the module of the system that distributes it in order is selected.

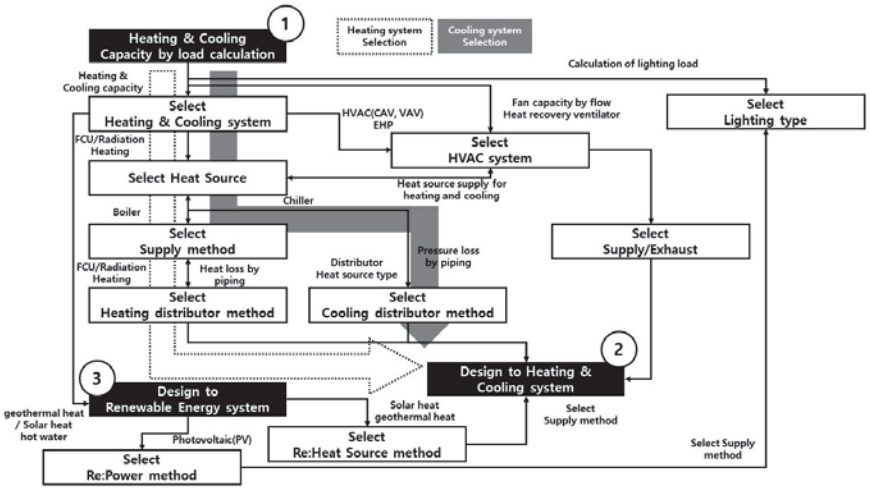

Figure 4. Process of the active technical package.

In the heating module, a boiler (or heat source) is selected according to the selection of the heating method, and a pump attached to the heat source equipment and the supply distribution-related equipment can be selected. The heating module is configured according to the product of the boiler facility. For this reason, a module of a structure that depends on the heat source product is configured via a product type DB. In addition, when utilizing renewable energy equipment, it can be integrated into or replaced by the air conditioning renewable energy module. The cooling module selects the refrigeration equipment according to the cooling mode selection, and selects the pump and the supply distribution-related equipment attached to the refrigerator equipment. The cooling module is configured according to the product of the refrigerating machine equipment. Refrigerator products are selected by DB for each type of product, and modules are configured with a structure that depends on this. Additionally, when utilizing renewable energy equipment such as a heating facility, the refrigerator can be integrated into or replaced by a cooling/heating renewable energy module. The configuration of the air conditioning ventilation module can be changed by an air conditioner and a fan installed based on the cooling/heating method inside the building and the internal ventilation method. Accordingly, a module of a structure that is dependent on the product is configured so that the accessory materials and equipment required for the configuration of the air conditioner (or fan) can be selected. The lighting module consists of main lighting and accessory material. The main lighting considers the purpose of the lighting's installation place and the arrangement of the lighting equipment. The lighting module thus constitutes a module via the lighting fixture and the accessory material DB. The renewable energy heat source module consists of solar power generation and geothermal power that can supply heating and cooling energy for buildings. Solar power generation systems convert solar radiation energy into thermal energy. This system consists of a solar collector and a condenser. The geothermal system utilizes the thermal energy of soil, rock and ground-water to utilize the temperature difference from the atmosphere. Additionally, in order to distribute and utilize the produced cooling and heating energy, cooperation with the heating/cooling module is considered, so the renewable energy module is structured to be compatible with other modules. The renewable energy power module utilizes renewable energy equipment for the purpose of producing necessary electricity for buildings. The photovoltaic power generation system is a representative module. In the module, the production module corresponding to the generator that generates electricity is composed of a power storage device with a power storage function, a power conversion device, etc., accessory.

3.5. Passive and Active Technology Packaging Materials and Equipment DB Composition

The building material DB constituting the passive module is made up of a wall material (Material); a glass part (Glazing) and a window frame (Frame); an inquiry core material of doors (Material) and attached materials (Accessories); a solar control device component (Material) and a driving motor (Motor). The wall material consists of DB of insulation material/structure/exterior material/ interior material. So, the material information was composed of the company name, model name, manufacturer, country of manufacture, density (kg/m^3), and specific heat (J/kg·K). The performance information was composed of thickness (mm) and thermal conductivity (W/m·K). The glass part (Glazing) of the windows was constructed to be able to enter the company name, model name, manufacturer, manufacture and type of glass and air gap details. The performance information composed of the heat transmission coefficient (W/m^2·K) of the glass part, SHGC, and visible light transmittance (VT). As for the glazing, the material of the window frame was made up of the company name, model name, manufacturer, and country of manufacture. As for the material of the window frame, material, thermal break and drawings are included. The performance information of the window frame was selected by the heat transmission coefficient (W/m^2·K). As a result, it is possible to confirm the thermal performance according to the area of the glazing and the window frame. The material DB of the door was composed of a core material (insulation material)/constituent material/thermal break. Material information was composed of the company name, model name, manufacturer, country of manufacture, density (kg/m^3), specific heat (J/kg·K), absorption rate, and tensile properties. Performance information consisted of thickness (mm) and thermal conductivity (W/m·K). Attachment material DB includes hinge/door lock/other attached hardware. Material information is composed of the company name, model name, manufacturer, type, material, and shape (drawing). The constituent material DB of the solar control device included slat/louver and the like, and the material information was composed of the performance of the company name, model name, manufacturer, country of manufacture, type, solar discoloration and discoloration. In the case of the drive motor, the material information was composed of the company name, model name, manufacturer, type, driving power, and repeated driving performance. The facility product DB constituting the active module can be classified into a heat source, a cooling source, a pump, air conditioning (AHU), a fan, lighting, a renewable heat source, and a renewable power source. We constructed DB for all equipment. Heat sources are domestic gas boilers, electric air-conditioners, multi-electric heat pump systems, gas boilers for industrial purposes and buildings, direct-fire absorption-type cold water heater, oil combustion hot water boiler, gas heat pump (GHP), and gas vacuum hot water boiler of the equipment DB. Each piece of equipment information is configured in a different way, but the thermal efficiency (%), the heating capacity (kW), and the supply water/return water temperature (°C) are commonly configured for the performance information. The cooling source can be electric heaters, electric air-conditioners, multi-electric heat pump systems, centrifugal screw refrigerators, direct-fire absorption type cold and hot water heaters, gas heat pumps (GHP), and medium temperature absorption refrigerators. Similar to the heat source, each piece of equipment information was constructed in a different way, but the capacity (W), the efficiency (%), the coefficient of performance (COP), and the supply water/return water temperature (°C) are common to the performance information. Since the pump is applied to various heat sources and equipment, the equipment information is composed of the company name, model name, manufacturer, country of manufacture, format, capacity, efficiency (%), rotation speed (rpm), and discharge amount (m^3/min). For performance information, we chose power (kW). The equipment information in the DB of the air conditioner was composed of the company name, model name, manufacturer, and control method. The performance information includes the maximum air volume (CMH), supply air volume (CMH), exhaust air volume (CMH), air supply fan pressure loss (Pa), exhaust fan pressure loss (Pa), heat recovery rate (%) and fan efficiency (%). In the case of a fan DB, the device information includes the company name, model name, manufacturer, and manufacturing. Performance information consisted of power (kW) and pressure loss (Pa).

In the case of lighting, LED lamp/LED appliances were constructed by separating equipment information by company name, model name, format, power factor, lighting factor, compensation rate, light source color, and harmonic content ratio. The performance information consisted of initial luminous flux (lm), light efficiency (lm/W), color temperature, color rendering property and power (W). The heat source of renewable energy was classified into solar heat and geothermal heat pump. The equipment information consisted of company name, model name, manufacturer, and type of driving. In the case of solar heat, the type of system and the type of heat collector were added. The performance information of solar heat was classified into capacity (kW), efficiency (%), pump power, and thermal storage tank capacity (L). The performance information of the geothermal source was capacity (kW), rated capacity (kW) of the heat exchanger, COP (cooling/heating), pump power (kW), presence and amount of expansion tank, total pipe length (m), and thermal conductivity of piping (W/m·K). The photovoltaic (PV) equipment information was classified into company name, model name, manufacturer, country of manufacture. The performance information was selected for capacity (kW). Figure 5 shows an example of passive technology package DB.

Passive Package−Wall Material DB

☑ No. 00 Insulation/Exterior/Interior

☑ Information of product

Company	OOO Coporation
Model name	TKR−002
Manufactuer	OOO Coporation
Country of manufacture	
Density(kg/㎥)	20.000
Specific heat(J/kg·K)	1.400.000

☑ Information of performance

Category	Unit	Value
Thickness	(mm)	50
Thermal conductivity	(W/m·K)	0.025

Passive Package DataBase Input − Version 2.0

Figure 5. Example of passive technology package DB.

4. Proposed Performance Standard of Passive and Active Technology Packages

4.1. Performance Classification of the Passive Technology Package

The performance of building materials for zero energy buildings can be divided into energy performance and other performance. Energy performance is classified into insulation materials and airtight performance, which affect the energy consumption of buildings. Other performance is related to the durability and weather resistance of materials. The performance items of the materials constituting the wall module were classified into heat insulation materials and internal and external materials.

The performance of building materials for zero energy building can be divided into energy performance and other performance. Energy performance is classified into insulation materials and airtight performance, which affect the energy consumption of buildings. Other performance is related to the durability and weather resistance of materials. The performance items of the materials constituting the wall module were classified into heat insulation materials and internal and external materials. Thermal insulation was classified into thermal conductivity of energy performance and other performance, fire resistance and absorption rate. Since the inner and outer packaging material varies according to the shape of the material and the method being applied to the structure, the energy

performance can be divided into the heat transmission coefficient, the thermal conductivity, and the thermal resistance. In addition, other performances can be confirmed by the properties of each material, adhesion strength, length change rate, fire protection performance, peel resistance, moisture content, salt spray test, and impact resistance. The window set module is divided into a glass part and a window frame. The energy performance of the glass part consists of the heat transmission coefficient and the solar heat gain coefficient (SHGC). Additionally, sound insulation performance is checked further. The window frame confirms the energy performance through the heat transmission coefficient. In addition, the modules of the door set were classified as insulation. The thermal conductivity of the insulation was chosen as the energy performance. The solar heat gain coefficient was chosen as the energy performance of the solar control device module separated by a slat, louver and blind. It was classified on the basis of the internally and externally installed materials. It consisted of wind speed resistance, salt spray, tensile strength, yield strength, elongation, and accelerated weather resistance of externally placed material. Tension strength, yield strength, elongation, and accelerated weather resistance were taken into consideration for the internally installed materials. Furthermore, the loading load, head trapping, durability of the fixing device, prevention of entanglement and cumulative confirmation performance were taken into consideration. The performance of the drive motor takes into consideration the performance of repeated operation. Table 2 shows the material performance list.

The performance criteria of each module were suggested by the testing method of the constituent materials and the testing method of the modules. The wall module selected thermal insulation performance as energy performance. Energy performance of the window set module consists of the performance of the heat transmission coefficient, the air flow rate and the solar heat gain coefficient. Other performance consists of condensation prevention, wind pressure, water-tightness, discoloration/bleach prevention, handle strength, opening and closing forces, repetitive operation of opening and closing and sound insulation.

In addition, the energy performance of the door set module consists of the heat transmission rate and the air flow rate. So, other performance of the door set module consists of condensation prevention, wind pressure, water-tightness, fire-proof, smoke penetration prevention, stability, opening and closing forces, discoloration/bleach prevention and sound insulation. Finally, energy performance of the solar control device module consists of the solar heat gain coefficient. For other performance, wind pressure, proof against climate performance, durability, repetitive operation and stability were selected. Table 3 shows the module performance list.

Table 2. Material performance contents.

Category	Material Type	Name of Performance	Type of Performance *
Wall-Material	Insulation	Thermal conductivity	E.P
		Fireproof	O.P
		Water absorption	O.P
	Interior/Exterior	Thermal conductivity	E.P
		U-value	E.P
		Thermal resistance	E.P
		Bond strength	O.P
		Length change	O.P
		Fireproof	O.P
		Peel resistance	O.P
		Water absorption	O.P
		Salt spray resistance	O.P
		Impact resistance	O.P
Window-Glazing	Glazing	U-value	E.P
		Solar heat gain coefficient (SHGC)	E.P
		Flame interruption performance (LIP)	O.P
Window-Frame	Frame	U-value	E.P
Door-Material	Insulation	Thermal conductivity	E.P
Solar Control Device-Material	Slat/Louver/Blind (Exterior)	Solar heat gain coefficient (SHGC)	E.P
		Wind pressure	O.P
		Salt spray resistance	O.P
		Tensile strength	O.P
		Yield strength	O.P
		Elongation	O.P
		Accelerated weathering	O.P
	Slat/Louver/Blind (Interior)	Solar heat gain coefficient (SHGC)	E.P
		Tensile strength	O.P
		Yield strength	O.P
		Elongation	O.P
		Accelerated weathering	O.P
		Weight load	O.P
		Head stuck	O.P
		Durability	O.P
		Prevention of tangling	O.P
		Accumulation device	O.P
Solar Control Device-Motor	Motor	Repetitive operation	O.P

* E.P: Energy Performance, O.P: Other performance.

Table 3. Module performance contents.

Category	Name of Performance	Type of Performance
Wall-Module	U-value	E.P
	Linear transmittance	E.P
Window Set-Module	U-value	E.P
	Air flow rate	E.P
	Solar heat gain coefficient (SHGC)	E.P
	Condensation prevention (TDR)	O.P
	Wind pressure	O.P
	Water-tightness	O.P
	Discoloration/Bleach prevention (DBP)	O.P
	Handle strength	O.P
	Opening and closing forces (OCF)	O.P
	Repetitive operation of opening and closing (ROOC)	O.P
	Sound insulation(R)	O.P
Door Set-Module	U-value	E.P
	Air flow rate	E.P
	Condensation prevention (TDR)	O.P
	Wind pressure	O.P
	Water-tightness	O.P
	Fireproof	O.P
	Smoke penetration prevention (SPP)	O.P
	Stability	O.P
	Opening and closing forces (OCF)	O.P
	Discoloration/Bleach prevention (DBP)	O.P
	Sound insulation(R)	O.P
Solar Control Device-Module	Solar heat gain coefficient (SHGC)	E.P
	Wind pressure	O.P
	Proof against climate performance (PACP)	O.P
	Durability	O.P
	Repetitive operation (RO)	O.P
	Stability	O.P

4.2. Method of Measureing the Performance of the Passive Technology Package and Minimum Performance Standard

In order to construct a zero energy building, the components of the passive technology package should be constructed of high efficiency/high performance construction materials. The performance of construction materials should be evaluated under the same conditions using a certified measurement method. The minimum performance criteria and performance test methods are proposed for zero energy buildings. The performance test method was based on the KS standard provided by the National Institute of Technology Standards. Additionally, in some cases, we selected the national examination and the performance measurement method of the material.

In the case of wall insulation, KS L 9106, KS F 2277 and "Building Energy Conservation Design Standard (BEDS)" were selected according to the test method of energy performance. Other performance test methods referred to KS F ISO1192, KS F ISO 5660-1, KS F 2271, KS M ISO 2896, and KS M ISO 4898. The performance test method and performance standard for thermal conductivity, fire protection performance and the absorption rate of wall free insulation material are proposed. The test methods and performance standard of the interior and exterior materials suggested thermal conductivity, thermal transmittance, and thermal resistance performance of energy performance.

We also proposed test methods and performance standards for other performances such as Bond strength, Length change, Fireproof, Peel resistance, Water absorption, Salt spray resistance and Impact resistance. In relation to the glazing, the author proposed the test method and performance standard of the U-value of energy performance and the performance of the solar heat gain coefficient.

The authors also proposed the test method of Fire resistance performance (F.R.P) which is the other performance. Frame and door insulation test methods were proposed for U-value and thermal conductivity test methods, and BEDS performance standards were selected. The slats/louvers/blinds

of the solar control device were divided into indoor and outdoor, and performance test methods and the performance standard were proposed, respectively. The solar heat gain coefficient of energy performance is commonly applied to the other performances (Wind pressure, Salt spray resistance, Tensile strength, Yield strength, Elongation, Accelerated weathering, Weight load, Head stuck, Durability, Prevention of tangling, Accumulation device) individually. In addition, for the drive motor, we have proposed a performance test method and performance standard for repetitive operation performance. Table 4 shows the Test methods and performance reference of the material [10–28].

Table 4. Test methods and performance reference of the material.

Material Type	Name of Performance (Unit)	Performance	Test Method	Performance Standard
Insulation	Thermal conductivity (W/m·K)	▼ 0.034	KS L 9106	BEDS
	Fireproof (-)	Pass	KS F ISO 1182 KS F ISO 5660-1 KS F 2271	BEFS
	Water absorption (%)-EPS	▼ 6	KS M ISO 2896	KS M ISO 4898
	Water absorption (%)-XPS	▼ 1		
	Water absorption (%)-PUR	▼ 4		
	Water absorption (%)-PF	▼ 4		
Interior/Exterior material	Thermal conductivity (W/m·K)	▼ 0.15	KS F 2277	BEDS
	U-value (W/m^2·K)	▼ 0.071	KS L 9016	KS F 4040
	Thermal resistance (m^2·K/W)	▲ 0.043	KS F 2277	KS F 3504
	Bond strength (N/mm^2)	▲ 0.1	KS F 4716	KS F 4040
	Length change (%)	▼ 0.5	KS F 2424	KS F 4040
	Fireproof (-)	Pass	KS F ISO 1182 KS F ISO 5660-1 KS F 2271	BEFS
	Peel resistance (-)	Pass	KS F 3504	KS F 3504
	Water absorption (%)	▼ 3	KS F 3504	KS F 3504
	Salt spray resistance (-)	Pass	KS F 9502	KS F 4760
	Impact resistance (-)	Pass	KS F 4760	KS F 4760
Glazing	U-value (W/ m^2·K)	▼ 0.9	KS F 2278	BEDS
	SHGC (-)	▲ 0.5	KS L 9107	PHI
	F.I.P (min)	-	KS F 2845	-
Frame	U-value (W/m^2·K)	▼ 0.9	KS F 2278	BEDS
Door Insulation	Thermal conductivity (W/m·K)	▼ 0.034	KS L 9106	BEDS
Slat/Louver/ blind (Exterior)	SHGC (-)	-	KS L 9107	-
	Wind pressure (-)	Pass	ASTM 331	ASTM 331
	Salt spray resistance (RN)	▲ 8	KS D 9502	KS D8334
	Tensile strength (N/ mm^2)	200 ~ 260	KS B 0802	KS B 0802
	Yield strength (N/ mm^2)	200 ~ 240	KS B 0802	KS B 0802
	Elongation (%)	5 ± 3	KS B 0802	KS B 0802
	Accelerated weathering (-)	Pass	KS C 8568	KS C 8568
Slat/Louver/ blind (Interior)	SHGC (-)	-	KS L 9107	-
	Tensile strength (N/mm^2)	200 ~ 260	KS B 0802	KS B 0802
	Yield strength (N/ mm^2)	200 ~ 240		
	Elongation (%)	5 ± 3		
	Accelerated weathering (-)	Pass	KS C 8568	KS C 8568
	Weight load (-)	Pass		
	Head stuck (-)	Pass		
	Durability (-)	Pass	APP.7	APP.7
	Prevention of tangling (-)	Pass		
	Accumulation device (-)	Pass		
Motor	Repetitive operation (Time)	▲ 100,000	KS C 6021	KS C 6021

▲: or More ▼: or less.

In the case of passive modules, the performance can be verified by the coupling of performance between materials, and the performance can be verified through the actual physical testing method of the module. At this time, it provides the durability of the module and other performances to satisfy the basic required performance. It can also confirm the energy performance suitable for the purpose of the zero energy building, as well as various performance test methods and the proposed performance standard. In the case of the wall module, the test method of U-value and linear U-value is proposed and the performance standard of BEDS is proposed. The performance test method and performance standard of the window module are proposed. The performance standard of U-value, air tightness, and solar heat gain performance to energy performance is also proposed. Additionally, the performance test method and performance standard of other performances are proposed. For the door module, the author determined the performance test method of U-value and air tightness performance, and proposed other performance (TDR, Wind pressure, Water-tightness, Fireproof, SPP, Stability, OCF, DBP, sound insulation) test methods and performance standards. In order to satisfy the energy performance, a performance test method of solar heat gain performance was proposed in the solar control device module. To ensure the durability and maintain the function, we also proposed various other performance test methods and performance standards. Table 5 shows test methods and the performance reference of the module [29–42].

4.3. Performance Classification of the Active Technology Package

Unlike passive technology packages, active technology packages applied to zero energy buildings select the products of each facility in order to determine the cooling/heating, lighting, ventilation equipment, etc., required for each building. Therefore, we confirmed the performance of the products of each facility. We also confirmed and configured the performance confirmation items of the conventional high efficiency certified products that can reduce energy consumption and the highest grade products of the efficiency evaluation. The equipment of the active technology package is divided into heat source, cooling source, pump, fan, lighting and renewable heat source.

Moreover, on the basis of each installation product, the heat source comprised domestic gas-fired boilers, electric chillers and heaters, a multi electric heat pump system, gas-fired boilers for industry and buildings, direct fired absorption cold and hot water dispensers, oil-fired hot water boilers, gas-fired heat pumps, and gas-fired vacuum hot water boilers. The cooling source comprised refrigerators, electric chillers and heaters, a multi electric heat pump system, centrifugal and screw chillers, direct fired absorption cold and hot water dispensers, gas-fired heat pumps and medium-temperature absorption chillers. The pump consisted of a single item and the fan consisted of an energy recovery ventilator and a centrifugal fan. The lighting equipment consisted of external convertor-type LED lamps, recessed LED luminaires and fixed LED luminaires, tubular LED lamps and LED lamps for replacing fluorescent lamps. Additionally, the renewable heat source consisted of solar thermal collectors and the ground source heat pump unit. Table 6 shows the performance contents of the equipment.

Table 5. Test methods and performance reference of the modules.

Category	Name of Performance (Unit)	Performance	Test Method	Performance Standard
Wall-Module	U-value ($W/m^2 \cdot K$)	▼ 0.15	KS F 2277	BEDS
	Linear U-value (W/m·K)	▼ 0.4	ISO 10221-1	BEDS
Window Set-Module	U-value ($W/m^2 \cdot K$)	▼ 0.9	KS F 2278	BEDS
	Air flow rate ($m^3/h \cdot m^2$)	▼ 1.0	KS F 2292	ESL
	SHGC (-)	▲ 0.5	KS L 9107	PHI
	TDR (-)-by each local area	▼ Standard	KS F 2295	DCCP
	Wind pressure (-)	Pass	KS F 2296	KS F 3117
	Watertightnes s(-)	Pass	KS F 2293	KS F 3117
	DBP (-)	Pass	KS C 8568	KS C 8568
	Handle strength (-)	Pass	KS F 2239	KS F 3117
	OCF(N)	▼ 50	KS F 2237	KS F 3117
	ROOC (time)	▲ 10,000	KS F 3109/4534	KS F 3117
	R (dB, 500 Hz)	▼ 40	KS F ISO 10140-2	KS F ISO 10140-2
Door Set-Module	U-value ($W/m^2 \cdot K$)-Door	▼ 0.9	KS F 2278	BEDS
	U-value ($W/m^2 \cdot K$)-Fire door	▼ 1.4		
	Air flow rate ($m^3/h \cdot m^2$)	▼ 1.0	KS F 2292	HEC
	TDR (-)-by each local area	▼ Standard	KS F 2295	DCCP
	Wind pressure (-)	Pass	KS F 2296	KS F 3109
	Watertightness (-)	Pass	KS F 2293	KS F 3109
	Fireproof (-)	Pass	KS F 2268-1	KS F 2268-1
	SPP ($m^3/min \cdot m^2$, △25 Pa)	▼ 0.9	KS F 2846	KS F 2846
	Stability (-)	Pass	KS F 3109	KS F 3109
	OCF (N)	▼ 50	KS F 2237	KS F 3109
	DBP (-)	Pass	KS C 8568	KS C 8568
	R (dB, 500 Hz)	▼ 40	KS F ISO 10140-2	KS F ISO 10140-2
Solar Control Device-Module	SHGC (-)	-	KS L 9107	-
	Wind pressure (-)	Pass	ASTM 331	ASTM 331
	Salt spray resistance (RN)	▲ 8	KS D 9502	KS D8334
	Tensile strength (N/mm^2)	200 ~ 260	KS B 0802	KS B 0802
	Yield strength (N/mm^2)	200 ~ 240	KS B 0802	KS B 0802
	Elongation (%)	5 ± 3	KS B 0802	KS B 0802
	Accelerated weathering (-)	Pass	KS C 8568	KS C 8568
	Weight load (-)	Pass		
	Head stuck (-)	Pass		
	Durability (-)	Pass	APP.7	APP.7
	Prevention of tangling (-)	Pass		
	Accumulation device (-)	Pass		
	Repetitive operation (Time)	▲ 100,000	KS C 6021	KS C 6021

▲: or More ▼: or less.

Table 6. Performance contents of the equipment.

Category	Equipment Name	Name of Performance
Heat Source	Domestic gas-fired boilers	Heating thermal efficiency
	Electric chillers and heaters	HSPF
	Multi electric heat pump system	COP
	Gas-fired boilers for industry and buildings	Thermal efficiency
	Direct fired absorption cold and hot water dispensers	IPLV
	Oil-fired hot water boilers	Heating efficiency
	Gas-fired heat pumps	Heating COP
	Gas-fired vacuum hot water boilers	Heating efficiency
Cooling Source	Refrigerators	CSPF
	Electric chillers and heaters	CSPF
	Multi electric heat pump system	IEER
	Centrifugal and screw chillers	Energy efficiency
	Direct fired absorption cold and hot water dispensers	IPLV
	Gas-fired heat pumps	Cooling COP
	Medium-temperature absorption chillers	IPLV
Pump	Pump	Efficiency
Fan	Energy recovery ventilators	Heat transfer efficiency
	Centrifugal fans	Efficiency
Lighting	External convertor type LED lamps	Luminous efficiency
	Recessed LED luminaires and fixed LED luminaires	Luminous efficiency
	Tubular LED lamps	Luminous efficiency
	LED lamps for replacing fluorescent lamps	Luminous efficiency
Renewable Heat Source	Solar thermal collectors	Collector performance
	Ground Source Heat Pump Unit	COP

4.4. Method of Measuring the Performance of the Active Technology Package and Minimum Performance Standard

As mentioned above, the active technology package is composed of each facility based on the proposed module configuration of the technology package, so this chapter proposes the performance test method and performance standard of each facility product. These products are used based on the "Energy Efficiency Labeling and Standard (ELS)" and "High-efficiency Appliance Certification (HEC)" managed by the Korea Energy Corporation, and the performance test methods provided by each rule are used. It was divided into performance item and performance standard based on whether the performance standard was met.

For the performance test method and performance standard of the heat source, the highest performance of Energy Efficiency Labeling and Standard to heating thermal efficiency, the heating season power efficiency (HSPF) and COP were selected. Additionally, integrated power level value (IPLV), heating COP, and thermal coefficient were selected by referring to High-efficiency Appliance Certification. The cooling season performance efficiency (CSPF) and the integrated electric energy rate (IEER) were selected as the testing method and performance standard of the cooling source, respectively, referring to the highest rating of Energy Efficiency Labeling and Standard. Additionally, with reference to High-efficiency Appliance Certification, the authors proposed energy efficiency, integrated performance level value (IPLV), and cooling coefficient of performance. The pump performance standard and test method were selected based on the efficiency of Energy Efficiency Labeling and Standard as the performance standard. The performance of the fan was selected based on the heat transfer efficiency of the High-efficiency Appliance Certification and the nominal efficiency was selected as the performance standard. The luminous efficiency of the lighting was selected with reference to High-efficiency Appliance Certification. The performance standard and test method of renewable heat sources were divided into the solar power generation system and the geothermal heat

pump system. This selection was determined with reference to KS B8295 and KS B8292, respectively, as well as the performance of the collector and the heating and cooling efficiency. Table 7 shows the test methods and performance reference of the equipment [43,44].

Table 7. Test methods and performance reference of the equipment.

Equipment Name	Name of Performance (Unit)	Performance	Reference Standard
Domestic gas-fired boilers	Heating thermal efficiency (%)	▲91.0	ELS
Electric chillers and heaters	HSPF (-)	▲5.0	ELS
Multi electric heat pump system	COP (-)	▲5.0	ELS
Gas-fired boilers for industry and buildings	Thermal efficiency (%)	▲88	HEC
Direct fired absorption cold and hot water dispensers	IPLV (-)	▲1.41	HEC
Oil-fired hot water boilers	Heating efficiency (%)	▲82	HEC
Gas-fired heat pumps	Heating COP (-)	▲1.4	HEC
Gas-fired vacuum hot water boilers	Heating efficiency (%)	▲88	HEC
Refrigerators	CSPF (-)	▲5.0	ESL
Electric chillers and heaters	CSPF (-)	▲5.0	ESL
Multi electric heat pump system	IEER (-)	▲5.0	ESL
Centrifugal and screw chillers	Energy efficiency (-)	▼0.7	HEC
Direct fired absorption cold and hot water dispensers	IPLV (-)	▲1.41	HEC
Gas-fired heat pumps	Cooling COP (-)	▲1.2	HEC
Medium-temperature absorption chillers	IPLV (-)	▲0.83	HEC
Pump	Efficiency (-)	Pass	HEC
Energy recovery ventilators	Heat transfer efficiency (%)	▲45 (Cooling) ▲70 (Heating)	HEC
Centrifugal fans	Efficiency (-)	Pass	HEC
External convertor type LED lamps	Luminous efficiency (lm/W)	▲85	HEC
Recessed LED luminaires and fixed LED luminaires	Luminous efficiency (lm/W)	▲95	HEC
Tubular LED lamps	Luminous efficiency (lm/W)	▲130	HEC
LED lamps for replacing fluorescent lamps	Luminous efficiency (lm/W)	▲105	HEC
Solar thermal collectors	Collector performance (MJ/m^2)	▲7.64	KS B 8295
Ground Source Heat Pump Unit	COP (-)	▲3.78	KS B 8292

▲: or More ▼: or less.

5. Conclusions

In order to set up a zero energy building, the authors confirmed the conventional concept of zero energy building introduced in Korea and proceeded with research based on the existing research results. In this study, we proposed a package of passive and active technologies to facilitate the spread of zero energy buildings that suit Korea's situation through the application of appropriate building materials and building equipment. The results of this study are as follows:

(1) In Korea, ECO2 is used in building design. Therefore, in order to construct a technology package and express energy performance, it is necessary to indicate the performance value required by ECO2. Therefore, this study proposes measures to improve ECO2 by comparing analysis tools. The zero energy building concept in Korea and the energy performance evaluation tool for constructing zero energy buildings were confirmed. Then, the performance of the building materials and building equipment required for zero energy buildings was derived. Based on these results, it was necessary to unify the method used to test the performance of building materials and building equipment by utilizing the energy performance evaluation tool for buildings. Also confirmed was the necessity of declaring the method used to test the performance. We also confirmed that it is necessary to consider the extensibility by introducing technology packaging to convert DBs of building materials and building facilities.

(2) Based on building materials, we provided passive technology packages, and proposed active technology packages based on building equipment. Using passive and active technology packages, we confirmed that the technology of each technology parameter is necessary, and confirmed the detailed requirements of each technology. We implemented passive and active technology

packages using the proposed configuration, and we proposed the necessary DB configuration for this.

(3) We analyzed and classified the Korean building materials testing methods and performance standards, and proposed passive and active technology packages, modules, material performance testing methods and minimum requirement performance standards. Based on these results, we proposed the technical performance required for a zero energy building—not a simple energy saving technology description.

The results of this study can be used as the basic data of the future technology level. The passive and active technology packages provided by this research will be updated in the future as each DB is converted. Additionally, it is necessary to improve the test method required for DB and derive a new test method. Through future research, we will try to derive the performance test method of the technology package and the required performance standard at the package level.

As the Korea Zero Energy Building Technology Package represents an area of ongoing research, there are no concrete results yet. However, as a result of this research, the concept of the technology package is applied and DB is constructed, as in Figure 5. In future research, we will present the results of the development of specific technology packages.

Author Contributions: U.-J.S. managed the project and wrote the manuscript. S.-H.K. reviewed the concept of the technical package and edited the manuscript.

Funding: This work was supported by the Korea Institute of Energy Technology Evaluation and Planning (KETEP) and the Ministry of Trade, Industry & Energy (MOTIE) of the Republic of Korea (No. 20162010104270).

Conflicts of Interest: The authors declare no conflict of interest.

References

1. Cho, S.; Han, S.Y.; Sung, U.K.; Kim, S.H. An Suggestion of Improvement Plan and Analysis of Comparison about the Energy Performance Evaluation Tools for Application of the Technical Package in Zero Energy Building. *J. KIAEBS* **2017**, *11*, 319–330.
2. Cho, S.; Sung, U.K.; Rim, M.Y.; Kim, S.H. A Fundamental Study on the Technical Package in Zero Energy Building. *J. KIAEBS* **2018**, *12*, 253–263.
3. Sung, U.K.; Rim, M.Y.; Kim, S.H.; Cho, S. A Study on the Performance Measuring Methods and Standard for the Technical Package in Zero Energy Building. *J. KIAEBS* **2018**, *12*, 543–556.
4. Shim, J.S.; Song, D.S.; Kim, J.W. The Economic Feasibility of Passive Houses in Korea. *Sustainability* **2018**, *10*, 3358. [CrossRef]
5. Mahdavi, A.; Doppelbauer, E. A performance comparison of passive and low-energy buildings. *Energy Build.* **2010**, *42*, 1314–1319. [CrossRef]
6. Audenaert, A.; De Cleyn, S.H.; Vankerckhove, B. Economic analysis of passive houses and low-energy houses compared with standard houses. *Energy Policy* **2008**, *36*, 47–55. [CrossRef]
7. Kim, Y.W.; Yu, K.H. Study on Policy Marking of Passive Level Insulation Standards for Non-Residential Buildings in South Korea. *Sustainability* **2018**, *10*, 2554. [CrossRef]
8. Oh, J.Y.; Hong, T.H.; Kim, H.P.; An, J.B.; Jeong, K.B.; Koo, C.W. Advanced Strategies for Net-Zero Energy Building: Focused on the Early Phase and Usage Phase of a Building's Life Cycle. *Sustainability* **2017**, *9*, 2272. [CrossRef]
9. Faustino, P.C.; Armesto, J.; Faustino, P.B.; Bastos, G. Perspectives on Near ZEB Renovation Projects for Residential Buildings: The Spanish Case. *Energies* **2016**, *9*, 628.
10. Korea Agency for Technology and Standard. KS L 9016: Test Methods for Thermal Transmission Properties of Thermal Insulations. 2017. Available online: https://www.kssn.net/en/search/stddetail.do?itemNo=K001010106453 (accessed on 30 April 2019).
11. Korea Agency for Technology and Standard. KS F ISO 1182: Test Method of Non-Combustibility of Building Products. 2018. Available online: https://www.kssn.net/en/search/stddetail.do?itemNo=K001010110234 (accessed on 30 April 2019).

12. Korea Agency for Technology and Standard. KS F ISO 5660-1: Reaction to Fire Test—Heat Release. Smoke Production and Mass Loss Rate—Part 1: Heat Release Rate (Cone Calorimeter Method). 2017. Available online: https://www.kssn.net/en/search/stddetail.do?itemNo=K001010118692 (accessed on 30 April 2019).
13. Korea Agency for Technology and Standard. KS F 2271: Testing Method for Gas Toxicity of Finish Materials of Buildings. 2016. Available online: https://www.kssn.net/en/search/stddetail.do?itemNo=K001010109594 (accessed on 30 April 2019).
14. Korea Agency for Technology and Standard. KS M ISO 2896: Rigid Cellular Plastics—Determination of Water Absorption. 2015. Available online: https://www.kssn.net/en/search/stddetail.do?itemNo=K001010105494 (accessed on 30 April 2019).
15. Korea Agency for Technology and Standard. KS M ISO 4898: Rigid Cellular Plastics-Thermal Insulation Products for Buildings-Specifications. 2013. Available online: https://www.kssn.net/en/search/stddetail.do?itemNo=K001010121096 (accessed on 30 April 2019).
16. Korea Agency for Technology and Standard. KS F 2277: Thermal Insulation—Determination of Steady-State Thermal Transmission Properties—Calibrated and Guarded Hot Box. 2017. Available online: https://www.kssn.net/en/search/stddetail.do?itemNo=K001010113351 (accessed on 30 April 2019).
17. Korea Agency for Technology and Standard. KS F 4040: Insulating Mortar. 2014. Available online: https://www.kssn.net/en/search/stddetail.do?itemNo=K001010101533 (accessed on 30 April 2019).
18. Korea Agency for Technology and Standard. KS F 3504: Gypsum Boards. 2018. Available online: https://www.kssn.net/en/search/stddetail.do?itemNo=K001010118690 (accessed on 30 April 2019).
19. Korea Agency for Technology and Standard. KS F 4716: Cement Filling Compound for Surface Preparation. 2016. Available online: https://www.kssn.net/en/search/stddetail.do?itemNo=K001010109879 (accessed on 30 April 2019).
20. Korea Agency for Technology and Standard. KS F 2424: Standard Test Method for Length Change of Mortar and Concrete. 2015. Available online: https://www.kssn.net/en/search/stddetail.do?itemNo=K001010108274 (accessed on 30 April 2019).
21. Korea Agency for Technology and Standard. KS F 4760: Raised Access Floor. 2016. Available online: https://www.kssn.net/en/search/stddetail.do?itemNo=K001010113113 (accessed on 30 April 2019).
22. Korea Agency for Technology and Standard. KS F 2278: Standard Test Method for Thermal Resistance for Windows and Doors. 2017. Available online: https://www.kssn.net/en/search/stddetail.do?itemNo=K001010113352 (accessed on 30 April 2019).
23. Korea Agency for Technology and Standard. KS L 9107: Testing Method for the Determination of Solar Heat Gain Coefficient of Fenestration Product Using Solar Simulator. 2014. Available online: https://www.kssn.net/en/search/stddetail.do?itemNo=K001010099475 (accessed on 30 April 2019).
24. ASTM international. ASTM 331: Standard Test Method for Water Penetration of Exterior Windows, Skylights, Doors, and Curtain Walls by Uniform Static Air Pressure Difference. 2016. Available online: http://www.astm.org/ (accessed on 30 April 2019).
25. Korea Agency for Technology and Standard. KS D 9502: Methods of Neutral Salt Spray Testing (Neutral Salt, Acetic Acid and Cass Test). 2014. Available online: https://www.kssn.net/en/search/stddetail.do?itemNo=K001010100937 (accessed on 30 April 2019).
26. Korea Agency for Technology and Standard. KS D 8334: Methods of Corrosion Resistance Test of Metallic Coatings. 2015. Available online: https://www.kssn.net/en/search/stddetail.do?itemNo=K001010106704 (accessed on 30 April 2019).
27. Korea Agency for Technology and Standard. KS B 0802: Method of Tensile Test for Metallic Materials. 2013. Available online: https://www.kssn.net/en/search/stddetail.do?itemNo=K001010122930 (accessed on 30 April 2019).
28. Korea Agency for Technology and Standard. KS C 8568: Daylight Collecting System. 2015. Available online: https://www.kssn.net/en/search/stddetail.do?itemNo=K001010105683 (accessed on 30 April 2019).
29. International Organization for Standardization. ISO 10211-1: Thermal Bridges in Building Construction—Heat Flows and Surface Temperatures—Part 1: General Calculation Methods. 1995. Available online: https://www.iso.org/ (accessed on 30 April 2019).
30. Korea Agency for Technology and Standard. KS F 2292: The Method of Air Tightness for Windows and Doors. 2013. Available online: https://www.kssn.net/en/search/stddetail.do?itemNo=K001010122343 (accessed on 30 April 2019).

31. Korea Agency for Technology and Standard. KS F 2295: Test Method of Dew Condensation for Windows and Doors. 2014. Available online: https://www.kssn.net/en/search/stddetail.do?itemNo=K001010101501 (accessed on 30 April 2019).
32. Korea Agency for Technology and Standard. KS F 2296: Windows and Door Sets—Wind Resistance Test. 2014. Available online: https://www.kssn.net/en/search/stddetail.do?itemNo=K001010101502 (accessed on 30 April 2019).
33. Korea Agency for Technology and Standard. KS F 3117: Window Sets. 2015. Available online: https://www.kssn.net/en/search/stddetail.do?itemNo=K001010105704 (accessed on 30 April 2019).
34. Korea Agency for Technology and Standard. KS F 2293: Test Method of Water Tightness for Windows and Doors. 2013. Available online: https://www.kssn.net/en/search/stddetail.do?itemNo=K001010122344 (accessed on 30 April 2019).
35. Korea Agency for Technology and Standard. KS F 2239: Doors and Windows—Test Method for Mechanical Deformation of Edge Rail. 2013. Available online: https://www.kssn.net/en/search/stddetail.do?itemNo=K001010122342 (accessed on 30 April 2019).
36. Korea Agency for Technology and Standard. KS F 2237: Windows and Doors—Standard Test Method for Determination of Opening and Closing Forces. 2017. Available online: https://www.kssn.net/en/search/stddetail.do?itemNo=K001010113986 (accessed on 30 April 2019).
37. Korea Agency for Technology and Standard. KS F 3109: Door Sets. 2013. Available online: https://www.kssn.net/en/search/stddetail.do?itemNo=K001010110206 (accessed on 30 April 2019).
38. Korea Agency for Technology and Standard. KS F 4534: Fittings for Sash Windows. 2016. Available online: https://www.kssn.net/en/search/stddetail.do?itemNo=K001010110218 (accessed on 30 April 2019).
39. Korea Agency for Technology and Standard. KS F ISO 10140-2: Acoustics-Laboratory Measurement of Sound Insulation of Building Elements—Part 2: Measurement of Airborne Sound Insulation. 2016. Available online: https://www.kssn.net/en/search/stddetail.do?itemNo=K001010109202 (accessed on 30 April 2019).
40. Korea Agency for Technology and Standard. KS F 2268-1: Fire Resistance Test for Door Assemblies. 2014. Available online: https://www.kssn.net/en/search/stddetail.do?itemNo=K001010103912 (accessed on 30 April 2019).
41. Korea Agency for Technology and Standard. KS F 2846: Methods for Measuring Smoke Penetration through Door Assemblies. 2013. Available online: https://www.kssn.net/en/search/stddetail.do?itemNo=K001010122917 (accessed on 30 April 2019).
42. Korea Agency for Technology and Standard. KS C 6021: Endurance (Mechanical) Testing Method for Electronic Components. 2014. Available online: https://www.kssn.net/en/search/stddetail.do?itemNo=K001010103862 (accessed on 30 April 2019).
43. Korea Agency for Technology and Standard. KS B 8295: Solar Thermal Collectors (Flat Plate, Evacuated-Tube, Fixed Concentrating Type). 2015. Available online: https://www.kssn.net/en/search/stddetail.do?itemNo=K001010105690 (accessed on 30 April 2019).
44. Korea Agency for Technology and Standard. KS B 8292: Water-to-Water Ground Source Heat Pump Unit. 2015. Available online: https://www.kssn.net/en/search/stddetail.do?itemNo=K001010105689 (accessed on 30 April 2019).

energies

MDPI

Article

Energy Renovation versus Demolition and Construction of a New Building—A Comparative Analysis of a Swedish Multi-Family Building

Lina La Fleur [1,*], Patrik Rohdin [1] and Bahram Moshfegh [1,2]

[1] Division of Energy Systems, Department of Management and Engineering, Linköping University, 581 83 Linköping, Sweden; patrik.rohdin@liu.se (P.R.); bahram.moshfegh@liu.se (B.M.)

[2] Division of Building, Energy and Environment Technology, Department of Technology and Environment, University of Gävle, 801 76 Gävle, Sweden

* Correspondence: lina.la.fleur@liu.se; Tel.: +4613-281156

Received: 3 May 2019; Accepted: 6 June 2019; Published: 11 June 2019

Abstract: This study addresses the life cycle costs (LCC) of energy renovation, and the demolition and construction of a new building. A comparison is made between LCC optimal energy renovations of four different building types with thermal performance, representing Swedish constructions from the 1940s, 1950s, 1960s, and 1970s, as well as the demolition of the building and construction of a new building that complies with the Swedish building code. A Swedish multi-family building from the 1960s is used as a reference building. LCC optimal energy renovations are identified with energy saving targets ranging between 10% and 70%, in addition to the lowest possible life cycle cost. The analyses show that an ambitious energy renovation is not cost-optimal in any of the studied buildings, if achieving the lowest LCC is the objective function. The cost of the demolition and construction of a new building is higher compared to energy renovation to the same energy performance. The higher rent in new buildings does not compensate for the higher cost of new construction. A more ambitious renovation is required in buildings that have a shape factor with a high internal volume to heated floor area ratio.

Keywords: renovation; energy renovation; demolition; new construction; energy use; energy performance; life cycle cost; optimization; OPERA-MILP; multi-family buildings

1. Introduction

More than one quarter of the energy use in the European Union takes place in residential buildings [1]. In cold climates, more than 60% of the total energy demand in residential buildings is needed for space heating [2]. Of the existing European buildings, 75% are considered energy inefficient compared to modern energy performance requirements [3]. By implementing energy efficiency measures (EEMs), the energy performance of buildings can be significantly improved.

Around 35% of the European building stock is more than 50 years old, and many buildings are in need of renovation [3]. Building renovations that include EEMs are sometimes referred to as energy renovations. The Energy Performance of Buildings Directive [4] recognized that there is an opportunity to reduce the cost of implementing EEMs when buildings are in need of renovation. Several studies have shown significant reductions in space heating demand by implementing EEMs during the renovation of buildings [5–7]. Renovation can also increase the value of the building [8], increase pride [9], and improve the indoor environment [10–12], which are all important additional benefits from a renovation.

Common approaches for reducing energy use in existing building include thermal improvement of the building envelope by adding insulation [10,12–15]. The potential for a reduction in energy

use from insulation is revealed to be enormous. A significant reduction in heat demand has also been achieved by installing a balanced mechanical ventilation system with heat recovery as part of buildings renovation [12,13,16]. Several studies have shown that the implementation of EEMs in energy renovation of buildings have the potential to reduce the energy demand to a low energy building, passive house, or nearly-zero energy building standard [6,9,17,18].

The importance of the cost-effectiveness of energy renovation is highlighted in the Energy Performance of Buildings Directive, which also states that a cost-optimal level should be sought, where the cost of investing in EEMs should be balanced against the total costs during the life cycle of the building [4]. A life cycle cost (LCC) approach is common in a building context, because of the long life cycle of buildings. The LCC is the present value of the current and future costs of the construction, installation, maintenance, and operation of a building during its life cycle [19]. Several studies have used an LCC perspective when studying the cost-effectiveness of implementing EEMs in building renovation [20–23]. The cost-effectiveness of EEMs will vary between building types, thermal performance before implementing EEMs, and the costs of EEMs and supplied energy. As the cost-effectiveness is dependent on the building and context, several studies have used optimization approaches to find the cost-optimal level of improved energy efficiency as part of building renovations [20,21,24–28]. For example, Niemelä et al. [25] found that it was not cost-optimal to implement EEMs in Finish multifamily buildings from the 1960 that had a primary energy use of 165 kWh/m^2, before implementing any EEMs. However, Kuusk et al. [29] found that façade insulation significantly reduced the global cost in the Estonian multi-family building stock with a heat demand of up to 280 kWh/m^2. Other studies have also identified improvement of the building envelope as being cost-effective in buildings with a poor thermal performance [20,21].

Instead of implementing EEMs in existing buildings, an alternative approach to reducing energy use in the building stock would be to demolish old buildings with a poor energy performance, and construct new modern buildings with a better energy performance. Although there are many studies addressing renovation and the demolition and construction of a new building from a life cycle analysis perspective or based on environmental impacts [30–35], there are few studies addressing the life cycle costs of renovation and the demolition and construction of a new building, especially when considering buildings that are not damaged. Morelli et al. [36] studied a Danish apartment building constructed between the years 1850–1930, and found that renovation was more cost-effective than the demolition and construction of a new building. Previous studies of the choice between the rehabilitation of damaged buildings and demolition and new construction [37], and studies of buildings in need of structural reinforcement as part of the renovation [35] have shown that the demolition and the construction of a new building should be considered. Alba-Rodríguez et al. studied a building in an urgent condition after a construction failure, and concluded that the cost of rehabilitating the building was 21% lower than demolition and new construction [37]. Ferreria et al. [35] found, by comparing the costs for the renovation of a building and new construction in the same area, that it was more economical to construct new buildings than to improve the seismic strength of the building as part of a structural renovation. The reasons for demolishing a building could be other than those related to costs, such as comfort of living or indoor environment [36]. Sadick and Issa [38] showed that there was a statistically significant difference between the perceived indoor environmental quality in new or renovated school buildings compared to non-renovated buildings. They found no statistical difference between the new and renovated school buildings. Bullen and Love [39,40] found other drivers that can be important in the choice between renovation and demolition and reconstruction. If a building is perceived as being no longer viable for its intended use, demolition is often considered instead of renovation or restoration. For rental buildings, another factor in the choice between renovation and the demolition and construction of a new building is the rent. When buildings are renovated in a Swedish context, the rent is increased in accordance with the improvement in living standards [41]. The rent after a major renovation is usually around 70%–80% of the rent for newly constructed buildings [42]. Although this could be a driver for demolition and new construction, Power [32] argues that the

demolition and construction of a new building instead of renovation can disadvantage economically weak families. Buildings with formally protected cultural heritage value have limitations in the possibilities of changing the aesthetics of the building, thus making both extensive energy renovation measures and demolition unsuitable [20,21,26].

The aim of this study is to compare and analyze the LCC of energy renovation of a multi-family building with the demolition and construction of a new building. The analysis is based on four building types with different thermal performances, and an optimization approach is used to identify the lowest LCC based on proposing different combinations of EEMs for reducing space heating demand so as to achieve different energy saving targets in the studied buildings. The LCC and energy use after energy renovation are compared to the demolition of the building and the construction of a new building that fulfils the design requirements in the Swedish building code.

2. Renovation and Building Costs in a Swedish Context

2.1. Renovation

An analysis of five different Swedish renovation projects with a focus on energy showed that there were significant differences between the costs for EEMs in the different projects [43]. The reduction in energy use varied between 45% and 70%, and all of the renovations included thermal improvement of the building envelope and installation of a heat recovery unit in the ventilation system (see Table 1). Other EEMs were replacement of the existing windows with windows with a better thermal performance rating, improvement of airtightness, individual metering and charging for heat and domestic hot water, adjustment to the heating system, control systems, and solar collector panels. One of the renovations (Brogården) involved extensive demolition, and only the load bearing structure and roof were kept [44]. The renovations were performed between 2000 and 2011, and the costs for renovation that are presented in Table 1 have been adjusted for the increase in building construction up until 2017, based on the figures from Statistics Sweden [45].

Table 1. Summary of energy renovation performed in Sweden.

Con-struction Year	Project Name	Extensive Demo-lition	Insu-lation of Building Envelope	New Windows	Heat Reco-very	Improved Air-Tightness	Indivi-dual Metering and CHarging	Control System	Bal-ancing Heating System	Solar COLlec-tors	Energy Use[1] (kWh/m^2)		Energy Renovation Cost [2] SEK[3]/m^2	Total Renovation Costs (SEK/m^2)	Ref
											Before	After			
1969–1972	Gårdssten		X		X	X	X	X		X	263	145	2736	17,055	[43]
1971–1973	Brogården	X	X	X	X	X	X				177	58	7441	24,714	[43,44,46]
1971	Katjas gata		X		X	X	X				176	52	3986	19,266	[43,47]
1974	Nystad 7		X	X	X				X		164	78	1751	16,167	[43]
1974	Trond-heim 4		X	X	X				X		214	94	2290	19,670	[43]

[1] Energy use per heated area (above 10 °C); [2] Renovation cost per apartment or other rentable area. Costs are calculated at the current cost, based on an increase in construction from the renovation year to 2017, reported by Statistics Sweden [45]; [3] Exchange rate 1 Euro = 10.6 SEK.

2.2. New Construction

The cost of newly constructed buildings has increased drastically in Sweden, and between 2000 and 2017, the cost of new construction increased by 107% in central Sweden, and by 138% in Stockholm (the capital of Sweden) [45], adjusted for inflation. In 2017, the total cost of a newly constructed building was 36.7 kSEK per square meter of apartment area in central Sweden, and 62.1 kSEK/m^2 in Stockholm (exchange rate: 1 Euro = 10.6 SEK).

The Swedish National Board of Housing, Building, and Planning studied the cost of a newly constructed building in Linköping, Sweden. The total cost was 17.2 kSEK/m^2 when the building was finalized in 2005, after 18 months of construction [48]. Adjusted for the increase in costs for new construction and the cost of land in central Sweden between 2004 and 2017, the cost would be 35.7 kSEK/m^2 in total, and 32 kSEK/m^2 excluding the cost of land. The division of cost is shown in Figure 1. Around 66% of the total cost relates to the building construction contract. The cost of the building body and interior is 15.0 kSEK/m^2. In two reference buildings included in a Swedish database of construction costs [49], the construction of the building skeleton structure represented 29% and 36% of the total cost of the building body and interior.

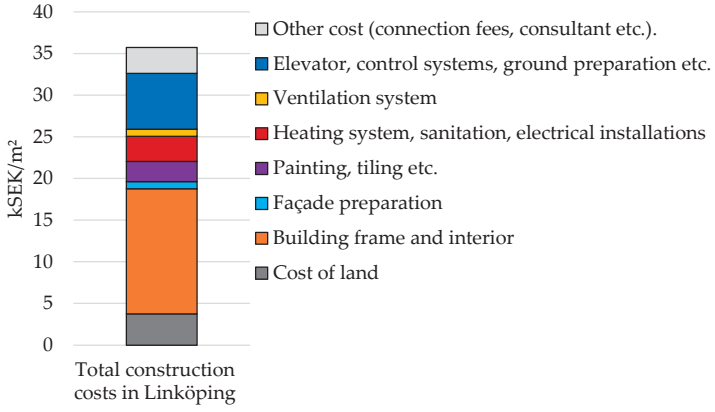

Figure 1. Building costs for newly constructed multi-family buildings in Linköping, Sweden, based on findings from [48] and corrected to current cost based on increase in construction costs in central Sweden [45].

3. Case Description

The analysis is based on the geometry of an existing 1960s building located in central Linköping, Sweden. The building underwent renovation in 2014, and the effects on the building from the renovation have been previously been studied with regard to energy demand and indoor environment, using an empirically validated whole building energy simulation model [16,50]. To address the choice between energy renovation and the demolition and construction of a new building with regard to the differences in thermal performance, three additional construction types have been included in the analysis. The buildings have a thermal performance representing common original Swedish constructions from the 1940s, 1950s, and 1970s. A comparison is made with the demolition and the construction of a new building with the same external geometry as the reference building. The new building meets the minimum requirements for new Swedish buildings in the building code. All of the buildings are assumed to be heated with district heating as the energy carrier, which is common in larger Swedish municipalities.

3.1. Reference Building

The reference building was constructed in 1961, and originally had a lightweight concrete construction and was ventilated with an exhaust air ventilation system. The building has five stories, with a ceiling height of 2.5 m. The top four floors have three apartments each, and the ground floor compromises a storage area and office premises. The façade and a building cross section can be seen in Figure 2.

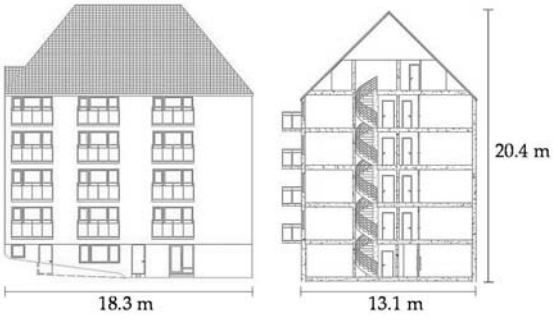

Figure 2. Façade facing south (left) and cross section of building (right).

The geometry, construction, and U-values of the building are seen in Table 2.

Table 2. Description of the reference building.

Building Segment	Area (m^2)	Original Construction	*U*-Value [1] ($W/m^2 \cdot °C$)
External walls	569.9	0.01 m plasterboard, 0.25 m lightweight concrete, cladding	0.43
Windows	112.8 [2]	three-pane	1.9 [3]
Floor	216.5	0.2 m concrete, 0.1 m insulation Ground [4]	0.2
Attic	194.5	0.05 m concrete, 0.12 m mineral wool, 0.2 m concrete	0.25 [5]

[1] U-values calculated in accordance with international standard ISO 6946—building components and building elements—thermal resistance and thermal transmittance [51]; [2] 22.5 m^2 per floor; [3] Glazing U-value; [4] Ground properties and floor U-value calculated in accordance with ISO 13370—thermal performance of buildings—heat transfer via the ground (calculation methods [52]); [5] Including the insulating capacity of the external roof (0.15 m concrete, 0.04 m cork, roofing tile).

3.2. Typical Building Types

Three building constructions that were common in Sweden in the 1940s, 1950s, and 1970s are applied to the external geometry of the reference building [53] to be able to compare the costs of the energy renovation of the buildings with different thermal performance and construction. The 1970s building is assumed to have a similar thermal performance as the reference building, but has an insulated cavity wall construction. The two older buildings are assumed to have brick façades and natural ventilation. It is common for older buildings in Sweden to have high ceilings. The 1940s and 1950s buildings are therefore assumed to have one less floor. The total internal height of the building means that each floor has a height of 3.1 m. The studied building types are presented in Table 3, and the U-values in Table 4. All of the buildings are assumed to have a ground slab with a U-value ranging between 0.2 and 0.3 $W/m^2 \cdot °C$, which cannot be insulated. The window area per floor is assumed to be the same for all of the buildings.

Table 3. Construction and ventilation systems of the analyzed building types.

Building Type	Wall Construction (thickness)	Attic Construction	Window Type	Number of Floors	Number of Apartments	Ventilation System	Space Heating Demand (kWh/m^2·year)
1940s	1$\frac{1}{2}$ brick wall (440 mm)	Wood beams and sawdust insulation	two-pane	4	9	Natural	188.0
1950s	Insulated brick wall (350 mm)	Wood beams and sawdust insulation	two-pane	4	9	Natural	157.0
1960s	Lightweight concrete (260 mm)	Insulated concrete joist	three-pane	5	12	Exhaust	113.5
1970s	Insulated concrete cavity wall with external brick (400 mm)	Insulated concrete joist	three-pane	5	12	Exhaust	116.2

Table 4. Assumed U-values for all of the buildings included in the analysis.

Building Segment	1940	1950	1960	1970
Wall U-value (W/m^2·°C)	1.03	0.77	0.45	0.42
Attic U-value (W/m^2·°C)	0.5	0.5	0.25	0.25
Window U-value (W/m^2·°C)	2.7	2.7	1.9	1.9
Floor U-value (W/m^2·°C)	0.3	0.3	0.2	0.2
Average U-value (W/m^2·°C)	0.94	0.79	0.51	0.50

The buildings are all assumed to have the same external geometry. This means that the internal surface areas will differ, depending on the wall thickness. With thicker walls, the rentable area and the heated area will be smaller. The heated area and rentable apartment area are shown in Table 5.

Table 5. Heated area and rentable apartment are in the studied building types.

Type of Area	1940s	1950s	1960s	1970s
Heated area (m^2)	804.7	834.6	1072.5	1032.9
Rentable apartment area (m^2)	683.1	698.9	918.4	886.2

The airtightness of the reference building was measured prior to and after the performed renovation using the blower door technique [50], and the results were used for the reference building and the building from 1970 prior to renovation. Air tightness measurement was also performed in a building constructed in 1950, and serves as the infiltration prior to renovation in the 1940s and 1950s buildings. The building is located in the same area as the reference building, had old two-pane windows, and a lightweight concrete structure. In addition to the infiltration, the 1940s and 1950s buildings are assumed to have an air exchange corresponding to the lowest recommended ventilation flow of 0.35 l/s·m^2. The lowest minimal required exhaust air flow has been used for the 1960s and 1970s buildings. As the building has small apartments, the exhaust air flow is relatively high in relation to the floor area. All of the buildings have an airing corresponding to 2 l/s·apartment [54]. A summary of the building air tightness and airflows is seen in Table 6.

Table 6. Air tightness, ventilation flows, and airing of the studied buildings.

Air Exchange	1940s	1950s	1960s	1970s
Specific air leakage at ± 50 Pascal [1] (l/s·m^2)	0.46	0.46	0.35	0.35
Exhaust air flow [2] (l/s·m^2)	-	-	0.58	0.60
Natural ventilation flow[1] (l/s·m^2)	0.35	0.35	-	-
Airing (l/s·apartment)	2	2	2	2

[1] per external area of building envelope; [2] per heated floor area.

As the buildings have different assumed constructions, the renovation measures will vary slightly. The renovation measures are divided into two categories, namely: inevitable renovation measures, and EEMs that are performed with the purpose of reducing the heat demand and operation costs of the building. The study includes the minimal maintenance of the building body as an inevitable renovation cost. In addition to this, the thermal performance of the building envelope can be improved by insulation and by changing to windows with lower U-values. A summary of the renovation measures and EEMs is shown in Table 7.

Table 7. Inevitable renovation measures and energy efficiency measures (EEMs) of the different building segments.

Building Segment	Inevitable Renovation Measures	Energy Efficiency Measures
Façade	Façade cleaning and repainting of lightweight concrete structure, none for brick structure	Insulation with mineral wool, new façade plaster
Attic and roof	Replacement of roof tiles and repair of roof foundation	Insulation of attic with mineral wool
Windows	New wood framed windows with original U-value	New aluminum framed windows with U-value 1.1 or 0.8 W/m^2·°C
Ventilation system	None	Supply and exhaust air ventilation system with heat recovery
Heating system	Replacement of district heating exchanger	-

4. Methodological Approach

The study is divided into three parts, as follows: (1) Identifying LCC optimal EMMs with energy saving targets ranging between 10%–70% in the four building types using the optimization tool OPtimal Energy Retrofit Advisory-Multiple integer Linear programming (OPERA-MILP); (2) calculation of the LCC of the demolition of the four building types and the construction of a new building; and (3) the identification of the LCC optimal EEMs for achieving the same energy performance as the new building used in part two, and a comparison between the costs for energy renovation and the demolition and construction of a new building. The cost-optimal EEMs are identified using OPERA-MILP, as in part one. The process can be seen in Figure 3.

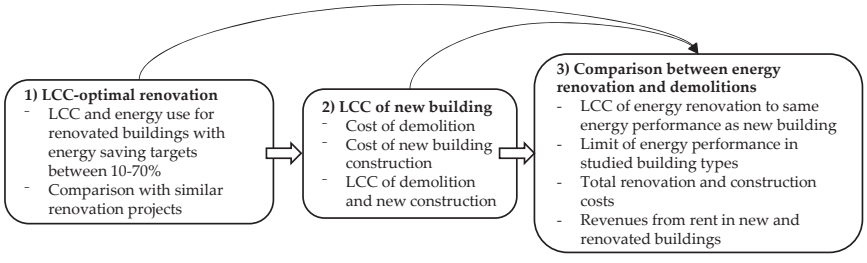

Figure 3. Overview of methodological approach and results from the three parts. LCC—life cycle cost.

The heating demand of the building is calculated using a quasi-steady state heat balance calculation. The district heating tariff at the building's location in Linköping, Sweden, is used to calculate heating costs.

The analysis is primarily focused on the cost of the building skeleton structure and the parts of the building that have an influence on energy use. An analysis is performed using additional costs from Swedish examples to contrast to the higher revenues from the rent in newly constructed buildings.

4.1. LCC Optimal Energy Renvoation

The long-life cycle of a building makes an LCC approach suitable for comparing the costs of different renovation measures in a building. By adding present and discounted future costs, different

investment alternatives can be compared [19]. In a building context, the LCC consists of costs related to the construction, technical installations, operation, and maintenance. When the investment in an EEM is lower than the cost saving for operation, the measure is profitable. The study and comparison between energy renovation and the construction of a new building focuses on the building skeleton structure, windows, installation of a heating system and a ventilation system, and heating of the building. The LCC does not include the costs for interior or other installations.

The optimization tool OPtimal Energy Retrofit Advisory (OPERA) was originally designed in the 1980s to identify which EEMs lead to the lowest LCC (LLCC) during a selected life cycle [55]. Increased focus on the cost-effective reduction in energy use of buildings leads to the development of a constraint on maximal energy use using multiple integer linear programming (MILP), so that the most suitable EEMs can be identified for a predefined target. The tool has been used in several studies of multi-family buildings and historic buildings [20,21,26,56–58]. The validation of the heat demand calculated in OPERA-MILP has been performed using a dynamic whole building simulation [21,59] in the simulation tool IDA Indoor Climate and Energy (IDA ICE). IDA ICE has been validated in accordance with Standard 140-2004 from the American Society of Heating, Refrigerating and Air-Conditioning Engineers [60], European CEN Standard EN 15255-2007 and 15265-2007 [61], and CEN Standard EN 13791 [62]. A test cell validation was performed with measurements in IEA's Solar Heating and Cooling Programme Task 34, with good agreement between the prediction and measurements [63].

As OPERA-MILP is designed for finding the lowest LCC, it is possible that the actual energy saving from the suggested EEMs is higher than the target. If a higher energy saving than the target is optimal, the LCC for the actual target is calculated by removing the measures with the highest increase in LCC per reduced kWh. Note that these EEMs are not cost-optimal, and are calculated to illustrate how different energy saving targets for an energy renovation can affect the selected measures and LCC.

OPERA-MILP calculates the LCC of a renovated building ($LCC_{renovation}$) using the discounted sum of maintenance costs ($LCC_{maintenance}$), the cost of installing a heating system (LCC_{HS}), the cost of investments in EEMs (LCC_{EEM}) that are implemented in the building to reduce heat demand, and the operation cost of heating the building during the selected life cycle ($LCC_{heating}$). Any residual value (RV) is subtracted from the LCC if the investment has a value at the end of the selected life cycle.

$$LCC_{renovation} = LCC_{maintenance} + LCC_{HS} + LCC_{EEM} + LCC_{heating} - RV \quad (1)$$

The present values for non-recurring investments (PV_N) in building maintenance, the heating system, and EEMs are calculated in Equation (2).

$$PV_N = N \times (1 + r)^{-a} \quad (2)$$

where N is the non-recurring cost, r is the real interest rate, and a is the number of years until the cost occurs. A new investment is made if the technical life cycle is shorter than the period for which the LCC is calculated.

For the operation cost that recurs annually, in this case heating, the present value (PV_R) is calculated in Equation (3).

$$PV_R = R \times \frac{1 - (1 + r)^{-b}}{r} \quad (3)$$

where R is the annually recurring cost of space heating, and b is the number of years that R occurs during the life cycle. The heating demand for the building is calculated with a quasi-steady state heat balance calculation with twelve time steps. The LCC is calculated during a lifetime of 40 years, and a real interest rate of 5% is used.

Maintenance costs are inevitable costs, and occur regardless of whether or not EEMs are implemented in the building. The EEMs of the building envelope consist of thermal insulation. The cost of the building envelope ($C_{envelope}$ (SEK/m^2)), is calculated in Equation (4).

$$C_{envelope} = CE_1 + (CE_2 + CE_3 \times t) \quad (4)$$

where CE_1 is the inevitable maintenance cost (SEK/m^2), CE_2 is costs related to insulating the envelope independent of the insulation thickness (SEK/m^2), CE_3 is costs related to insulating the envelope dependent on and linear to the insulation thickness (SEK/m^2·m), and t is the thickness of the insulation (m). The cost function for the maintenance and insulation of the building envelope is visualized in Figure 4.

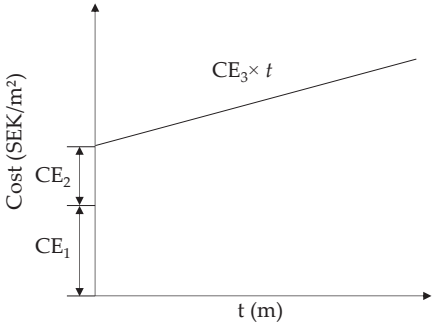

Figure 4. Cost function for insulation of the building envelope.

The cost of the window replacement is based on the inevitable costs for replacing windows with new windows (CE_1) with the same U-value as the original windows. OPERA-MILP also includes different window types with lower U-values, which have different additional costs (CE_2).

The investment cost of the heating system ($C_{heating\ system}$ (SEK)) is dependent on the maximum installed power of the system, and is calculated in Equation (5).

$$C_{heating\ system} = HS_1 + HS_2 \times P + HS_3 \times P \quad (5)$$

where HS_1 is the cost of installing a new heating system regardless of maximum power (SEK), HS_2 is the cost of installing a new heating system and is linear to the maximum power of the heating system (SEK/kW), P is the maximum power of the heating system (kW), and HS_3 is the costs related to the systems needed in connection with the heating system, such as pipes, a chimney, or a bore hole (SEK). The heating systems (HS_1 and HS_2) and related systems (HS_3) can have different technical lifetimes.

Heat losses can be reduced by increasing the airtightness of the building by weather-stripping. The cost of each unit that is weather-stripped, an interval for how often the measure has to be performed, and the changes in resulting air exchange rate have to be defined. The function can also be used for heat recovery ventilation measures by giving the cost of a new heat recovery ventilation system (HRX system) and the reduction in air exchange rate that corresponds to the heat exchanger efficiency.

Cost of Renovation Measures

Renovation costs will differ depending on the original building construction and geometry, as well as the geographic location. The Swedish database Wikells Sektionsfakta was used to summarize the cost of all of the renovation measures, technical installations, and demolition included in the study. Wikells Byggberäkningar AB is a Swedish company that offers a database with costs for the construction and labor for building parts and technical installations in buildings, and is a common

database for cost calculations for new buildings and renovations in Sweden [49]. The costs for wall and attic insulation (CE_2 and CE_3) have been linearized from insulation with a thickness ranging between 50 and 200 mm. The costs for installing windows (CE_1) are the same regardless of thermal, but the lifetime is shorter for wood frame windows. A window with a better thermal performance has a higher CE_2 cost. The cost of a new district heating exchanger is linearized based on district heating exchangers with a thermal power ranging between 40 and 100 kW. The costs are summarized in Table 8. To be able to compare this with a newly constructed building, the roof tiles are exchanged and the roof foundation is renovated. The cost of this is 285 kSEK, which is added to the total renovation costs for all of the buildings.

Table 8. Costs for different renovation measures and heating systems.

Insulation Measures	**CE_1 (SEK/m^2)**	**CE_2 (SEK/m^2)**	**CE_3 (SEK/m·m^2)**	**Thermal Conductivity (W/m·°C)**	**Technical Lifetime**
Attic (max 400 mm)	0	248	544	0.037	40 years
Lightweight concrete façade (max 400 mm)	409	1256	1283	0.037	40 years
Brick façade (max 400 mm)	0	1665	1283	0.037	40 years
Window Measures	**CE_1 (SEK/m^2)**	**CE_2 (SEK/m^2)**	**CE_3**	**Window *U*-Value (W/m^2·°C)**	**Technical Lifetime**
Original windows [1]	7895	0	-	1.9	30 years
Window type 1 [2]	7895	441	-	1.1	40 years
Window type 2 [2]	7895	1367	-	0.8	40 years
Heating System	**HS_1 (SEK)**	**HS_2 (SEK/kW)**	**HS_3 (SEK/kW)**	-	**Technical Lifetime**
District heating exchanger	33,336	53	535	-	20 years [3]

[1] Wood-framed three pane windows (non-gas filled), *g*-value 0.68; [2] Aluminum-framed windows (gas filled), *g*-value 0.43; [3] Technical lifetime of pipes and ventilation ducts is 40 years.

The HRX system that was installed in the reference building during the actual renovation was used in the optimization. The heat recovery efficiency was measured at 57.4% during one month of operation [50]. The cost is slightly higher per apartment area for the naturally ventilated buildings that require exhaust air ducts. The cost of new shafts is assumed to be the same in all buildings. The infiltration rate is based on the blower door measurements performed in the reference building after it was renovated and fitted with an HRX system, and represents 0.49 l/s per external surface area [50]. The total cost and the corresponding air exchange rate with an HRX system are shown in Table 9. Note that this is not the actual air exchange rate, only the corresponding losses due to infiltration and ventilation after heat recovery.

Table 9. Air exchange rate before and after installation of an heat recovery ventilation (HRX) system, and the cost of the new ventailtion systems.

HRX Properties	**1940s**	**1950s**	**1960s**	**1970s**
Corresponding air exchange rate with HRX [1]	0.47 h^{-1}	0.45 h^{-1}	0.51 h^{-1}	0.52 h^{-1}
Cost HRX	1.3 MSEK	1.3 MSEK	1.32 MSEK	1.32 MSEK

[1] The reduction in air exchange rate corresponds to the reduction in heat losses from ventilation due to the heat recovery in the HRX system.

4.2. LCC of Newly Constructed Building

The LCC of a newly constructed building is calculated in a similar way as the LCC for the renovation cases. The LCC is the sum of the total cost of demolition ($C_{demolition}$ (SEK)), the discounted sum of the construction costs ($LCC_{construction}$ (SEK)), the installation costs for the heating system

(LCC_{HS} (SEK)), and the operation cost for heating the building during the entire life cycle ($LCC_{heating}$ (SEK)), minus any residual value, as in Equation (6).

$$LCC_{new\ constriction} = C_{demolition} + LCC_{construction} + LCC_{HS} + LCC_{heating} - RV \quad (6)$$

The LCC for construction, heating system and heating in Equation (6) is calculated in accordance with Equations (2) and (3).

Demolition and Construction Costs

The analysis includes the cost from Wikells Sektionsfakta for demolishing the old building prior to the construction of a new building [49]. As the construction varies between the different building types, they will have different demolition costs. Building constructions with a high thickness or a large mass have higher demolition costs than thin and light constructions, and hence the cavity wall from the 1970s building has a significantly higher cost per square meter of wall area. The newer buildings with more windows also have slightly higher demolition costs related to the window demolition. The demolition costs are summarized in Table 10.

Table 10. Demolition costs for building parts in the 1940s, 1950s, 1960s, and 1970s buildings from Wikells Sektionsfakta [49].

Building Segment	1940s	1950s	1960s	1970s
Wall demolition (SEK/m^2)	1074	870	603	2747
Demolition of joist and internal floors (SEK/m^2)	1140	1140	1140	1140
Roof demolition (SEK/m^2)	878	878	878	878
Window and door demolition (kSEK)	28.5	28.5	35.4	35.4

The Swedish building code is established by the National Board of Housing, Building, and Planning, and states that a newly constructed multi-family building in central Sweden should have a maximal energy demand of 85 kWh of primary energy per square meter of heated area and year, including domestic hot water and facility electricity. Electricity has a primary energy factor of 1.6, and all other energy carriers have a primary energy factor of 1.0 [64]. As a basis for the building constructed in accordance with the building code, a building model from the Swedish Association of Public Housing Companies was used [65]. The building model can be built up to eight floors high, with four to eight apartments per floor, and some contractors [66] offer a building model with prefabricated elements for faster construction. The building construction, U-values, and energy performance can be seen in Table 11.

4.3. Calculation of Space Heating Demand and Heating Costs

The energy demand of the building and the cost of annual space heating are calculated with a quasi-steady heat balance calculation, including twelve time steps. The heat balance summarizes the heat losses from the building envelope, ventilation, and infiltration (see Equation (7)).

$$E_{heating} = (Q_{transmission} + Q_{ventilation} + Q_{infiltration}) \times DH - E_{IHG} - E_{solar} \quad (7)$$

where $Q_{transmission}$ is the envelope transmission losses (W/°C), $Q_{ventilation}$ is the losses from ventilation (W/°C), $Q_{infiltration}$ is the losses from infiltration (W/°C), DH are the degree hours (°Ch), E_{IHG} is the internal heat gain from appliances and occupants (Wh), and E_{solar} is the useful solar radiation (Wh). The monthly mean temperature, the indoor temperature, and the number of hours during the same month are used for calculating the degree hours. The accuracy of the quasi-steady heat balance included in OPERA-MILP have been tested against the dynamic simulation of building energy use with good agreement [21].

Table 11. Construction, U-values, and energy performance of the new building designed in accordance with the Swedish building code.

Building Segment	Construction	U-value	Area	Cost per m^2 [49]
Walls	Prefabricated sandwich elements (thickness 270 mm)	0.29 W/m^2·°C	591.6 m^2	2310 SEK
Attic	160 mm concrete 200 mm mineral wool 80 mm concreteRoof	0.16 W/m^2·°C	194.0 m^2	1830 SEK
Floor	Insulated ground slab	0.2 W/m^2·°C	216.0 m^2	1096 SEK
Windows	Three-pane, low emissivity	0.8 W/m^2·°C	112.8 m^2	9262 SEK
Internal floor	Reinforced concrete joists (thickness 300 mm)	-	864 m^2	1527 SEK
Roof	Concrete tiles of wood frame foundation	-	344.5 m	770 SEK
Other information				
Heated area		1069.5 m^2		
Rentable area		916.0 m^2		
Number of floors		5		
Annual heat demand		49.6 MWh		
Space heat demand		46.4 kWh/m^2·year		
Energy demand [1]		84.9 kWh/m^2·year		
Maximum power [2]		31.1 kW		
Heat supply system		District heating		

[1] Including standard domestic hot water (25 kwh/m^2·year when included in rent) based on findings from a Swedish setting [54], and facility electricity use from the renovated reference building (1749 kWh for lighting and other facility use, 7288 kWh for HRX ventilation); [2] At the winter outdoor design temperature of −17.6°C.

District Heating Tariffs

Many of the district heating tariffs in Sweden are divided up into a power demand fee and a cost related to the amount of used energy. In most cases, the cost varies during the year, and is higher during cold periods with a high heating demand. The district heating tariff that is used in the case study can be seen Table 12.

Table 12. Cost of district heating in Linköping, Sweden.

Maximal Power	Demand Fee (SEK/year)	Demand Fee (SEK/kW [1])	Heating Price Jan–Feb, Dec (SEK/kWh)	Heating Price Mar–Apr, Oct–Nov (SEK/kWh)	Heating Price May–Sep (SEK/kWh)
5–50 kW [1]	1200	931	0.45	0.32	0.08
51–250 kW [1]	4700	856	0.45	0.32	0.08

[1.] For power demand when the outdoor temperature is −17.6°C.

4.4. Comparison between Renvoation and Demolition and Construction of New Building

The LCC of energy renovation varies with different energy saving targets. OPERA-MILP is thus used to identify the EEMs with the lowest LCC that achieves the same energy performance in the four studied building types as the new building. As the heated area varies, the buildings have slightly different electricity demands for facility purposes and mechanical ventilation, which affects the maximal allowed space heating demands. The primary energy factor of 1.6 is used for electricity and 1 for district heating, in accordance with the Swedish building code [64].

To be able to compare energy renovation and the demolition and construction of a new building from a broader perspective, an analysis is performed where the additional costs related to the renovation and new construction from Swedish examples are included. In the three renovation projects most similar to the energy renovation included in this analysis (Katjas gata, Trondheim 2, and Nystad 7; see Table 1), the costs for renovation that do not affect energy use ranged between 14.4 to 17.4 SEK/m^2 apartment area. The highest costs have been included in the analysis. The costs of the construction of a multi-family building, presented in Figure 1, are used for the additional costs related to new

constructions. The rent in the renovated reference building and the rents from the newly constructed building in the same area are used for calculating the present value of the revenues from the rents during the life cycle, in accordance with Equation (3). The renovation that was performed in the reference building took six months to perform, which means six months without rental revenues. The new construction is assumed to take 18 months [48]. A summary of the costs, rent, and time requirement are in Table 13.

Table 13. Costs per apartment area for other renovations, excluding EEMs, additional costs for new construction, rent, and time requirement for performing renovation or demolition and construction.

Renovation or Construction Characteristics	Renovation (kSEK/m^2)	Demolition and New Construction (kSEK/m^2)	Ref
Renovation and maintenance costs	17.4	-	[43]
Technical installations	-	9.8	[48]
Interior installations	-	13.4	[48]
Other costs	-	2.6	[48]
Rent	0.99	1.23	-
Time requirement	6 months	18 months	[48]

5. Results and Analysis

5.1. Life Cycle Costs of Renovation

The combinations of EEMs that are found to be cost-optimal vary between the buildings. In the buildings with a building envelope with a poor thermal performance (1940s and 1950s buildings), it is cost-effective to add thermal insulation to the attic to achieve the LLCC. In the buildings with a relatively good thermal performance, such as the typical buildings from the 1960s and the 1970s, it is not cost-effective to implement EEMs to achieve the LLCC.

The LLCC in the 1940s building is achieved by insulating the attic with 0.22 m, and a reduction in heat demand of 13.3% is achieved (see Table 14). With an energy saving target above 20%, the most cost-effective approach is to insulate the attic with 0.24 m and the façade with 0.16 m. Other energy saving levels are not optimal from a cost perspective. Ventilation measures are not cost-optimal because of the low air exchange rate prior to renovation, and should only be applied when an energy saving target of 70% is set.

The EEMs that are cost-effective in the 1950s building are similar to those in the 1940s building (see Table 15). The LLCC measures mean a reduction in heat demand of 15.9%. As with the 1940s building, an energy saving target between 20% and 50% gives a more ambitious renovation as the most cost-optimal solution, with a reduction in space heating demand of 53.9%, by adding 0.16 m insulation to the façade and 0.24 m to the attic.

In the 1960s building with better energy performance prior to renovation than the two older buildings, no EEMs are found to be cost-optimal to implement in order to reduce the heat demand (see Table 16). The windows are changed to modern three-pane windows that have a longer lifetime than the original window type. When the energy saving target is above 40%, the installation of an HRX system is a cost-effective EEM. It should be noted that the actual reduction in heat demand is higher than the target, as the reduction is not linear in the same way as insulation. A reduction in the heat demand of 40% cannot be achieved by insulation measures and window replacement alone. In contrast to the two older buildings without mechanical ventilation, significant heat losses occur from ventilation, and the reduction in heat losses is greater with an HRX system.

Similar to the 1960s building, an HRX system is a cost-effective measure in the 1970s building, but above an energy saving target of 10% (see Table 17). Reducing the heat demand by 10%, 20%, or 30% from insulation measures involves a higher cost than the optimal level of 44.2%, which includes an HRX system and replacing the windows with modern three-pane windows, but no other thermal improvements of the building envelope. As in the 1960s building, it is not possible to achieve a reduction of 40% without ventilation measures.

Table 14. EEMs at different energy saving targets between 10% and 70% for the 1940s building. LLCC—lowest LCC.

Energy Saving Target	Window *U*-Value (W/m^2·°C)				Additional Insulation (m)		HRX	Energy Use (kWh/m^2·y)	Power Demand (kW)	Reduced Heat Demand	LCC	Optimal
	North	*East*	*South*	*West*	*Façade*	*Attic*						
Original	2.7	2.7	2.7	2.7	-	-	-	188.0	62.0	-	3.08	No
10%	1.1	1.1	1.1	1.1	-	0.02	-	169.3	55.1	10.0%	2.86	No
LLCC	1.1	1.1	1.1	1.1	-	0.24	-	160.5	52.9	14.6%	2.81	Yes
20%	1.1	1.1	1.1	1.1	0.01	-	-	150.5	50.5	20.0%	3.69	No
30%	1.1	1.1	1.1	1.1	0.02	-	-	131.5	45.8	30.0%	3.54	No
40%	1.1	1.1	1.1	1.1	0.05	-	-	112.7	41.0	40.0%	3.40	No
50%	1.1	1.1	1.1	1.1	0.07	0.24	-	93.9	36.2	50.0%	3.32	No
20%–50%	1.1	1.1	1.1	1.1	0.16	0.24	-	76.7	31.7	59.2%	3.24	Yes
60%	1.1	1.1	1.1	1.1	0.18	0.24	-	75.1	31.2	60.1%	3.24	Yes
70%	1.1	0.8	1.1	1.1	0.26	0.36	Yes	56.3	26.1	70.0%	4.45	Yes
Max.	0.8	0.8	0.8	0.8	0.40	0.40	Yes	48.1	23.9	74.7%	4.57	No

Table 15. EEMs at different energy saving targets between 10% and 70% for the 1950s building.

Energy Saving Target	Window *U*-Value (W/m^2·°C)				Additional Insulation (m)		HRX	Energy Use (kWh/m^2·y)	Power Demand (kW)	Reduced Heat Demand	LCC	Optimal
	North	*East*	*South*	*West*	*Façade*	*Attic*						
Original	2.7	2.7	2.7	2.7	-	-	-	157.0	56.1	-	2.87	No
10%	1.1	1.1	1.1	1.1	-	-	-	141.3	49.9	10.0%	2.68	No
LLCC	1.1	1.1	1.1	1.1	-	0.24	-	129.7	46.9	17.4%	2.60	Yes
20%	0,8	1.1	0,8	1.1	-	0.30	-	125.5	45.8	20.0%	2.64	Yes
30%	1.1	1.1	1.1	1.1	0.04	-	-	110.0	41.7	30.0%	3.41	No
40%	1.1	1.1	1.1	1.1	0.04	0.24	-	94.2	37.7	40.0%	3.27	No
50%	1.1	1.1	1.1	1.1	0.11	0.24	-	78.5	33.3	50.0%	3.25	No
20%–50%	1.1	1.1	1.1	1.1	0.16	0.24	-	72.8	31.7	53.7%	3.23	Yes
60%	0.8	1.1	0.8	0.8	0.26	0.32	-	62.8	28.9	60.0%	3.31	Yes
70%	0.8	1.1	0.8	0.8	0.30	0.34	Yes	47.0	24.4	70.0%	4.49	Yes
Max.	0.8	0.8	0.8	0.8	0.40	0.40	Yes	44.0	23.7	72.0%	4.56	No

Table 16. EEMs at different energy saving targets between 10% and 70% for the 1960s building.

Energy Saving Target	Window *U*-Value (W/m^2·°C)				Additional Insulation (m)		HRX	Energy Use (kWh/m^2·y)	Power Demand (kW)	Reduced Heat Demand	LCC	Optimal
	North	*East*	*South*	*West*	*Façade*	*Attic*						
Original	1.9	1.9	1.9	1.9	-	-	-	113.5	57.4	-	3.30	No
LLCC	1.1	1.1	1.1	1.1	-	-	-	109.5	53.6	3.5%	3.13	Yes
10%	0.8	1.1	0.8	0.8	-	0.30	-	102.1	51.0	10.0%	3.21	Yes
20%	1.1	1.1	1.1	1.1	0.12	-	-	90.2	46.9	20.5%	3.75	Yes
30%	1.1	0.8	0.8	0.8	0.22	0.36	-	79.4	43.1	30.0%	3.83	Yes
40%	1.1	1.1	1.1	1.1	-	-	Yes	65.2	38.1	42.5% [1]	3.93	Yes
50%	1.1	1.1	1.1	1.1	0.03	-	Yes	56.7	35.0	50.0%	4.60	No
50%	1.1	1.1	1.1	1.1	0.12	-	Yes	46.7	31.4	58.8%	4.54	Yes
60%	1.1	1.1	1.1	1.1	0.16	-	Yes	44.6	30.6	60.7%	4.54	Yes
70%	0.8	0.8	0.8	0.8	0.26	0.36	Yes	34.0	26.6	70.0%	4.67	Yes
Max.	0.8	0.8	0.8	0.8	0.40	0.40	Yes	31.9	25.8	71.9%	4.75	No

[1] Reduction from HRX is higher than 40%. A reduction of 40% cannot be achieved by insulation measures alone.

Table 17. EEMs at different energy saving targets between 10% and 70% for the 1970s building.

Energy Saving Target	Window *U*-Value (W/m^2·°C)				Additional Insulation (m)		HRX	Energy Use (kWh/m^2·y)	Power Demand (kW)	Reduced Heat Demand	LCC	Cost Optimal
	North	*East*	*South*	*West*	*Façade*	*Attic*						
Original	1.9	1.9	1.9	1.9	-	-	-	116.2	56.4		3.04	No
LLCC	1.1	1.1	1.1	1.1	-	-	-	112.1	52.6	3.5%	2.86	Yes
10%	0.8	1.1	0.8	1.1	-	0.30	-	104.5	50.1	10.0%	2.94	No
20%	1.1	1.1	1.1	1.1	0.14	-	-	93.0	46.2	20.0%	3.75	No
30%	0.8	0.8	0.8	0.8	0.22	0.40	-	81.3	42.4	30.0%	3.86	No
10%–40%	1.1	1.1	1.1	1.1	-	-	Yes	64.8	36.6	44.2% [1]	3.65	Yes
50%	1.1	1.1	1.1	1.1	0.03	-	Yes	58.1	34.3	50.0%	4.57	No
50%	1.1	1.1	1.1	1.1	0.12	-	Yes	47.8	30.7	58.9%	4.52	Yes
60%	1.1	1.1	1.1	1.1	0.16	-	Yes	45.8	30.0	60.6%	4.53	Yes
70%	0.8	0.8	0.8	0.8	0.26	0.40	Yes	34.8	26.0	70.0%	4.66	Yes
Max.	0.8	0.8	0.8	0.8	0.40	0.40	Yes	32.5	25.1	72.1%	4.74	No

[1] Reduction from HRX is higher than 40%. A reduction of 40% cannot be achieved by insulation measures alone.

The increase in LCC between different energy saving targets is far from linear, and also varies between the different building types (see Figure 5).

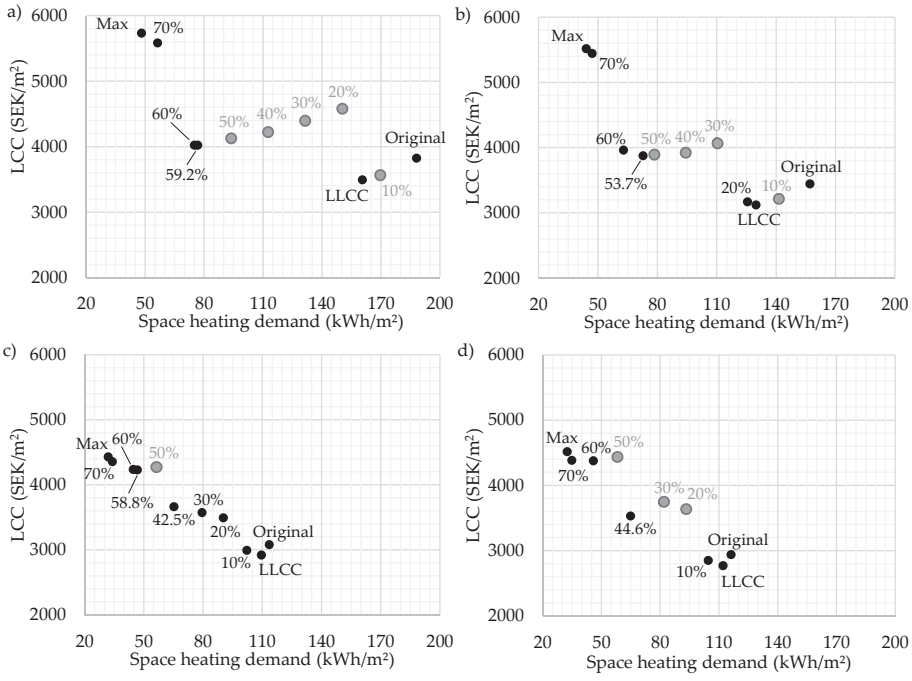

Figure 5. Increase in LCC for different energy saving targets for the buildings from the 1940s (**a**), the 1950s (**b**), the 1960s (**c**), and the 1970s (**d**). Gray indicates that the combination of energy efficiency measures is not optimal. LLCC—lowest LCC.

They gray dots in Figure 5 are the cost of achieving the exact energy saving targets, and are not cost-optimal. Although these will have a smaller investment cost at the time of renovation, they will have a large increase in LCC, as the reduction in heat demand is too small to compensate for the investment. In three of the buildings, the optimal level of renovation is a level that has a much lower heat demand than many of the lower energy saving targets. In fact, in the oldest buildings, the LCC for a reduction in heat demand between 20% and 50% is higher than a combination of EEMs that achieve a reduction of heat demand by 60%. In the 1960s building, a reduction of heat demand between 20% and 30% does yield a lower LCC, but is still relatively close to a reduction in heat demand of 44.9% (HRX installation) in terms of LCC. This highlights the importance of identifying the renovation measures that are suitable in the specific context. Although a general energy saving target might have been set for an energy renovation, a higher reduction might be a more cost-effective approach when considering the life cycle of a building. The type of construction should also be considered as well as its condition. If the façade is in need of maintenance, part of the costs related to adding thermal insulation, such as scaffolding, are already needed, and thus reduce the cost of thermal insulation if it is not implemented as part of a renovation.

Comparison with Other Renovation Projects

In the most ambitious renovations (60% and 70% energy saving targets), investments in EEMs represent more than 50% of the total LCC. The cost of the energy renovation per apartment area for the 1960s and 1970s buildings is seen in Figure 6. The costs for EEMs presented in this study are

similar to those found in Katjas gata, Trondheim 2, and Nystad 7 (presented in Table 1). These three energy renovations also have similar renovation measures to the ones identified for the 1960s and 1970s buildings.

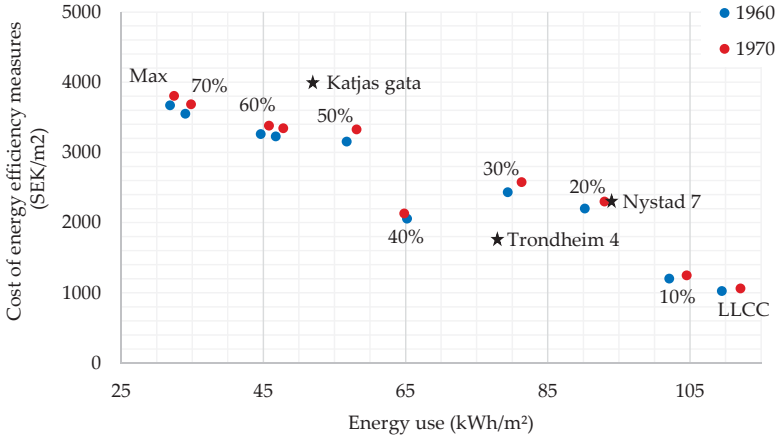

Figure 6. Cost of energy renovation per apartment area at the different energy saving targets compared to three other energy renovated buildings from the 1960s and the 1970s (presented in Table 1).

5.2. Cost of Demolition and the Construction of a New Building

A large proportion of the cost of constructing a new building is related to the demolition of the existing building (see Figure 7). The 1940s, 1950s, and 1960s buildings have external walls with relatively light materials (brick and lightweight concrete), and are thus less expensive to demolish and dispose compared with the concrete frame of the 1970s building. The cost of demolition and disposal is more than twice as high for the 1970s concrete wall compared to the three other wall types included in the analysis (see Table 10). A significant cost is also related to the construction of the internal floors. Together, they represent almost half the cost.

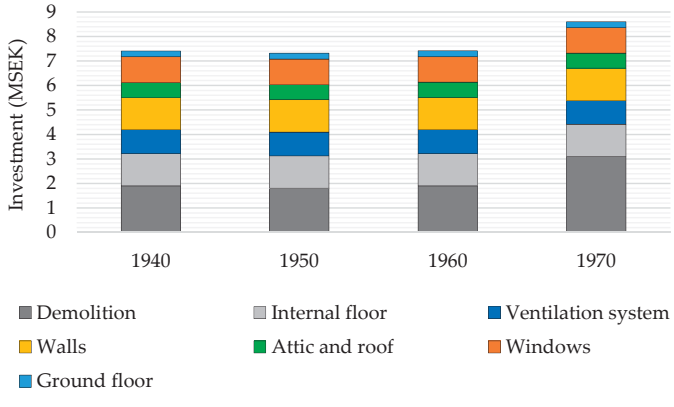

Figure 7. Investment cost of the demolition and construction of a building skeleton structure and ventilation system.

During the lifecycle of the building, the construction remains the largest part of the LCC (see Figure 8). The operation of the building (power demand fee and energy demand fees) represents around 10% of the total LCC in all of the buildings, except the 1970s building.

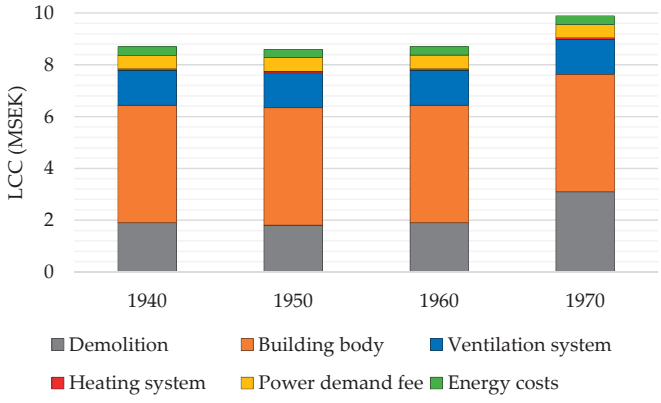

Figure 8. LCC for the demolition and construction of a new building for the buildings from the 1940s, 1950s, 1960s, and 1970s.

5.3. Comparison between the Renovation and the Construction of a New Building

The renovated buildings included in this analysis vary not only in construction, but also in the relationship between the internal volumes and floor area, because of the differences in ceiling height. This means that although the costs of renovation are similar with regard to, for example, the façade area, attic area, and ventilation unit, the rentable area and heated area are significantly smaller in the two buildings with higher ceiling heights. This means that a more ambitious energy renovation is required in order to achieve a similar energy performance per heated area compared with a building with a smaller internal volume to floor area ratio. The two newest buildings have similar or larger heated and rentable areas compared to the new building, which means that it is cheaper to renovate them so that they achieve similar energy performance as a new building. To allow for a comparison between energy renovation and the construction of a new building, an optimization was performed for each of the four buildings to find the LCC of an energy renovation to reach the same energy performance as the new building included in the analysis. All of the renovations include installing an HRX system, and the average required U-value and energy performance for all buildings are summarized in Table 18. The 1940s building cannot be improved to match the energy performance of the newly constructed building, and the best energy performance that can be achieved by implementing all of studied EEMs is 87.9 kWh/m^2·y. The 1950s building has a slightly higher heated area and better thermal performance of the building envelope prior to renovation compared to the 1940s building, and can thus be renovated to the same energy performance as the new building, although a significant amount of insulation is needed (0.34 m attic insulation and 0.36 m façade insulation). The higher ceiling height of the two older buildings compared with the two newer buildings and the newly constructed building means that a more ambitious energy renovation approach is needed. The buildings from the 1960s and the 1970s can be renovated to the same performance as the new building by installing HRX and insulating the façade with 0.13 m and 0.16 m, respectively.

The costs for renovation or construction and the LCC are summarized in Table 19. The cost of renovating the buildings from the 1940s and the 1950s is around 5 kSEK/m^2 of apartment area. Note that the 1940s building does not reach the same energy performance as the newly constructed building included in the analysis. The cost for the 1960s and 1970s buildings is around 3.5 kSEK/m^2. The cost of the construction of a new building is around 8 kSEK/m^2 for the demolition of the 1940s, 1950s, and

1960s buildings, and around 9.4 kSEK/m^2 for the 1970s building. The total LCC is approximately 1.4 kSEK/m^2 higher than the renovation or construction costs for the five story buildings (1960s, 1970s, and new building), and approximately 1.6 kSEK/m^2 for the four story buildings (1940s and 1950s buildings), because of the smaller apartment area.

There is currently no energy performance requirement when Swedish buildings undergo renovation. Tables 18 and 19 have already shown that it would not be possible to reach the energy performance requirement set for newly constructed buildings in the oldest building included in the study. The building from the 1950s can be renovated to the standard of a new building, but the maximum energy performance that is possible with the EEMs included in the study means that the best possible energy performance that could be achieved is 83.3 kWh/m^2 (see Figure 9). The 1960s and 1970s buildings can be renovated to an energy performance of 70.4 and 71.5 kWh/m^2, respectively, with the EEMs included in this analysis.

Table 18. Average U-value of the building envelope needed in order to achieve the required energy performance for the newly constructed buildings heated with district heating in central Sweden.

Building Type	$U_{average}$ ($W/m^2 \cdot °C$)	Annual Space Heating Demand (MWh)	Power Demand (kW)	Space Heating Demand [1] ($kWh/m^2 \cdot y$)	Facility Electricity [1] ($kWh/^{m2} \cdot y$)	Domestic Hot Water [1] ($kWh/m^2 \cdot y$)	Energy Performance [1] ($kWh/^{m2} \cdot y$)
1940s	0.18	38.7	23.9	48.1	14.8	25	87.9
1950s	0.19	38.1	24.0	45.6	14.3	25	84.9
1960s	0.29	49.8	31.3	46.4	13.5	25	84.9
1970s	0.28	47.3	30.0	45.9	14.0	25	84.9
New	0.30	49.6	31.1	46.4	13.5	25	84.9

[1] Primary energy use according to primary energy factors in the Swedish building code [64].

Table 19. Total LCC, LCC per apartment area, and renovation or construction cost per apartment area for the construction of a new building and renovation to the same energy performance as a new building (presented in Table 18).

Cost and Energy Use	1940s		1950s		1960s		1970s	
	Renovate	Rebuild	Renovate	Rebuild	Renovate	Rebuild	Renovate	Rebuild
LCC (MSEK)	4.57	8.70	4.53	8.60	4.54	8.70	4.53	9.90
LCC (SEK/m^2)	6685	9496	6485	9391	4947	9498	5114	10,799
Renovation/construction cost (SEK/m^2)	5153	8147	4984	8044	3596	8150	3752	9451
Energy performance (kWh/m^2)	88.0	84.9	84.9	84.9	84.9	84.9	84.9	84.9

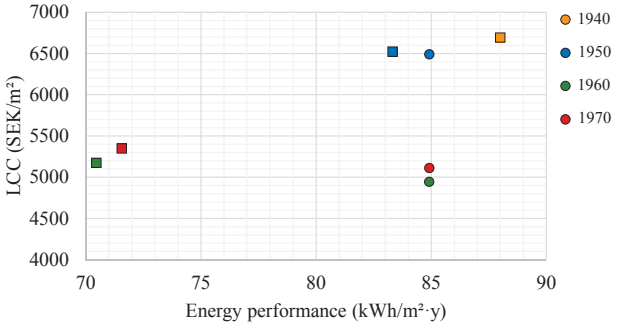

Figure 9. LCC for renovation to energy performance requirement in newly constructed building (circles), and highest energy performance achieved with all of the EEMs included in the analysis (squares).

A comparison between a renovated building and a newly constructed building means that several aspects have to be considered. There are also differences in rent levels in larger and smaller cities, city layout, and accessibility of the building, as well as the competence and economy of the building owner. This means that any comparison is highly contextualized. As previous results have indicated, the costs and suitable EEMs also depend on the buildings type.

The cost of renovating the building skeleton structure has been shown, in previous sections, to be lower than demolishing and constructing a new building. However, the revenue from rent is higher for newly constructed buildings compared with renovated buildings, which means that part of the additional costs for the construction of a new building are compensated for. Figure 10 shows the LCC of renovation and demolition and new construction with additional costs from a Swedish setting included (see Table 13). The LCC is significantly higher for new construction. Even though the rent is higher for newly constructed buildings, it remains the most expensive approach in all of the building types included in the analysis.

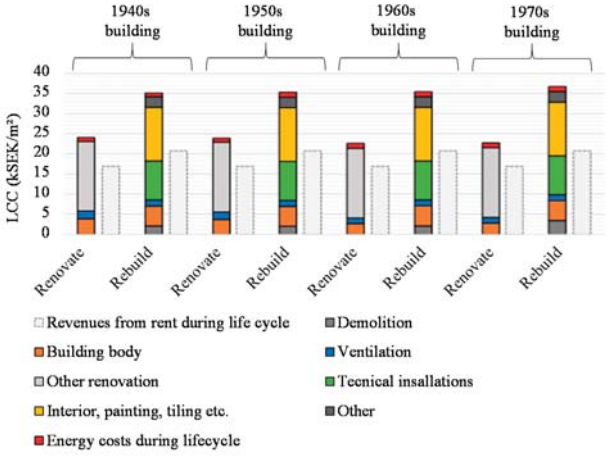

Figure 10. LCC for renovation and demolition and construction, as well as the revenues from rent during the building life cycle.

6. Discussion

This study analyzes the cost of energy renovation of a multi-family building in Sweden, and compares it to demolishing the building and constructing a new building. The focus is on the costs

for the building skeleton structure. The study uses an optimization approach to find the life cycle cost (LCC) optimal energy efficiency measures for four different building types, representing common Swedish building types from the 1940s, 1950s, 1960s, and 1970s. The LCC for demolishing the building and constructing a new building is calculated for each building type. The new building included in the analysis fulfils the design requirement of the Swedish building code.

The energy renovation costs identified in the study are similar to the costs related to the energy efficiency measures (EEMs) implemented in other similar Swedish energy renovations. The analysis shows that it is cost-effective to add thermal insulation to the attic in the two buildings with the poorest thermal performance of the building envelope (1940s and 1950s). The cost of attic insulation is relatively low, and none of the more extensive EEMs, such as façade insulation or the installation of a mechanical ventilation system, are cost-optimal. In the studied buildings with a slightly better thermal performance (1960s and 1970s), no EEMs are found to be cost-effective when the lowest LCC is the objective function. The building with the poorest thermal performance prior to energy renovation remains the building with the poorest thermal performance after energy renovation. In three of the buildings, it is more cost-effective to aim for higher energy savings than a low energy saving target. This indicates that it is important to carefully consider the building's characteristics when choosing an energy renovation approach. The analysis suggests that ventilation measures are not suitable for the naturally ventilated buildings. The losses from ventilation are significantly lower, and the majority of the heat is lost because of the poor thermal performance of the building envelope in the building types with natural ventilation included in the study. The buildings included in the study are assumed to be relatively air tight. In a building with significant air leakage due to infiltration, air tightness improvements should be considered.

In the case of the demolition and construction of a new building, the demolition of the building body and the construction of the internal concrete floors represent almost half of the LCC. The demolition costs are especially high in buildings with a concrete building structure. A comparison was made between renovating the four building types to the same energy performance (according to the Swedish building code) as the newly constructed building included in the analysis. The 1940s building would be the most expensive building to renovate, and because of the poor thermal performance prior to energy renovation and the high volume to floor area ratio, it is not possible to reach the same energy performance as the new building with the energy efficiency measures included in the analysis. The best energy performance that can be achieved is 87.9 kWh/m^2 at an LCC of 6.7 kSEK/m^2. The building with the lowest cost for energy renovation to the standard of the new building is the building from the 1960s. Although the building does not have the best thermal performance of the building envelope among the buildings included in the analysis, it has the largest heated area, which means that a less ambitious energy renovation approach is needed. The 1960s building can achieve an energy performance of 84.9 kWh/m^2 at an LCC of 5.0 kSEK/m^2. Demolishing the 1940s and 1960s building, and constructing a new building with an energy performance of 84.9 kWh/m^2, has an LCC of 9.5 kSEK/m^2. The thermal performance is thus not the only parameter that will influence the choice between energy renovation and the demolition and construction of a new building; the shape factor of the volume to floor area ratio also has a significant impact on the LCC/m^2 and the possibility of achieving energy saving targets in a cost-effective manner. The increase in revenues from rent in newly constructed buildings is not able to compensate for the higher costs of the demolition and construction of a new building.

Several aspects have to be considered in the choice between energy renovation and the demolition and construction of a new building. This study has isolated the cost of the building skeleton structure and the parts of the building that affect the energy use of the building to analyze the LCC of energy renovation versus the demolition and the construction of a new building. Although energy performance is central to national construction goals, several other aspects are also important, such as aesthetics and comfort, rent for renovated and newly constructed apartments, and suitability for intended use.

7. Conclusions

The demolition and construction of a new building has a higher LCC than energy renovation of existing buildings. The higher rent in the newly constructed buildings compared to the renovated buildings does not compensate for the total costs related to new construction. With a large volume to floor area ratio common in older buildings, the LCC of energy renovation is higher, and a more ambitious energy renovation is required in order to achieve the same energy performance as a new building. An ambitious energy renovation is not cost-optimal in any of the studied building types if the lowest LCC is the main objective. The LCC of the energy renovation is highly dependent on the building type and thermal performance prior to energy renovation. Among the studied buildings, the highest cost has been identified for the building with the smallest apartment area in relation to the internal volume and poorest thermal performance of the building envelope.

Author Contributions: Conceptualization, L.L.F., P.R. and B.M.; Data curation, L.L.F.; Formal analysis, L.L.F.; Funding acquisition, B.M.; Investigation, L.L.F.; Methodology, L.L.F., P.R. and B.M.; Project administration, B.M.; Supervision, P.R. and B.M.; Visualization, L.L.F.; Writing—original draft, L.L.F.; Writing—review & editing, L.L.F., P.R. and B.M.

Funding: This study has been financed by the Swedish Research Council Formas.

Acknowledgments: The authors are grateful for the support in calculating the building demolition costs by Wikells Sektionsfakta AB, Sweden.

Conflicts of Interest: The authors declare no conflict of interest.

References

1. European Commission. EU Energy Statistical Pocketbook and Country Datasheets|Energy. Available online: https://ec.europa.eu/energy/en/data/energy-statistical-pocketbook (accessed on 10 June 2019).
2. Gynther, L.; Lapillonne, B.; Pollier, K. Energy Efficiency Trends and Policies in the Household and Tertiary Sectors—An Analysis Based on the ODYSSEE and MURE Databases. Available online: http://www.odyssee-mure.eu/publications/br/energy-efficiency-trends-policies-buildings.pdf (accessed on 10 June 2019).
3. European Commission. Energy Performance of Buildings. Available online: https://ec.europa.eu/energy/en/topics/energy-efficiency/buildings (accessed on 10 June 2019).
4. European Parliament. Directive 2010/31/EU of the European Parliament and of the Council—on the Energy Performance of Buildings. Available online: https://eur-lex.europa.eu/legal-content/EN/TXT/?uri=CELEX%3A32010L0031 (accessed on 10 June 2019).
5. Lechtenböhmer, S.; Schüring, A. The potential for large-scale savings from insulating residential buildings in the EU. *Energy Effic.* **2011**, *4*, 257–270. [CrossRef]
6. Morelli, M.; Rønby, L.; Mikkelsen, S.E.; Minzari, M.G.; Kildemoes, T.; Tommerup, H.M. Energy retrofitting of a typical old Danish multi-family building to a "nearly-zero" energy building based on experiences from a test apartment. *Energy Build.* **2012**, *54*, 395–406. [CrossRef]
7. Liu, L.; Moshfegh, B.; Akander, J.; Cehlin, M. Comprehensive investigation on energy retrofits in eleven multi-family buildings in Sweden. *Energy Build.* **2014**, *84*, 704–715. [CrossRef]
8. Popescu, D.; Bienert, S.; Schützenhofer, C.; Boazu, R. Impact of energy efficiency measures on the economic value of buildings. *Appl. Energy* **2012**, *89*, 454–463. [CrossRef]
9. Ferreira, M.; Almeida, M.; Rodrigues, A. Impact of co-benefits on the assessment of energy related building renovation with a nearly-zero energy target. *Energy Build.* **2017**, *152*, 587–601. [CrossRef]
10. Thomsen, K.E.; Rose, J.; Mørck, O.; Jensen, S.Ø.; Østergaard, I.; Knudsen, H.N.; Bergsøe, N.C. Energy consumption and indoor climate in a residential building before and after comprehensive energy retrofitting. *Energy Build.* **2016**, *123*, 8–16. [CrossRef]
11. Prasauskas, T.; Martuzevicius, D.; Kalamees, T.; Kuusk, K. Effects of Energy Retrofits on Indoor Air Quality in Three Northern European Countries. *Energy Procedia* **2016**, *96*, 253–259. [CrossRef]
12. Liu, L.; Rohdin, P.; Moshfegh, B. Evaluating indoor environment of a retrofitted multi-family building with improved energy performance in Sweden. *Energy Build.* **2015**, *102*, 32–44. [CrossRef]

13. Mørck, O.; Almeida, M.; Ferreira, M.; Brito, N.; Thomsen, K.E.; Østergaard, I. Shining examples analysed within the EBC Annex 56 project. *Energy Build.* **2016**, *127*, 991–998. [CrossRef]
14. Kuusk, K.; Kalamees, T.; Link, S.; Ilomets, S.; Mikola, A. Case-study analysis of concrete large-panel apartment building at pre- and post low-budget energy-renovation. *J. Civ. Eng. Manag.* **2017**, *23*, 67–75. [CrossRef]
15. Blomqvist, S.; La Fleur, L.; Amiri, S.; Rohdin, P.; Ödlund, L. The impact on system performance when renovating a multifamily building stock in a district heated region. *Sustainability* **2019**, *11*, 2199. [CrossRef]
16. La Fleur, L.; Rodhin, P.; Moshfegh, B. Energy use and perceived indoor environment in a Swedish multifamily building before and after major renovation. *Sustainability* **2018**, *10*, 766. [CrossRef]
17. Wrålsen, B.; O'Born, R.; Skaar, C. Life cycle assessment of an ambitious renovation of a Norwegian apartment building to nZEB standard. *Energy Build.* **2018**, *177*, 197–206. [CrossRef]
18. Friesen, C.; Malbert, B.; Nolmark, H. Renovating to Passive Housing in the Swedish Million Programme. *Plan. Theory Pract.* **2012**, *13*, 115–131. [CrossRef]
19. Gluch, P.; Baumann, H. The life cycle costing (LCC) approach: A conceptual discussion of its usefulness for environmental decision-making. *Build. Environ.* **2004**, *39*, 571–580. [CrossRef]
20. Liu, L.; Rohdin, P.; Moshfegh, B. LCC assessments and environmental impacts on the energy renovation of a multi-family building from the 1890s. *Energy Build.* **2016**, *133*, 823–833. [CrossRef]
21. Milić, V.; Ekelöw, K.; Moshfegh, B. On the performance of LCC optimization software OPERA-MILP by comparison with building energy simulation software IDA ICE. *Build. Environ.* **2017**. [CrossRef]
22. Spickova, M.; Myskova, R. Costs Efficiency Evaluation using Life Cycle Costing as Strategic Method. *Procedia Econ. Financ.* **2015**, *34*, 337–343. [CrossRef]
23. Brown, N.W.O.; Malmqvist, T.; Bai, W.; Molinari, M. Sustainability assessment of renovation packages for increased energy efficiency for multi-family buildings in Sweden. *Build. Environ.* **2013**, *61*, 140–148. [CrossRef]
24. Almeida, M.; Ferreira, M. Cost effective energy and carbon emissions optimization in building renovation (Annex 56). *Energy Build.* **2017**, *152*, 718–738. [CrossRef]
25. Niemelä, T.; Kosonen, R.; Jokisalo, J. Cost-effectiveness of energy performance renovation measures in Finnish brick apartment buildings. *Energy Build.* **2017**, *137*, 60–75. [CrossRef]
26. Liu, L.; Rohdin, P.; Moshfegh, B. Investigating cost-optimal refurbishment strategies for the medieval district of Visby in Sweden. *Energy Build.* **2018**, *158*, 750–760. [CrossRef]
27. Tokarik, M.S.; Richman, R.C. Life cycle cost optimization of passive energy efficiency improvements in a Toronto house. *Energy Build.* **2016**, *118*, 160–169. [CrossRef]
28. Murray, S.N.; Walsh, B.P.; Kelliher, D.; O'Sullivan, D.T.J. Multi-variable optimization of thermal energy efficiency retrofitting of buildings using static modelling and genetic algorithms—A case study. *Build. Environ.* **2014**, *75*, 98–107. [CrossRef]
29. Kuusk, K.; Kalamees, T.; Maivel, M. Cost effectiveness of energy performance improvements in Estonian brick apartment buildings. *Energy Build.* **2014**, *77*, 313–322. [CrossRef]
30. Itard, L.; Klunder, G. Comparing environmental impacts of renovated housing stock with new construction. *Build. Res. Inf.* **2007**, *35*, 252–267. [CrossRef]
31. Verbeeck, G.; Cornelis, A. Renovation versus demolition of old dwellings Comparative analysis of costs, energy consumption and environmental impact. In Proceedings of the PLEA2011—27th International conference on Passive and Low Energy Architecture, Louvain-la-Neuve, Belgium, 13–15 July 2011; pp. 1–6.
32. Power, A. Does demolition or refurbishment of old and inefficient homes help to increase our environmental, social and economic viability? *Energy Policy* **2008**, *36*, 4487–4501. [CrossRef]
33. Power, A. Housing and sustainability: Demolition or refurbishment? *Urban Des. Plan.* **2010**, *163*, 205–216. [CrossRef]
34. Weiler, V.; Harter, H.; Eicker, U. Life cycle assessment of buildings and city quarters comparing demolition and reconstruction with refurbishment. *Energy Build.* **2017**, *134*, 319–328. [CrossRef]
35. Ferreira, J.; Duarte Pinheiro, M.; De Brito, J. Economic and environmental savings of structural buildings refurbishment with demolition and reconstruction—A Portuguese benchmarking. *J. Build. Eng.* **2015**, *3*, 114–126. [CrossRef]
36. Morelli, M.; Harrestrup, M.; Svendsen, S. Method for a component-based economic optimisation in design of whole building renovation versus demolishing and rebuilding. *Energy Policy* **2014**, *65*, 305–314. [CrossRef]

37. Alba-Rodríguez, M.D.; Martínez-Rocamora, A.; González-Vallejo, P.; Ferreira-Sánchez, A.; Marrero, M. Building rehabilitation versus demolition and new construction: Economic and environmental assessment. *Environ. Impact Assess. Rev.* **2017**, *66*, 115–126. [CrossRef]
38. Sadick, A.; Issa, M.H. Differences in teachers' satisfaction with indoor environmental quality and their well-being in new, renovated and non-renovated schools. *Indoor Built Environ.* **2018**, *27*, 1272–1286. [CrossRef]
39. Bullen, P.A.; Love, P.E.D. The rhetoric of adaptive reuse or reality of demolition: Views from the field. *Cities* **2010**, *27*, 215–224. [CrossRef]
40. Bullen, P.; Love, P. A new future for the past: A model for adaptive reuse decision-making. *Built Environ. Proj. Asset Manag.* **2011**, *1*, 32–44. [CrossRef]
41. Swedish Association of Public Housing Companies; Fastigehetsägarna (Swedish Assisiation for Property Owners); Swedish Union of Tenants. Att Arbeta med Hyressättningsmodeller—En Handledning för Systematisk Hyressättning. Available online: https://www.sabo.se/trycksaker/att-arbeta-med-hyressattningsmodeller/ (accessed on 10 June 2019).
42. Lind, H. *Leder Hyreslagens Regler Till Rätt Renoveringar: Analys och Förslag*; Building and Real Estate Economics, Real Estate and Construction Management, School of Architecture and the Built Environment (ABE), KTH: Stockholm, Sweden, 2015.
43. Byman, K.; Jernelius, S. Ekonomi vid Ombyggnader med Energisatsningar. Stockholm, Sweden, 2012. Available online: https://insynsverige.se/documentHandler.ashx?did=96754 (accessed on 10 June 2019).
44. Martinsson, L. Uvärdering av prefabricerad vägg—System för tilläggsisolering vid renovering av flerbostadshus Byggbarhet i produktion Prefab i renovering. 2014. Available online: https://www.bebostad.se/library/1846/utvaerdering-av-prefabricerad-vaegg-slutrapport.pdf (accessed on 10 June 2019).
45. Statistics Sweden Priser för Nyproducerade Bostäder. Available online: https://www.scb.se/hitta-statistik/statistik-efter-amne/boende-byggande-och-bebyggelse/byggnadskostnader/priser-for-nyproducerade-bostader/ (accessed on 17 December 2018).
46. BeBo Brogården—Passivhusrenovering. Available online: http://www.bebostad.se/library/1777/godaex-brogaarden-2014.pdf (accessed on 17 December 2018).
47. BeBo Backa Röd—Lågenergirenovering. Available online: http://www.bebostad.se/library/1776/godaex-backa-roed-2014.pdf (accessed on 17 December 2018).
48. Swedish National Board of Housing Building and Planning. *Produktionskostnader för nyproduktion av flerbostadshus*; Swedish National Board of Housing Building and Planning: Karlskrona, Sweden, 2009; ISBN 9789186045555.
49. Wikells Byggberäkningar AB Kalkylprogram och kalkylböcker inom Bygg, El och VVS—Wikells Byggberäkningar. Available online: http://www.wikells.se/omwikells.aspx (accessed on 10 June 2019).
50. La Fleur, L.; Moshfegh, B.; Rohdin, P. Measured and predicted energy use and indoor climate before and after a major renovation of an apartment building in Sweden. *Energy Build.* **2017**, *146*, 98–110. [CrossRef]
51. International Standard ISO 6946:2007. Building Components and Building Elements—Thermal Resistance and Thermal Transmittance—Calculation Method 2007. Available online: https://www.iso.org/standard/40968.html (accessed on 11 June 2019).
52. International Standard ISO 13370:2007. Thermal Performance of Buildings—Heat Transfer via the Ground—Calculation Methods 2007.
53. Adalberth, K.; Wahlström, Å.; Abel, E.; Tućan, B. *Energibesiktning av byggnader: Flerbostadshus och Lokaler*; SIS förlag: Stockholm, Sweden, 2009; ISBN 9789171627551.
54. Sveby Brukarindata bostäder. Available online: http://www.sveby.org/ (accessed on 10 June 2019).
55. Gustafsson, S.-I. *Optimal Energy Retrofits on Existing Multi-Family Buildings*; Linköping Studies in Science and Technology. Dissertation No. 0280-7971; Linköping University: Linköping, Sweden, 1986; ISBN 91-7870-118-X.
56. Gustafsson, S.-I. Mixed integer linear programming and building retrofits. *Energy Build.* **1998**, *28*, 191–196. [CrossRef]
57. Gustafsson, S.I. Optimal fenestration retrofits by use of MILP programming technique. *Energy Build.* **2001**, *33*, 843–851. [CrossRef]
58. Gustafsson, S.I.; Bojic, M. Optimal heating-system retrofits in residential buildings. *Energy* **1997**, *22*, 867–874. [CrossRef]

59. La Fleur, L.; Rohdin, P.; Moshfegh, B. Investigating cost-optimal energy renovation strategies for a multifamily building in Sweden. *Energy Build.* **2019**, submitted.
60. Equa Simulation AB. Validation of IDA Indoor Climate and Energy 4.0 Build 4 with Respect to ANSI/ASHRAE Standard 140-2004. Solna, Sweden, 2010. Available online: http://www.equaonline.com/iceuser/validation/ASHRAE140-2004.pdf (accessed on 10 June 2019).
61. Equa Simulation AB. Validation of IDA Indoor Climate and Energy 4.0 with Respect to CEN Standards EN 15255-2007 and EN 15265-2007. Solna, Sweden, 2010. Available online: http://www.equaonline.com/iceuser/validation/CEN_VALIDATION_EN_15255_AND_15265.pdf (accessed on 10 June 2019).
62. Kropf, S.; Zweifel, G. Validation of the Building Simulation Program IDA-ICE According to CEN 13791 "Thermal Performance of Buildings—Calculation of Internal Temperatures of a Room in Summer Without Mechanical Cooling—General Criteria and Validation Procedures"; Hochschule Technik+Architektur Luzern. HLK Engineering. 2001. Available online: http://www.equaonline.com/iceuser/validation/ICE_vs_prEN%2013791.pdf (accessed on 10 June 2019).
63. Loutzenhiser, P.; Manz, H.; Maxwell, G. *Empirical Validations of Shading/Daylighting/Load Interactions in Building Energy Simulation Tools*; A Report from the International Energy Agency´s SHC Task 34/ECBCS Annex 42 Project C; International Energy Agency: Paris, France, 2007.
64. Swedish National Board of Housing Building and Planning. *The Swedish Building Code*; Swedish National Board of Housing Building and Planning: Karlskrona, Sweden, 2018; ISBN 9789175635804.
65. Swedish Association of Public Housing Companies SABOs Kombohus Plus. Available online: https://www.sabo.se/nyproduktion/sabo-kombohus/sabos-kombohus-plus/ (accessed on 16 January 2019).
66. Skanska Kombohus. Available online: https://www.skanska.se/vart-erbjudande/byggentreprenader/byggkoncept/kombohus/ (accessed on 16 January 2019).

energies

MDPI

Article

Evaluation of Energy Efficiency Potential for the Building Sector in the Arab Region

Moncef Krarti

Building Systems Program, University of Colorado Boulder, Boulder, CO 80309, USA; krarti@colorado.edu

Received: 23 October 2019; Accepted: 8 November 2019; Published: 9 November 2019

Abstract: The paper overviews the current energy demand trends in the building sector for the Arab region using reported historical energy consumption. Moreover, the paper describes the current energy efficiency policies and regulations for all the Arab countries specific to both residential and commercial buildings. Finally, the paper evaluates potential benefits for large-scale energy efficiency programs specific to new and existing building stocks within the Arab region using a bottom-up analysis approach. The analysis of the available energy consumption for all the Arab countries has shown that the Arab region presents a significant variation in energy consumption levels between its sub-regions and countries. Indeed, the Arab region includes oil-producing countries such as Saudi Arabia with the largest energy use per capita in the World with over 9000 kWh/person of electricity used annually in buildings. However, the same region has the least developed countries such as Sudan and Yemen with the lowest energy use per capita in the World with barely 100 kWh/person/year of electrical consumption. The review of the existing regulations has indicated that several Arab countries have not implemented any energy efficiency codes and standards for building envelope, lighting, heating and cooling equipment, and appliances. A cost-effectiveness analysis has indicated that the Arab region can incur significant benefits in upgrading the energy efficiency of its new and existing buildings especially its households. Specifically, the adoption and the enforcement of stringent energy efficiency codes for new residential and commercial buildings can result in a reduction of 12.7 TWh/year in final annual energy consumption for the Arab region. Moreover, retrofit programs targeting existing buildings can save up to 470 TWh or a third of the building sector final energy consumption per year after 2030. Combining comprehensive energy efficiency requirements for new buildings and extensive retrofit programs for existing buildings would reduce the total final energy consumption of the building sector in the Arab region by 600 TWh by 2030 and by 900 TWh by 2050 if all the energy programs start to be implemented by 2020.

Keywords: Arab region; building sector; energy efficiency; energy productivity; GCC; Maghreb; Mashreq

1. Introduction

From 1990 to 2015, the total primary energy supply (TPES) in the Arab region (The Arab region includes the following countries: Algeria, Bahrain, Egypt, Iraq, Jordan, Kuwait, Lebanon, Libya, Mauritania, Morocco, Oman, Palestine, Qatar, Saudi Arabia, Sudan, Syria, Tunisia, United Arab Emirates, and Yemen.) has increased three-fold following the same trend of population growth as noted in Figure 1a using recent International Energy Agency (IEA) data [1]. However, the gross domestic product (GDP) has increased only 60% during the same period indicating an increase in energy intensity and ultimately a decrease in the energy productivity of the overall Arab region economy (The energy productivity, defined as the inverse of the energy intensity, is the ratio of GDP per total primary energy supply). Specifically and during the 1990–2015 period, the per capita GDP in the Arab region has been only slightly above the World averages but has remained significantly less than similar indicators reported for the European Union (EU) and the United States (US) as noted in Figure 1b. It should

be noted, however, that the per capita GDP varies significantly within the Arab region, especially between the Gulf Cooperation Council (GCC) countries and other countries. During the 1990–2015 period, the Arab region's primary energy use (expressed in ton of oil equivalent or TOE) per capita has increased steadily and has reached the World average of 2.0 TOE/person during 2015 as indicated in Figure 1c. Both the EU and US have significantly higher energy use per capita values which have been declining since 2008 to settle at 3.0 TOE/person and 7.0 TOE/person levels during 2015 [1].

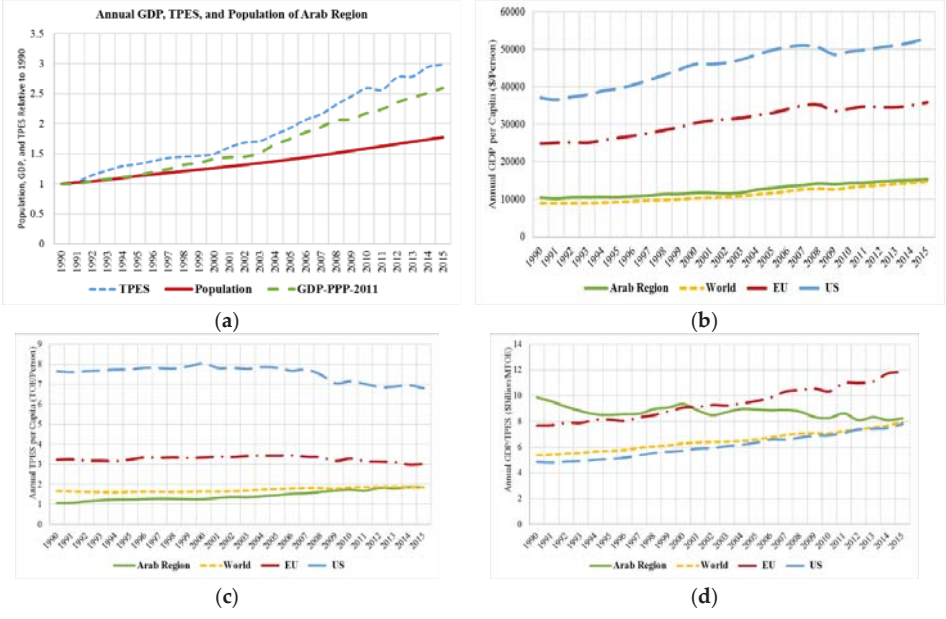

Figure 1. Annual variation gross domestic product (GDP), Total primary energy supply (TPES), and population of the Arab region compared to those of US, EU, and World. (**a**) GDP, TPES, population index to 1990; (**b**) per capita GDP; (**c**) per capita TPES; (**d**) GDP per TPES (Data Source: International Energy Agency (IEA) [1]).

Because of these trends for both GDP and TPES, the overall energy productivity, defined as the ratio of GDP and TPES, has been decreasing in the Arab region while it is increasing in the rest of the World including EU and US as shown in Figure 1d. It has been argued that energy productivity value provides an indicator of a country's economy, energy, and environmental performance and helps to allocate energy resources to optimize economic growth [2,3]. In particular, the EU has been able to improve its energy productivity by more than 50% between 1990 and 2015 most likely through diversification of its economy in order to rely less on energy-intensive industries and more on the service sector. The improvement in energy productivity can also be associated with enhancements of energy efficiency for the building and transport sectors. Similar arguments have been given to justify the increase in energy productivity, albeit less significant compared to that of EU region, in several countries including the US [4].

The relative decrease in the energy productivity for the Arab region shown in Figure 1d can be attributed to a wide range of factors. In particular, the region has experienced in the last two decades a growing rate of urbanization and a rising standard of living. These two factors have resulted in a sharp increase in energy consumption especially for services that are not directly related to the productive sectors. In addition, the significant reliance in some Arab countries on energy-intensive activities (i.e., industry) with low value added has resulted in a significant increase in energy consumption

outpacing the rise in the GDP level. Another significant factor for low energy productivity is the reduced penetration of high energy efficiency practices and best available technologies in all economic sectors. In order to improve its energy productivity and decouple its energy consumption from its GDP creation, the Arab region has to start diversifying its economy and most importantly improving the energy efficiency of all its sectors (i.e., industry, transport, and buildings). In this paper, potential benefits of large-scale implementation in the Arab region of energy efficiency programs are evaluated for the building sector. First, general trends of energy consumption are assessed for the Arab region and are compared to other regions in the World. In particular, contributions of the building sector to the total primary and final energy consumptions are estimated based on available historical data. Current energy efficiency indicators, as well as energy policies related to the building sector, are then presented for the Arab region, sub-regions, and various countries. Finally, potential benefits from specific energy efficiency programs targeting new and existing residential and commercial buildings in all Arab countries are analyzed. In particular, predictions of the impacts of large-scale implementation of these energy policies on future energy demands in the building sector are estimated for various countries of the Arab region.

The analyses conducted in this study are based on well-documented data sets, methods, and models as noted throughout this paper. However, the study provides a unique application of these analyses to consider the potential energy, economic, and environmental benefits of improving the energy efficiency of new and existing buildings in all the countries of the Arab region.

2. Overall Energy Consumption Trends

2.1. Analysis for Arab Region

2.1.1. Primary Energy Supply

Throughout the last two decades, the Arab region consumed mostly oil products and natural gas to power its economy. During 2015, the Arab region relied mainly on oil products (50%) and natural gas (46%) to meet its primary energy needs. Besides biofuels and waste (2%) and hydro (1%), insignificant other renewable energy resources are utilized as noted in Figure 2 which compares the primary energy mix of the Arab region to that reported for the World, the EU, and the US during 2015 [1]. Unlike the case of the Arab region, coal has been used to meet a significant part of the energy needs of other regions in the World contributing respectively 28%, 16%, and 17% of the total primary energy supply (TPES) specific to the World, the EU, and the US. Nuclear, hydro, and renewables (i.e., sources with no carbon emissions) are also prominent in other regions of the World serving up to 18% (World), 28% (EU), and 17% (US) of TPES.

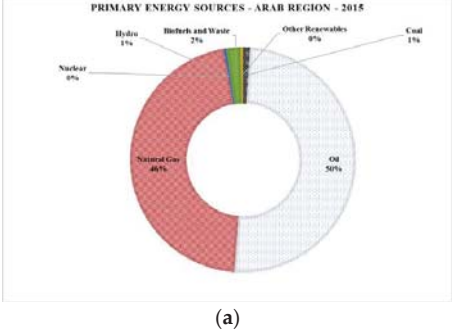

(**a**)

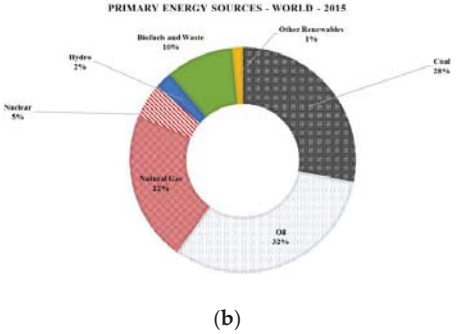

(**b**)

Figure 2. *Cont.*

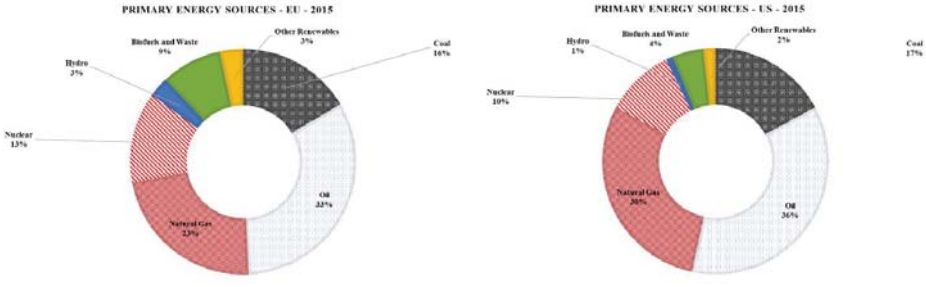

(**c**) (**d**)

Figure 2. Primary energy resources for (**a**) Arab region, (**b**) World, (**c**) EU, and (**d**) US during 2015 (Source of the data: IEA [1]).

2.1.2. Final Energy Consumption

Figure 3 presents the annual variation and distribution of total final energy consumption (TFEC) in the Arab region during the 1990–2015 period using reported data [1]. As noted in Figure 3, the Arab region has seen a significant increase in energy consumption with an average annual growth rate of 10% since 1990. During 2015, the Arab region consumed almost 5000 TWh of energy to meet its economy's needs. Most of these needs are attributed to the industry and transport sectors with 31% and 32%, respectively. However, the contribution of the building sector, estimated at 21% during 2015, has been steadily increasing especially during the last decade. Indeed, the increase in energy used by non-residential buildings has more than doubled compared to the annual growth of the overall TFEC for the Arab region. Specifically, the annual growth rate in energy consumption specific to commercial and public services buildings has averaged almost 25% during the period between 1990 and 2015 [1]. As noted in Figure 8, the annual growth rate of the energy used by the residential buildings follows closely that reported for the overall Arab region TFEC during the 1990–2015 period.

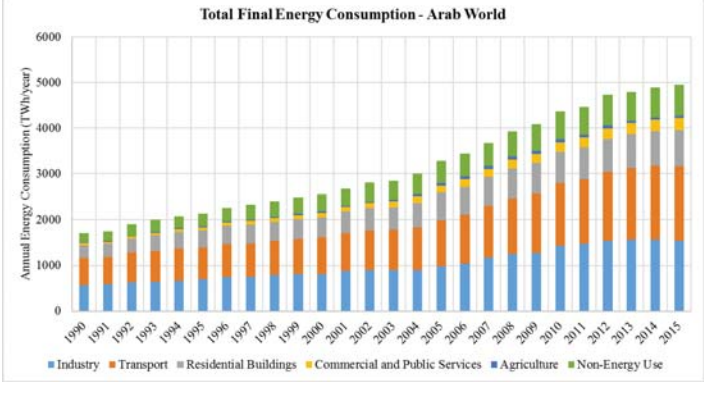

Figure 3. Annual total final energy consumption in the Arab region between 1990 and 2015.

The overall Arab region per capita final energy consumption, electricity use, and carbon emission are rather low as noted in Figure 4 comparing the annual energy indicators with those reported for the World, US, and EU [5]. Overall, the per capita energy use and electricity consumption in the Arab region are close to the World averages but significantly lower than those reported for EU and US as clearly indicated in Figure 4a,b. Due to this low per capita energy use, the Arab region generates slightly less carbon emissions per person than the World average and significantly less than the EU and US as noted by Figure 4c. However, the per

capita energy use and carbon emissions have been steadily increasing in the Arab region while decreasing in EU and the US especially during the last decade. The trend for higher energy consumption including electricity demand in the Arab region is expected to continue over the next decade especially in the building sector due to a high population growth, a significant urbanization rate, as well as rising standards of living associated with aspirations for greater comfort. The increase in energy consumption in the Arab region is also aided by reduced prices of some household equipment, often with very poor efficiency ratings, making them affordable to an increasingly high number of potential consumers. Indeed, the annual urban population growth rates in Arab countries range between 2% to 6% with an average for the region of 3.8% [6]. Moreover, a total of 4.3 USD trillion is forecast to be spent on construction in the Arab region over the next decade, representing cumulative growth of 80% [7,8].

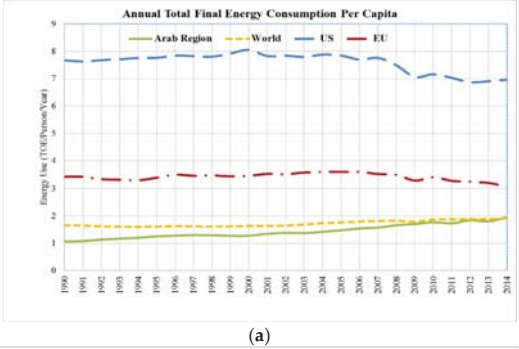

(**a**)

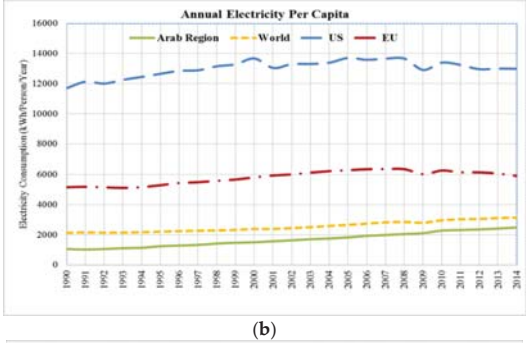

(**b**)

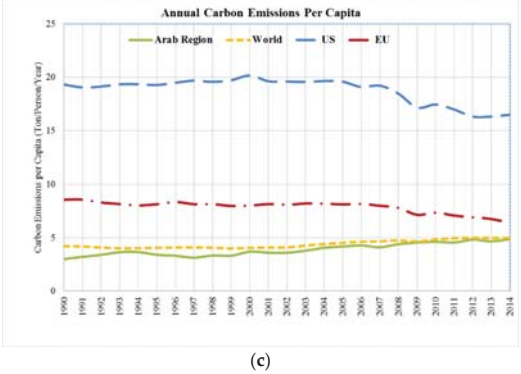

(**c**)

Figure 4. Annual per capita (**a**) final energy consumption (**b**) electricity use, and (**c**) carbon emissions in Arab region compared to averages for EU, US, and the World for the period 1990–2014 (Source of the data: World Bank [5]).

2.2. Analysis of Sub-Regions

The Arab region is generally divided into four sub-regions as defined in Table 1 based on several criteria including geographical locations, cultural tendencies, and living standards. These sub-regions include:

- Gulf Cooperation Council (GCC) countries with Bahrain, Kuwait, Oman, Qatar, Saudi Arabia, and the United Arab Emirates
- Mashreq countries with Egypt, Iraq, Jordan, Lebanon, Palestine, and Syria
- Maghreb countries with Algeria, Libya, Morocco, and Tunisia
- Least developed countries (LDC) including Mauritania, Sudan, and Yemen.

Table 1. Characteristics of Arab sub-regions including countries, population, GDP per capita, and TPES per capita.

Sub-Region	List of Countries	Population (Million)	GDP/Capita (USD/person)	TPES/Capita (TOE/person)
Gulf Cooperation Council (GCC)	Bahrain; Kuwait; Oman; Qatar; Saudi Arabia; United Arab Emirates	52.70	55,601	7.87
Mashreq	Egypt; Iraq; Jordan; Lebanon; Palestine; Syria	164.67	9915	0.94
Maghreb	Algeria; Libya; Morocco; Tunisia	91.58	10,805	1.11
Least Developed Countries (LDC)	Mauritania; Sudan; Yemen	71.24	3296	0.29

Table 1 summarizes the population, the GDP per capita, and the total primary energy supply (TPES) per person for each sub-region based on 2015 data [1]. The GCC with the lowest population has the highest values for both primary energy use as well as GDP per person. The Mashreq and the Maghreb have similar economic and energy indicators even though the Mashreq has almost double the population due to the inclusion of Egypt. As expected, the LDC region has the lowest energy use and GDP per capita for all the Arab sub-regions.

Figure 5 illustrates the variation during the 1990–2015 period in the Arab sub-regions of the per capita GDP, per capita TPES, and energy productivity (i.e., ratio of GDP and TPES). As expected, the GCC region has significantly higher levels for both economic output and energy consumption per person. Meanwhile the LDC sub-region has the lowest economic and energy use indicators among not only the Arab region but the World. The GDP and the TPES per person follow the same trend during the entire 1990–2015 period for both the Mashreq and Maghreb regions. When considering the energy intensity or the economic output per unit of primary energy supply, referred to as the energy productivity, the LDC region has higher and increasing energy productivity levels during the last decade among all Arab sub-regions. Meanwhile, the GCC region has the lowest and decreasing energy productivity values since 2000 as illustrated in Figure 5c. The energy productivity levels of the Mashreq and Maghreb regions are between those of GCC and LDC with the Mashreq energy productivity exhibiting an increasing trend while that of the Maghreb is decreasing since 2007.

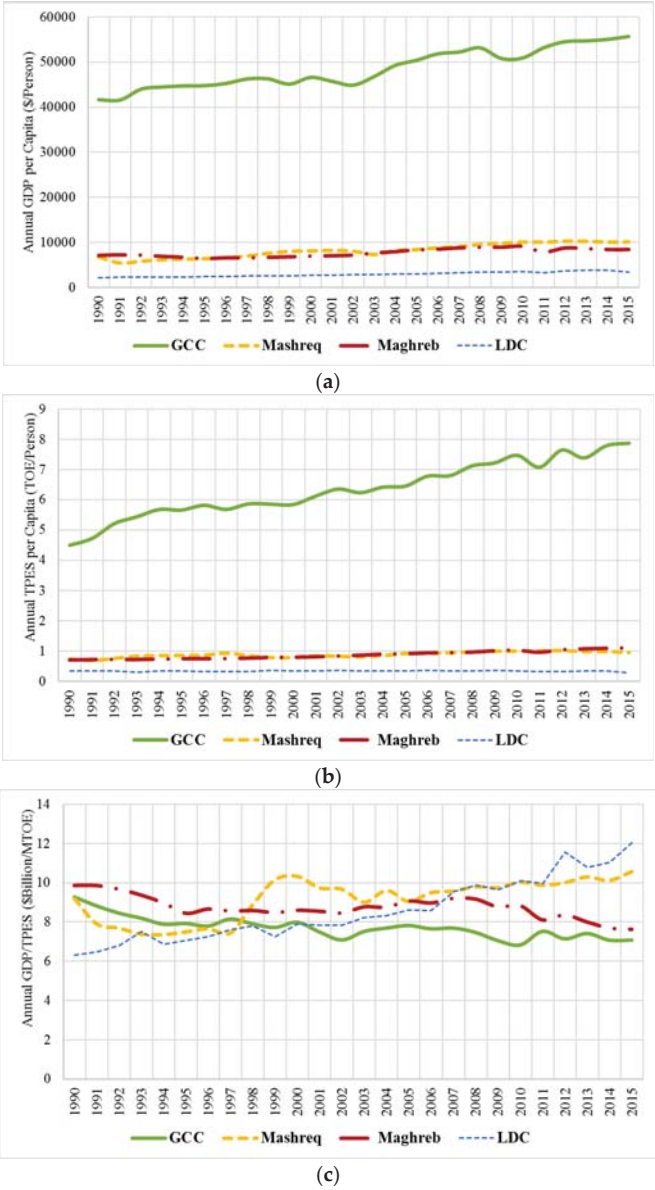

Figure 5. Annual variation of (**a**) per capita GDP, (**b**) per capita TPES, and (**c**) energy productivity for the Arab sub-regions.

2.3. Country-Specific Analysis

Basic macro-economic indicators for the Arab countries are listed in Table 2 based on 2015 data except for Palestine where 2013 data for 2013 are used [1,5,9]. Moreover, annual variations of these macro-economic indicators for representative countries of the Arab sub-regions are presented in Figure 6. Specifically, Figure 6a–c shows the annual variation of during 1990–2015 period in Saudi Arabia (KSA), Egypt, Tunisia, and Yemen respectively, the per capita GDP the TPES per capita,

and the GDP/TPES ratio. As expected, KSA as a representative of GCC sub-region has significantly higher values for both economic output and energy consumption per person. Meanwhile, Yemen representing the LDC sub-region has the lowest economic and energy use indicators. The GDP and the TPES per person follow the same trend during the entire 1990–2015 period for both Egypt and Tunisia representing respectively, the Mashreq and Maghreb sub-regions. Figure 15 indicates that KSA has lower and decreasing energy productivity (i.e., inverse of energy intensity) while Egypt and Tunisia have stagnant energy productivity over the last decade and Yemen is exhibiting a higher albeit inconsistent energy productivity levels.

Table 2. Summary of basic macro-economic indicators for Arab countries for 2015 (colors refer to the sub-regions: green for GCC, yellow for Mashreq, maroon for Maghreb, and blue for LDC).

Country	Population (Million)	GDP/Capita [1] (2011 PPP USD/person)	TPES/Capita (TOE/person)	TEPS/GDP (TOE/1000 USD)
Algeria	39.67	13,725	1.36	0.10
Bahrain	1.38	43,926	10.34	0.24
Egypt	91.51	10,096	0.87	0.09
Iraq	36.42	14,929	1.31	0.09
Jordan	7.60	8491	1.13	0.11
Kuwait	3.89	68,476	8.91	0.13
Lebanon	5.85	13,353	1.306	0.10
Libya	6.28	13,048	2.75	0.21
Mauritania	4.17	3602	0.31	0.30
Morocco	34.38	7286	0.56	0.08
Oman	4.49	40,139	5.65	0.15
Qatar	2.24	119,749	20.29	0.15
Palestine [2]	4.79	1860	0.33	0.18
Saudi Arabia	31.54	50,724	7.03	0.14
Sudan	40.24	4037	0.39	0.10
Syria	18.50	2030	0.54	0.27
Tunisia	11.25	10,750	0.97	0.09
United Arab Emirates	9.16	65,975	8.00	0.12
Yemen	26.83	2641	0.13	0.05

[1]: Data of GDP are from World Bank [5] except for Syria, the data is from IEA [1]; [2]: Data for Palestine are based on 2013 UN data [9].

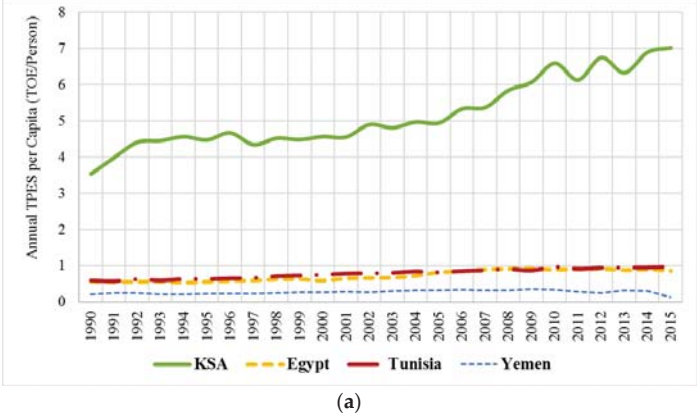

(**a**)

Figure 6. *Cont.*

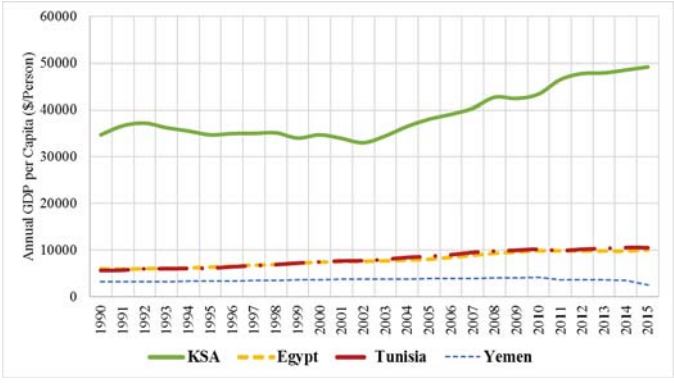

(**b**)

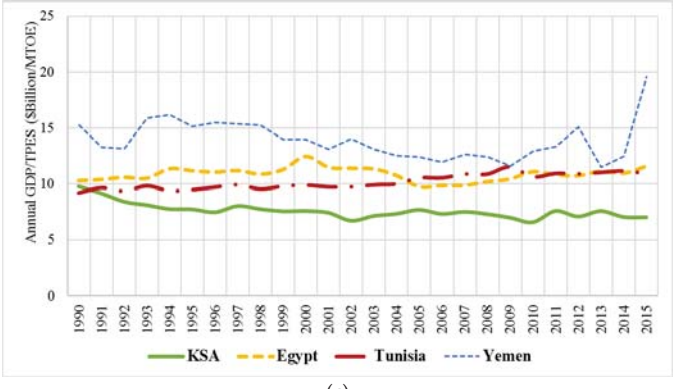

(**c**)

Figure 6. Annual variation of (**a**) per capita GDP, (**b**) per capita TPES, and (**c**) energy productivity for Saudi Arabia (KSA), Egypt, Tunisia, and Yemen.

3. Building Sector Energy Consumption

First, the main drivers for energy use in the building sector are described for the Arab region including the climatic conditions, building stock size, penetration rates of air conditioning systems, and energy subsidies, and current regulations and standards. Then, energy consumption trends for the building sector are presented at various scales including the overall Arab region, the four sub-regions, and the individual countries. Finally, energy efficiency metrics of both residential and non-residential buildings are estimated for the Arab region and its sub-regions with a discussion of typical end-uses for both residential and commercial buildings in the region and representative countries.

3.1. Climate Characteristics

Using hourly weather data for 162 cities, degree-days for both heating and cooling have been estimated throughout the Arab region [10]. Figure 7a shows a contour map of annual heating degree-days (HDD) (Heating degree-days represent the number of degrees for all days in a season with average temperatures below 18 °C) with a base temperature of 18 °C obtained for the Arab region where hourly climatic data are available. Figure 7b presents a similar map obtained for the annual cooling degree-days (CDD) (Cooling degree-days represent the number of degrees for all days of the year with average temperatures above 18 °C) with a base temperature of 18 °C [10]. As indicated in Figure 7a, HDD values of the cities close to coastal areas in the Mediterranean region (characterized by temperate climates using CSa of Koppen–Gieger classification) are higher than in the Arabian Desert

region (dominated by arid and semi-arid climates using BWh/BWk and Bsh/BSk of Koppen–Gieger classifications). Therefore, Mediterranean cities would have higher space heating energy requirements in order to maintain acceptable indoor thermal comfort in conditioned buildings during the heating season. In contrast, Figure 7b clearly indicates that sites located in the Arabian Desert are extremely hot and thus require significant energy use to cool buildings compared to sites located in the Mediterranean region. In hot climates such as those in the GCC region, energy consumption for the building sector follows the climatic conditions since most of the buildings are air-conditioned as noted by analyses conducted by Krarti [11] and Krarti et al. [12]. For Saudi Arabia, for instance, the monthly total electricity consumption closely follows the average ambient temperatures [12]. The strong correlation between the electricity consumption and the ambient temperature clearly reflects the importance of air-conditioning during the summer months when electrical demands double compared to levels reported during the winter period.

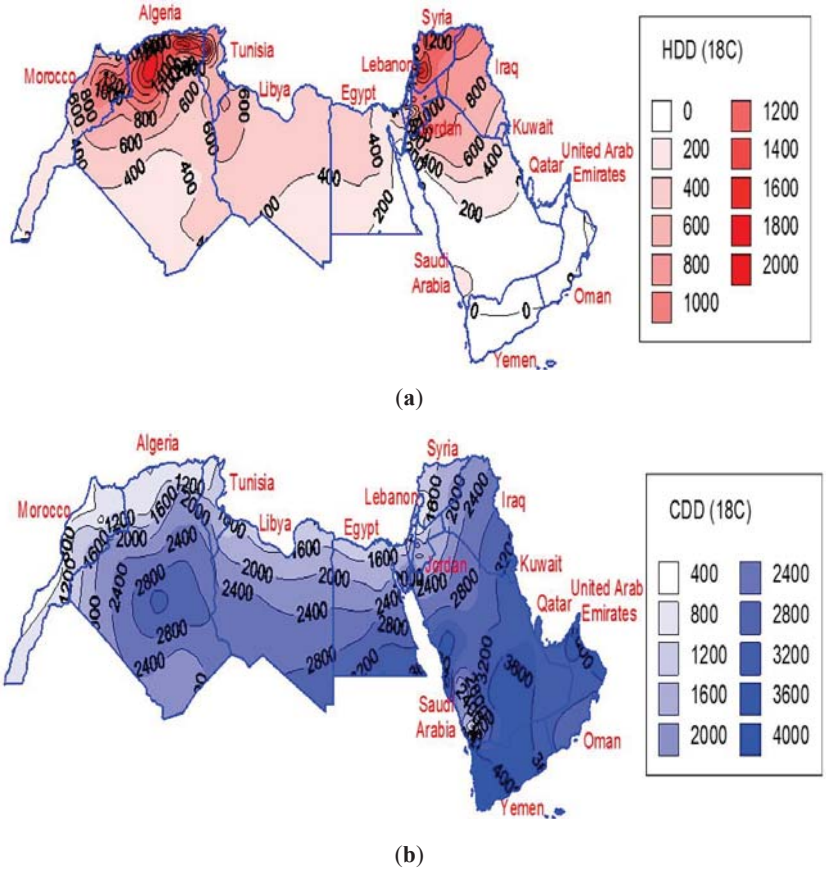

Figure 7. Contour map of Arab region for annual (**a**) heating and (**b**) cooling degree-days with a base temperature of 18 °C (Source: [10]).

3.2. Building Stock Floor Area

Detailed census data for building stock and especially building floor area in the Arab region is almost inexistent. However, some studies have utilized limited available census data to estimate the building floor area for residential and non-residential buildings for few Arab countries. Table 3

summarizes these studies, the reported estimated building floor area, and the calculated per capita floor area based on the population data reported by the United Nations (UN) for the census year.

Table 3. Reported total floor area for buildings in Arab countries based on census data.

Country, Type of Buildings	Census Year	Total Building Floor Area (million m^2)	Per Capita Floor (m^2/person)	Reference
Egypt, Residential	2006	1476	19	[13,14]
Tunisia, Residential	2006	274	27	[15]
Tunisia, Non-Residential	2006	28	3	[15]
Saudi Arabia, Residential	2010	652	24	[16]

Models for estimating building floor areas have been developed and utilized to assess the energy performance of various building types for countries and regions. In particular, Navigant has indicated that the Middle East and North Africa (MENA) region, which includes most of the Arab countries, has a total building floor area of 4.5 billion m^2 during 2014 or 11.5 m^2/person [17]. Moreover, another study [18] has reported that the MENA region has 8 billion m^2 of building floor area or 18.65 m^2/person, a close to the estimate of 20.5 m^2/person provided by Harvey et al. [19]. IEA developed based on existing data, a model that provides per capita floor area for residential buildings as a function of GDP per capita for a country or a region [20]. Using the IEA building sector model, Table 4 summarizes the average, minimum, and maximum values per capita household floor area

Table 4. Residential floor area per capita as a function of GDP per capita [20].

GDP per Capita (2012 PPP USD/person)	Average	Minimum	Maximum
0	12 m^2/person	7 m^2/person	30 m^2/person
10,000	23 m^2/person	9 m^2/person	50 m^2/person
20,000	34 m^2/person	17 m^2/person	62 m^2/person
30,000	44 m^2/person	25 m^2/person	68 m^2/person
40,000	49 m^2/person	30 m^2/person	71 m^2/person
50,000	51 m^2/person	31 m^2/person	72 m^2/person
60,000	52 m^2/person	32 m^2/person	73 m^2/person

Using the GDP data for the Arab region, per capita residential building floor area is estimated to range between 11.6 m^2/person and 48.1 m^2/person with an average of 24.2 m^2/person, a metric that is close to the values listed in Table 3 for Tunisia and Saudi Arabia, and to a lesser extent, to that found for Egypt. Indeed, the reported per capita residential floor area of 19 m^2/person for Egypt (GDP = 10,000 USD/person) is lower than the average of 23 m^2/person, as it may be expected for a country with densely populated urban areas, but is still higher than the minimum value of 9 m^2/person.

For non-residential buildings, the estimation of the floor area is even more challenging for the Arab region. Only a few models have been reported with a large variation in per capita floor area estimations for the MENA region and include (i) 5.5 m^2/person [21]; (ii) 4.5 m^2/person [20]; (iii) 4.0 m^2/person [19], and (iv) 2.5 m^2/person [22]. The per capita floor area of 2.8 m^2/person found for non-residential buildings in Tunisia seems to be in the low range of the reported model's estimates. Using the range of 2.5 to 5.5 m^2/person, the non-residential floor area for the Arab region can be estimated as a function of the population size. In particular, the total floor area for non-residential buildings during 2015 is estimated to range from 950 million m^2 to 2091 million m^2 with a mean value of 1521 million m^2.

3.3. Penetration Rates of Air Conditioning Systems

As noted in Figure 7, the vast majority of the Arab region is characterized by a cooling dominated climate. Thus, air conditioning (AC) systems are generally required to maintain desired indoor thermal comfort for both residential and commercial buildings. Moreover, refrigerators are required to preserve food longer and prevent it from spoiling quickly. The use of AC in buildings, however, depends on the Arab sub-regions. While, AC is available for almost all buildings within the GCC region (i.e., 100% penetration rate, that is, all the buildings have AC systems), the use of active systems (i.e., mechanical equipment) to cool buildings depend on the country and its standard of living. Reported penetration rates of AC systems, as well as refrigerators, are listed in Table 5 for residential buildings for some Arab countries representatives of the Mashreq, Maghreb, and LDC sub-regions. The AC penetration rates forecasted for the Maghreb countries are also provided [23]. As noted in several studies, the penetration rate of AC systems and appliances depends significantly on the income level per capita in each country. The penetration rate of AC systems for residences in the Maghreb and Mashreq ranges currently between 40% and 50% and are forecasted to exceed 80% by 3030 [23]. In the LDC region, the AC penetration rate as well refrigerators are low and do not exceed 30%

Table 5. Penetration rates of air conditioning (AC) systems and refrigerators in residential buildings for some Arab countries.

Country	AC Penetration Rate (Year)	Forecasted AC Penetration Rate (2030)	Refrigerator Penetration Rate (Year)	References
Algeria	37.2% (2015)	84.5%	90% (2009)	[23]
Morocco	9.3% (2015)	49.0%	85% (2009)	[23]
Syria	9% (2009)	NA	40% (2009)	[24]
Tunisia	40.3% (2015)	84.5%	80% (2009)	[23]
Yemen	12% (2009)	NA	30% (2009)	[24]
Lebanon	50% (2010)	NA	100% (2010)	[25]

Within the Arab region, the GCC sub-region is and will remain in the next decade a significant market for the AC industry. Table 6 lists the number of AC sold during the 2011–2016 period in the Arab region itemized by country using reported data [26]. As indicated in Table 6, GCC represents over 80% of the total AC demand in the Arab region. However, the AC demand in most of the GCC countries has stabilized and has been even slightly decreasing in the last two years most likely to slower economic activities associated with low oil prices.

Table 6. The total number of AC units (in thousands) sold in the Arab region during the 2011–2016 period [26].

Country	2011	2012	2013	2014	2015	2016
Saudi Arabia	1581	1666	2226	2238	2164	1926
UAE	497	493	713	737	763	731
Oman	248	217	297	321	320	296
Qatar	189	179	275	284	286	278
Kuwait	144	147	214	217	225	211
Iraq	274	296	315	320	193	187
Bahrain	77	82	82	78	77	80
Lebanon	69	68	69	77	76	80
All Others	181	168	162	173	174	168
Arab Region	3260	3316	4353	4445	4278	3958

3.4. Energy Subsidies

Energy prices are highly subsidized in the Arab region as depicted in Table 7 providing total energy subsidies as well as subsidies per capita based on the 2015 International Monetary Fund (IMF) data [27]. Table 8 lists electricity rates for typical households as well as available electricity generating capacity, electricity consumption per capita, and carbon emissions per capita for most Arab countries [1,5,28,29]. As indicated in Table 7, the energy subsidies especially for GCC and oil-exporting countries are among the highest in the World and may explain the high electricity consumption and carbon emissions per person prevalent in several Arab countries as illustrated in Table 8. According to reported IEA data, the Arab countries are among the largest subsidizers of energy in the World. Indeed, six of the World's ten largest subsidizers are from the Arab region, led by Kuwait, Saudi Arabia, and Qatar [30,31]. Moreover, GCC countries have the highest electricity consumption per capita in the World due to the significant air conditioning loads for buildings, especially during the summer months. However, there is a wide variation in energy consumption levels between Arab countries. Indeed, the Arab region includes some of the highest (i.e., GCC countries as noted earlier) but also some of the lowest users of electricity in the World. For instance, an average person in Yemen consumes only 147 kWh per year, as noted in Table 8, most likely due to low energy accessibility in rural areas.

Table 7. Energy subsidies in the Arab region (Source, International Monetary Fund (IMF) [27]).

Country	Total Energy Subsidies [1] (Billions USD)	Percent GDP (%)	Subsidies of Total Energy Per Capita (USD/person)	Subsidies of Electricity per Capita (USD/person)
Algeria	23.870	10.0	604.70	59.83
Bahrain	3.940	11.2	3224.74	1179.72
Egypt	32.349	10.0	365.79	33.20
Iraq	0.495	0.2	13.37	0.00
Jordan	1.424	3.6	208.67	89.90
Kuwait	14.097	7.8	3429.95	409.78
Lebanon	5.246	10.3	1151.99	465.14
Libya	6.442	10.2	1021.64	0.00
Mauritania	0.058	1.3	15.53	15.53
Morocco	1.957	1.6	58.41	NA
Oman	7.267	8.9	1718.97	102.13
Qatar	14.471	6.4	5995.25	1041.12
Saudi Arabia	106.556	13.2	3395.03	352.54
Sudan	1.375	2.1	35.77	NA
Tunisia	2.004	4.0	180.37	115.28
United Arab Emirates	28.961	6.6	3022.85	337.03
Yemen	0.359	0.7	12.69	6.08
Arab region	250.868	8.3	715.65	85.31

[1] The price-gap method, based on global reference energy costs, is used to estimate energy subsidies.

Table 8 indicates that the Arab region has 232,675 MW of available electric power generating capacity with 6% coming from renewable resources mostly from hydroelectric plants (about 11,000 MW). As part of their national renewable energy plans, most of the Arab countries have set ambitious targets to meet between 10% to 100% of the electricity needs using renewable energy resources by 2030 [29].

Table 8. Electricity prices, energy use, and carbon emissions indicators for Arab countries.

Country	Cost of Electricity (USD/kWh) [1]	Electricity Generation Capacity (MW) [2]	Electricity Consumption per Capita (kWh/person) [3]	Total Final Energy Consumption per Capita (TOE/person) [3]	CO_2 Emissions per Capita (tons/person) [4]
Algeria	0.051	13,000	1451	0.944	3.717
Bahrain	0.008	3889	20,190	4.568	23.450
Egypt	0.033	32,483	1754	0.604	2.199
Iraq	0.009	25,600	1218	0.496	4.812
Jordan	0.092	4882	2288	0.73	3.003
Kuwait	0.007	18,000	14,951	4.523	25.224
Lebanon	0.046	2710	2861	0.835	4.296
Libya	0.016	10,000	1656	1.322	9.187
Morocco	0.123	8202	892	0.435	1.744
Oman	0.026	8750	6588	4.548	15.443
Qatar	0.022	8900	17460	8.769	45.423
Saudi Arabia	0.013	46,400	9926	4.6	19.529
Sudan	0.049	3253	264	0.265	0.309
Syria	0.004	3154	811	0.357	1.599
Tunisia	0.127	4491	1458	0.7	2.587
UAE	0.080	29,348	12,916	5.805	23.202
Yemen	0.041	1500	147	0.095	0.865

[1]: Average prices in 2014 for residential buildings estimated based on 500 kWh of consumption [28]; [2]: Data for 2015 obtained from IRENA [29]; [3]: Data for 2015 are obtained from IEA [1]; [4]: Data for 2014 (except for Sudan 2013) are obtained from World Bank [5].

3.5. Building Sector Energy Consumption Trends

In this section, the energy consumption specific to the building sector is compiled for the Arab region, sub-regions, and individual countries based on reported data over the last two decades [1]. In particular, the general trends of energy consumption and mix for both residential and non-residential (i.e., commercial and services) buildings are evaluated and discussed.

3.5.1. Overall Trends for the Arab Region

As shown in Figure 8, the total final energy consumption (TFEC) attributed to the building sector has been increasing steadily in the Arab region since 1990 with a clear transition from oil products to electricity use. Indeed, and as clearly illustrated in Figure 8a, the energy mix for the building sector has transitioned from a preference for oil products during 1990 representing 41% of the overall buildings TFEC to a dominance of electricity used to meet over 60% of the total Arab region-building sector needs during 2015. Moreover, the annual total final energy consumption of the buildings has increased consistently since 1990 as indicated in Figure 8b showing a linear trend between years and total building energy uses. If the linear trend continues unchanged, buildings in the Arab countries would consume 1450 TWh by 2030 doubling the 2006 energy consumption level and 2000 TWh by 2050 almost doubling the 2015 energy use level. The share of the building sector in TFEC remained in the range of 18% to 23% over the 1990–2015 period mostly dominated by households' energy use. Using the reported efficiencies for converting primary energy supply to final energy consumption, the share of the building sector in TPES is estimated for the Arab region has increased over the year from 22% in 1990 to 28% in 2015. Specifically and during 2015, buildings in the Arab countries consumed 1062 TWh mostly electricity (60%) to operate increasing demands attributed mainly to lighting, appliances, and cooling systems [10]. For commercial and public buildings, electricity represents 88% of the total energy consumed in the Arab region. While for residential buildings, electricity covers 50% of the

energy needs in most Arab countries. Oil products, natural gas, and renewables provide respectively 21%, 10%, and 9% of TFEC associated with the building sector to meet most likely non-electrical energy demands specific to domestic hot water, cooking, and space heating needs [10].

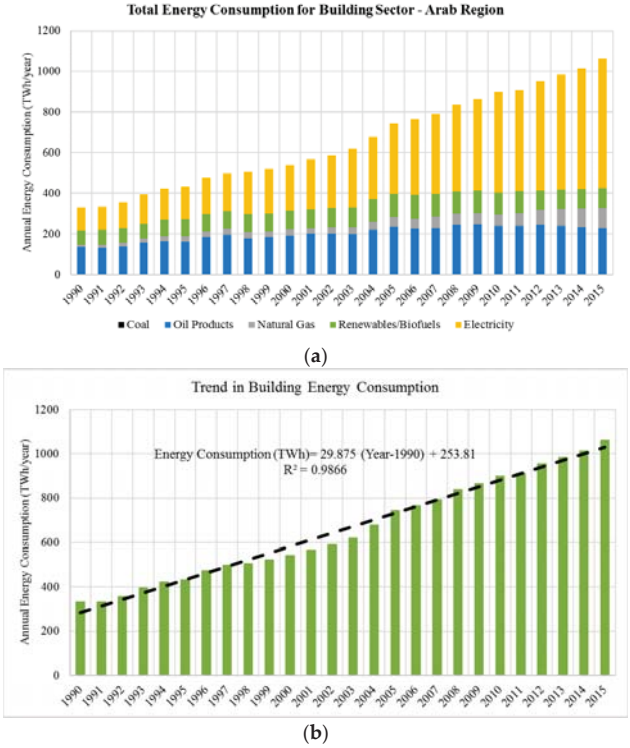

Figure 8. Total annual energy use of the building sector in the Arab region between 1990 and 2015. (**a**) Energy mix; (**b**) trend between energy consumption and year.

It should be noted that while electricity represents 60% of the energy used by buildings, it accounts for only 18% of the overall TFEC for the Arab region during 2015. Electricity is generated primarily from natural gas (65%) and oil products (30%) with renewables (3%) and coal (2%) providing minor contributions.

3.5.2. Trends for Arab Sub-Regions

The annual energy consumption associated with the building sector varies significantly among the Arab sub-regions. Since 2010, GCC consumes the most energy attributed to buildings among all four sub-regions due to the drivers outlined in Sections 3.1–3.4. However, the building sector represents less than 13% of the overall GCC in the GCC TFEC, one of the lower shares with the Arab region as illustrated in Figure 9. In particular, buildings are responsible during the period 2010–2015 for 27%, 28%, and 42% of TFEC for respectively, the Mashreq, Maghreb, and LDC.

When considering the primary energy requirements to generate electricity commonly used in buildings within the Arab region, the building sector share to TPES increases in all the sub-regions as shown in Figure 10 for 2015. In particular, the building sector share for the GCC sub-region increases from 13% relative to TFEC to 32% relative TPES due to the heavy reliance on electricity to meet the energy needs of buildings.

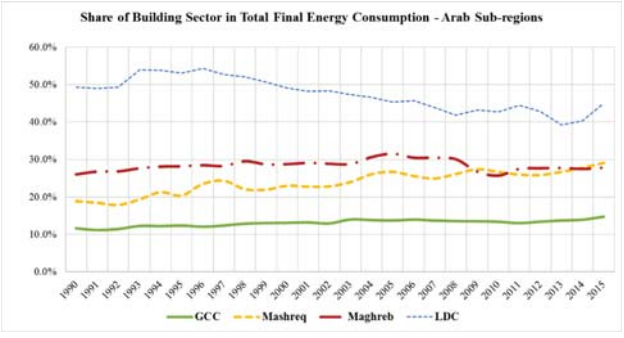

Figure 9. Annual share of the building sector of the overall total final energy consumption (TFEC) for the Arab sub-regions.

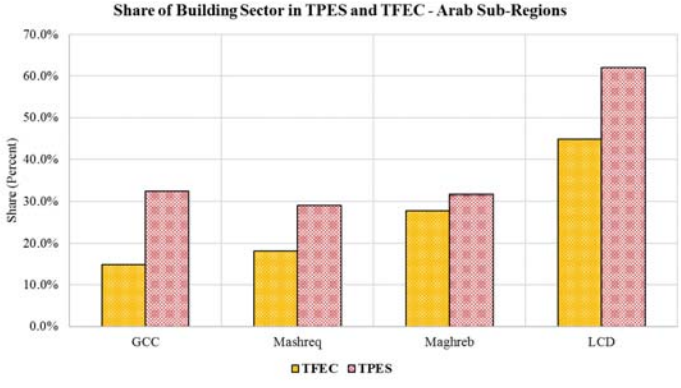

Figure 10. Share of the building sector in the Arab Sub-regions TPES and TFEC for 2015.

3.5.3. Trends for Individual Arab Countries

The contribution of the building sector in the national total final energy consumption (TFEC) varies also significantly among countries within the Arab region. Figure 11a shows the annual contribution of the building sector in national TFC for three years 1990, 2000, and 2015 for all the Arab countries with reported data [1]. Among the Arab countries, the TFEC share of the building sector is highest for Sudan (57% in 2015) and is the lowest for Qatar (10% in 2015). For all the Arab countries, residential buildings consume more energy than commercial/public buildings as indicated in Figure 11b.

During 2015, residential buildings in the entire Arab region have consumed 791 TWh of total final energy representing 75% of all energy used by the building sector. Figure 12a illustrates the energy mix used by households in each Arab country during 2015 [1]. Similarly, Figure 12b shows the energy mix for commercial and public buildings specific to the Arab countries with available data during 2015. Generally, the GCC countries utilize mostly electricity while other countries combine electricity with fossil fuels to meet the energy needs for their residential and commercial building stocks. As indicated in Figure 12, Sudan relies heavily on hydroelectric power to cover the electricity needs of its buildings including 84% of the total energy consumed by households. Among all the Arab countries, Saudi Arabia consumes the highest energy for both residential and commercial buildings. Indeed, buildings in Saudi Arabia have consumed 260 TWh during 2015 representing a third of the total final energy used by the building sector in the Arab region.

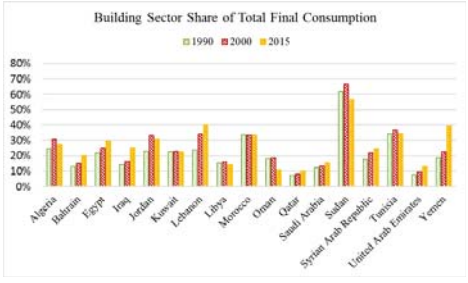

(**a**)

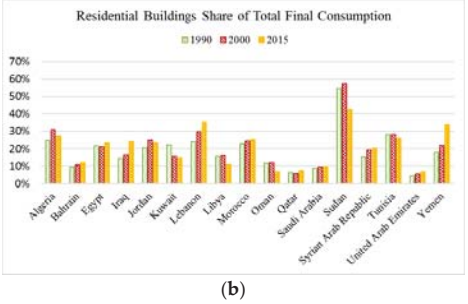

(**b**)

Figure 11. Share of (**a**) entire building sector and (**b**) the residential buildings in total final energy consumption in most countries within the Arab region for 1990, 2000, and 2015.

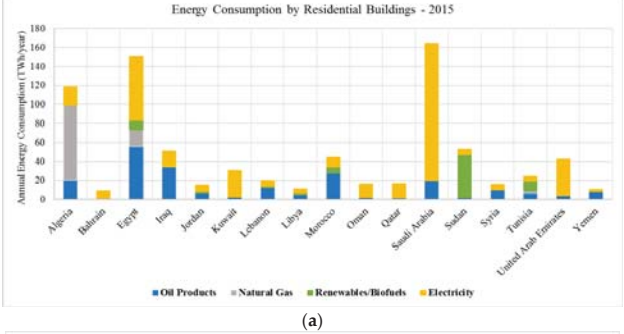

(**a**)

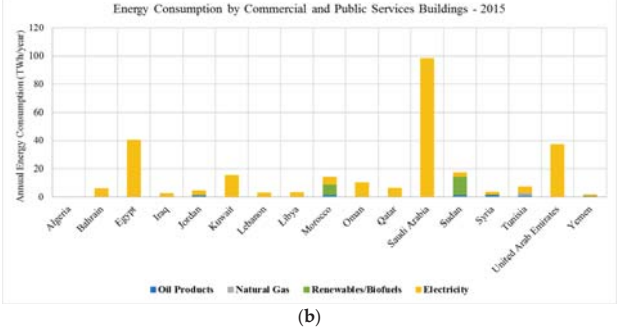

(**b**)

Figure 12. Total final consumption by energy sources for (**a**) residential and (**b**) non-residential (i.e., commercial and public) buildings for most Arab countries during 2015.

3.6. Energy Efficiency Indicators

Typically, two indicators are considered to assess the energy efficiency of the building sector: energy use per capita and energy use per floor area. In this section, estimations of these energy efficiency indicators are provided for the Arab region and its sub-regions.

3.6.1. Building Energy Use per Capita

The average building energy consumption per capita for the Arab region has been steadily increasing to almost double from 1990 (1475 kWh/person) to 2015 (2665 kW/person). However, the Arab region per capita building energy use remains low compared to the values reported for the World and the developed countries including EU and especially US as illustrated in Figure 13a [1]. It should be noted that the building energy consumption per capita for EU and US has started to decline since 2009 even though they remain significantly higher than the global average. Similar observations can be made about the building electricity consumption per capita as outlined in Figure 13b. Since 2010, buildings in the Arab region consume slightly more electricity per capita than the average reported for the World. Moreover, electricity meets increasingly higher percentage of the energy needs of the building sector jumping from 34% in 1990 to 60% in 2015.

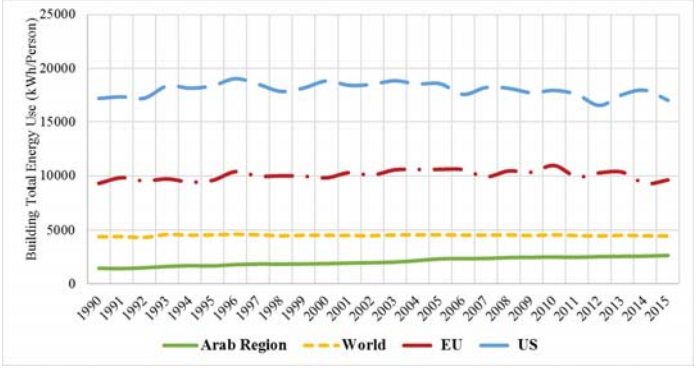

(**a**)

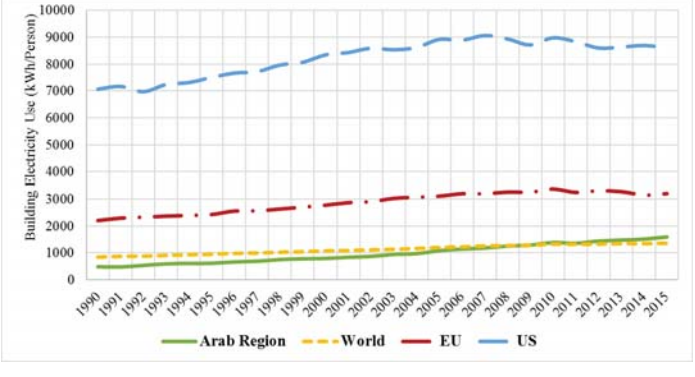

(**b**)

Figure 13. Annual per capita building (**a**) total final energy consumption and (**b**) total electricity consumption of the Arab region compared to those of the US, EU, and World.

The per capita building total energy consumption as well as electricity energy use vary widely within the Arab region as clearly shown in Figure 14 for both sub-regions and representative countries. It is clear that buildings in the GCC countries consume significantly more total energy use and electricity per capita than those in the other sub-regions. As noted earlier, electricity constitutes increasingly the vast majority of the energy used by buildings in the GCC and to a lesser extent in the other sub-regions.

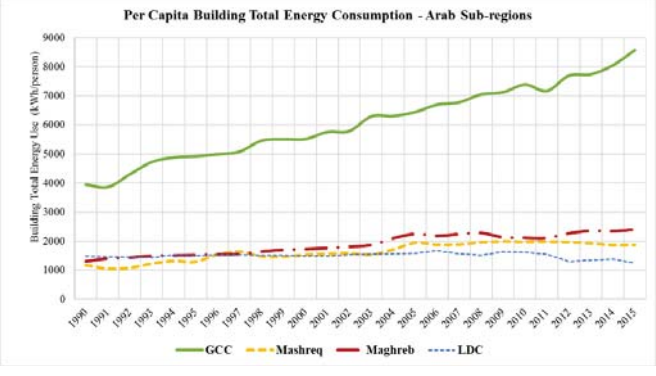

(**a**)

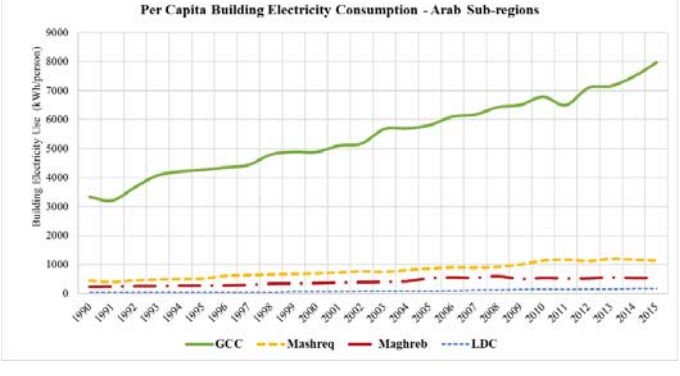

(**b**)

Figure 14. Annual per capita building (**a**) total energy consumption and (**b**) electricity consumption of the Arab sub-regions during the 1990–2015 period.

The total energy use per capita as well electricity use per capita for both residential and non-residential buildings in the four Arab sub-regions are illustrated in Figures 15 and 16, respectively. The results confirm the observations made earlier: the GCC sub-region's energy use per capita is significantly higher for both types of buildings compared to the other sub-regions. On the other hand, the LDC sub-region has the lowest energy use per capita not only of the Arab region but of the World.

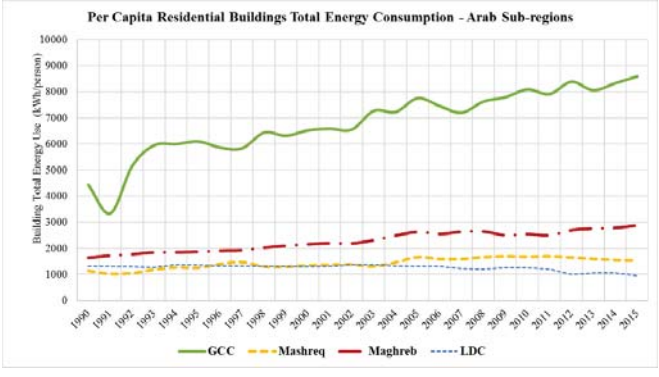

(**a**)

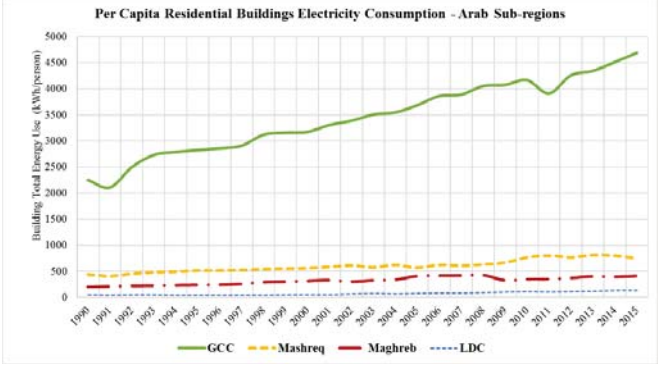

(**b**)

Figure 15. Annual per capita residential building (**a**) total energy consumption and (**b**) electricity consumption per capita of the Arab sub-regions during the 1990–2015 period.

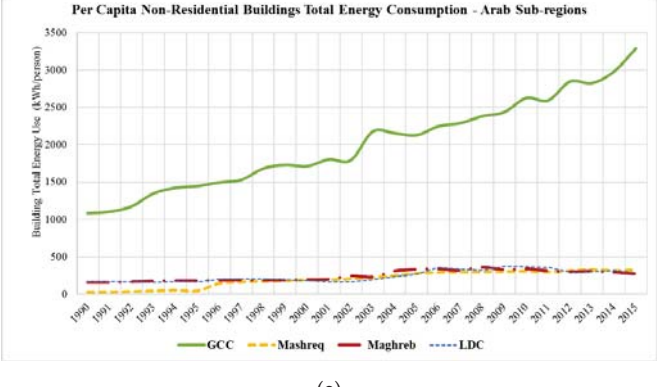

(**a**)

Figure 16. *Cont.*

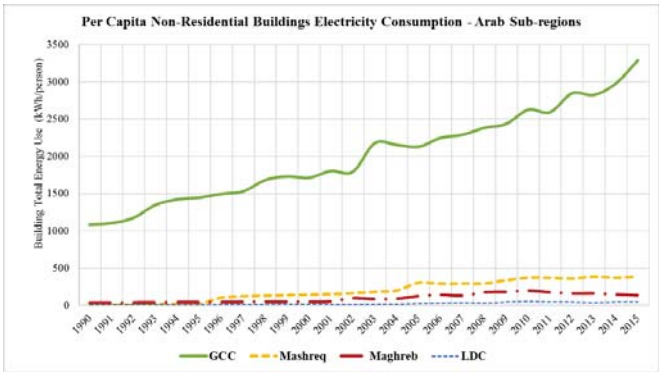

(**b**)

Figure 16. Annual per capita non-residential building (**a**) total energy consumption and (**b**) electricity consumption for the Arab sub-regions during the 1990–2015 period.

3.6.2. Building Energy Use per Floor Area

Building energy use per floor area provides another measure of building energy performance using the total occupied space. However, the use of this metric has to be considered with other factors such as the number of occupants and the type of equipment present within the building. For instance, improvements to the envelope, lighting, and heating/cooling systems typically reduce the overall building energy use and thus the building energy use per floor area. However, the addition of spaces may increase the building energy use while decreasing the building energy use per floor areas.

Table 9 lists reported energy use per building floor area, commonly known as energy use intensity (EUI), for the World, EU, US, China, and India [32]. The EUI values for the Arab region, estimated based on the IEA energy consumption data and the average floor area estimates outlined in Section 3.2, are also listed in Table 9 [32].

Table 9. Energy use intensity (EUI) (expressed in kWh/m^2) for the building sector for Arab region, World, US, EU, China, and India estimated for 2000, 2006, and 2016.

Country Region	2000	2006	2012
World	200	175	165
EU	223	215	187
US	212	207	197
China	131	108	102
India	195	180	165
Arab region *	72	89	96

(*) Estimated using the average building floor area estimations discussed in Section 3.2.

Two observations can be made from the EUI values summarized in Table 9. First, the Arab region EUI for the building sector has increased during the 2000–2012 period. This increase may be attributed to improvement in living standards and the use of energy-consuming devices such as air conditioning equipment, lighting, and appliances. The EUI values for the building sector in other regions of the World are significantly higher than that of the Arab region, but they have been decreasing. Worldwide, EUI for the building sector has decreased 17.5% in 2012 relative to 2000 levels most likely driven by the adoption and the implementation of significant energy efficiency programs in large economies and countries including US, EU, China, and India.

However, as noted earlier for the building energy consumption per capita, the EUI values vary widely among countries within the Arab region. Figure 17 shows the EUI variations for the 1990–2015 period for the four Arab sub-regions. The GCC sub-region has seen its building EUI doubles from 150 kWh/m^2 in 1990 to 300 kWh/m^2 in 2015. Meanwhile, the building sector EUI for the Mashreq and Maghreb sub-regions has slightly increased from 45 kWh/m^2 in 1990 to respectively 66 kWh/m^2 and 85 kWh/m^2, in 2015. The EUI for the LDC sub-region has remained constant at about 50 kWh/m^2 during the entire 1990–2015 period most likely due to stagnant and low living standards as well as lack of energy-intensive equipment in the building sector including AC systems as discussed in Section 3.3.

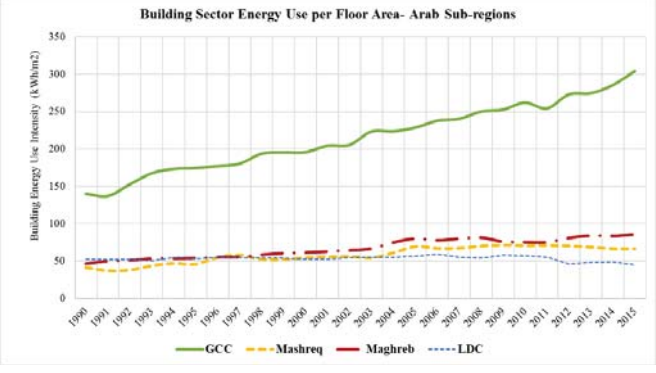

Figure 17. Building sector energy use per floor area for Arab sub-regions for the 1990–2015 period.

Figure 18 shows the EUI variations for the total final energy and electricity consumed by residential buildings during the 1990–2015 period for the four Arab sub-regions. The EUI values outlined in Figure 18 are consistent with reported energy use data of existing residential buildings in some Arab countries that represent three sub-regions: GCC, Mashreq, and Maghreb as summarized in Tables 10 and 11. In particular, Table 10 summarizes the compiled total residential building floor areas for Tunisia, Egypt, and Saudi Arabia [1]. Table 11 lists data obtained for a wide range of sources for some Arab countries using surveys or audits of existing residential buildings [25,33–36].

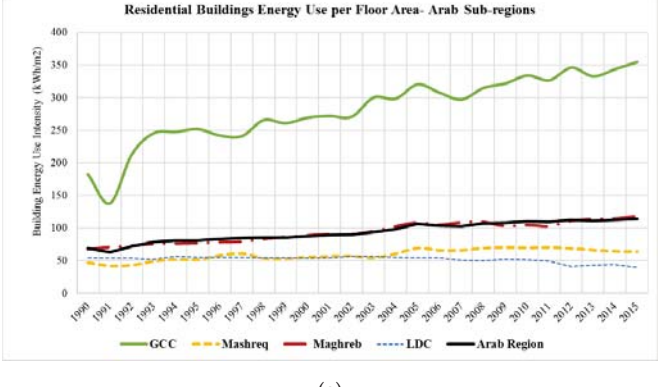

(**a**)

Figure 18. *Cont.*

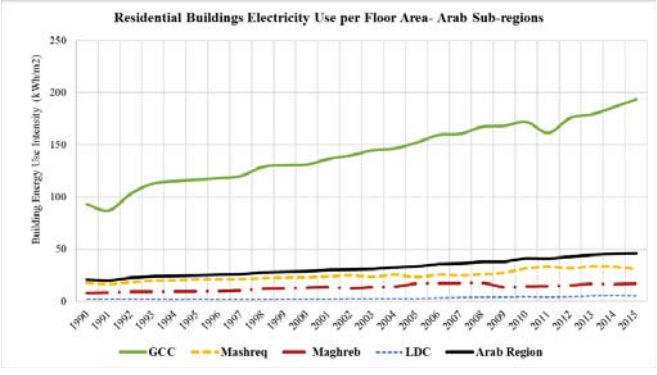

(**b**)

Figure 18. Annual residential buildings energy use intensity for (**a**) total energy use and (**b**) electricity consumption specific to the Arab Region and its sub-regions during the 1990–2015 period.

Figure 19 shows the EUI variations for non-residential buildings during the 1990–2015 period for the four Arab sub-regions. The EUI values outlined in Figure 19 are consistent with reported energy use data of existing non-residential buildings in some Arab countries that represent three sub-regions: GCC, Mashreq, and Maghreb as summarized in Table 12.

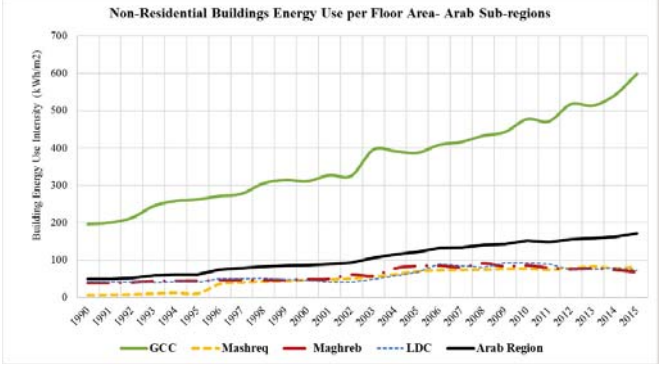

Figure 19. Annual non-residential buildings energy use intensity of the Arab sub-regions during the 1990–2015 period.

Table 10. Estimation of EUI for residential buildings based on data reported for three Arab countries.

Country	Census Year	Total Building Floor Area (million m^2)	Energy Consumption (TWh/year) *		Energy Use Intensity (kWh/m^2)	
			Total	Electricity	Total	Electricity
Egypt	2006	1476.463	99.967	36.603	67.7	24.8
Tunisia	2006	274.254	21.708	2.969	79.2	10.8
Saudi Arabia	2010	651.616	127.582	108.647	195.8	166.7

(*) Source of data: [1].

Table 11. Reported EUI values for residential buildings in select Arab countries.

Country (City)	Year of Reported Data	Type of Analysis	Energy Use Intensity (kWh/m^2/year)	References
Lebanon (Entire Country)	2013	Survey	135 (Total) 47 (Elec. Only)	[25] *
Tunisia (Entire Country)	2013	Survey	79 (Total) 12 (Elec. Only)	[25]
Saudi Arabia (Jeddah)	2011	Audit, Apartment	350	[33]
Saudi Arabia (Riyadh)	2015	Calibrated Modeling, Villa	228	[34]
UAE (Al-Ain)	2008	Audit, Villa	306	[35]
UAE (AL-Ain)	2008	Audit, Villa	269	[35]

(*) Average housing unit in Lebanon is set to 120 m^2 [36].

Table 12. Reported EUI values for non-residential buildings in select Arab countries.

Country (City)	Year of Reported Data	Type of Analysis	Energy Use Intensity (kWh/m^2/year)	References
Egypt (Entire Country)	2009	Survey		[37]
Office Buildings			84	
Shopping Malls			770	
Hotels			730	
Tunisia (Entire Country)	2006	Survey		[15]
Office Buildings			21	
Retail Stores			231	
Hotels			266	
Banks			284	
Universities			26	
All Non-Residential Buildings			87	
Saudi Arabia (Dammam)	2011	Audit, Shopping Malls	268	[38]
Saudi Arabia (Dammam)	2010	Audit, Six Shopping Malls	250–276	[39]
Kuwait (Kuwait-City)	2011	Audit, Educational Buildings	300–600	[40]
Bahrain (Manama)	2007	Audit, Office Buildings	100–805	[41]

4. Analysis of Energy Efficiency Potential for the Building Sector

The potential for improving the energy performance of buildings in the Arab region is significant for both new and existing building stocks due to the lack of any stringent energy efficiency codes and practices in most Arab countries. Indeed, several opportunities are available to reduce energy consumption and enhance the sustainability of buildings in the Arab region through well designed and targeted energy policies. In this section, some of these opportunities are compiled and evaluated based on detailed analyses and reported studies. In particular, the potential benefits of large-scale implementation of selected energy efficiency programs are presented for both new and existing building stocks. The analysis is based on a bottom-up approach of the building stock to account for the characteristics of the building stock in the Arab region. The details of the bottom-up approach, as well as the specific characteristics of the building energy models used in the simulation and optimization analyses are outlined in the literature for various countries in the Arab region [2,10–12,42–46].

4.1. Benefits for Improved MEPS

The potential benefits of setting minimum energy performance standards (MEPS) based on currently available energy efficiency equipment and appliances commonly used in buildings have been estimated by a study reported by United for Energy Efficiency [47]. In particular, the analysis has considered energy-consuming products commonly used in residential buildings including air conditioners, refrigerators, and lighting. The potential annual savings in both electricity consumption and carbon emissions during 2030 for several Arab countries are summarized in Table 13 (lighting), Table 14 (refrigerators), and Table 15 (room air conditioners) based on the implementation of stricter MEPS in 2020 [47]. While refrigerators are specific to residential buildings, lighting, and room air conditioners can affect energy consumption of both residential and commercial buildings.

Table 13. Potential annual benefits attributed to lighting minimum energy performance standards (MEPS) in the Arab region.

Country	Electricity Use [1] (TWh/year)		Energy Cost [1] (USD Million/year)		Carbon Emissions [2] (Million Tonnes/year)	
	2025	2030	2025	2030	2025	2030
Algeria	2.365	2.371	70.9	71.1	1.470	1.474
Bahrain	0.305	0.316	7.0	7.3	0.207	0.215
Egypt	1.711	2.198	78.7	101.1	0.840	1.079
Iraq	1.333	1.387	10.7	11.1	1.351	1.406
Jordan	0.442	0.468	88.4	93.6	0.284	0.300
Kuwait	1.571	1.618	15.7	16.2	1.355	1.396
Lebanon	0.452	0.477	28.9	30.5	0.344	0.363
Libya	1.417	1.418	42.5	42.5	1.023	1.024
Morocco	1.479	1.476	177.5	177.2	1.118	1.115
Oman	0.725	0.746	37.7	38.8	0.593	0.610
Palestine	0.150	0.156	23.7	24.6	0.119	0.124
Qatar	1.395	1.437	34.9	35.9	0.693	0.714
Saudi Arabia	8.000	8.200	400.1	412.4	6.400	6.600
Syria	0.251	0.325	2.5	3.3	0.163	0.212
Sudan	0.180	0.225	8.4	10.4	0.061	0.076
Tunisia	0.771	0.715	69.4	64.3	0.383	0.355
UAE	3.100	3.200	361.1	367.3	2.038	2.072
Yemen	0.109	0.114	3.0	3.1	0.075	0.078
Total	25.756	26.847	1461.1	1510.7	18.517	19.213

[1]: Source: [47]; [2]: Estimated based on IEA carbon emission factors for each country [1].

Table 14. Potential annual benefits attributed to MEPS for refrigerators in the Arab region.

Country	Electricity Use [1] (TWh/year)		Energy Cost [1] (USD Million/Year)		Carbon Emissions [2] (Million Tonnes/year)	
	2025	2030	2025	2030	2025	2030
Algeria	0.803	1.545	24.1	46.4	0.499	0.960
Bahrain	0.047	0.090	1.1	2.1	0.032	0.061
Egypt	1.901	3.963	87.40	182.3	0.933	1.945
Iraq	0.511	1.020	4.1	8.2	0.518	1.034
Jordan	0.117	0.243	23.4	48.6	0.075	0.156
Kuwait	0.180	0.325	1.8	3.3	0.156	0.280
Lebanon	0.094	0.189	6.0	12.1	0.072	0.144
Libya	0.136	0.262	4.1	7.9	0.098	0.189
Morocco	0.458	0.897	55.0	107.7	0.346	0.678
Oman	0.069	0.137	3.6	7.1	0.056	0.112
Palestine	0.074	0.153	11.7	24.2	0.059	0.112
Qatar	0.035	0.072	0.90	1.8	0.017	0.036
Saudi Arabia	0.800	1.500	40.4	77.20	0.600	1.200
Syria	0.376	0.756	3.8	7.6	0.245	0.493
Sudan	0.608	1.255	28.3	58.4	0.206	0.425
Tunisia	0.177	0.336	15.9	30.2	0.088	0.167
UAE	0.400	0.700	40.9	85.7	0.231	0.484
Yemen	0.186	0.408	5.0	11.0	0.127	0.280
Total	6.972	13.851	357.5	721.8	4.358	8.756

[1]: Source: [47]; [2]: Estimated based on IEA carbon emission factors for each country [1].

Table 15. Potential annual benefits attributed to improved MEPs for room air-conditioners in the Arab region.

Country	Electricity Use Savings [1] (TWh/year)		Carbon Emissions Reduction [2] (Million Tons/year)	
	2025	2030	2025	2030
Algeria	0.392	0.756	0.215	0.415
Bahrain	0.021	0.033	0.008	0.012
Egypt	0.687	1.266	0.275	0.507
Iraq	0.683	1.246	0.693	1.264
Jordan	0.105	0.18	0.061	0.105
Kuwait	0.055	0.091	0.039	0.065
Lebanon	0.072	0.122	0.056	0.094
Libya	0.122	0.201	0.237	0.391
Morocco	0.252	0.484	0.140	0.269
Oman	0.117	0.2	0.057	0.097
Palestine	0.003	0.006	0.002	0.005
Qatar	0.051	0.085	0.015	0.026
Saudi Arabia	2.2	3.6	1.258	2.058
Sudan	0.346	0.852	0.081	0.199
Sudan	0.346	0.852	0.183	0.451
Tunisia	0.133	0.238	0.063	0.113
UAE	1.1	1.7	0.499	0.770
Yemen	0.04	0.082	0.083	0.170
Total	6.448	11.271	3.965	7.012

[1]: Source: [47]; [2]: Estimated based on IEA carbon emission factors for each country [1].

As noted in the results shown in Table 13 through Table 15, the overall annual electrical savings that can be achieved by 2030 from updating, implementing, and enforcing MEPS in the Arab region are highest for lighting (26.847 TWh/year) followed by refrigerators (13.851 TWh/year) and then room air conditioners (11.271 TWh/year). Based on business as usual (BAU) projections for 2030, these savings represent 1.9% (lighting), 0.9% (refrigerators), and 0.8% (room air conditioners) of the final energy consumption of the building sector in the Arab region.

Table 16 summarizes the cumulative savings in both electricity energy use and carbon emissions due to improved MEPS for lighting, residential refrigerators, and room air conditioners for each Arab country [47]. It is clear that improved lighting standards have the highest impact among all three options with potential savings over the 10 year period (2020 through 2030) of 227 TWh in electricity consumption and 144 million tonnes in carbon emissions, three times the benefits of improving MEPS for either residential refrigerators or room air-conditioners.

Table 16. Cumulative from 2020 to 2030 benefits attributed to improved MEPs for, lighting, residential refrigerators, and room air-conditioners in the Arab region.

Country	Lighting		Residential Refrigerators		Air Conditioners	
	Electricity Use Savings [1] (TWh)	Carbon Emissions Reduction [2] (Million Tonnes)	Electricity Use Savings [1] (TWh)	Carbon Emissions Reduction [2] (Million Tonnes)	Electricity Use Savings [1] (TWh)	Carbon Emissions Reduction [2] (Million Tonnes)
Algeria	20.5	11.2	8.7	4.8	4.3	2.4
Bahrain	2.7	1.0	0.5	0.2	0.2	0.1
Egypt	16.3	6.5	21.3	8.5	7.3	2.9
Iraq	11.8	12.0	5.6	5.7	7.3	7.4
Jordan	3.9	2.3	1.3	0.8	1.1	0.6
Kuwait	13.8	9.8	1.9	1.4	0.6	0.4
Lebanon	4	3.1	1	0.8	0.7	0.5
Libya	12.3	23.9	1.5	2.9	1.3	2.5
Morocco	12.8	7.1	5	2.8	2.7	1.5
Oman	6.4	3.1	0.8	0.4	1.2	0.6
Palestine	1.3	0.8	0.8	0.7	0	0.0
Qatar	12.2	3.7	0.4	0.1	0.5	0.2
Saudi Arabia	70.3	40.2	8.7	5.0	22.5	12.9
Syria	2.4	0.6	4.2	1.0	0.7	0.2
Sudan	1.7	0.9	6.8	3.6	4.2	2.2
Tunisia	6.6	3.1	1.9	0.9	1.4	0.7
UAE	27.2	12.3	4	1.8	10.7	4.8
Yemen	1	2.1	2.1	4.4	0.5	1.0
Total	227.2	143.7	76.5	45.6	67.2	40.9

[1]: Source: [47]; [2]: Estimated based on IEA carbon emission factors for each country [1].

4.2. Impact of LED Systems for Commercial Buildings

For commercial and public buildings, LED fixtures integrated with advanced control capabilities are now becoming more widespread due their ease of installation and lower costs. In particular, LED fixtures with integrated control systems allow a reduction in both lighting power density and lighting energy use since they can act as sensors in small or open spaces and provide daylight dimming controls. A field study has demonstrated and documented the performance of the integrated control LED fixtures for two commercial buildings in the US [48]. Each integrated control LED unit includes LED lamp, driver, a set of daylighting controls, and an occupancy sensor. The LED units are designed to replace T-8 and T-12 fluorescent fixtures using existing wiring systems [48]. The analysis of the reported experimental studies, as well as other simulation based analyses, have shown that integrated controls LED units can save more than 50% of the lighting energy consumption as well as 30% of

lighting power density in commercial buildings [48–50]. In this section, a large-scale replacement program of fluorescent lighting systems with integrated control LED units is considered for both commercial and public buildings in the Arab region with a 10 year implementation plan starting by 2020. Conservative savings of 40% and 20%, respectively, in electricity energy use and peak demand, are considered for the Arab countries. The conservative estimates are made to take into account that electrical peak demands may not occur at the same time for all building types and all countries. In recent years, however, the vast majority of Arab countries have their highest electricity demands occur during the hot summer days.

The potential benefits for such a program are summarized in Table 17 for each Arab country for both 2025 and 2030 including savings in electricity consumption, peak electrical demand, and carbon emissions using the same approach as detailed in [47]. The overall reduction in annual electrical energy use is estimated at 21.660 TWh at the end of 2030 representing 1.5% of total final energy consumed by the building sector in the Arab region. It should be noted that this program can be implemented and enforced through a retrofit program specific to commercial and public buildings. Moreover, it should be noted that while lighting MEPS affect only the power density installed, the control LED lighting units result in lower time of use of the lighting systems and thus are more effective in reducing in electricity consumption as illustrated by their potential savings shown in Table 17 for non-residential buildings. These savings have the same order of magnitude as those estimated for improved lighting MEPS applied to both residential and non-residential buildings listed in Table 13.

Table 17. Potential annual benefits attributed to using integrated control LED lighting units in commercial and services buildings in the Arab region.

Country	Electricity Use Savings (TWh/year)		Peak Demand Reduction (MW)		Carbon Emissions Reduction (Million Tons/year)	
	2025	2030	2025	2030	2025	2030
Algeria	0.000	0.000	258.960	517.920	0.000	0.000
Bahrain	0.246	0.491	77.220	154.440	0.090	0.180
Egypt	1.607	3.214	929.500	1859.000	0.644	1.288
Iraq	0.101	0.202	762.960	1525.920	0.103	0.205
Jordan	0.184	0.368	132.200	264.400	0.107	0.214
Kuwait	0.615	1.229	720.000	1440.000	0.438	0.875
Lebanon	0.113	0.227	76.680	153.360	0.088	0.175
Libya	0.133	0.266	309.600	619.200	0.258	0.517
Morocco	0.568	1.137	216.808	433.616	0.316	0.632
Oman	0.402	0.804	269.500	539.000	0.195	0.391
Qatar	0.251	0.501	228.908	457.816	0.075	0.150
Saudi Arabia	3.930	7.861	1545.660	3091.320	2.247	4.494
Sudan	0.690	1.380	109.873	219.746	0.161	0.323
Syria	0.137	0.273	78.750	157.500	0.072	0.145
Tunisia	0.300	0.600	134.280	268.560	0.142	0.285
United Arab Emirates	1.487	2.973	994.740	1989.480	0.674	1.347
Yemen	0.066	0.133	57.600	115.200	0.138	0.276
Total	10.830	21.660	6903.239	13806.478	5.748	11.496

4.3. Impact of EE Programs for New Buildings

As noted earlier, there are no specific mandatory building energy efficiency codes (BEECs) in several Arab countries. BEECs includes a set of mandatory design requirements to improve the energy performance of buildings. Since the 1970s, BEECs have been developed and enforced successfully in several countries and have been shown to be effective in reducing energy consumption of buildings. In particular, the implementation of mandatory BEECs has resulted in significant energy use reduction of households for most EU countries [32]. Typically, two approaches are commonly considered for the development and adoption of BEECs specific to new buildings including:

- Prescriptive-based approach: In this case, the BEECs include sets of minimum energy performance requirements for each component of the building—windows, walls, and heating and cooling equipment.
- Performance-based approach: In this option, the BEECs are based on sets of performance requirements and targets for the overall building energy consumption. Thus, performance-based BEECs encourage integrated design approach to account for interactions between building components in order to optimize the energy performance for the entire building.

Based on a detailed review of existing energy efficiency regulations related to the building sector, Table 18 summarizes the status of building energy efficiency regulations for various Arab countries [2,6,10–12,43–46,51]. Moreover, Table 18 lists the Regulatory Indicators for Sustainable Energy (RISE) score provided for each country for their efforts to implement energy efficiency policies [52]. In particular and as indicated in Table 18, Tunisia has the highest score mostly due to its adoption and enforcement of building energy efficiency codes for both residential and commercial buildings. Indeed, the energy efficiency code for Tunisia for new buildings is one of the most comprehensive in the Arab region and includes both prescriptive and performance paths for compliance.

4.3.1. Building Envelope Thermal Performance

In this section, the benefits of improved building envelope thermal performance are evaluated for those Arab countries without mandatory codes. While the addition of thermal insulation may not be always beneficial to reduce overall energy consumption of buildings, especially those located in temperate climates [53], analyses specific to both residential and commercial buildings located in all Arab countries have indicated that thermal insulation applied to walls and roofs result in reduction of heating and cooling energy end-uses [10,45]. Moreover, it has been shown that the addition of insulation can be beneficial even for non-conditioned buildings since it can improve indoor thermal comfort while may not affect significantly the buildings energy consumption [10]. Recent analyses have shown that dynamic insulation systems that can change their thermal properties depending on the seasons and even outdoor conditions can achieve even more energy savings and indoor thermal comfort than conventional static insulation systems [54,55]. However, affordable prototypes of these systems are still not commercially available.

If 50 mm polystyrene thermal insulation for walls and roofs as well as double-pane glazing for windows are required for new buildings, an estimated average reduction of annual energy consumption of at least 10% reduction in energy consumption and electrical peak demand can be achieved for new buildings in the Arab region [10,45]. The savings for countries with hot climates such as GCC countries are expected to be higher as noted in the previous section. Using the bottom-up analysis carried by Krarti [11], the economic and environmental benefits of the thermal insulation requirements on new buildings are estimated for the Arab countries as summarized in Table 19. Only countries with no building energy efficiency codes prior to 2014 (refer to Table 18) are included in estimating the analysis summarized in Table 19. The carbon emissions for generating electricity are based on each country's emission factor [1]. The analysis assumes that the annual contribution of energy consumption due to new buildings is 4% [11].

Table 18. Status of building energy efficiency regulations in Arab countries.

Country	Building EE Regulation (Year of Implementation)	Type of Compliance	Mandatory/Voluntary	EE RISE Score (Max. 100)
Algeria	Thermal Insulation for building envelope (2005)	Prescriptive	Mandatory	56
Bahrain	Thermal Insulation Requirements for commercial buildings (1999) and other building types (2013)	Prescriptive	Mandatory	25
Egypt	Energy Efficiency code for residential (2005), commercial (2009), and public buildings	Prescriptive and Performance	Mandatory	48
Iraq	Energy Efficiency Specifications for Buildings (2012)	Prescriptive	Voluntary	NA
Jordan	Energy Conservation Building Code (2010)	Prescriptive	Mandatory	57
Kuwait	Energy Conservation Code of Practice No. R-6 (1983 updated 2014)	Prescriptive	Mandatory	30
Mauritania	None	NA	NA	9
Morocco	Energy Efficiency Code (2015)	Prescriptive and Performance	Mandatory	42
Lebanon	Thermal Insulation Requirements ARZ Building Rating System for Existing Buildings (LBGC, 2011)	Prescriptive Evidence-based building rating systems for existing commercial buildings	Voluntary Voluntary	35
Libya	None	NA	NA	NA
Oman	None	NA	NA	
Palestine	Energy Efficiency Code for Buildings (2004)	Prescriptive	Voluntary	NA
Qatar	Global Building Assessment System (GSAS): All new Public Buildings (2012) All new Commercial Buildings (2016) All new Residential Buildings (2020)	Sustainable Building Label System	Mandatory	50
Saudi Arabia	Thermal Performance Code (2014)	Prescriptive	Mandatory	49
Sudan	None	NA	NA	19
Syria	Thermal Insulation Code (2009)	Prescriptive	Mandatory	NA
Tunisia	Energy Efficiency code for residential (2009) and select commercial and institutional buildings (2008)	Prescriptive and Performance	Mandatory	68
United Arab Emirates (Dubai)	Thermal Insulation requirements (2003) Green Building Regulations and Specifications (2011)	Prescriptive Performance	Mandatory Voluntary	63
Yemen	None	NA	NA	12

Table 19. Economic and environmental benefits for requiring better-insulated building envelope systems for all new buildings in the Arab region (only countries without any building energy efficiency codes (BEECs) prior to 2014 are considered as listed in Table 18).

Building Type	Annual Energy Use Savings (TWh/year)	Peak Demand Savings (MW)	Annual CO_2 Emissions Savings (Million Tons/year)
Residential Buildings	1.263	228	0.39
Commercial and Public Buildings	0.532	96	0.17
Total	1.795	324	0.560

4.3.2. Integrated Building Energy Performance

When combined, proven energy efficiency strategies can be effective in significantly reducing building energy consumption in the Arab region [31,33,34,56–58]. Indeed, when appropriate energy efficiency strategies are applied to new buildings, over 30% of energy use can be saved relative to the current construction practices in the Arab region. In particular, the potential energy savings and implementation costs associated to design high-performance residential buildings in the Arab region have been evaluated for the Arab countries using the integrated analysis approach described in [8,10]. This approach involves modeling the energy performance of representative buildings as well as optimization analysis to select among various energy efficiency measures using the life-cycle cost (LCC) method and has already been applied to several Arab countries [8,10,33,34,57,58]. Table 20 summarizes the results of the analysis for the Arab countries including the annual electrical energy consumption, reduction in life-cycle costs for 30 years, and increase in construction costs to achieve optimal energy efficiency designs [8]. The optimal analysis for villas located in various Arab cities is detailed in [8]. The increase in construction costs listed in Table 20 considers additional capital costs required to integrate energy efficiency designs. As shown in Table 20, a savings range of 31% to 56% in energy use is found in all Arab cities considered in the analysis. The optimal design for the residential buildings has lower LCC values with a reduction ranging from 13% to 25% relative to the baseline cases. It should be noted that the additional costs to implement the optimized energy efficiency options are rather reasonable with an increase of construction costs relative to that of the baseline designs varying between 2% and 20% depending on the climate and the set of energy-efficiency measures to implement [8]. The reduction of the LCCs is mainly attributed to lower operating costs associated with the decrease in annual energy consumption. Over the building lifetime, the annual energy cost reduction outweighs the increase in building construction costs to implement more energy-efficient features [8].

As noted in Table 20, annual primary energy savings ranging between 35% and 55% can be achieved using optimal designs. The highest savings are achieved for hot climates especially in the GCC region while the lowest savings are obtained for regions with mild climates.

Based on the reported literature, more effective building energy efficiency codes (BEECs) can be developed throughout the entire Arab region and for all new buildings. As illustrated in Table 20, 35% to 55% savings can be achieved using integrated and optimal designs for residential buildings [8]. For this study, the impact of integrated design based BEEC is assumed to be 30% savings in both energy consumption and peak demand associated with the new building stock in the Arab region. This conservative saving level is used in this analysis specific to the Arab region to account for the diversity of climate conditions, behavioral changes, and energy efficiency rebound effects [59–61]. In particular, the impacts of occupant behavior on the energy efficiency of the built environment can be significant even though these impacts depend on several factors and remain difficult to quantify for a large-scale analysis [62–64]. The benefits of integrated design based BEECs applied to the new buildings are estimated and are summarized as shown in Table 21.

Table 20. Summary of energy use savings and normalized life-cycle cost (LCC) values and implementation costs for minimizing LCC to achieve optimal designs for residential buildings in select Arab cities.

Country	City	Optimal Energy Saving [%]	Optimal LCC Reduction [%]	Construction Cost Increase for Optimal Design *
Algeria	Oran-Senia	33	14	5
Egypt	Cairo	31	13	4
Jordan	Amman	45	15	17
Kuwait	Kuwait	56	25	20
Lebanon	Beyrouth	32	14	3
Libya	Tripoli	47	16	17
Morocco	Rabat	33	15	2
Oman	Salalah	32	14	2
Qatar	Doha	47	17	14
Saudi Arabia	Riyadh	55	22	20
Syria	Damascus	49	18	17
Tunisia	Tunis	47	16	17
UAE	Abu-Dhabi	43	16	11

(*): The construction costs considered in the analysis include those of walls, roofs, heating, air conditioning, and lighting systems [8].

Table 21. Economic and environmental benefits for implementing integrated BEECs for all new buildings in the Arab region.

Building Type	Annual Energy Use Savings (TWh/year)	Peak Demand Savings (MW)	Annual CO_2 Emissions Savings (Million Tons/year)
Residential Buildings	9.490	1543	2.960
Commercial and Public Buildings	3.249	528	1.014
Total	12.739	2071	3.974

The baseline (i.e., BAU) scenario for future energy consumption for buildings in the Arab region can be estimated based on a regression analysis of the trend shown in Figure 20. The regression analysis indicates an average annual growth rate from 2015 to 2050 of 3.1%. This growth rate is consistent with the rates considered for the MENA region of 3.6% by IEA specific to the building sector and of 2.9% for the electricity demand [1].

As indicated in the projection profiles of Figure 20, the implementation starting from 2020 of the two BEEC types outlined above reduces future energy consumption slowly as the building stock is replaced by new construction over time. To account for new construction addition including demolition and renovation of the existing building stock, a 4% annual rate is considered for the addition of new construction for the Arab region [12]. The impact of improving building envelope systems (i.e., through the addition of thermal insulation) is rather minimal since most of the Arab countries have already mandatory thermal insulation code requirements and are not included in the analysis of this study. However, the implementation starting from either 2020 (Figure 20a) or 2030 (Figure 20b) of an integrated design based BEEC has the potential to reduce substantially the energy demand of the building sector. Specifically, when the integrated design based BEEC requirements are set to start in 2020, the annual savings in the Arab region can reach 127 TWh and 382 TWh by 2030 and 2050, respectively. Lower annual savings of only 210 TWh are obtained for 2050 when the integrated BEEC is required by 2030.

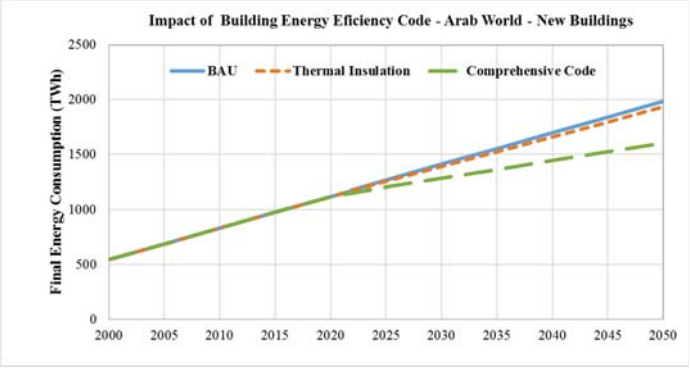

(**a**)

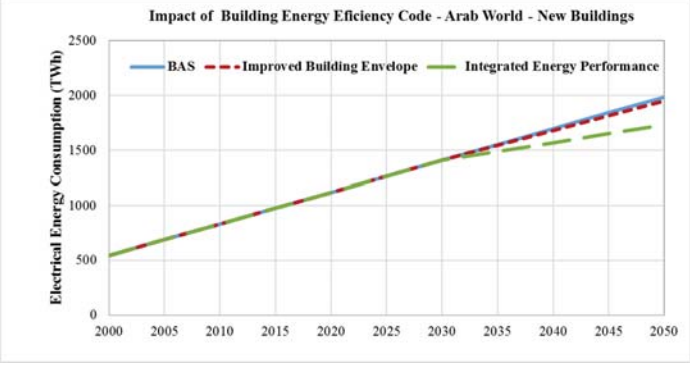

(**b**)

Figure 20. Impact on total final energy consumption of buildings due to implementation of energy efficiency codes for new buildings in the Arab region with the start of implementation in (**a**) 2020 and (**b**) 2030.

4.4. Impact of EE programs for Existing Buildings

In order to improve the energy performance of existing building stock, three levels of building retrofits are typically considering with different capital cost requirements and varying energy saving potentials and ultimately economic and environmental benefits. These three levels of energy retrofits of existing buildings include [50,60]:

- ***Level-1 of energy retrofit:*** This basic retrofit involves mostly low-cost energy efficiency measures such as replacement of lighting fixtures with LED units and weatherization of building shells to reduce air infiltration. As detailed in several other studies, the estimated average savings from a Level-1 retrofit program are about 8% for all building types based on the simulation analysis carried out for several Arab countries as well as case studies reported for residential, commercial, and governmental buildings [2,10,42–46,56–58].
- ***Level-2 of energy retrofit:*** In addition to Level-1 measures, this retrofit includes the use of energy-efficient equipment as well as temperature and lighting controls. Based on reported studies in the Arab region as well as from the simulation results outlined in this study for Arab countries, average savings of about 23% can be achieved for Level-2 retrofits for all building types [2,42–46].
- ***Level-3 of energy retrofit:*** This type of retrofit, known as a deep retrofit, requires the implementation of capital-intensive measures including the addition of roof thermal insulation,

cooling system replacement, and installation of automated control systems. While deep retrofits are typically costly, they can provide significant energy use savings exceeding 50% as noted in several reports and as noted for the optimal analysis conducted for the Arab region [2,10,42–46].

The specific measures of each retrofit level have to be tailored to the building type and the climate. Table 22 illustrates three options of specific energy efficiency measures that can be considered for residential building types based on a study performed for Oman for all three retrofit levels [2]. Table 22 provides estimates for the annual energy savings associated with each option and retrofit level.

Table 22. Options for energy efficiency measures specific to three retrofit levels of Omani residential buildings (source: [2]).

Recommended Options	Retrofit Description [(a)]	Retrofit Level for Residential Buildings		
		Level-1	**Level-2**	**Level-3**
1.	List of EEMs	EEM-1	EEM-1, EEM-2, and EEM-3	EEM-1, EEM-2, EEM-3, and EEM-4
	Energy Use Savings	12%	28%	54%
	Range of reduction in savings due to behavioral and rebound effects [(b)]	0%–6%	0%–6%	0%–6%
2.	List of EEMs	EEM-2	EEM-4	EEM-2, EEM-3, and EEM-6
	Energy Use Savings	10.0%	29%	51.0%
	Range of reduction in savings due to behavioral and rebound effects [(b)]	0%–4%	0%–4%	0%–4%
3.	List of EEMs	EEM-3	EEM-5	EEM-5, and EEM-6
	Energy Use Savings	10%	28%	52%
	Range of reduction in savings due to behavioral and rebound effects [(b)]	0%–4%	0%–6%	0%–6%

Notes:

(a) Description of EEMs:

- EEM-1: Increase the cooling set from 21 °C to 23 °C, from 22 °C to 24 °C, or from 23 °C to 25 °C depending on the existing operating conditions.
- EEM-2: Replace existing lighting fixtures by LEDs.
- EEM-3: Seal air leakage sources around the building envelope (i.e., window and door frames so ACH = 0.21).
- EEM-4: Replace the existing AC unit by a high-efficiency system (COP = 4.0).
- EEM-5: Better lighting controls including dimming daylighting and occupancy sensors for commercial buildings.
- EEM-6: Insulate the roof using RSI-3.

(b) The behavioral and rebound effects are estimated based on previous studies. Typically, the effects are higher for measures that relay on temperature and lighting controls (i.e., EEM-1 and EEM-5).

Table 23 summarizes the annual energy use, electricity peak demand, carbon emissions savings for Level-1, Level-2, and Level-3 building energy efficiency retrofit programs applied to the entire existing building stock in the Arab region. As clearly shown in Table 23, significant energy and environmental benefits can be achieved for all the levels of the building energy retrofit programs. While requiring higher implementation costs, higher benefits can be achieved for the Level-2 and Level-3 retrofit programs compared to the Level-1 retrofit program. The economic and environmental benefits that can be realized for residential buildings are significantly higher than those obtained for commercial and public buildings for all energy retrofit levels. Indeed, over 74% of the overall benefits can be achieved by solely retrofitting residential buildings in the Arab region as indicated in Table 23.

Table 23. The energy and environmental benefits for three levels of building energy efficiency retrofit programs for the Arab region [*].

Retrofit Program	Level-1	Level-2	Level-3
Annual Energy Savings (TWh/year)			
• Residential Buildings	63.269	166.523	344.180
• Commercial Buildings	21.660	59.346	125.623
Total Existing Building Stock	84.929	225.870	469.803
Peak Demand Savings (MW)			
• Residential Buildings	9720	24,301	49,074
• Commercial Buildings	3328	8318	16,358
Total Existing Building Stock	13,048	32,619	65,432
Annual CO_2 Savings Tons/year)			
• Residential Buildings	19.764	52.561	109.326
• Commercial Buildings	6.729	17.896	37.224
Total Existing Building Stock	26.493	70.458	146.550

(*) The benefits are estimated when the entire existing building stock within the Arab region is retrofitted.

It is expected that the implementation of large-scale building energy retrofit programs to be gradual requiring several years due to two main reasons: (i) the significant investments needed for renovating the entire existing building stock, and (ii) the lack of qualified energy efficiency contractors in most Arab countries requiring at least few years to develop and train. However, any of the three energy retrofit programs can result in significant economic and environmental benefits for the Arab region even when only a small fraction of the existing stock is targeted as noted in the results shown in Table 23. The energy retrofit programs for the existing building stock have significant impacts on both final energy consumption, peak electrical demand, and carbon emissions in the Arab region even when implemented gradually over a 10 year period starting either (a) in 2020 or (b) in 2030 as noted in Figure 21. As expected, a Level-3 retrofit has the highest impact with an annual energy consumption reduction of 470 TWh as well as a decrease in electricity demand of 65 GW and 146 million tons per year of carbon emissions when the program is fully implemented by 2030. A basic Level-1 retrofit program would still save 85 TWh in annual final energy consumption without significant investment requirements [12].

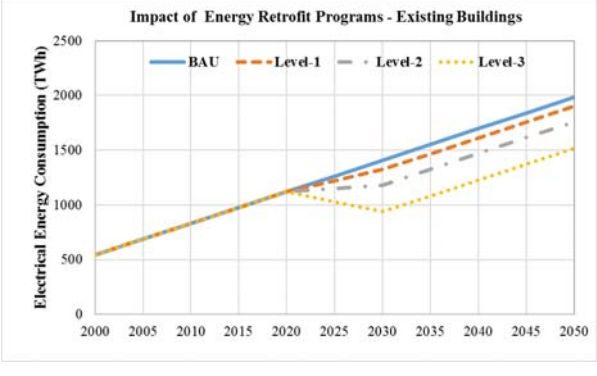

(a)

Figure 21. *Cont.*

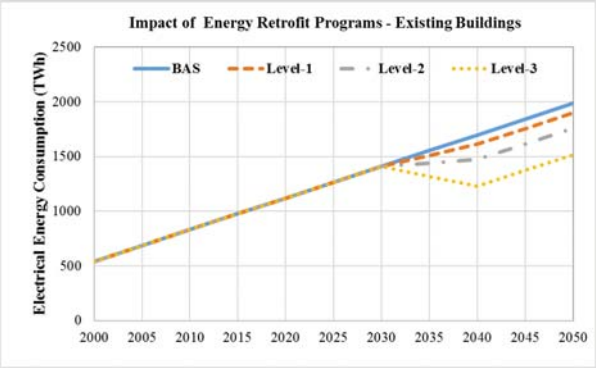

(**b**)

Figure 21. Impact on load profiles for electrical energy consumption due to implementation of energy retrofit programs for the entire existing building stock when the programs start during (**a**) 2020 and (**b**) 2030.

The retrofit programs can start initially with non-residential buildings since they provide higher energy savings per unit floor area than residential buildings for the Arab region [56]. Moreover, it is easier to perform energy audits and retrofits for larger non-residential buildings through ESCOs than it is for smaller residential buildings. In addition, retrofitting residential buildings offer specific privacy and cultural sensitivity challenges in several countries within the Arab region [12]. As indicated in Figure 21, the potential benefits depend on when the programs are actually initiated and the rate of the retrofit. The results of Figure 21 assume a 10% rate of retrofit (that is that 10% of the existing building stock is retrofitted each year). If lower retrofit rates are considered, the potential benefits will be reduced accordingly.

The highest impact scenario for reducing the final energy use and peak demand would be to simultaneously (i) implement integrated BEEC for new buildings and (ii) upgrade over a 10 year span the entire existing building stock using Level-3 energy retrofit. Figure 22 shows that there is a significant potential saving in annual energy consumption of buildings especially when Level-3 energy retrofit program is implemented during a 10 year period and new buildings are constructed using an integrated energy efficiency code starting in 2020 as illustrated in Figure 22a or in 2030 as indicated in Figure 22b. In particular, if the code and the retrofit program are implemented by 2020 the total Arab region's annual final energy consumption could be reduced by 597 TWh (or 43%) from a projected 1409 TWh per year under baseline scenario (BAU) to be only 812 TWh per year. Similar reductions in both electrical peak demands and carbon emissions can be achieved. While the required investments to implement these energy efficiency programs can be significant as highlighted later for the special case of Saudi Arabia in Table 23, the economic benefits can be substantial for most Arab countries as documented for the GCC countries [2,42–46].

The cost of the retrofit programs varies with the level and the country. For instance, Table 24 summarizes the required investments and the potential benefits of the three retrofit levels, outlined earlier in this section, for the entire existing residential and non-residential buildings of the Kingdom of Saudi Arabia (KSA). Specifically, it is found that [12]:

- Given the low electricity prices in Saudi Arabia, it makes little sense for households and other private organizations to invest in energy efficiency. The subsidies for energy prices have to be reduced in order for building owners and/or operators to cost-effectively invest in energy efficiency.
- When the economic benefits from avoided fuel consumption and reduced need for electricity generation capacity are considered, energy-efficiency investments by the KSA government for retrofitting existing buildings are highly cost-effective. For instance, a basic retrofit (i.e., Level-1)

of households can pay for itself within less than one year. Indeed this program can avoid the construction of 22,900 MW in power plant capacity and the consumption of 100,000 GWh electrical energy per year.

- Other benefits include the reduction of carbon emissions as well as employment creation in energy auditing. Specifically, over 76 million tons of carbon emissions can be eliminated when the Level-3 retrofit program is implemented for the existing KSA building stock. In addition, the Level-3 retrofit program would create 247,000 new jobs per year over a 10 year implementation period for a total of 2,470,000 job-years created.
- Innovative financing mechanisms need to be developed to incentivize the private sector to undertake large-scale energy efficiency investments. For instance, the creation of energy service companies can be initiated by the government using the concept of performance contracting as a means of financing energy efficiency based on future savings.
- The successful implementation of any energy efficiency program for both new and existing buildings requires the development of strong institutional and labor force capacity.

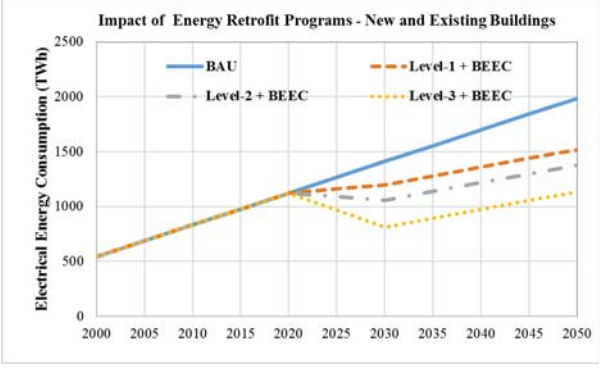

(**a**)

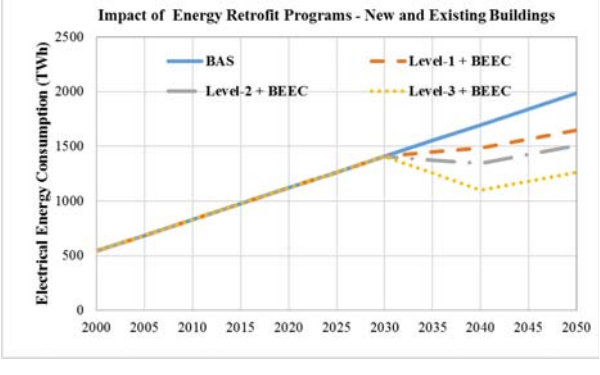

(**b**)

Figure 22. Impact on final energy consumption due to the implementation of both comprehensive energy efficiency code for new buildings and energy retrofit programs for the entire existing building stock when the programs start during (**a**) 2020 and (**b**) 2030.

Table 24. Summary of investments and benefits for building energy retrofit programs in Saudi Arabia (Source: [12]).

Retrofit Program	Level 1	Level 2	Level 3
Investments Required (USD Billion)	10	104	207
Avoided Electricity Consumption (GWh/year)	16,000	46,000	100,000
Value of Avoided Electricity Consumption (USD Billion/year)	0.5–1.7	1.4–4.9	3.0–10.5
Avoided Electricity Generation Capacity (MW)	3700	10,500	22,900
Value of Avoided Electricity Capacity (USD Billion)	2.8	7.9	17.2
Jobs Created (per year for a 10-year period)	12,000	123,000	247,000
Reduced Carbon Emissions (million ton/year)	12	35	76

4.5. Impact of Integrated Renewable Energy with Buildings

In this section, the integration of renewable energy systems in buildings is evaluated for the Arab region through the installation of rooftop photovoltaic (PV) panels. Recent studies have assessed the implementation costs and the benefits of installing PV systems on roofs of existing Saudi Arabia housing stock [16]. Table 25 summarizes the main findings of these studies specific to Saudi Arabia as well as results from a similar analysis conducted for Tunisia. In particular, Table 25 estimates the annual avoided carbon emissions and the electrical energy that can be generated when rooftop PV systems can be installed on top of all available roof areas for the existing residential building stock within Saudi Arabia and Tunisia. The new analysis for the PV rooftop systems for Tunisia is based on statistical data for the number and type of housing units obtained from the most recent census [65]. As noted in Table 25, the potential rooftop PV electricity generation is 51.0 TWh/year in Saudi Arabia representing about the third of current electricity needs for the residential buildings. For Tunisia, the rooftop PV panels can provide 15.2 TWh/year of energy equivalent to the overall current electricity consumption of the entire housing stock.

Table 25. Size and benefits of photovoltaic (PV) systems installed on roofs of the entire existing residential buildings in Saudi Arabia and Tunisia.

Size/Benefits	Saudi Arabia	Tunisia
PV Roof Area Available for Housing Units (Million m^2)	221.8	70.0
Size of Roof-PV Systems (GW)	38.0	10.5
Annual Electricity Generated by PV (TWh/year)	51.0	15.2
Carbon Emissions Avoided (Million Tons/year)	29.2	7.2

One approach to promote integration of PV systems in buildings is to require net-zero energy buildings (NZEBs) for new housing units. NZEB requirements are set in several regions of the World include EU and select US states. The analysis for prototypical residential buildings throughout the Arab region has shown that NZEB designs are possible based on integration of proven energy efficiency measures with rooftop PV systems [46]. Figure 23 presents the impact of NZEB requirements starting for all new residential buildings on the future final energy consumption of the Arab region buildings for two starting dates (a) 2020, and (b) 2030. When the program starts is set to 2020, annual energy savings are expected to reach 221 TWh by 2030 and 664 TWh by 2050 compared to BAU scenario. The main challenge for implementing the NZEB program would be the capital investments needed to install the PV rooftop systems. Based on 2500 USD/kW installation cost, the required capital costs

for the rooftop PV panels are estimated to be 90.6 USD Billion in Saudi Arabia and 25.4 USD Billion in Tunisia [16]. However, the cost of PV panels is expected to decrease further in the coming years possibly making NZEB designs cost-effective for most Arab countries especially when energy subsidies are reduced or eliminated. When the NZEB requirements for residential buildings are implemented to start in 2030, the potential benefits are delayed and reduced for 2050 to 450 TWh.

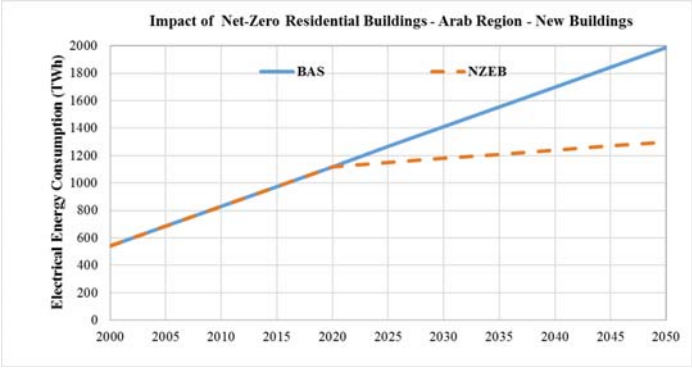

(**a**)

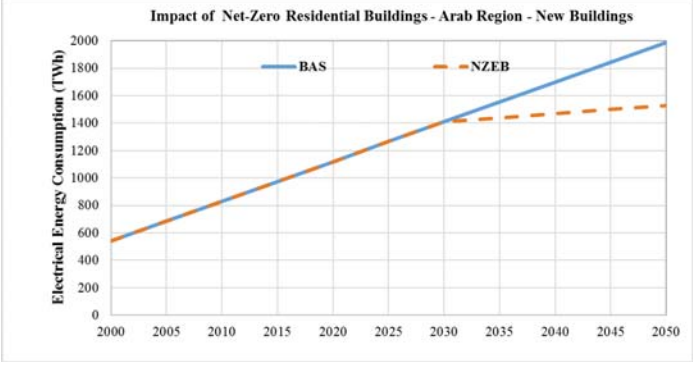

(**b**)

Figure 23. Impact on load profiles for electrical energy consumption due to implementation starting in (**a**) 2020, and (**b**) 2030 of net-zero residential buildings for the new housing stock in the Arab region.

5. Summary and Conclusions

In the study summarized in this paper, past and current energy consumption trends in the building sector are first analyzed for the Arab region and sub-regions. While the building sector contributes only 21% of the total final energy consumed in the Arab region, the energy used by households has doubled between 2005 and 2015. The set of analyses presented in the paper has clearly shown that the Arab region is not homogeneous in both past and current energy consumption trends and future energy challenges.

In particular, past and current energy consumption trends have shown that there is a large inequity between energy consumption between Arab countries and sub-regions. The inequities in per capita use of electricity for the building sector are as significant as the inequities in per capita use of overall primary energy. In 2015, the average citizen in the Gulf Cooperation Council sub-region used 8500 kWh of electricity. In contrast, the average citizen in the least developed countries used 1200 kWh. The per

capita average use of electricity for the built environment in the Mashreq and Maghreb sub-regions was 1900 kWh and 2100 kWh, respectively, during 2015. These sub-regionally aggregated figures mask even starker disparities among Arab countries. For instance, a citizen in Yemen consumes only 147 kWh of electricity annually while a citizen in Bahrain uses almost 20,200 kWh per year.

A comprehensive overview of current energy policies related to buildings has indicated that several countries have only recently adopted either minimum energy performance standards (MEPS) for air conditioners, lighting fixtures, and appliances. Moreover, more than half of the Arab countries have adopted energy efficiency codes for new buildings. However, these codes are typically limited to prescriptive requirements and consist of thermal insulation addition to walls and roofs and the use of double-pane glazing for windows. The enforcement of these recently adopted MEPS and building energy efficiency codes are still a challenge for most Arab countries.

As part of the analyses outlined in the second part of this paper, the benefits of large-scale implementation of energy efficiency programs for the building sector in the Arab region are quantified. The analysis includes strategies to improve the energy performance of both new and existing building stocks as well as improved minimum energy performance standards (MEPS). Specifically, implementing MEPS for energy-intensive equipment in buildings (i.e., lighting, appliances, and air conditioners) can be a good first step to reduce energy consumption and carbon emissions in the Arab region. Indeed, adoption of more stringent MEPS can achieve an annual energy savings of about 51.9 TWh by 2030 if these MEPS are implemented and strictly enforced starting in 2020. Moreover, the analysis presented in this paper shows that the replacement of existing fluorescent lamps by integrated controls LED units in commercial and public buildings can save additional 21.7 TWh annually. As a second phase, the adoption and the implementation of integrated and comprehensive energy efficiency codes for both residential and commercial buildings can result in an additional reduction of 12.7 TWh/year in final energy consumption for the overall Arab region. Finally, the analysis presented in this paper has clearly indicated that the most significant potential to save energy in the Arab region lies in retrofitting existing building stock. Indeed, even with a basic retrofit program with no significant capital investments about 85 TWh/year can be saved for the Arab region by 2030. A more aggressive retrofit program can save up to 470 TWh or the third of building sector final energy consumption per year after 2030. When combining the adoption of comprehensive energy efficiency codes for new buildings and the implementation of extensive retrofit programs for existing buildings, the annual energy consumption by the building sector in the Arab region can be lowered by 600 TWh by 2030. In addition, these programs can create significant high skilled jobs, avoid the need for additional future power plants, and reduce substantially carbon emissions.

Acknowledgments: The research was funded by United Nations ESCWA program, grant number 2500114522.

Conflicts of Interest: The author declares no conflict of interest.

Nomenclature

AC	Air Conditioners
BAU	Business as Usual
BEEC	Building Energy Efficiency Code
CDD	Cooling Degree Days
CFL	Compact Fluorescent Lamp
COP	Coefficient of Performance
EEM	Energy Efficiency Measure
EER	Electrical Efficiency Ratio
EU	European Union
EUI	Energy Use Intensity

GCC	Gulf Cooperation Council
GDP	Gross Domestic Product
HDD	Heating Degree Days
IEA	International Energy Agency
IMF	International Monetary Fund
KSA	Kingdom of Saudi Arabia
LCC	Life Cycle Cost
LDC	Least Developed Countries
LED	Lighting Emitting Diode
LEED	Leadership in Energy and Environment Design
MENA	Middle East and North Africa
MEPS	Minimum Energy Performance Standard
NZEB	Net Zero Energy Building
PV	Photovoltaic
TFEC	Total Final Energy Consumption
TOE	Ton of Energy Equivalent
TPES	Total Primary Energy Supply
UAE	United Arab Emirates
US	United States
USD	US Dollar (1 USD = 0.90 EURO)

References

1. IEA. *International Energy Agency Statistics: Energy Balance*; IEA: Paris, France, 2017; Available online: http://www.iea.org/statistics (accessed on 16 January 2018).
2. Krarti, M.; Dubey, K. Energy productivity evaluation of large scale building energy efficiency programs for Oman. *Sustain. Cities Soc.* **2017**, *29*, 12–22. [CrossRef]
3. KAPSARC. *Global Shift: The Energy Productivity Transformation*; KAPSRAC Energy Workshop Series; The King Abdullah Petroleum Studies and Research Center: Riyadh, Saudi Arabia, 2015; Available online: http://www.kapsarc.org (accessed on 18 December 2017).
4. KAPSARC. *The Case of Energy Productivity: It's Not Just Semantics*; KAPSRAC Discussion Paper; The King Abdullah Petroleum Studies and Research Center: Riyadh, Saudi Arabia, 2014; Available online: http://www.kapsarc.org (accessed on 18 December 2017).
5. World Bank. World Development Data. 2017. Available online: http://databank.Worldbank.org/data/home.aspx (accessed on 11 December 2017).
6. UN-Habitat. States of Arab Cities 2012. In *Challenges of Urban Transition*; United Nations Human Settlements Programme: Nairobi, Kenya, 2013.
7. GCOOE. Oxford Economics and Global Construction Perspectives. In *Global Construction 2020*; Executive Report; Global Construction Perspectives and Oxford Economics: Oxford, UK, 2011.
8. Asif, M. Growth and sustainability trends in the buildings sector in the GCC region with particular reference to the KSA and UAE. *Renew. Sustain. Energy Rev.* **2016**, *55*, 1267–1273. [CrossRef]
9. United Nations. Statistical Data, UN Statistics Division. 2017. Available online: https://unstats.un.org/unsd/databases.htm (accessed on 15 January 2018).
10. Krarti, M.; Ihm, P. Evaluation of Net-Zero Energy Residential Buildings in the MENA Region. *Sustain. Cities Soc.* **2016**, *22*, 116–125. [CrossRef]
11. Krarti, M. Evaluation of large scale building energy efficiency retrofit program in Kuwait. *Renew. Sustain. Energy Rev.* **2015**, *50*, 1069–1080. [CrossRef]
12. Krarti, M.; Dubey, K.; Howarth, N. Evaluation of building energy efficiency investment options for the Kingdom of Saudi Arabia. *Energy* **2017**, *134*, 595–610. [CrossRef]
13. USAID. *Housing Study for Urban Egypt*; Final Report for US Agency for International Development: Washington, DC, USA, 2018. Available online: http://pdf.usaid.gov/pdf_docs/Pnady276.pdf (accessed on 10 January 2018).
14. CAPMAS. *Census Data for Egypt*; Central Agency for Public Mobilization and Statistics: Cairo, Egypt, 2017; Available online: http://egypt.opendataforafrica.org/tadpaqg/egypt-census-data (accessed on 15 December 2017).

15. ANME. Elaboration d'un Plan pour la Rénovation Thermique et Energétique des Bâtiments Existants en Tunisie. In *Partie-1: Connaissance et Analyse du Secteur*; Technical Report by TEMA Consulting and CESEEN for Agence Nationale pour la Maitrise de l'Energie; ANME: Tunis, Tunisia, 2010.
16. Khan, M.M.A.; Asif, M.; Stach, E. Rooftop PV Potential in the Residential Sector of the Kingdom of Saudi Arabia. *Buildings* **2017**, *7*, 46. [CrossRef]
17. Navigant. *Global Building Stock Database Commercial and Residential Building Floor Space by Country and Building Type: 2014–2024*; Navigant: Boulder, CO, USA, 2015.
18. GABC. Towards Zero-Emission Efficient and Resilient Buildings, Global Alliance for Building and Construction. 2016. Available online: http://www.planbatimentdurable.fr/IMG/pdf/gabc_report.pdf (accessed on 12 December 2017).
19. Harvey, L.D.D.; Korytarovab, K.; Luconc, O.; Roshchankada, V. Construction of a global disaggregated dataset of building energy use and floor area in 2010. *Energy Build.* **2014**, *76*, 488–496. [CrossRef]
20. IEA-ETP. Annex E: Buildings Sector Model, Energy Technology Perspectives. Available online: https://www.iea.org/media/etp/etp2016/AnnexE_UrbanBuildingsEnergyEstimationMethodology_web.pdf (accessed on 22 December 2017).
21. McNeil, M.A.; Letschert, V.E.; de la Rue du Can, S.; Ke, J. Bottom-up energy analysis system (BUENAS)—An international appliance efficiency policy tool. *Energy Effic.* **2013**, *6*, 191–217. [CrossRef]
22. Ürge-Vorsatz, D.; Petrichenko, K.; Antal, M.; Staniec, M.; Ozden, E.; Labzina, E. *Best Practice Policies for Low Carbon & Energy Buildings Based on Scenario Anal-Ysis*; Centre for Climate Change and Sustainable Policy (3CSEP) for the GlobalBuildings Performance Network: Paris, France, 2013.
23. WBG. *Energy-Efficient Air Conditioning: A Case Study of the Maghreb Opportunities for a More Efficient Market*; Khalfallah, E., Missaoui, R., el Khamlichi, S., Hassine, H.B., Eds.; World Bank Group: Washington, DC, USA, 2016; Available online: http://http://documents.Worldbank.org/curated/en/754361472471984998/pdf/105360-REVISED-PUBLIC-MENA-Digital-Print-English-sep-2016.pdf (accessed on 15 January 2018).
24. RCREEE. *Energy Efficiency Indicators in The Southern and Eastern Mediterranean Countries*; Missaoui, R., Hassine, H.B., Mourtada, A., Eds.; RCREEE: al-Qāhira, Egypt, 2012; Available online: http://http://www.rcreee.org/sites/default/files/rs_eeindicatorsinthesouthernandeasternmediterraneancountries_2012_en.pdf (accessed on 24 January 2018).
25. MEDENER. Energy Efficiency Trends in Mediterranean Countries, Report Prepared by Eenerdata. 2013. Available online: http://medener-indicateurs.net/uk/download/094 (accessed on 21 December 2017).
26. JRAIA. *World Air Conditioner Demand by Region*; Japan Refrigeration and Air Conditioning Industry Association: Tokyo, Japan, 2017; Available online: https://www.jraia.or.jp/english/World_AC_Demand.pdf (accessed on 27 January 2018).
27. IMF. *How Large Global Energy Subsidies?* Country level estimates, International Monetary Fund, Fiscal Affairs Department: Washington, DC, USA, 2015.
28. RCREEE. *Arab Future Energy Index 1015—Energy Efficiency*; Regional Center for Renewable Energy and Energy Efficiency (RCREEE): Cairo, Egypt, 2015; Available online: www.rcreee.org (accessed on 15 December 2017).
29. IRENA. *Renewable Energy in the Arab Region: Overview of Developments*; Report in Collaboration with Arab LAS and RCREEE, International Renewable Energy Agency; IRENA: Abu Dhabi, UAE, 2016.
30. Fattouh, B.; El-Katiri, L. Energy Subsidies in the Arab Region, Research Paper Series on Arab Human Development Report for United Nations Development Programme—Regional Bureau of Arab States. 2012. Available online: http://www.undp.org (accessed on 21 December 2017).
31. Ameer, B.; Krarti, M. Impact of Subsidization on High Energy Performance Designs for Kuwaiti Residential Buildings. *Energy Build.* **2016**, *116*, 249–262. [CrossRef]
32. IEA. *Building Energy Performance Metrics, Supporting Energy Efficiency Progress in Major Economies*; International Energy Agency: Paris, France, 2015.
33. Taleb, H.M.; Sharples, S. Developing sustainable residential buildings in Saudi Arabia: A case study. *Appl. Energy* **2011**, *88*, 383–391. [CrossRef]
34. Alaidroos, A.; Krarti, M. Optimal design of residential building envelope systems in the Kingdom of Saudi Arabia. *Energy Build.* **2015**, *86*, 104–117. [CrossRef]
35. Radhi, H. Evaluating the potential impact of global warming on the UAE residential buildings—A contribution to reduce the CO_2 emissions. *Build. Environ.* **2009**, *44*, 2451–2462. [CrossRef]

36. Ecofys. *A Roadmap for Developing Energy Indicators for Buildings in Lebanon, Energy Efficiency in the Construction Sector in the Mediterranean*; Final Report for MED-NEC; Ecofys: Utrecht, The Netherlands, 2013; Available online: http://https://www.ecofys.com/files/files/med-enec-2013-roadmap-ee-indicators-buildings-lebanon.pdf (accessed on 20 December 2017).
37. UNEP. Development of a System of Energy Intensity Indicators for the Egyptian Economy, Report for United Nations Environment Program by Environics. 2011. Available online: http://www.mdgfund.org/sites/default/files/ENV_STUDY_Egypt_Development%20of%20Energy%20Indicactor%20System.pdf (accessed on 10 January 2018).
38. Fasiuddin, M.; Budaiwi, I. HVAC system strategies for energy conservation in commercial buildings in Saudi Arabi. *Energy Build.* **2011**, *43*, 3457–3466. [CrossRef]
39. Fasiuddin, M.; Budaiwi, I.; Abdou, A. Zero-investment HVAC system operation strategies for energy conservation and thermal comfort in commercial buildings in hot-humid climate. *Int. J. Energy Res.* **2010**, *34*, 1–19. [CrossRef]
40. Alajmi, A. Energy audit of an educational building in a hot summer climate. *Energy Build.* **2012**, *47*, 122–130. [CrossRef]
41. Radhi, H.; Sharples, S. Benchmarking carbon emissions of office buildings in Bahrain. In Proceedings of the PLEA 2007—24th Conference on Passive and Low Energy Architecture, Singapore, 22–24 November 2007.
42. Krarti, M.; Dubey, K. Review Analysis of Economic and Environmental Benefits of Improving Energy Efficiency for UAE Building Stock. *Renew. Sustain. Energy Rev.* **2018**, *82*, 14–24. [CrossRef]
43. Krarti, M.; Ali, F.; Alaidroos, A.; Houchati, M. Macro-economic benefit analysis of large-scale building energy efficiency programs in Qatar. *Int. J. Sustain. Built Environ.* **2018**. [CrossRef]
44. Krarti, M.; Dubey, K. Evaluation of High Performance of Residential Buildings in Bahrain. *J. Build. Eng.* **2018**, *18*, 40–50. [CrossRef]
45. Ihm, P.; Krarti, M. Design optimization of energy efficient office buildings in Tunisia. *ASME J. Sol. Energy Eng.* **2013**, *135*. [CrossRef]
46. Ihm, P.; Krarti, M. Design optimization of energy efficient residential buildings in Tunisia. *Build. Environ.* **2012**, *58*, 81–90. [CrossRef]
47. U4E. United for Energy Efficiency, Country Assessments. 2017. Available online: http://united4efficiency.org (accessed on 27 December 2017).
48. Shackelford, J.; Robinson, A.; Rubinstein, F. *Retrofit Demonstration of LED Fixtures with Integrated Sensors and Controls*; Lawrence Berkeley National Laboratory Report Prepared for US General Services Administration: Berkeley, CA, USA, 2015.
49. Khilifi, A.; Krarti, M. Genetic Algorithm Based Controls for Daylighting. In Proceedings of the ASME Solar Energy Conference, Denver, CO, USA, 13–18 July 2016.
50. Krarti, M. *Energy Audit of Building Systems: An Engineering Approach*, 2nd ed.; CRC Pres: Boca Raton, FL, USA, 2011.
51. Liu, F.; Meyer, A.S.; Hogan, J.F. *Mainstreaming Building Energy Efficiency Codes in Developing Countries, Global Experiences and Lessons from Early Adopters*; Paper No. 204; The World Bank: Washington, DC, USA, 2010; Available online: http://www.Worldbank.org (accessed on 12 December 2017).
52. RISE. Regulatory-Indicators-for-Sustainable-Energy (RISE). Report by World Bank. 2015. Available online: http://documents.Worldbank.org/curated/en/538181487106403375/pdf/112828-REVISED-PUBLIC-RISE-2016-Report.pdf (accessed on 10 March 2018).
53. Kwag, B.C.; Adamu, B.M.; Krarti, M. Analysis of high-energy performance residences in Nigeria. *Energy Effic.* **2019**, *12*, 681–695. [CrossRef]
54. Park, B.; Srubar, W.V.; Krarti, M. Energy performance analysis of variable thermal resistance envelopes in residential buildings. *Energy Build.* **2015**, *103*, 317–325. [CrossRef]
55. Menyhart, K.; Krarti, M. Potential energy savings from deployment of Dynamic Insulation Materials for US residential buildings. *Build. Environ.* **2017**, *114*, 203–218. [CrossRef]
56. Al-Ragom, F. Retrofitting residential buildings in hot and arid climates. *Energy Convers. Manag.* **2003**, *44*, 2309–2319. [CrossRef]
57. Znouda, E.; Ghrab-Morcos, N.; Hadj-Alouane, A. Optimization of Mediterranean building design using genetic algorithms. *Energy Build.* **2007**, *39*, 148–153. [CrossRef]

58. Al-Sanea, S.A.; Zedan, M.F.; Al-Hussain, S.N. Effect of thermal mass on performance of insulated building walls and the concept of energy savings potential. *Appl. Energy* **2012**, *89*, 430–442. [CrossRef]
59. Jacobsen, G.D.; Kotchen, M.J. Are building codes effective at saving energy? Evidence from residential billing data in Florida. *Rev. Econ. Stat.* **2013**, *95*, 34–49. [CrossRef]
60. ASHRAE. *Procedures for Commercial Building Energy Audits*, 2nd ed.; Guide Developed; The American Society for Heating, Refrigerating, and Air Conditioning Engineers: Atlanta, GA, USA, 2011.
61. Campisi, D.; Simone Gitto, S.; Morea, D. An Evaluation of Energy and Economic Efficiency in Residential Buildings Sector: A Multi-Criteria Analysis on an Italian Case Study. *Int. J. Energy Econ. Policy* **2018**, *8*, 185–196.
62. Yan, D.; O'Brien, W.; Hong, T.; Feng, X.; Gunay, H.B.; Tahmasebi, F.; Mahdavi, A. Occupant behavior modeling for building performance simulation: Current state and future challenges. *Energy Build.* **2015**, *107*, 264–278. [CrossRef]
63. D'Oca, S.; Hong, T.; Langevin, J. The human dimensions of energy use in buildings: A review. *Renew. Sustain. Energy Rev.* **2018**, *81*, 731–742. [CrossRef]
64. Pereira, P.F.; Ramos, N.M. Occupant behaviour motivations in the residential context—An investigation of variation patterns and seasonality effect. *Build. Environ.* **2019**, *148*, 535–546.
65. ST. Statistiques de Tunisie, Census Data of 2014: Number of Housing Units by Governorate, Area and Type. 2014. Available online: http://regions.ins.tn (accessed on 20 January 2018).

MDPI
St. Alban-Anlage 66
4052 Basel
Switzerland
Tel. +41 61 683 77 34
Fax +41 61 302 89 18
www.mdpi.com

Energies Editorial Office
E-mail: energies@mdpi.com
www.mdpi.com/journal/energies

MDPI
St. Alban-Anlage 66
4052 Basel
Switzerland

Tel: +41 61 683 77 34
Fax: +41 61 302 89 18

www.mdpi.com

ISBN 978-3-03928-703-1